Eindevaluatie pilot Langsdammen in de Waal

Hydromorphological data and observations

enabling delta life

Eindevaluatie pilot Langsdammen in de Waal

Hydromorphological data and observations

Authors
Jurjen de Jong
Victor Chavarrías
Willem Ottevanger

Front page: Longitudinal training wall at Dreumel (photo by Frank Collas)

Deltares

Eindevaluatie pilot Langsdammen in de Waal

Hydromorphological data and observations

Client	Rijkswaterstaat Water, Verkeer en Leefomgeving
Contact	de heer J. Sieben
Reference	Eindevaluatie en analyse WaalSamen, pilot Langsdammen, zaaknummer 31154483
Keywords	Langsdammen, longitudinal training walls, Waal, rivieren, hydrodynamica, morfodynamica

Document control

Version	1.0
Date	2021-12-15
Project number	11204644-018
Document ID	11204644-018-ZWS-0001
Pages	560
Status	final

Author(s)

	Jurjen de Jong	Deltares
	Victor Chavarrías	Deltares
	Willem Ottevanger	Deltares

Doc. version	Author	Reviewer	Approver	Publish
1.0	Jurjen de Jong	Kees Sloff	Johan Boon	

Executive summary

In the river Waal, longitudinal training walls (LTW) have been built in 2015 near Tiel as a pilot to replace the groynes. Combined with the realisation, also a measurement campaign of multiple years was started to study the effects of the LTW on water levels, flow velocities and bed level. In this report these measurements have been processed and analysed to answer the research questions posed by Rijkswaterstaat.

Measurements

Water levels have been obtained from longitudinal water level measurements ('verhanglijnmetingen'), from the national LMW-network, and from measurements with divers. The longitudinal measurements have been executed biweekly from 2018 onwards, and several times per year for the period before. Small changes in water level can not be found as the measurements are strongly influenced by ship waves. Measurements with divers were installed at both river kilometre (rkm) 911.5 and 922 and at the head of all three LTW. The measurements by divers at rkm 911.5 and 922 were only available for the period between August 2013 and December 2016 and did not include periods of low discharge. Data of the divers at the head of the LTW was only available between October 2020 and December 2020. The data from the divers was thus considered insufficient for the analyses.

Flow velocity measurements were executed for many runs at the LTW with the use of ADCP. From 2018 onwards the frequency of the measurements was increased to biweekly campaigns. In each campaign, measurements were done at multiple location in the main channel and auxiliary channel, and each locations was measured in multiple runs. The ADCP measurements have been compared with four reference measurements of the situation before construction of the LTW. In addition, the flow field at the inlets is studied.

Bed level measurements are available from yearly soundings ('JMP') and from additional campaigns that were performed every eight weeks. Every campaign covers both the main channel and the auxiliary channel. The yearly sounding make it possible to compare with the situation before construction of the LTW. The soundings have been analysed using the 'P-map' method by Rijkswaterstaat, where statistics of the distribution in bed level soundings are derived for both short reaches (100 m) and long reaches.

It is found very valuable that the longitudinal training wall pilot was combined with an extended measurement campaign. However, data should not be merrily stored, but inspected and made available in a processed and uniformed format by an experienced party. This would allow all researches at universities over the past years to also include this extended dataset.

Effect on the water levels

Measurements at Tiel show a lowering of the water level for equal discharge as a result of bed erosion in the period before construction of the LTW. After construction of the LTW the water level at Lobith discharges below 2000 m^3/s remains stable or show a small increase in water level of several centimetres per year (figure 0.1). For average and high discharge, the water levels after construction have been lowered by approximately 20 cm as a result of removal of the groynes (figure 0.2). At high discharge the lowering of the water levels is also effected by the realisation of the side channel Passewaaij (right bank at Dreumel) and the lowering of the groynes downstream of the LTW.

The effect of changes in the inlets could unfortunately not be noticed in the measurements. Even though as a result of the closing of the inlet at Wamel (April 2018), it was found (in ADCP measurements) that the discharge in the auxiliary channel reduced which should have an effect of 10 to 20 cm on the water levels. Unfortunately, stationary (diver) measurements were not available at the inlet of Wamel and the effect is too small to be noticeable in the longitudinal measurements.

The effect of the withdrawal of river discharge through the Prins Bernhardsluizen is clearly visible in the water levels at Tiel. Days where a high discharge was measured through the Amsterdam-Rijnkanaal (up to 68 m^3/s) correspond with an approximately 15 cm lower water level.

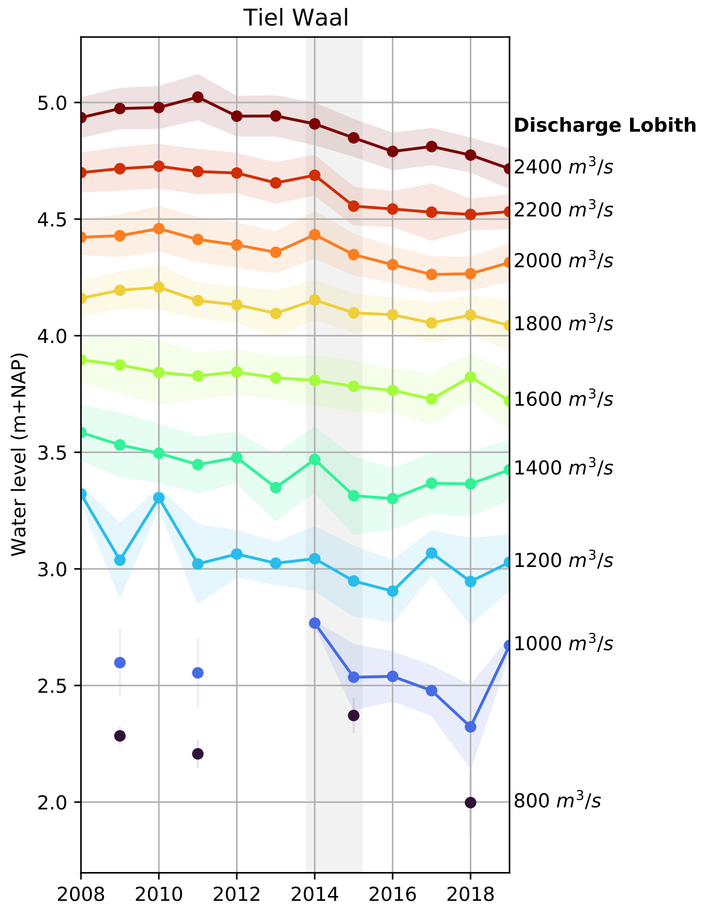

Figure 0.1 Trends in water level at Tiel, showing the mean and standard-deviation per discharge bin (+/- 100 m^3/s). The years influenced by construction are marked in grey.

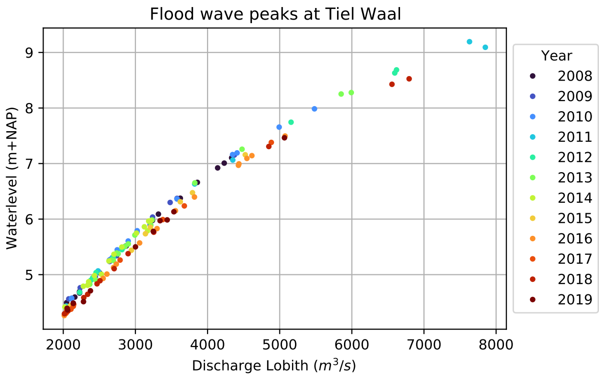

Figure 0.2 Trend in flood peaks per year at Tiel Waal.

Effect op flow velocity and sediment transport

From ADCP measurements a reduction in flow velocity of 2% to 15% is concluded for conditions where the dam is submerged (discharge Lobith above 3000 m^3/s (figure 0.3). It is expected that as a result the sediment transport capacity has decreased with approximately 40%. This is expected to result in sedimentation.

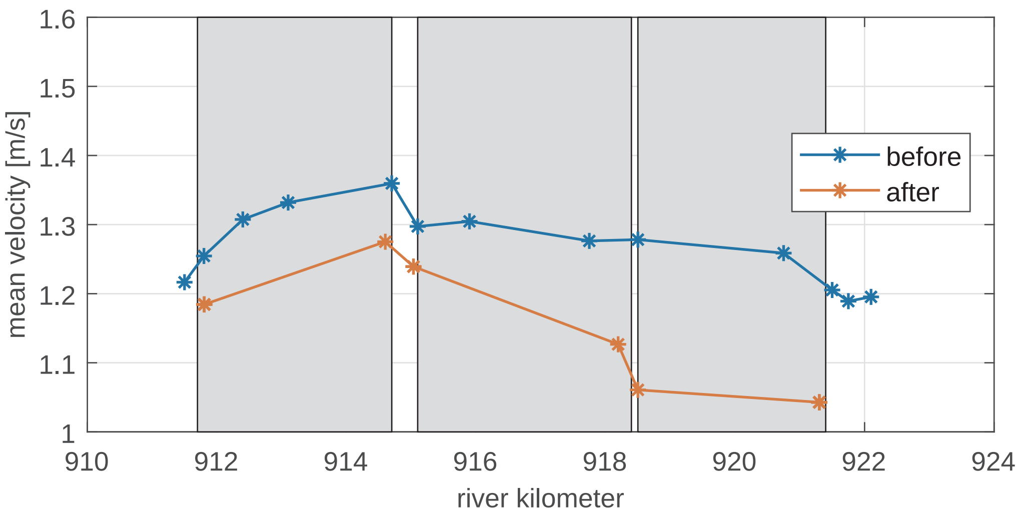

Figure 0.3 Cross-sectional and depth-averaged streamwise velocity at the central 100 m of main channel before intervention (1 Februari 2013) and after intervention (15 and 16 January 2019) for Condition 2 (2500 to 3500 m^3/s at Lobith).

Effect on bed level and water depth

From the P-map analyses (figure 0.4) it is concluded that prior to construction of the LTW the bed level had an small eroding trends at Dreumel, Wamel and upstream, and a small sedimentation trend at Ophemert and downstream of the LTW. During construction of the LTW, the bed level at Wamel and Ophemert shows a strong erosion. After construction at Ophemert the sedimentation is dominant, while at Wamel and Dreumel reaches of erosion and sedimentation are alternating. After the raising of the inlet of Wamel (April 2018), the discharge in the main channel increased and the bed level shows a stronger erosion trend. The smaller adjustments to the inlets of Dreumel and Ophemert, are not showing a change in trend in the measurements. On average the eroding trend (prior to construction) has been stopped and changed into a small sedimentation trend, which is in line with the ADCP measurements.

In combination with the stabilisation of the water levels, the higher bed results in a reduction of the average water depth. As the ADCP measurements show a reduction in flow velocities, this suggests an increase in the flow width. The effect on the local water depth is studied by comparing the bed level to the OLR reference level. This shows that especially at Ophemert the depth has decreased after construction, but that during periods of low discharge (OLA) this depth does not drop below 2.8 m, probably as result of maintenance.

The analyses using P-map can not conclude on the effect of the LTW on river dunes.

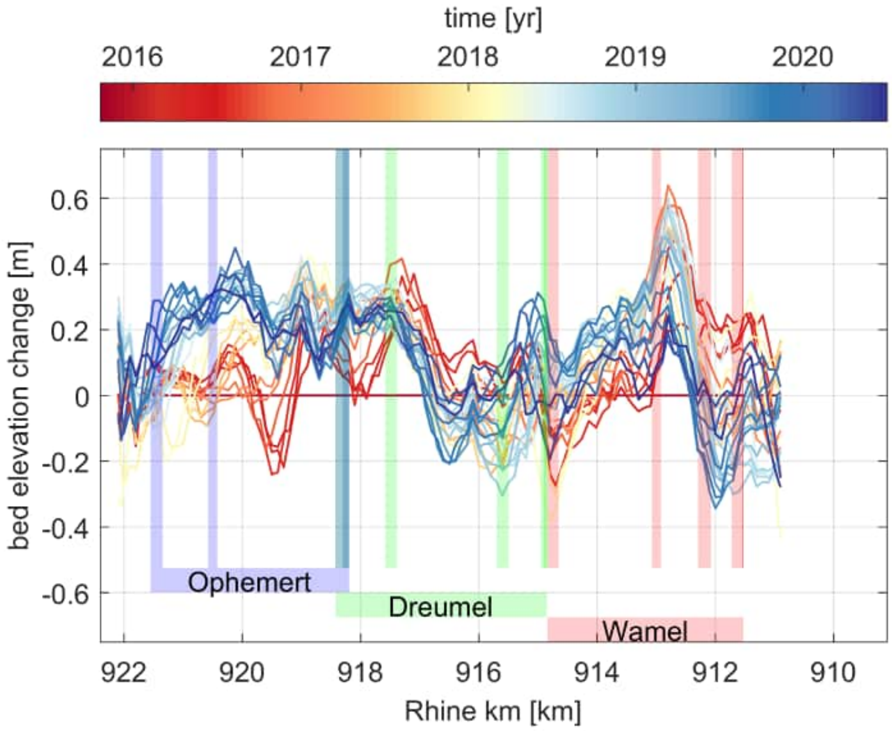

Figure 0.4 Average bed level development based on P-map analysis (averaged over 250 m upstream and downstream) relative to 2015 week 42

Contents

	Executive summary	**4**
1	**Introduction**	**12**
2	**Water level**	**14**
2.1	Introduction	14
2.2	Available data	14
2.2.1	Processing of longitudinal measurements	14
2.2.2	Processing of water level measurement stations	17
2.3	Effect of the longitudinal training walls	18
2.3.1	Water level change in longitudinal water level measurements	18
2.3.2	Water level change at (LMW) measurement stations	22
2.3.3	Change in head difference between measurement stations	25
2.4	Effect of changing in inlet openings	26
2.4.1	Effect of openings on the water level in the river axis	26
2.4.2	Effect of openings on the water level slope in the auxiliary channel	27
2.5	Effect of opening the Prins Bernhardsluizen	34
2.6	Waves in the auxiliary channel	35
2.7	Discussion of the applicability of longitudinal measurements	37
2.8	Conclusions and recommendations	38
3	**Flow velocity**	**39**
3.1	Introduction	39
3.2	Available data	39
3.3	Changes in flow due to the construction of the longitudinal training walls	41
3.3.1	Methodology and results of the analysis of the flow changes	41
3.3.2	Methodology and results of the analysis of the discharge partitioning	55
3.3.3	Discussion of the results of the analysis of the changes in flow and recommendations	58
3.4	Transverse velocity near the inlets	61
3.4.1	Methodology and results of the analysis of the transverse velocity	61
3.4.2	Discussion of the results of the analysis of the transverse velocity near inlets and recommendations	67
3.4.3	Conclusions and recommendations	67
4	**Bed level**	**68**
4.1	Introduction	68
4.2	Available data	68
4.2.1	Yearly multibeam measurements 2000-2017	68
4.2.2	8 weekly multibeam measurements	68
4.2.3	P-map procedure	68
4.2.4	Reference plane OLR	70
4.2.5	Channel widths and analysis polygons	70
4.3	Methodology	72
4.4	Results	74
4.4.1	Main channel development	74
4.4.2	Effect of the change in inlets on the bed level trends in the main channel	79
4.4.3	Auxiliary channel development	81
4.4.4	Bank erosion in the auxiliary channels	83
4.4.5	Effect on navigation	84
4.5	Conclusions and recommendations	88

5	**Conclusions and recommendations**	**91**
5.1	Water levels	91
5.2	Velocity and Discharge	92
5.3	Sediment transport	92
5.4	Bed levels	93
5.5	Dune height	94
5.6	Navigation	94
5.7	Recommendations	95
5.7.1	Further research on different effects at low discharge	95
5.7.2	Distribution of the water in the Rhine at low discharge	96
5.7.3	Change in sediment transport capacity	96
5.7.4	Improvements to systematic storing of the data	97
5.7.5	Reconsider of longitudinal water level measurements	97
6	**References**	**98**
A	**Design and developments of the longitudinal training walls**	**100**
A.1	Asbuilt design drawings	100
A.2	Dimensions of the inlets	102
A.3	Fixed Layers	105
A.4	Timeline of development in the region of the LTW	108
A.5	Discharge regimes	108
B	**Longitudinal water level measurements**	**111**
B.1	Processing	111
B.2	Overview	113
B.3	Details per measurement	116
B.4	Average of longitudinal measurements	202
B.4.1	Aslijn	202
B.4.2	Wamel	208
B.4.3	Dreumel	211
B.4.4	Ophemert	214
B.5	Head difference to main channel	217
B.5.1	Wamel	217
B.5.2	Dreumel	220
B.5.3	Ophemert	223
B.6	Effect on curvature	226
C	**Water level measurements at stations**	**227**
C.1	LMW-measurements	227
C.1.1	Processing	227
C.1.2	Rating curves	229
C.1.3	Water level trends	232
C.1.4	Head Difference trends	236
C.1.5	Peaks and troughs	239
C.1.6	Peak water level trends	241
C.1.7	Trough water level trends	244
C.1.8	Discharge Amsterdam-Rijnkanaal	246
C.2	Diver measurements	246
D	**ADCP**	**250**
D.1	Summary of all ADCP profiles along the Waal River.	250
D.2	Summary of ADCP profiles used in the analysis of conditions prior/post intervention.	281

Deltares

D.3 Comparison of the flow pattern before and after intervention 283
D.3.1 Condition 1 283
D.3.2 Condition 2 287
D.3.3 Condition 3 326
D.3.4 Condition 4 365
D.4 Summary of ADCP profiles used in analysis of velocity at entrances. 404
D.5 Transverse velocity near inlets 405
D.5.1 Ophemert upstream 405
D.5.2 Wamel inlet 1 433
D.5.3 Wamel inlet 2 437
D.5.4 Wamel upstream 441
D.5.5 Wamel-Dreumel 471
D.6 Discharge partitioning between auxiliary channel and main channel 503

E Bed level 515
E.1 Pre-defined sections for bed level analyses 515
E.2 Comparison to the findings of Czapiga *et al.* (2021) 518
E.3 Development in main channel for different reaches 520
E.4 Development in auxiliary channels 540
E.5 Analysis of bed levels with respect to OLR 542
E.6 Wamel inlet 550
E.7 Dreumel inlet 550
E.8 Ophemert inlet 550
E.9 Overall sedimentation erosion 551

F MGD registrations 559

Preface

Het riviersysteem van de Rijn, met daarin alle Nederlandse Rijntakken, kent problemen met onder meer hoogwaterveiligheid, insnijding van de zomerbedbodem, daling van laagwaterstanden en grondwaterstanden, de kwaliteit van het rivierecosysteem, en het gebruik van de rivier als vaarweg. De laatste decennia wordt onderkend dat de sectorale aanpak niet efficiënt is. De beleidsdirecties van het ministerie van Infrastructuur en Waterstaat hebben de wens uitgesproken voor een meer innovatieve systeem- en gebiedsgerichte aanpak, met integrale aandacht voor alle probleemvelden tegelijk. Deze integrale aanpak beoogt de som van alle problemen te reduceren in plaats van slechts de problemen van een beperkt aantal sectoren.

Voor deze integrale aanpak heeft Rijkswaterstaat Oost-Nederland een idee gelanceerd onder de werknaam WaalSamen. Dit is een plan voor herinrichting van het zomerbed in de gehele Waal. De herinrichting wijzigt het principe van het bestaande normalisatiesysteem door het zomerbed te verdelen in twee parallelle stroomgeulen, gescheiden door een langsdam. Om de eigenschappen van deze systeemwijziging in de praktijk te beproeven is over een lengte van tien kilometer de pilot Langsdammen uitgevoerd. Het doel daarvan is een proof of concept, om meer zekerheid te verkrijgen over de integrale werking en de potenties van een dergelijke systeemwijziging.

Voor de pilot werd het Waaltraject Wamel-Ophemert (km 911.5-921.5) bij Tiel gekozen. Om redenen van efficiëntie werd de pilot tegelijk uitgevoerd met Fase III van het project Kribverlaging Waal van het programma Ruimte voor de Rivier. Hiervoor leverde Rijkswaterstaat Oost-Nederland op 30 juni 2011 de producten van een SNIP-3-besluit op aan de Programmadirectie Ruimte voor de Rivier van Rijkswaterstaat, inclusief een omwisselbesluit om geplande kribverlaging te vervangen door langsdammen. De Staatssecretaris van Verkeer en Waterstaat bekrachtigde dit eind 2011. De langsdammen tussen Wamel en Ophemert werden vervolgens in de periode van augustus 2014 tot maart 2016 gerealiseerd.

Voor, tijdens en na de aanleg van de langsdammen is een uitgebreid monitorings- en onderzoeksprogramma uitgevoerd door de partners van de samenwerkingsovereenkomst ‘WaalSamen’. Dit programma is afgesloten met een integrale eindevaluatie, onderverdeeld in 12 inhoudelijke deelprojecten die worden aangeduid met “WP” (werkpakket). Voor u ligt het deelrapport van WP0 over het onderdeel van de evaluatie van het tweegeulensysteem met langsdammen dat gericht is op hydromorphologische data en observaties. De deelrapporten vormen de ondergrond van het hoofdrapport, maar de inzichten en conclusies zijn bij het opstellen van dat hoofdrapport integraler beschouwd, verder geëvolueerd en verduidelijkt. Waar dat mogelijk tot verschillen heeft geleid, zijn de conclusies van het hoofdrapport leidend.

1 Introduction

In the river Waal, longitudinal training walls (LTW) have been built in 2015 near Tiel as a pilot to replace the groynes. Combined in construction plan, also a measurement campaign of multiple years was started. Each year, tens of measurement campaigns were executed, measuring velocities with ADCP, water levels as longitudinal tracks, and bed levels with multibeam soundings. In PhD- and MSc- research projects many of the measurements have been analysed, but a large part has never been processed before. In the evaluation of this pilot in 2020/2021 it became apparent that multiple research questions were still open which could possibly be answered by using this data. As a result, the evaluation was extended with a subproject for data analyses. This report gives the result of the data analyses.

The report has been divided into three chapter discussing the influence of the longitudinal training walls on the water level, on the velocity and discharge and on bed levels. For each of these data, the research questions are introduced, different analyses are performed, and results of the analysis are discussed related to the different research questions. Finally a combined chapter discusses all of the results combined. In addition, some recommendations are provided for some additional analyses based on available data.

The comparison to the numerical models has not been done in this report, as it is our impression that including those results will distract the message that the data is conveying on its own. The comparison of the model results to the data will be included in WP1 Paarlberg and Omer (2021).

In figure 1.5 an overview of the location of the longitudinal training walls is given with respect to the river kilometres. The map shows the inlet end outlet of all dams, as well as the (1 or 2) intermediate openings per dam.

A general description of the Asbuilt design, the dimensions of the inlets (and changes per year), the location of fixed layers are given in appendix A. This appendix also contains a timeline of measures in the region around the longitudinal training walls.

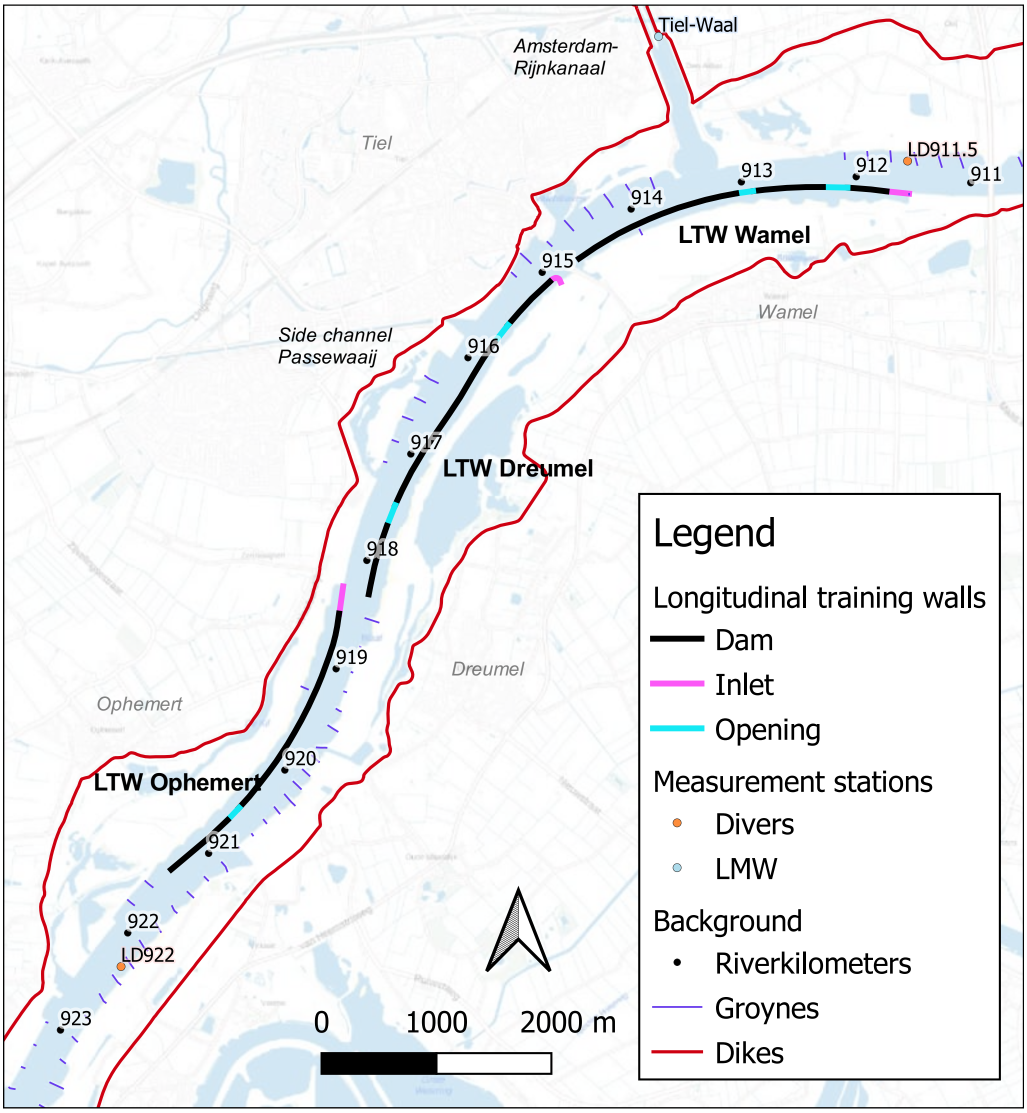

Figure 1.5 Overview map showing the location of the longitudinal training walls including the inlets, intermediate openings and outlets

2 Water level

2.1 Introduction

This chapter analyses several water level measurements that have been performed at the longitudinal training walls. By using these measurements we will be analysing the effect of the LTW on the water levels as well as the effect of the openings on hydraulics of the LTW.

The following research questions are posed:
1 What is the effect of LTW on the water level in the main channel?
2 What is the effect of openings on the discharge in the auxiliary channels and the effect on the main channel water level?

These questions are answered for both the conditions at low discharge and high discharge. Additional analysis is done to show the quality of using longitudinal measurements for local measures.

2.2 Available data

To answer these questions the following data were analysed:
- longitudinal measurements of water level and bed level. From 2008 to 2017 on average 3 measurements per year. From 2018 to 2020 this increased to 19 measurements per year (see B.2).
- time series from the Landelijk Meetnet Water (LMW) (also referred to as MWTL, Monitoring Waterstaatkundige Toestand des Lands) consisting of (amongst others) measured water levels at Zaltbommel, Tiel and Dodewaard and of discharges at Tiel and Lobith (derived from rating curves) from January 2008 up to July 2020.
- time series of water level measurements using a diver at the longitudinal training walls at rkm 911.5 and rkm 922. These measurements are only available from August 2013 to December 2016.
- time series of depth measurements using a diver at the head of all longitudinal training walls. These measurements are only available from October 2020 to December 2020.

In the sections below the processing of these measurements is described.

2.2.1 Processing of longitudinal measurements

In all recent years (from 2017) each set of longitudinal measurements of bed level and water level consists of multiple parallel tracks. Besides the track in the river axis ('aslijn') there are measurement at the left bank ('L-oever') and the right bank ('R-oever'), and in the auxiliary channels Wamel, Dreumel and Ophemert. Details on each set of measurements are given in appendix B.3. An example is given in Figure 2.1. For each measurement the following subplots are given:
- Top left: Map of all measurements, showing the exact location and date of all tracks. The title of this plot is the label of the dataset at Rijkswaterstaat.
- Top right: Time of measurements (orange) with the discharge at Lobith. The discharge at the mean of the time span is used as the representative discharge for the post-processing.
- Centre figure: Longitudinal plot. Averaging is applied to make it more readable. Exact height and width of all openings is shown as dashed line (including the

changes in the dimensinos as given in appendix A.2).
- Lower figure: Difference in longitudinal measurements to the river axis. Vertical lines indicate the location of the inlet, outlets and openings.

Based on this sheet the following can be interpreted for this (randomly picked) single measurement. The measurement was taken during a falling discharge, this means that at the LTW the discharge might have been slightly higher, and also that later measurement will have been at a lower discharge. For this campaign they first measured the river axis, than the three auxiliary channels and than the right and left bank. These measurements took 6 hours.

From the longitudinal plot it shows that the inlets of Ophemert and Dreumel are fully flowing, while the inlet of Wamel, as well as all intermediate openings, are just about to be over-topped. From the longitudinal difference plot it shows that in tha auxiliary channel of Ophemert the water level is more or less equal to the river axis. This unlike the channels at Wamel and Dreumel which have a lower water level slope than the main channel, resulting in a head difference. This head difference only starts building upstream of the last (downstream) intermediate opening, showing that apparently this last opening has some role in the exchange of discharge, either by over-topping or due to the higher permeability of these sections.

On a more detailed level there are also some spikes in the difference plot. A spike in all lines indicate that the actual jump was in the reference (the river axis). These spikes are caused by passing ships (further mentioned below) and possibly other waves. Comparing the location of the spikes between measurement campaigns showed no correspondence.

The tracks have a high temporal resolution (approximately 1 second). With a vessel speed of 3 m/s (upstream direction) to 5 m/s (downstream direction) this results in a spatial resolution of several metres. In figure 2.2 and figure 2.3 unfiltered measurements of 20-08-2018 around rkm 920 are shown. Both figures clearly show a large scatter of approximately +/- 5 cm (macro turbulence). The measurements also show the effect of wind and ship waves on the local water level and thereby on the measurement vessel. Most apparent are the water level depressions of passing (i.e. encountering) vessels (at rkm 920.8) with a height of -15 cm and a length scale of 75 m (equal to 15 seconds). Assuming the measurement vessel is only small and that the relative velocity to the passing vessel is 8.5 m/s, this gives a water level depression with a length scale of 130 m. This is equal to the water level depression (induced by the return current) of a large Rhine vessel (ship type M9 or M12). Also note the increase in vessel velocity as a result of the return current.

For the analysis of the measurements we are mostly interested in the large scale impacts on the water levels. Therefore the results are filtered to remove the scatter and to remove the effect of waves. Several filters and filter parameters have been tested (see appendix B.1). As a result the longitudinal measurements have been processed into two products for different typical applications:
- a Savitsky-Golay filter[1] with a window of 81 m, which performs very well for only removing the scatter and keeping all local variation (Savitzky and Golay, 1964).
- a rolling average with a window of 1000 m, which removes both the large scatter as well as the local variation. However, this rolling average will have (slightly) lower water levels than the undistributed water levels due to water level depressions.

[1] A Savitsky Golay filter can be interpreted like a rolling polynomial fit. In this study a second order fit is applied.

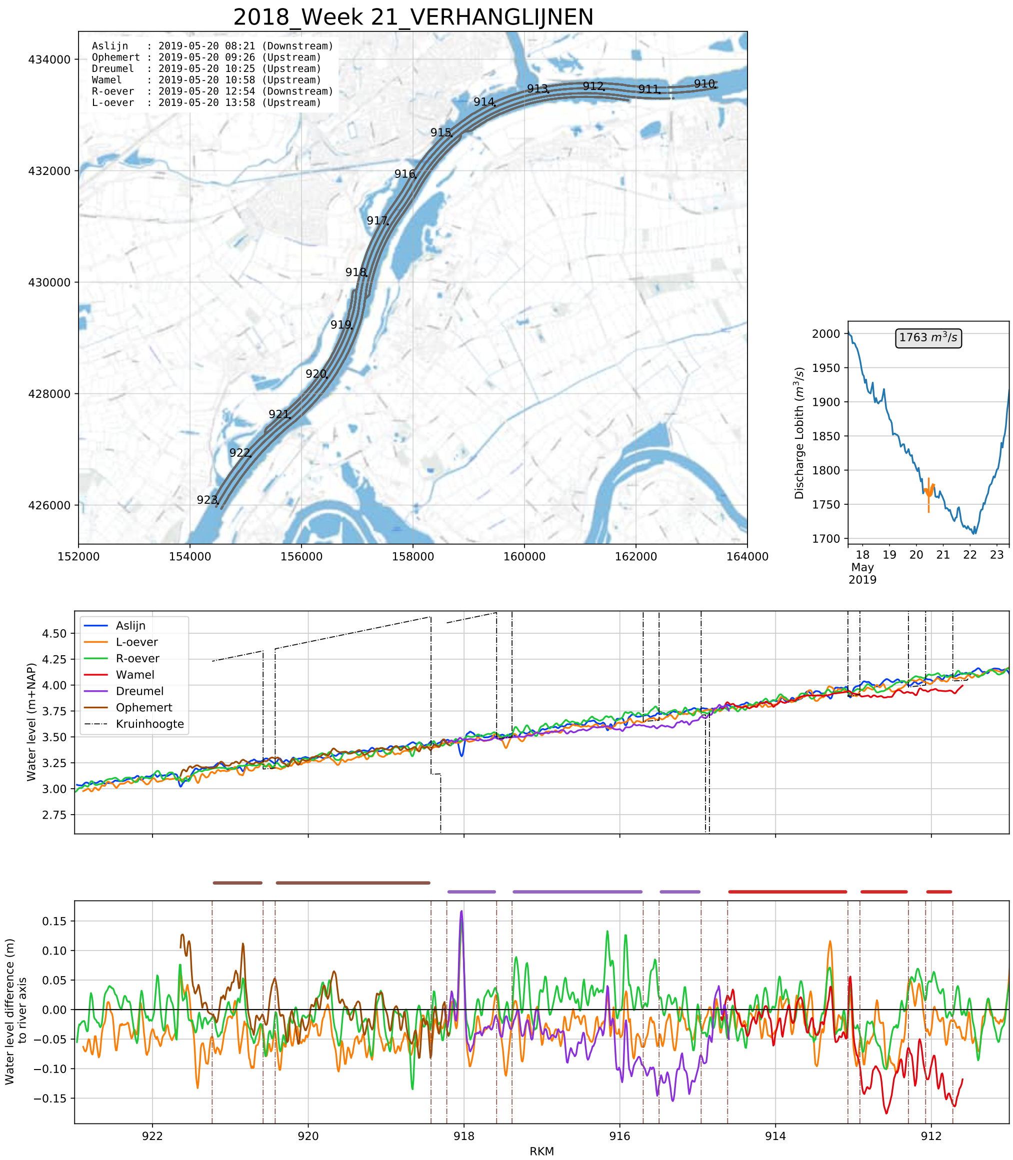

Figure 2.1 Example of the details given for each set of longitudinal water level measurements. A description of all lines in each subplot is given above

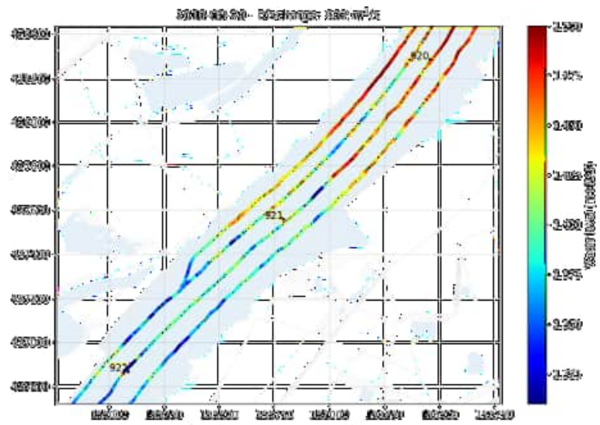

Figure 2.2 Map of longitudinal water level measurements between rkm 919.8 and 921.2 (date measurements: 20-08-2018)

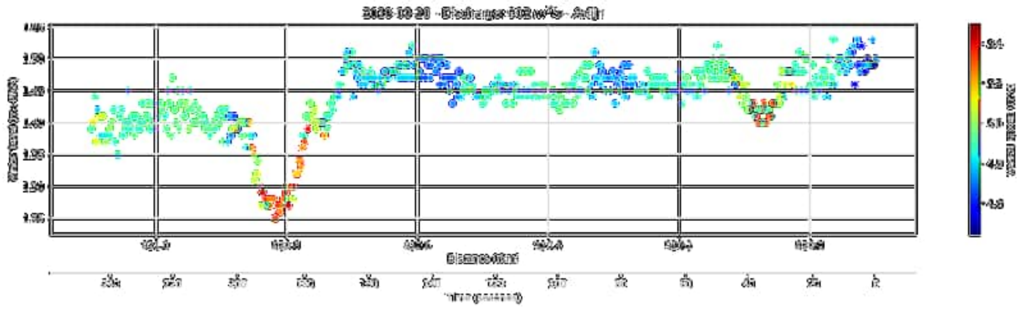

Figure 2.3 Longitudinal plot of water level measurements around rkm 920 (date measurements: 20-08-2018)

Each measurement campaign took multiple hours to several days. For (steeply) falling or rising discharges this can result in a bias in the different tracks up to several decimetres. In the analyses of the results, parameters are chosen such that are influenced by this bias as little as possible.

2.2.2 Processing of water level measurement stations

For the measurements from LMW and the diver stations no significant post-processing was required. An overview of the available measurements is given in figure C.1 for the LMW measurements and in figure C.37 and C.38 for the diver measurements. Both measurements are delivered with a temporal resolution of 1 hour.

For the measurements by divers at rkm 911.5 and rkm 922 only data up to November 2016 was made available. Although it is expected the divers are still in operation, more recent data could not been found by Rijkswaterstaat. For the divers at the head of all longitudinal training walls data was only available from October 2020 to December 2020. Although it is expected that the divers have been operationally for a longer period of time, data of the earlier period could not be found by Rijkswaterstaat.

2.3 Effect of the longitudinal training walls

In this section an analysis is given of the effectivity of the LTW in setting up the water levels. In this section we look at the entire section and the cumulative effect upstream of all LTW. In section 2.3.1 we try to get conclusions from the longitudinal measurements, but it is concluded that these effects are better analysed by using the water level timeseries at the LMW-stations which are given in section 2.3.2.

In the next section (section 2.4) the effect of each individual dam is analysed, taking into account the different configurations of the inlets.

2.3.1 Water level change in longitudinal water level measurements

A subset of all longitudinal measurements for discharges at Lobith between 1000 and 1500 m^3/s is included in figure 2.4. The difference in line style indicates if the measurement is done prior or after construction of the LTW. By using the rolling average local variation has been filtered. The effect of the LTW can be summarised by looking at the total head difference over the LTW between rkm 911.5 and rkm 922. This result is given in figure 2.5.

Results are split in a dataset before construction (all measurements until july 2014), during construction, and after construction (from november 2015). The water level difference has been plot against both the discharge at Lobith and the water level at rkm 922 on the x-axis. By plotting against the water level we correct for (short-term[2] and long-term[3]) changing discharge distribution on the Rhine branches (and upstream withdrawals, see section 2.5) and for the time offset between the Lobith and the LTW (the alternative to plot to the (rating curve) discharge at Tiel is discarded as the quality of this discharge has a negative bias[4]). However, also the water level at rkm 922 is influenced by measures (groyne lowering, effective at higher discharges) and by other external forcings like the wind set-up and tide (most significant at lower discharges[5]). Combined with the scatter from macro turbulence and ship waves in the measurements itself, this results in a plot with a large scatter.

From these measurements no conclusions can be drawn for the effect of the LTW on the water levels at rkm 911.5 at low discharges (lower than 1500 m^3/s). The point cloud in the measurements before and after construction seems very identical, i.e. the water levels of the in the new situation fall well within the point cloud band-width of the old situation. The large variation in the situations with low discharge (below 1200 m^3/s can also be the result of the withdrawal of discharge to the Amsterdam-Rijnkanaal, as the Prins Bernhardsluizen are opened in these conditions. This effect is further analysed in section 2.5.

For higher discharge (higher than 2000 m^3/s) the longitudinal water level measurements do show a reduction in water levels. However, the measurements

[2] Short-term variation in discharge distribution is the result of the operation of the weir at Driel. By Rijkswaterstaat an analyses is performed of the difference between the measured water levels and discharge at Driel (and other weirs) with the expected water levels and discharge from the weir operations ('stuwprogramma'). From the analyses it can be concluded that the difference can be many decimetres (too high) and over 100 m^3/s (too low). However, these deviations were not during the lower and very high discharges and therefor do not influence the analyses.

[3] Long-term changes in dicharge distribution are the result of bed degradation around the bifurcations points. Over time the fraction of the discharge to the Waal is increasing.

[4] Sieben (2020) mentions that the current MWTL Waal discharge recordings currently underestimate the discharge compared to ADCP measurements

[5] From model simulations it is approximated that the tide at rkm 922 is approximately 7 cm at a discharge of 700 m^3/s and reduces to 4 cm at a discharge of 2000 m^3/s and below 1 cm for discharges above 9000 m^3/s. At Tiel the tidal amplitude is never larger than 1 cm.

before construction are only scarce and not sufficient for definitive conclusions on the effect of the LTW.

For higher discharge (between 1500 and 3000 m^3/s) the longitudinal water level measurements show that the water levels have become lower after construction of the LTW. The purple markers are clearly below the orange markers, even when considering the scatter bandwidth. At these discharges the intermediate openings are submerged, and the dam itself is just slightly over-topping at the high end of this spectrum (see also figure fig:dimensions). During these conditions the flow width (and area) has increased in the new situation. However, the higher 'before construction' measurements could also be the result of long term trends in the data set. It contains many measurements around 2000 to 3000 m^3/s between 2008 and 2011 with many more years of ongoing bed erosion (see also the analyses of LMW Tiel in section 2.3.3).

For higher discharges (larger than 3000 m^3/s only 1 valid measurement is available for the situation before construction.[6] No conclusions can be drawn from the longitudinal water level measurements for these conditions.

The longitudinal water levels are only a limited data set when it comes to long scale effects. In section 2.4 more analyses will be done on local effects from these measurements.

[6] The two odd measurements at 7500 m^3/s seem to have been caused by a (overnight) break during the measurement campaign for a falling discharge (see also appendix B.13 and B.14).

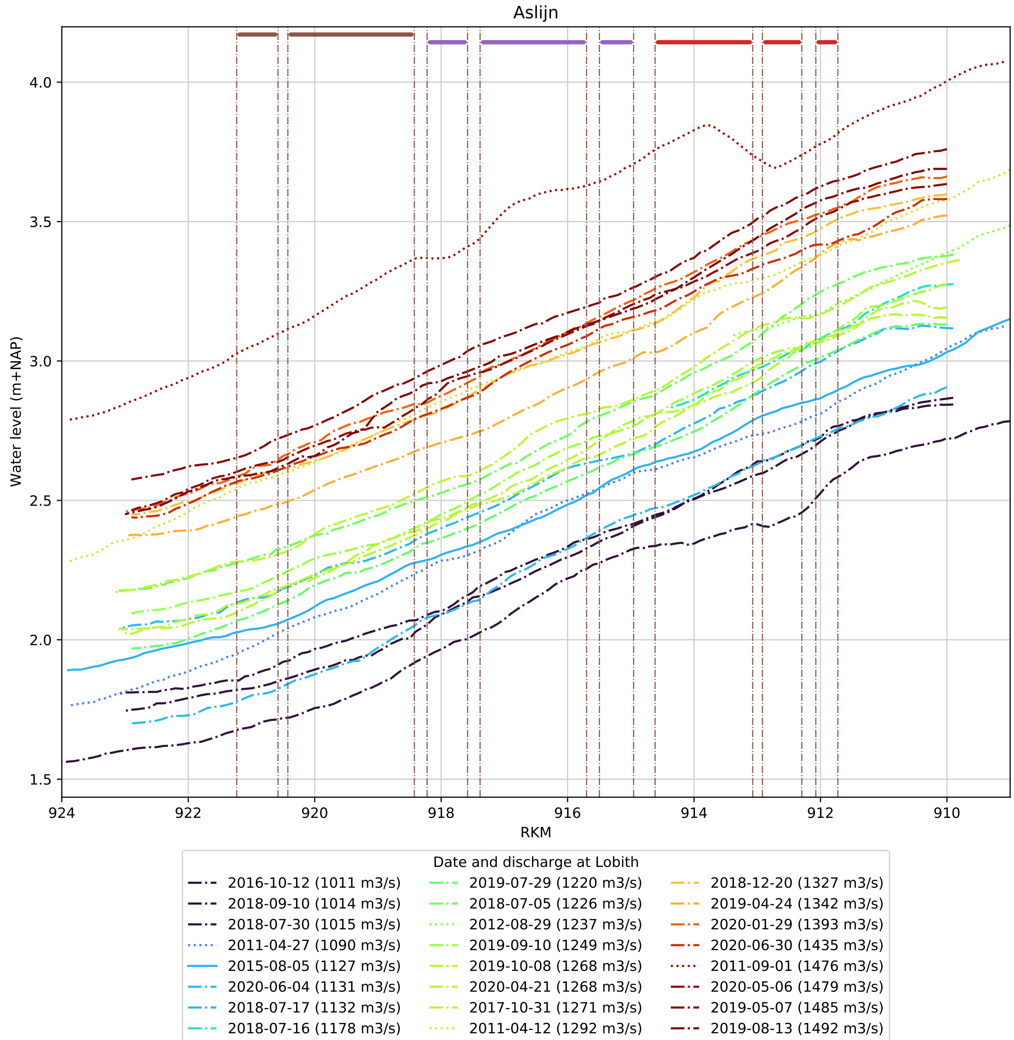

Figure 2.4 Longitudinal measurements at the river axis for a discharge at Lobith between 1000 and 1500 m^3/s. The data has been filtered using a rolling average over 1000 m. The line style indicated if the data is before construction (dotted), during construction (solid) or after construction (dash-dot).

Deltares

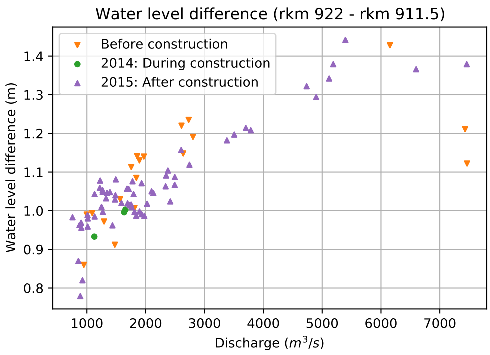

(a) Plot against discharge at Lobith

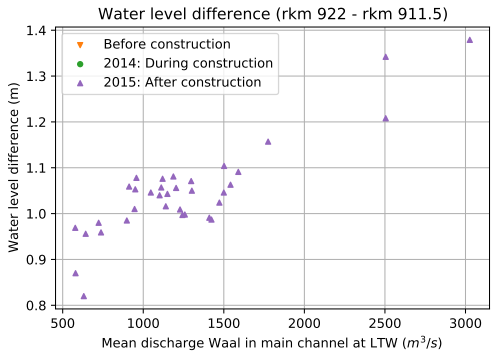

(b) Plot against mean measured discharge on the Waal at the LTW. A tollerance of +/- 2 days is applied to increase the data set from 18 to 37 measurements.

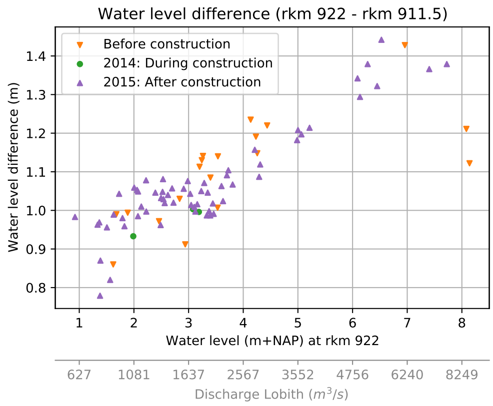

(c) Plot against water level just downstream of the LTW. The discharge is based on the betrekkingslij-nen

Figure 2.5 Water level difference (between rkm 922 minus rkm 911.5) from the longitudinal water level measurements based on all available longitudinal measurements, split in categories of before, during and after construction of the LTW.

2.3.2 Water level change at (LMW) measurement stations

In the remainder of this section the focus is on the water level measurements at the LMW measurement stations. The diver measurements did not add conclusive results, possibly due to the short time span of these measurements (less than one year after construction). Results are included in appendix C.2.

2.3.2.1 Mean water level per discharge Lobith

Similar to the analyses in WP10 of this evaluation (Chavarrías *et al.* (2021)) the water level measurements are analysed by discretising the discharge at Lobith in bins (of 200 m^3/s) and plotting the mean and standard deviations of each bin. This procedure and its limitations are further explained in appendix C.1.2, including results at various other stations along the Waal. Downsides of the usage of the discharge at Lobith as a reference parameter are given in section 2.3.1. As the period prior to construction contained a lowering trend in water levels, the grouping over long periods will include a (positive) bias. Therefore the analyse is split in groups of each individual years (2008 to 2019), this method is explained in appendix C.1.3 and shown for Tiel Waal in figure 2.6.

Although the variation per year includes some odd year to year variations, it is clear that the water levels showed a declining trend prior to constructing the LTW. After construction this has stabilised for lower discharges (smaller than 2400 m^3/s), while at higher discharges the declination in water levels continues.

The water level increase at lower discharges is not as significant as was expected from model studies. This is partly caused by the effect of downstream measures which have reduced the water levels (see section 2.3.3), but also show that the LTW are less effective than expected. Possible explanations, which may explain this water level reduction are (i) a reduction of the alluvial roughness, (ii) the lack of horizontal mixing (previously caused by groynes), (iii) the porosity of the longitudinal training wall structure, (iv) too much water entering the auxiliary channels, (v) changes in the bed level during and after construction, or (vi) the increase in flow velocity (due to an M2 backwater curve). Unfortunately, we have not been able to quantify which of these effects are most important.

The change in discharge distribution over the Rhine branches (as a result of bed degradation) probably results in an increasing discharge to the Waal for the same discharge at Lobith. This trend is expected to be present for both the period before as after construction. Without this additional discharge, the declination in water levels would have been larger. For very low discharges (below 1200 m^3/s) the withdrawal of discharges through the Amsterdam-Rijnkanaal (see section 2.5) might result in a reduction in discharge on the lower Waal, which could be the reason of the large dip in 2018 (also visible at Zaltbommel and St. Andries in figures C.5 and C.6).

The lowering of the water levels at the medium to high discharges in this plot (2500 to 5000 m^3/s at Lobith) show the expected water level lowering, but for an analysis at discharges waves (so most higher discharges) it is more effective to look at the peaks (see section 2.3.2.2).

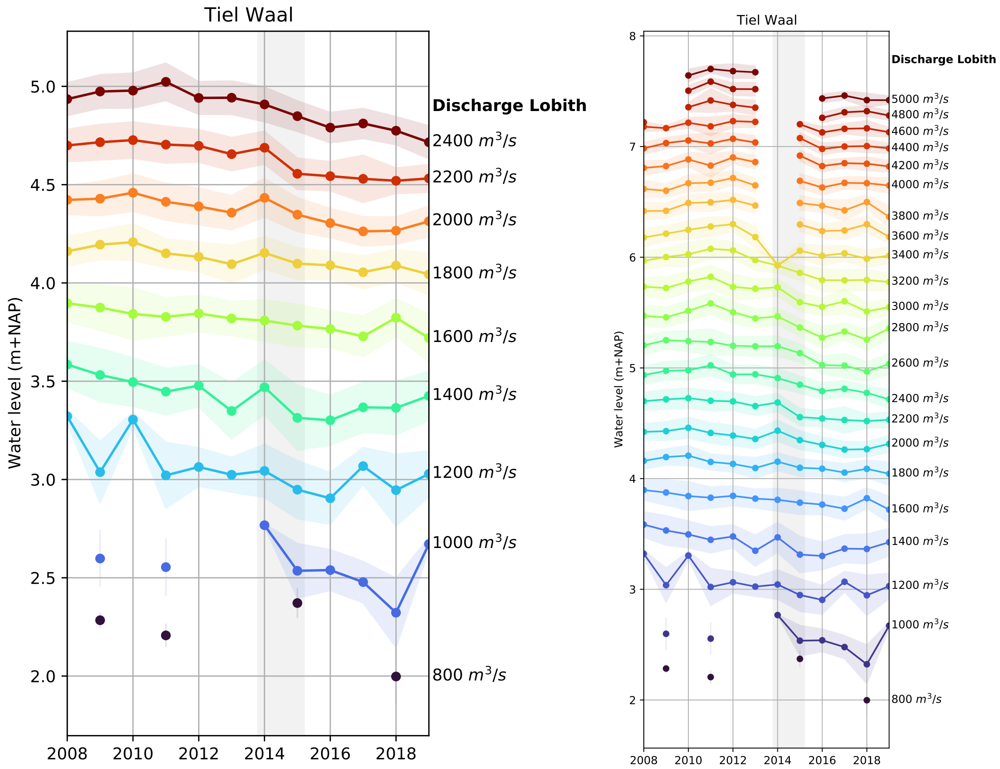

Figure 2.6 Trends in water level at Tiel, showing the mean and standard-deviation per discharge bin (+/- 100 m^3/s). The left plot shows the effect up to 2400 m^3/s, the right plot shows the effect up to 5000 m^3/s. The years influenced by construction are marked in grey.

2.3.2.2 Effect on peaks and troughs

As a final analyses of the water levels each peak and trough of the period 2008 to 2019 has been analysed (see appendix C.1.5). The results at Tiel are shown in figure 2.7. This further repeats the earlier conclusions or lower discharges, but additional shows the effect at the very high discharges (above 5000 m^3/s). At these higher discharge a similar water level reduction of 20 cm is concluded.

The construction of the LTW coincides with the lowering of the groynes (all groynes upstream of rkm 911.5 and downstream of rkm 922). And during the period also additional measures in the flood plains were constructed (e.g. side channel Passewaaij). It can therefore not be concluded that these effects are solely the effect of the LTW, but that they are the effect of these measures combined.

However, this trend might be biased due to other measures or due to a trend in the 'Before' period. To exclude these effects, the analyses is repeated for each seperate year in the data set, resulting in the point cloud of figure 2.8. Because all points are located on the diagonal, making it hard to spot the (relatively) small difference between the years, the right figure is added in which the water levels are corrected to a polynomial fit (more explanation in appendix C.1.6). This figure can also be interpreted as rotating the previous figure by 45 degree. In this plot the change over the years is more apparent: there is a clear reduction in water level for all measurements after 2015 to the measurements before 2014 for discharges of 2500 m^3/s and higher. This coincides with the construction of the LTW, but also with the lowering of the groynes and the side channel at Passewaaij (see appendix A.4). The reduction in peak water levels is approximately 20 cm.

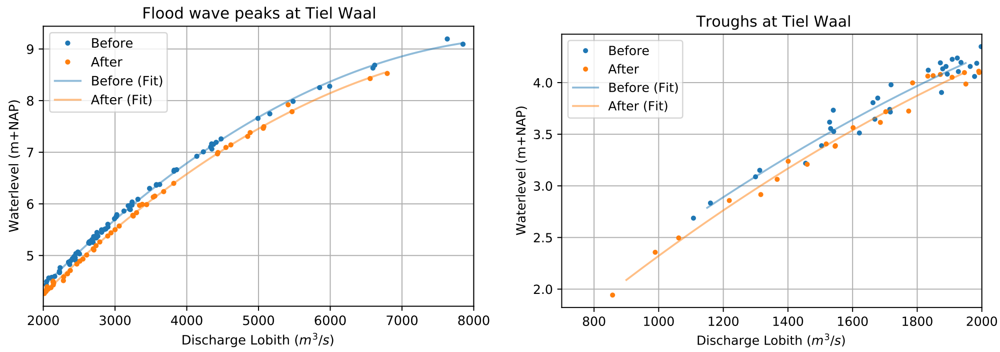

Figure 2.7 Peaks and troughs at Tiel Waal for the period January 2008 to March 2020. Including a least square second order polynomial fit.

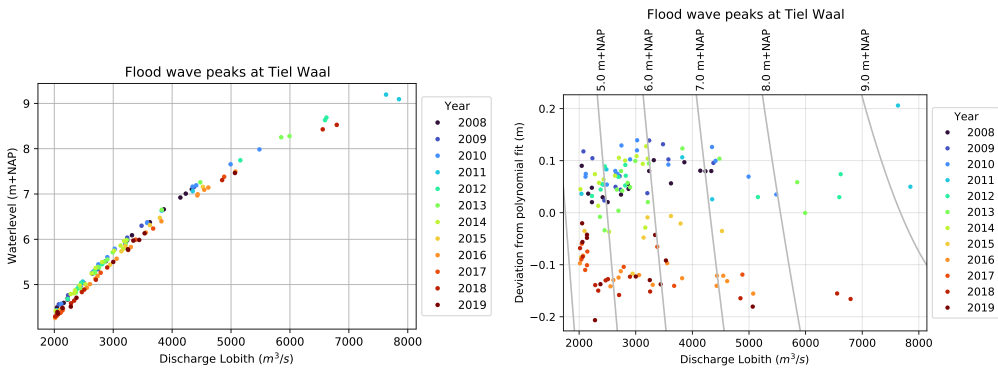

Figure 2.8 Trend in flood peaks per year at Tiel Waal. Left: Absolute water level; right: Water level after subtracting a polynomial fit for increased readability.

2.3.3 Change in head difference between measurement stations

In the earlier paragraph the absolute water levels were analysed. Those are also influenced by effects downstream of the LTW and might show deviation from the trend due to uncertainty in the discharge. To isolate the effect of the LTW this section analyses the difference in water level between the stations Tiel Waal and St. Andries. Most of this reach includes the longitudinal training walls. In figure 2.9 the trends are shown. The lower subplot includes the bed level over the entire 'trajectvak' (see also chapter 4) as an indicator for the reach scale bed level trends.

The figure show a gradual reduction in the head difference over the period 2008 to 2014. The reduction in head difference is more than the observed bed level trends in the lower plot. The reason for this is unsure, but possibly the average bed level is not representative for the flow area. From the start of the construction of the LTW, initially the water levels drop even further in 2015 to 2016, possibly as a result of the situation during construction. From 2017 onwards the head difference has recovered to the situation pre-construction and shows a slight increase in head difference over the years.

This trend in head difference shows a strong correlation with the trend in bed level as shown in the lower subplot. The drop in the average bed level in 2015, corresponds well with the reduction in head difference in 2015 and 2016. This suggests that (as expected) the head difference is very closely related to the bed level. There is a slight phase lag (the water level drop is later than the bed level drop), which might be the result of both the averaging over the reach, as the averaging over a full year: local and temporal information might be missed. The bed level change downstream of the LTW is not included, but might also influence the water levels up to Tiel.

For the evaluation of the LTW a clean comparison is necessary. To prevent side effects of the discharge withdrawal at the ARK (see section 2.5), we look at discharges above 1200 m^3/s. For these conditions the discharge in the auxiliary channels is larger than 12 % (apart from Wamel, see figure 3.18) resulting in the expectation of a reduced water level slope (as derived from theory in Sieben (2020)). To prevent the effect of bed level we look at years with approximately the same level: 2013 versus 2017. For these conditions, the lowering of the water levels is between 1 and 3 cm. This effect is most likely caused by the LTW.

Plots for other stations are included in appendix C.1.4. Although these plots show interesting trends, they are not further analysed as they are not in the scope of this project.

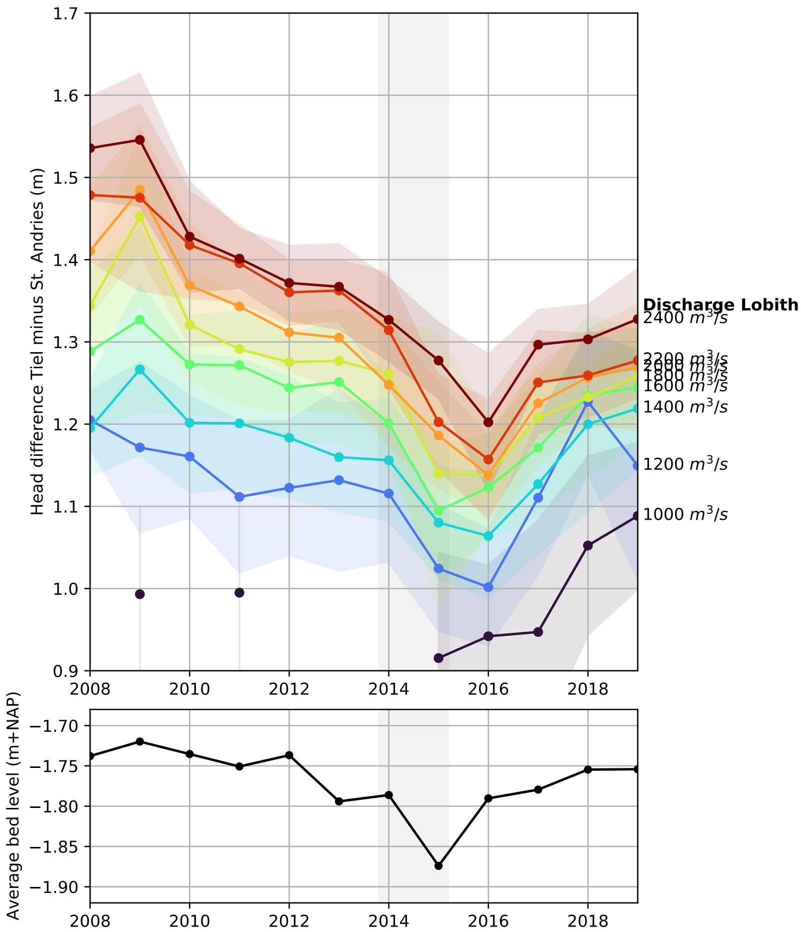

Figure 2.9 Trends in water level difference Tiel minus St. Andries, showing the mean and standard-deviation per discharge bin (+/- 100 m^3/s). The lower subplot includes the bed level over the entire 'trajectvak' (see also chapter 4)

2.4 Effect of changing in inlet openings

In this section we focus on the effect of the individual dams (section 2.4.1). An analysis is given of the effect of the openings on the water level just upstream of each dam, as well as the effect of the openings on the slope within each auxiliary channel (section 2.4.2).

2.4.1 Effect of openings on the water level in the river axis

Similar as the analysis in section 2.3, the water level difference at each LTW (upstream minus downstream) has been plotted against the water level downstream of Ophemert in figure 2.10. For each dam all phases of inlet design are show with different markers (see also appendix A.2 for dimensions and photos of the different inlet designs).

Similar to the analysis in section 2.3, also in these plots the scatter in results is very significant. As a result, no conclusions can be given with certainty because the (scarce) events can easily contain a bias as a result of the external forcing or geometry (assuming this is the cause of the scatter). More measurements, or different measurements are necessary gain more confidence in the results. Taking into account these possible pitfalls some crude interpretations can be made.

At Wamel the construction of the LTW seems to have caused (again) the lowering of water levels at median discharges (between 3 and 5 m+NAP at rkm 922). At low discharge insufficient measurements before construction are available to get any conclusion. There is also no significant effect of the lowering and rising of the inlet in 2018 and 2020. Unfortunately also the stationary measurements are not on the right location (Tiel is too far downstream of inlet Wamel) or have insufficient data (all diver measurements). The water level prior to the construction at the highest discharges, are outliers and should be ignored (these measurements contain an overnight break).

At Dreumel conclusions are very similar. After construction, the water level is reduced at median discharge (between 3 and 5 m+NAP at rkm 922), but also seems to have reduced at low discharge. The reducing of the width might have resulted in a slight increase in water levels, but only measurements are available for median to high discharges. The lowering of the inlet (2019; purple triangles) seems to have resulted in higher water levels (e.g. at 2 m+NAP at rkm 922), but as this is not the expected response, it is probably caused by other changes in forcing or geometry. At the highest discharges there is no visible difference between the situations before and after construction.

At Ophemert the measurements again show a clear lowering of the water levels at median discharge (between 3 m+NAP and 5 m+NAP at rkm 922). At low discharge little measurements were available before construction, but they indicate a significant reduction in water level. By reducing the width (in 2019) the water levels seem to have slightly increased.

2.4.2 Effect of openings on the water level slope in the auxiliary channel

Unlike the water level in main channel, the slope in longitudinal direction in the auxiliary channel is very significantly influenced by changes in the inlet and for changing discharge (for the times and dimensions of changes see appendix A.2). This can be seen in longitudinal plots of water level in Wamel in Figure 2.11. Both the Savitsky-Golay filtering and the rolling average are shown. The Savitsky-Golay shows so much information that it can be hard to comprehend, while the rolling average smoothens away many interesting details. Similar figures for all auxiliary channels and all discharges are given in appendix B.4 (only including the Savitsky-Golay filter). In appendix B.5 additional figures are included of the difference in water level to the main river axis (only including the rolling average).

From a discharge of 1700 m^3/s at Lobith the raised inlet (solid lines) is slightly over-topping and the intermediate openings start (more slightly) over-topping. Still the (right) figure shows that the slope has a knick-point between rkm 913.5 and 914 with the steepest downstream of this point, where there are no intermediate openings. This is most probabaly caused by the construction of a fixed layer in the auxiliary channel as bed protection for pipes (see also figure A.10).

For all lower discharges the slope in the entire channel is horizontal as there is no discharge in the channel (see figure B.95, except for the one measurement in 2017 before raising the inlet, which does contain a slope). The newest measurement of May 2020 shows a steep slope in the upstream part of the channel because of the lower of the inlet that was constructed. All other measurements since this alteration do not show any significant change.

The slope at the auxiliary channels of Dreumel and Ophemert is given in figure 2.12 for median discharges (1500 m^3/s to 2000 m^3/s at Lobith). Only the Savitsky-Golay filter is shown here, as these provide most information. Figures of other discharges are included in appendix B.4.

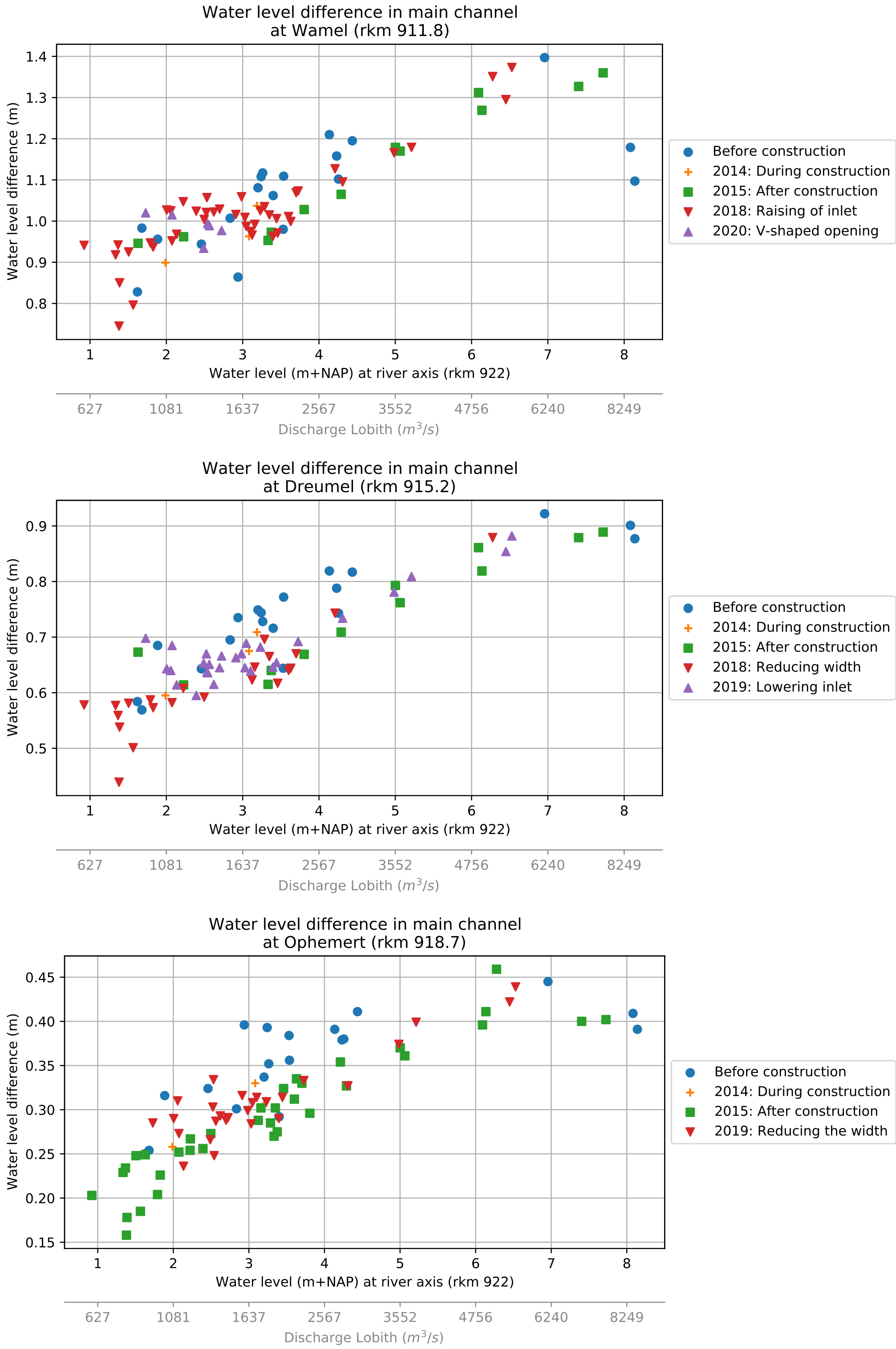

Figure 2.10 Effect of openings on the upstream water levels (minus water level at rkm 922) as a function of the downstream water level (rkm 922) (and the discharge estimated from betrekklingslijnen 2018).

The water level slope at Dreumel at low discharge is small but constant for the entire auxiliary channel (see appendix B.4). At median discharge (1500 m^3/s to 2000 m^3/s, see figure 2.12) the upstream end of the channel suddenly develops a much steeper slope. At these discharges the water level in the main channel (and at the inlet) has a

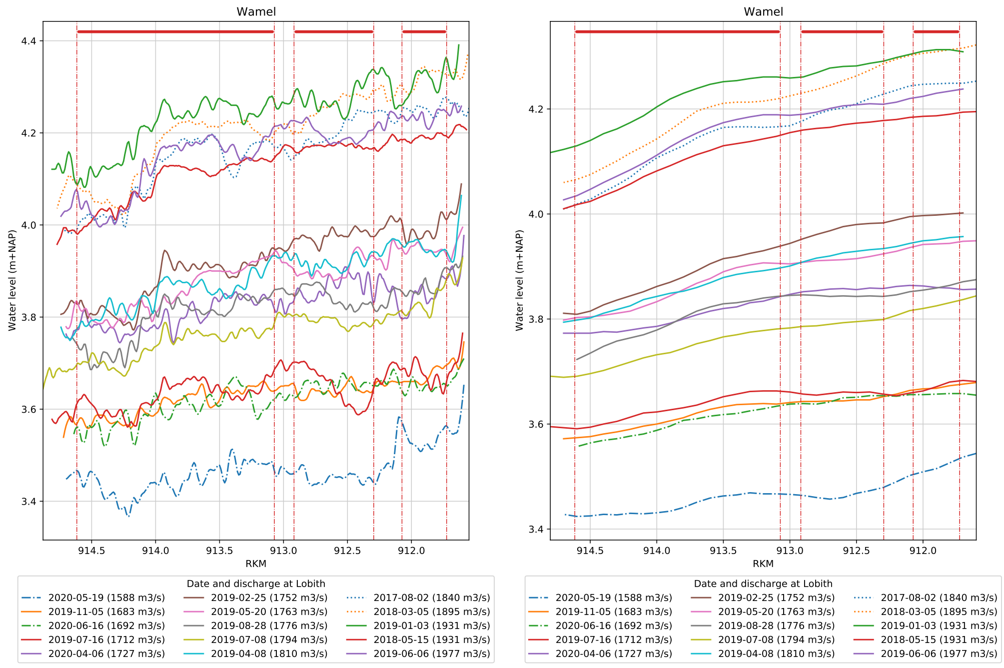

(a) Savitsky-Golay filtered **(b)** Rolling average

Figure 2.11 Longitudinal water level in the auxiliary channel at Wamel for all discharges between 1500 m^3/s and 2000 m^3/s. The linestyle indicates the situation just after construction (dotted), after raising the inlet (solid) and after construction of the V-shaped opening (dash-dot). The intermediate openings of Wamel are at rkm 912.3 and rkm 913.0.

higher slope than the water level in the auxiliary channel resulting in a head difference of over 10 cm at the inlet of Dreumel (see appendix B.5). This steep slope was far less significant in the measurements that were done before reducing the with of the inlet in April 2018 (dotted lines, measurements of 2017-08-02 and 2019-03-05). The slight widening of the inlet in April 2019 (the solid lines) does not show a significant effect.

Similarly, the auxiliary channel at Ophemert shows a very constant slope at all discharges and both opening configuration. There is no notable effect of the change in opening dimensions (see figure 2.12). Only at the downstream end the downward slope suddenly increases for these median discharges, which indicates that the water level in the auxiliary channel is higher than the main channel (mostly visible for discharges between 1200 and 2000 m^3/s). The outlet itself appears to be causing this local set-up. In contrast to the other auxiliary channels the discharge is relatievely high (see figure 3.17) and the design of the outlet also has a more sharp bend (see the map in figure 1.5). On photo A.8 it is also visible that a large part of the flow is not going through the opening, but flows in downstream direction over the (lowered) weir.

All of the measurements show fluctuations in the water level with a height up to 10 cm and length scales up to hundred metres. Most of those fluctuations do not show a consistent trend. Similar to section 2.2.1 these might be a temporal change as a result of passing ships. It is not clear how these waves arrive in the auxiliary channel. This could either be caused by the porosity of the dam, or as a result of a ship passing an opening (most probably the outlet) and introducing a translation wave in the channel, or a reflection of any of these waves.

At some locations (for example 2020-05-19 at Ophemert rkm 918.7) the effect appears to present in multiple measurements. Inspection of the bed level shows that this water

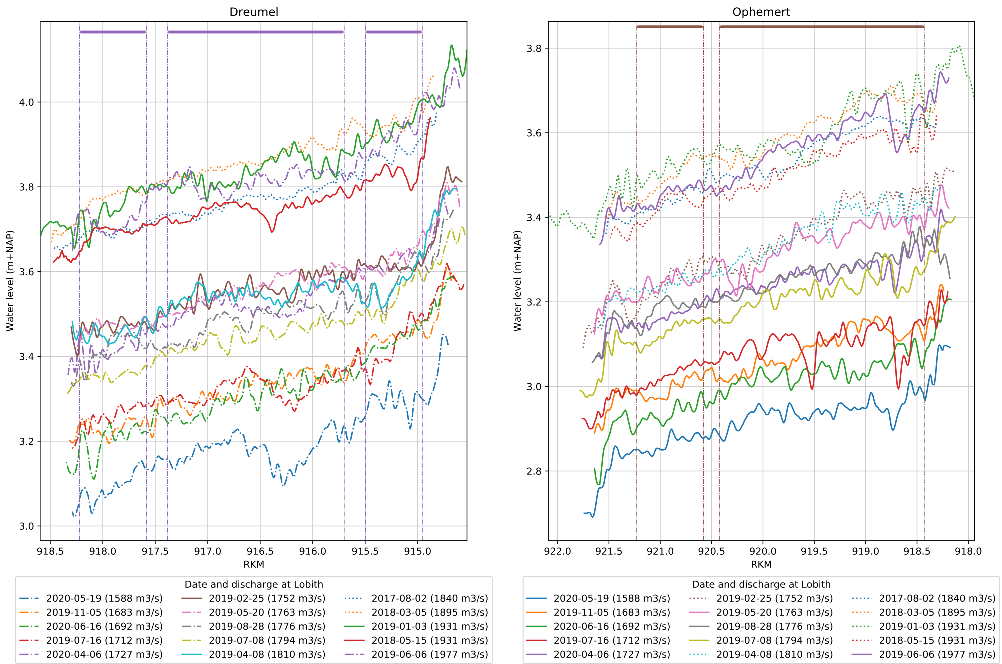

Figure 2.12 Longitudinal water level in Dreumel (left) and Ophemert right) for all measurements at discharges between 1500 m^3/s and 2000 m^3/s. For Dreumel the linestyles indicates the situation just after construction (dotted), after reducing the width of the inlet (solid) and after lower the inlet (dash-dot). For Ophemert the linestyles indicate just after construction (dotted), and after reducing the width (solid).

level depression is at the location of a shoal (see figure 2.13). The lowering of the water level is the result of Bernoulli's principle, which states that an increase in flow velocity results in a lowering of the water level. From theoretical approximations, it is expected that the local flow velocity at the shoal is over 1.5 ms, which gives a lowering of the water level of approximately 1 decimetre. As the measurement vessel is sailing against the flow, it has a relative sailing speed of over 4 m/s which should also result in an additional water level depression of approximately 1 decimetre. From the measurements it cannot be derived if the water level depression is caused by the undistrurbed flow, or by the return current.

To summarise all results in one figure per LTW, the mean slope of each measurement is computed. It is plotted in figure 2.14 (the standard deviation is on average 3.5 cm). The effect on the slope is only visible during lower discharge. The single measurement

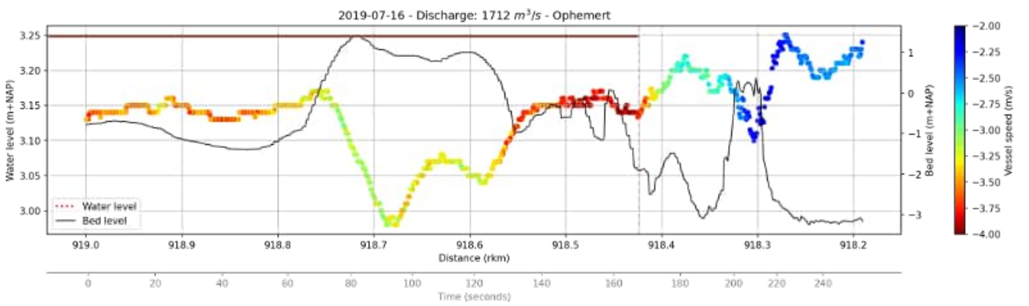

Figure 2.13 Water level (colored dots, left axis) and bed level (right axis) in the auxiliary channel Ophemert near the inlet. The color represents the sailing speed of the measurement vessel (negative means that it's sailing in upstream direction).

at Wamel before raising the inlet clearly shows a much larger slope.

A similar plot is also given in figure 2.15, but plotted to the measured discharge in each auxiliary channel. As not all longitudinal measurements have a discharge measurement in the same period (a tolerance of 2 days is applied), the number of measurements has been reduced to the previous plot. The figure show the relation between the discharge through the auxiliary channel and the slope. A strong correlation is expected, as slope should mainly be the result of this discharge. This correlation is most clear at Wamel, because very low discharges have been measured in this channel. At all auxiliary channels the slope has a variation in the point cloud of around 0.02 m/km. At Wamel a reducing trend seems visible in 2019 compared to 2018, which can be result of the change in inlet design: the same discharge occurs at a much higher water depth. The slight reduction in slope at Ophemert might be explained by the increase in flow area due to bank erosion (see section 4.4.3).

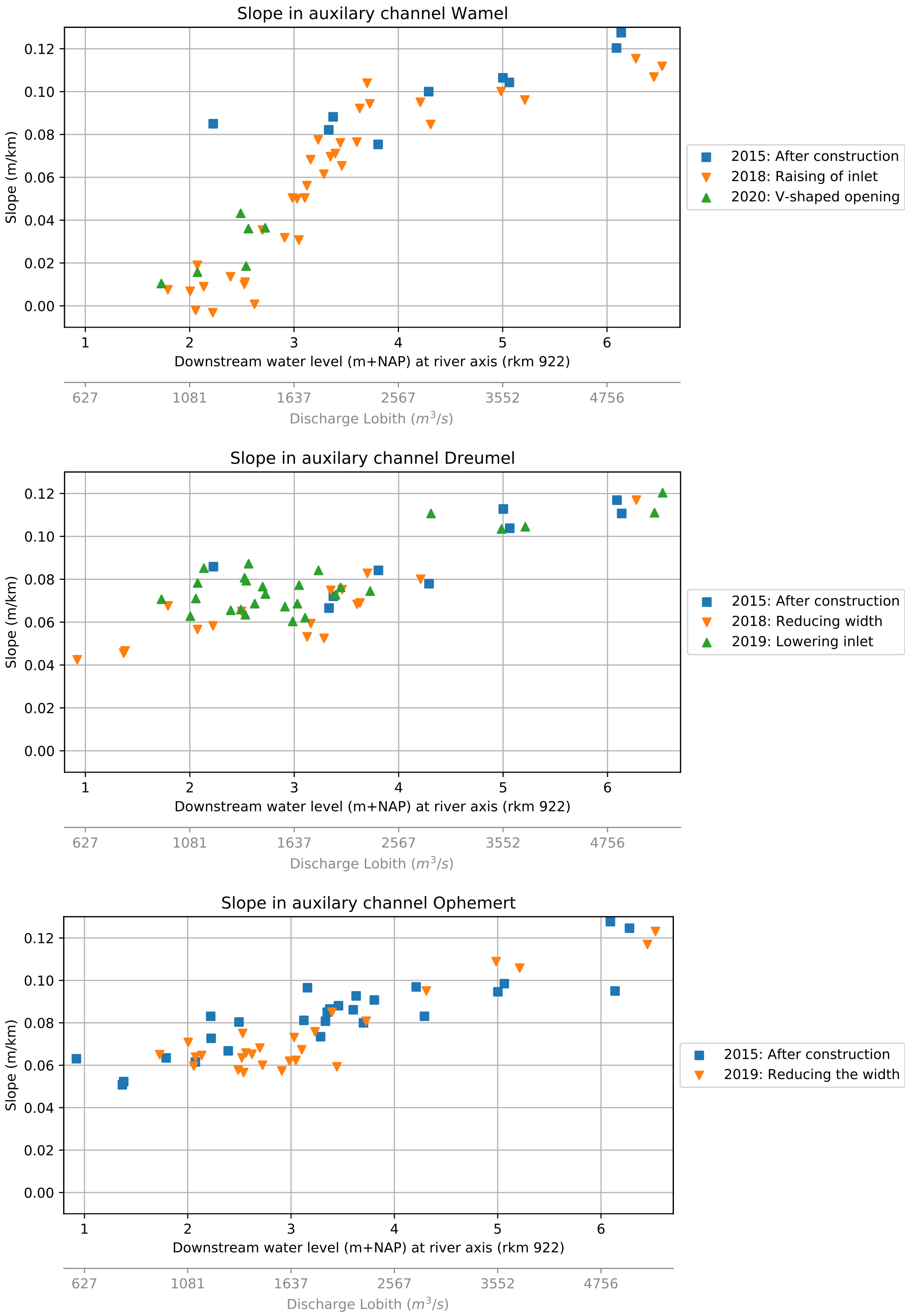

Figure 2.14 Average slope within de auxiliary channel plotted against the downstream water level (and the discharge at Lobith from betrekkingslijnen 2018). The measurements close to inlet and outlet are excluded. Each group of measurements visualises a different design of the inlet.

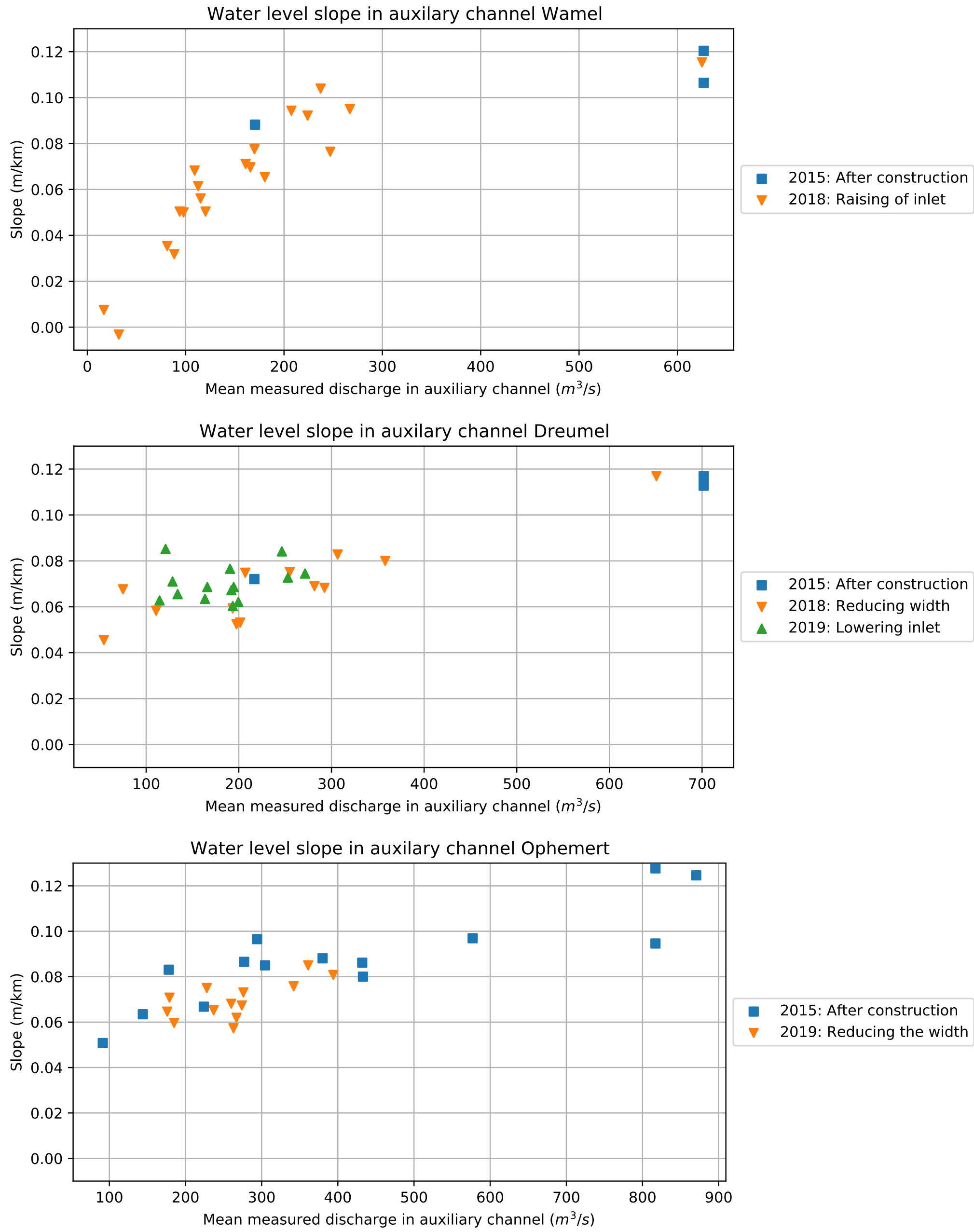

Figure 2.15 Average slope in de auxiliary channel plotted against the *measured discharge in the auxiliary channel*. For coupling to the ADCP measured discharge a tolerance of 2 days is applied to increase the data set from 10-12 measurements to 23-30 measurements.

2.5 Effect of opening the Prins Bernhardsluizen

During low discharge (water level Tiel below 3.0 m+NAP, approximately a discharge Lobith of 1200 m^3/s) the Prins Bernhardsluizen resulting in an open connection between the Waal and the Amsterdam-Rijnkanaal (and also the Nederrijn between Hagestein and Amerongen). During open conditions water from the Waal can also be used in northern parts of the Netherlands to prevent salinity intrusion (on the Lek and Noordzeekanaal) and as fresh water supply (through KWA+). This results in a high discharge that is being withdrawn from the Waal, which lowers the water level on the Waal. A basic rule of thumb is that every loss of 1 m^3/s, lowers the water level with approximately 3 mm at Tiel (and 2 mm at St. Andries).

The discharge through the Amsterdam-Rijnkanaal (ARK) has been measured with ADCP on several days, with a maximum measured discharge of 68 m^3/s. In figure 2.16 the water level at Tiel is plotted to the discharge at Lobith, with annotations of all ADCP-measurements. As expected, the higher measurements correlate to the lower water levels. An increase in ARK-discharge of 60 m^3/s lowers the water levels with approximately 15 cm. There are also some measurements that might have had an even higher discharge withdrawn for the Waal (for example around 900 m^3/s), but these conditions remain unmeasured.[7]

In appendix C.1.8 an analyse is also made of the head difference over the Prins Bernhardsluizen. A time series has been generated of all moments that the locks were presumably open (a head difference lower than 3 cm). The head difference is also correlated to the discharge, but the correlation is only very weak. Based on this conclusion it is not possible to differentiate within the measurements for timespans with high discharges in ARK and situations with lower discharges.

[7] The discharge through the Betuwepand can be estimated from the volumebalance and the discharge stations at Hagestein and Wijk bij Duurstede (Van Putten (2021)). Although on first sight, the results show a deviation to the ADCP-measurements, the longer time series might provide a better and more continous respresentation of the daily average discharge.

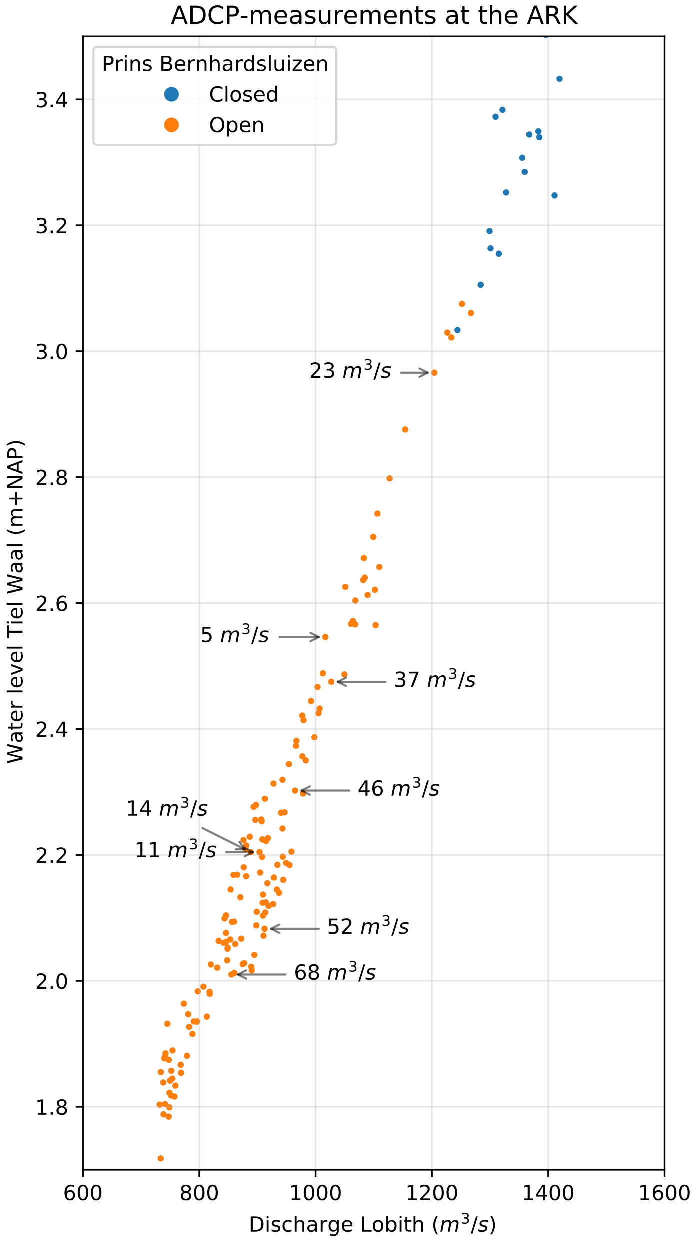

Figure 2.16 Relation between daily averaged discharge at Lobith and water level at Tiel Waal (including a correction of 17 hours) with annotation of the discharge from ADCP measurements at the ARK in 2018. The discharge is the average of multiple runs and has a large standarddeviation: between 10.6 and 37.5 m^3/s.

2.6 Waves in the auxiliary channel

As explained earlier, a large part of the small fluctuations in the longitudinal water level is probably caused by the heave of the ship as a result of various waves in the channel. It is expected that onboard technology on the survey vessel will correct for the ship movements (like the pitch), but is not able to correct for waves that move the entire vessel up and down. In this section these fluctuations are analysed for trends as a result of a changing flow regime (a higher or lower discharge). To isolate the variations, the difference between the Savitzky-Golay filtering and the Rolling average is taken. The root mean square (RMS) of this 'longitudinal difference' is used as an indicator for the height of the waves. In figure 2.17 this wave indicator is plotted to the discharge at Lobith. It should be noted that the length of a wave in a longitudinal profile is also dependent on the speed (as a result of sailing direction) of the measurement vessel. This inaccuracy is expected to be of only small effect.

From the figure it can be concluded that the wave indicator is highest at discharges around 2000 m^3/s. Although this might be partially caused by the larger dataset during these discharges, but can also explained by the design of the LTW. During these average discharges the channel is narrow and has one hard side. In these conditions waves entering the channel are well reflected and can propagate for some time. At these discharges waves can enter the channel both through the inlet and outlet, as well as over the intermediate openings (see the design in figure A.2).

At lower discharges (1000 m^3/s and lower) the wave indicator is lower at the auxiliary channels of Wamel and Dreumel. At these conditions the intermediate openings are no longer overtopping and also the inlets are significantly more closed (most measurements are after April 2018). As the core material of the intermediate openings consists of large rip rap (see as built design in appendix A), it is expected that the porosity of the intermediate openings is higher than the other parts of the dam (with a core of sand). The effects of a higher porosity can not be seen in the measurements.

At higher discharges (3000 m^3/s and above) the entire dam is overtopping. This means that more waves from a passing vessel can enter the channel, but also that the waves are less reflected and dampen out quicker. Also, at higher water depths the height of ship waves reduces, as a result of the reduction in water level depression of the return current.

This figure does not indicate local difference in wave climate within the channel. To study this local variation, all individual longitudinal measurements (see appendix B.4) have been inspected. These longitudinal profiles show variation of the auxiliary channel, but do not show a consistent trend the different measurements. The larger waves that appear might be caused by a ship passing closer by the dam or any of the openings. It can also be that the waves are partially caused the measurement vessel it self. Especially the translation wave caused by the vessel entering the auxiliary channel might reflect on the other end, and end up in the measurements.

For a more in depth analyses of how the waves propagate in the auxiliary channel it is advised to apply stationary measurements on multiple locations in the auxiliary channel at the same moment. Both the situation with and without overtopping intermediate openings should be measured. A simulation of the wave propagation can also help with understanding the waves in the auxiliary channel.

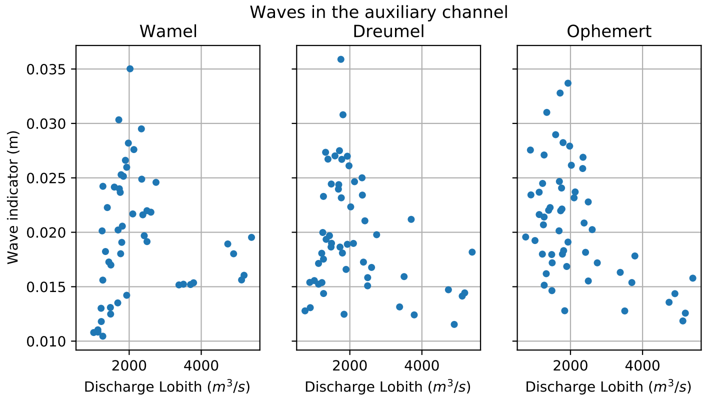

Figure 2.17 Wave indicator as a function of the discharge in the three auxiliary channels. The wave indicator is defined as the RMS of the difference between the Savitzky-Golay filter and the rolling average.

2.7 Discussion of the applicability of longitudinal measurements

In the analysis of the paragraph before, the longitudinal measurements did not proof valuable for detecting all the expected impacts. The effects on the water levels due to both the construction of the longitudinal training wall as well as the changes in inlet dimensions are too small to be measured, as they are marginal compared to the scatter. The effect of temporal variation by ship waves and possible spatial variation by small bed and bank features, is of a similar or higher order than those effects. Large smoothing or filtering is required, but this also reduces the value of the measurements.

The measurements provide a valuable insight in the highly variable slope in the auxiliary channel. But for these insights only few measurements would have been necessary. The large data set now available did not provide a necessary addition, because the scatter in the measurements do not allow further detailing.

Analysing the slope in cross direction of the different parallel runs is not included in this report as no valuable insights were gained from this. The bias between those parallel runs due to the different moment in time (a couple of hours up to a day later) are too large to make a useful comparison. A small study on the relation between curvature and cross slope is included in B.6, but neither gave any insights.

It is advised to reconsider the usage of longitudinal measurement for measurement campaigns of local measures with relatively small impacts compared to the expected fluctuations and scatter in water levels.

2.8 Conclusions and recommendations

From the measurements of the water level the following is concluded:

- From water level measurements it at the LMW-station at Tiel, it is concluded that at high discharge the water levels have been reduced by 10 to 20 cm as a result of the construction of the LTW and the other measures in this region.
- At low and median discharge, the water levels at Tiel have been stabilised since construction of the LTW: the downward trend in the period before construction is stopped. The water level at the station St. Andries (just downstream of the LTW) does show an continuous decline in the period after construction (expect for the lower discharges), which means that the head difference between the stations Tiel and St. Andries has actually increased. This effect can be contributed to the LTW.
- The effect of the change in the openings is not significant enough to conclude from the water level measurements. Only the raising of the inlet and Wamel was significant enough to show in the water level measurements of the auxiliary channel.
- An increased discharge through the Amsterdam-Rijnkanaal results in a reduction of the water levels on the Waal. The measured discharges at Tiel support the model simulation that every 1 m^3/s results in a water level reduction of 3 mm.
- From the experience in analysing the longitudinal measurements, it is advised to reconsider the application of this technique for measurement campaigns of local measures with relatively small impacts in relation to the large fluctuations in the longitudinal water levels. Although a single run can be used for analysing the bigger pictures, it can not be easily compared to other runs due to this macro turbulence. To increase the accuracy, it could be decided to measure on moments of lower ship intensity (less ship waves, e.g. at night), to sail at lower speed (not make waves with the vessel it self) and to do multiple runs of each measurement. However, larger time series at measurement stations (possibly at divers) is expected to provide better insights.
- In the pilot the costs to build many measurement stations was too high. Only a couple of divers could be placed to measure the water level. However, none of these stations have been retreived frequently nor checked for quality, resulting in a data set that was not usuable in this evaluation. It is adviced to have a clear ‘data owner’ in future evaluation projects that requests and validates the data during the project.

3 Flow velocity

3.1 Introduction

This chapter focuses on the data obtained by means of ADCP measurements. One important point of the longitudinal training walls is the morphodynamic changes they induce due to the change in sediment transport capacity. Another point of attention is the transverse velocities occurring at the inlets and outlets, which may hamper navigation. Hence, the following research questions are posed:

1 What is the influence of the longitudinal training walls regarding sediment transport capacity?
2 What is the influence of the longitudinal training walls regarding the transverse velocity near the inlets?

This chapter is organized as follows. In Section 3.2, the data used in this part of the project is described. Section 3.3 focuses on assessing the sediment transport capacity changes. Section 3.4 describes the transverse velocity profiles.

3.2 Available data

The data available to answer the research questions (Section 3.1) consists of ADCP measurements obtained between 2013 and 2020. The measurements were taken as:

- cross-sections in the main channel,
- cross-sections in the auxiliary channel,
- longitudinal sections in the main channel,
- longitudinal sections in the auxiliary channel,
- longitudinal sections in the surroundings of the inlet.

For obtaining one measurement several “rounds” (also referred to as “runs”) were taken. A round is a single sample, for instance, from the left bank to the right bank. The same cross-section is sampled several times (i.e., several rounds are taken) and the successful rounds comprise a single measurement.

In total there are 13,117 files. The data is in two different format types. Both formats are given as ASCII files and contain for each position (x, y) the velocity in north and east directions. Only one of the data types has information on the vertical velocity. Table D.12 summarizes all measurements. Only one round per measurement is shown by not showing measurements on the same day separated less than 10 m. The river kilometre is computed as the mean of all the points in the profile.

Coordinates are given in different reference systems and velocities in different units, amongst other differences. All files have been read, uniformed, and saved in Matlab® format.

Each of the 13,117 files have been plotted for inspection and are available for interested readers. In these figures, processing is minimal and it concerns only flipping of the measurement rounds such that the direction is the same in all cases, and projection of the velocity in the direction of the measurement plane based on the first and last positions. Figure 3.1 provides an example of a cross-sectional measurement. A positive crosswise velocity is defined in increasing distance along the section (see colorbar indicating distance along section). In all cases, the same and most recent satellite image in Google Earth® is used in the background. Hence, in the figures of the situation before construction of the longitudinal training walls, the walls are shown in the image although they were not present at that moment. It is remarkable that the vertical velocity shows an unrealistic profile. This will be discussed later in Section 3.3.3.2.

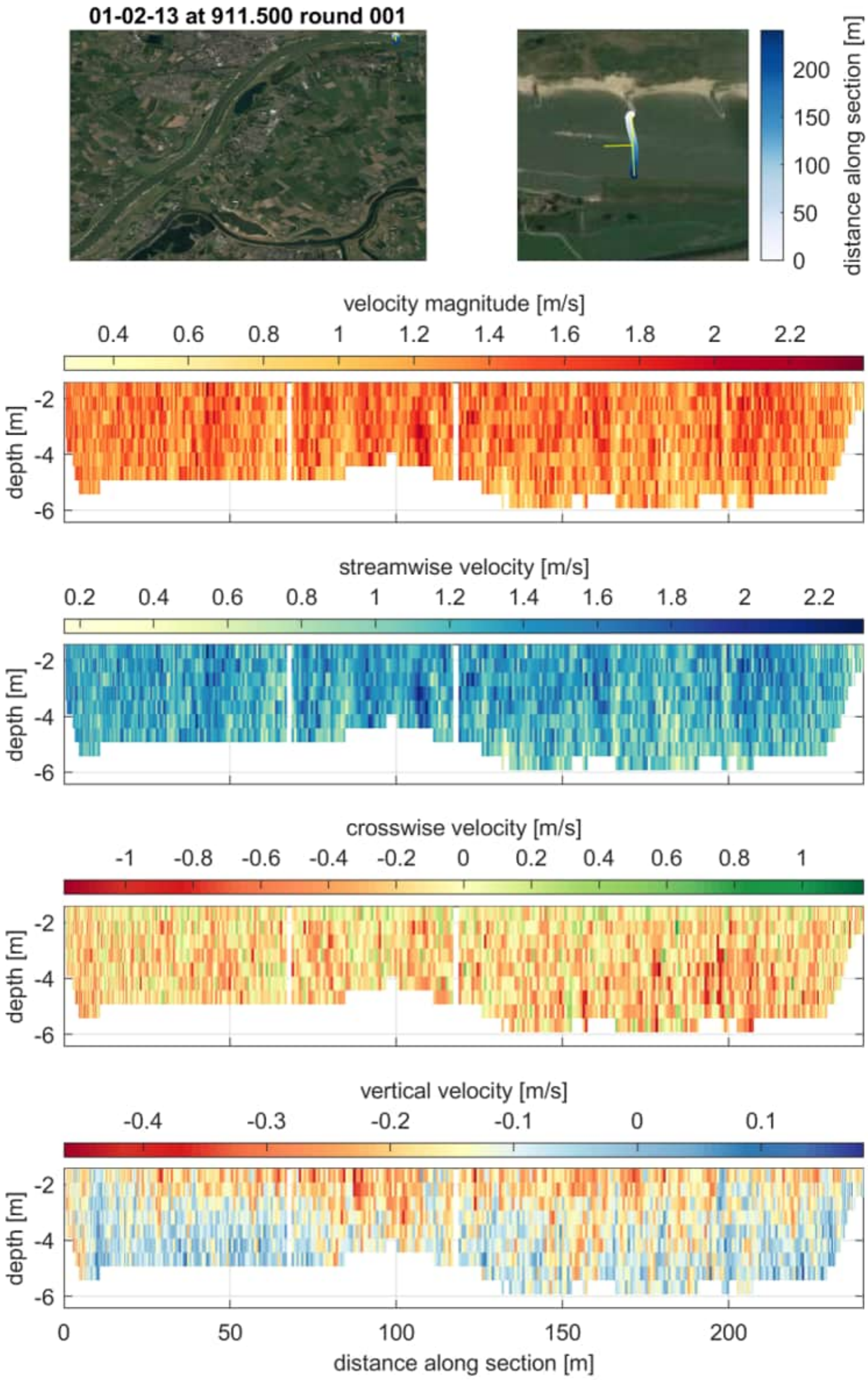

Figure 3.1 Example of a cross-sectional measurement.

Sieben (2020) conducted a preliminary analysis of the discharge measurements. His data-set is available to us as an Excel sheet in which the day, the river kilometre, whether the measurement was conducted along the main channel or the auxiliary channel, and the discharge is recorded.

3.3 Changes in flow due to the construction of the longitudinal training walls

This section focuses on analysing changes in sediment transport capacity due to the construction of the longitudinal training walls (i.e., answering Research Question 1). In analysing changes in sediment transport, flow patterns before construction of the longitudinal training walls are compared with flow patterns after intervention.

3.3.1 Methodology and results of the analysis of the flow changes

During a rising-flow event between the 1st and the 4th of February 2013 a measurement campaign was conducted. This serves as the basis of the situation prior to intervention. The discharge at Lobith and at Tiel during the measurement campaign are shown in Figure 3.2. It is not possible to speak about a single discharge for each measurement, as the time needed for sampling the whole river is substantial. Still, the data received labels the three measurements with the discharges 2380 m^3/s, 3870 m^3/s, and 4690 m^3/s, respectively. The labelling seems to be based on the discharges of the DVR model (Ottevanger *et al.*, 2015) but it does not seem to be consistent with the actual river discharge.

The lowest discharge in the 2013 campaign is already relatively high. For this reason, a measurement on the 17th of November of 2011 when the discharge at Lobith was approximately 922 m^3/s is also considered. This measurement forms part of a set of measurements conducted only at Tiel.

Overall, four conditions are considered which are labelled as Condition 1, 2, 3, and 4 in increasing discharge (Table 3.1).

label	date	discharge at Lobith at 12:00 [m^3/s]	locations
Condition 1	17-11-2011	922	1
Condition 2	01-02-2013	3436	13
Condition 3	02-02-2013	4170	13
Condition 4	04-02-2013	5087	13

Table 3.1 Conditions used to study the situation prior to intervention.

The water level at Tiel at 00:00 on the day of the measurement is obtained, which is then used to match with the measurement after construction of the longitudinal training walls in which the water level was closest to that which occurred during the measurement taken before construction (Figure 3.3). The absolute differences in water level between the situations before and after intervention for Conditions 1, 2, 3, and 4 are equal to 4 cm, 2 cm, 9 cm, and 14 cm, respectively. These relatively low values indicate that data can be compared, although attention needs to be paid when extracting quantitative conclusions.

Matching locations based on the water level at Tiel before and after intervention

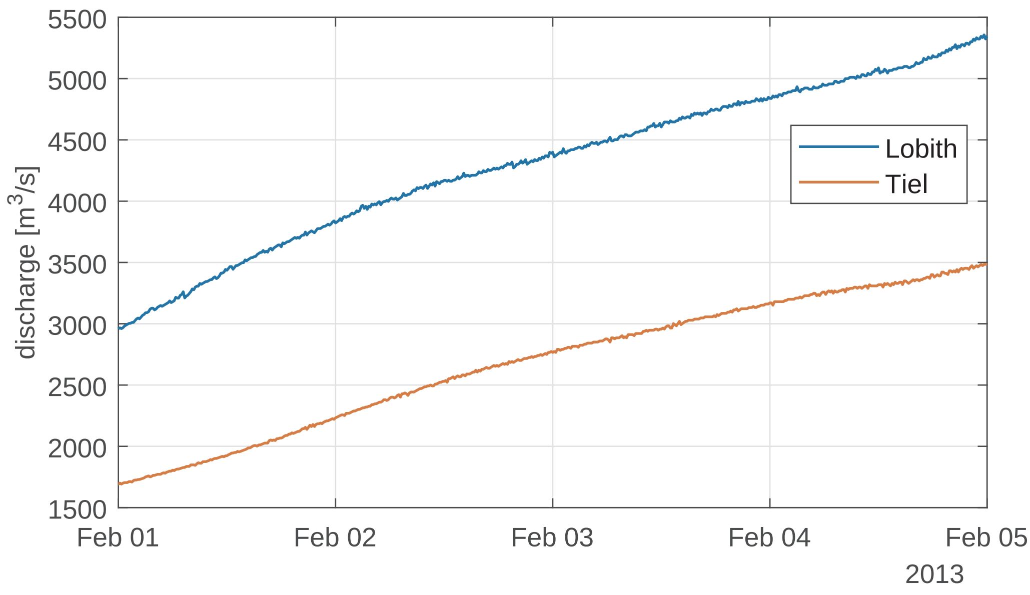

Figure 3.2 Water discharge at Lobith and Tiel during the measurement campaign before construction of the longitudinal training walls.

presents several limitations such as the fact that the intervention is expected to change the water level. One would prefer to match based on discharge, but this is also problematic due to the fact that a measurement at the auxiliary channel and the main channel at the same location needs to exists, conducted at the time in which the discharge was similar to the one prior to construction. Considering the variability it was found best to match on discharge. This and other limitations are further discussed in Section 3.3.3.

In each measurement campaign before intervention for Conditions 2, 3, and 4, 13 cross-sections were measured. For each of these locations, the closest measurement location inspected on the selected date is obtained. Hence, 13 locations after intervention for each of the three different discharges are selected to compare with the same locations before intervention (Figures 3.5, 3.6, and 3.7). Table D.13 summarizes the profiles that have been used.

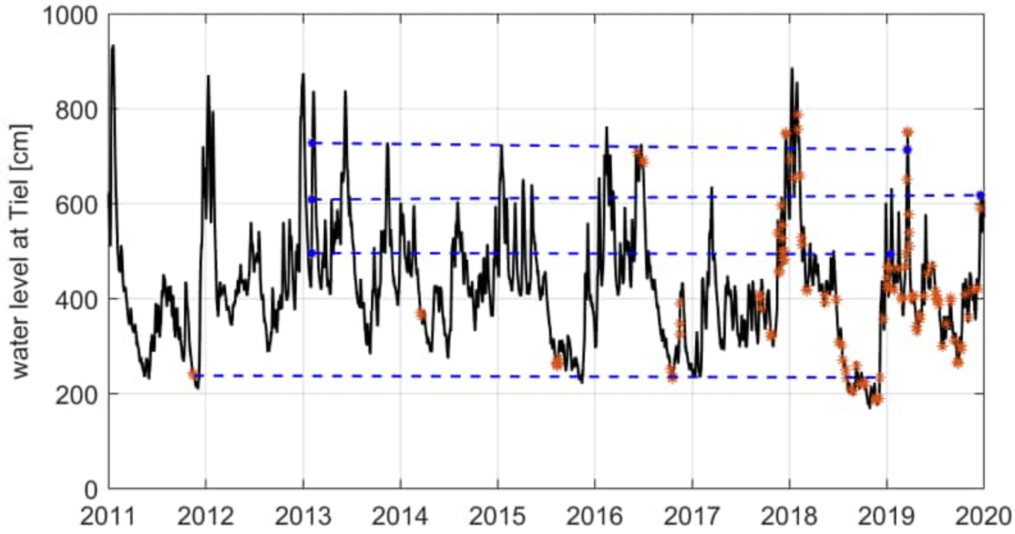

Figure 3.3 Water level at Tiel with time (black line) and times when each measurement campaign was done (red asterisks). The blue dashed line matches measurements taken before construction with measurements taken after construction which have a most similar water level.

Figure 3.4 Location of the cross-sectional measurements before and after intervention for condition 1. For this condition measurements were only conducted at one location. For each measurement before construction (square marker with number) the matched measurement after construction (circle marker) is given the same color.

Figure 3.5 Location of the cross-sectional measurements before and after intervention for condition 2. . For each measurement before construction (square marker with number) the matched measurement after construction (circle marker) is given the same color.

Figure 3.6 Location of the cross-sectional measurements before and after intervention for condtion 3. . For each measurement before construction (square marker with number) the matched measurement after construction (circle marker) is given the same color.

Figure 3.7 Location of the cross-sectional measurements before and after intervention for condition 4. . For each measurement before construction (square marker with number) the matched measurement after construction (circle marker) is given the same color.

At each location, all rounds are averaged for obtaining a representative cross-sectional measurement. Figure 3.8 shows an example of the averaging of all rounds at the same location as Figure 3.1. Note how the resulting averaging procedure filters the data.

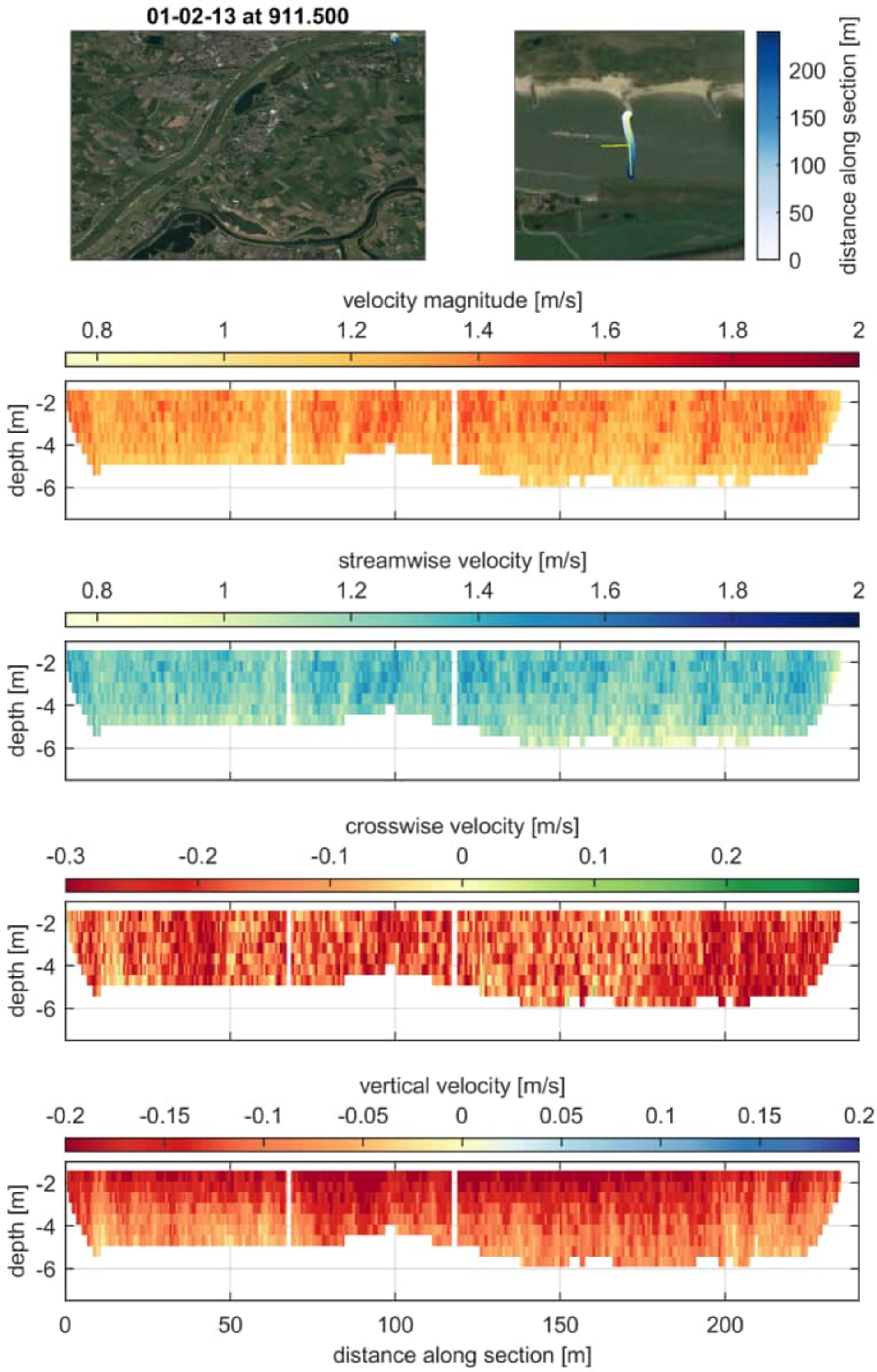

Figure 3.8 Cross-sectional measurements on 01-02-13 (discharge at Lobith at 12:00 equal to 3436 m^3/s) at rkm 911.500 projected on measurement plane.

The measurement plane does not exactly align with the transverse direction (i.e., it is

Deltares

not normal to the streamwise direction). For proper comparison of the situation before and after intervention it is desired that the measurement plane coincides with the transverse direction of the flow in all cases such that one can speak about velocity in the flow direction and in the transverse direction. This is necessary to be able to visualise the secondary flow circulation and for an accurate computation of the total discharge. It is especially necessary when comparing flow fields that were not on the exact same sailing track.

To this end, the streamwise direction is numerically found by minimization of the cross-sectional discharge (Figure 3.9). Worded differently, the cross-sectional discharge is computed for an arbitrary plane as the sum for all bins (in cross-wise and vertical direction) of the product of the velocity parallel to that plane and the flow depth of the bin. Then, the plane with smaller cross-sectional discharge is selected (this is a common method, e.g. Dietrich and Smith (1983)). In this way, measurements with zero cross-sectional discharge are found (Figure 3.10).

Figure 3.11 presents the measurements after intervention that is associated with the data before intervention as given in Figure 3.10.

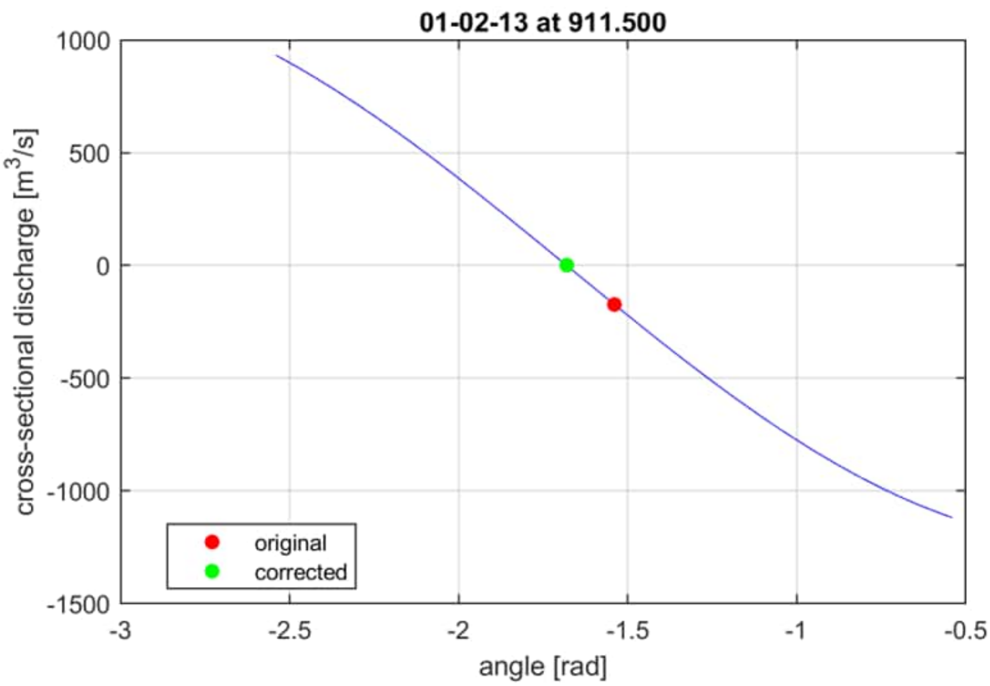

Figure 3.9 Cross-sectional discharge on 01-02-13 (discharge at Lobith at 12:00 equal to 3436 m^3/s) at rkm 911.500 as a function of the direction of the projection plane (blue line). The original measurement plane and the corrected plane are marked in red and green, respectively.

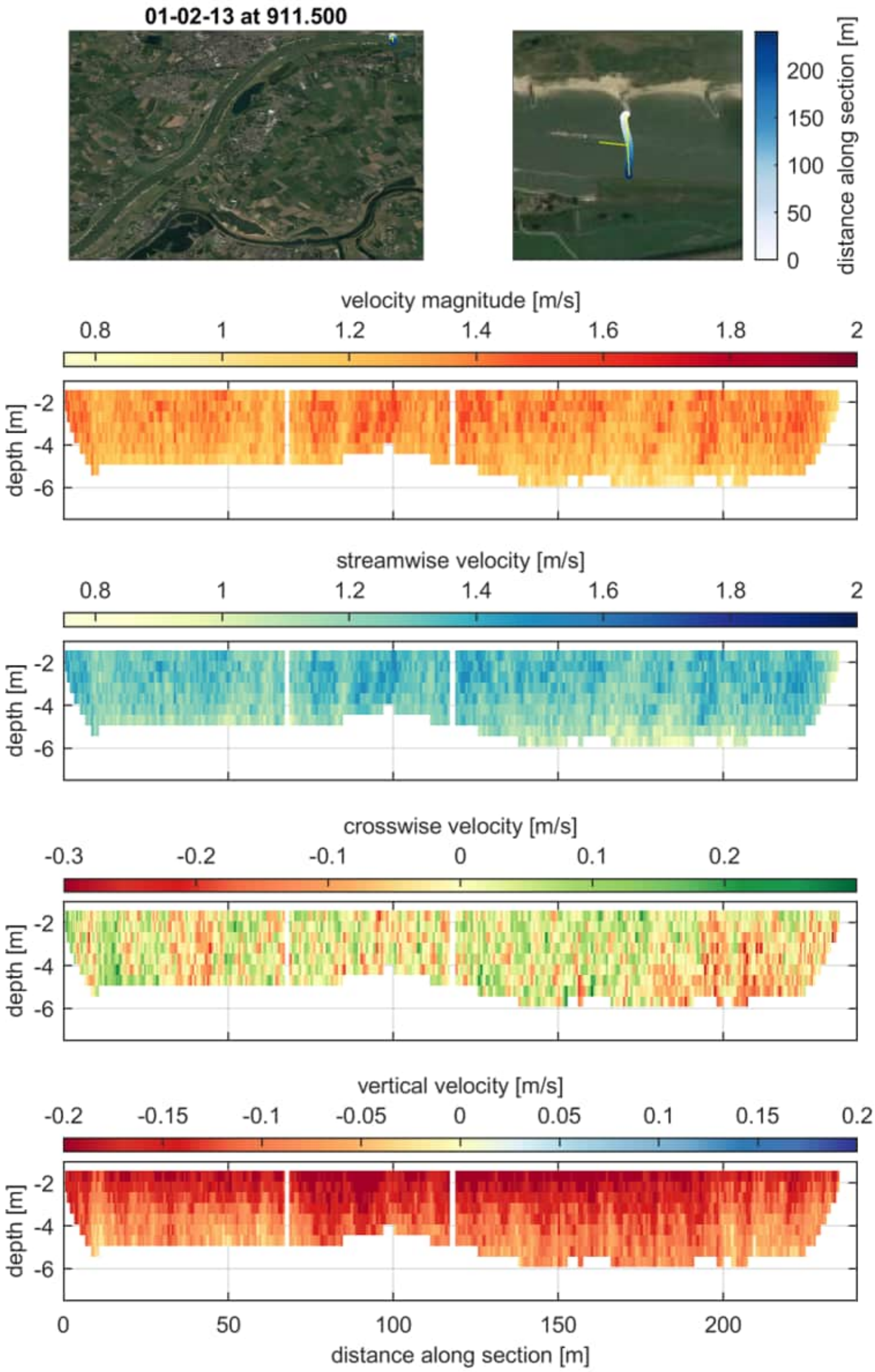

Figure 3.10 Cross-sectional measurements on 01-02-13 (discharge at Lobith at 12:00 equal to 3436 m^3/s) at rkm 911.500 projected on crosswise plane.

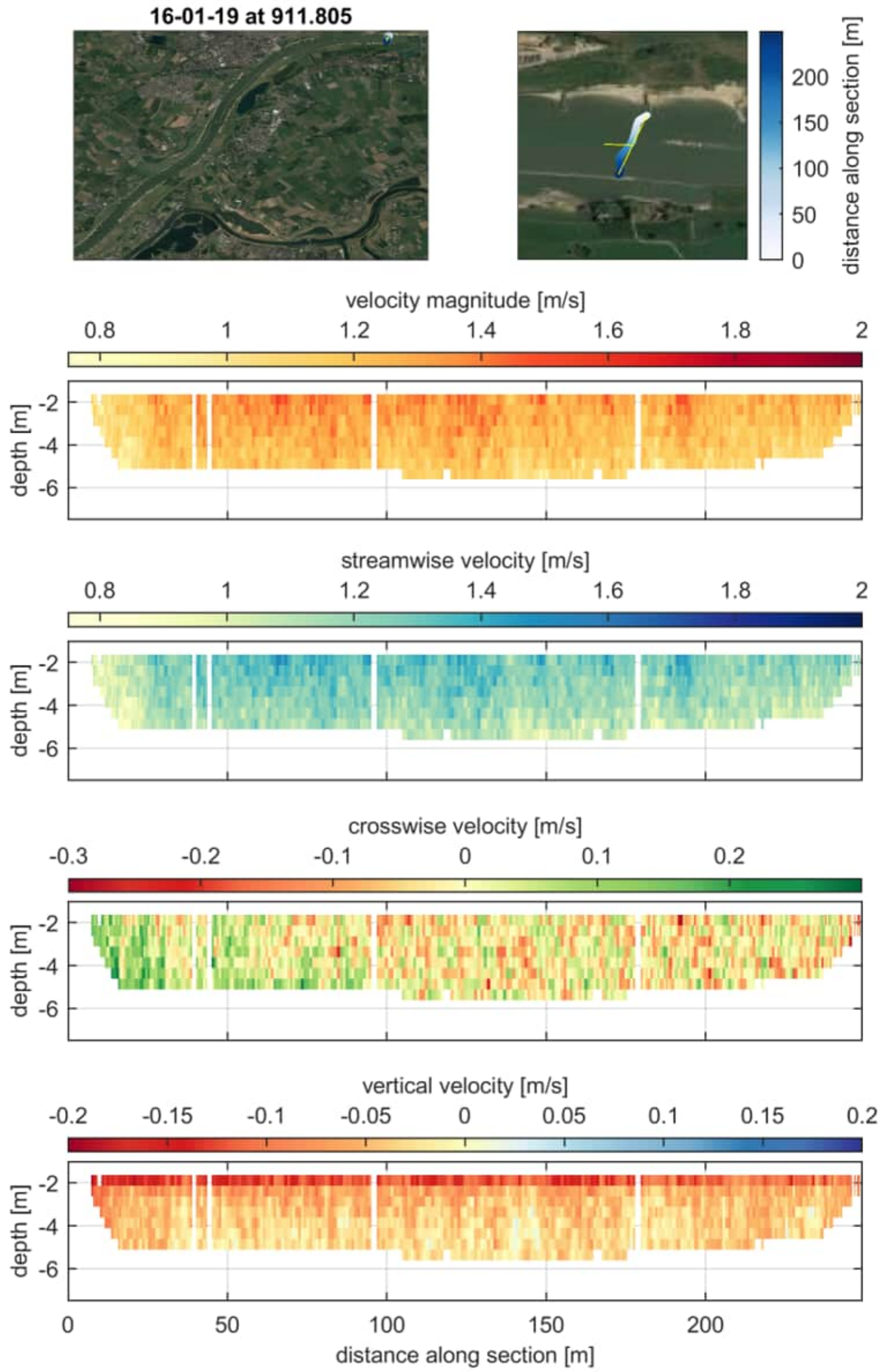

Figure 3.11 Cross-sectional measurements on 16-01-19 (discharge at Lobith at 12:00 equal to 3022 m^3/s) at rkm 911.805 projected on crosswise plane.

The last step consist of considering the data around the centre of the channel to study the effect of the intervention on the main channel velocity. To this end, the point of each measured profile closest to the river axis is found and the data 50 m to the left and right of the point is selected. The vertical profiles before and after intervention are averaged in transverse direction to obtain a representative velocity profile. Figure 3.12) shows one example. The thin lines in the background show all the velocity profiles in the central 100 m of the main channel. The thick lines are the average profiles. The error bars identify one standard deviation in each direction.

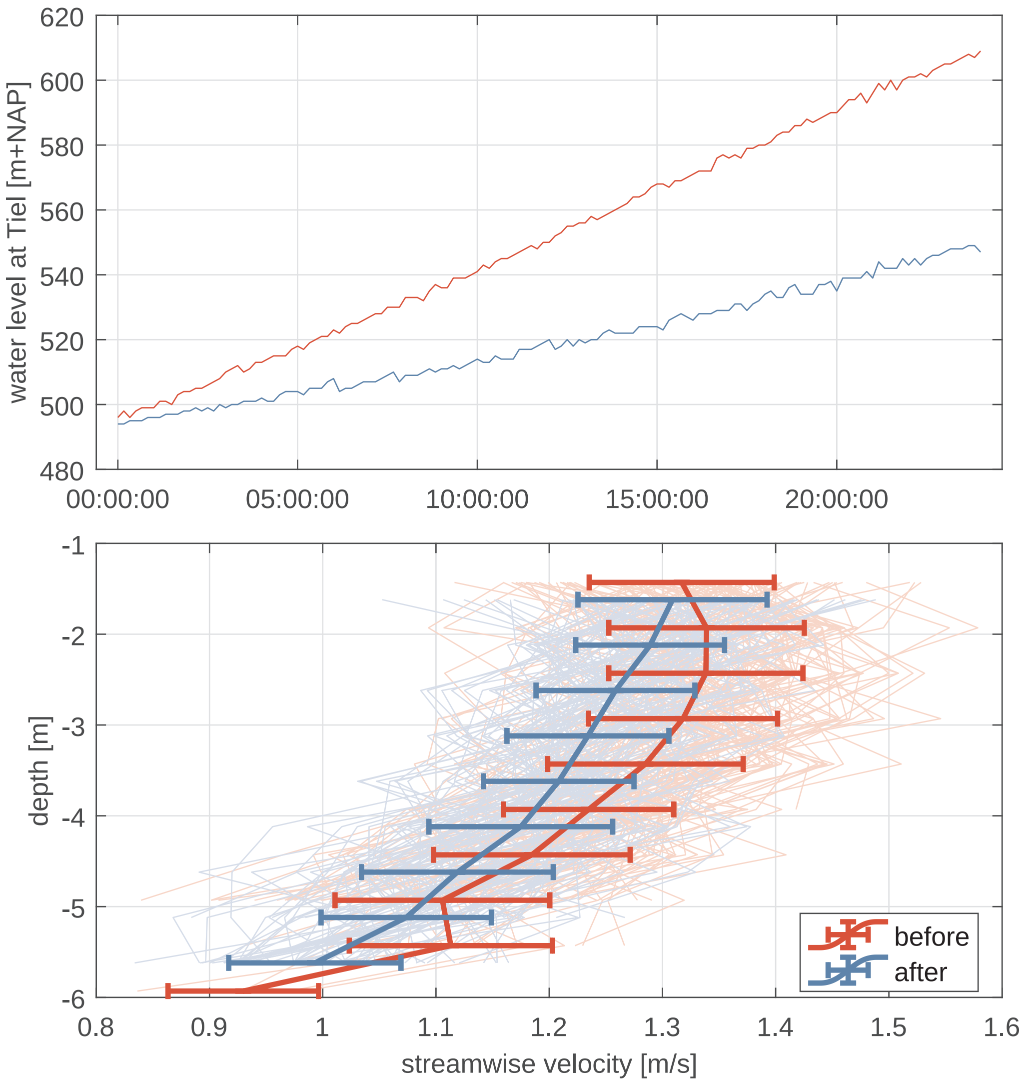

Figure 3.12 Streamwise velocity at the central 100 m of channel before (01-02-13, discharge at Lobith at 12:00 equal to 3436 m^3/s, rkm 911.500) and after (16-01-19, discharge at Lobith at 12:00 equal to 3022 m^3/s, rkm 911.805). Condition 2. (Note that the measurements are matched on the water level at Tiel. The time lag to Lobith in combination with the different water-rising speed causes a large difference in discharge.)

Appendix D.2 contains all the figures showing the flow pattern before and after intervention for all discharges. Tables 3.2, 3.3, 3.4, and 3.5 summarize the data for the four conditions. The velocity is shown in Figures 3.14, 3.15, and 3.16, respectively.

location [-]	rkm before	distance [km]	velocity before [m/s]	standard deviation before [m/s]	velocity after [m/s]	standard deviation after [m/s]	velocity change [%]
1	916	0.00	0.78	0.11	0.87	0.12	10.79

Table 3.2 Change in streamwise flow velocity for condition 1. “location” indicates the location number,“distance” indicates the distance between the two compared locations, “velocity” is the cross-sectional and depth-averaged flow velocity in the 50 m to the right and left of the river axis, and “standard deviation” is the mean of the standard deviation of the depth-averaged velocity. The water level Tiel is given in appendix D.2.

location [-]	rkm before	distance [km]	velocity before [m/s]	standard deviation before [m/s]	velocity after [m/s]	standard deviation after [m/s]	velocity change [%]
1	912	0.30	1.22	0.08	1.18	0.07	-2.64
2	912	0.00	1.25	0.08	1.18	0.07	-5.59
3	912	0.60	1.31	0.07	1.18	0.07	-9.41
4	913	1.30	1.33	0.09	1.18	0.07	-11.07
5	915	0.10	1.36	0.09	1.28	0.09	-6.21
6	915	0.07	1.30	0.08	1.24	0.08	-4.48
7	916	0.87	1.30	0.08	1.24	0.08	-5.02
8	918	0.45	1.28	0.07	1.13	0.09	-11.72
9	919	0.00	1.28	0.11	1.06	0.07	-17.01
10	921	0.55	1.26	0.08	1.04	0.07	-17.15
11	922	0.20	1.21	0.08	1.04	0.07	-13.48
12	922	0.45	1.19	0.08	1.04	0.07	-12.31
13	922	0.80	1.20	0.08	1.04	0.07	-12.76

Table 3.3 Change in streamwise flow velocity for condition 2. “location” indicates the location number,“distance” indicates the distance between the two compared locations, “velocity” is the cross-sectional and depth-averaged flow velocity in the 50 m to the right and left of the river axis, and “standard deviation” is the mean of the standard deviation of the depth-averaged velocity. The water level Tiel is given in appendix D.2.

location [-]	rkm before	distance [km]	velocity before [m/s]	standard deviation before [m/s]	velocity after [m/s]	standard deviation after [m/s]	velocity change [%]
1	912	0.30	1.34	0.08	1.33	0.10	-0.12
2	912	0.00	1.39	0.07	1.33	0.10	-4.02
3	912	0.60	1.42	0.08	1.33	0.10	-6.23
4	913	1.30	1.43	0.09	1.33	0.10	-6.78
5	915	0.10	1.36	0.09	1.41	0.10	3.48
6	915	0.07	1.50	0.09	1.33	0.11	-11.72
7	916	0.87	1.45	0.09	1.33	0.11	-8.33
8	918	0.45	1.37	0.09	1.37	0.10	-0.05
9	919	0.03	1.33	0.10	1.21	0.11	-8.88
10	921	0.55	1.41	0.08	1.30	0.12	-7.62
11	922	0.20	1.31	0.08	1.30	0.12	-0.56
12	922	0.45	1.41	0.08	1.30	0.12	-7.93
13	922	0.80	1.40	0.08	1.30	0.12	-6.83

Table 3.4 Change in streamwise flow velocity for condition 3. “location” indicates the location number,“distance” indicates the distance between the two compared locations, “velocity” is the cross-sectional and depth-averaged flow velocity in the 50 m to the right and left of the river axis, and “standard deviation” is the mean of the standard deviation of the depth-averaged velocity. The water level Tiel is given in appendix D.2.

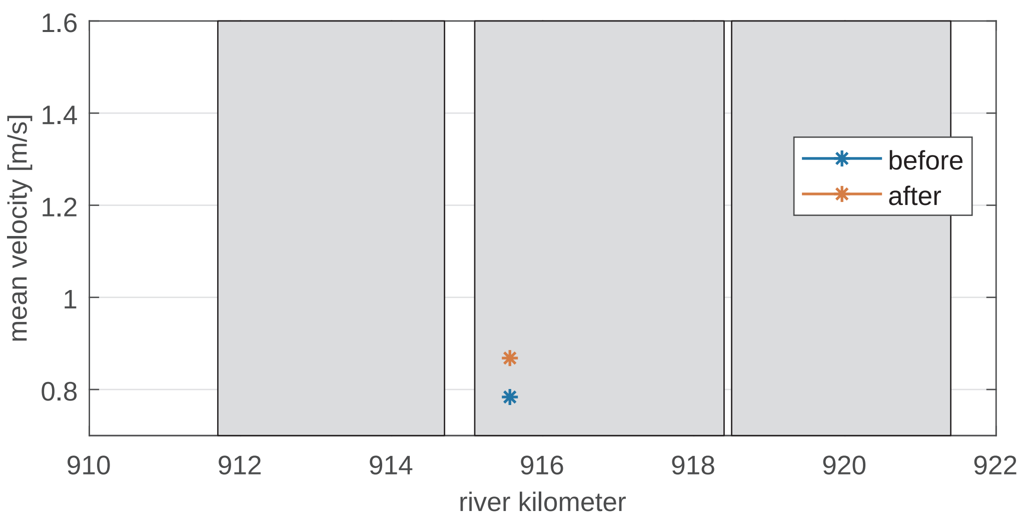

Figure 3.13 Cross-sectional and depth-averaged streamwise velocity at the central 100 m of main channel before and after intervention for Condition 1.

location [-]	rkm before	distance [km]	velocity before [m/s]	standard deviation before [m/s]	velocity after [m/s]	standard deviation after [m/s]	velocity change [%]
1	912	0.30	1.44	0.08	1.39	0.06	-3.42
2	912	0.00	1.43	0.08	1.39	0.06	-2.78
3	912	0.05	1.50	0.09	1.42	0.04	-5.44
4	913	0.01	1.57	0.09	1.50	0.06	-4.50
5	915	0.10	1.49	0.08	1.50	0.05	0.54
6	915	0.07	1.52	0.08	1.55	0.07	2.11
7	916	0.08	1.48	0.09	1.45	0.05	-2.23
8	918	0.01	1.48	0.08	1.41	0.05	-4.92
9	919	0.03	1.38	0.09	1.31	0.05	-5.32
10	921	0.03	1.48	0.08	1.45	0.04	-2.40
11	922	0.20	1.42	0.08	1.42	0.05	0.50
12	922	0.25	1.50	0.08	1.50	0.04	-0.03
13	922	0.10	1.49	0.07	1.50	0.04	0.78

Table 3.5 Change in streamwise flow velocity for condition 4. “location” indicates the location number,“distance” indicates the distance between the two compared locations, “velocity” is the cross-sectional and depth-averaged flow velocity in the 50 m to the right and left of the river axis, and “standard deviation” is the mean of the standard deviation of the depth-averaged velocity. The water level Tiel is given in appendix D.2.

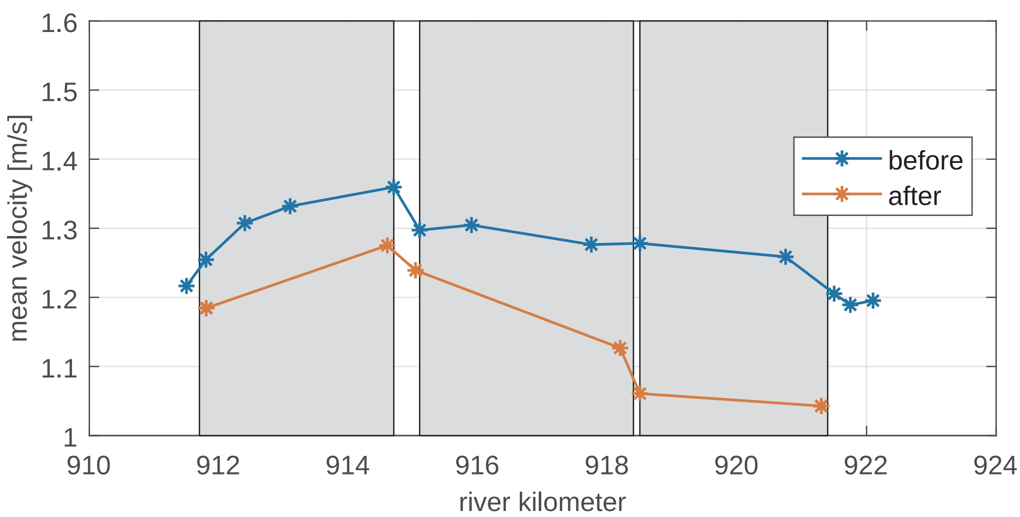

Figure 3.14 Cross-sectional and depth-averaged streamwise velocity at the central 100 m of main channel before and after intervention for Condition 2.

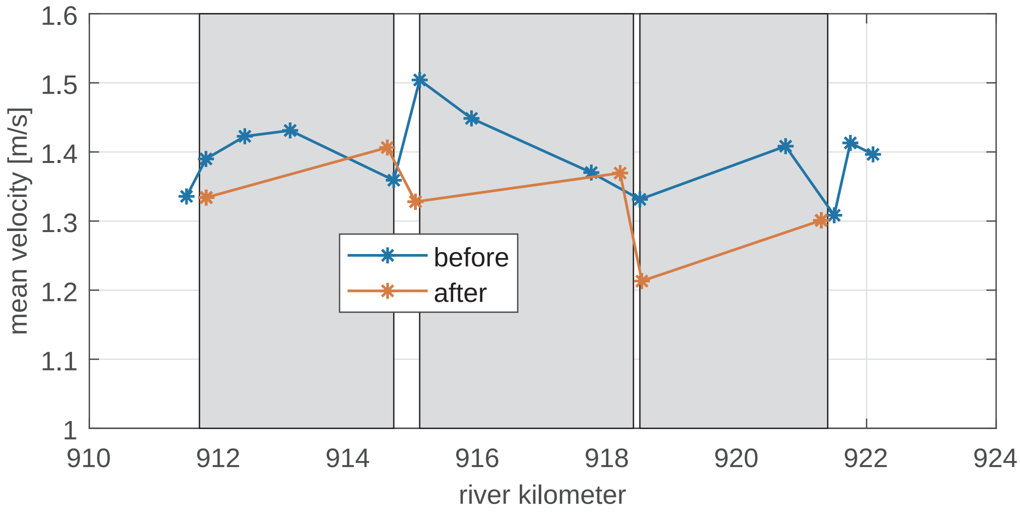

Figure 3.15 Cross-sectional and depth-averaged streamwise velocity at the central 100 m of main channel before and after intervention for Condition 3.

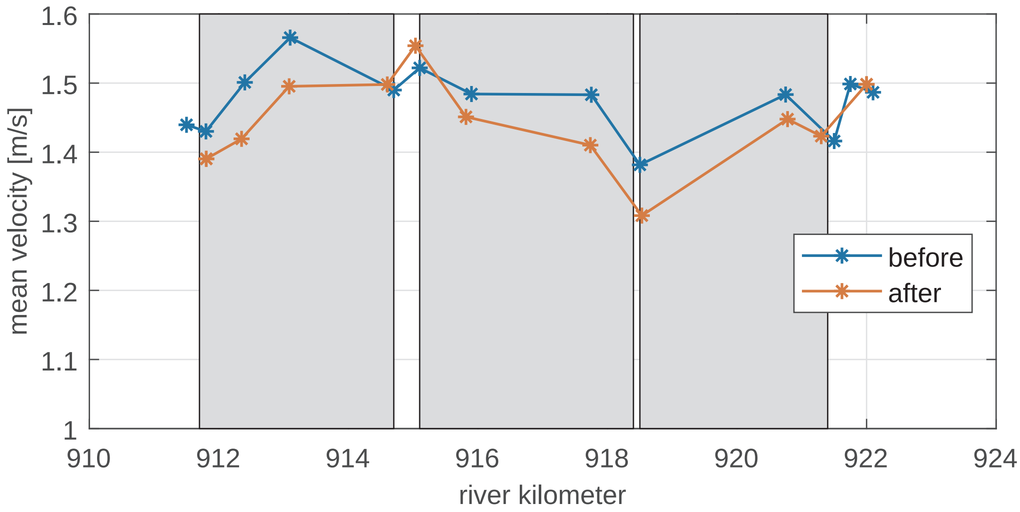

Figure 3.16 Cross-sectional and depth-averaged streamwise velocity at the central 100 m of main channel before and after intervention for Condition 4.

The velocity for the lowest discharge increases significantly (10%) after intervention. Unfortunately, there is only one measurement for this condition, which hinders generalization. For Conditions 2, 3, and 4, the velocity after intervention is smaller than before the construction of the longitudinal training walls. The change in flow velocity between the situation before and after intervention increases as the discharge decreases. Worded differently, for a low discharge, the effect of the longitudinal training walls on the main channel flow velocity is larger than for a high discharge.

The largest change in velocity occurs at Ophemert (Locations 9-13) for Condition 2. In this case, it is larger than 10%, even reaching 17% at the upstream end. At Wamel and Dreumel it is in the order of 5%. It is relevant to remind the reader that the discharge in the measurement before interventions is certainly different than in the measurement after intervention given the limitations in the analysis (see Section 3.3.3). Yet, the reduction flow velocities appears to be consistent among most measurements, although varying in magnitude. This suggest that the change is indeed due to the longitudinal training walls and not to limitations in the methodology.

3.3.2 Methodology and results of the analysis of the discharge partitioning

The data compiled by Sieben (2020) is used for studying the effect of the inlet openings on the discharge distribution. From all the measurements, those for which there is a measurements in the auxiliary channel and in the main channel on the same day and river kilometre are selected and matched.[1] These selected measurements are discretized according to the date at which they where taken as (see appendix A.2):

- from construction until May 2018,
- from May 2018 until May 2019,
- from May 2019 until present.

In summary, in April 2018 the inlets at Wamel and Dreumel were raised and in April 2019 the inlet at Dreumel was lowered and the one at Ophemert was narrowed.

Figures 3.17 and 3.18 present the fraction of the discharge along the auxiliary channel as a function of the river kilometre and the total discharge in the cross section, respectively. The total discharge is computed by adding the ADCP measurement of the main channel to the measurement in the auxiliary channel. As a result, measurement campaigns without measurements on both location are excluded. In Appendix D.6 the figures for each river kilometre are shown.

The amount of discharge along the auxiliary channel varies between less than 5% and more than 25% of the total discharge. For a larger total discharge, a larger fraction is transported along the auxiliary channel. This is the expected behaviour: for low discharges flow is concentrated in the main channel and as the discharge increases a larger proportion is transported along the auxiliary channel.

In general, the effect of varying the inlets is not visible in the data. For instance, Figure 3.19 shows the inlet of Dreumel. The measurements before and after intervention do not cluster at different locations. For a discharge equal to 1000 m^3/s one may conclude that after May 2019 the auxiliary channel transports a larger proportion of water than before. This may be in line with the fact that the inlet was lowered. At discharges of approximately 1400 m^3/s the figure does not show differences between the situation before and after intervention.

[1] In Sieben (2020) also measurements are presented that had could not be matched between main and auxiliary channel. The discharge fraction through the channel is computed based on an assumed discharge (through regression with Lobith). This also results in discharge fractions higher than 100%. The discharge analysis by Sieben also includes discharge extractions towards the Tiel-Kanaal.

At Wamel, the figures cannot be used to show the effect of the change in inlet (May 2018), because no measurements prior to May 2018 are available with a matching to main channel measurements. The available measurements show with the closed inlet show very low discharges through the channel: 1 to 2 % at a Waal discharge between 600 and 1000 m^3/s. This shows that the closing of the inlet resulted in a low (but not 0) discharge. Estimates by Sieben (2020) show that before construction the discharge through the channel was approximately higher than 12 %.

Further downstream in the auxiliary channel of Wamel, the discharge increases. Probably as a result of the porosity of the dams. The porosity of the dams is probably the highest at the inlet and intermediate openings as these are only constructed of coarse material (40 - 100 kg), see figure A.1.

Sieben (2020) shows that, from theory, when the discharge in the main channel is 88 % or more of the total Waal discharge, this will result in an increase in water levels compared to the situation prior to construction. This is the same as a discharge through the auxiliary channel of less than 12 %, which can be concluded from either figure 3.18 or from Sieben (2020). At Wamel, for a discharge at Lobith lower than 2500 m^3/s is lower than 12 % of total Waal discharge, which should in theory result in an increase in water levels compared to prior to construction. At Dreumel, the only at Boven-Rijn discharges of roughly 1250 m^3/s and lower the auxiliary channel discharge is lower than 12 % of the total Waal discharge. At Ophemert the auxiliary channel discharge is never below 12 %.

The main limitation is that, while there are 650 measurements, only 160 pairs of points are useful for the analysis considering that they need to be taken on the same day and location. Moreover, measuring the discharge accurately is challenging and even more in the shallow auxiliary channel.

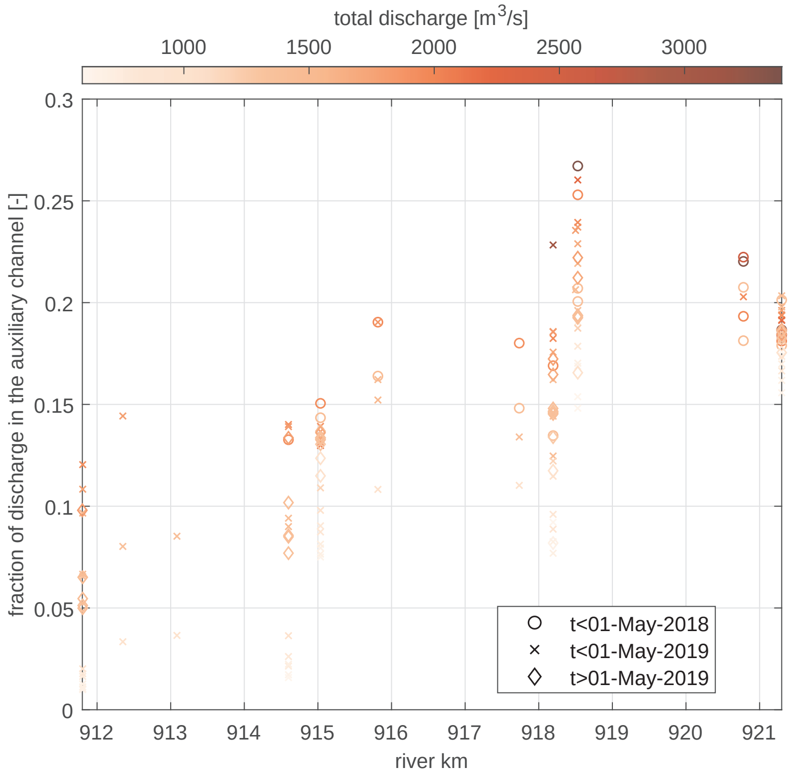

Figure 3.17 Fraction of discharge along the auxiliary channel for a varying river kilometre.

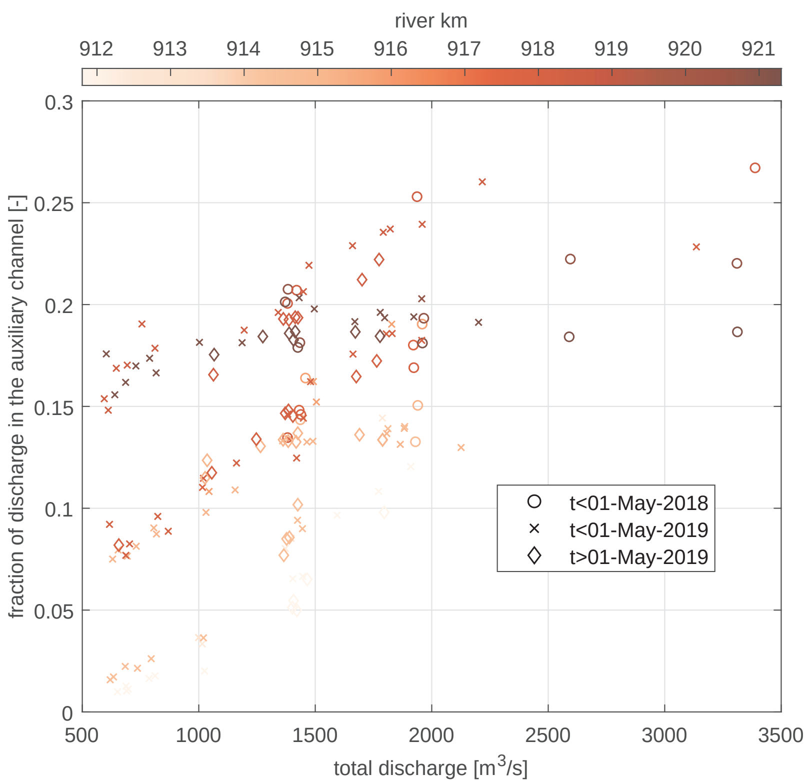

Figure 3.18 Fraction of discharge along the auxiliary channel for a varying total discharge.

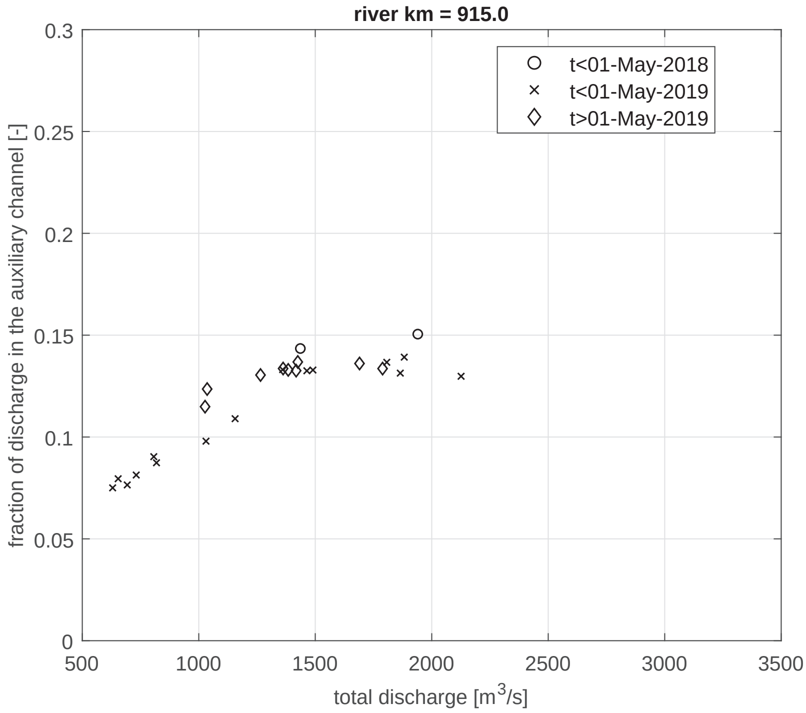

Figure 3.19 Fraction of discharge in the auxiliary channel as a function of the total discharge for the measurements at river km 915.0

3.3.3 Discussion of the results of the analysis of the changes in flow and recommendations

3.3.3.1 Consequences for sediment transport

For Condition 1 with low-flow (922 m^3/s), a velocity increase after intervention is observed. This is reasonable given that the width of the main channel has been reduced. This results in an increase in sediment transport. However, these low discharges only occur a couple of days per year and are measured along the LTWWamel, while the inlet was fully raised. At other LTW this increase in velocity might not be present, due to a higher discharge in the auxiliary channel. Also at higher discharges, when the auxiliary channels become more active, the velocity increase might not be present.

For a discharge at Lobith equal to 3436 m^3/s and higher (i.e., Conditions 2, 3, and 4), the mean flow velocity in the main channel appears to have decreased due to the construction of the longitudinal training walls. At this discharge overtopping of the longitudinal training wallsoccurs (Section A.5) and the expected outcome of the river intervention is, as measured, a decrease of the flow velocity in the main channel, as more flow is transported through the auxiliary channel (which before intervention was a high-friction groyne field).

The implications for sediment transport capacity can be derived by assuming a power 5 relation between mean flow velocity and sediment transport capacity (Engelund and Hansen, 1967). In this case, a 10% reduction in flow velocity (representative of low-flow conditions) causes a 40% reduction in sediment transport capacity and a 1% reduction in flow velocity (representative of high-flow conditions) causes a 5% reduction in sediment transport capacity. The sediment transport rate is higher during high-flow than during low-flow condition, but low-flow conditions occur over a longer period. For the sake of exemplifying what the yearly implications of the reductions are, we assume that low flow occurs during 11 months a year with a velocity equal to 1.3 m/s (approximated value from Table 3.3) and high flow during 1 month a year with a velocity equal to 1.45 m/s (approximated value from Table 3.5). In this case, the reduction in yearly sediment transport rate would be 36%.

A reduction in the sediment transport capacity is coherent with the aggradation (or reduction in degradation) observed in the bed level measurements and in the simulation results. It is relevant to have in mind that it seems from the velocity measurements that this is mainly due to the effect under low-flow conditions, rather than high-flow conditions, as the change in velocity is largest for the conditions with a lower flow.

3.3.3.2 Limitations and recommendations

Data has been delivered in two different formats, one of them without vertical velocity. The coordinates system varies between profiles. This lack of uniformity may have its origin in different contractors and organizations obtaining the measurements. Importantly, it unnecessary complicates data processing. Moreover, data is structured in a non-uniform and non-intuitive format. The names of the files and folders do not follow a convention. Furthermore, the folder names are used to provide information, rather than “readme” files and tables, which causes names so long that cannot processed with some software. We strongly recommend to structure data in a uniform machine-readable manner with proper meta-data.

Several observations follow from the raw ADCP measurements (e.g., Figure 3.8). In all profiles, the vertical velocity is unrealistically large and shows an unrealistic pattern in which the top part of the flow is directed downwards and the bottom part upwards. The expected magnitude of the vertical velocity may be too small to be captured by the ADCP using the configuration that was set, which seems to have been set to capture the streamwise velocity. The precise ADCP configuration is unknown to us which prevents us from assessing the device accuracy. Most probably, the ADCP was not configured to measure vertical velocities.

Similarly, the crosswise-velocity pattern does not show the details of secondary flow one would expect. Being two orders of magnitude smaller than the streamwise velocity, most probably the instruments and measurement campaign were not set and designed to capture these subtle characteristic of the flow.

A larger number of rounds for each measurement would help in filtering noise related to turbulence. If the main question to be answered is the flow velocity, a measurement at a fixed location in the main channel for a long time would be more helpful and cheaper than several rounds measuring the entire cross-section. Certainly, this would not provide information on discharge. Measurement at a fixed location is not trivial, as instruments cannot be placed in the navigational channel, but a ship could maintain a fixed location for a certain time. This is again not trivial given how busy is the Waal River. Still, such a measurement would allow filtering in time and obtaining a precise view of the vertical profile.

In comparing the situation before and after intervention, we are severely limited by the scarce number of measurements conducted before intervention. The extensive dataset available may serve other purposes than then ones treated here. Nevertheless, for assessing the impact of the construction, once the exact same locations measured before intervention have been measured for the exact same discharge occurring at that time, extra measurements do not add further information.

A second important limitation is the fact that measurements have not been conducted at always the same location. For instance, the closest location after intervention to Location 4 in 2013 for a low discharge (rkm 913.100,upstream of Amsterdam-Rijn Kanaal inlet) is 1300 m upstream. Comparison of these two locations is far from ideal. Some other locations are ideal for comparison. For instance, Locations 2 and 5 for all discharges are right at the same point before and after intervention.

Regarding the analysis, the water level at Tiel has been used to match measurements before and after intervention. A problem with this approach is that the construction of the longitudinal training walls affects the water level at Tiel. As it is expected that the water level is lowered thanks to the construction of the longitudinal training walls, by matching the water level the discharge (and flow velocity) after construction are underestimated. Hence, the change in flow velocity may be larger than estimated.

The construction of the longitudinal training walls is not the only source of change in water level at Tiel. Groynes downstream and upstream from the longitudinal training walls have been lowered and other interventions even affect the water partitioning at the Pannerdensche Kop. The flow conditions are also important. Following a flood wave a larger friction is expected due to bed forms.

It is relevant to mention that the lowering of the water level is not clearly visible in the data due to large scatter (see report of WP10). Moreover, its effect would be negligible compared to the standard deviation of the measurements and averaging procedure in depth and cross directions.

One could think about computing the discharge in all measurements and match data based on discharge. This approach presents several issues. The first is that the uncertainty in velocity and in discharge computed by integration in vertical and cross directions is large. Note the noise visible in the raw plots of the profiles and the standard deviation in velocity measurements. Hence, most probably this uncertainty is larger than the effect of a change in water level. Second, it would be necessary to add the discharge measured in the main channel to that in the auxiliary channel. This adds further uncertainty as sections in the main channel and auxiliary channel where not taken at the same time and at the same river kilometre. Measurements which are not taken at the same river kilometre are difficult to add, considering that it is known that there is flow through the walls. Moreover, seeing that the closest measured data already have a difference in water level between 2 and 14 cm, it is foreseeable that also if using discharge, a condition exactly equal (in terms of discharge) to the original one cannot be found. Overall, the best way to match conditions before and after is the water level at a station.

One clear effect of the construction of the longitudinal training walls on the main channel under low-flow conditions has been a reduction of the width. A secondary effect is the fact that while before there was an exchange of mass and momentum between groyne fields and main channel, now there is not. The consequences of such decrease in mixing have not been considered. A first assessment could be done by comparing results of three-dimensional schematized simulations of a river section with groynes and with a longitudinal training wall.

3.4 Transverse velocity near the inlets

3.4.1 Methodology and results of the analysis of the transverse velocity

This section focuses on analysing the flow pattern in the inlets and outlets with focus on navigation (i.e., answering Research Question 2).

An indicator of nautical safety is the transverse velocity. As an order of magnitude of the transverse velocity that is relevant for safety purposes, for small channels in which the streamwise velocity is smaller than 0.5 m/s, the transverse velocity should be smaller than 0.3 m/s (Koedijk, 2020). In rivers the conditions usually requires specific research. Here, we will use the value of 0.3 m/s in plots simply as an order of magnitude as this is not an actual threshold for navigation under the conditions in the longitudinal training walls.

In order to study the transverse velocity at the inlets, the focus is on analysing the profiles taken in streamwise direction at the inlets. The velocity is depth-averaged for:

- the entire flow depth, and
- the top 2 m of the water column.

The second averaging is done for the reason that the velocity affecting navigation is the one occurring on the top part of the flow, although the criterion is set for the depth-averaged velocity.

A grid is generated oriented following the flow and the values from the profiles are averaged on the grid to get a spatial view of the flow pattern (e.g., Figure 3.20). All the figures analysed are shown in Appendix D.5 grouped per inlet.

The maximum transverse velocity is in general observed along the inlet itself. As one moves towards the auxiliary channel, large transverse velocities are still observed, while the transverse velocity rapidly decreases towards the main channel. See, for instance, Figures D.137, D.145, D.181.

Figure 3.21 shows the maximum transverse velocity (averaged in the grid) for each of the conditions that have been analysed. Table D.14 describes the locations. In general, the maximum is below 1 m/s, although above 0.3 m/s. Nevertheless, the area in which the velocity is larger than 0.3 m/s is relatively small and it is concentrated in the inlet and towards the auxiliary channel. For comparison, in Figure D.167 there are 1948 m^2 in which the velocity is above threshold, which is representative of a location with a small area.

Another data-set for studying the transverse velocity is available. A limited number of longitudinal profiles have been taken along the main channel (e.g., Figure 3.22). In this figure we see how, at the inlet of Ophemert, a larger-than-average cross-wise velocity is observed. The main limitation of using this data-set is that only one profile was measured (i.e., there are no several rounds that can be averaged). Hence, it is not possible to filter several profiles in order to derive the mean-flow velocity from the instantaneous one. It is relevant to mention that we see in this profile the aggradation at the inlet at the same location where the increase in transverse velocity is observed. This is a sign to where influence of the inlet is noticeable on the flow field and indirectly on the bed level.

We attempt to study differences in flow pattern due to changes in the inlet shape. To this end, we focus on the upstream inlet at Wamel. Here, the crest-level change is largest, as it increased from 1 m+NAP to 4 m+NAP in April 2018 (Figure A.3).

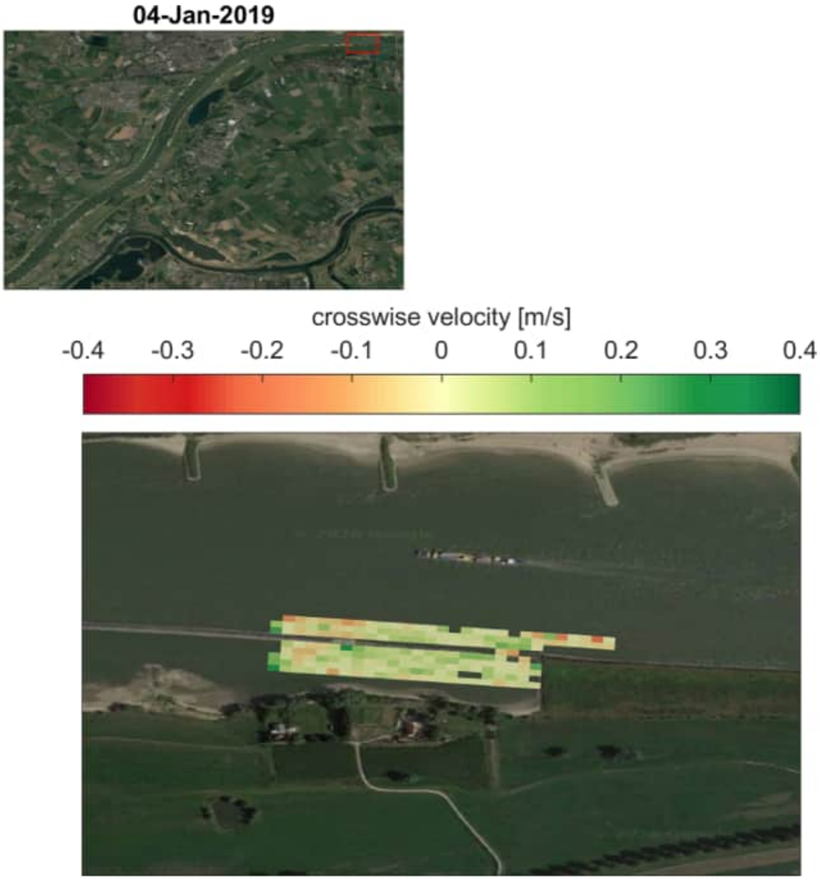

Figure 3.20 Depth-averaged velocity field considering the full water column on 04-01-19 (discharge Lobith: 1800 m^3/s).

We consider a situation before and after the change in crest level with flow conditions being as close as possible. On February 2, 2018, the water level at Tiel was 7.57 m+NAP. The closest water level in which measurements are available after changing the inlet were conducted on March 20, 2019, and the water level was equal to 7.50 m+NAP. The two figures showing the flow field in these cases are Figure 3.23 and Figure 3.24, respectively. No substantial changes in flow pattern can be observed.

Another comparison can be drawn between that situation on December 1 2017, when the water level at Tiel was 5.96 m+NAP. The closest water level in which measurements are available after changing the inlet were conducted on December 19, 2019, and the water level was equal to 6.18 m+NAP. The two figures showing the flow field in these cases are Figure D.177 and Figure D.167, respectively. The same conclusion can be extracted: no significant changes are observed and the changes can be associated the fact that the water discharge in the two situations we are comparing is not exactly the same.

Given that these are the largest changes expected to occur, we conclude that with the current approach the changes in depth-averaged flow pattern at the inlet due to a change in crest level are not appreciable.

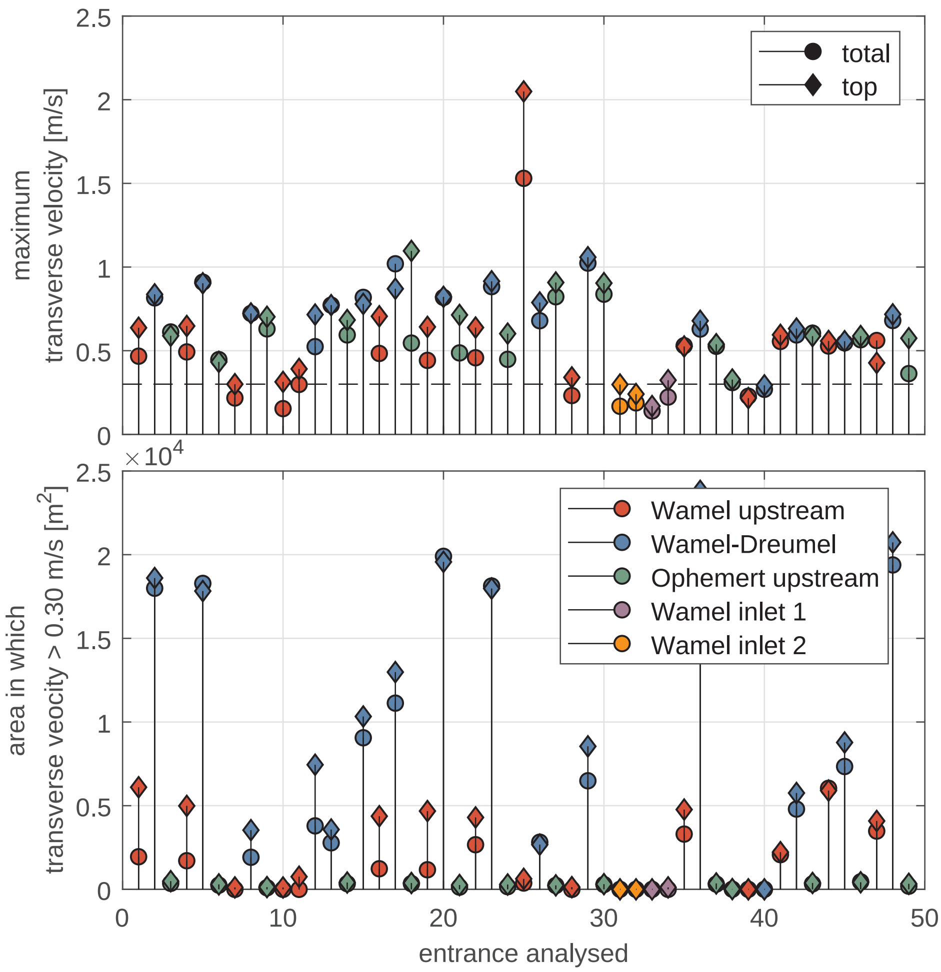

Figure 3.21 Maximum transverse velocity at each of the situations analysed (top figure) and area in which the transverse velocity is larger than 0.3 m/s (bottom figure). The analysis is conducted on the full depth-averaged velocity (total) as well as in the top 2 m of flow (top). 49 situations have been analysed at different times and locations (horizontal axis).

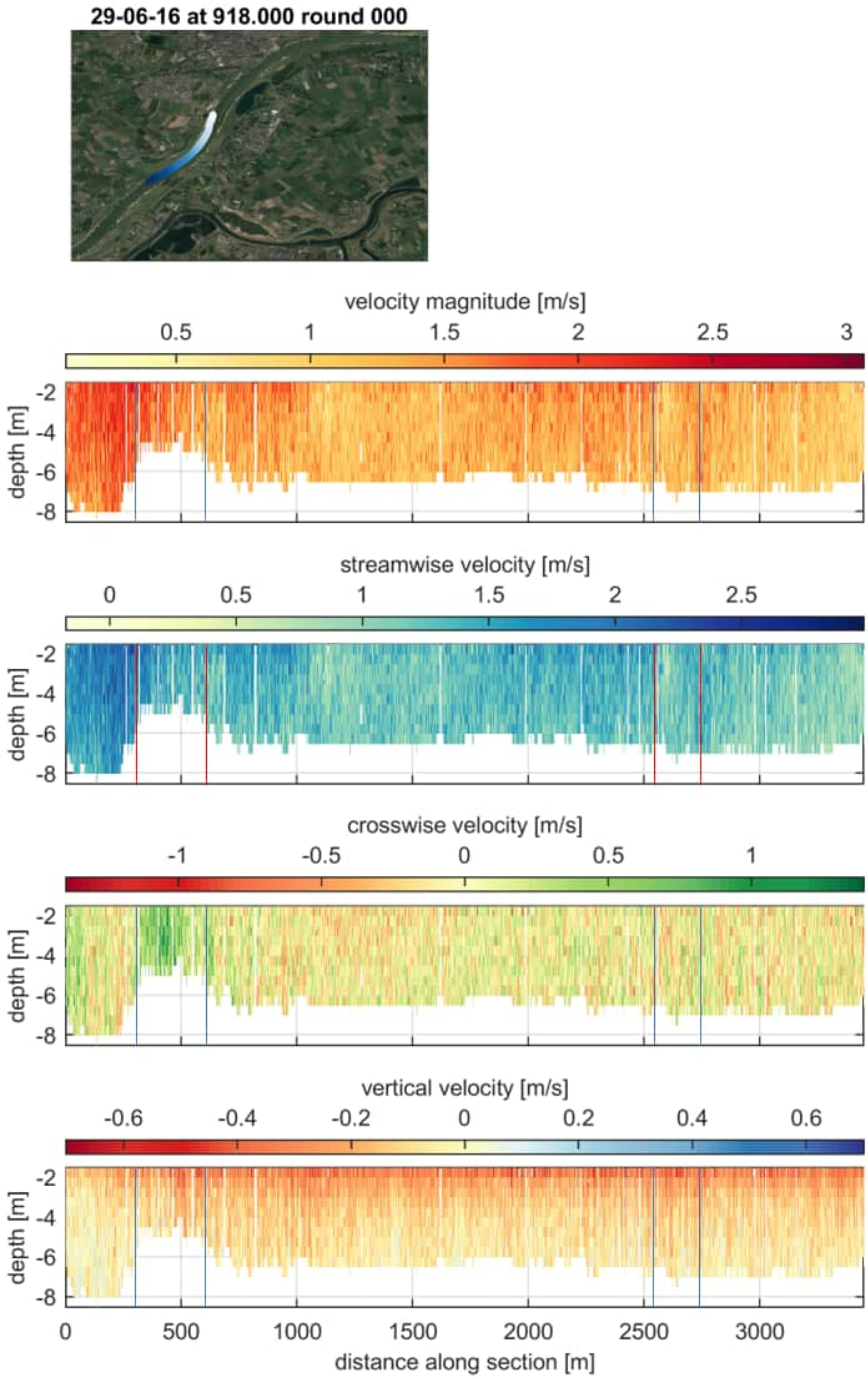

Figure 3.22 Velocity along a longitudinal profile. Positive cross-wise direction directed to the right bank. Vertical lines mark the inlet (at 500 m) and intermediate opening (at 2600 m) of the longitudinal training wall.

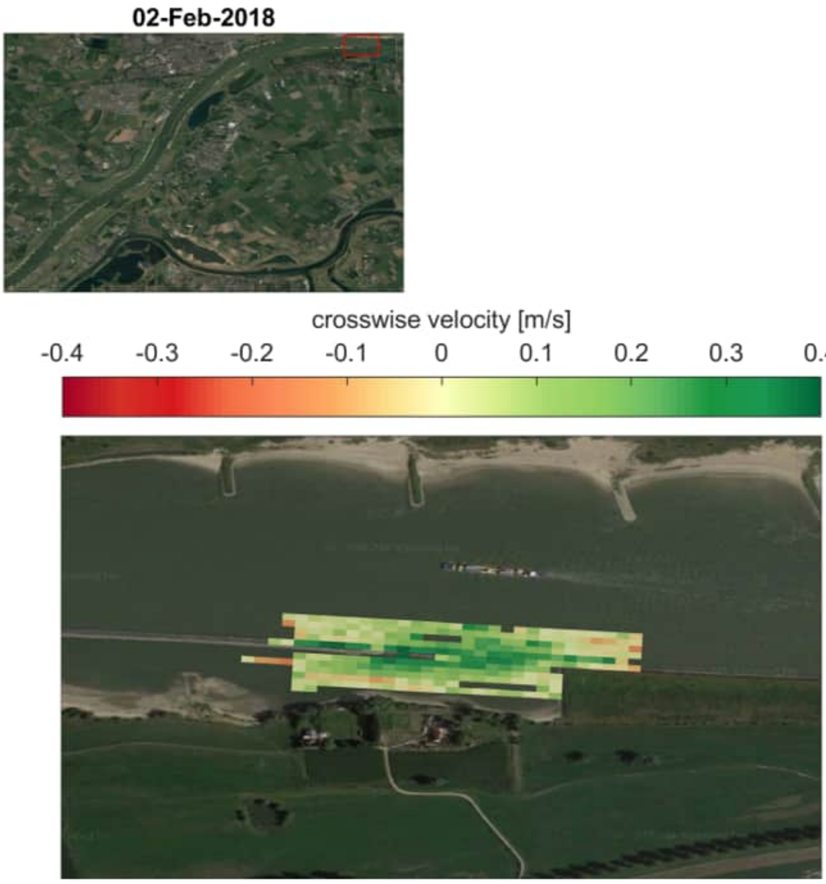

Figure 3.23 Depth-averaged velocity field considering the full water column on 02-02-18.

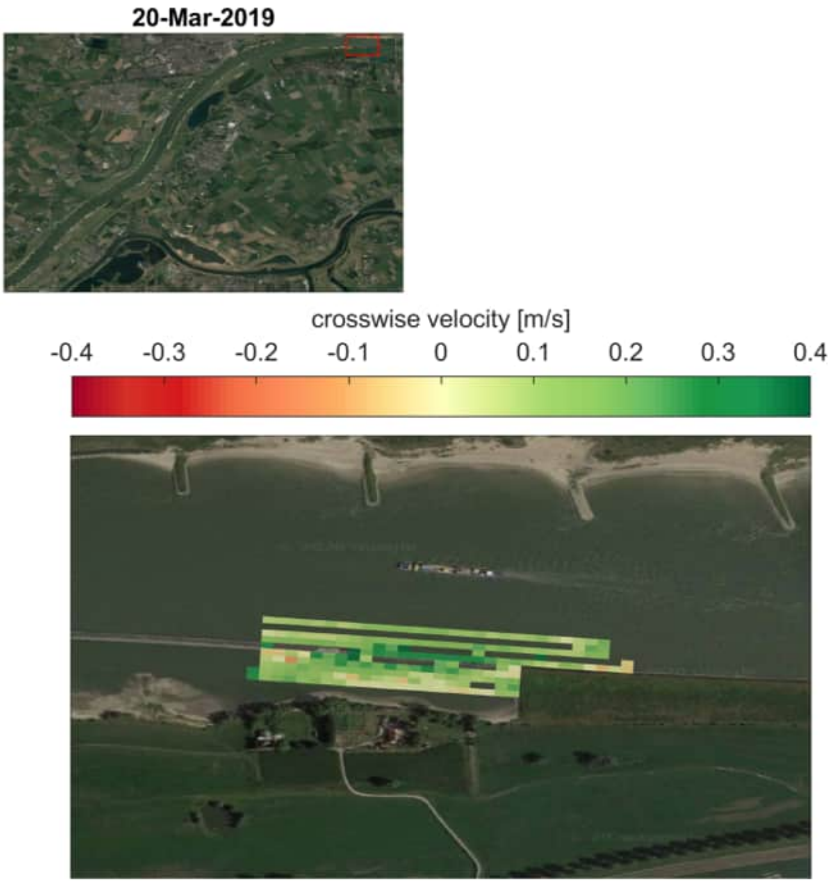

Figure 3.24 Depth-averaged velocity field considering the full water column on 20-03-19.

3.4.2 Discussion of the results of the analysis of the transverse velocity near inlets and recommendations

The depth-averaged flow fields reproduced in the results show the expected general patterns. They capture the flow in the main and auxiliary channel as well as the change in direction at the inlet and even eddies. The results show that inlets have no significant effect in the transverse velocity in the navigational fairway. At the inlet, the maximum transverse velocity is around 0.5 m/s.

Nevertheless, it relevant to mention that the same limitations discussed in Section 3.3.3.2 apply to this case. Namely, data seems to well capture the velocity in the main flow direction but not the flow subtleties in the vertical direction. Similarly, less data in time but under the same flow condition is more useful than more data in time under different flow conditions.

We recommend to *a priori* set certain water levels at Tiel spanning the whole range of relevant water discharges at which measurements will be taken. In this way, a detail study of the effect of modifying the inlet shape is possible. Furthermore, if the question to be answered is the main channel transverse velocity, the most useful measurement is obtained by fixing the ADCP (i.e., the boat) in the main channel at a fixed position for a long enough time (order of minutes). This allows filtering of turbulence, ship waves, and all other disturbances affecting the results.

3.4.3 Conclusions and recommendations

From the ADCP measurements the following is concluded:

- From ADCP measurements the change in velocity is analysed. For a discharge at Lobith of 922 m^3/s, an increase in flow velocity in the order of 10% is observed. An increase in flow velocity was expected as flow is concentrated in the main channel thanks to the longitudinal training walls. For a discharge at Lobith equal to 3436 m^3/s, 4170 m^3/s, and 5087 m^3/s, a decrease in flow velocity was observed of approximately 15%, 5% and 2%, respectively. For these discharges the longitudinal training walls are fully submerged making the flow width wider than the situation prior to construction of the LTW.
- Based on a simple estimate based on Engelund and Hansen (1967) related to the average velocity before and after the construction of the longitudinal training walls, it is estimated that a low discharges the sediment transport is reduced by 40 % and at high discharges the sediment transport is reduced by roughly 5 %.
- A discharge through the auxiliary channel of less than 12 % is expected to be succesful in raising the water levels in the main channel. At Wamel, only the situation after raising the inlet is evaluated, after which the discharge is smaller than 12 % for all discharges smaller than 2500 m^3/s. At Dreumel, this only goes for discharges below 1250 m^3/s. At Ophemert, this never occurs. For more set-up in the main channel the discharge through the auxiliary channel should be reduced.
- Near the inlets, the transverse velocity is in general above 0.3 m/s, but below 1 m/s. Nevertheless, the area in which the velocity is larger than 0.3 m/s is relatively small.

4 Bed level

4.1 Introduction

This chapter discusses the data analysis based on multibeam measurements of the bed level. In this chapter the following research questions are considered.

1 How is the bed level and the bed level trend related to the overall degradation, influenced by the construction of the longitudinal training walls?
2 What is the effect of changes to the inlets?
3 How does the bed level develop in the auxiliary channels?
4 What is the influence of the longitudinal training walls on the navigation depth and width?

4.2 Available data

Before starting on the data analysis, first an overview is given of the available data, which will be described in further detail in the subsequent sections.

- Yearly multibeam measurements for the bed level
- Eight-weekly measurement campaigns from 2015 week 42 until 2020 week 26 covering the full with of the main channel
- Reference plane OLR of 2012
- Polygons for reach and hectometres, delineating different sections of river.
- P-map scripts for post-processing the bed levels from the multibeam and the eight-weekly measurement campaigns
- Auxiliary channel zones

4.2.1 Yearly multibeam measurements 2000-2017

Rijkswaterstaat kindly provided us with multbeam measurements.

The data is processed using the P-map method. The averaging polygons used are shown in Figure 4.4 in purple. These are the polygons before construction of the longitudinal training walls. The data was provided per year, the month of the measurement was estimated from the date of the last measurement done for that year (cf. Figure 4.1).

4.2.2 8 weekly multibeam measurements

In addition *Rijkswaterstaat* provided multibeam measurements from the period after 2015 week 42 until 2020 week 26 for the region at the longitudinal training walls both inside the navigation channel and in the auxiliary channels (see Figure 4.2). This data was provided in many different formats, with the vertical reference in either centimetres, decimetres or metres, the reference direction as positive up or down depending on the date of the measurement, and the data was stored in integer or float. Fortunately, all the data appeared to be consistent with the reference level NAP (Normaal Amsterdams peil). The horizontal resolution is 1 m.

4.2.3 P-map procedure

The procedure (Kater, 2014) to compute the bed level trends was also shared with us. The procedure consists of Arcgis python® scripts which combine subsequent multibeam data and obtain the average, minimum and maximum for each of the polygons as described in Section 4.2.5.

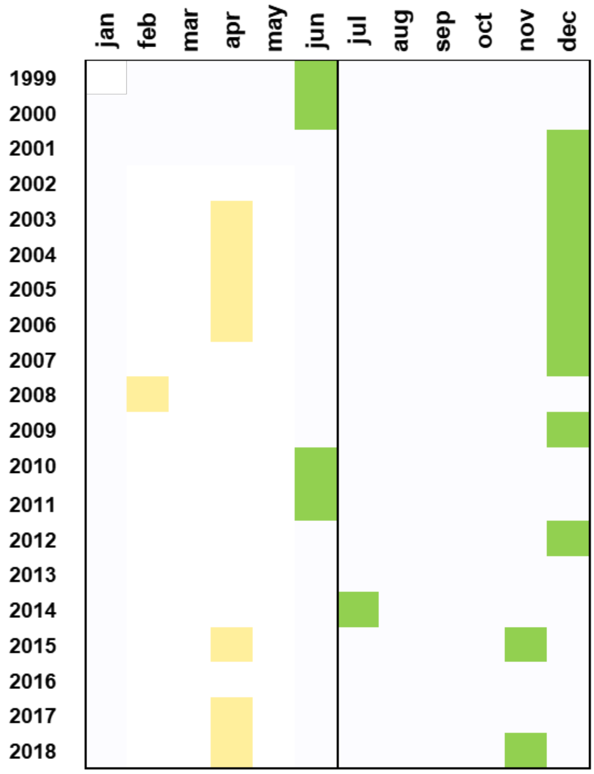

Figure 4.1 Overview of the provided yearly multibeam measurements. Sometimes multiple measurements are done in a year, but the month of the measurement is said to be the last measurement of the year (green, not the yellow).

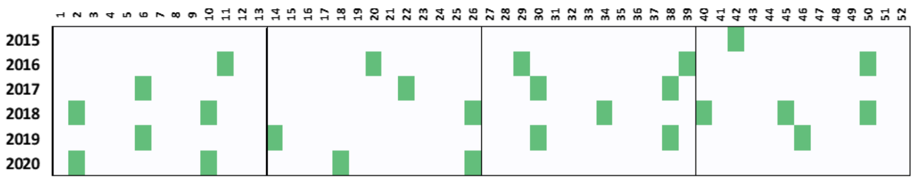

Figure 4.2 Overview of the provided 8 weekly measurements. The horizontal axis shows week numbers.

4.2.4 Reference plane OLR

OLR is the agreed upon low river reference level (in Dutch: Overeengekomen lage rivierstand) and this was provided to us by *Rijkswaterstaat* . For the Rhine branches the associated discharge is referred to as OLA (In Dutch: Overeengekomen lage afvoer), and its magnitude is 1020 m^3/s.

4.2.5 Channel widths and analysis polygons

Many definitions exist for the defining the width of the river or fairway on the river. In WP7 (Van der Wijk and Van der Mark, 2021) these definition have been written down carefully and sketched. As these widths are used for the analyses of the bed level, the sketch is included in Figure 4.3 and the definitions as used in this report are given below in Table 4.6. The location of the navigation channel has been adjusted since the construction of the longitudinal training walls, and only this new definition has been used throughout this research.

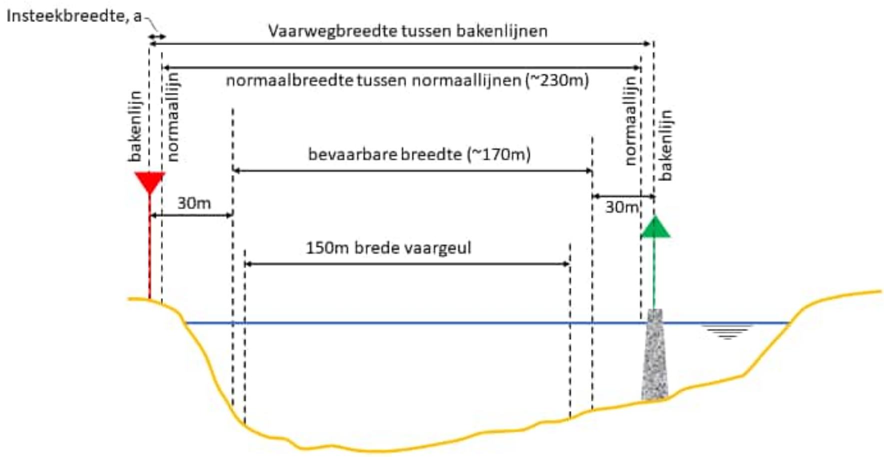

Figure 4.3 Definitions of widths of river and fairway. For more information see (Van der Wijk and Van der Mark, 2021).

Table 4.6 Definitions of widths of river and fairway For more information see (Van der Wijk and Van der Mark, 2021).

Definition (NL)	Definition (EN)	Description
'vaargeul'	navigation channel	Formal width of the fairway that is being maintained at a depth of 2.8 m (at OLA-discharge). It is following the deeper sections of the river. This width is 150 m for the middle and upper Waal.
'bevaarbare breedte'	navigable width	The part of the river that is located between 30 m from fixed beacons and 5 m from floating beacons. For this part of the river the MGD is registered. At the LTW this width is 170 m. In this bed level analyses it is agreed with RWS to design this polygon by applying a 10 m buffer to both sides of the navigation channel.
'zomerbed secties'	main channel section	Polygons defined by *Rijkswaterstaat* for the analyses of bed level effects. These are defined as the Normal Width minus 15 m on both sides. At the LTW this has a width of 200 m
Normaalbreedte	Normal width	Width between the 'normaallijnen', which on the Waal approximately follow the beacons. Upstream of the LTW this has a width of 260 m, which reduces to 230 m just after the inlet at Wamel and remains this width for the remainder of the LTW.

The auxiliary channel zones indicate the locations in the auxiliary channel near the main channel and near the river bank. These polygons are also split into 100 m sections. An example of these zones can be seen in Figure 4.4. They correspond to the sections Br, Bl, Cr and Cl in the figure in the same section. B refers to the near channel zone, while C refers to the near bank zone. The small letters l and r refers to left and right bank, respectively.

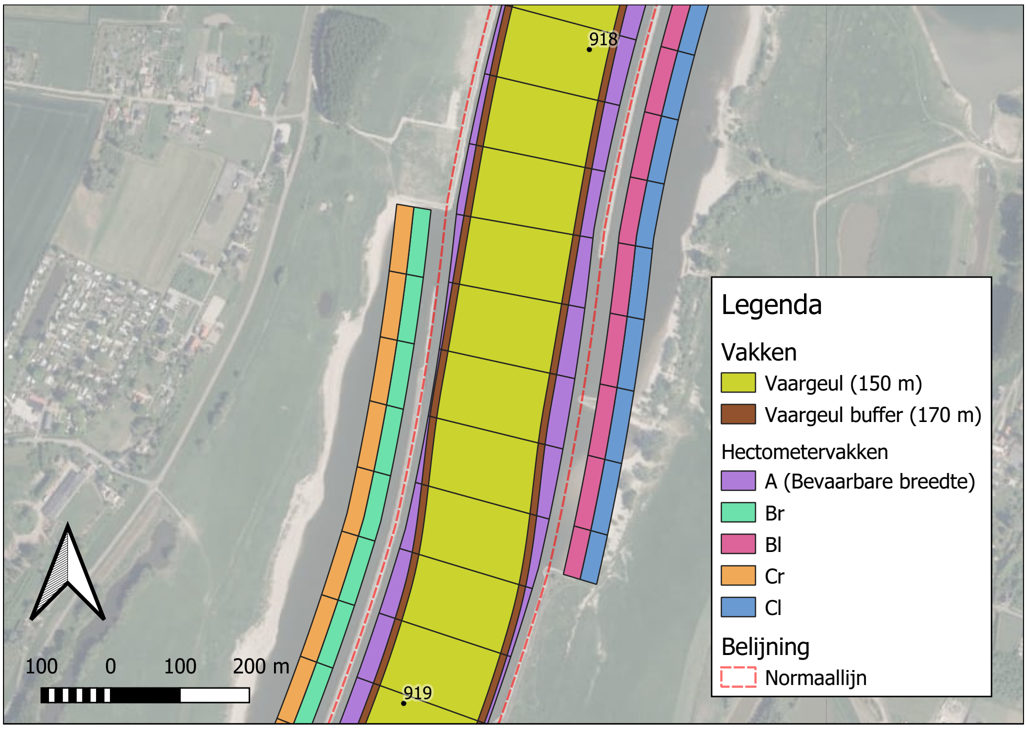

Figure 4.4 Averaging areas for the bed level 'zomerbed secties'. Note: the definition 'Bevaarbare breedte' was later in this study changed to 'zomerbed secties' (main channel section)

4.3 Methodology

The following steps are followed in this analysis of the bed levels:

- Data clean-up
- P-map analysis
- Processing and plotting based on available scripts (Chavarrías and Ottevanger, 2019)
- Additional scripts for computation of percentile of OLR - 2.8 m
- Sharing of cleaned data and scripts

For the provided multibeam data, each of these files had to be inspected manually to confirm the correctness, and be transformed to the form which could be used in combination with the P-map procedure. There was no meta-data available to describe how the data was stored. All the data was transformed to centimetres w.r.t. NAP, vertical positive up, and stored as an integer with a horizontal resolution of 1 m. The data was stored as an ESRI grid file.

The OLR data was also transformed into centimetres, positive up w.r.t. NAP. After this, rasters were computed of the difference OLR minus multibeam bed level. An example of this is shown in Figure 4.5.

Next the P-map approach was applied to the bed level measurements and the depths w.r.t. OLR for the navigation channel, navigable width and main channel section and different reach polygons shown in in Section E.1. For all analyses the location of the channels after construction of the LTW was used.

In addition, extra analysis was developed for determining the standard deviation and the percentile at which the depth is equal to 2.8 m w.r.t. OLR.

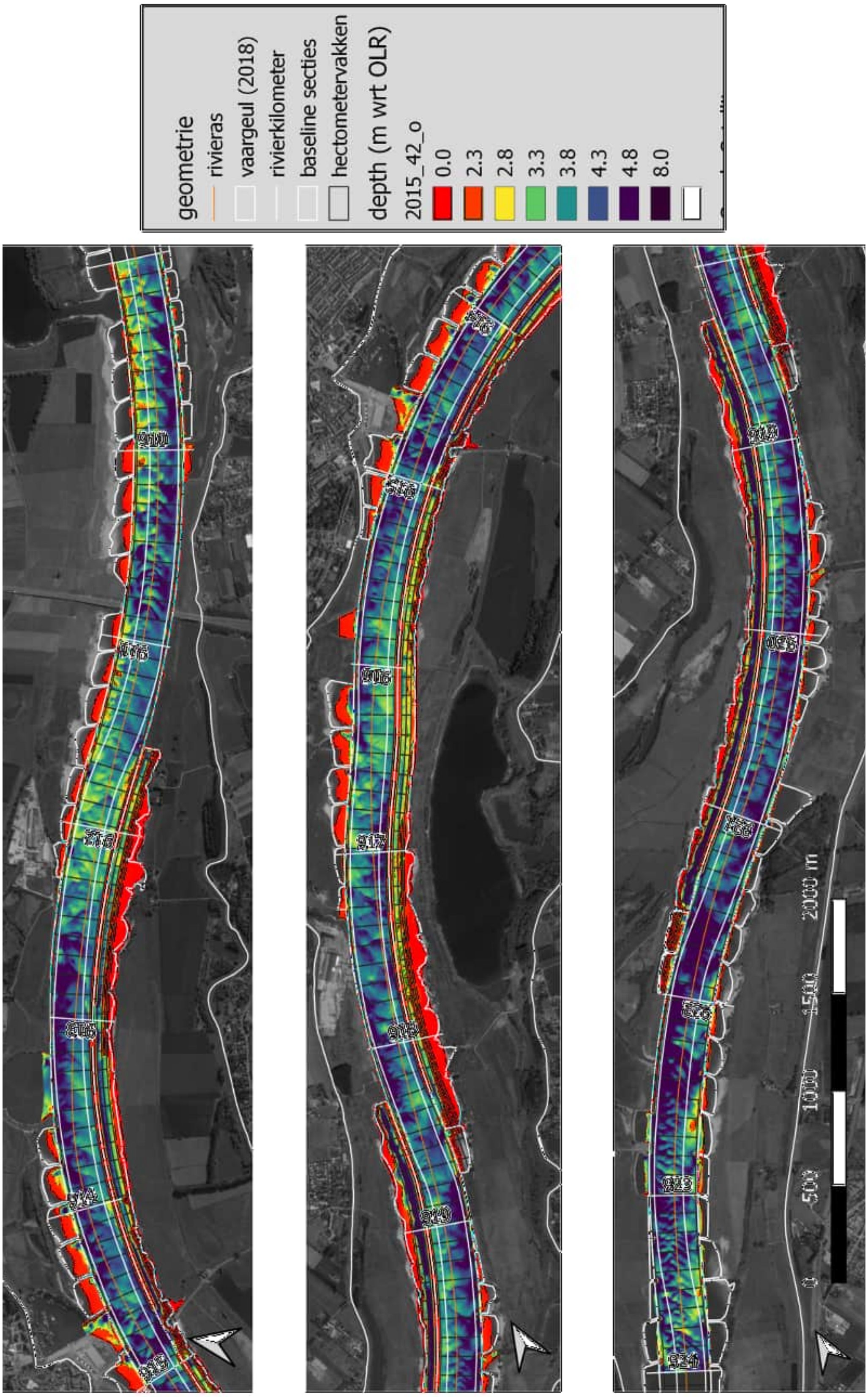

Figure 4.5 Depth w.r.t. OLR in 2015 week 42.

4.4 Results

4.4.1 Main channel development

Firstly, the P-map approach was applied to larger sections. The large scale polygons for which the analysis was done are shown in Appendix E.1. These data have been simplified to reaches upstream, downstream and at the three different auxiliary channels of Wamel, Dreumel and Ophemert (cf. Table 4.7).

location	river kilometre	
	start	end
Langsdam hoofdgeul Upstream	909.000	911.755
Langsdam hoofdgeul Wamel	911.755	914.750
Langsdam hoofdgeul Dreumel	914.750	918.450
Langsdam hoofdgeul Ophemert	918.480	921.550
Langsdam hoofdgeul Downstream	921.550	922.500

Table 4.7 Locations for averaging of the P-map results.

Figure 4.6 shows the P-map data for the sections as presented in Table 4.7.

Based on the yearly multibeam measurements, the Upstream, Wamel, Dreumel seem to have average bed levels which are stable over time until 2010. Wamel shows a slight degrading trend.

From 2015 to 2017 (or 2018) the bed levels, at Wamel, Ophemert and downstream the bed seems to be eroding. The construction of the longitudinal training walls took place from August 2014 until November 2015 (see appendix A.2), which implies that some of these changes happened during the construction phase. Based on the situation after construction, it appears that at the upstream and at Dreumel the bed level remains stable, while Wamel shows a bit of sedimentation until 2018. At Ophemert there appears to be sedimentation after 2018 and downstream the bed initially shows erosion and some sedimentation in the last two years (2019, 2020), but is still developing. This is apparent from the main channel average developments at Wamel, Ophemert and Downstream. A similar analysis for alternative reaches (for example the entire reach) is included in appendix E.3. In appendix E.2 a discussion to the findings of Czapiga *et al.* (2021) is included.

	1999-2015	**2015 – 2017**	**2017 -2019**	**2019-2020**
Upstream (909.0-911.8)	Minor degradation 7 mm/yr	Stable	Small degradation	Stable
Wamel (911.8-914.8)	Minor degradation 7 mm/yr	Degradation	Stable	Degradation
Dreumel (914.8-918.5)	Minor degradation 2 mm/yr	Stable	Stable	Stable
Ophemert (918.5-921.5)	Aggradation 5 mm/yr	Degradation/Stable	Aggradation	Stable
Downstream (921.5-922.5)	Aggradation 9 mm/yr	Lowering	Degradation	Aggradation

Table 4.8 Observed bed-level trends per section.

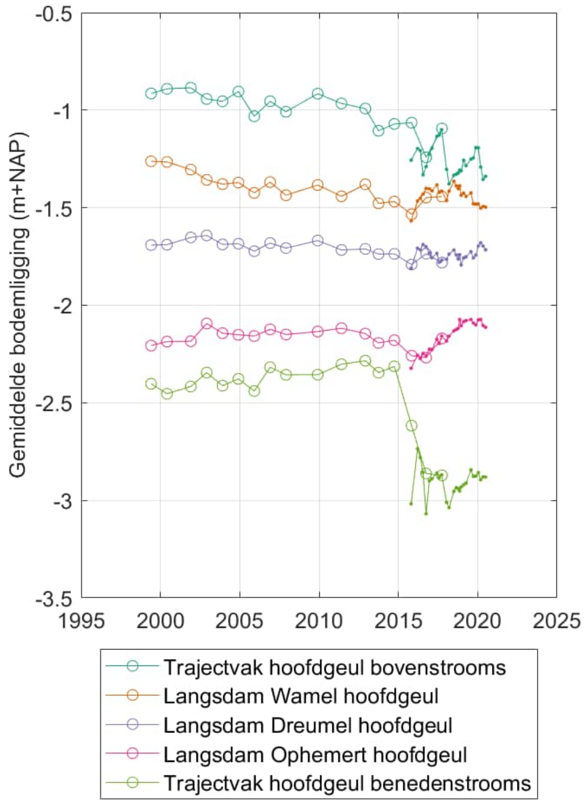

Figure 4.6 The average over different reaches of the P-map *average* bed level.

The minimum bed levels per for the sections in Table 4.7 as computed through the P-map analysis is shown in Figure 4.7. At the auxiliary channel locations the minimum bed level seems to increase slightly since the construction of the longitudinal training walls.

The maximum bed levels per section as computed through the P-map analysis is shown in Figure 4.8. It appears that the maximum bed level remains rather constant over time.

The standard deviations of the bed levels per section as computed through the updated P-map analysis is shown in Figure 4.9. It appears that the standard deviation is larger after construction than in the period 2005-2015. It is not clear if the yearly multibeam measurements are based on the situation after maintenance dredging, and whether the same holds for the 8 weekly measurements. This can possibly be refined by comparing with maintenance records (as visualised by Chavarrías *et al.* (2021)).

The standard deviation of the P-map approach is used to act as a proxy for the height of the bed forms, or at least indicative of it. From the analyses in figure 4.9 it shows that for the new data set the standard deviation follows the river discharge (cf. Figure 3.3). This is confirming the knowledge that at (and after) higher discharges higher bed forms appear (as expected). For the old data set the temporal resolution is lower, thence not showing the effects of individual discharge wave. The data since 2015 appear to show a larger standard deviation. It is not clear if this larger value is solely the effect of the moment in time at which was measured.

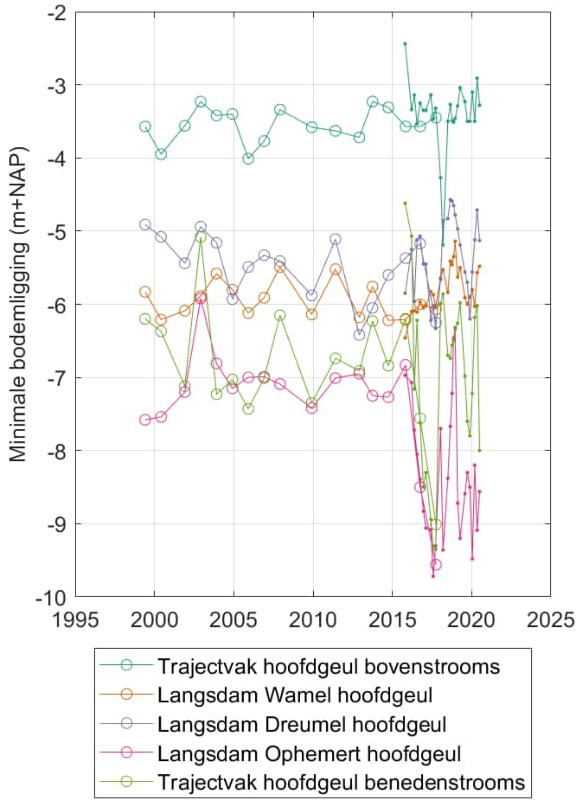

Figure 4.7 The average over different reaches of the P-map *minimum* bed level.

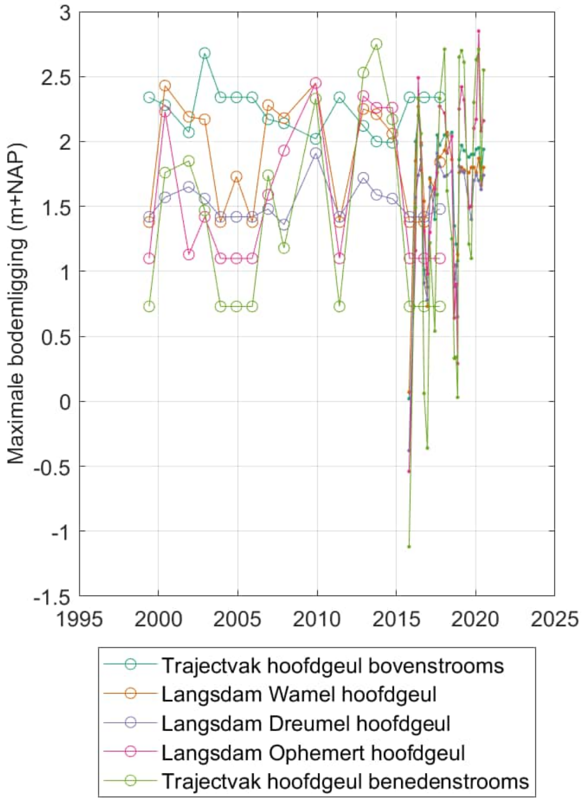

Figure 4.8 The average over different reaches of the P-map *maximum* bed level.

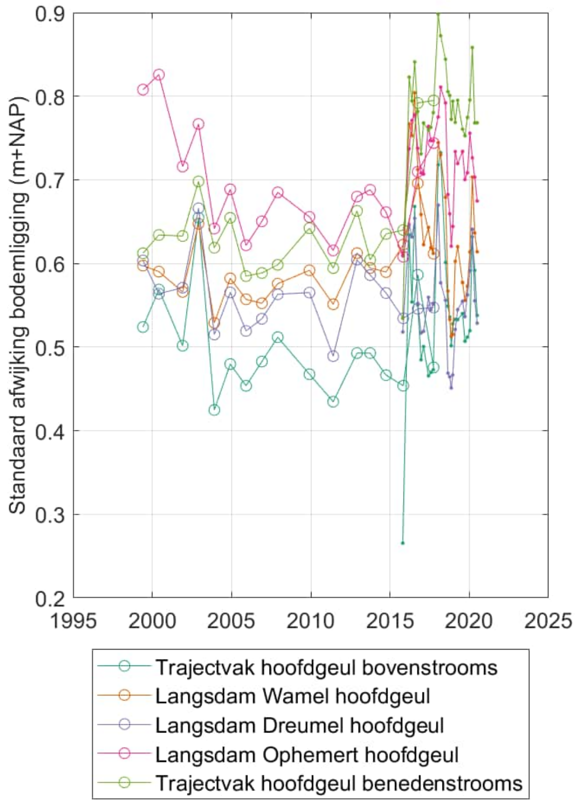

Figure 4.9 The average over different reaches of the P-map standard deviation of the bed level.

Finally, the trend is plotted per rkm for the eight-weekly measurements (cf. Figure 4.10). This figure contains a lot of variation probably caused for the most part by the seasonality. To remove this effect the bed level measurements have been spatially averaged over a length of 500 m, and plotted for the 8 weekly measurements only. The result of this action can be found in Figure 4.11. The relative bed level development is given in figure 4.12.

The figures shows a degrading trend upstream of Wamel. At the reach of Wamel, degradation in the upstream reach and sedimentation in the lower reach is visible. A similar trend can be seen at Dreumel with strong sedimentation up till the first opening along the LTW, from which point erosion is shown. The sedimentation in the Dreumel section coincides with the side channel Passewaaij on the right bank (see also figure 1.5). This side channel has been opened for permanent flow in 2015, so it adds to the sedimentation you see between 916.3 (entrance of the side channel) and 917.3 (exit).

At Ophemert the overall stretch seems to be agrading to about 0.3m on average higher than at the start of the 8 weekly measurements. Downstream of the last dam (Ophemert), an erosion wave appears to be progressing. It is interesting to see that exactly at the outflow of the Ophemert auxiliary channel (rkm 921.3) the bed level is showing some recovery by local sedimentation until 2018.

Upstream of the first intermediate opening of Ophemert a strong degradation is seen initially, similar but stronger than the other LTW, possibly caused by the larger discharge in Ophemert's auxiliary channel (see also Sieben (2020)).

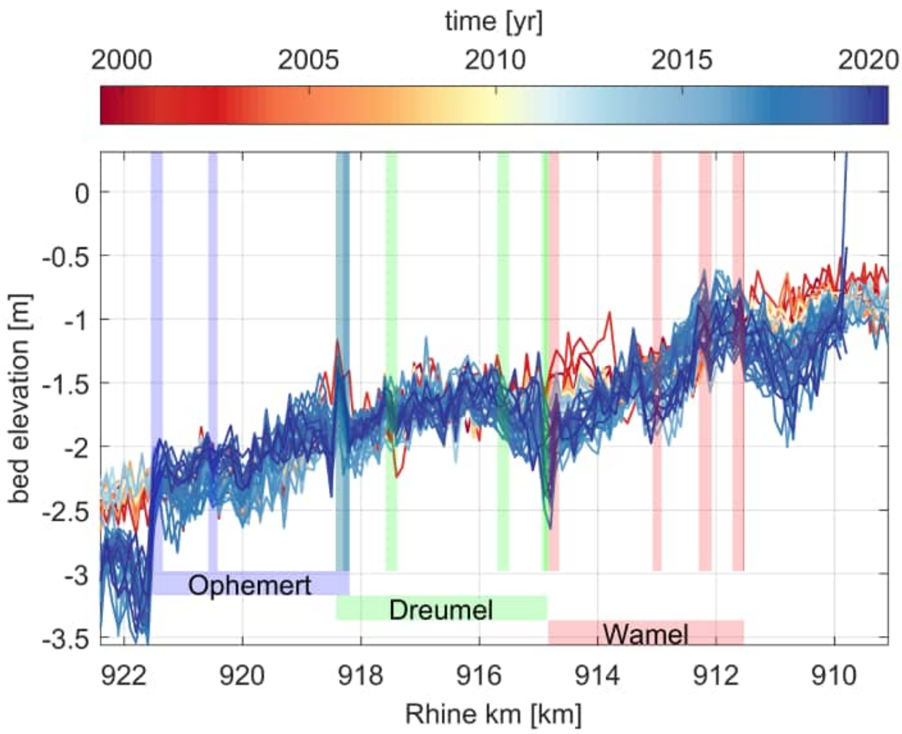

Figure 4.10 Average bed level development based on P-map analysis.

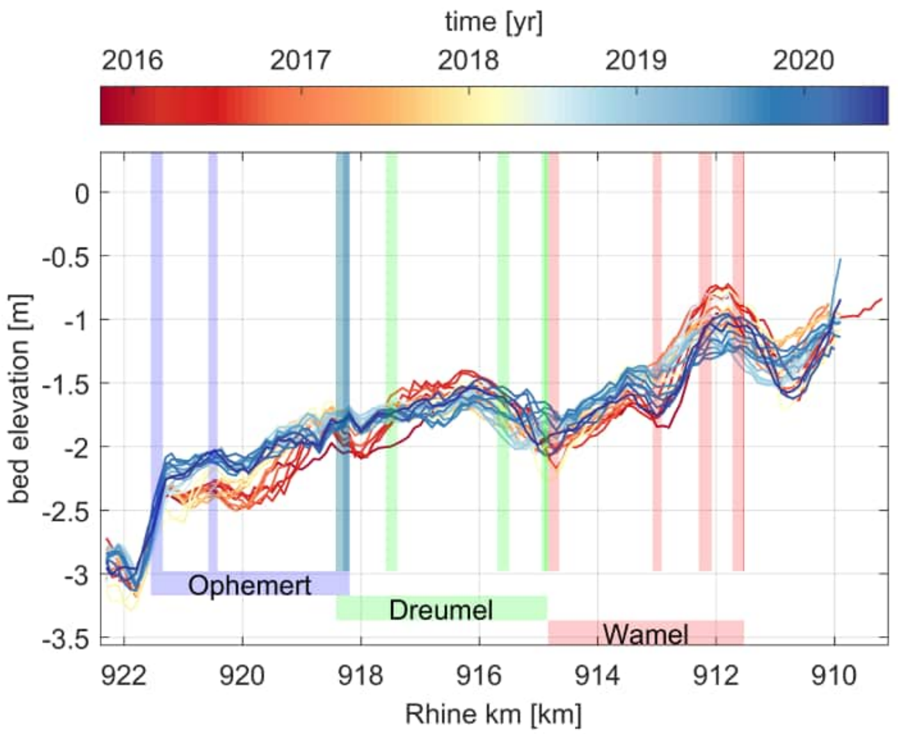

Figure 4.11 Average bed level development based on P-map analysis (averaged over 250 m upstream and downstream) from 2015 week 42

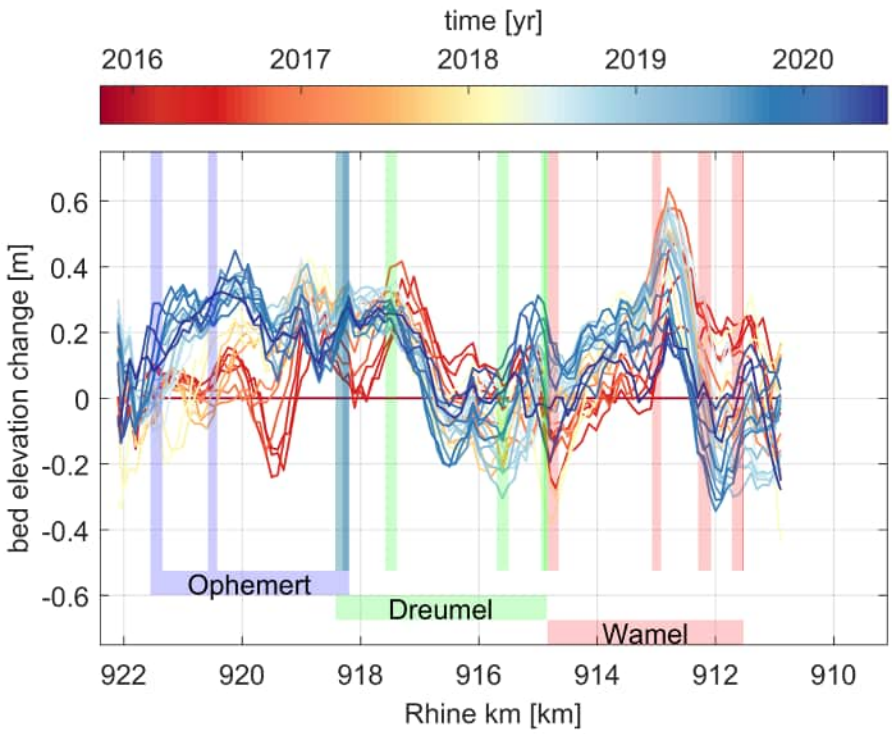

Figure 4.12 Average bed level development based on P-map analysis (averaged over 250 m upstream and downstream) relative to 2015 week 42

4.4.2 Effect of the change in inlets on the bed level trends in the main channel

We have tried to see the impact of the level of the inlets of the auxiliary channels to the bed level trends. The inlets of Wamel and Dreumel had a large adaptation in April 2018. At Ophemert the change was only done after April 2019, and at Dreumel a slight adaptation occurred in April 2019. Dimensions of the adaptations are given in appendix A.2.

To be able to use the data we look at trends between 2015 and April 2018, and after after April 2018 until 2020 week 26. The results of this analysis are shown in Figure 4.13 up till 2018, and in Figure 4.14 after 2018. As we do not have measurements of the sediment transport or its distribution between main and auxiliary channel, we look at the development of the average main channel bed level instead. As a word of caution, bed level changes in the main channel do not necessarily equate to differences in sediment entering the auxiliary channel.

At Wamel, a sedimentation wave develops after construction of the longitudinal training walls. In addition, erosion develops at the upstream region of Dreumel. From river kilometre 916 sedimentation occurs, reaching a maximum at the outflow of Dreumel and the inflow of Ophemert, which are located on opposite sides of the river. Further downstream towards the outflow of Ophemert, erosion is visible. As mentioned earlier, this might be related to the opening of the side channel at Passewaaij at the right bank.

After the update of the sill in April 2018, the behaviour in the main channel changes. At Wamel, the sediment transport is directed in the direction of the main channel, thereby reducing the sedimentation which took place up till April 2018. Interesting to mention is that it is possible that the observed change in trend after modification of the inlet is a coincidence. The bed level data shows degradation upstream of Wamel in week 2 of 2018 at rkm 910-911 which is possibly due to dredging. This trench propagates in downstream direction, and its location coincides with the location of the inlet. The erosion at the downstream end of Wamel gets filled up again after April 2018.

The bed level in the reach of Dreumel does not change much over time. Just downstream of the last intermediate opening of Dreumel (rkm 917.5), erosion occurs. Possibly, some maintenance dredging has taken place here. For the Ophemert reach, the upstream part does not change, and sedimentation occurs at the intermediate opening and the outlet (rkm 920.5 and rkm 922).

Although the trends appear to point in the direction that the raising of the sills indeed have an effect on the main channel bed levels, we remind the reader that only two years have passed since the construction. This implies that, the inherent variability of the river may also explain the changes which are observed. Furthermore, we have not considered effects of possible maintenance dredging in the evolution of the bed.

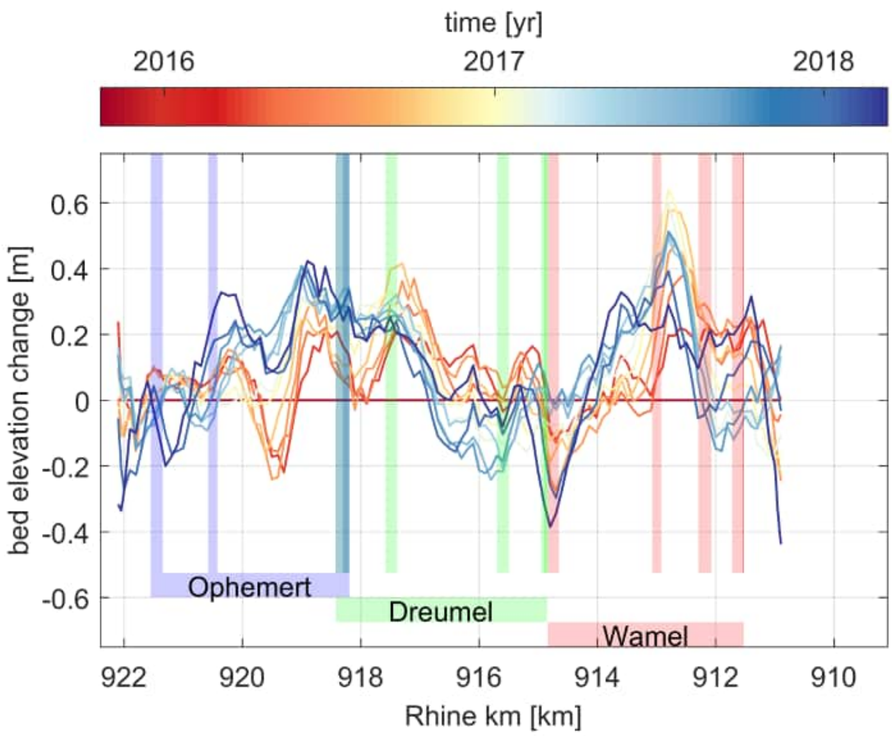

Figure 4.13 Bed level development (averaged over 250 m upstream and downstream) *before* adjustment of sill in April 2018. Bed level change relative to 2015 week 42.

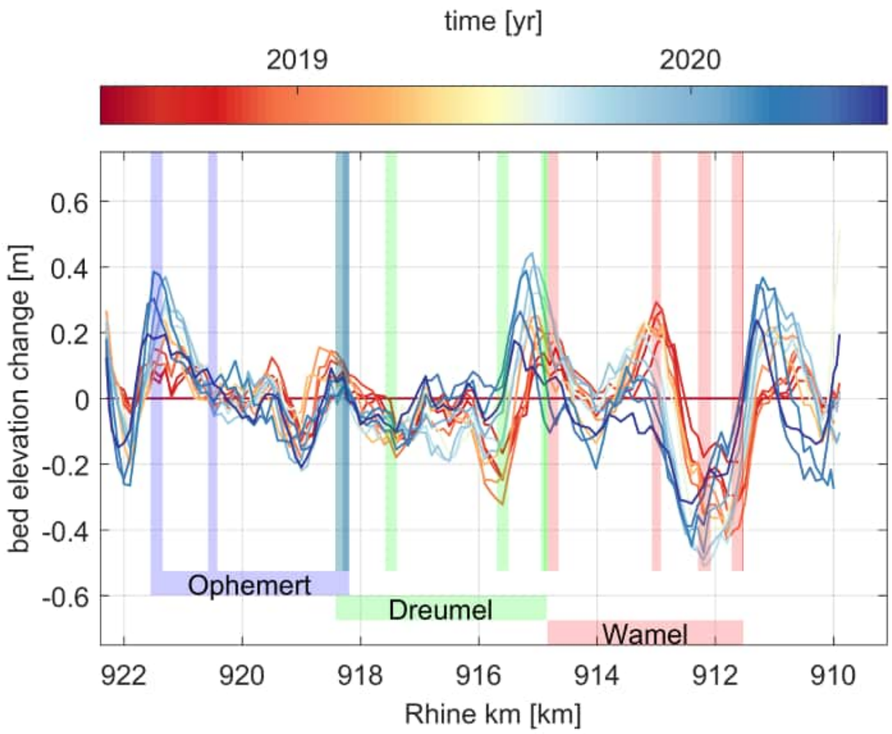

Figure 4.14 Bed level development (averaged over 250 m upstream and downstream) *after* adjustment of sill in April 2018. Bed level change relative to April2018.

4.4.3 Auxiliary channel development

De Ruijsscher *et al.* (2019, 2020) studied the effect of the inlet sill on the bed morphodynamics. Based on his flume experiments he developed a schematic overview of the sedimentation and erosion patterns in the auxiliary channel shown in Figure 4.15. Interestingly, he also mentions that remains of the former groynes in the region may limit erosive processes in the auxiliary channel and stabilize the bank. It is not clear if the wake causing the sedimentation at I really occured in the field, as the off-take is at a very small angle and will cause only little flow separation.

The development of the auxiliary channels Wamel and Dreumel is shown in Figure 4.16. This shows that although the main channel shows changes in the order of 0.5 m, the changes in the auxiliary channel can be much larger.

At the Wamel inlet the divergence bar (II in figure 4.15) is not visible, but the sedimentation pattern just downstream of the inlet is. From figure 4.16 it shows that the sedimentation (line BI) has a length scale of approximately 1 km and is thereby considerably larger than a possible wake (mentioned as I in figure 4.15). The erosion pit does not show (line CI; III in figure 4.15), but caution is advised using the C line as there is very little measured data initially 2015 week 42 (cf. Appendix E.4).

The raising of the inlet in April 2018, does seemingly not lead to large changes in the auxiliary channel. A slight increase in the erosion and sedimentation can be seen. Further details of the Wamel inlet can be found in Section E.6. Further downstream in the Wamel auxiliary channel, there is a large sedimentation, which seems to increase after the raising of the Wamel inlet sill in April 2018. This is probably caused by the decrease in sediment-transport capacity and the ongoing bank erosion.

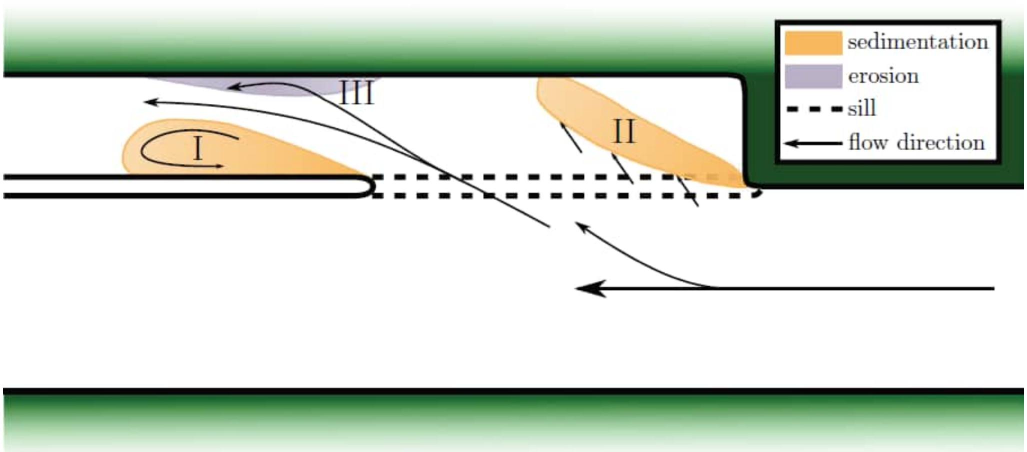

Figure 4.15 Schematic overview of the bed morphology at the bifurcation, highlighting (I) the inner-bend depositional bar caused by flow separation, (II) the divergence bar, induced by widening of the river at the auxiliary channel entrance and an increasing flow depth just behind the inlet, and (III) an erosion pit along the auxiliary channel bank, which might result from the solid flume wall. (From De Ruijsscher *et al.* (2019))

At Dreumel, the patterns at the inlet, are less pronounced than at Wamel. This is probably caused in part by the inlet location at the inner bend of the river, the fact that is more gradually departing from the main channel than the Wamel inlet, and it is close to the outlet of the Wamel auxiliary channel (see also Section E.7). According to Sieben (2020) the discharge into the auxiliary channel at Dreumel is similar to that at Wamel prior to the adaptation in April 2018 (after the adaptations the discharge in the auxiliary channel Wamel is greatly reduced). The Dreumel auxiliary channel can be considered as more or less a continuation of the Wamel channel, only partially separated by the 'veerstoep' (ferry landing) of Wamel. The feed into Dreumel is for a large part directly the outflow from Wamel channel with relative low sediment loads, although there is some limited exchange and attraction of the water from the main channel with sediment. That water is running around the Veerstoep is also causing a deep scour hole in front of the Veerstoep as seen in the figure E.38. It has not been measured how these processes work out at the entrance.

The development of the auxiliary channel at Ophemert is shown in Figure 4.17. Here strong sedimentation is found just downstream of the inlet. This side channel has the lowest sill level which was not adapted until the narrowing in April 2019. The bed in the side channel appears to be stable. The erosion and the sedimentation compared to the measurement of 2015, week 42 shows strong adjustment midway and at the end of the auxiliary channel.

The figures for the detailed development in the auxiliary channels can be found in the appendix from figure E.24 to E.27.

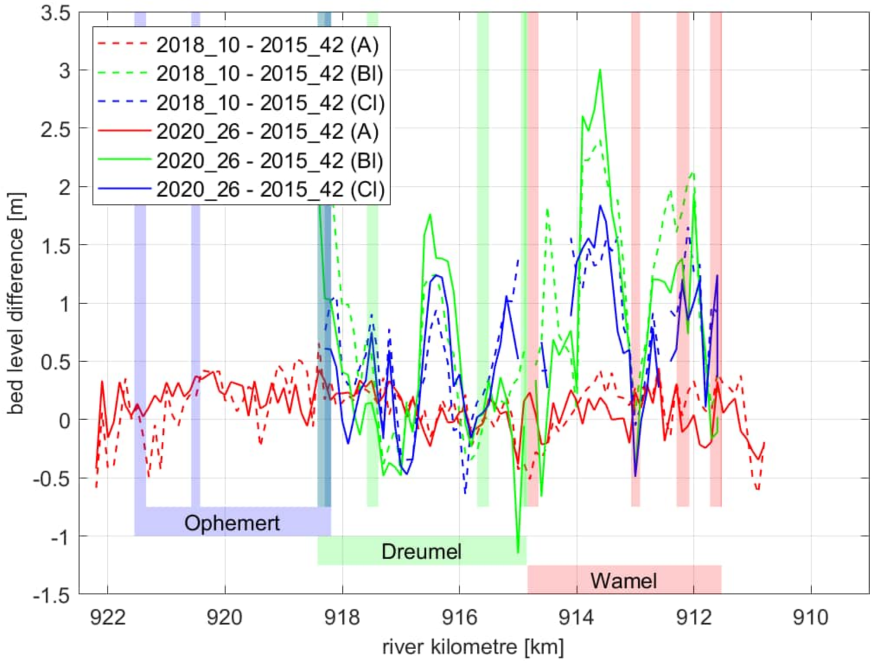

Figure 4.16 Development of the bed level in the auxiliary channels at Wamel and Dreumel. The lines indicate: A the main channel, Bl the left auxiliary channel zone, and Cl the left auxiliary channel bank zone (see 4.2.5).

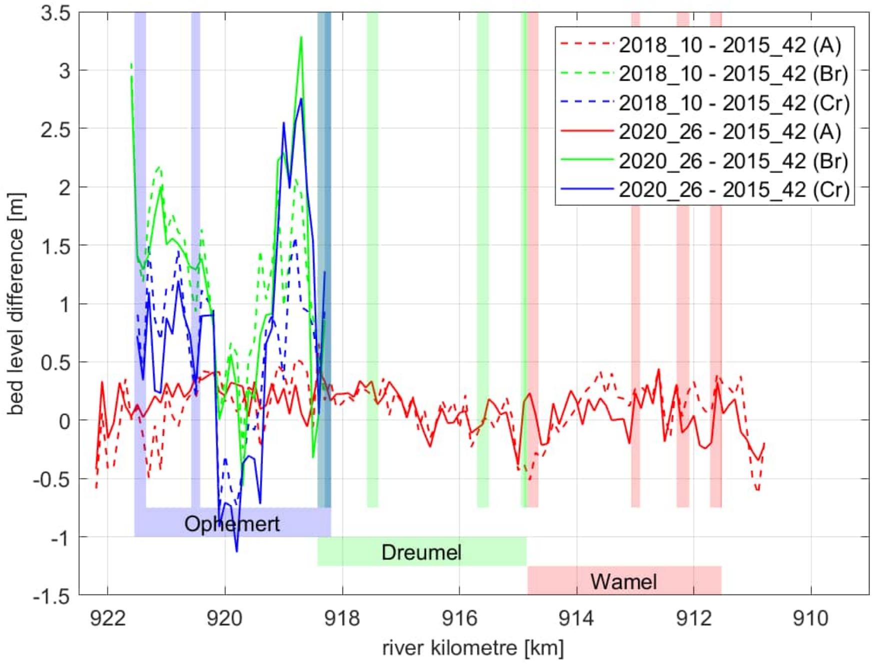

Figure 4.17 Development of the bed level in the auxiliary channel at Ophemert. The lines indicate: A the main channel, Bl the right auxiliary channel zone, and Cl the right auxiliary channel bank zone (see 4.2.5).

4.4.4 Bank erosion in the auxiliary channels

LiDAR measurements of the bank area have been taken on a yearly basis. These data have been combined by Flores *et al.* (2021) with multibeam echosounder data of the auxiliary channels to obtain a complete picture of the dynamics of shore with the objective of calculating net aggradation and degradation in the side channel.

It is observed that at the banks there is net degradation while close to the longitudinal training walls there is net aggradation. This seems to indicate bank erosion on one side and aggradation of the recreational navigational channel of the auxiliary channel on the other side. The bank lines in the bank area's that showed erosion were manually digitized. For Wamel this section has a length of 547 m and for Dreumel a length of 792 m. The yearly retreat of the bank line between 2014 and 2019 at Wamel and Dreumel oscillates between 0.1 m/year and 3.2 m/year with an average of 1.2 m/year at Wamel and 2.0 m/year at Dreumel (see also 4.18). No number for Ophemert is given. The rate of erosion decreases with time, which indicates stabilization.

Flores finds that the net reduction of volume in Dreumel bank zones is in the order of 156 000 m^3, or 4400 m^3 per 100 m. A rough estimate considering an average bank retreat of 1.2 m/year during 5 years and 4 m high bank equals 2400 m^3 per 100 m. Considering a width of the auxiliary channel of 90 m, the measured loss of sediment from the bank would equal 48 cm of homogeneous aggradation in the auxiliary channel, while it appears the recreational channels within the auxiliary channel have aggraded. These rough estimates provide evidence that the net loss of sediment in the side channels comes from bank erosion and not the recreational channels itself, which seem to aggrade.

It is relevant to take into consideration that the multibeam measurement that was taken as close as possible in time to the yearly LiDAR measurement is considered as representative for the whole year. This is a caveat given the dependence of the bed elevation in the underwater are from changes in the discharge. This effect should be filtered out when several measurements are taken or if the LiDAR measurements were obtained under similar flow conditions.

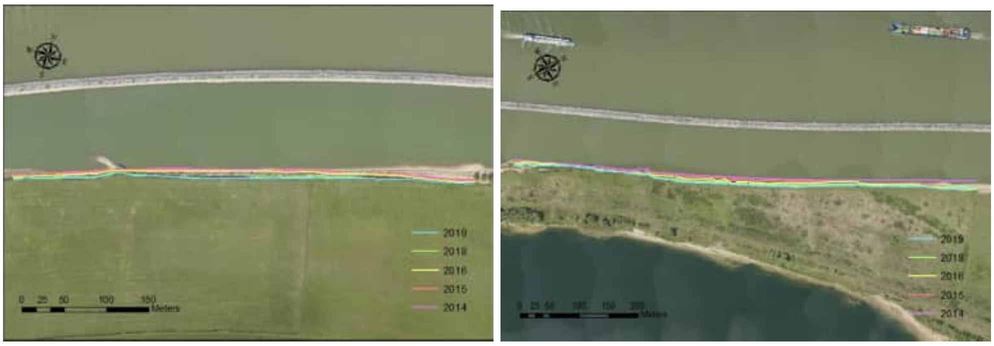

Figure 4.18 Digitized bank lines for the erosion areas in shore channels at Wamel (left) and Dreumel (right) in the river Waal. (Figure from Flores *et al.* (2021)).

4.4.5 Effect on navigation

For navigation, the question is if there is an increase in navigation depth due to a change in bed form heights and increase in water levels. In an earlier analyses (Figure 4.9) no conclusion could be made on the change in bed form dimensions. In this section the bed level is analysed with respect to OLR/OLW (later abbreviated to OLR). This 'depth' w.r.t. OLR is compared to the required navigational depth. This required depth is 2.8 m for most of the Rhine river, but increase towards the river mouth. According to Doornekamp (2019) within the area of interest, it increases slightly towards St. Andries w.r.t. OLR (from 2.8 m w.r.t OLR at river kilometre 917 to 2.92 m at river kilometre 922).

For the analyses of the bed level, the minimum bed level in the P-map results are subtracted from the bed level. Similar to the earlier analyses this is performed for different section widths ('vaargeul'of 150 m, 'bevaarbare breedte'of 170 m, 'zomerbed secties'of 200 m). In this section only figures of 'vaargeul'are included. Figures for the other widths are included in Appendix E.4.

Figure 4.19 show the minimum depth (most shallow location) for the 'vaargeul'(150 m) per hectometre. It shows that there are many locations along the reach of the longitudinal training walls where the requirement of 2.8 m is not satisfied. This is exceeded more for wider widths (Figure E.29 and E.30), as the bed outside the 'vaargeul'is not maintained by dredging. This figures gives an indication of the spatial variability, with the lowest depths around the inlets of Ophemert and Wamel. However, it does not clearly show the temporal variability nor its relation to the discharge.

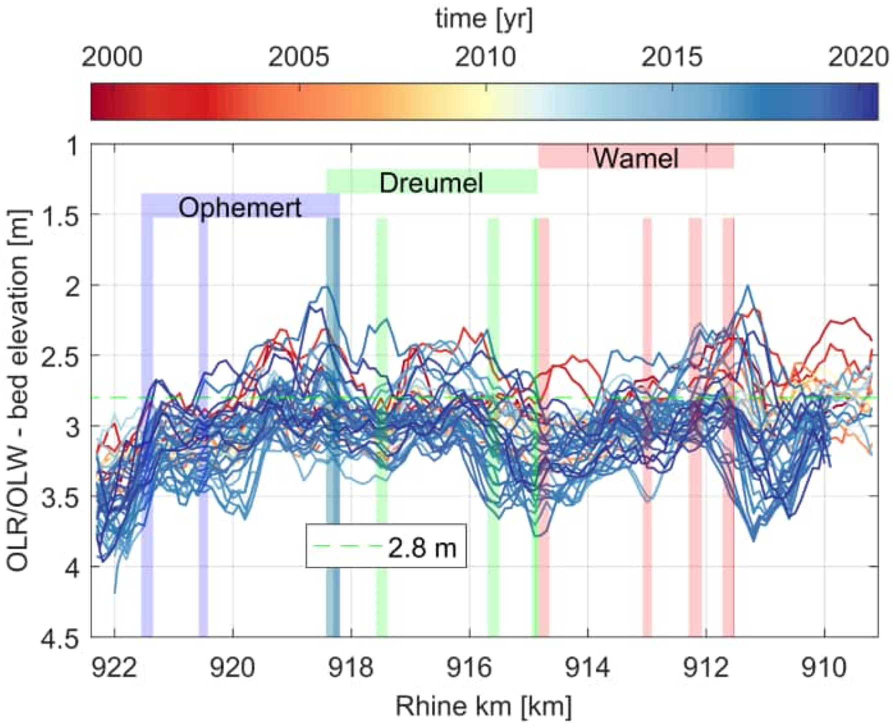

Figure 4.19 Minimum depth w.r.t. OLR/OLW in the hectometre area for the *'vaargeul' (150 m)* (averaged over 250 m upstream and downstream)

The minimum depth with respect to OLR/OLW in the 'vaargeul' (150 m) is shown in Figure 4.20 in the form of an heatmap. The discharge at Lobith is included in the plot as well. During higher discharges the height of the dunes increases, and the height decreases again during the lower discharges. During the high discharges the dredging activities are stopped as the depth is already sufficient for inland navigation. In the figure this is visible in the start of 2016, January 2018 and the first months of 2020, where the depth is lower than 2.8 m with respect to OLR (but the total depth is much larger). From the figure it can be concluded that in general the depth (w.r.t. OLR) is highest in the months with the low discharge (end of 2016, end of 2018). Partially because of the lower dune heights, but probably mostly due to dredging.

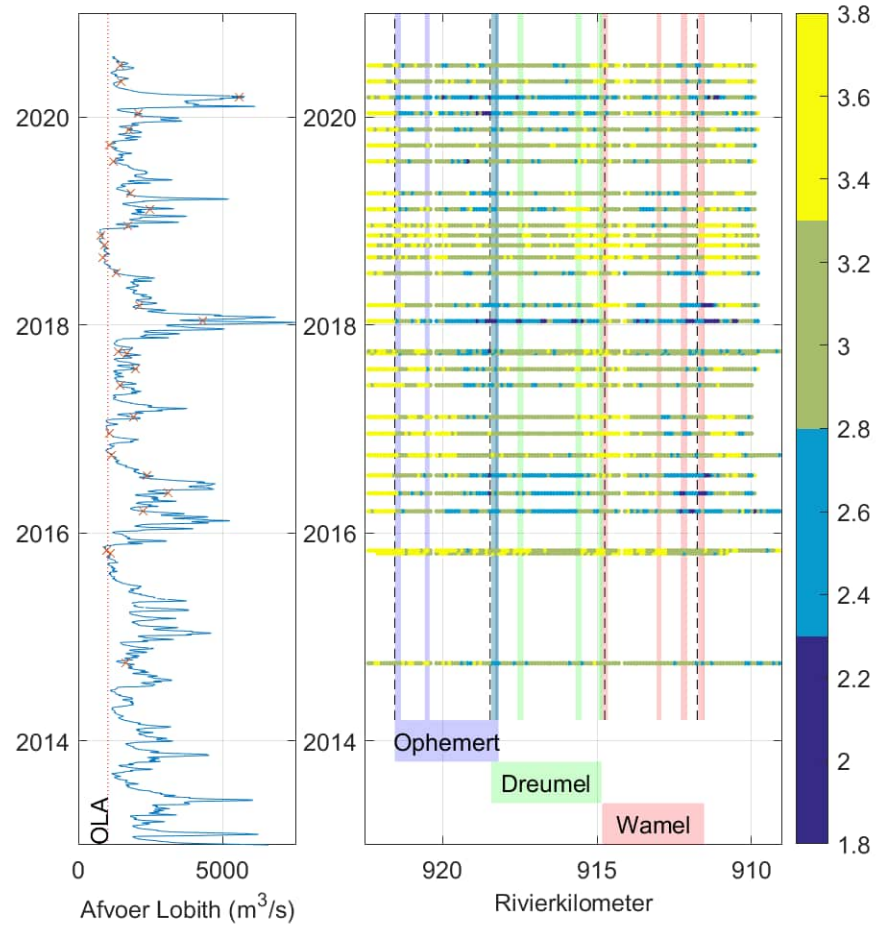

Figure 4.20 Minimum depth w.r.t. OLR/OLW in the hectometre area for the *'vaargeul' (150 m)* with comparison to discharge at Lobith

As an alternative analyses also a comparison is made of the percentile of the water depth within each channel definition is lower than 2.8 m at OLA, which can be found from Figure 4.21 for a channel width of 150 m (170 m is given in E.35 and 200 m in E.36). This analysis is less influenced by outliers and shows what fraction of the channel exceeds the required depth. For the period after the construction of the longitudinal training walls the largest percentiles are found near the inlet of Ophemert and the upstream end of Wamel (blue lines). However, both locations are also already limiting in the period before (red lines).

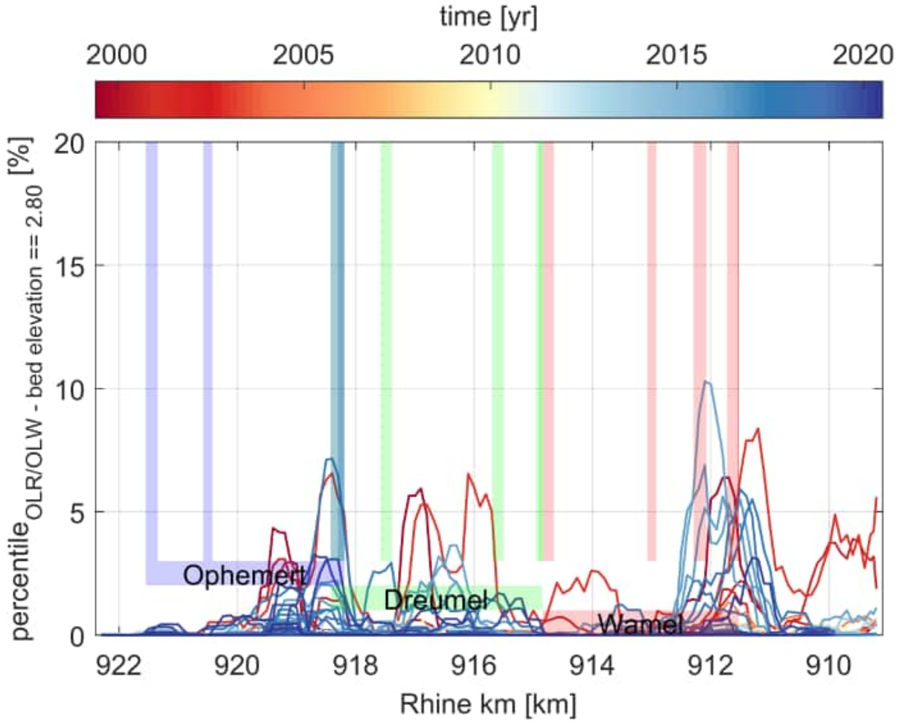

Figure 4.21 Percentage of the hectometre area for the *navigation channel (150m)* at which the depth is less than 2.80 w.r.t. OLR/OLW (averaged over 250 m upstream and downstream)

As an additional question it was asked if locations with an MGD are registered in the reach of the longitudinal training walls. Figure 4.22 shows that until 2013 most MGD's in this reach were found next to the Passewaaij flood plain with its large wetland and channel. From 2015, after construction of the longitudinal training walls, the depth around 919 next apparently reduced to such an extent that it caused the MGD to occur there rather than at Passewaaij. Even the opening of the side channel at Passewaaij and consequent sedimentation were less restrictive to the depth than the sedimentation next to the Ophemert longitudinal training wall.

For the period 2015 to 2018 MGD registrations are shown in appendix F. The MGD at Ophemert starts appearing in 2017, just downstream rkm 919. Starting in 2017 the MGD is registered for multiple reaches of the Waal. This has no effect on the lowest MGD (at rkm 876), but other MGD locations (like Ophemert) will show significantly more registrations. If the policy of only MGD for the Waal was followed, the number of registrations at MGD would have been reduced by half. In 2018 an MGD was hardly ever registered at Ophemert. Probably also as a result of dredging activities.

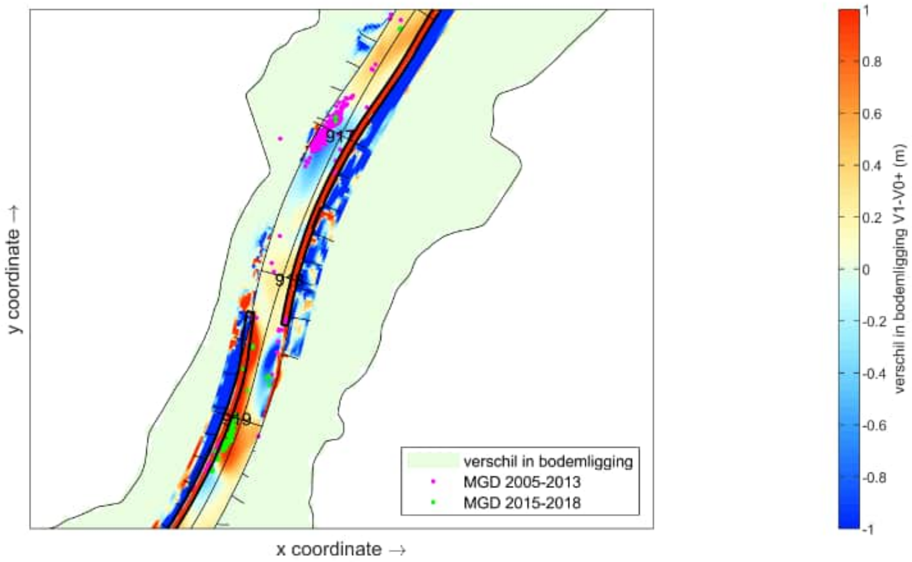

Figure 4.22 Locations of the MGD between 2005 and 2013 near rkm 917, and downstream of rkm 919 between 2015 and 2018 (Least measured depth, from Dutch: Minst gepeilde diepte) From: (Van der Wijk and Van der Mark, 2021).

4.5 Conclusions and recommendations

This chapter addresses the observed changes in bed level and water depth that have occurred after the construction of the longitudinal training walls.

How is the bed level and the bed level trend related to the overall degradation, influenced by the construction of the longitudinal training walls

Upstream of Wamel, prior to 2015 degradation is visible, and this continues after the construction of the longitudinal training walls. At the section of Wamel, prior to 2015 shows degradation and after construction shows sedimentation and slight degrdation in the last few years. At Dreumel, slight degradation is visible prior to 2015, and the appears stable, possibly showing slight sedimentation. At Ophemert the bed was stable prior to 2015, and shows overall sedimentation after construction. Downstream of Ophemert, the overall area was aggrading prior to constuction, and a strong lowering of the overall bed level is found after construction. These finding are found for the reach averaged behaviour. Locally in the Wamel and Dreumel sections, both erosion and sedimentation is found locally. Furthermore, the morphological response to the dams, as well as groyne lowering and opening of the side channel at Passewaaij, is still in a developing state. Also this transition makes it difficult to predict the long-term cumulative impacts of the measures.

For the average main channel bed level, the largest change which can be seen is the lowering of the average main channel bed level at Wamel, Ophemert and downstream of the longitudinal training walls, during construction (April 2014 - October 2015). It is hard to say if there is a change in the trend, as the river appears to still be adapting to the new conditions.

The minimum bed level appears to be increasing slighty at the locations of the auxiliary channels.

The maximum bed level cannot be compared one to one, but the maximum bed level appears to be constant over time, except during the construction phase.

The standard deviation of the bed level can also not be compared one-to-one, due to the different temporal frequency of the measurement sets. The impression is however that the standard deviation has increased compared to the period 2005-2015.

What is the effect of changes to the inlets?

The question about whether the sill levels have an influence on the sediment distribution and on the bed level development has been researched in the current study. The findings are that at Wamel, the bed level development is influenced by the raising of the sill in April 2018. This led to an reduction of the sedimentation which occurred until April 2018. Just prior to this a trench appears to be passing the location too. At the entrance to Dreumel, the effect of the sill adaptation is less pronounced, which is probably due to the location (inner bend and continuation of Wamel channel) and the fact that the adaptation was less extreme. At Ophemert the sill is not adjusted. What is apparent is that the MGD has been occurring just downstream over river kilometre 919, so there is apparently more sedimentation or larger bed forms in this reach. This point brings us to the final question on the navigation width. Although the trends appear to be clear, the time since the adaptation is short (two years) and the visible effects may also be due to river variability.

How does the bed level develop in the auxiliary channels? The bed level changes in the auxiliary channel are much larger than in the main channel.

At Wamel, aggradation occurs over the full length of the channel, but most significantly near the inlet (over +1 m aggradation) and after the last intermediate opening (over +2 m aggradation). The effects of raising the inlet of Wamel does seemingly not lead to large changes.

At Dreumel, the patterns are less pronounced than at Wamel, with alternating reaches of sedimentation (over +1 m) and erosion (-0.5 m). This is probably caused be the position of the channel in the wake of the ferry and the channel of Wamel.

At Ophemert, there is large sedimentation just downstream of the inlet (over 2 m). This reduces in downstream direction (around 0 m). Between the intermediate opening and the outlet the erosion is again higher (over 1 m).

What is the influence of the longitudinal training walls on the navigation depth and width?

For all P-map polygons (per hectometre) it is analysed what fraction of the polygon had a depth less than 2.8 m for each multibeam. Within the fairway (width of 150 m), this resulted in shallow locations at the Wamel inlet at 912, locally along the Dreumel (and Passewaaij) section at 917 and just downstream of the inlet at at Ophemert. For the opening at Wamel the size of the shallow area reduced in later years (most likely due to the raising of the sill). For the locations along Dreumel and just downstream of the Ophemert inlet at rkm 919, the shallow areas are more apparent in recent years. These conclusions also apply to the analyses with a width of 170 and 200 m.

Recommendations

Related to data there are some recommendations which are standardise the way that multibeam data are stored, and provide details of how the data was stored in the metadata document (vertical orientation, reference plane, units, horizontal resolution, etc. Furthermore, it is recommended to repeat some the bed level analyses based on the new polygons using the biweekly measurements prior to 2015.

5 Conclusions and recommendations

In this research a vast range of measurements of water levels, velocities and bed levels were used to analyse the effect of the longitudinal training walls on the river, compared to the situation prior to their construction. In this chapter we try to answer or discuss all research questions posed by Rijkswaterstaat. The questions have been translated, combined and rephrased to structure this section as much as possible. This chapter finishes with a list of recommendations for further research .

5.1 Water levels

What is the effect of the longitudinal training walls on the water levels at high discharge?

Based on the current analyses at high discharge, we conclude that the water levels are lowered, with respect to the situation prior to the construction of the longitudinal training walls. Analyses of the peak water levels show a lowering of 10 to 20 cm at station Tiel Waal for discharges higher than 2500 m^3/s (figure 2.8). The effect cannot be quantified as being solely dependent on the longitudinal training walls, as in the same period downstream of the longitudinal training walls the groynes were lowered and the side channel at Passewaaij was realised.

What is the effect of the longitudinal training walls on the water levels at low discharge?

By reducing the cross-sectional area at low river discharge, it is expected that the water depth increases during these conditions (discharges lower than 1500 m^3/s). The analyses of the water levels at station Tiel Waal shows that the lowering trend in water levels in the period before construction has been stopped for discharges below 2400 m^3/s (figure 2.6). This appears to be strongly linked to the bed level trends. The effect at very low discharge can not be accurately analysed due to the varying and unknown withdrawal through the ARK. From measurements a set-up of the water levels can not be concluded.

At the station Sint Andries Waal, downstream of the longitudinal training walls, the water levels show a lowering trend from 2017 onwards. This means that the head difference between Sint Andries and Tiel has actually increased in the period after construction of the LTW (see figure 2.9). It is expected that this increase is the result of the LTW.

5.2 Velocity and Discharge

What is the effects of the longitudinal training walls on the flow velocity

From ADCP measurements the change in velocity is analysed. For a discharge at Lobith of 922 m^3/s, an increase in flow velocity in the order of 10% is observed. An increase in flow velocity was expected as flow is concentrated in the main channel thanks to the longitudinal training walls. For a discharge at Lobith equal to 3436 m^3/s, 4170 m^3/s, and 5087 m^3/s, a decrease in flow velocity was observed of approximately 15%, 5% and 2%, respectively. For these discharges the longitudinal training walls are fully submerged making the flow width wider than the situation prior to construction of the LTW.

How is the the discharge distribution between main and auxiliary channel?

At Wamel, for a discharge at Lobith lower than 2500 m^3/s is lower than 12 % of total Waal discharge, which should in theory result in an increase in water levels compared to prior to construction.

At Dreumel, the only at Boven-Rijn discharges of roughly 1250 m^3/s and lower the auxiliary channel discharge is lower than 12 % of the total Waal discharge.

At Ophemert the auxiliary channel discharge is never below 12 %.

What is the effect of alterations to the inlets, and is there a view on the range to which the velocity can be influenced?

This was not clearly visible from the analysis of the velocity measurements. The patterns in the sedimentation and erosion after adjustment of the sill heights and the discharge analysis by Sieben (2020) show that there is an opportunity to influence the velocity in the main channel and thus indirectly also in the auxiliary channel. At this moment we are not able to quantify to what range the velocity can be influenced.

5.3 Sediment transport

What is the effect of the LTW on the sediment transport capacity in the main channel?

Based on a simple estimate based on Engelund and Hansen (1967) related to the average velocity before and after the construction of the longitudinal training walls, it is estimated that a low discharges the sediment transport is reduced by 40 % and at high discharges the sediment transport is reduced by roughly 5 %. The sediment transport is more significant at higher discharges (i.e., it relates non-linearly with velocity), but on the other hand the lower discharges occur more frequent. Therefore a weighing of both conditions is complex and requires numerical modelling. If the numerical simulations prove to correctly capture the flow velocity, these are the ideal tool for answering questions related to sediment transport. However, it is clear that the sediment transport capacity has reduced on average.

The raising of the sill height at Wamel showed that it was possible to influence the sediment transport in the main channel, and as such this may offer some possibilities for further refinement of the layout, particularly to optimise the water levels at low discharge.

These measurement are showing the initial morphological impact. The long term effects can show a very different response if due to the sedimentation the flow velocities increase again, resulting in the restoring of the transport capacity.

5.4 Bed levels

Has the trend in bed level evolution changed after construction of the longitudinal training walls?

An important objective of the longitudinal training walls, with regards to the bed level in the main channel is to stop the long term bed degradation. The long-term development before 2015 shows that upstream and along Wamel and Dreumel the bed has been degrading mildly, while at Ophemert and downstream a small aggrading trend has been observed. During the construction period between 2014 and 2015 some parts of the average main-channel bed level at Wamel and Ophemert show a strong lowering. After the construction of the dam was completed (and Phase 3 groyne lowering downstream), the analyses at Wamel, Dreumel and Ophemert appears to show that the eroding trend has stopped. The reach at Ophemert shows clear sedimentation, while at Wamel and Dreumel reaches of erosion and sedimentation are alternating.

The effect on the long term and large scale bed level changes cannot be determined on the basis of the current data, as the bed level is still adapting to the measure. In addition, for longer reaches and time scales, other Room for the River measures such as groyne lowering along the Waal, and others are also influencing the overall evolution of the bed which make it impossible to isolate the effect of the longitudinal training walls on the large scale behaviour from the data.

For both low and high discharge, the velocity is lower than prior to the construction of the longitudinal training walls. As indicated, this will lead to a lowering of the sediment transport in the reach, ultimately leading to a shallower section, which may hamper navigation and counteracts the reduce the water level reduction at high discharges as intended with this measure.

Do the sill levels have an influence on the sediment distribution between main and auxiliary channel?

The sill levels can be used to influence the sediment transport capacity in the main channel. This was illustrated by the different response to the change in inlet at Wamel, and also, but less pronounced at the Dreumel inlet. This change in functioning of both inlets is possibly caused by position of the inlet in relation to the curvature: offtakes in inner bends get more sediment and are therefore prone to close off. This was clearly apparent from the sedimentation prior to April 2018 and erosion after 2018 at the Wamel inlet shown in Figure 4.13 and Figure 4.14.

The bed levels in the side channel show sedimentation and erosion of larger magnitudes than in the main channel. At Wamel, the divergence bar is not visible, but the erosion and sedimentation patterns just downstream of the inlet are visible. After raising the sill at Wamel increased sedimentation is found after April 2018. It is however not directly clear what causes the sedimentation. At Dreumel the effects are less pronounced, and at Ophemert, where the sill level was never raised (but it was narrowed in April 2019), significant sedimentation occurs just downstream of the inlet.

Although the bank erosion might have a large contribution to the sediment and the bed level in the auxiliary channels, these have not been investigated in this report, but is being researched at the Radboud University.

5.5 Dune height

Do the bed level measurements show that the bed forms have lower amplitude in the reach of the longitudinal training walls?

Based on the P-map analysis of the bed levels, the standard deviation of the bed levels within certain polygons was defined as well. This value indicates what the variability of the bed level is and could refer to groyne flames, dunes, or any other variation in the bed level measurements (including the initial morphological response of the longitudinal training walls). According to the section averaged analysis the standard deviation of the bed level in the period 2015-2020, as derived from two-weekly multibeam soundings of the navigation channel, is larger than in the period 2005-2015 as derived from the yearly multibeam measurements.

As the temporal resolution of the 8 weekly measurements is higher than the yearly multibeam measurements, it may be that the effect is not as it appears. A possible explanation is that, although the amplitude of the local groyne flames are larger, overall there is more variation in the bed after construction of the longitudinal training walls. This analysis does not separate steady and migrating features, does not consider their distribution in space, and does not account for the propagation of dunes from upstream. This means that based on the current analysis, it is not possible to conclude that the dune heights are increasing along the longitudinal training wall reach. A recommendation is to redo the P-map analysis for the biweekly multibeam measurements prior to 2015. Furthermore alternative data-analysis methods should be applied for further detailing, e.g. wavelet, zero-crossing or similar for smaller frequencies.

Is it true that the lower bed forms are not a matter of smaller dune heights, but due to the suppression of groyne flames?

Unfortunately, this cannot be answered based on the current analysis.

5.6 Navigation

What is the effect of the longitudinal training walls on transverse currents, and how large are these currents and how do these extend over the transverse cross-section?

None of the flow velocity measurements showed strong cross-flow components larger than 0.3 m/s in the main channel. However, the data-set for answering this question is not ideal. Longitudinal ADCP measurements were taken, but not repeated. Hence, it is not possible to filter turbulence from mean-flow properties. The detailed measurements at the inlets have been used, but these do not extend enough towards the main channel.

Is there potential for reducing the requirements for the navigation depth due to a change in bedform height?

It is an interesting point that dunes could play a role in increasing the water level due to increased roughness, but at the same time form shallow locations limiting the navigable depth in the river. Based on the current data analysis we are unable to answer, how this works out in the field. A more detailed bed-form analysis on the multibeam data is required to judge whether the conditions have changed.

Are the locations where a MGD least measured depth is measured in the reach of the longitudinal training walls and where are the located?

Just downstream of rkm 919 at Ophemert, there is a location where the MGD often occurs (Figure 4.22), mainly in 2017. This location appears to become more restrictive to the depth than the location around river kilometre 917 at the side channel to Passewaaij which used to generate the MGD's in this section prior to the construction of the longitudinal training walls.

Are there locations in the reach of the longitudinal training walls, where the bed level exceeds OLW/OLR - 2.8 m for the 150 m navigation channel, the 170 m navigable width, or the 200 m main channel section, and if so when were these observed?

At various locations along the reach of the longitudinal training walls the requirement of 2.8 m is not satisfied (cf. Figures 4.19 and appendix E.5). This depth is exceeded more often for wider widths. Looking at the percentile of the bed level at -2.8 m w.r.t. OLR where this occurs, it can be seen that initially at the inlet of Wamel and midway the Dreumel structure. In more recent years the shallow section downstream near the Ophemert inlet appears (cf. Figure 4.22). These locations appear only at OLA discharges or smaller, indicating that the bed level could be maintained. The strict requirement of OLR/OLW - 2.8 m was not satisfied, but probably the water depth was sufficient at all times. It is recommended to formalise the unwritten maintenance rules for the situation with discharges above OLA and to analyse the temporal evolution of the water depth along the river.

5.7 Recommendations

5.7.1 Further research on different effects at low discharge

The increase in water levels at low discharges is less than expected from theory. We have put forward a number of different possibilities which could explain this, but we are currently not in a position to conclude based on the current data (analysis). Based on these points, recommendations for further analysis and measurements are provided:

5.7.1.1 Reduction of the alluvial roughness

Based on the current analysis, it was not possible to determine whether or not the bed form dimensions have reduced after construction of the longitudinal training walls. For this, we recommend to extend the P-map analysis in to the past using the biweekly bed level measurements, thereby removing the temporal uncertainty. Other techniques could also prove useful such as the wavelet analysis, or a zero crossing method, both to confirm the conclusions, but also as a check if the different methods provide similar insight. This analysis would also benefit the general change in the bed level trends for the area.

5.7.1.2 Reduction of horizontal mixing

A possible suggestion is that due to the removal of the groynes, large scale horizontal eddies are not generated as much as after the construction of the longitudinal training walls. On the other hand the roughness generated by the rockfill surface of the dams generates reasonable amount of friction. To check this we recommend to do measurements in which the horizontal stresses can be derived, and their impact on overall flow can be assessed. The most logical location for this would be just upstream of Wamel (in the groyne section) and further downstream, just upstream of the bend. A first assessment of this hypothesis could be done by comparing results of three-dimensional schematized simulations of a river section with groynes and with a longitudinal training wall.

5.7.1.3 Porosity of the longitudinal training wall

It is known that the dams are porous, and that water is flowing through the dam especially at low discharge when there is a head difference over the dam and especially at the openings which are constructed differently. The available ADCP and longitudinal measurements are not accurate enough to derive this quantity, therefore it is recommended to directly measure the flow through the longitudinal training wall. This could be achieved by more accurate ADCP surveys or the application of tracer measurements to track the flow through the porous medium.

5.7.1.4 Distribution of the water at the inlets

It would be good to have water level and velocity measurements just prior and just after adjustment of an inlet. Ophemert could possibly be a location for this, as it has not undergone any adjustment until now, and locally causes a water level lowering of 5 cm according to (Sieben, 2020) (although how this value is found is not immediately apparent, cf. Section 5.1), and appears to cause large sedimentation and is a location of where the MGD is measured.

In the past ships have been used to narrow the channel (an example is the IJsselkogge from the fifteenth century. Possibly, one of the inlets could be blocked by a barge, such that the effect of inlet closure on the water levels can be seen, but we realise, this may not be feasible.

5.7.2 Distribution of the water in the Rhine at low discharge

The trends in discharge distribution should be analysed further, and it would be good to have more insight into the discharge distribution at low discharges, preferably from measurements. The discharge currently given by MWTL is apparently lower than what can be concluded from available measurements. The MWTL product can be improved with for example more frequent measurements of the discharge for all river branches at all bifurcation points. It would be very valuable to include new insights in the discharge distributions in the officially distributed (MWTL) discharges.

5.7.3 Change in sediment transport capacity

We recommend to incorporate the insight from numerical models on this point, or to sediment transport measurements prior and just after the adjustment of a sill. Not only the sediment capacity, but also the grain-size fractions before and after the inlets would be of interest to better understand the seperation of the mixture and the type of sediment being transported in the auxiliary channels. Furthermore, other analysis based on the current adjustment at Wamel, may form interesting validation material for such numerical models.

5.7.4 Improvements to systematic storing of the data

For at least the velocity measurements and the multibeam data, the data was not stored in a clear and systematic method. It involved many iterations to obtain the correct orientation and magnitude of the provided data.

For the ADCP data the lack of a consistent naming convention may be the most limiting factor. Detailed recommendations are given in Section 3.3.3.2.

For the multibeam bed level data, the measurements were sometimes in centimetres, decimetres or metres, without any metadata explaining how it was organised. Similarly, sometimes the data was positive down, rather than positive up.

It is recommended to create guidelines/requirements for how different data should be stored, such that the next person working with it does not have to reprocess all the manual steps again.

Of a different nature is the registration of the water level measurements with divers. As these measurements were considered to be expensive, only 5 divers were placed. However, none of these measurements have been regularly loaded and saved. These potentially valuable measurements could therefore not be used.

During this pilot of the longitudinal training walls a data management system was set-up. It was hosted by Deltares, but the responsibilities for its content remained at Rijkswaterstaat. The data was hosted only passively without any active users. However, a similar system with active users could help in the ownership and quality assurance of the measurements. In other projects these collaborations have resulted in the set-up of a data house (‘datahuis’), which might also be a recommendation for riverine pilots.

5.7.5 Reconsider of longitudinal water level measurements

From the experience in analysing the longitudinal measurements, it is advised to reconsider the application of this technique for measurement campaigns of local measures with relatively small impacts compared to the expected fluctuations and scatter in water levels. Although a single run shows many interesting details, it can not be easily compared to other runs due to this macro turbulence.

6 References

Buijse, T., E. Mosselman, J. S. de Jong and M. Weeber, 2019. *Langsdammen beoordeling monitoring en synthese*. rapport, Deltares, Delft.

Chavarrías, V. and W. Ottevanger, 2019. *Morphological development of the bifurcation at Pannerden: Measurements, simulations and improving of graded-sediment modelling*. Tech. Rep. 11203682-007-ZWS-0005, Deltares, Delft, the Netherlands.

Chavarrías, V., K. Sloff and E. Mosselman, 2021. *Final evaluation longitudinal trainingwalls: WP10, morphology, operation and maintenance*. techreport 11204644-012-ZWS-0001, Deltares, Delft, the Netherlands.

Czapiga, M., A. Blom and E. Viparelli, 2021. *Efficacy of Longitudinal Training Walls to Mitigate Riverbed Erosion*. Powerpoint presentation, Delft University of Technology, Delft, the Netherlands.

Dietrich, W. E. and J. D. Smith, 1983. "Influence of the point bar on flow through curved channels." *Water Resources Research* 19 (5): 1173–1192. DOI: 10.1029/WR019i005p01173, URL https://agupubs.onlinelibrary.wiley.com/doi/abs/10.1029/WR019i005p01173.

Doornekamp, J., 2019. *Rivierkundig Beoordelingskader voor ingrepen in de Grote Rivieren*. Tech. rep., Ministerie van Infrastructuur en Waterstaat, Rijkswaterstaat Water, Verkeer en Leefomgeving. (in Dutch).

Engelund, F. and E. Hansen, 1967. *Monograph on sediment transport in alluvial streams*. Tech. Rep., Hydraulics Laboratory, Technical University of Denmark, Copenhagen, Denmark.

Flores, N. Y., F. P. L. Collas and R. S. E. W. Leuven, 2021. *Shore channel sedimentary processess, passability by migrating fish and habitat suitability*. Tech. rep., Radboud University, Nijmegen, the Netherlands.

Kater, E., 2014. *P-map Rijntakken RWS-ON 1999-2014: GIS-modules en datasets gemiddelde zomerbedhoogten per hectometervak, nautisch kilometervak en riviertraject*. Tech. rep., Rijkswaterstaat, Oost-Nederland. (in Dutch).

Koedijk, O. C., 2020. *Richtlijnen Vaarwegen 2020*. Tech. rep., Ministerie van Infrastructuur en Waterstaat, Rijkswaterstaat Water, Verkeer en Leefomgeving. (in Dutch).

Ottevanger, W., S. Giri and C. J. Sloff, 2015. *Sustainable fairway Rhinedelta II : effects of yearly bed stabilisation nourishments, Delta Program measures and training walls*. rapport, Deltares, Delft.

Paarlberg, A. J. and A. Y. A. Omer, 2021. *Eindevaluatie pilot Langsdammen in de Waal: Delft3D-berekeningen*. Tech. Rep. PR4153.10 (HKV), 11204644 (Deltares), HKV Lijn in Water and Deltares.

van Putten, D., 2021. *Effect onttrekkingen Betuwepand op waterstanden Waal*. Memo, Rijkswaterstaat, Arnhem, the Netherlands.

de Ruijsscher, T. V., A. J. F. Hoitink, S. Naqshband and A. J. Paarlberg, 2019. "Bed morphodynamics at the intake of a side channel controlled by sill geometry." *Advances in Water Resources* 134: 103452. DOI:

Deltares

10.1016/j.advwatres.2019.103452, ISSN 0309-1708, URL http://www.sciencedirect.com/science/article/pii/S0309170819301459.

de Ruijsscher, T. V., S. Naqshband, B. Vermeulen and A. J. F. Hoitink, 2020. "Morfodynamische effecten van langsdammen in de Waal." *H2O : tijdschrift voor watervoorziening en afvalwaterbehandeling* pages 20–23. ISSN 0166-8439. (in Dutch).

Savitzky, A. and M. J. E. Golay, 1964. "Smoothing and Differentiation of Data by Simplified Least Squares Procedures." *Analytical Chemistry* 36 (8): 1627-1639. DOI: 10.1021/ac60214a047, URL https://doi.org/10.1021/ac60214a047.

Sieben, A., 2020. *Overzicht afvoermetingen 2016-2019 project monitoring langsdammen*. Tech. rep., Rijkswaterstaat. (in Dutch).

van der Wijk, R. and R. van der Mark, 2021. *Evaluatie pilot langsdammen - Functie Vaarweg: WP7*. Concept report (in preparation) 11204644-009-ZWS-0003, Deltares, Delft, the Netherlands.

A Design and developments of the longitudinal training walls

A.1 Asbuilt design drawings

From the asbuilt design some indicative longitudinal profiles (‘langsdoorsneden’) and cross-sections (‘dwarsdoorsneden’) are shown in figure A.1.

- The *inlet* is fully built with large riprap (40 - 200 kg) on top of fascine mattress (‘zinkstuk’)
- The *dam* is built with multiple layers of rip rap on top of a core of sand (the dredged material: ‘cunet’). To prevent the erosion of this sediment, two filter layers are constructed on top of the core (‘filterlaag 1’ and ‘filterlaag 2’) of which the material is not specified. The top of the dam consists of riprap, but varies of the cross-sectin. The river side has the largest riprap (40-200kg), the top of the auxiliary channel is somewhat smaller (10-60 kg) and the toe at the auxiliary channel the smallest (1-60kg).
- The *intermediate opening* has the same design as the inlet with only large rip (40 - 200kg).
- The *outlet* has no specific design in these drawings.

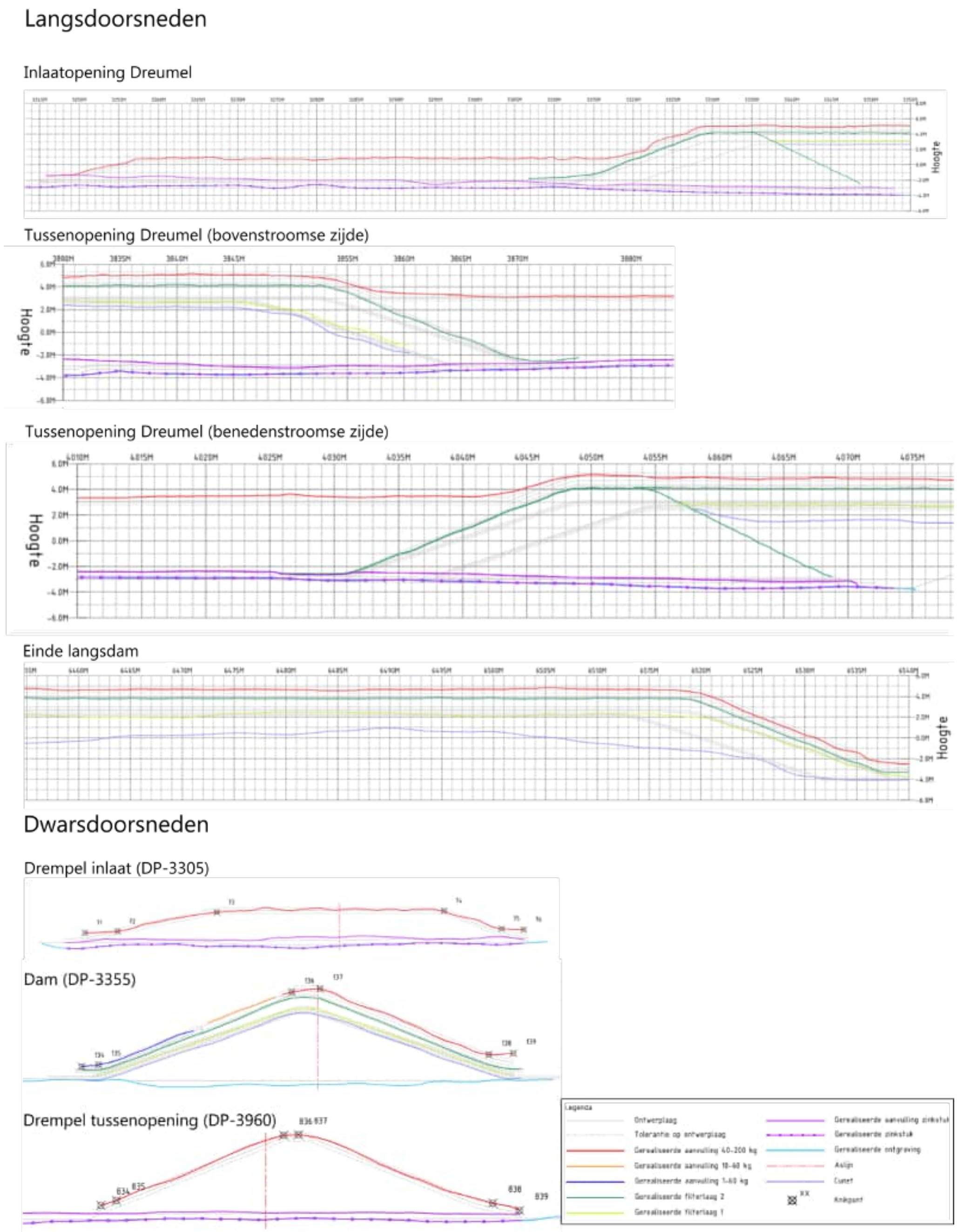

Figure A.1 Asbuilt design of the LTW Dreumel based on drawings of October/November 2015. From the hundreds of cross-sections only three are visualised that are representative for the different components of the dam. In the longitudinal plots the upstream end is to the left. In the cross-sections the auxiliary channel is to the left.

A.2 Dimensions of the inlets

In the overview below the dimensions are in reference to OLR/OLW 2002.

Inlet Wamel:
- August 2014 to November 2015: Construction at OLR - 1.75 m and a width of 190 m
- During April to the end of April 2018: Raising inlet to OLR + 1.25 m (NAP + 3.75 m)
- 8 April 2020: Construction of a V-shaped opening at the upstream end of the inlet with the lowest level at NAP + 2.0 m and a width ranging from 12 m (bed) to 16 m (at crest).

Inlet Dreumel:
- August 2014 to November 2015: Construction at OLR - 1.75 m and a width of approximately 110 m. The width is hard to quantify as the orientation is not parallel to the river axis
- 20 April 2018: Reduce width to 25 m (between the shipping beakens) by raising the remainder of the inlet to OLR + 1.25 m (NAP + 3.22 m ± 0.25 m)
- 18 April 2019: 15 m of the inlet is lowered to OLR -0.50 m.

Inlet Ophemert:
- August 2014 to November 2015: Construction at OLR - 1.75 m and a width of 230 m.
- 15 April to 2 May 2019: Reducing the width of the inlet to 85 m by building a dam connected to the longitudinal training dam at a height of OLR + 1.0 m (NAP + 3.14 m)

Intermediate openings have been constructed at OLR +1.25 m (or 1.25 m below the dam's crest level) and have not been altered since construction.

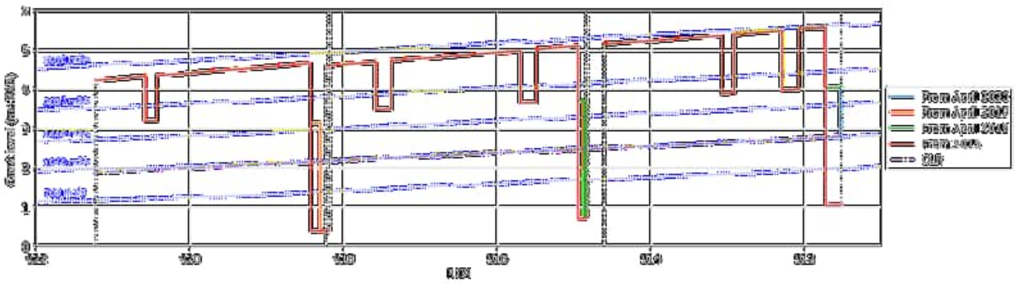

Figure A.2 Schematic drawing of the height of the longitudinal training walls from construction drawings ('Bijlage VSE-08 - Lengteprofiel langsdam.pdf'). Water level from betrekkingslijnen 2018 for the discharge at Lobith.

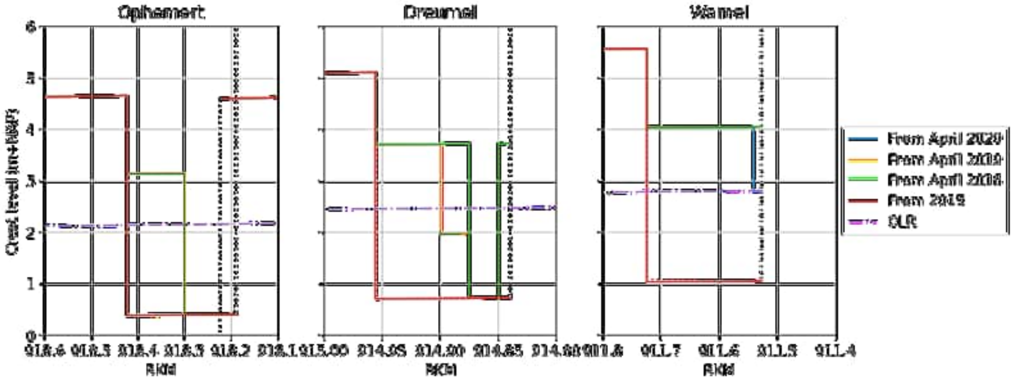

Figure A.3 Schematic drawing of the dimensions of the openings of the longitudinal training walls and the change over time. Note that for simplicity all slopes have been drawn either vertical while in the design a slope of 1:2.5 is applied.

Figure A.4 Inlet of Wamel in phase 1 (photo by Erik Mosselman), phase 2 (photo by Frank Collas) and phase 3 (photo by Kees Sloff)

Figure A.5 Inlet of Dreumel in phase 1 (photo by Frank Collas), phase 2 (photo by Frank Collas) and phase 3 (photo by Tom Buijse)

Figure A.6 Inlet of Ophemert in phase 1 (photo by Frank Collas), phase 2 (sattelite photo of September 2020, source: satellietdataportaal.nl)

Figure A.7 First intermediate opening of Wamel, and second intermediate opening of Dreumel (submerged) (photo's by Frank Collas)

Figure A.8 Flow at the outlet Ophemert. The photo shows the flow through the outlet (left of beacon) and over the groyne (photo by Jurjen de Jong on 2019-02-17

Figure A.9 Shallow area in auxiliary channel Dreumel near rkm 917.9 (photo by Frank Collas)

A.3 Fixed Layers

At the location of cables and pipes (in Dutch: kabels and leidingen or K&L) a certain coverage is required to protect these K&L. This protection can be in the form of regulation to not allow any dredging ('niet-baggerlocaties') or have a protective layer on top of the K&L. The location of the locations is shown in figure A.10. The design of the protective layers at Wamel are shown in figure A.11 and A.12.

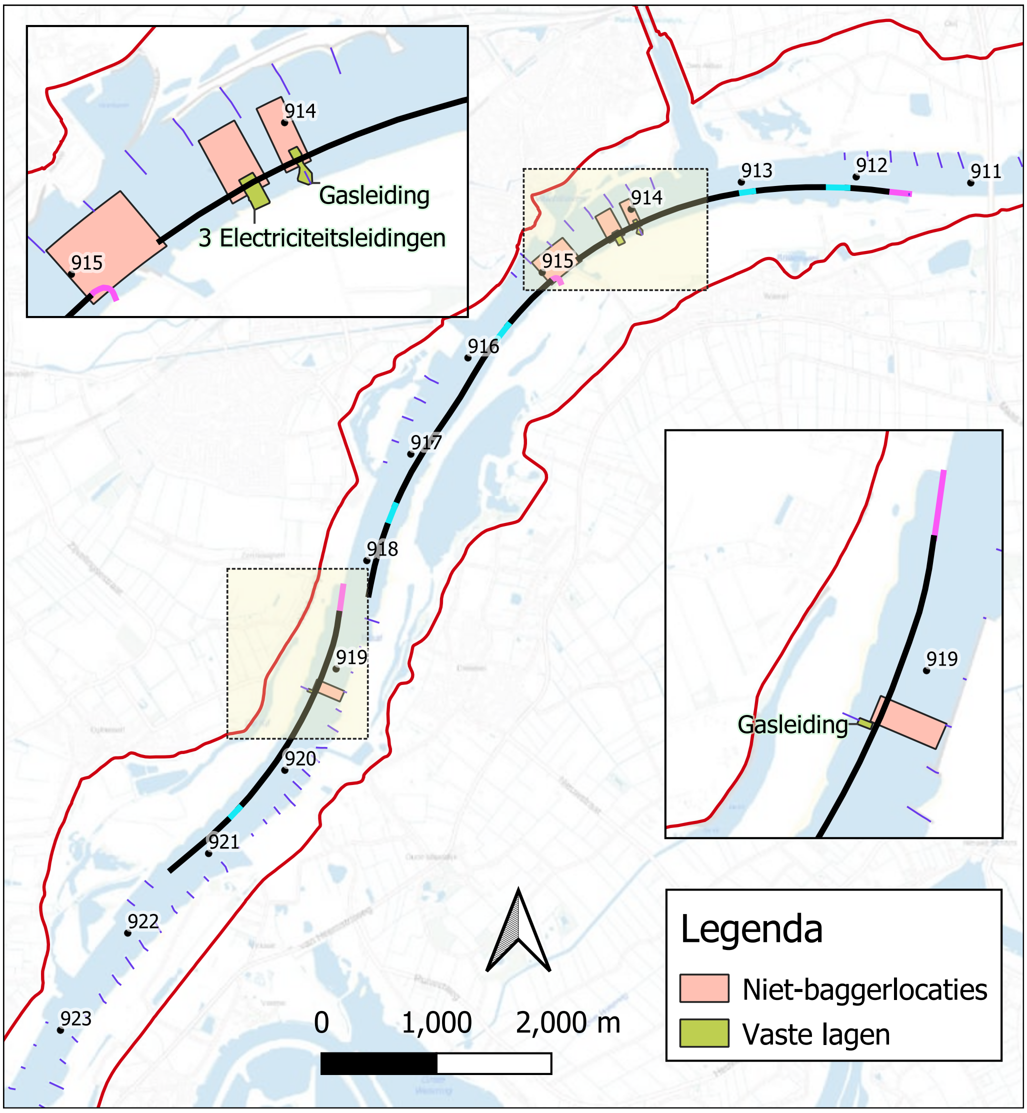

Figure A.10 Overview of locations where dredging is not allowed ('niet-baggerlocaties') and locations where bed protection is applied ('vaste lagen')

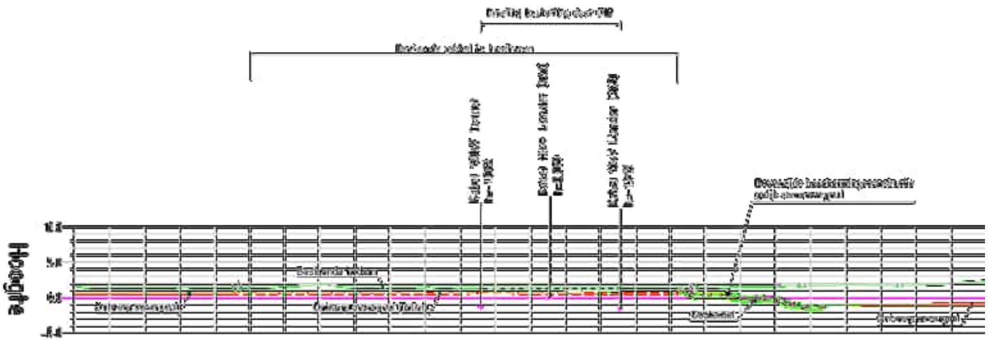

Figure A.11 Bed protection at the electricity lines at Wamel rkm 914.3.
Source: CHB-TEK-A-061 bescherminginsconstructie K&L KP 3.200 Wamel-blad4.pdf

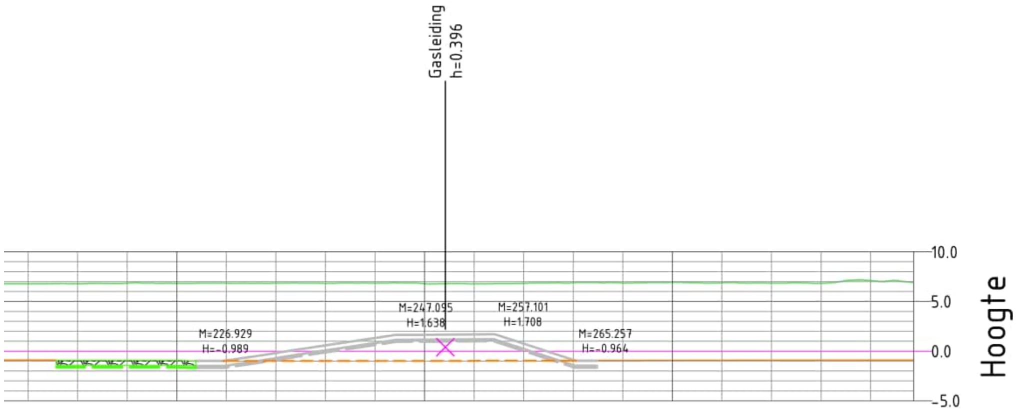

Figure A.12 Bed protection at the gas pipeline at Wamel rkm 914.1.
Source: CHB-TEK-A-061 bescherminginsconstructie K&L KP 3.200 Wamel-blad4.pdf

A.4 Timeline of development in the region of the LTW

Table A.9 contains an overview of several projects that were executed over the period of the analyses. The information is provided by Rijkswaterstaat.

Table A.9 Timeline of developments in the region of the LTW

Period	RKM	**Developments**
2014-2015	911-922	Construction of the LTW
2014-2015	upstream 911 and downstream 922	Lowering of the groynes directly downstream of the LTW and adjustment of the shape of the lowered groynes directly upstream of the LTW. Expected effect of 6 to 12 cm at design discharge.
2014-2015	916-918	Construction of a side channel and lowering of the flood plain at Wetland Passewaaij, on the right bank opposite LTW Dreumel
2015-2019	925-928	Construction of KRW-measure Herinrichting Heesseltsche Uiterwaarden with expected lowering of the water levels of 5.5 cm at design discharge
2016	everywhere	Execution of the program Stroomlijn with large scale removal of vegetation in the flood plains
2017	915-918	Dredging in the outlet of auxiliary channel Dreumel and around the inlet of the auxiliary channel Wamel. Total approximately 30,000 m^3
From 2018	913	Also opening the lock Bernardsluis Tiel at waterlevels higher than 3.00 m+NAP at station Tiel-Waal (up to approximately +3.20 m+NAP) for extracting discharge from the Waal for freshwater supply and preventing salinity intrusion on the Lek and Amsterdam-Rijnkanaal.
Continuous	920-922	Extraction of clay from the Stiftse Waard (behind on the summer dike on the floodplains next to auxiliary channel Ophemert)

A.5 Discharge regimes

Based on the analyses of the previous paragraphs, the following discharge regimes are used in the interpretation of the measurements.

Table A.10 Discharge regimes of the LTW

Discharge Lobith (m^3/s)	Description
Lower than 1200	The Prinsbernhardsluizen are opened, resulting in an additional loss in discharge on the Waal
Above 1500 to 1700	The inlet of Wamel and the increased part of the inlets at Ophemert and Dreumel are overtopping
Around 1700	All intermediate openings are overtopped.

Between 2500 and 3000	The dams of all LTW are overtopped. Downstream of the LTW the lowered groynes (see figure A.13 are overtopped.
Around 4000	Discharge through side channel Passewaaij (see figure 1.5) increases
Between 4000 and 6000	Indundation and flowing of the flood plains

Figure A.13 Groynes that were lowered on the Waal in the program Ruimte voor de Rivier. Source: Buijse *et al.* (2019)

B Longitudinal water level measurements

This appendix provides additional detail on the longitudinal water level measurements (Dutch: 'Verhanglijnmetingen'). It contains a description of the processing method (B.1), an overview of all measurement campaigns (B.2), a full page with details of each individual measurement campaigns (B.3), longitudinal plots (B.4), and the relation between curvature and gradient in transverse direction (B.6).

B.1 Processing

For each measurement the steps given below were required.
- Uniforming column names (for correcting typo's and changing standards)
- Recomputing the RKM values where necessary. Necessary to fix: older measurement did not yet have a RKM-column; many measurements had a 1 km error in the RKM of the auxiliary channel of Ophemert; some measurements had rkm in meters. Where the original data seemed correct, it has not been adjusted.
- Uniforming datetime notation
- Gathering meta-info for all measurements. The mean data per campaign is used for determining the current waterlevel (at Tiel) or discharge (at Lobith or Tiel).

This uniformed data is exported as 'raw data' to Excel (one file per measurement) and as a combined data set of all measurements to an h5 database.

After uniforming, additional post-processing steps were carried out. Further details on the averaging techniques is given below.
- Crop data between rkm 909 and 924
- Reindex to a spatial resolution of 1 m
- Apply rolling average on the reindexed data for analysing long length scales
- Apply Savitsky Golay filter on to reindex data for analysing short length scales

Also this data is exported in a combined file in both Excel and pkl format.

Three spatial filtering techniques have been compared: a rolling average (window of 80, 300 and 1000 m), a low pass filter (frequency of 1/70, 1/200 and 1/500 m^{-1}) and a Savitsky Golay filter (second order with window of 81, 401 and 701 m). A test of main channel measurements (in downstream sailing direction) is given in B.1. For keeping local variations either the low pass or Savintsky Golay filter gave satisfactory results. Choosen it use a Savitsky Golay of 81 m. For the large scale effects the rolling average performs best with a window of 1000 m, especially at the outer ends of the measurements.

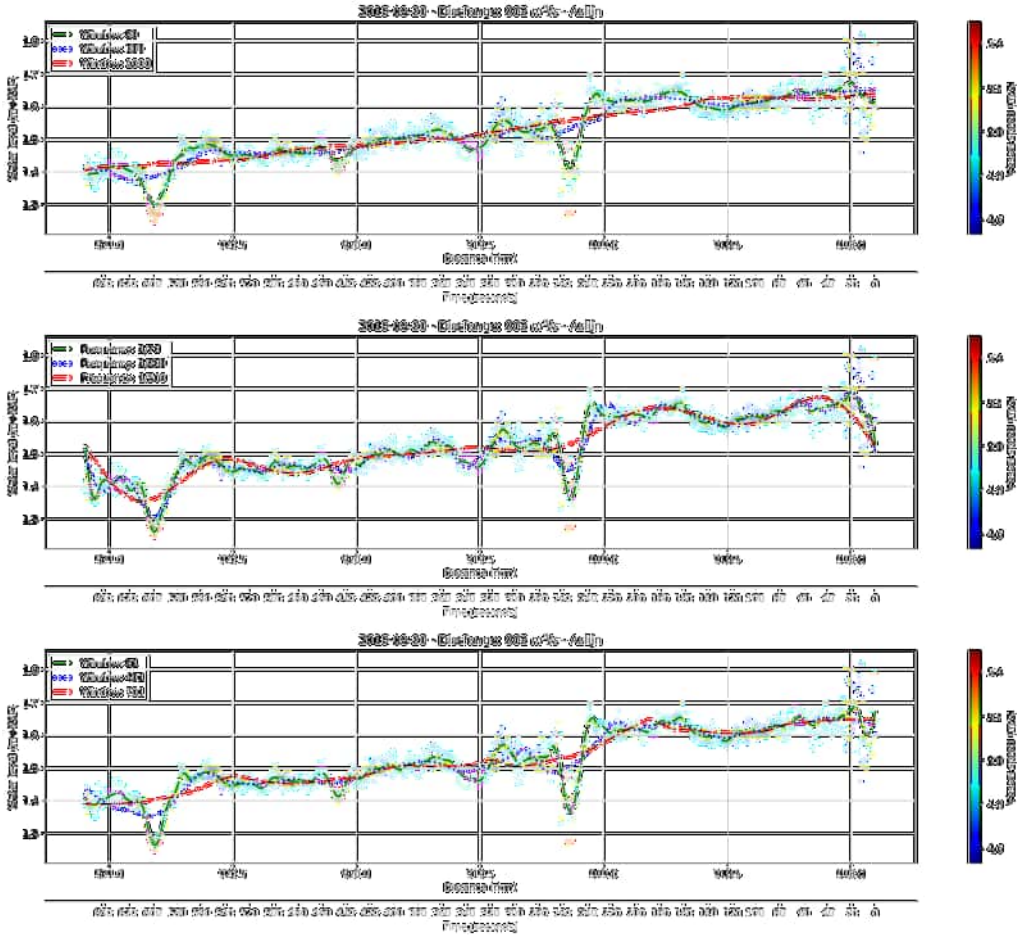

Figure B.1 Test of filtering techniques for longitudinal measurements

B.2 Overview

	Date	Duration (hours)	Q Lobith (m^3/s)	WL Tiel (m+NAP)	RKM start	RKM end	Aslijn	R-oever	L-oever	Wamel	Dreumel	Ophemert
verhanglijnwaal_20080205-07	2008-02-05	29.2	2731	5.35	867.1	933.0	X					
verhanglijnwaal_20080527-29	2008-05-28	52.5	1855	4.22	867.1	933.3	X					
20090427-29_Verhanglijn waal_afvoer 1900	2009-04-28	48.3	1969	4.43	853.5	933.3	X					
2009060304_Verhanglijn waal afvoer 1750	2009-06-03	31.6	1841	4.27	862.2	933.3	X					
2009060910_verhanglijn waal afvoer 1630	2009-06-09	27.0	1754	4.16	862.2	933.3	X					
2009100102_1277_verhanglijnwaal_afvoer_890	2009-10-01	24.6	949	2.37	857.0	952.0	X					
2009111112_Verhanglijn Waal_afvoer 1500	2009-11-11	27.3	1565	3.71	862.2	933.2	X					
100629tm0705_verhanglijn Waal afvoer 1800	2010-07-02	145.5	1810	4.24	852.1	953.4	X					
201008310901_Verhanglijn Waal_afvoer 2500	2010-08-31	25.7	2804	5.33	862.2	933.1	X					
11010405_Verhanglijn Waal afvoer 2500	2011-01-04	28.7	2609	5.42	857.2	953.1	X					
11011314ZH1277_Verhanglijn Waal_HW	2011-01-13	29.2	7430	9.13	862.0	955.0	X					
11011819ZH1277_Verhanglijn Waal_HW	2011-01-18	28.6	7463	9.15	862.0	955.7	X					
11041213c1277_Verhanglijn Waal_1250	2011-04-12	26.3	1292	3.28	862.2	934.8	X					
11042728c1277_Verhanglijn Waal_1000	2011-04-27	27.5	1090	2.68	862.1	935.0	X					
11051718BE1277_Verhanglijn Waal_940	2011-05-18	27.8	997	2.47	862.2	951.9	X					
11090102c1277_Verhanglijn Waal_1400	2011-09-01	26.7	1476	3.79	862.2	951.8	X					
12022122C1277_Verhanglijn Waal_afvoer 1750	2012-02-21	28.3	1893	4.24	862.2	951.9	X					
120829c1277_Verhanglijn Waal_afvoer 1230	2012-08-29	4.7	1237	3.08	862.2	913.5	X					
1302050607C1277_verhanglijn Waal_afvoer 5500	2013-02-06	49.8	6152	8.14	862.2	951.8	X					
78202_201407160717_Verhanglijn Waal_2500m3	2014-07-17	26.1	2638	5.25	853.2	955.6	X					
78202_201430091001_Verhanglijn Waal_1600m3	2014-09-30	28.1	1634	3.94	854.1	955.0	X					
78202_20150706+07_Verhanglijn Waal_1600m3_Rev01	2015-07-06	24.6	1656	3.9	856.7	955.0	X					
78202_20150805+06_Verhanglijn Waal_1000m3	2015-08-05	27.3	1127	2.78	853.4	955.4	X					
16WAL1277ml10_01_Verhanglijn Waal_1000kuub	2016-10-12	7.9	1011	2.46	849.7	955.0	X					
2017_845-895_VERHANGLIJNEN	2017-08-02	12.5	1840	4.12	909.8	923.1	X	X	X	X	X	X
1277_FLEX_201710315_VERHANGLIJNEN	2017-10-31	4.2	1271	3.06	909.8	923.3	X	X	X	X	X	X
2017_965-1015_VERHANGLIJNEN	2017-11-19	3.9	2495	5.17	909.8	923.1	X	X	X	X	X	X
2017_1105-1155_VERHANGLIJNEN	2017-12-01	5.0	3506	6.07	909.8	923.1	X	X	X	X	X	X
2017_1240-1290_VERHANGLIJNEN	2017-12-16	5.0	4898	7.22	909.8	923.1	X	X	X	X	X	X
2018_1105-1155_VERHANGLIJNEN	2018-01-02	4.1	3787	6.04	909.8	923.2	X	X	X	X	X	X
2018_1240-1290_VERHANGLIJNEN	2018-01-04	4.1	5119	7.21	909.8	923.1	X	X	X	X	X	X
FLEX_20180110_VERHANGLIJNEN	2018-01-10	3.6	7458	8.86	909.8	923.1	X	X	X			
FLEX_20180129_VERHANGLIJNEN	2018-01-29	2.9	6597	8.55	909.8	923.1	X	X	X			
2018_845-895_VERHANGLIJNEN	2018-03-05	4.2	1895	4.18	909.8	923.1	X	X	X	X	X	X
2018_965-1015_VERHANGLIJNEN	2018-03-15	4.7	2493	4.68	909.8	923.1	X	X	X	X	X	X
FLEX-VL_20180515_VERHANGLIJNEN	2018-05-15	5.2	1931	4.15	909.8	923.1	X	X	X	X	X	X
FLEX_VL20180705_VERHANGLIJNEN	2018-07-05	4.9	1226	3.07	909.8	923.1	X	X	X	X	X	X
FLEX_20180716_VERHANGLIJNEN	2018-07-16	2.8	1178	2.96	909.7	923.1	X	X	X			
1277_2018_725-775_VERHANGLIJNEN	2018-07-17	4.6	1132	2.87	909.7	923.1	X	X	X	X	X	X
1277_FLEX_20180730_VERHANGLIJNEN	2018-07-30	4.4	1015	2.5	909.8	923.1	X	X	X	X	X	X
1277_FLEX_20180820_VERHANGLIJNEN	2018-08-20	3.7	902	2.07	909.8	923.2	X	X	X		X	X
1277_FLEX_20180827_VERHANGLIJNEN	2018-08-27	2.9	856	2.02	909.8	923.1	X	X	X			
1277_FLEX_20180910_VERHANGLIJNEN	2018-09-10	2.9	1014	2.55	909.8	923.1	X	X	X			
1277_FLEX_20180924_VERHANGLIJNEN	2018-09-24	3.1	925	2.2	909.8	923.2	X	X	X			
1277_FLEX_20181009_VERHANGLIJNEN	2018-10-09	2.8	907	2.26	909.8	923.2	X	X	X			
1277_FLEX_20181115_VERHANGLIJNEN	2018-11-15	3.6	874	2.09	909.7	923.1	X	X	X			
2018_Week 47_VERHANGLIJNEN	2018-11-23	32.0	756	1.84	909.9	923.1	X	X	X		X	X
2018_Week 49_VERHANGLIJNEN	2018-12-04	43.8	888	2.12	909.9	923.0	X	X	X		X	X
2018_Week 51_VERHANGLIJNEN	2018-12-20	48.4	1327	3.49	909.9	923.1	X	X	X		X	X
2018_Week 01_VERHANGLIJNEN	2019-01-03	4.5	1931	4.32	909.9	923.1	X	X	X	X	X	X
2018_Week 03_VERHANGLIJNEN	2019-01-14	18.5	2418	4.63	909.9	923.0	X	X	X	X	X	X
2018_Week 05_VERHANGLIJNEN	2019-01-30	5.2	2130	4.3	909.9	923.1	X	X	X	X	X	X
2018_Week 07_VERHANGLIJNEN	2019-02-11	5.0	2339	4.48	909.9	923.0	X	X	X	X	X	X
2018_Week 09_VERHANGLIJNEN	2019-02-25	4.3	1752	4.06	909.8	923.1	X	X	X	X	X	X
2018_Week 11_VERHANGLIJNEN	2019-03-12	4.4	2348	4.63	909.9	923.2	X	X	X	X	X	X
2018_Week 12_VERHANGLIJNEN	2019-03-19	25.1	5188	7.49	909.9	923.1	X	X	X	X	X	X
2018_Week 13_VERHANGLIJNEN	2019-03-26	3.9	2603	5.24	909.9	923.1	X	X	X	X	X	X
2018_Week 15_VERHANGLIJNEN	2019-04-08	4.5	1810	4.05	909.8	923.1	X	X	X	X	X	X
2018_Week 17_VERHANGLIJNEN	2019-04-24	5.1	1342	3.3	910.0	923.1	X	X	X	X	X	X
2018_Week 19_VERHANGLIJNEN	2019-05-07	4.7	1485	3.55	909.9	923.0	X	X	X	X	X	X
2018_Week 21_VERHANGLIJNEN	2019-05-20	6.7	1763	4.01	909.9	923.0	X	X	X	X	X	X
2018_Week 23_VERHANGLIJNEN	2019-06-06	4.4	1977	4.32	910.0	923.0	X	X	X	X	X	X
2018_Week 25_VERHANGLIJNEN	2019-06-21	3.8	2378	4.73	910.0	923.0	X	X	X	X	X	X
2019_Week 28_VERHANGLIJNEN	2019-07-08	4.6	1794	3.98	910.0	923.0	X	X	X	X	X	X
2019_Week 29_VERHANGLIJNEN	2019-07-16	4.7	1712	3.86	909.9	923.0	X	X	X	X	X	X
2019_Week 31_VERHANGLIJNEN	2019-07-29	11.8	1220	2.97	910.0	923.0	X	X	X	X	X	X
2019_Week 33_VERHANGLIJNEN	2019-08-13	23.4	1492	3.55	909.9	923.0	X	X	X	X	X	X
2019_Week 35_VERHANGLIJNEN	2019-08-28	4.7	1776	3.98	910.0	923.0	X	X	X	X	X	X
2019_Week 37_VERHANGLIJNEN	2019-09-10	7.8	1249	3.09	909.9	923.0	X	X	X	X	X	X
2019_Week 41_VERHANGLIJNEN	2019-10-08	8.5	1268	3.08	910.0	923.1	X	X	X	X	X	X
2019_Week 43_VERHANGLIJNEN	2019-10-24	24.6	2100	4.39	910.0	923.1	X	X	X	X	X	X

2019_Week 45_VERHANGLIJNEN	2019-11-05	22.3	1683	3.79	910.0	923.1	X	X	X	X	X	X
2019_Week 51_VERHANGLIJNEN	2019-12-20	3.6	3381	6.12	910.0	923.0	X	X	X	X	X	X
2020_Week 3_VERHANGLIJNEN	2020-01-15	3.5	2024	4.44	909.9	923.0	X	X	X	X	X	X
2020_Week 5_VERHANGLIJNEN	2020-01-29	54.3	1393	3.45	909.9	923.1	X	X	X	X	X	X
2020_Week 7_VERHANGLIJNEN	2020-02-10	3.7	4736	7.66	910.0	923.0	X	X	X	X	X	X
2020_Week 9_VERHANGLIJNEN	2020-02-24	3.6	3703	6.39	910.0	923.0	X	X	X	X	X	X
2020_Week 11_VERHANGLIJNEN	2020-03-12	3.4	5395	7.76	910.0	923.0	X	X	X	X	X	X
2020_Week 13_VERHANGLIJNEN	2020-03-23	3.6	2744	5.37	910.0	923.0	X	X	X	X	X	X
2020_Week 15_VERHANGLIJNEN	2020-04-06	4.0	1727	4.01	910.0	923.1	X	X	X	X	X	X
2020_Week 17_VERHANGLIJNEN	2020-04-21	50.4	1268	3.14	909.9	923.1	X	X	X	X	X	X
2020_Week 19_VERHANGLIJNEN	2020-05-06	121.6	1479	3.47	909.9	923.0	X	X	X	X	X	X
2020_Week 21_VERHANGLIJNEN	2020-05-19	3.4	1588	3.69	910.0	923.0	X	X	X	X	X	X
2020_Week 23_VERHANGLIJNEN	2020-06-04	19.0	1131	2.75	909.9	923.0	X	X	X	X	X	X
2020_Week 25_VERHANGLIJNEN	2020-06-16	26.6	1692	3.72	909.9	923.0	X	X	X	X	X	X
2020_Week 27_VERHANGLIJNEN	2020-06-30	24.4	1435	3.49	909.9	923.1	X	X	X	X	X	X

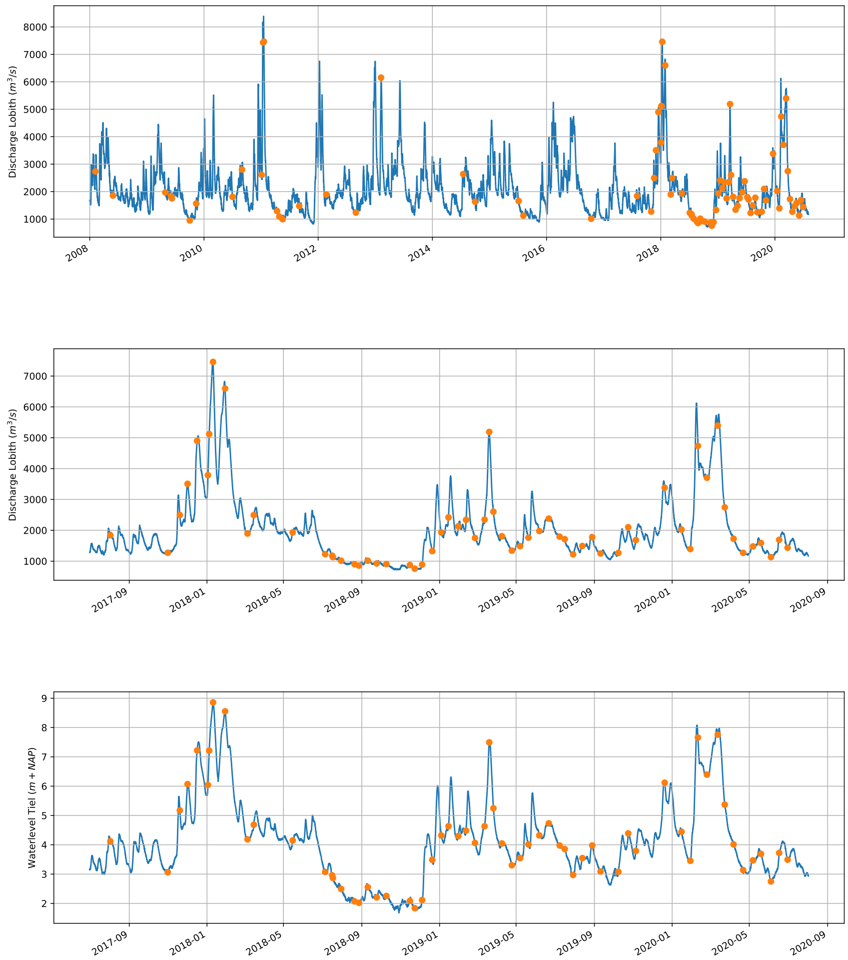

Figure B.2 Dates of longitudinal water level measurements

B.3 Details per measurement

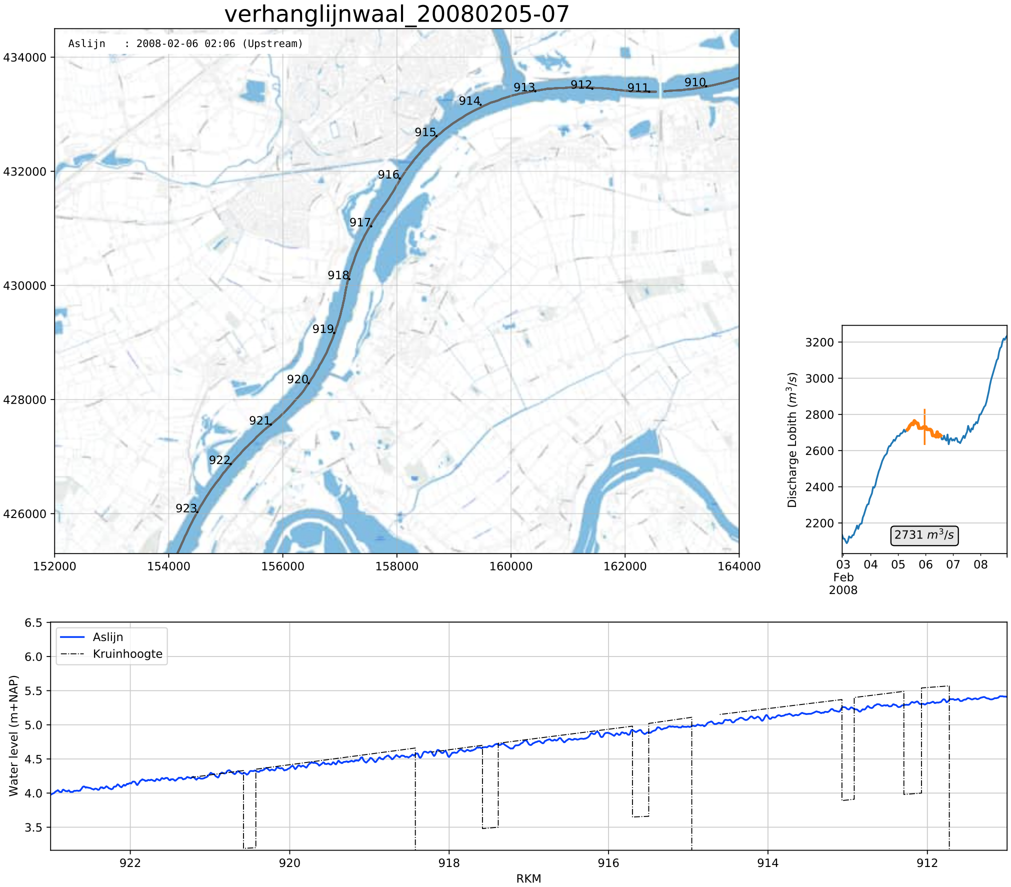

Figure B.3 Verhanglijnmeting van 2008-02-05 (afvoer Lobith: 2731 m^3/s)

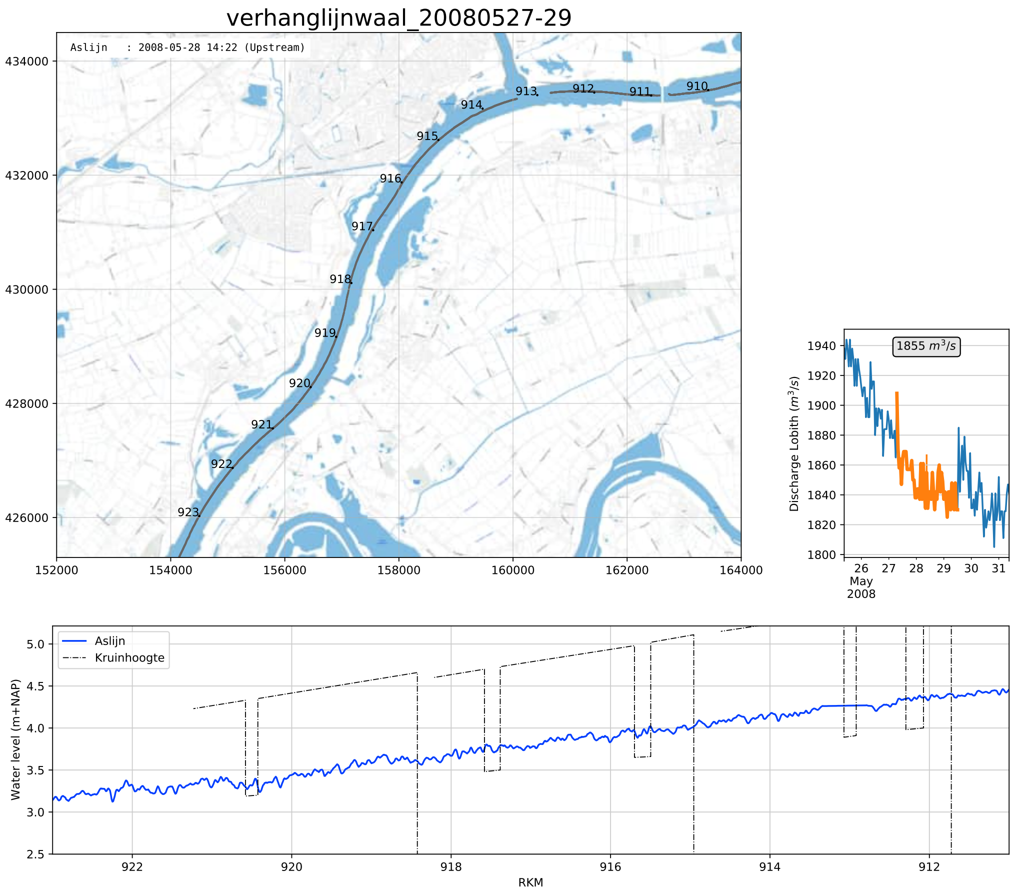

Figure B.4 Verhanglijnmeting van 2008-05-28 (afvoer Lobith: 1855 m^3/s)

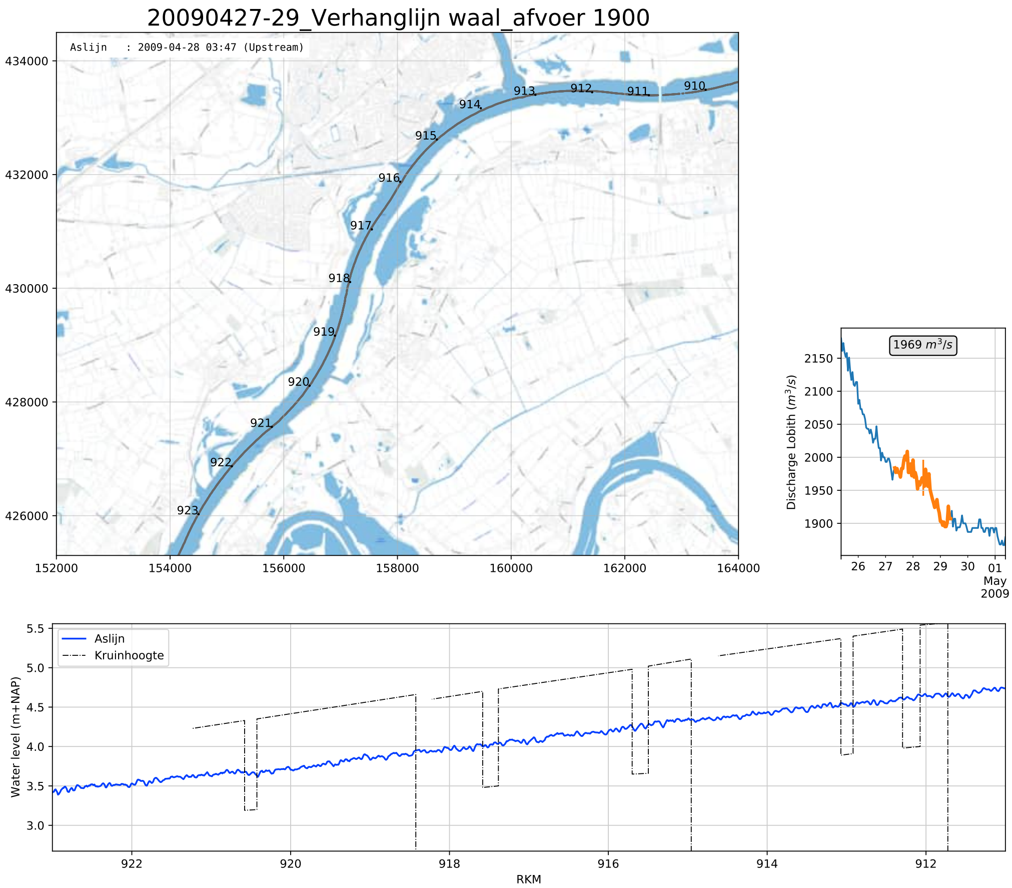

Figure B.5 Verhanglijnmeting van 2009-04-28 (afvoer Lobith: 1969 m^3/s)

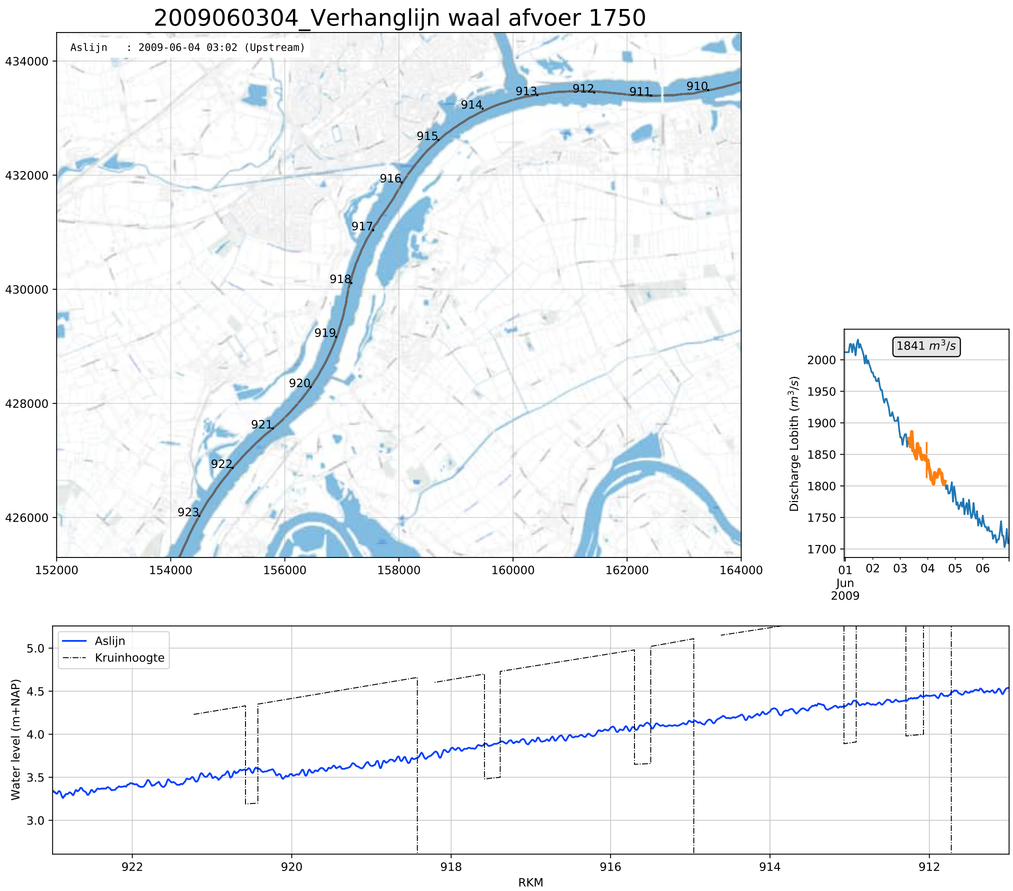

Figure B.6 Verhanglijnmeting van 2009-06-03 (afvoer Lobith: 1841 m^3/s)

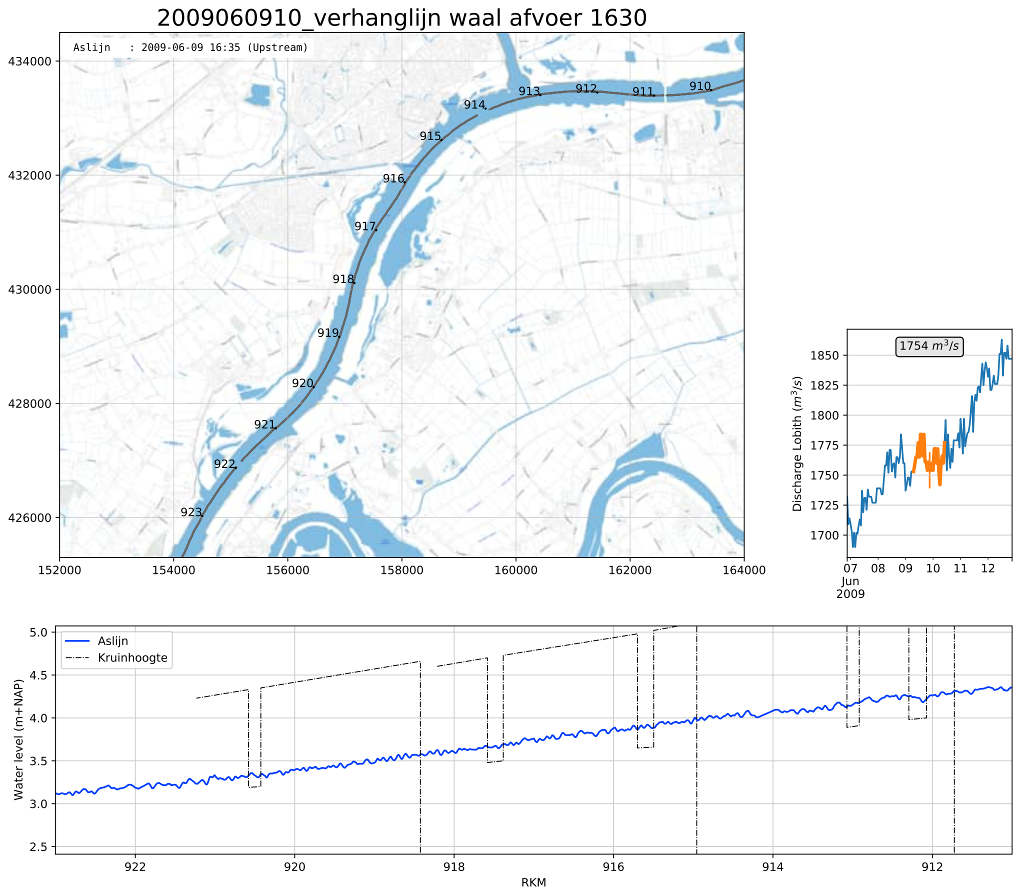

Figure B.7 Verhanglijnmeting van 2009-06-09 (afvoer Lobith: 1754 m^3/s)

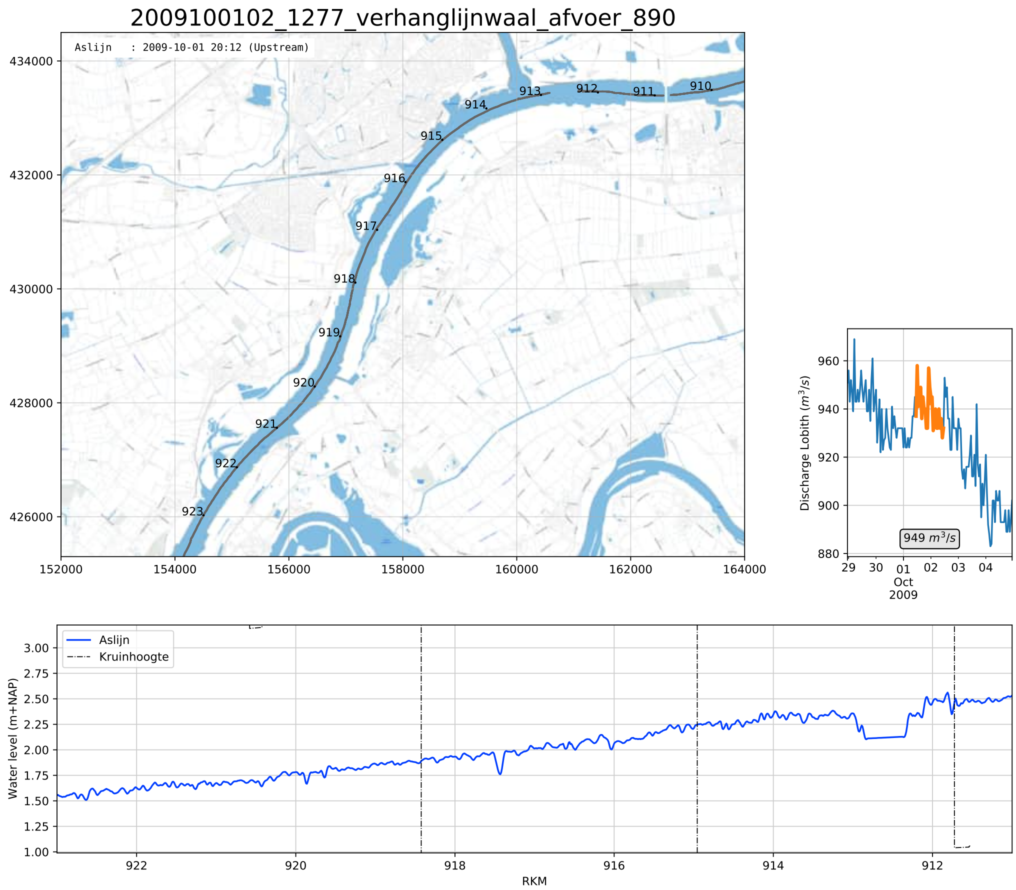

Figure B.8 Verhanglijnmeting van 2009-10-01 (afvoer Lobith: 949 m^3/s)

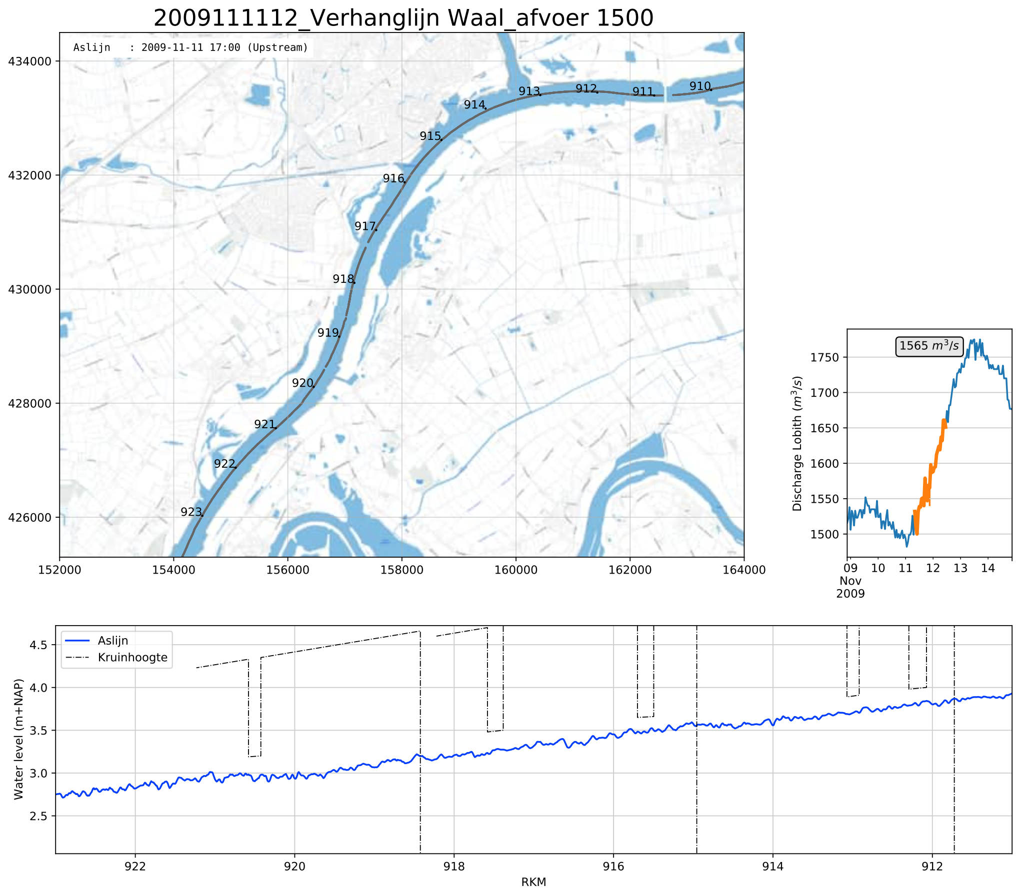

Figure B.9 Verhanglijnmeting van 2009-11-11 (afvoer Lobith: 1565 m^3/s)

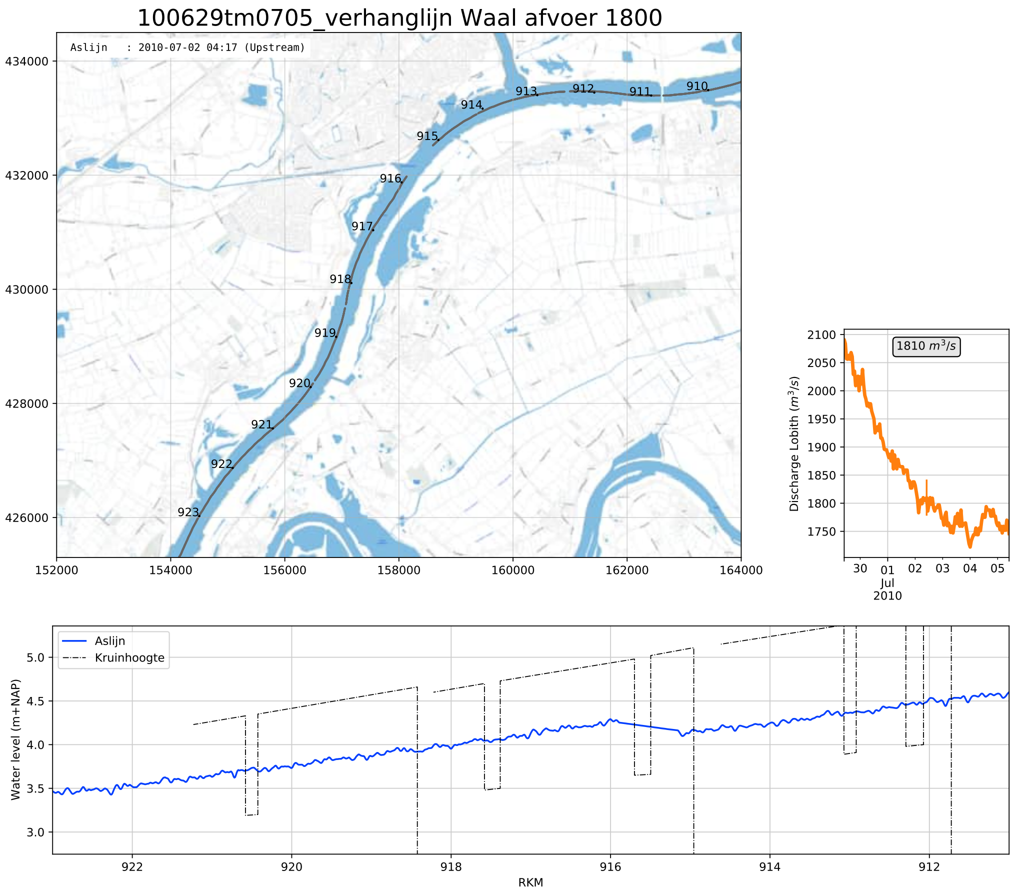

Figure B.10 Verhanglijnmeting van 2010-07-02 (afvoer Lobith: 1810 m^3/s)

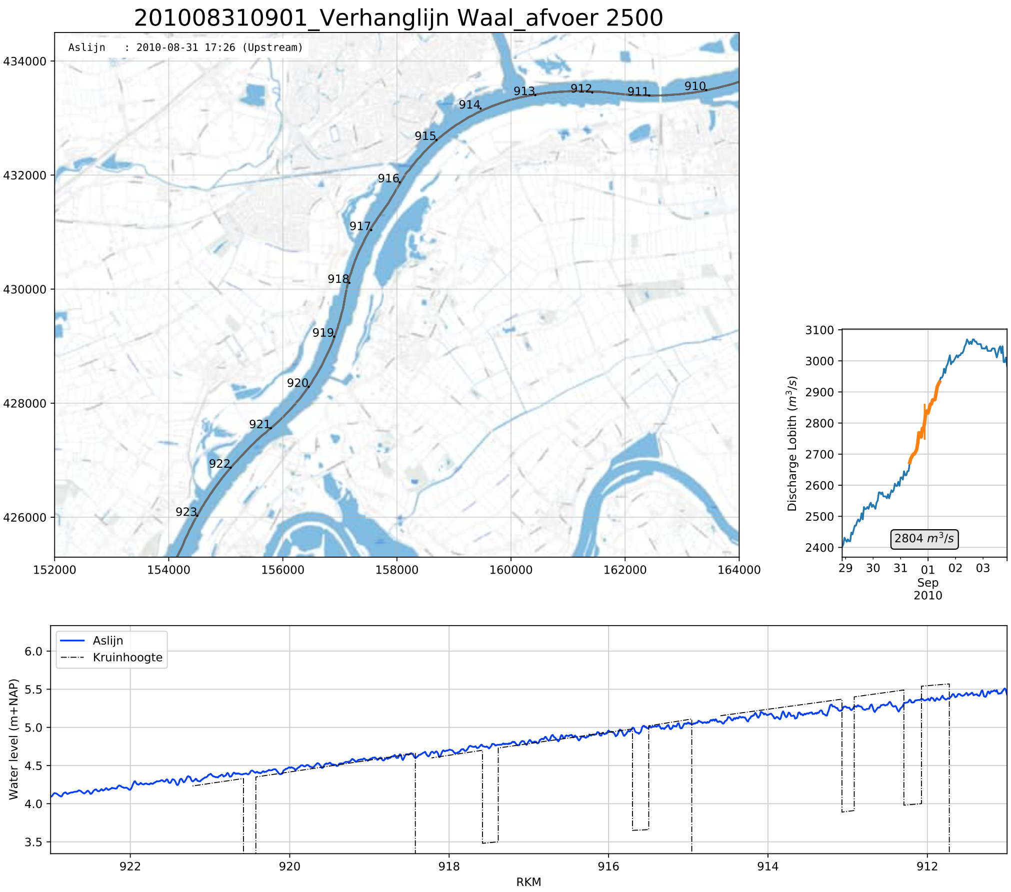

Figure B.11 Verhanglijnmeting van 2010-08-31 (afvoer Lobith: 2804 m^3/s)

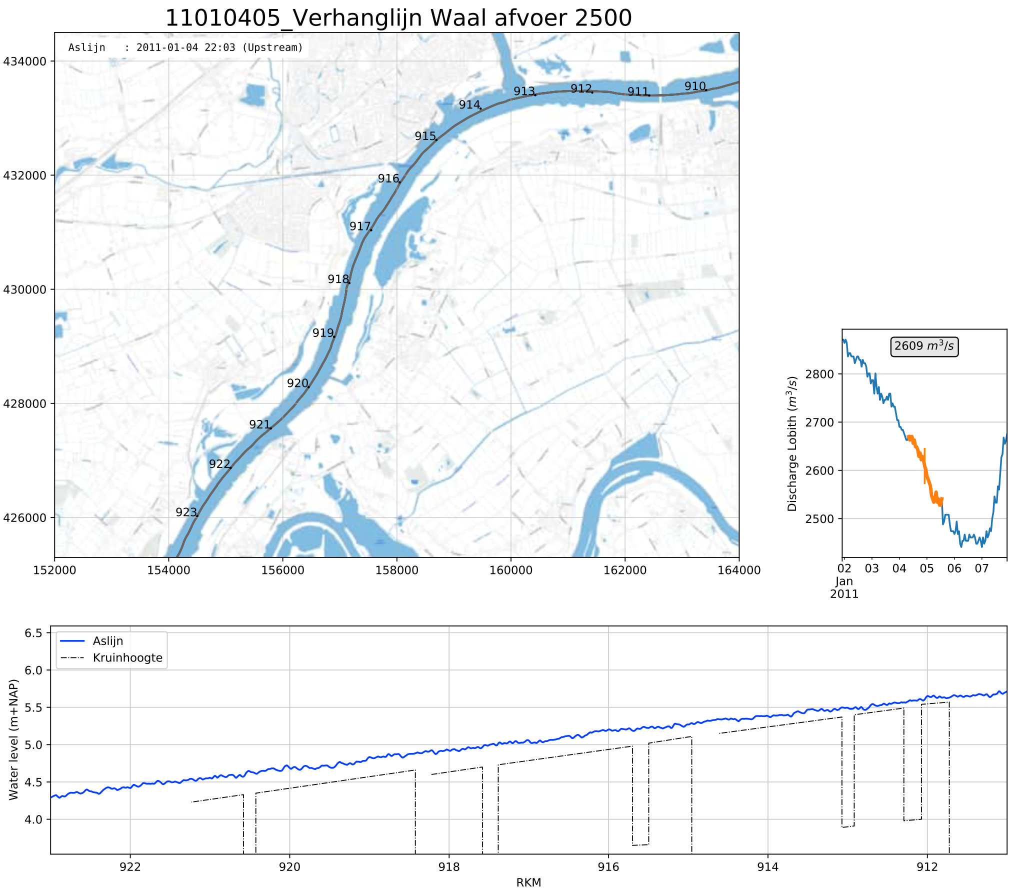

Figure B.12 Verhanglijnmeting van 2011-01-04 (afvoer Lobith: 2609 m^3/s)

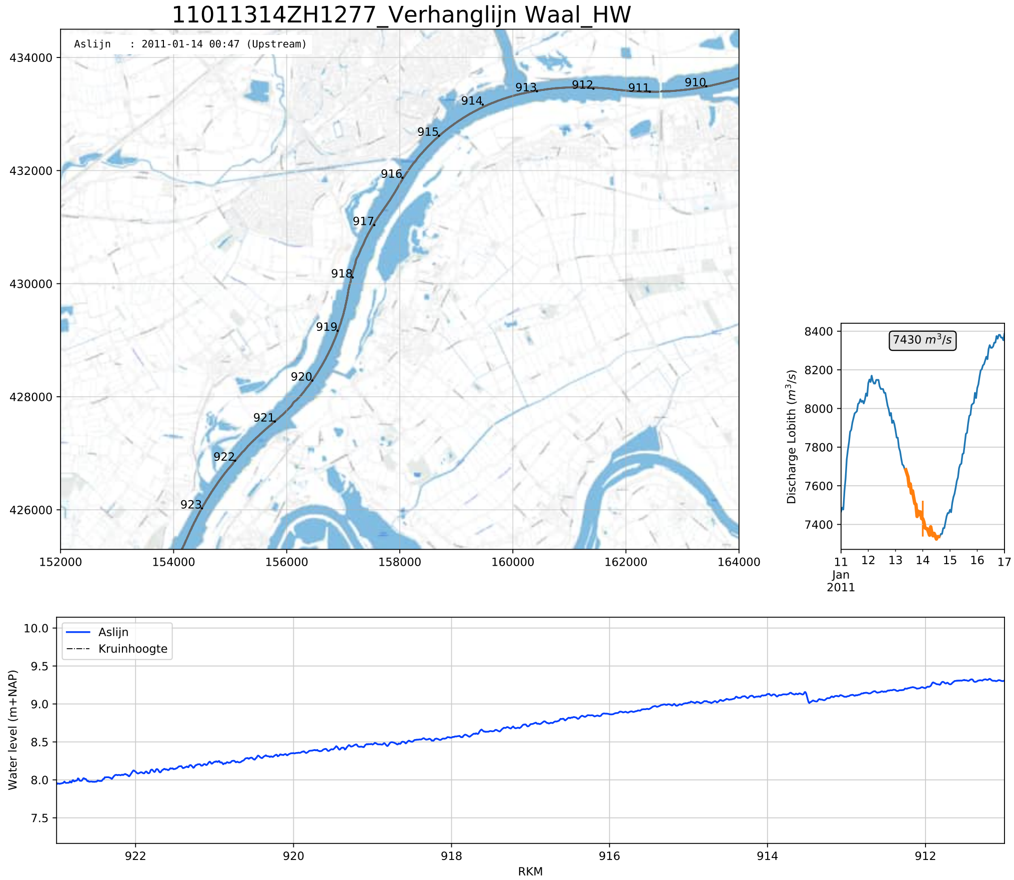

Figure B.13 Verhanglijnmeting van 2011-01-13 (afvoer Lobith: 7430 m^3/s)

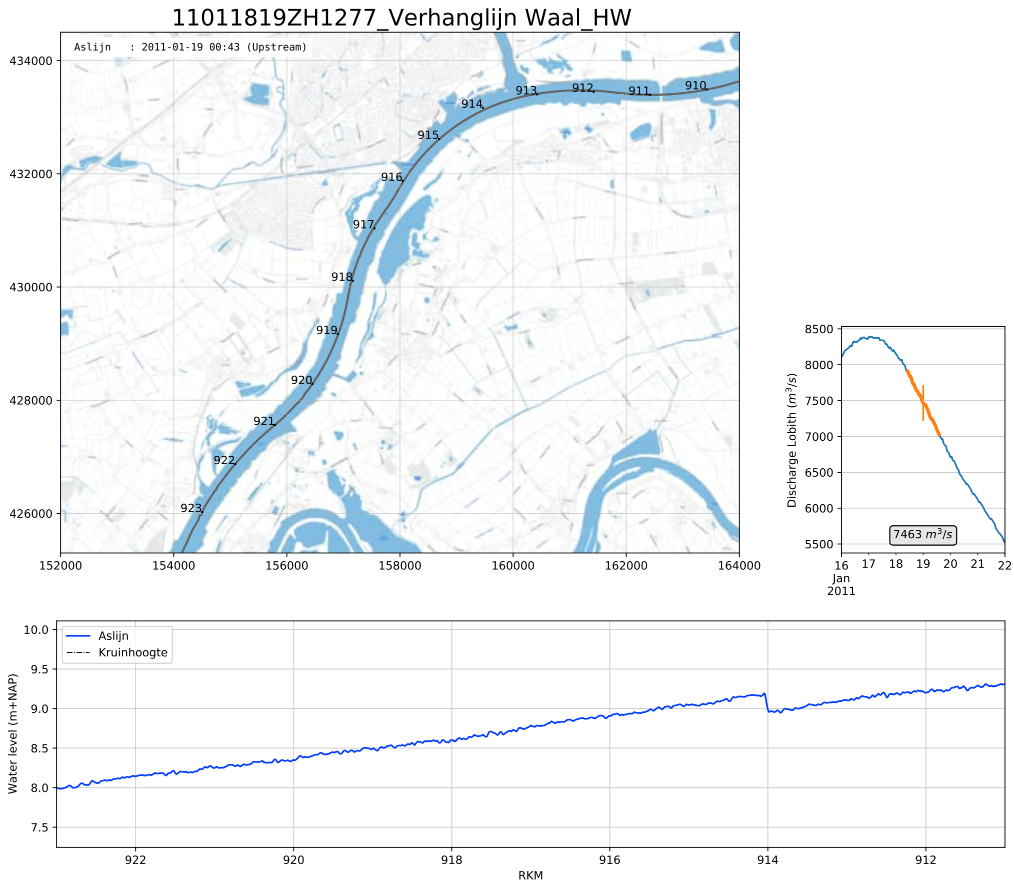

Figure B.14 Verhanglijnmeting van 2011-01-18 (afvoer Lobith: 7463 m^3/s)

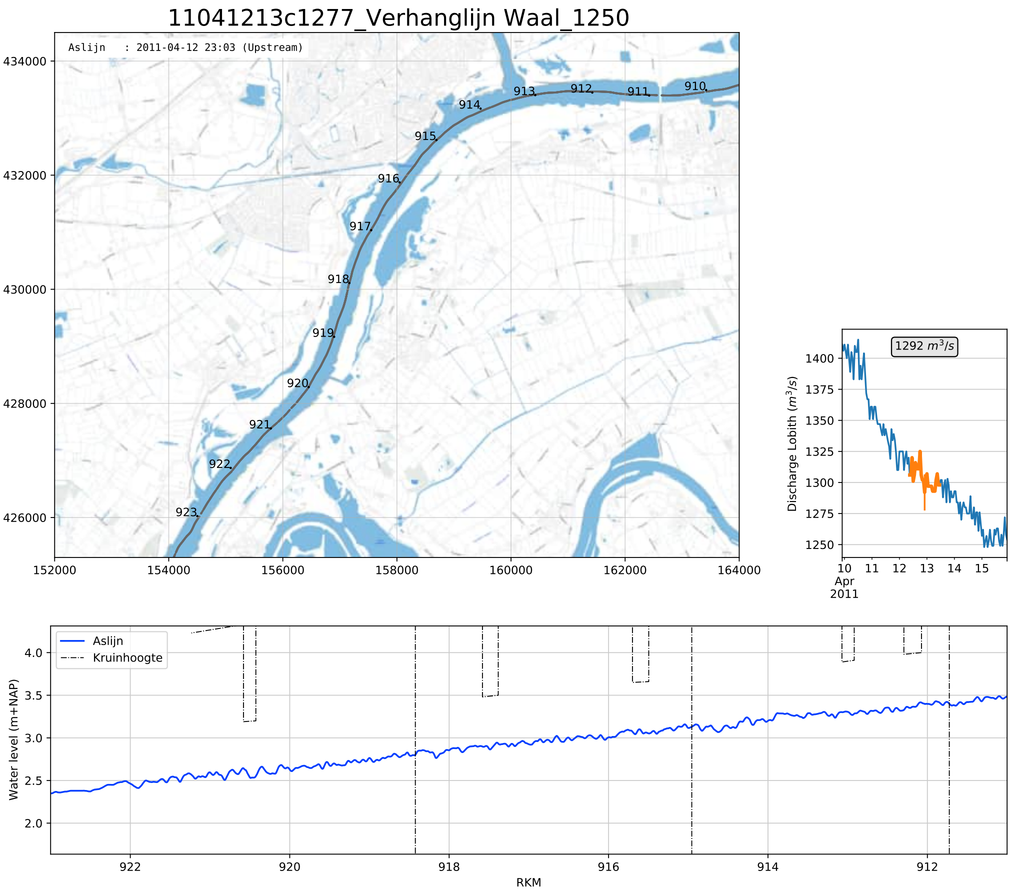

Figure B.15 Verhanglijnmeting van 2011-04-12 (afvoer Lobith: 1292 m^3/s)

Deltares

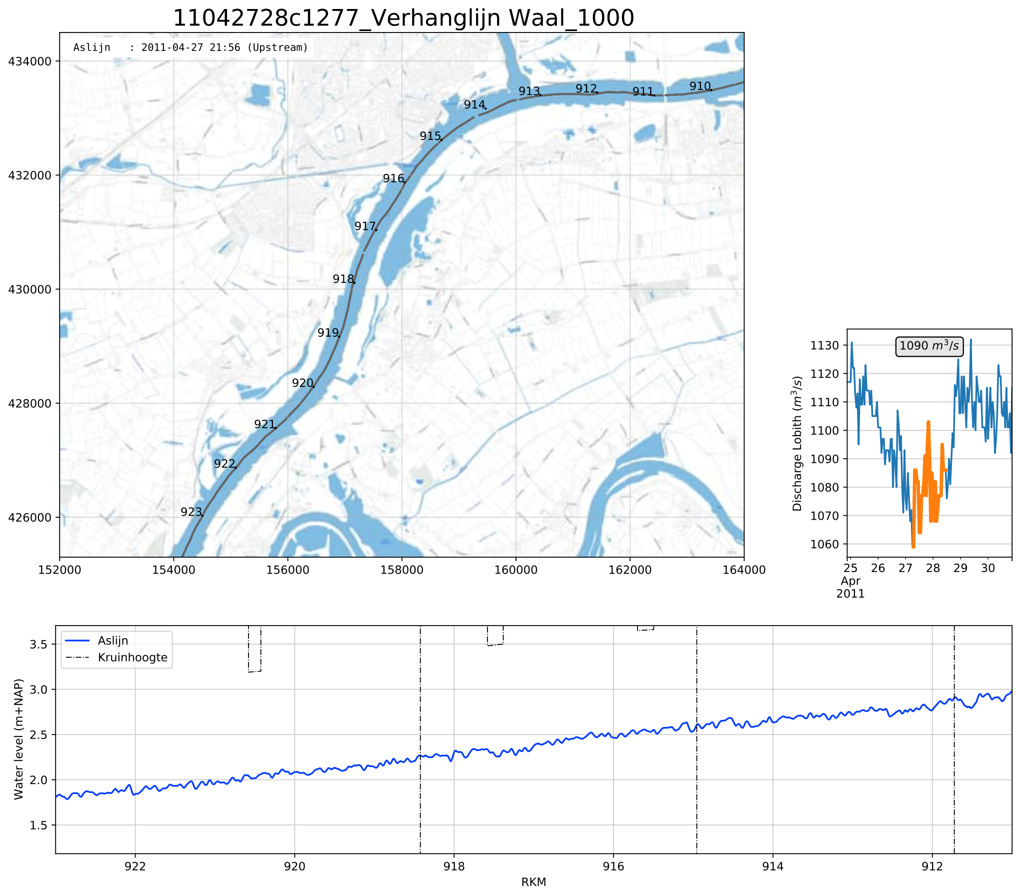

Figure B.16 Verhanglijnmeting van 2011-04-27 (afvoer Lobith: 1090 m^3/s)

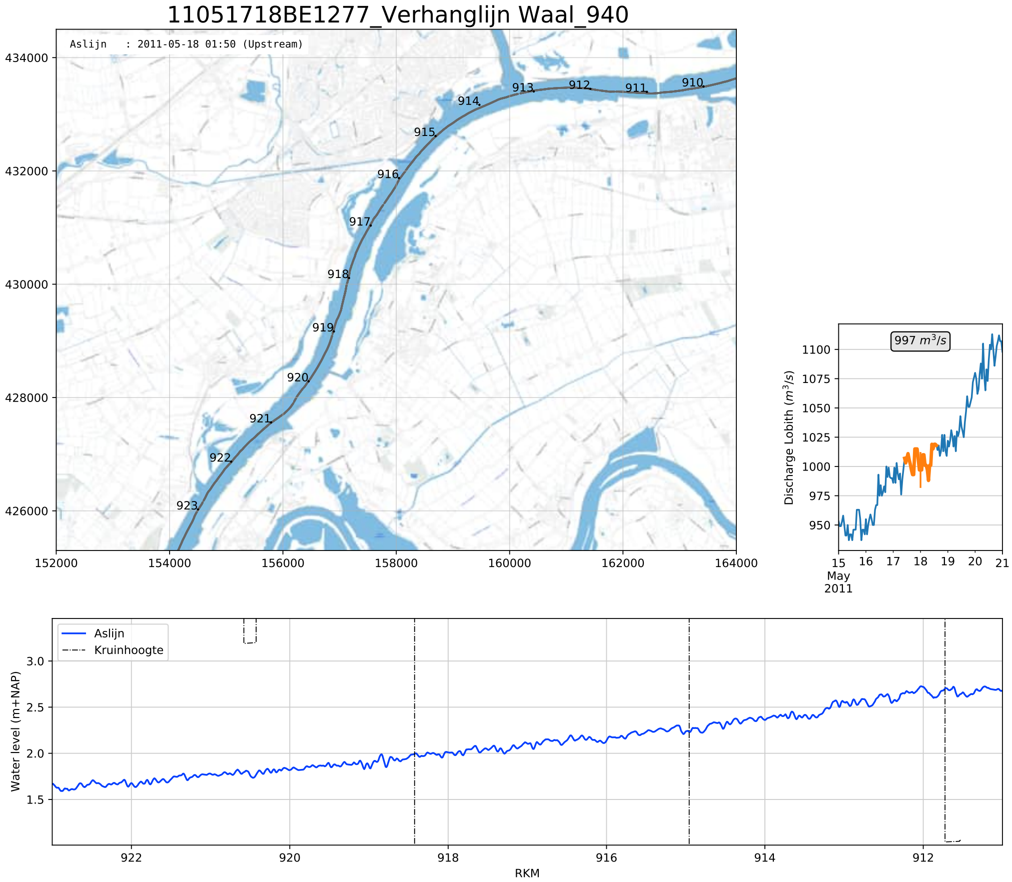

Figure B.17 Verhanglijnmeting van 2011-05-18 (afvoer Lobith: 997 m^3/s)

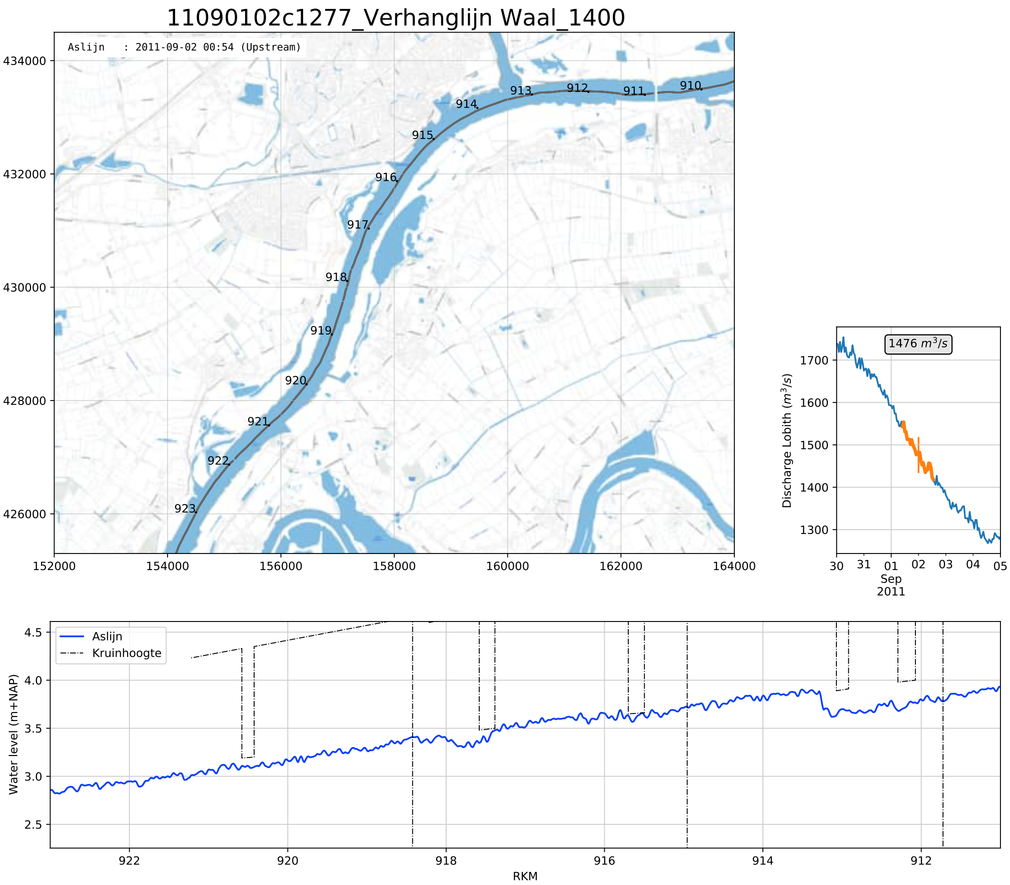

Figure B.18 Verhanglijnmeting van 2011-09-01 (afvoer Lobith: 1476 m^3/s)

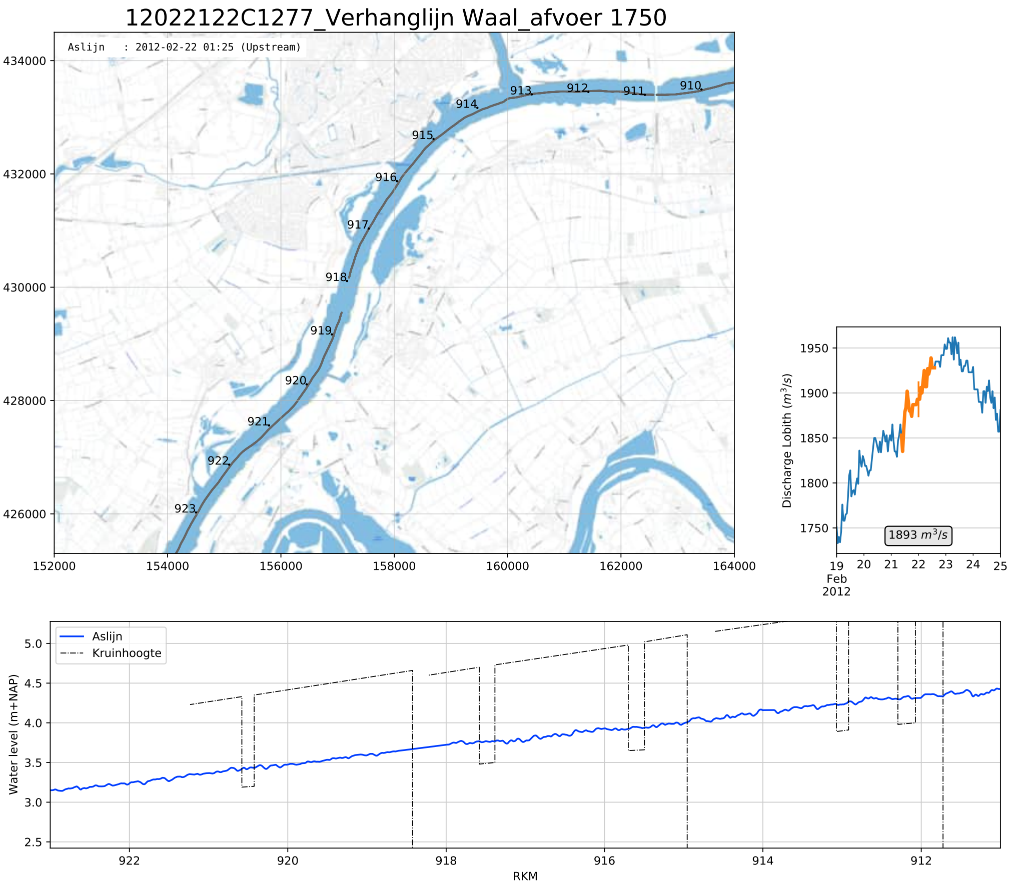

Figure B.19 Verhanglijnmeting van 2012-02-21 (afvoer Lobith: 1893 m^3/s)

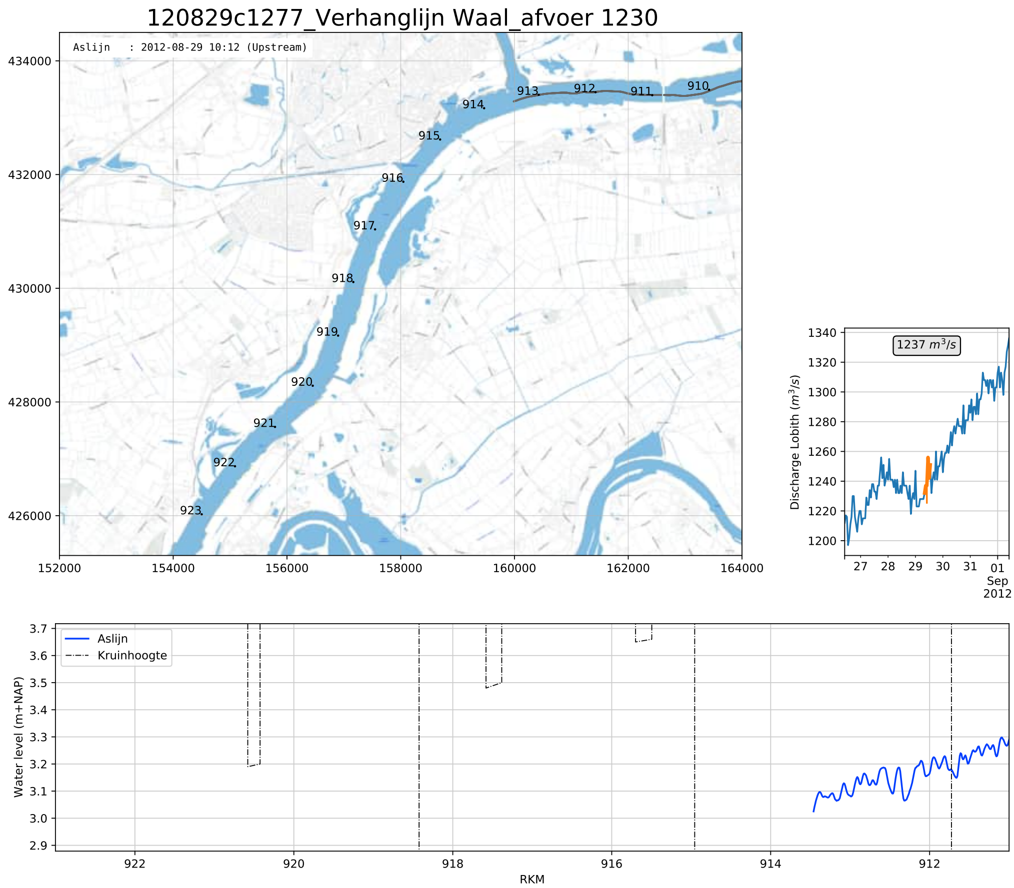

Figure B.20 Verhanglijnmeting van 2012-08-29 (afvoer Lobith: 1237 m^3/s)

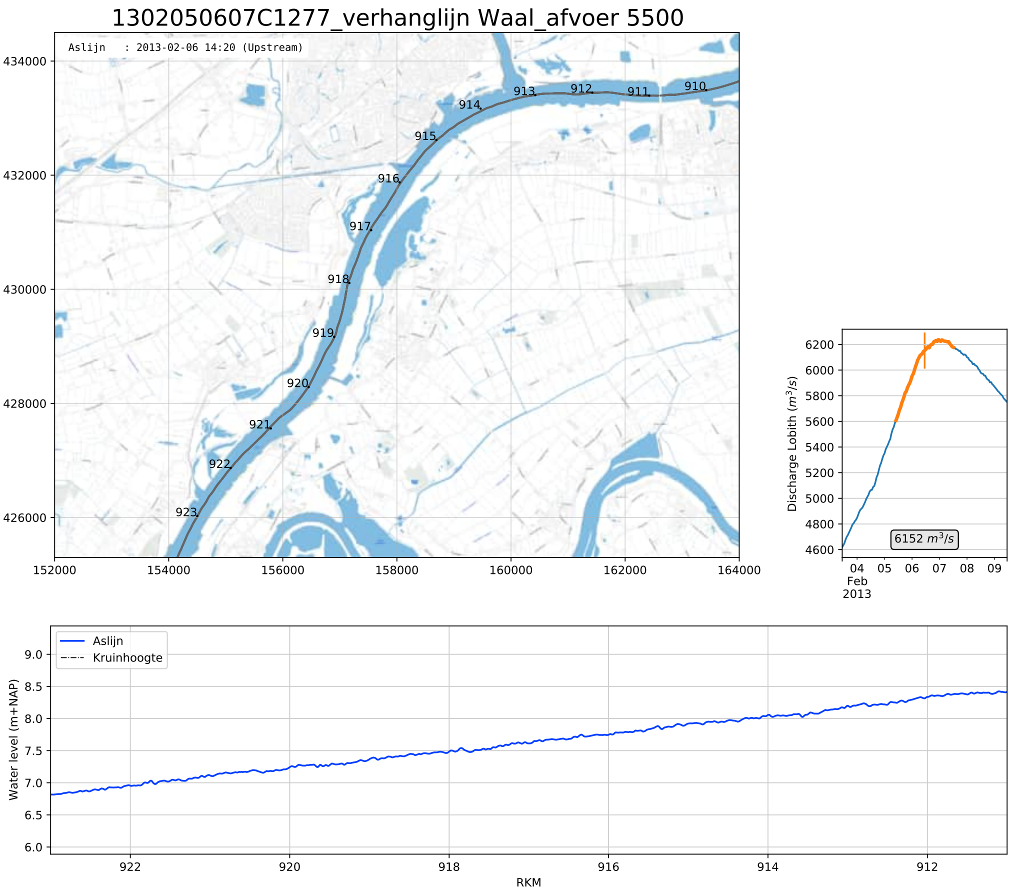

Figure B.21 Verhanglijnmeting van 2013-02-06 (afvoer Lobith: 6152 m^3/s)

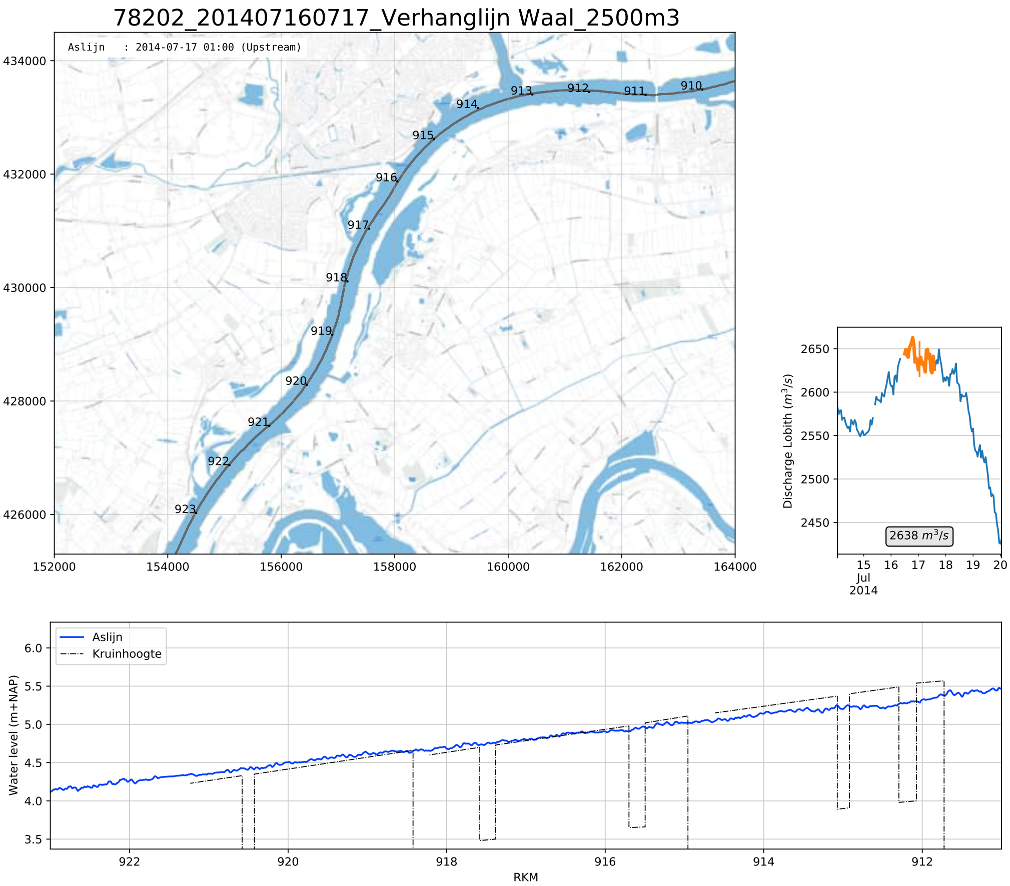

Figure B.22 Verhanglijnmeting van 2014-07-17 (afvoer Lobith: 2638 m^3/s)

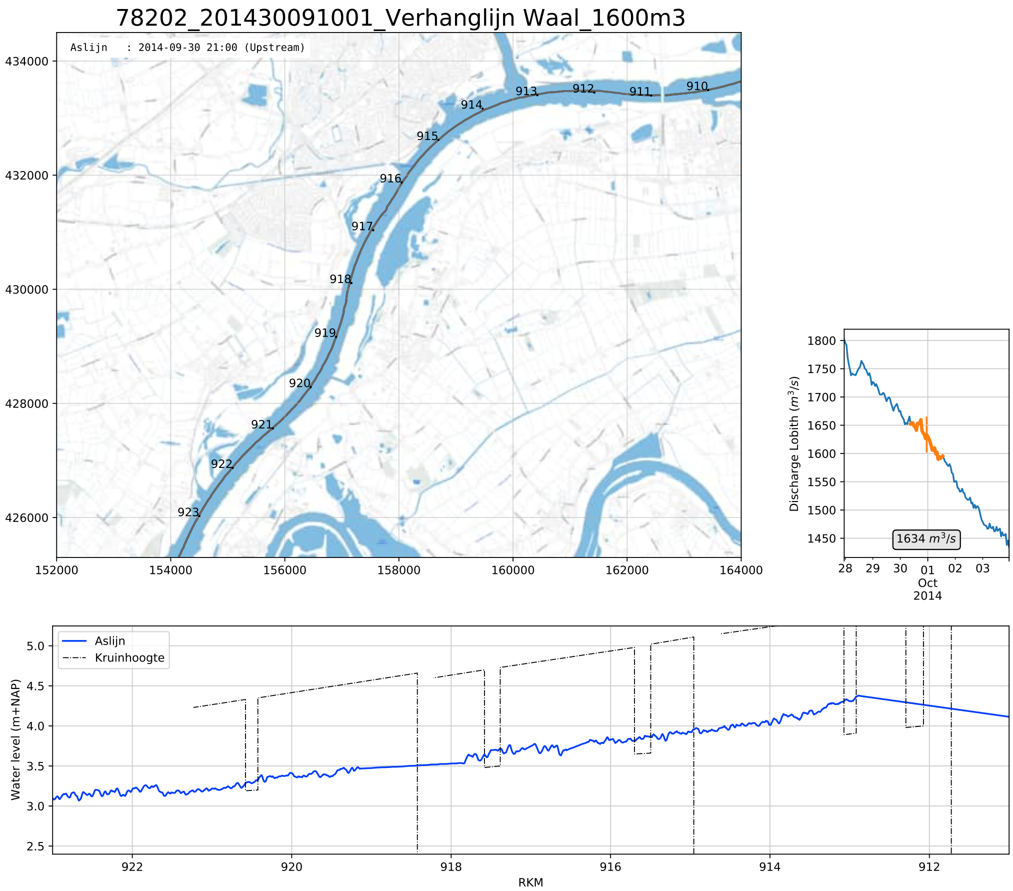

Figure B.23 Verhanglijnmeting van 2014-09-30 (afvoer Lobith: 1634 m^3/s)

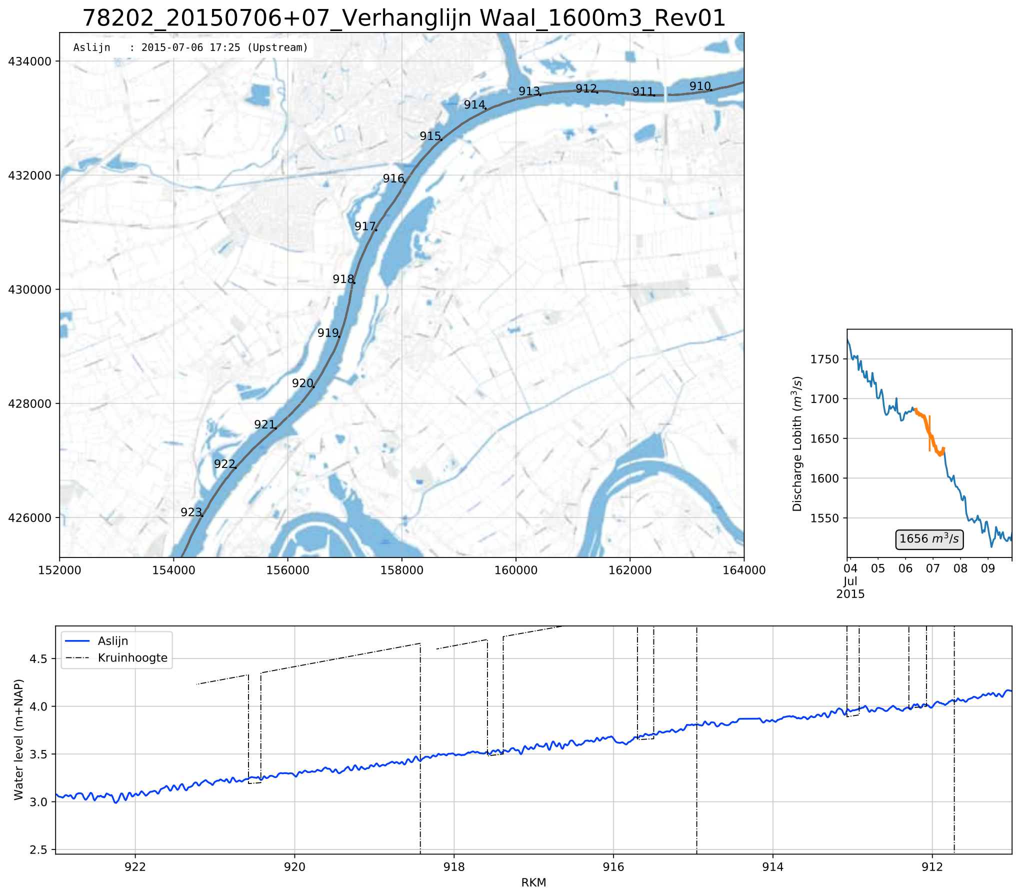

Figure B.24 Verhanglijnmeting van 2015-07-06 (afvoer Lobith: 1656 m^3/s)

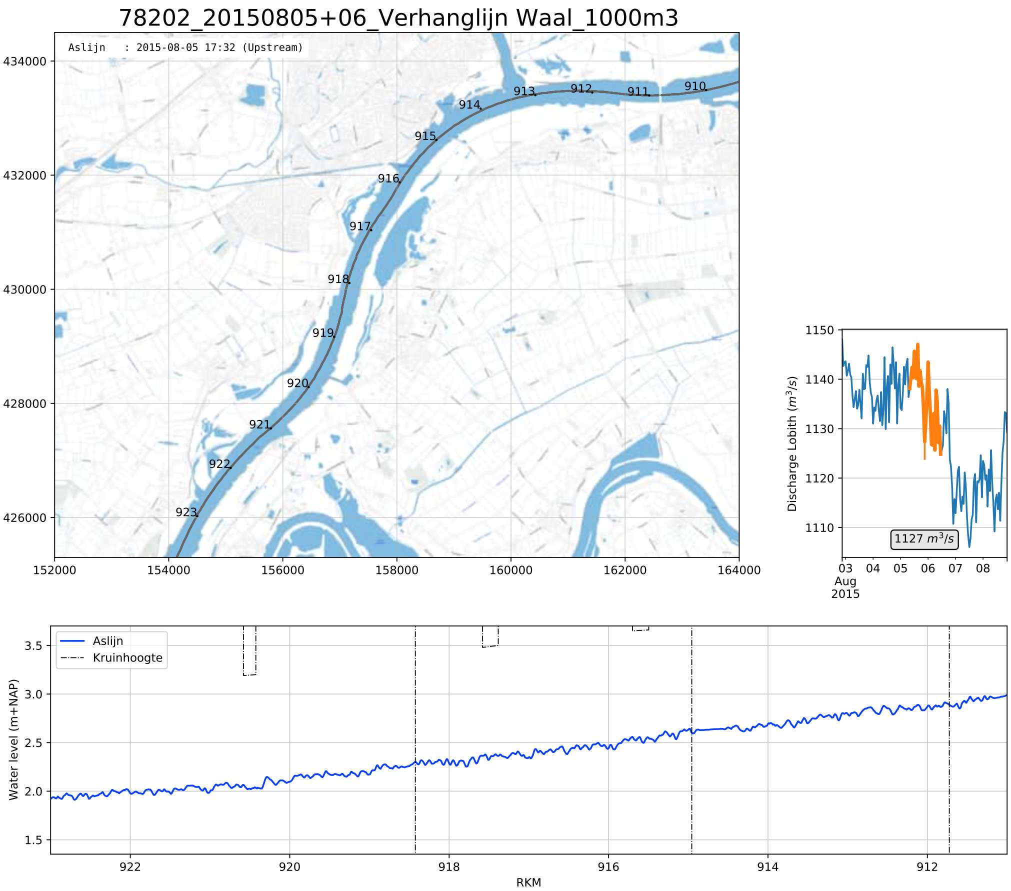

Figure B.25 Verhanglijnmeting van 2015-08-05 (afvoer Lobith: 1127 m^3/s)

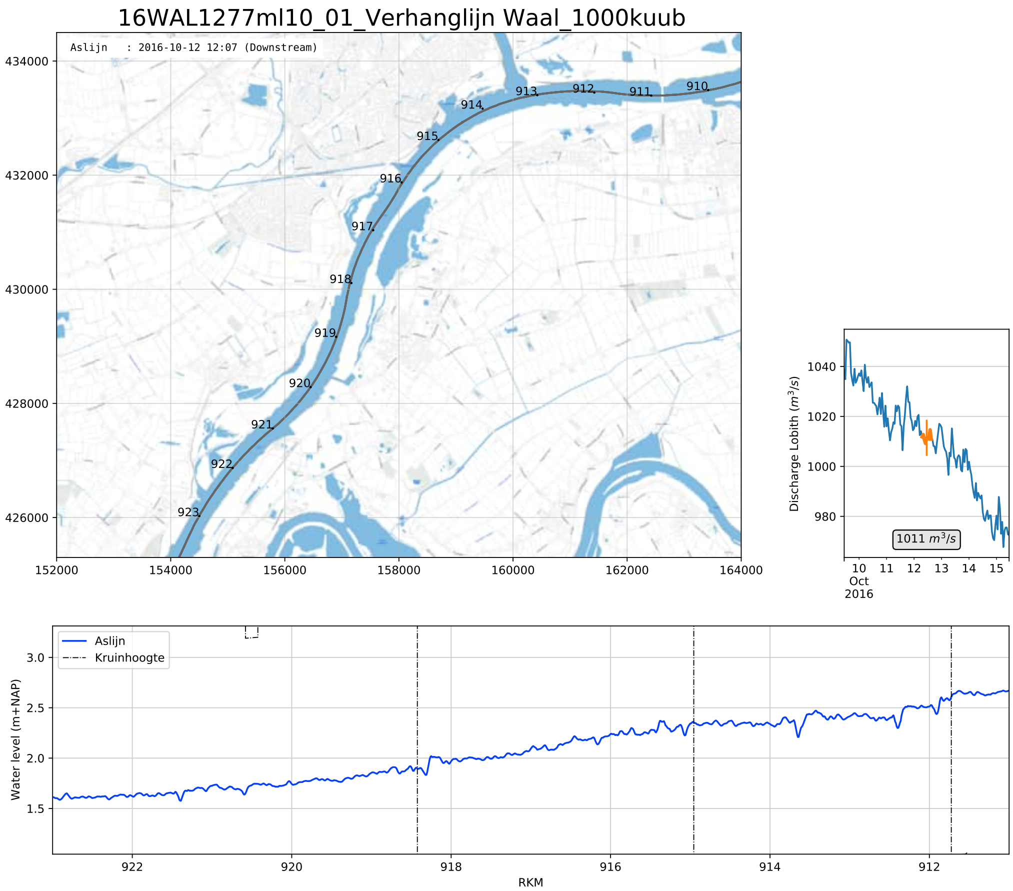

Figure B.26 Verhanglijnmeting van 2016-10-12 (afvoer Lobith: 1011 m^3/s)

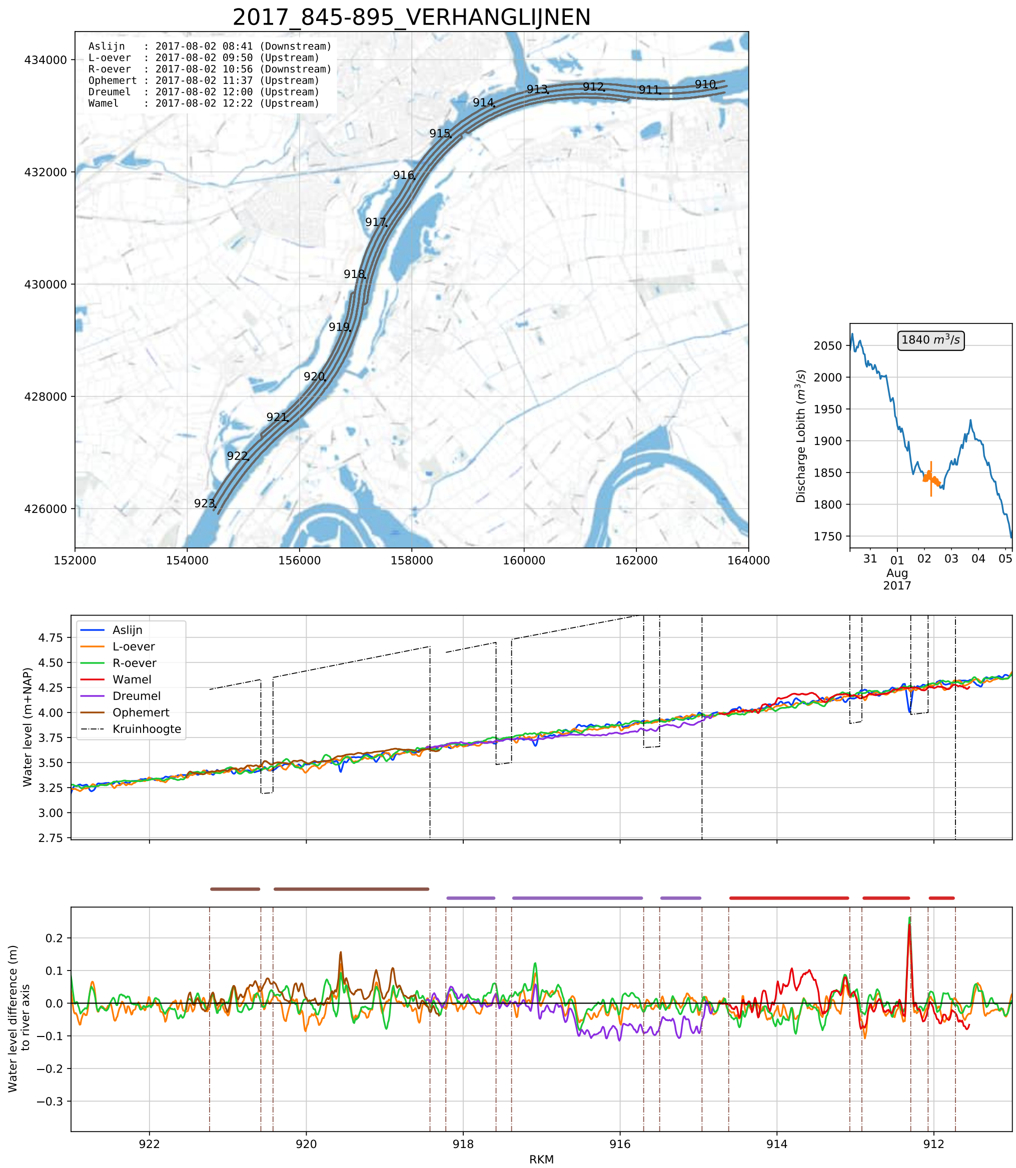

Figure B.27 Verhanglijnmeting van 2017-08-02 (afvoer Lobith: 1840 m^3/s)

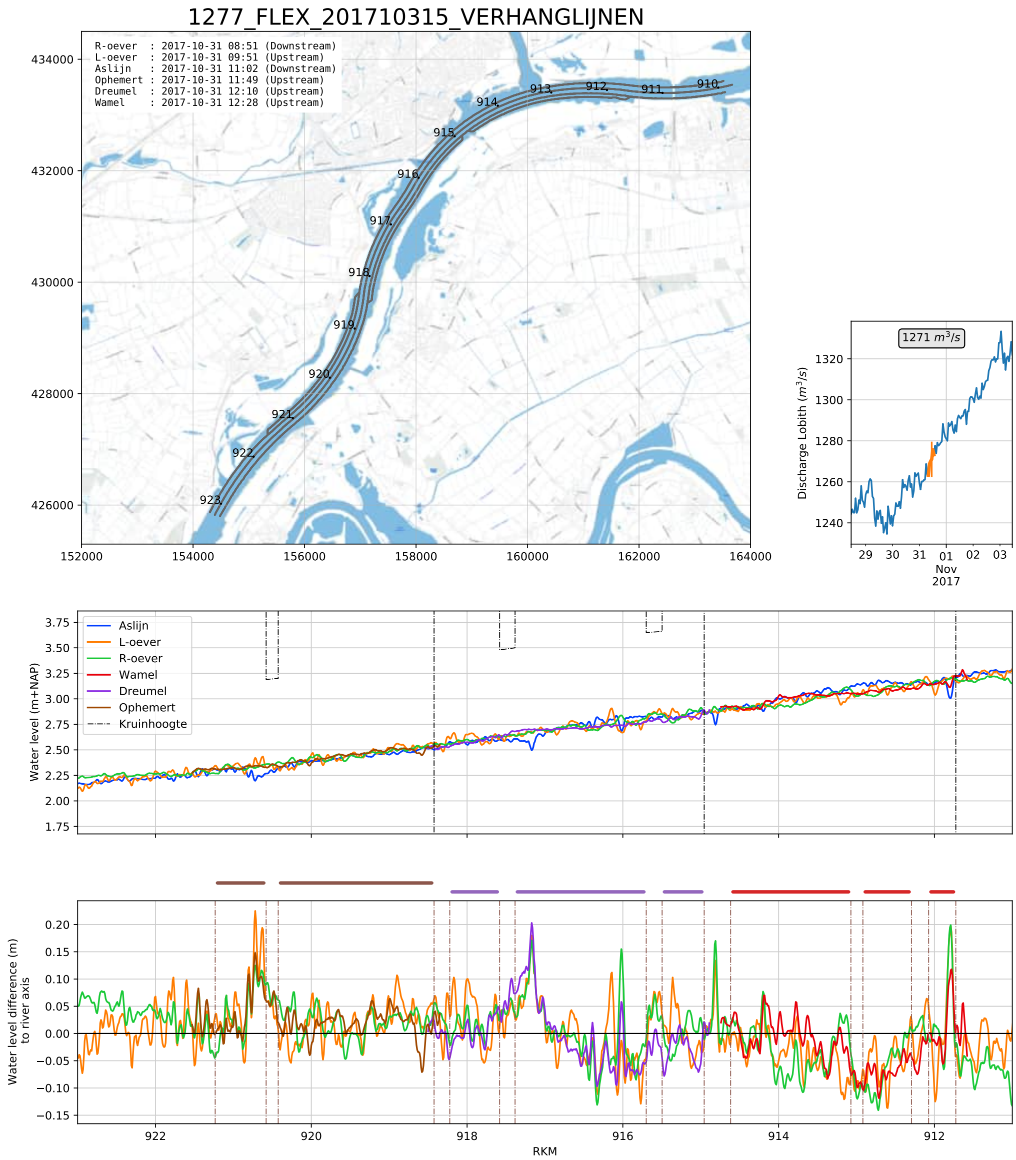

Figure B.28 Verhanglijnmeting van 2017-10-31 (afvoer Lobith: 1271 m^3/s)

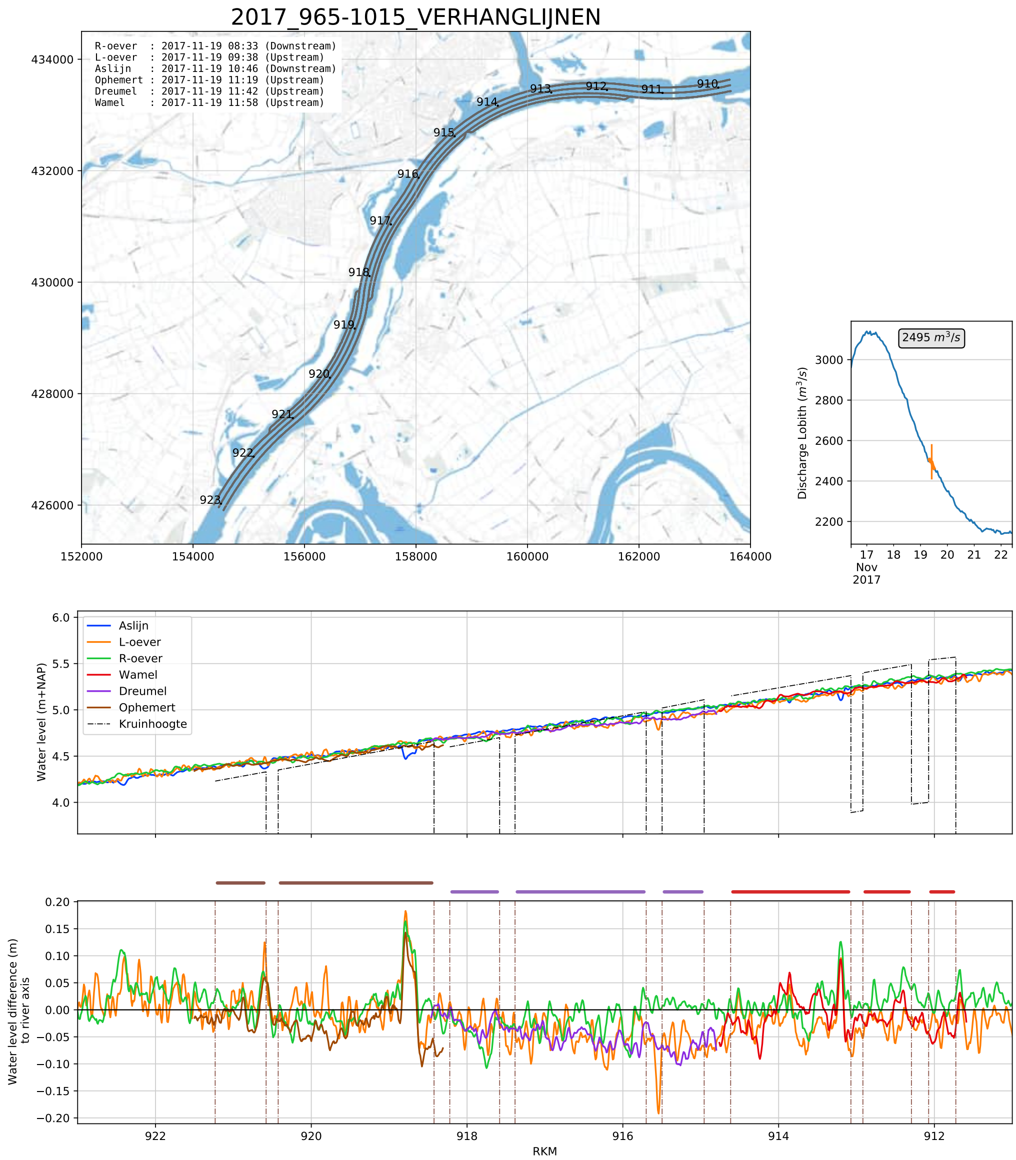

Figure B.29 Verhanglijnmeting van 2017-11-19 (afvoer Lobith: 2495 m^3/s)

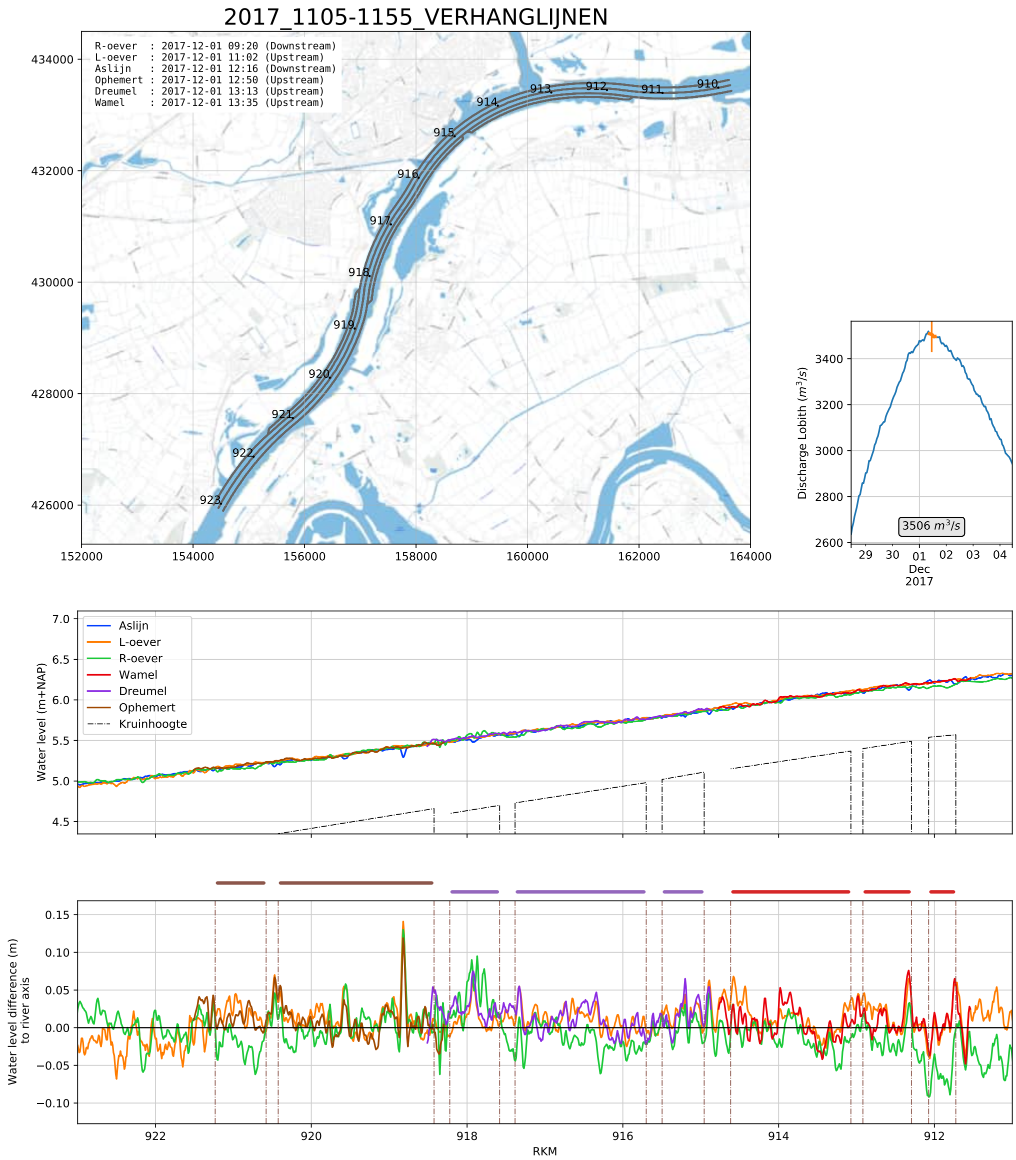

Figure B.30 Verhanglijnmeting van 2017-12-01 (afvoer Lobith: 3506 m^3/s)

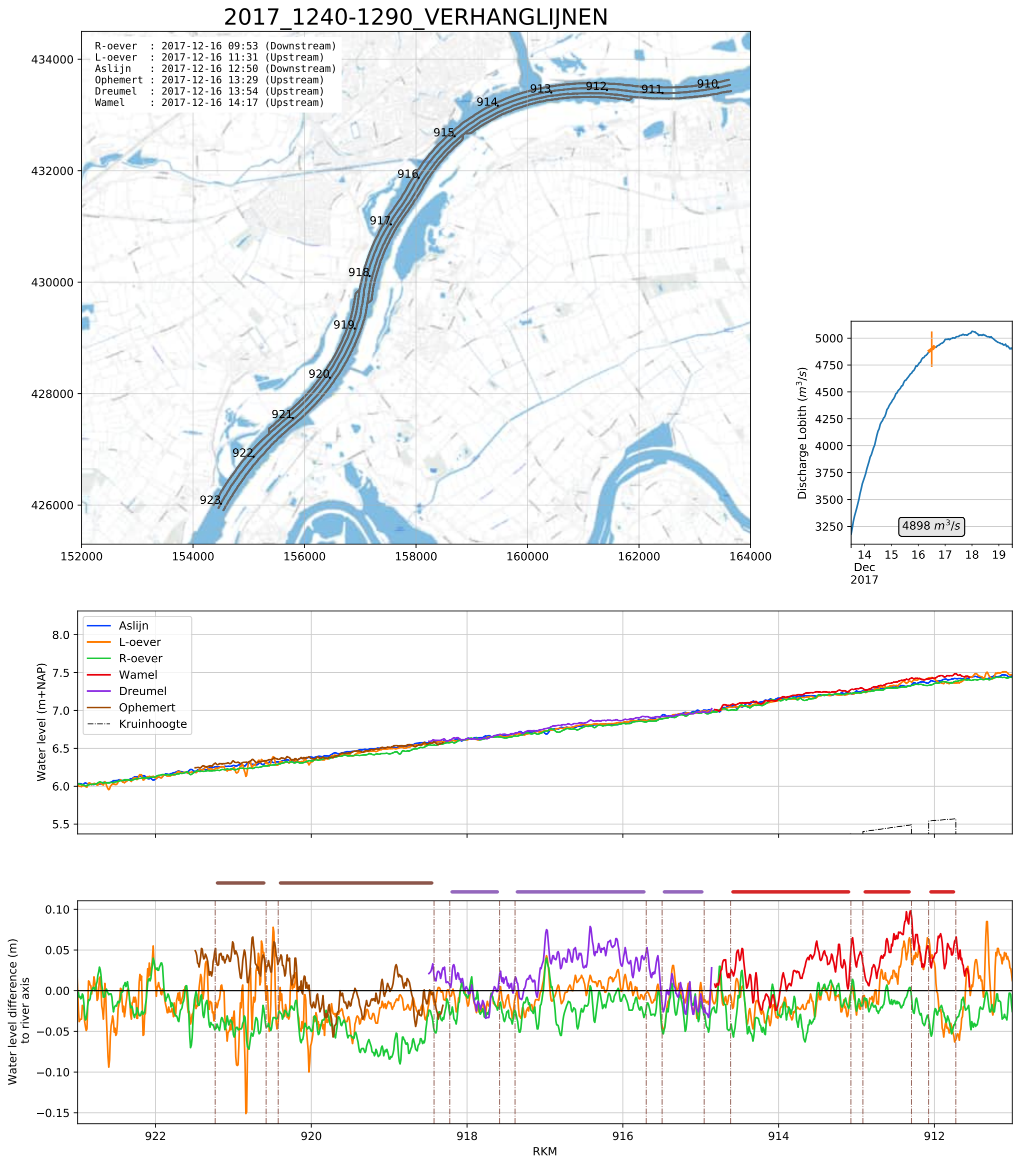

Figure B.31 Verhanglijnmeting van 2017-12-16 (afvoer Lobith: 4898 m^3/s)

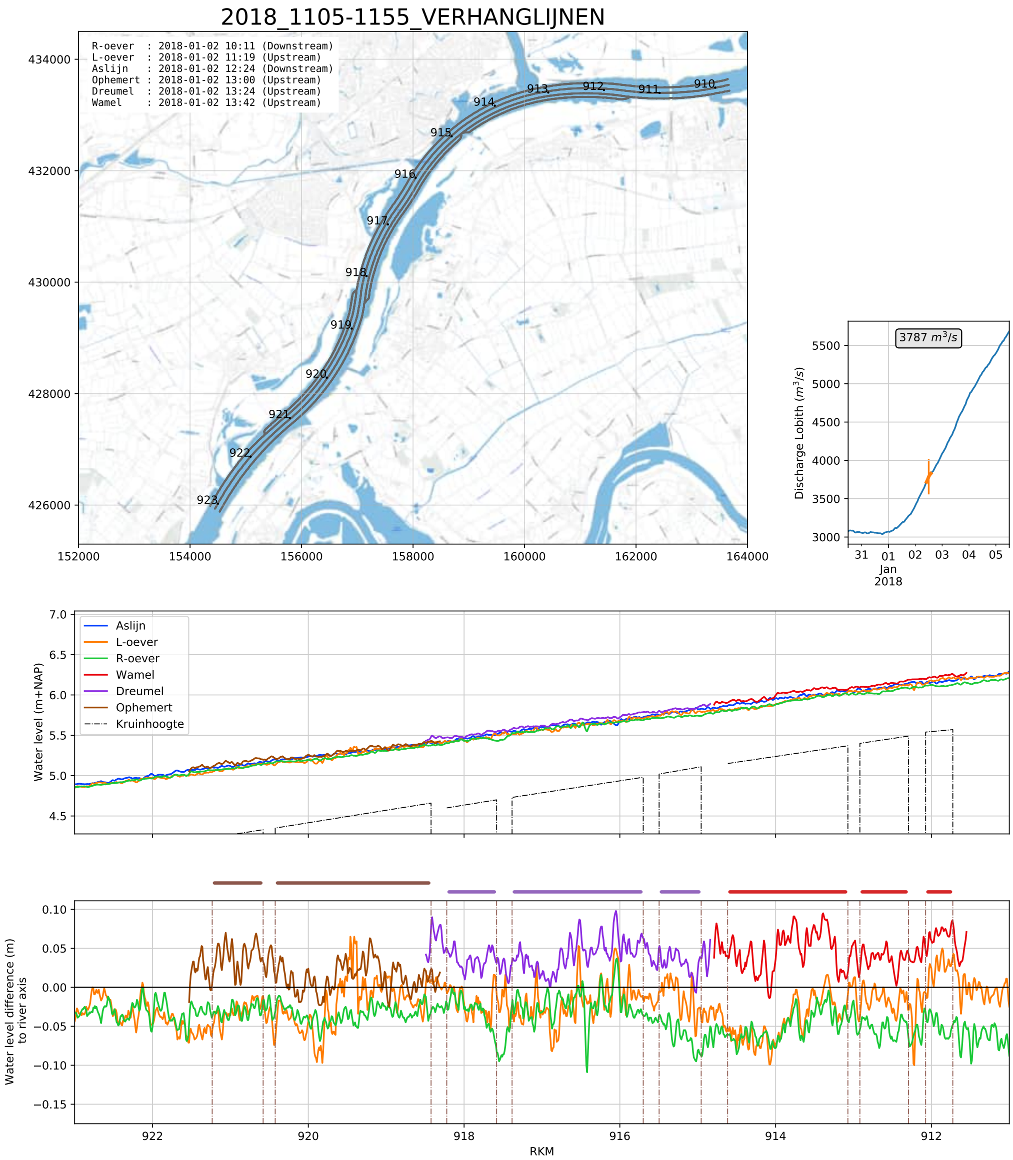

Figure B.32 Verhanglijnmeting van 2018-01-02 (afvoer Lobith: 3787 m^3/s)

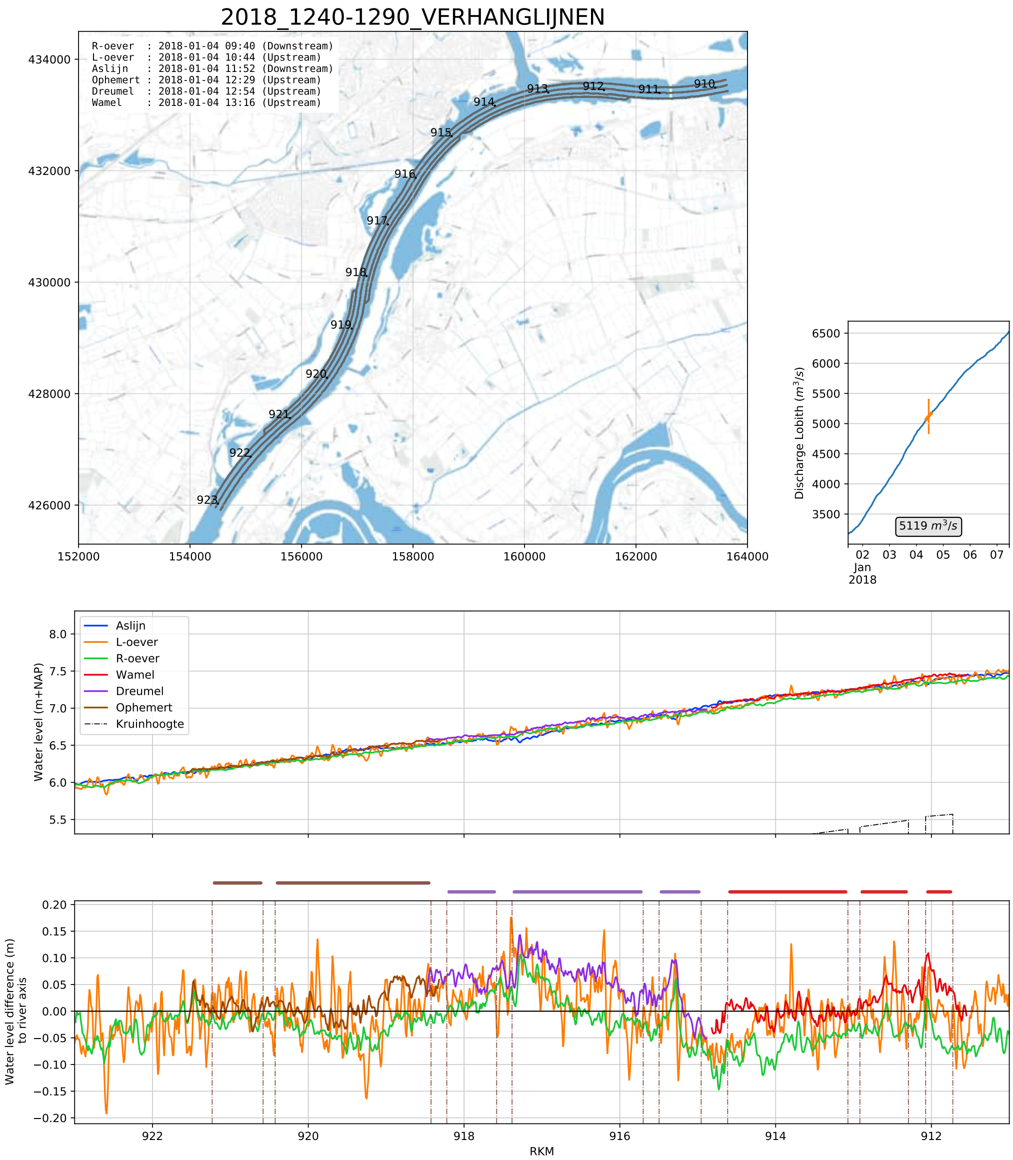

Figure B.33 Verhanglijnmeting van 2018-01-04 (afvoer Lobith: 5119 m^3/s)

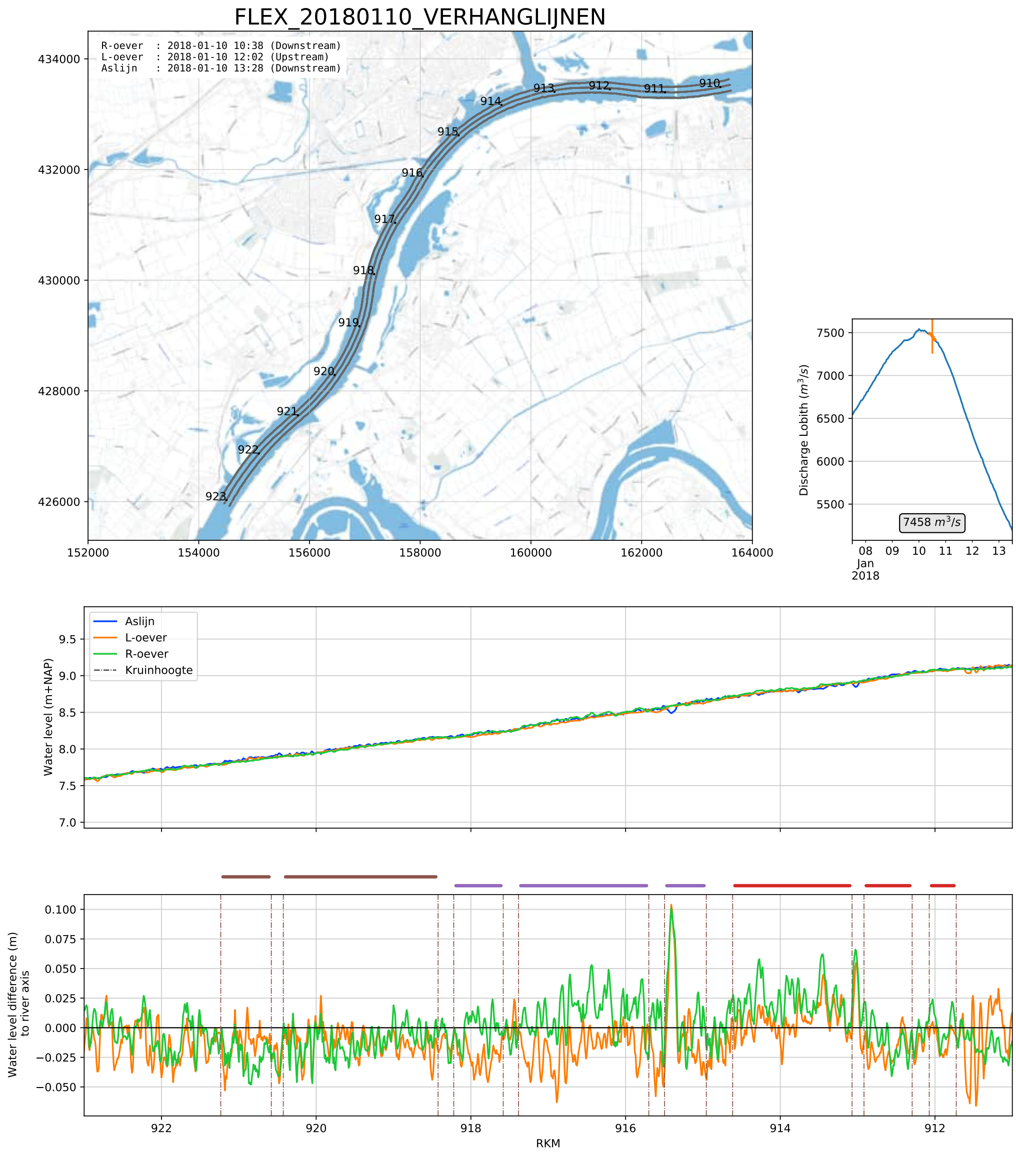

Figure B.34 Verhanglijnmeting van 2018-01-10 (afvoer Lobith: 7458 m^3/s)

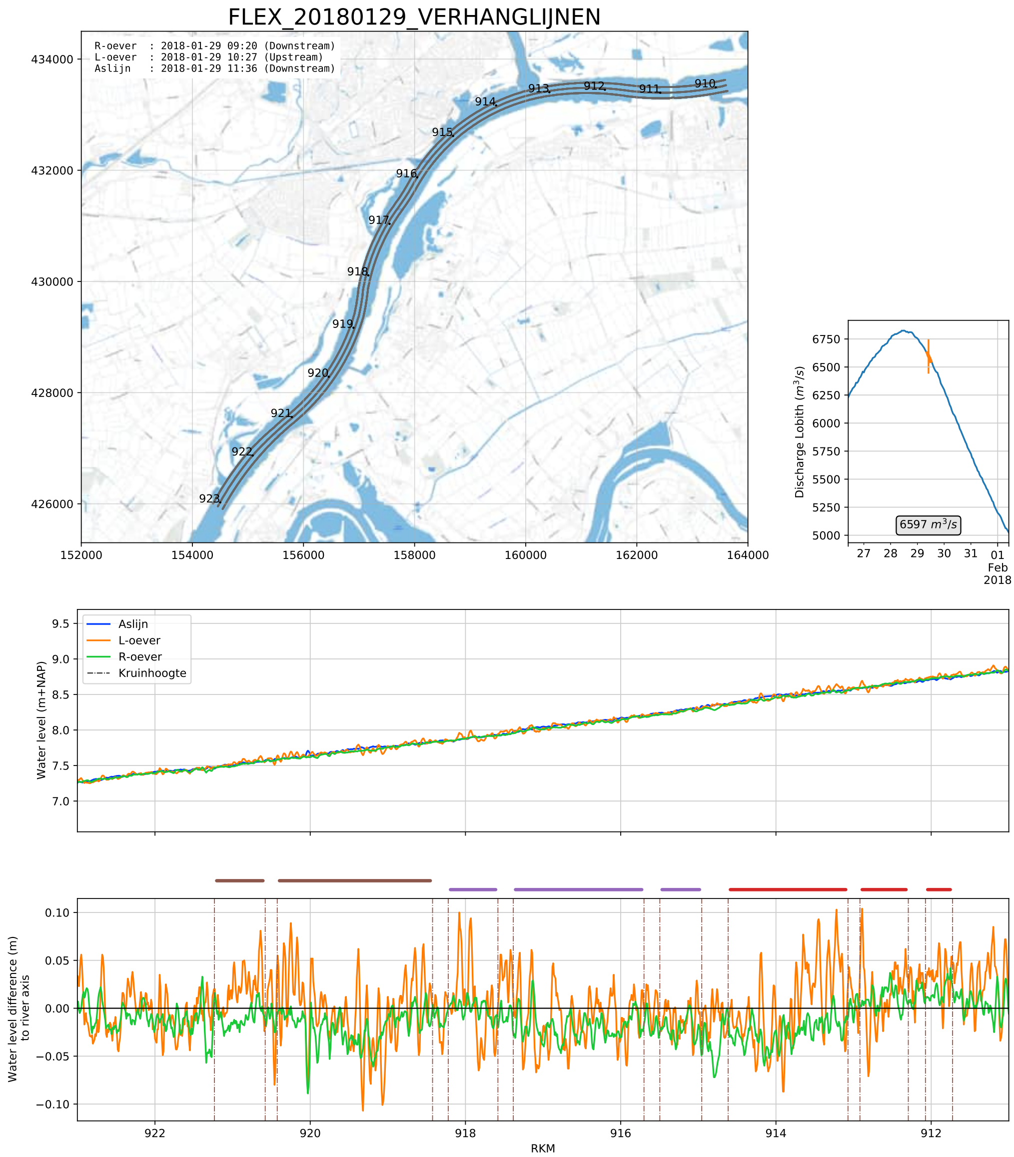

Figure B.35 Verhanglijnmeting van 2018-01-29 (afvoer Lobith: 6597 m^3/s)

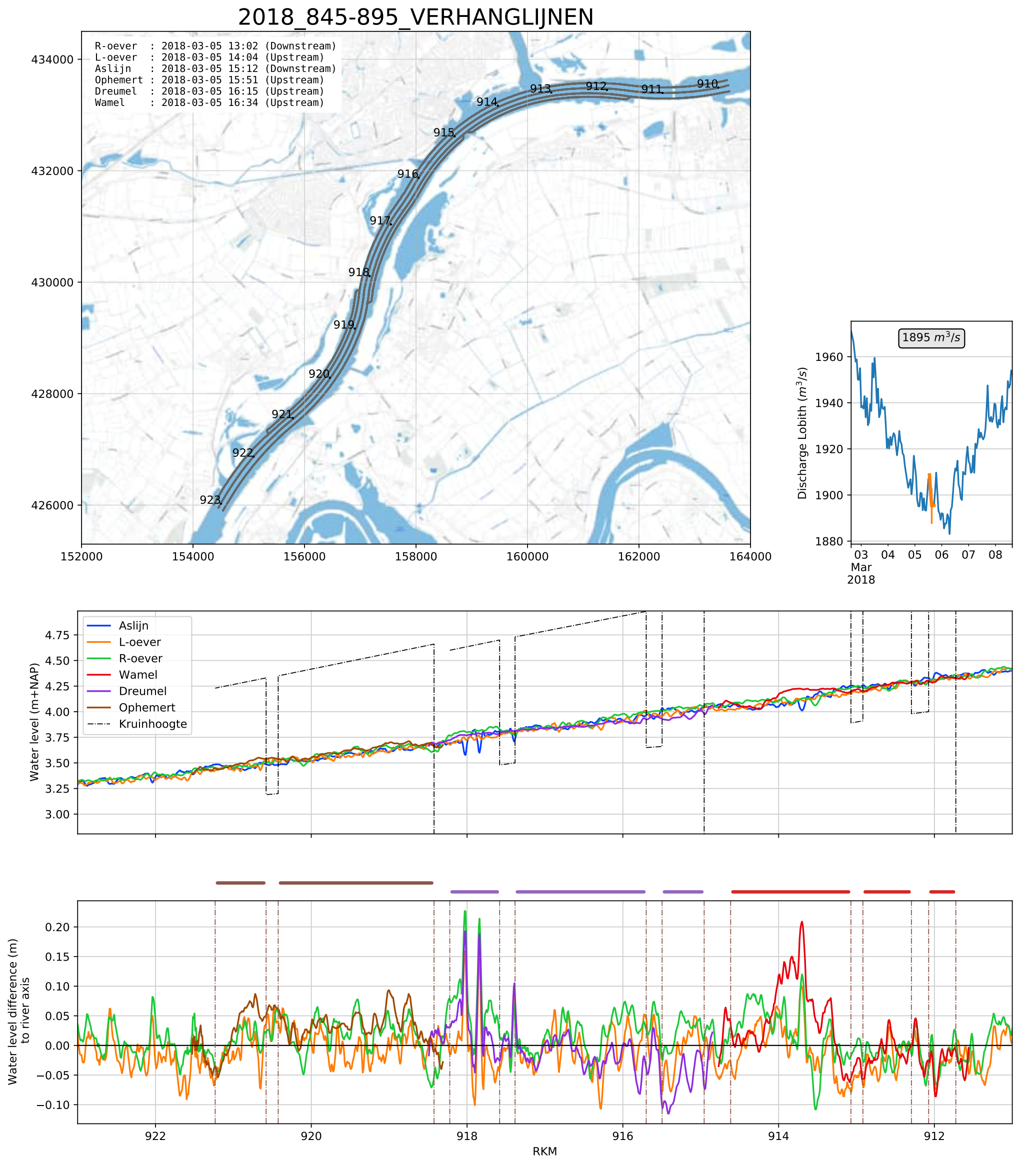

Figure B.36 Verhanglijnmeting van 2018-03-05 (afvoer Lobith: 1895 m^3/s)

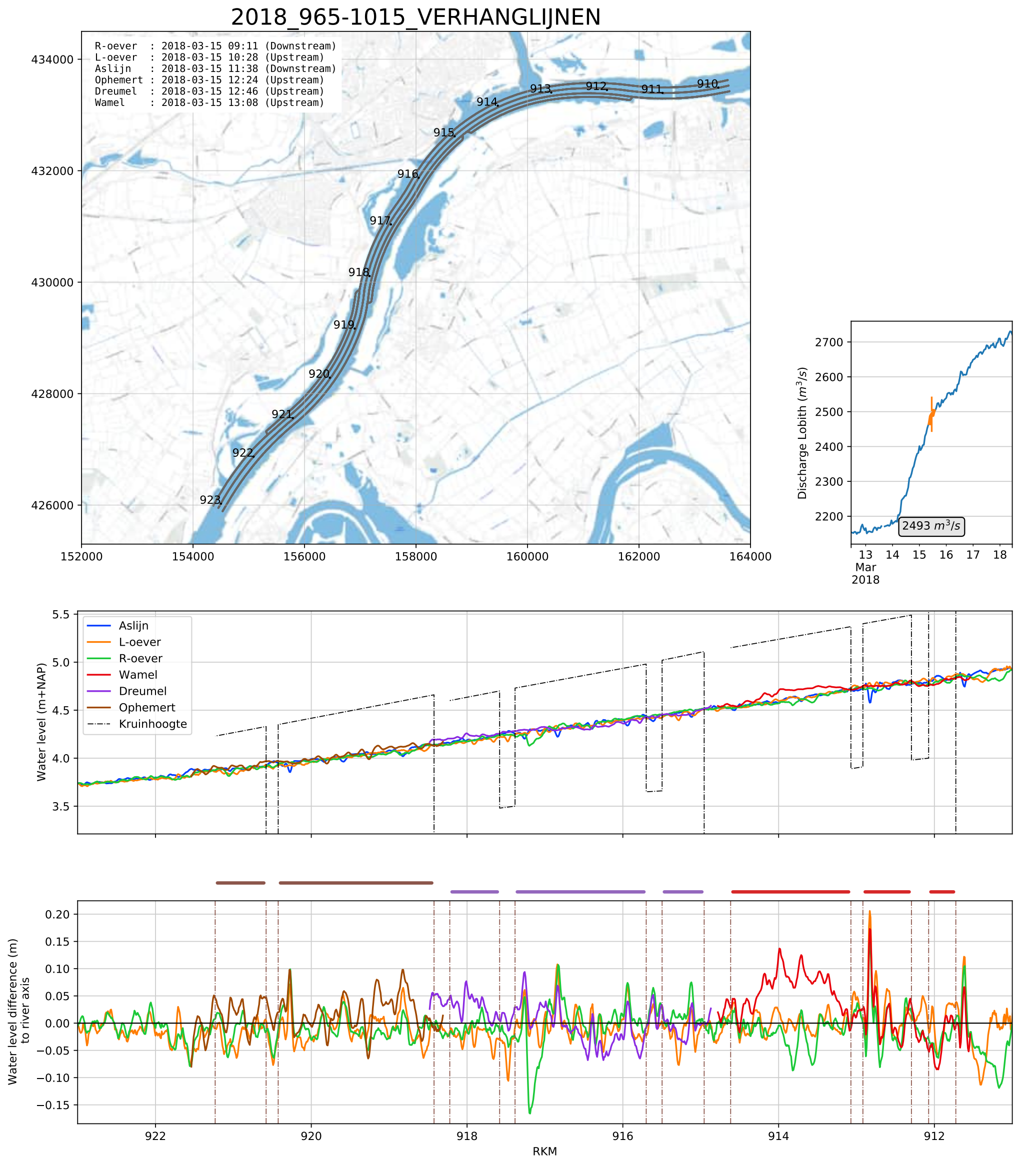

Figure B.37 Verhanglijnmeting van 2018-03-15 (afvoer Lobith: 2493 m^3/s)

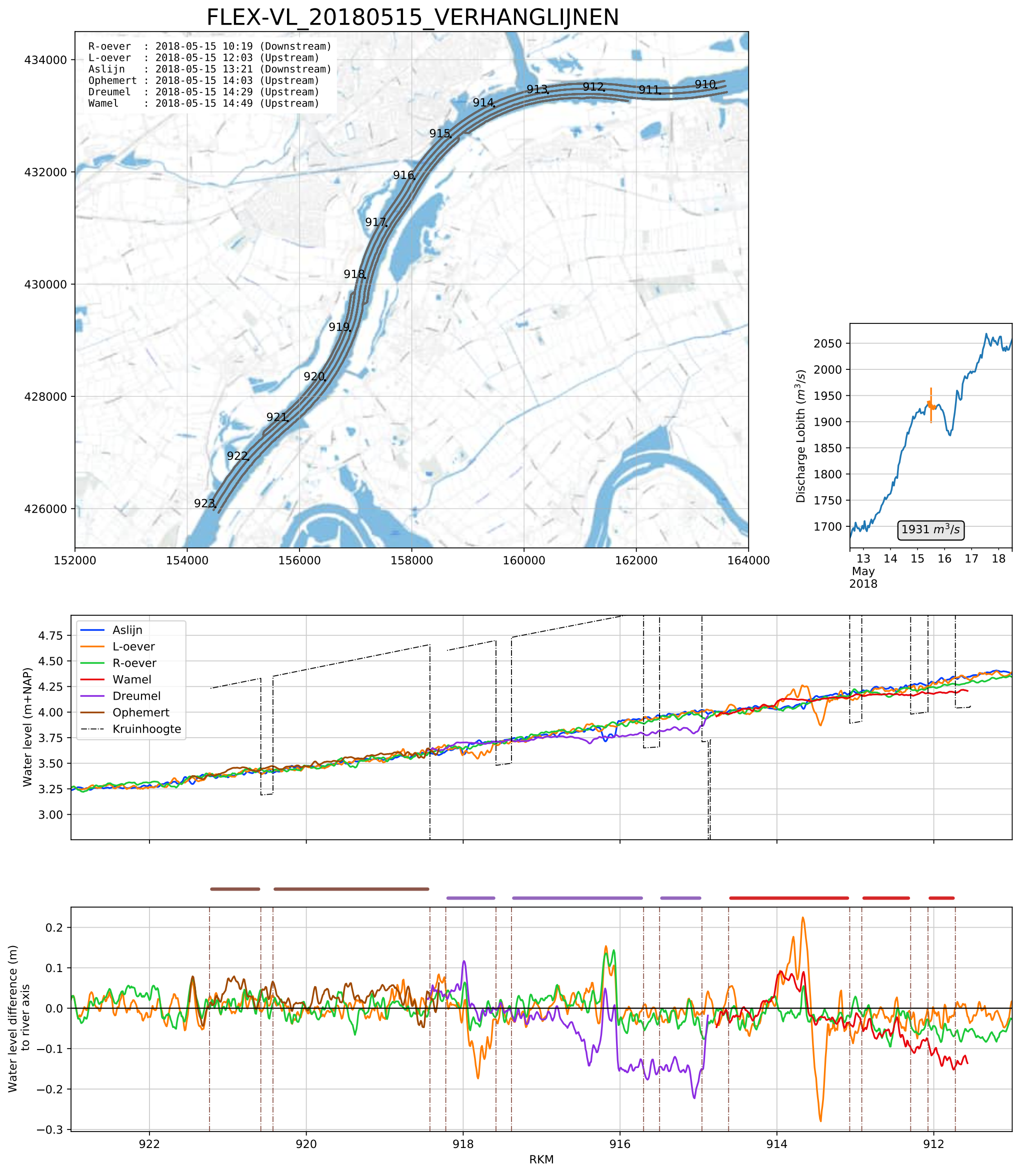

Figure B.38 Verhanglijnmeting van 2018-05-15 (afvoer Lobith: 1931 m^3/s)

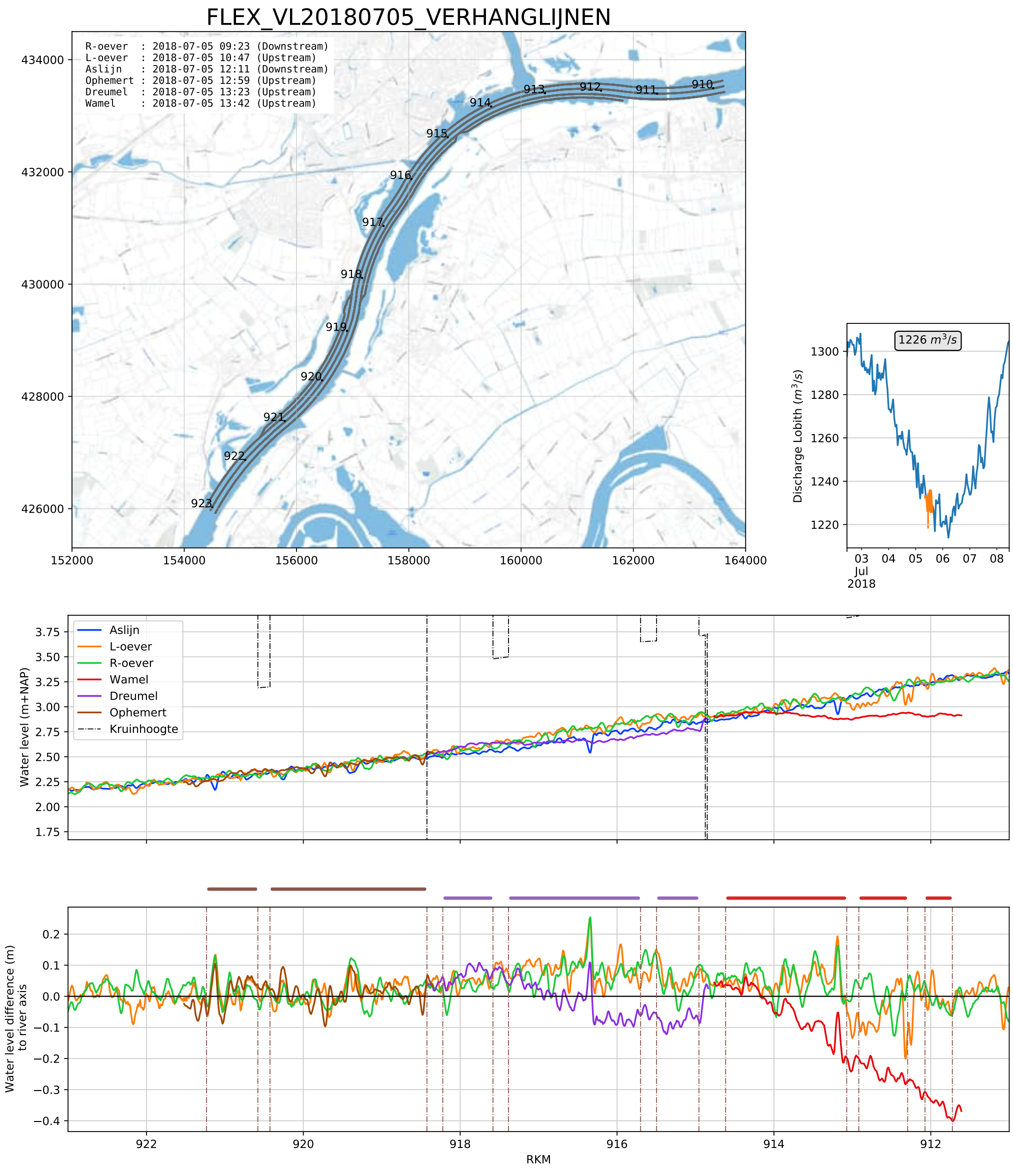

Figure B.39 Verhanglijnmeting van 2018-07-05 (afvoer Lobith: 1226 m^3/s)

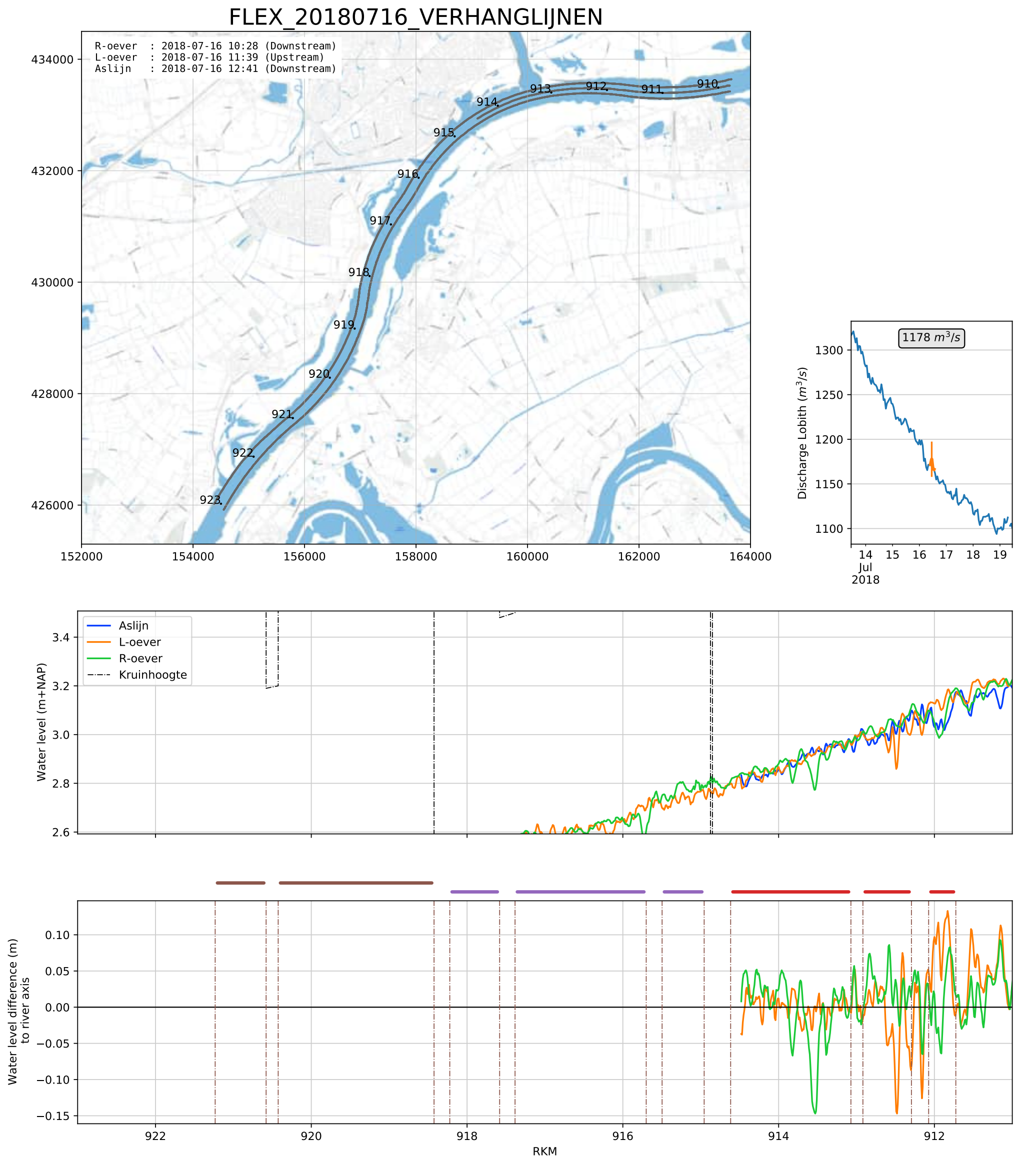

Figure B.40 Verhanglijnmeting van 2018-07-16 (afvoer Lobith: 1178 m^3/s)

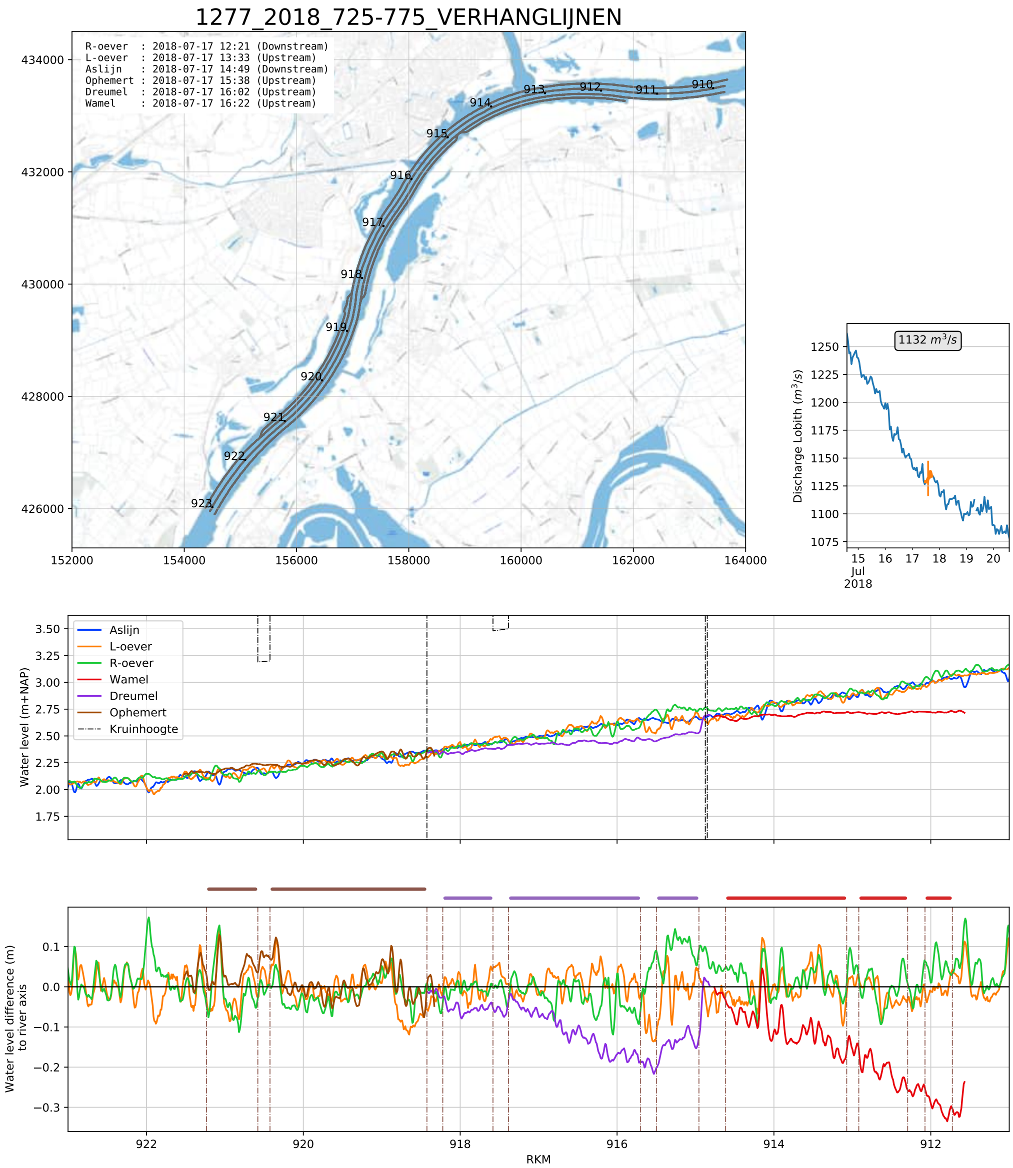

Figure B.41 Verhanglijnmeting van 2018-07-17 (afvoer Lobith: 1132 m^3/s)

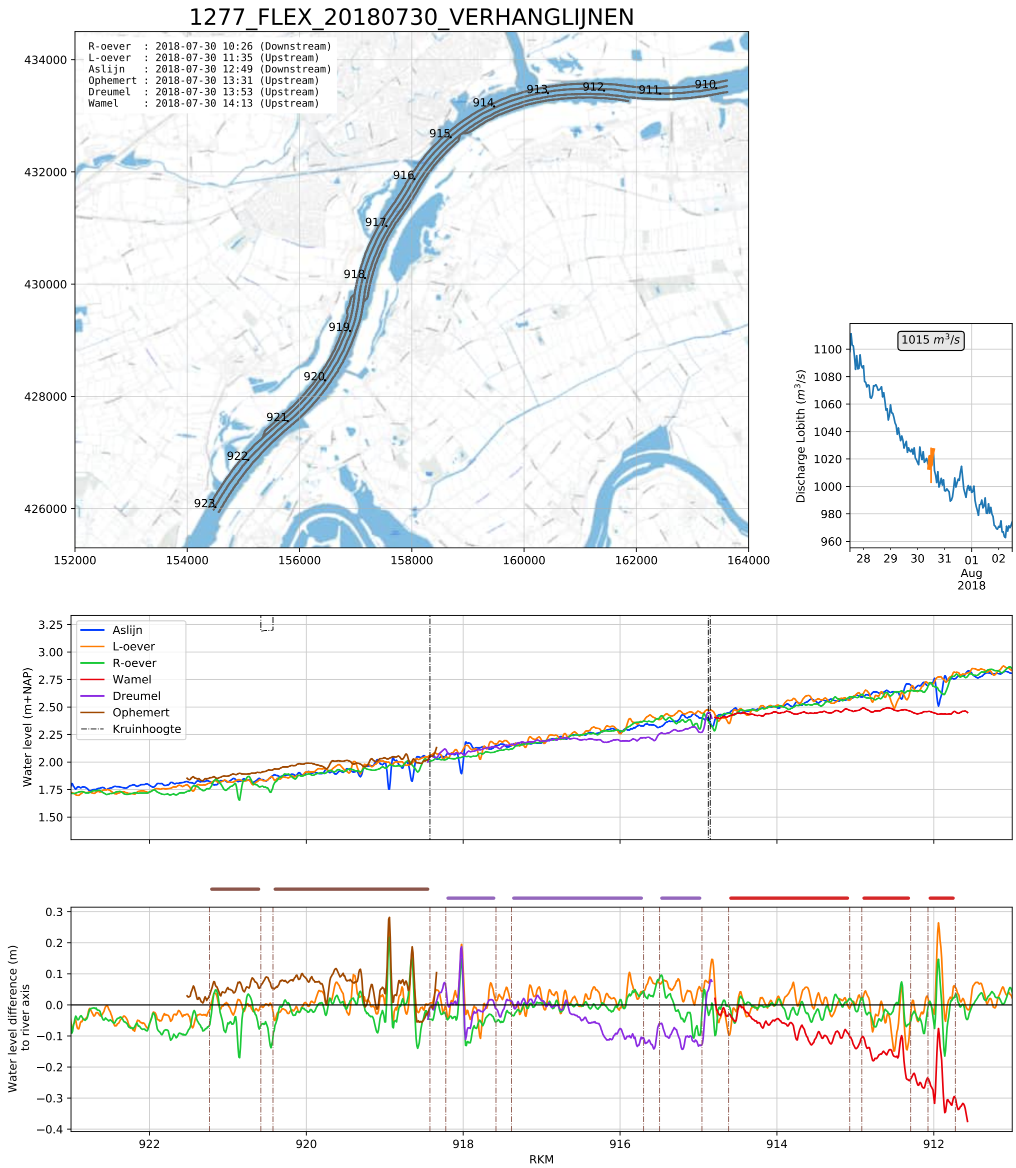

Figure B.42 Verhanglijnmeting van 2018-07-30 (afvoer Lobith: 1015 m^3/s)

Deltares

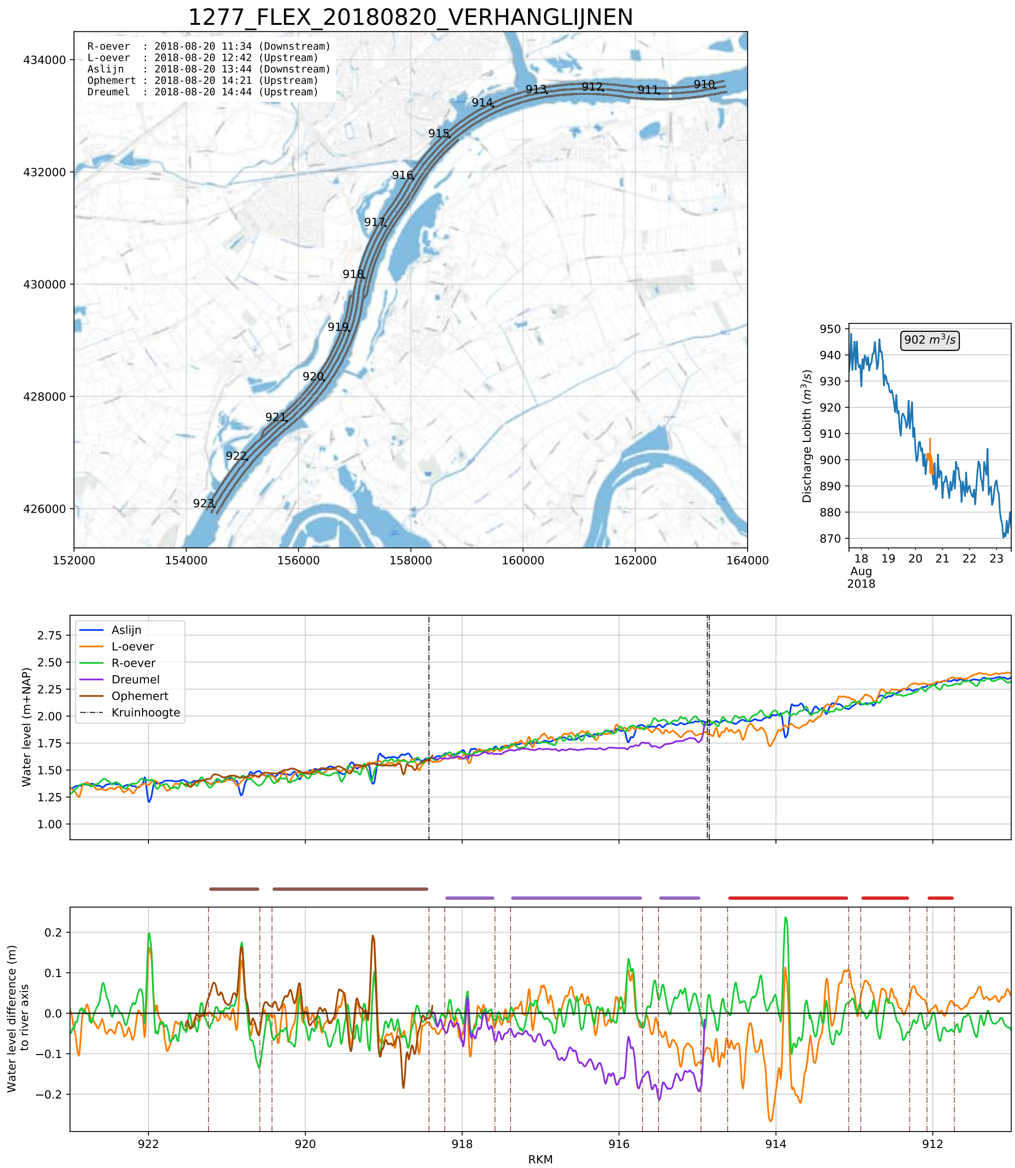

Figure B.43 Verhanglijnmeting van 2018-08-20 (afvoer Lobith: 902 m^3/s)

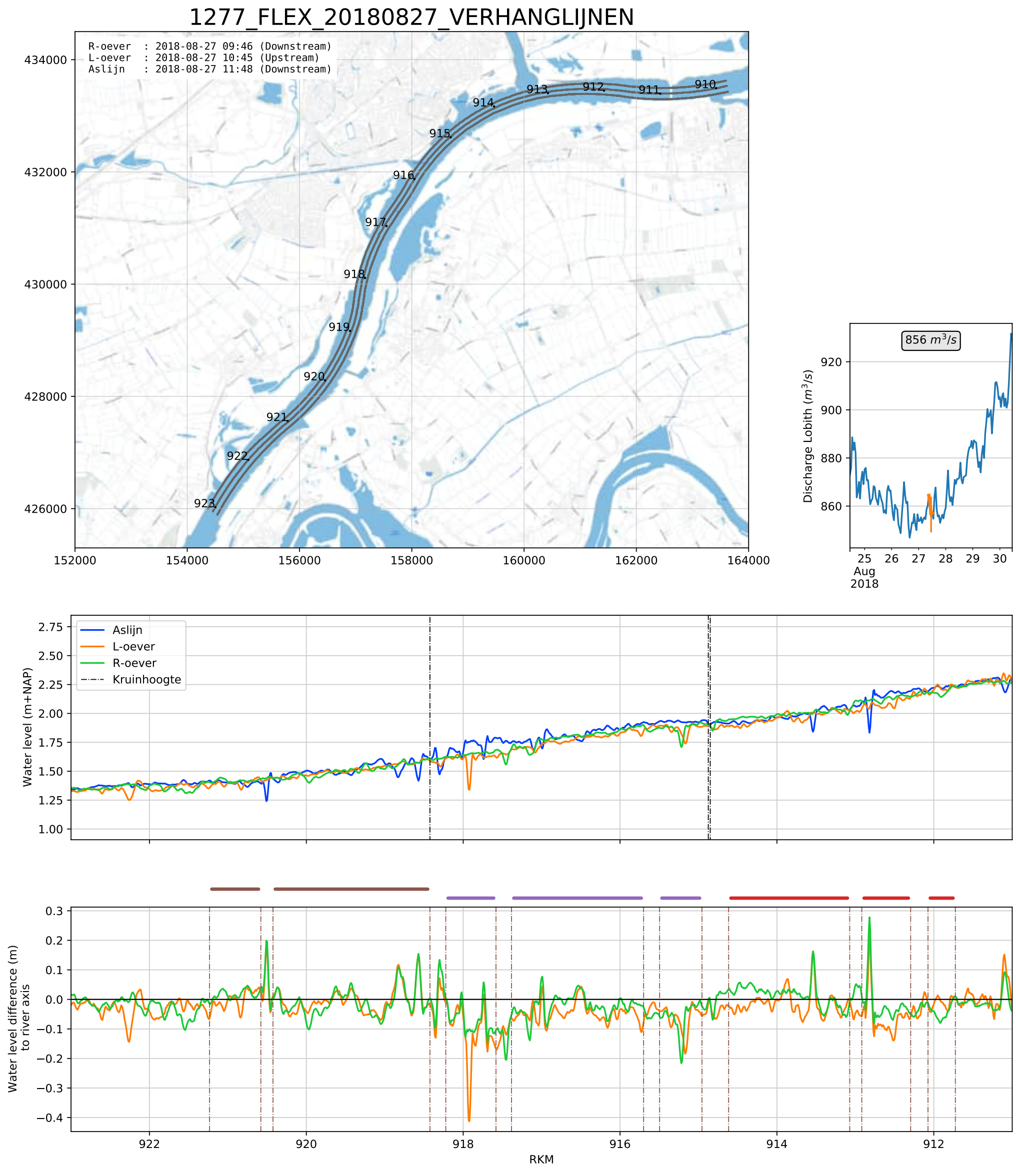

Figure B.44 Verhanglijnmeting van 2018-08-27 (afvoer Lobith: 856 m^3/s)

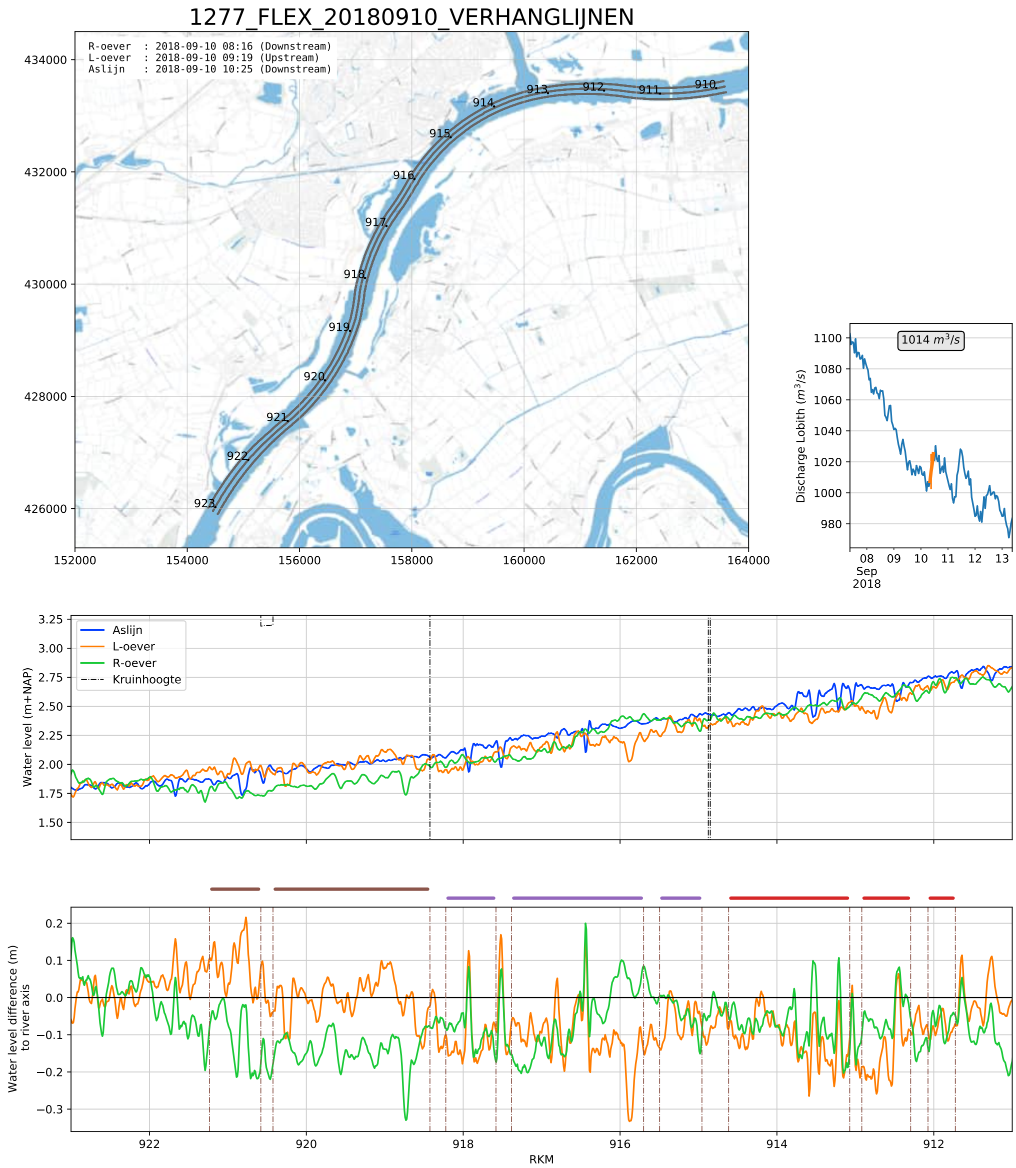

Figure B.45 Verhanglijnmeting van 2018-09-10 (afvoer Lobith: 1014 m^3/s)

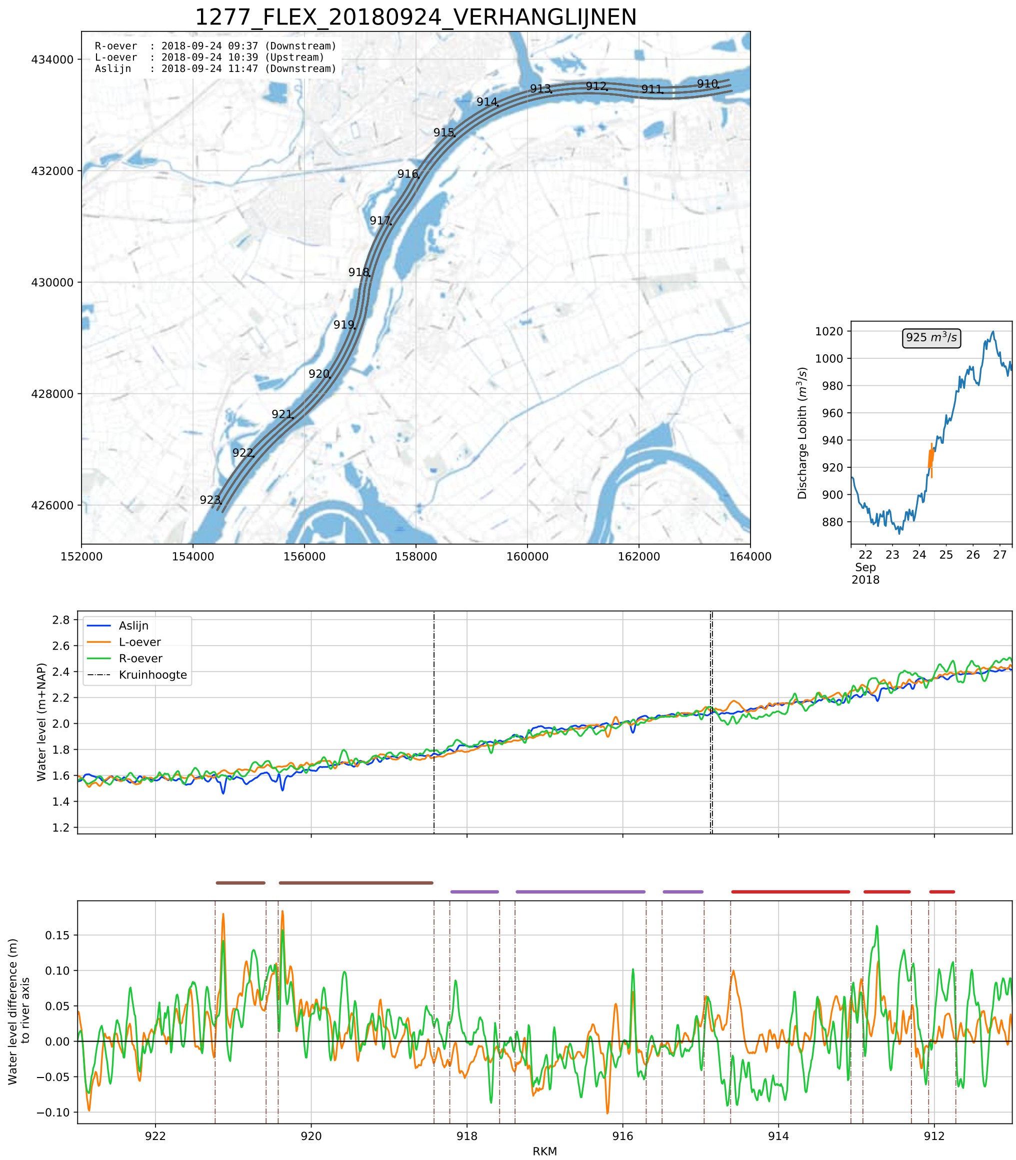

Figure B.46 Verhanglijnmeting van 2018-09-24 (afvoer Lobith: 925 m^3/s)

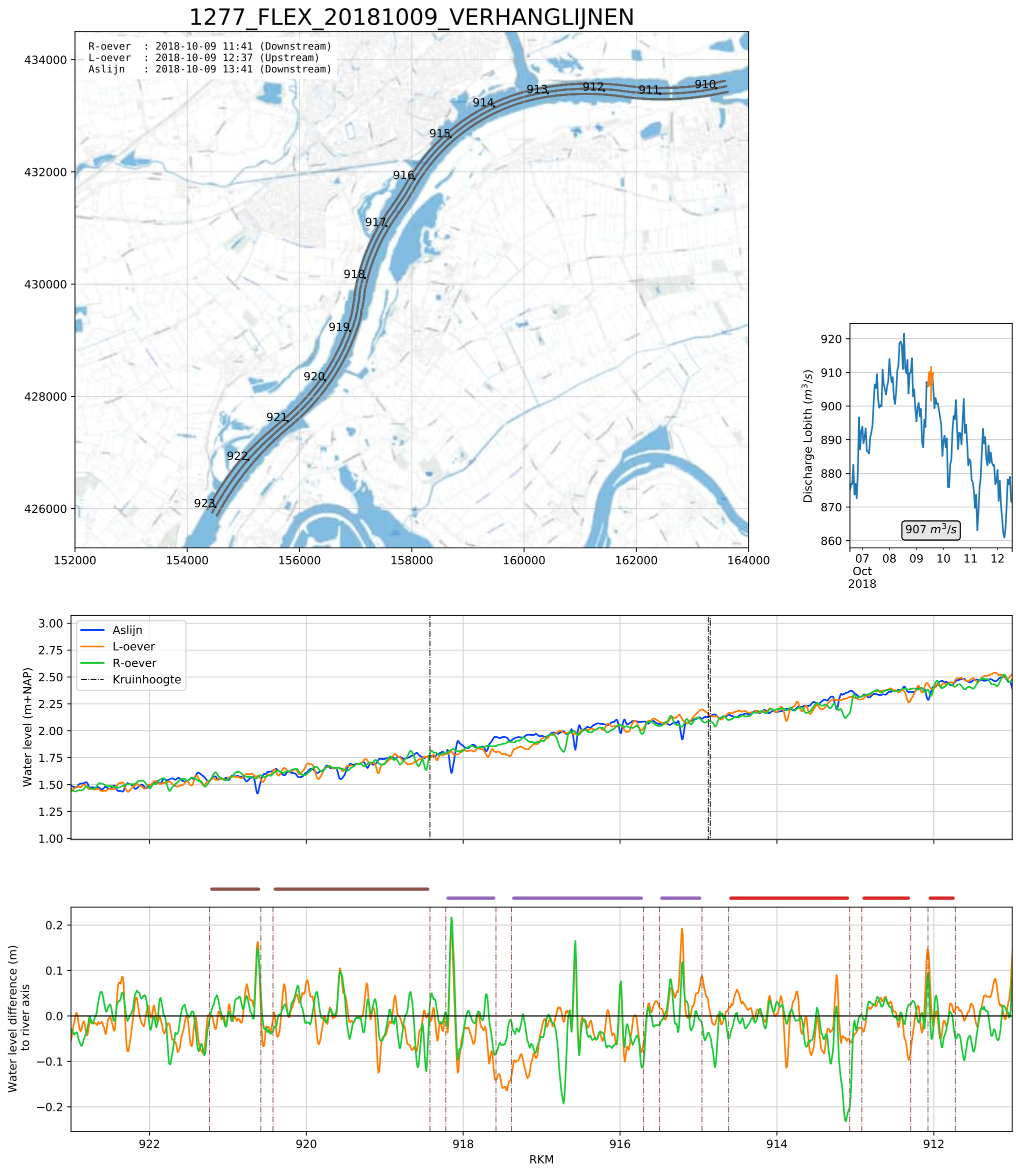

Figure B.47 Verhanglijnmeting van 2018-10-09 (afvoer Lobith: 907 m^3/s)

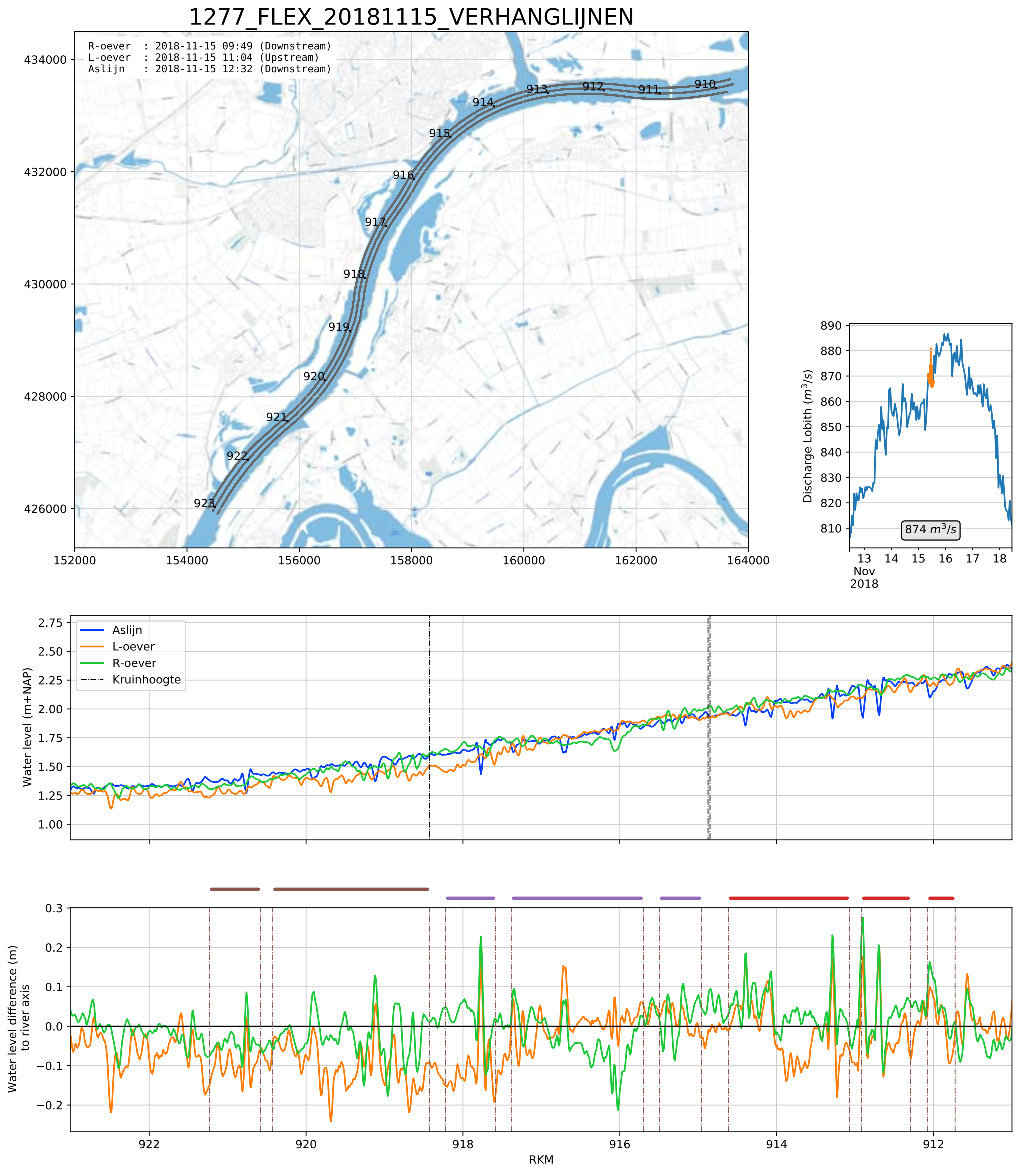

Figure B.48 Verhanglijnmeting van 2018-11-15 (afvoer Lobith: 874 m^3/s)

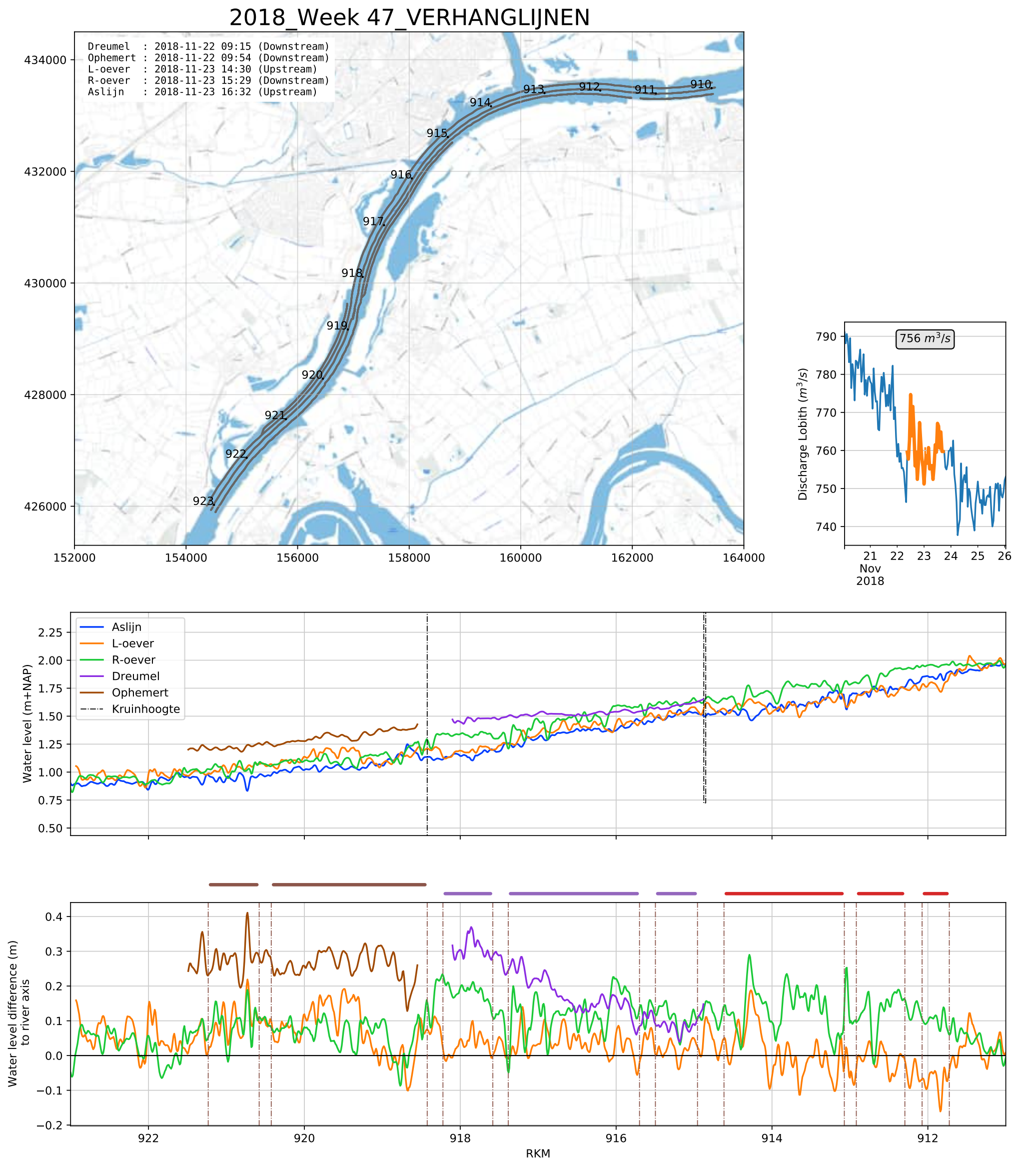

Figure B.49 Verhanglijnmeting van 2018-11-23 (afvoer Lobith: 756 m^3/s)

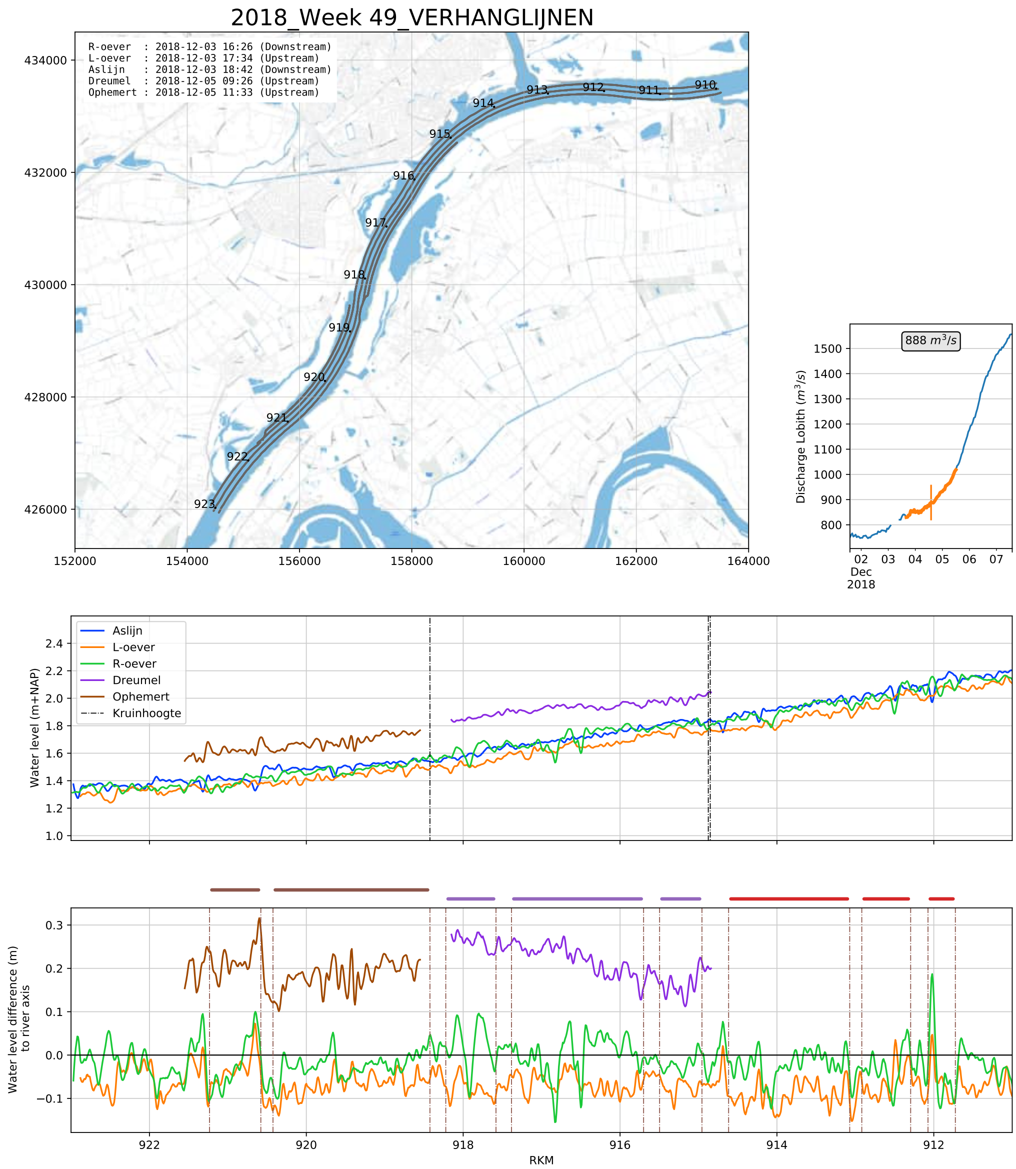

Figure B.50 Verhanglijnmeting van 2018-12-04 (afvoer Lobith: 888 m^3/s)

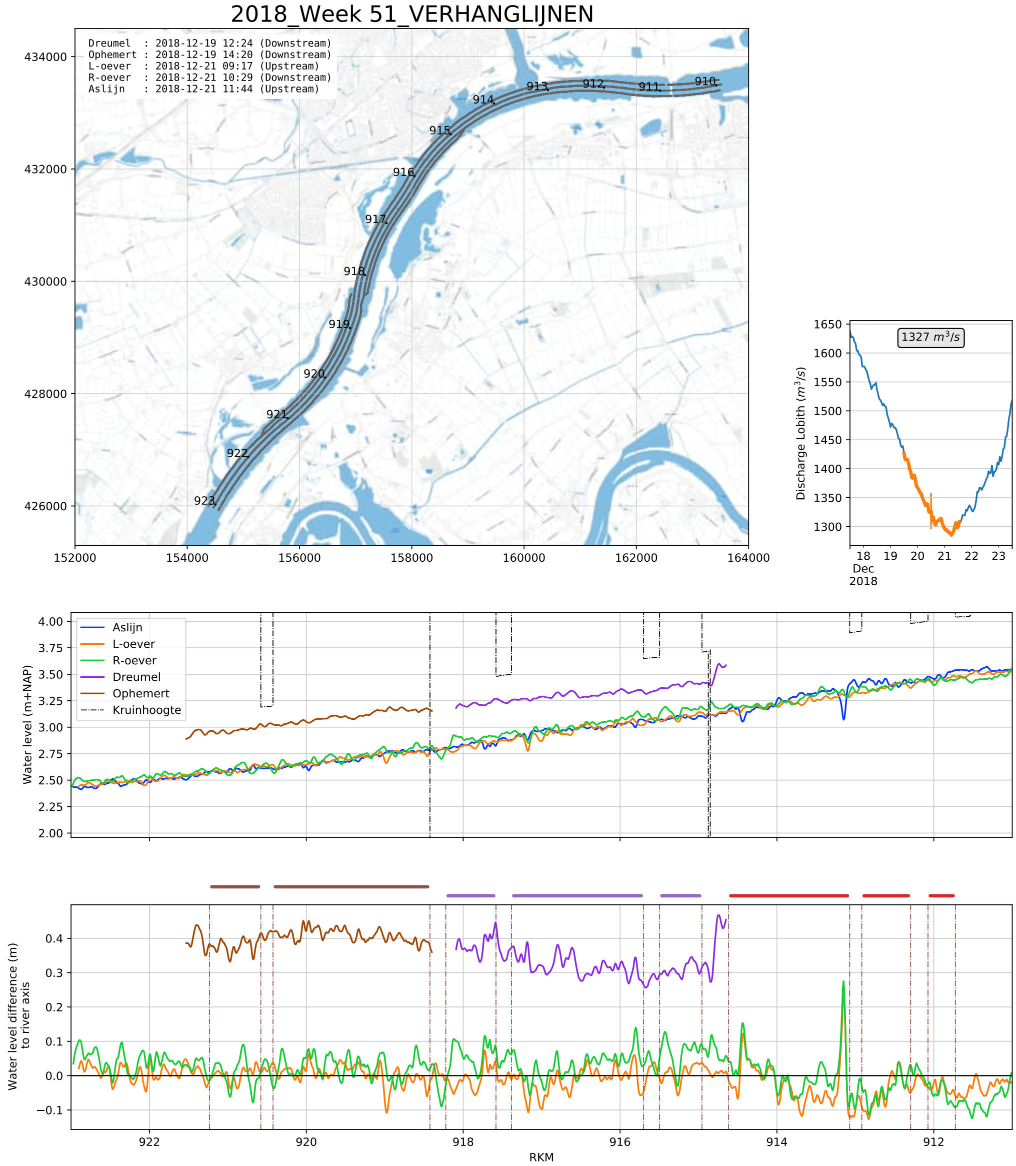

Figure B.51 Verhanglijnmeting van 2018-12-20 (afvoer Lobith: 1327 m^3/s)

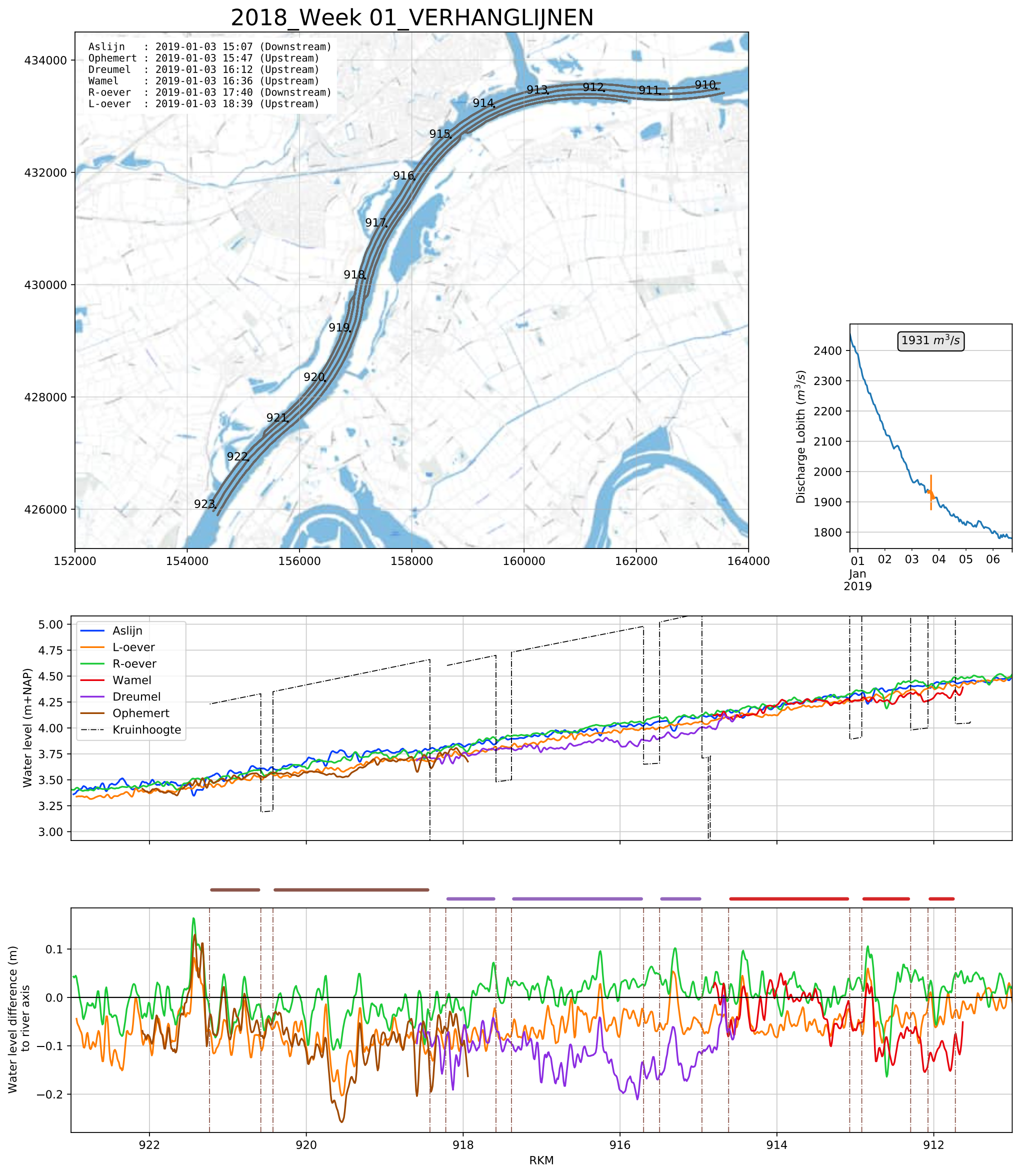

Figure B.52 Verhanglijnmeting van 2019-01-03 (afvoer Lobith: 1931 m^3/s)

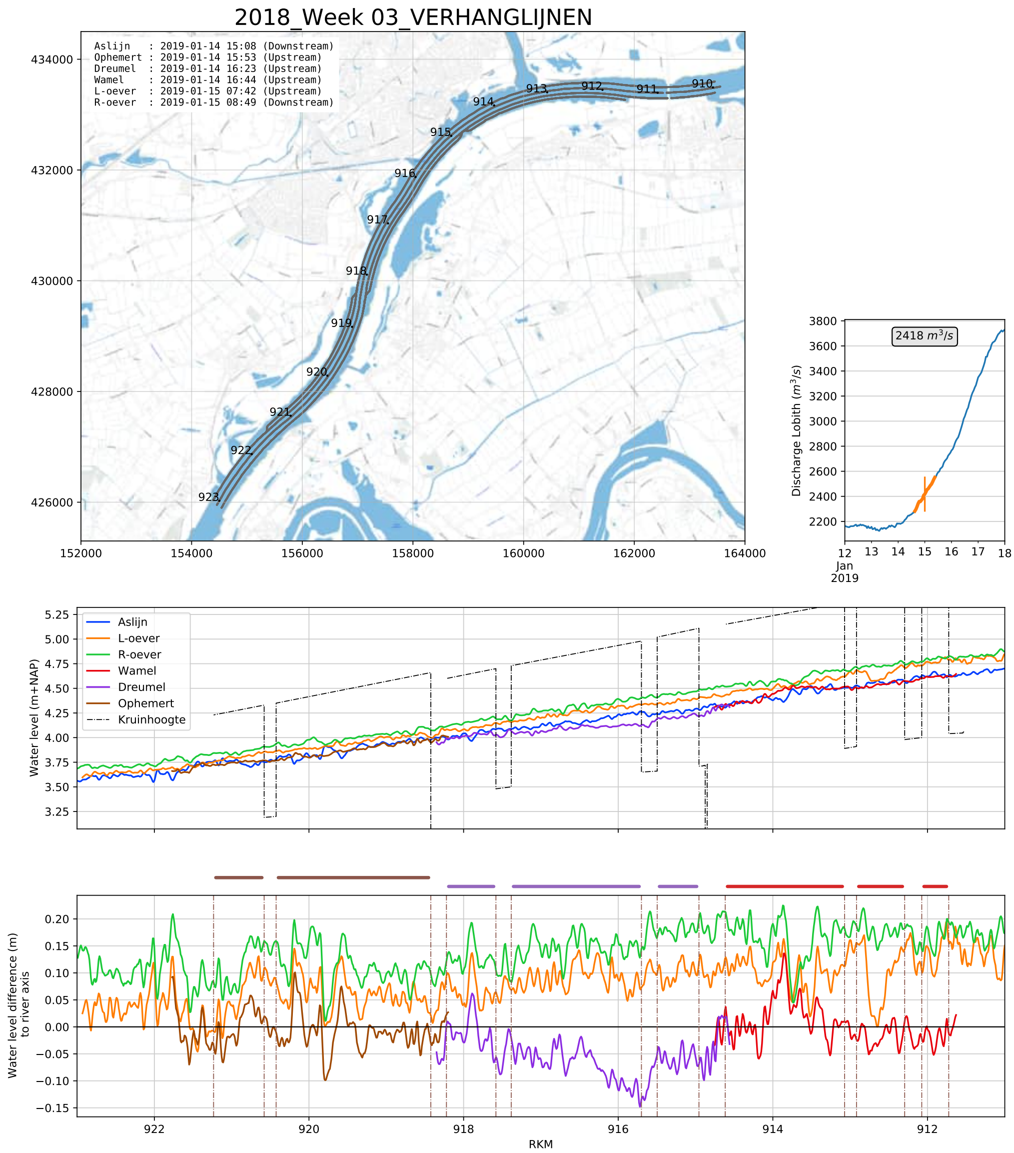

Figure B.53 Verhanglijnmeting van 2019-01-14 (afvoer Lobith: 2418 m^3/s)

Deltares

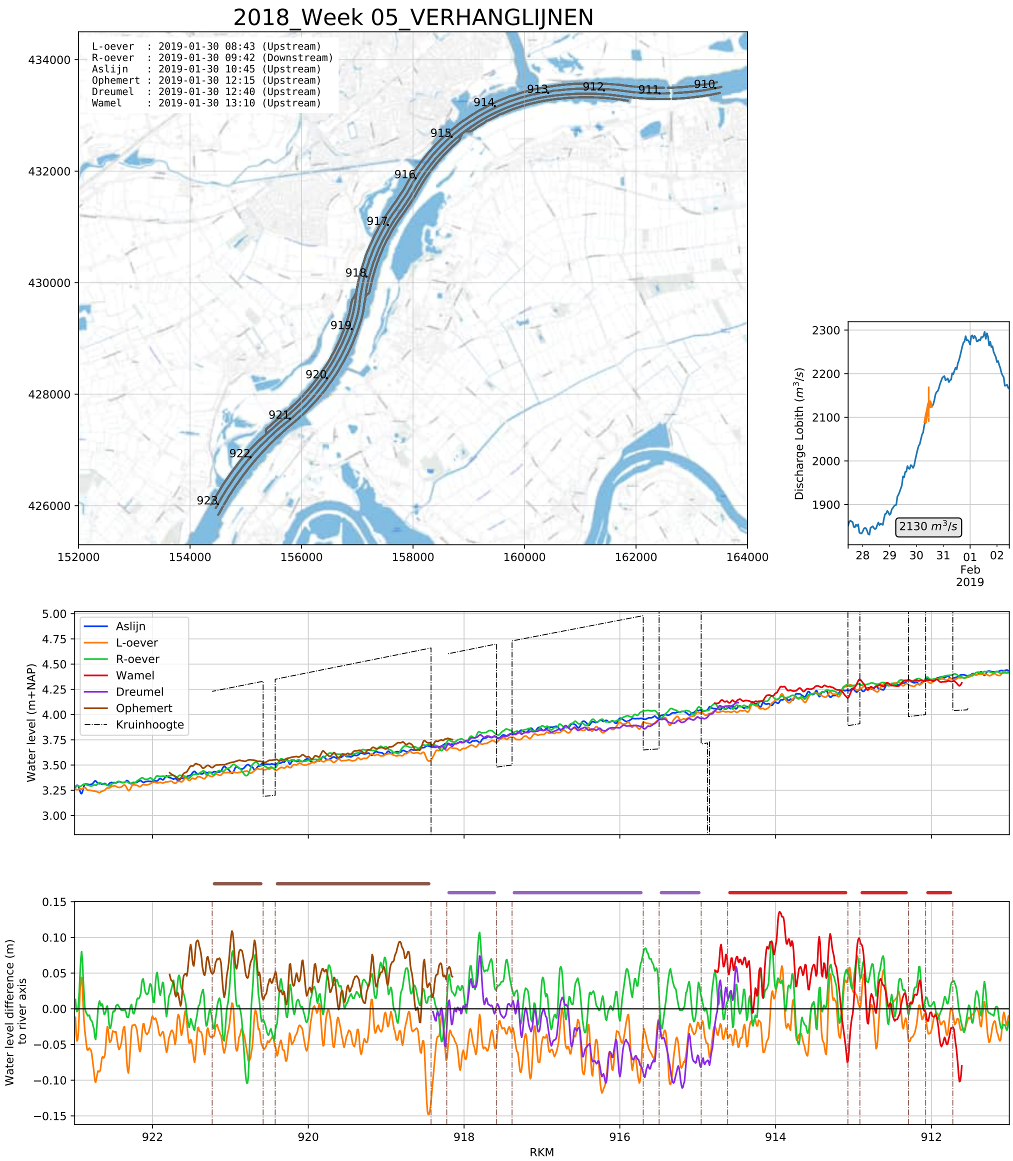

Figure B.54 Verhanglijnmeting van 2019-01-30 (afvoer Lobith: 2130 m^3/s)

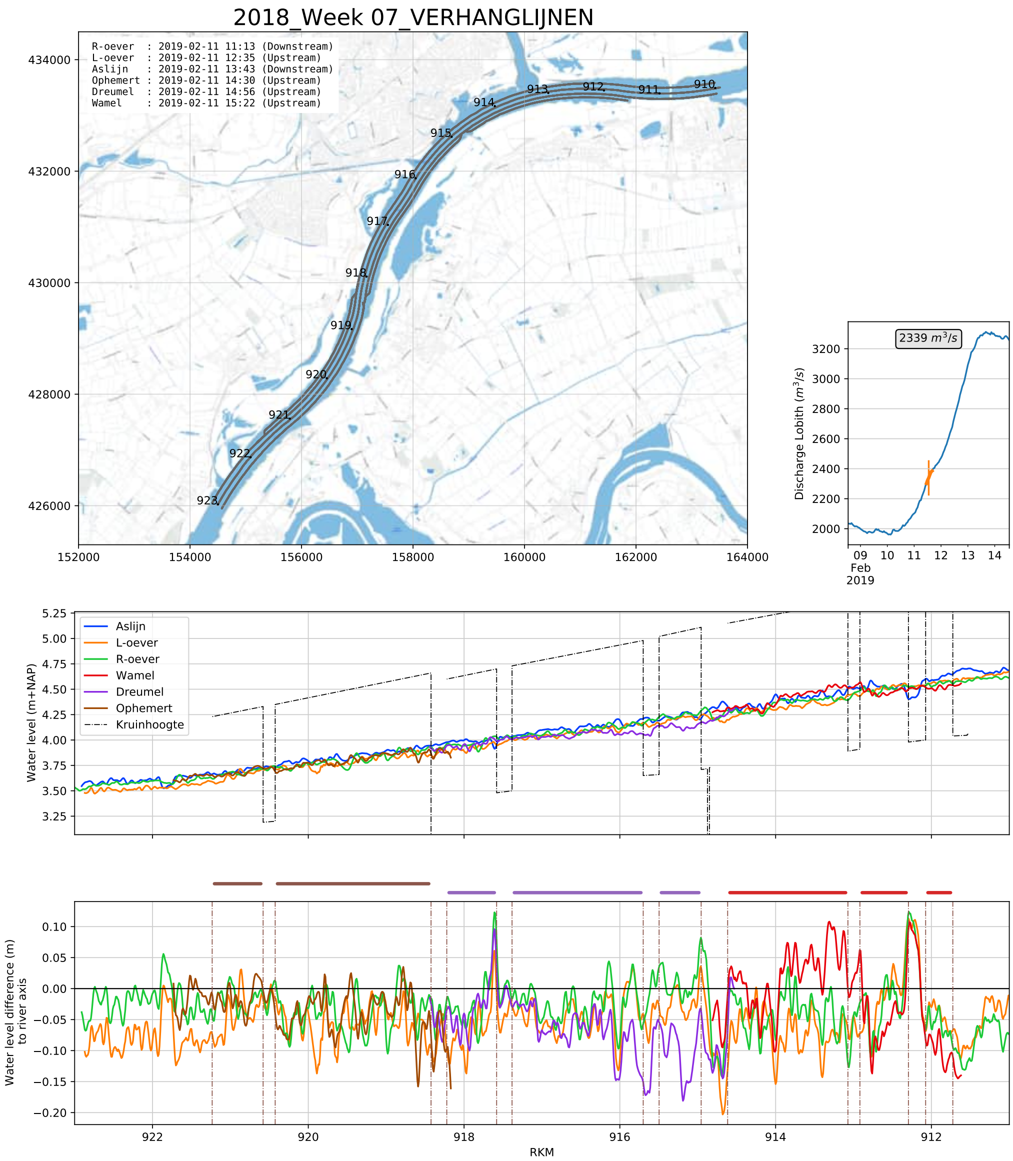

Figure B.55 Verhanglijnmeting van 2019-02-11 (afvoer Lobith: 2339 m^3/s)

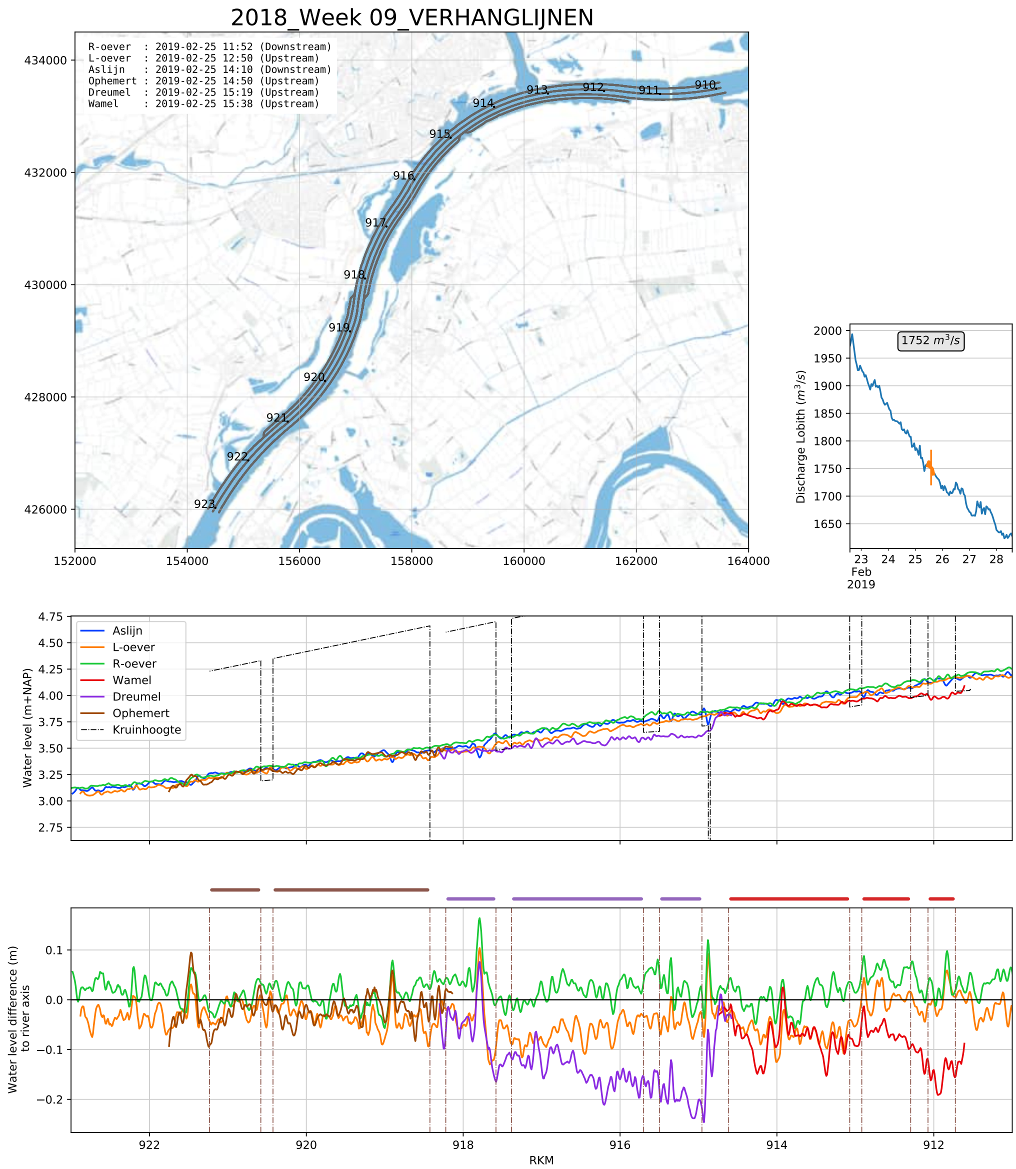

Figure B.56 Verhanglijnmeting van 2019-02-25 (afvoer Lobith: 1752 m^3/s)

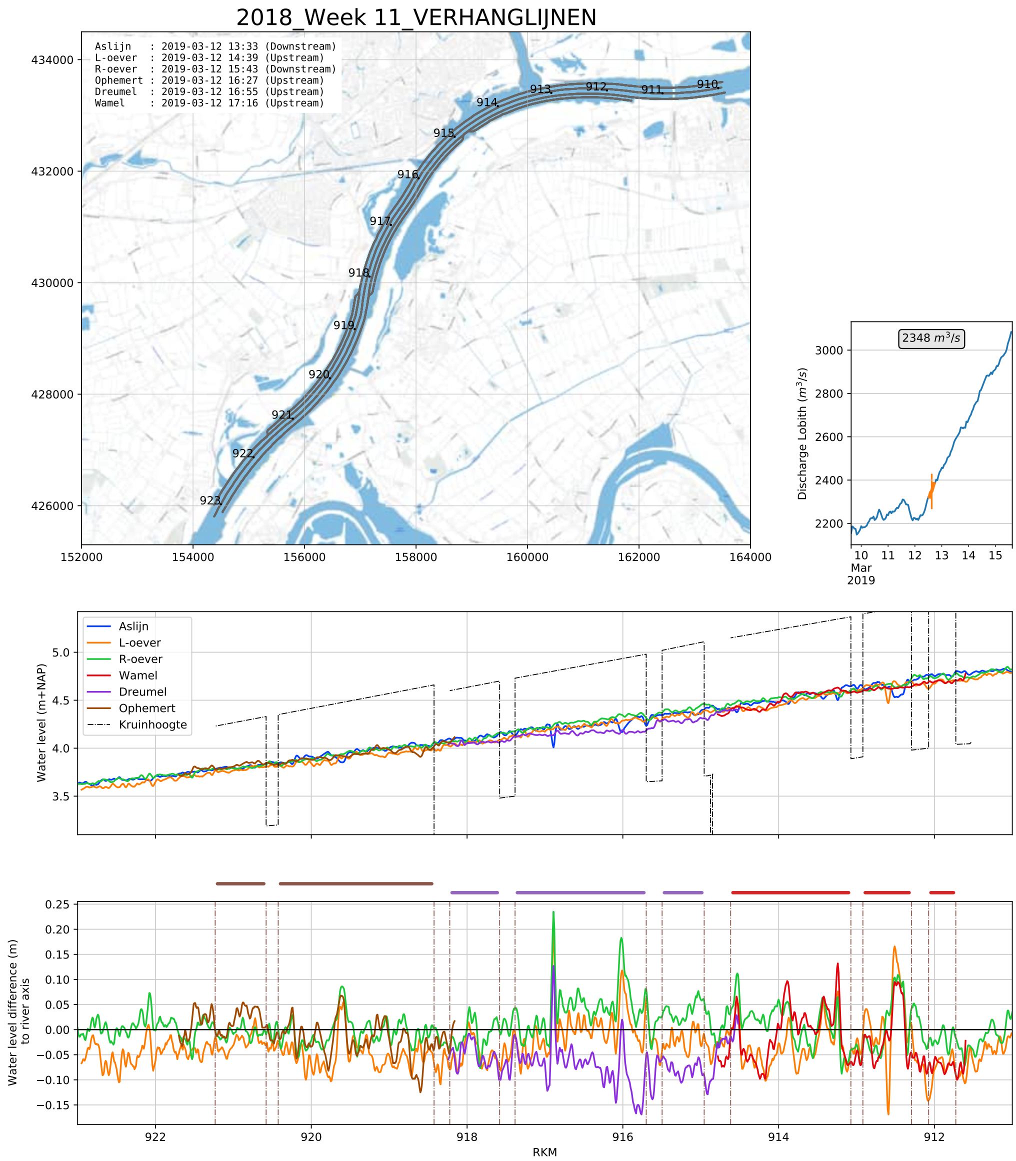

Figure B.57 Verhanglijnmeting van 2019-03-12 (afvoer Lobith: 2348 m^3/s)

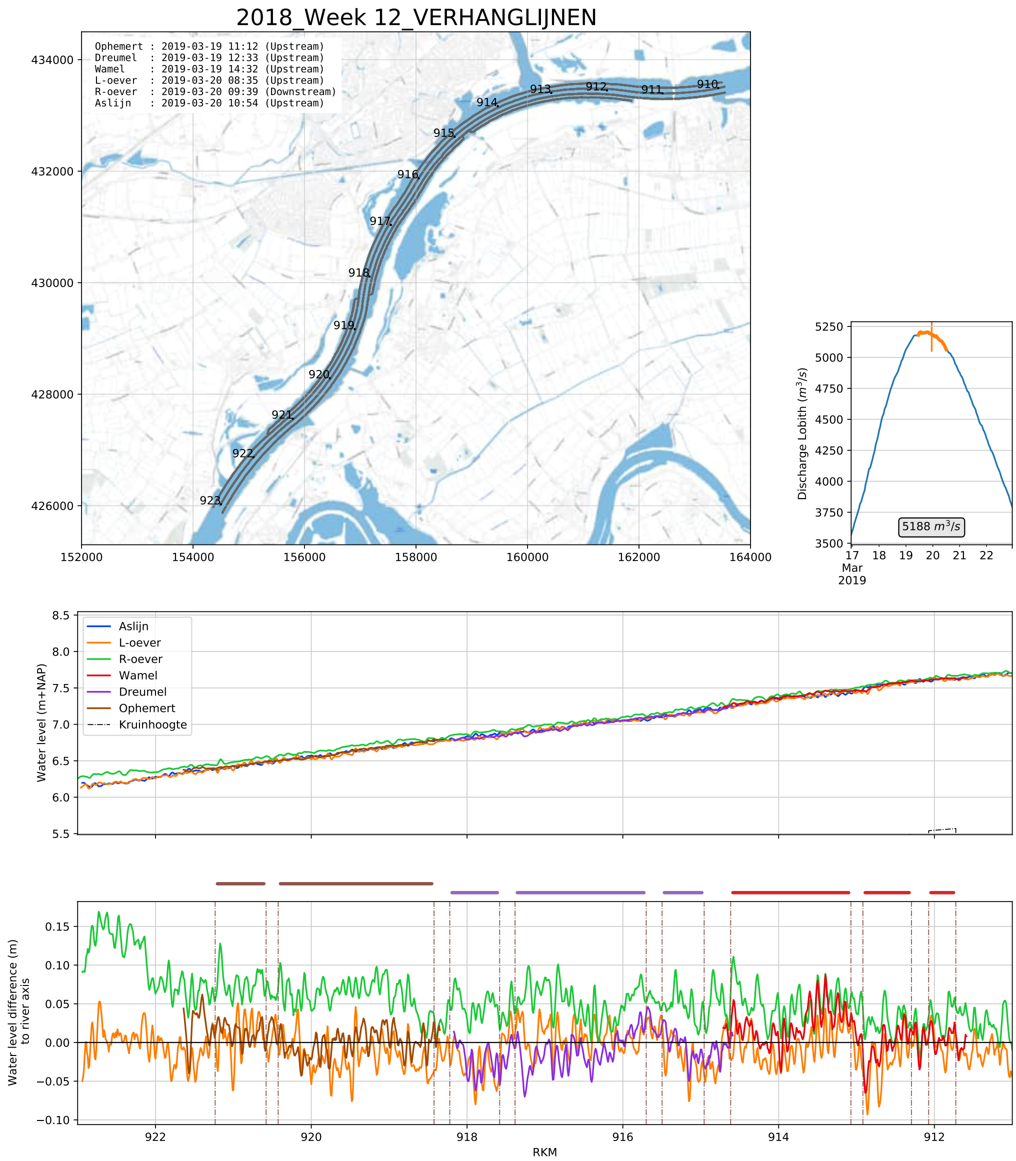

Figure B.58 Verhanglijnmeting van 2019-03-19 (afvoer Lobith: 5188 m^3/s)

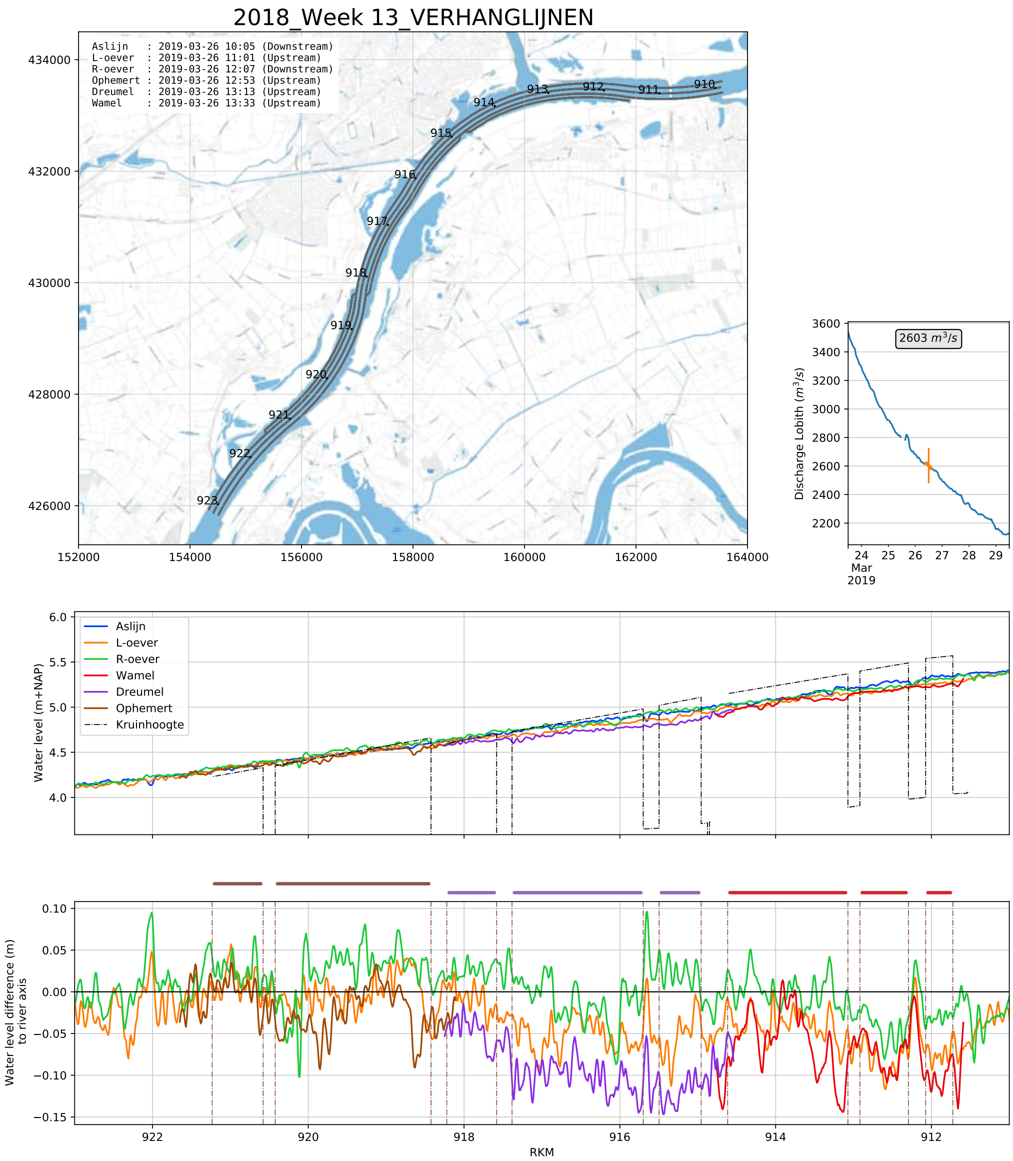

Figure B.59 Verhanglijnmeting van 2019-03-26 (afvoer Lobith: 2603 m^3/s)

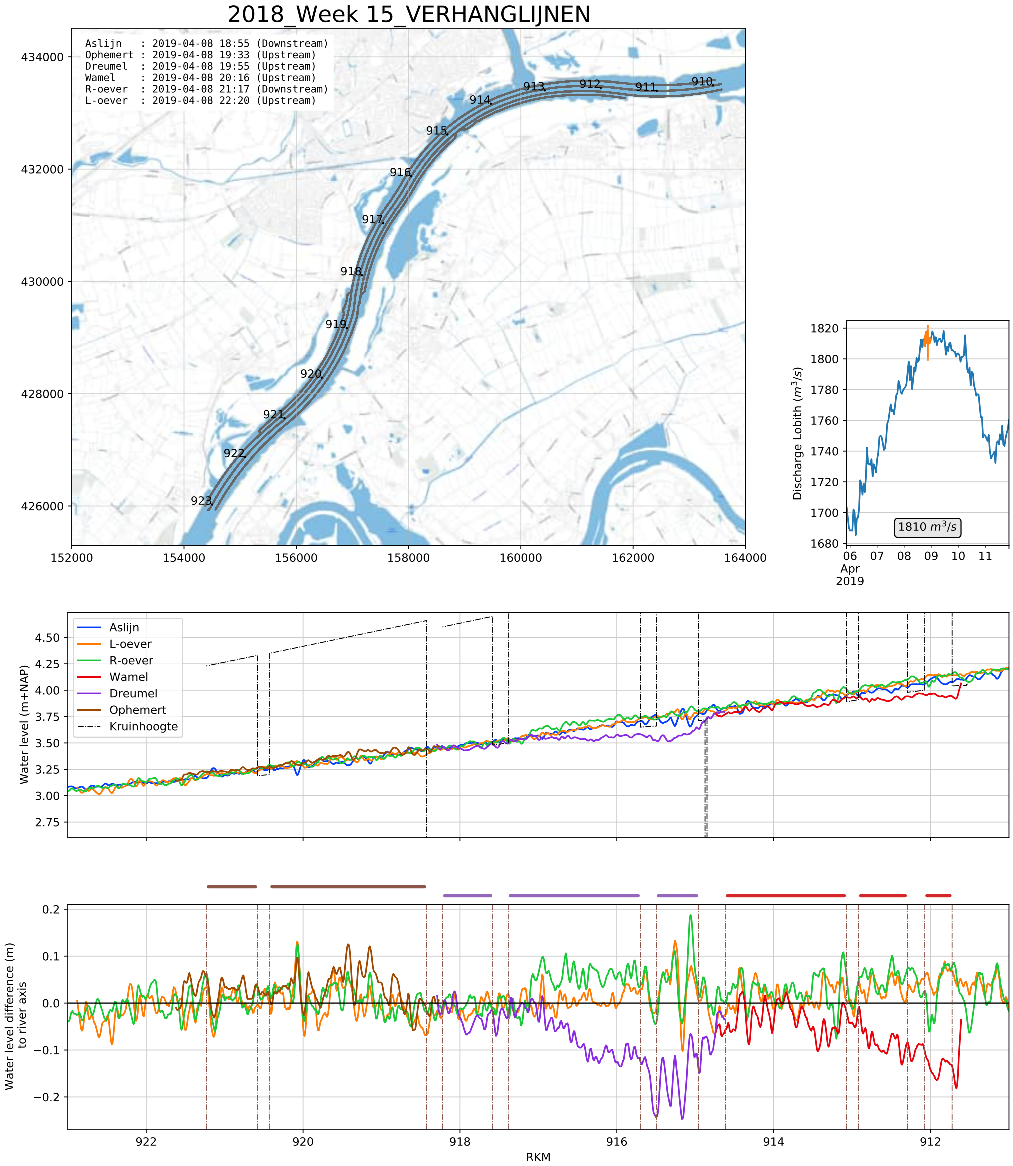

Figure B.60 Verhanglijnmeting van 2019-04-08 (afvoer Lobith: 1810 m^3/s)

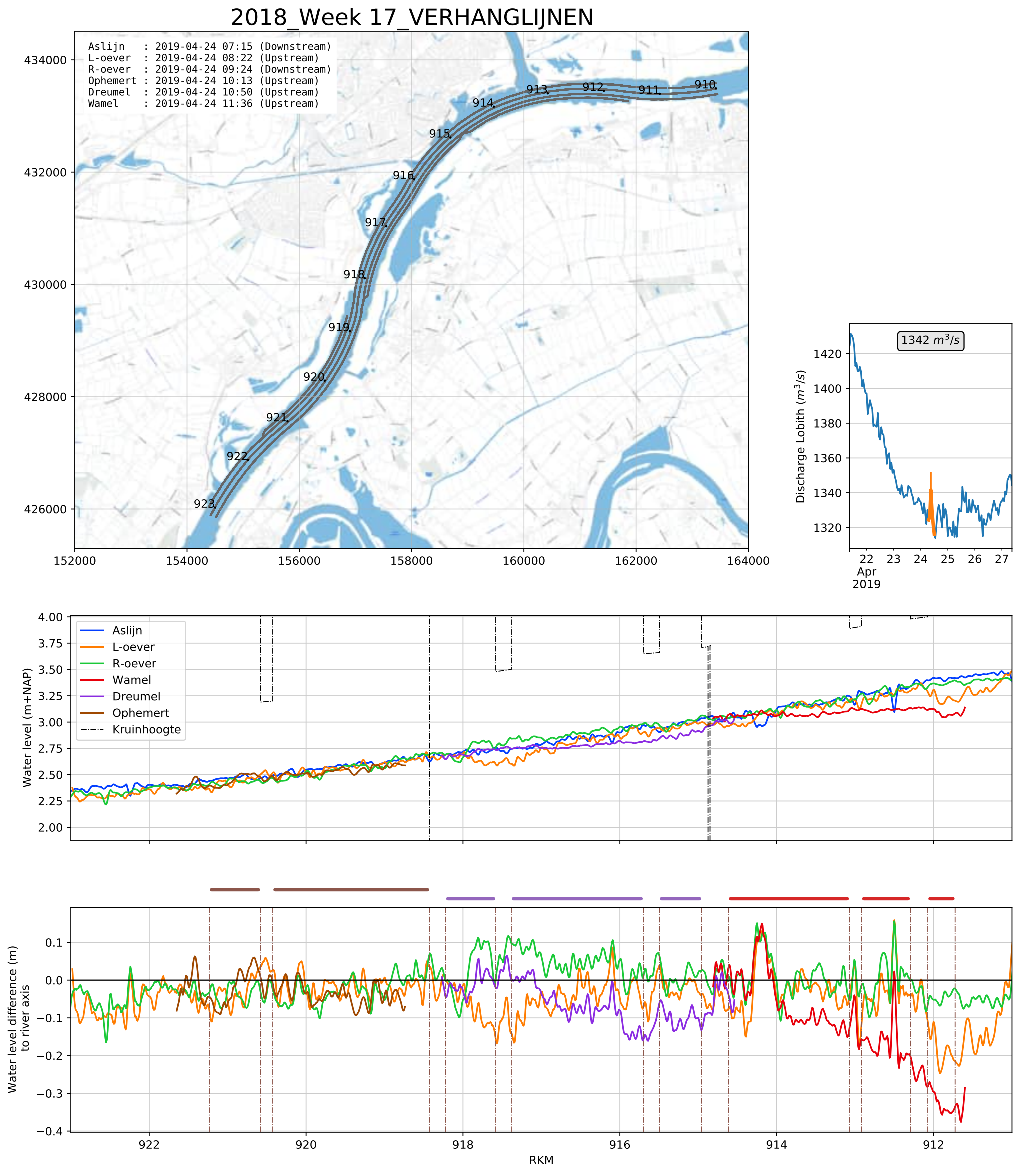

Figure B.61 Verhanglijnmeting van 2019-04-24 (afvoer Lobith: 1342 m^3/s)

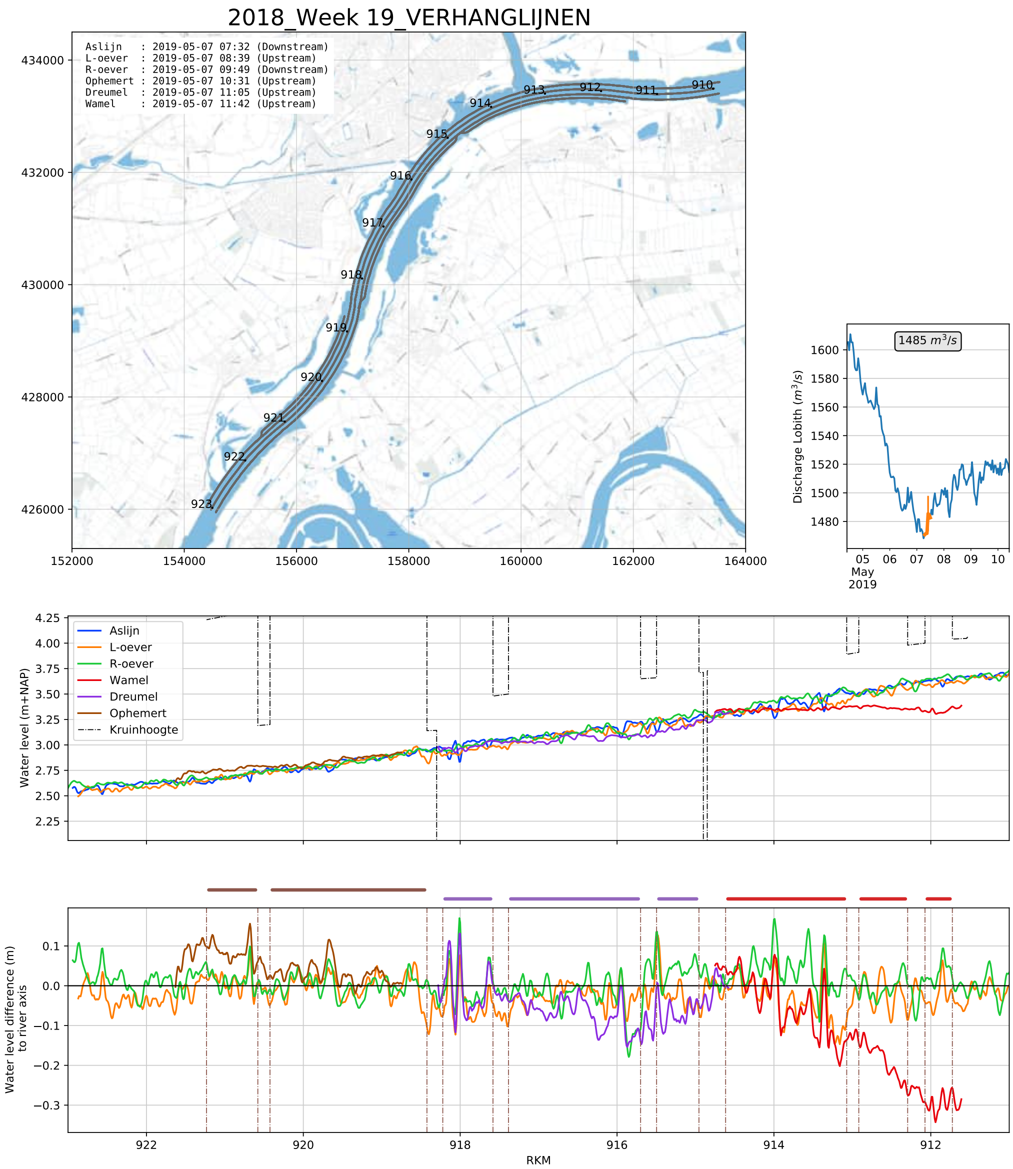

Figure B.62 Verhanglijnmeting van 2019-05-07 (afvoer Lobith: 1485 m^3/s)

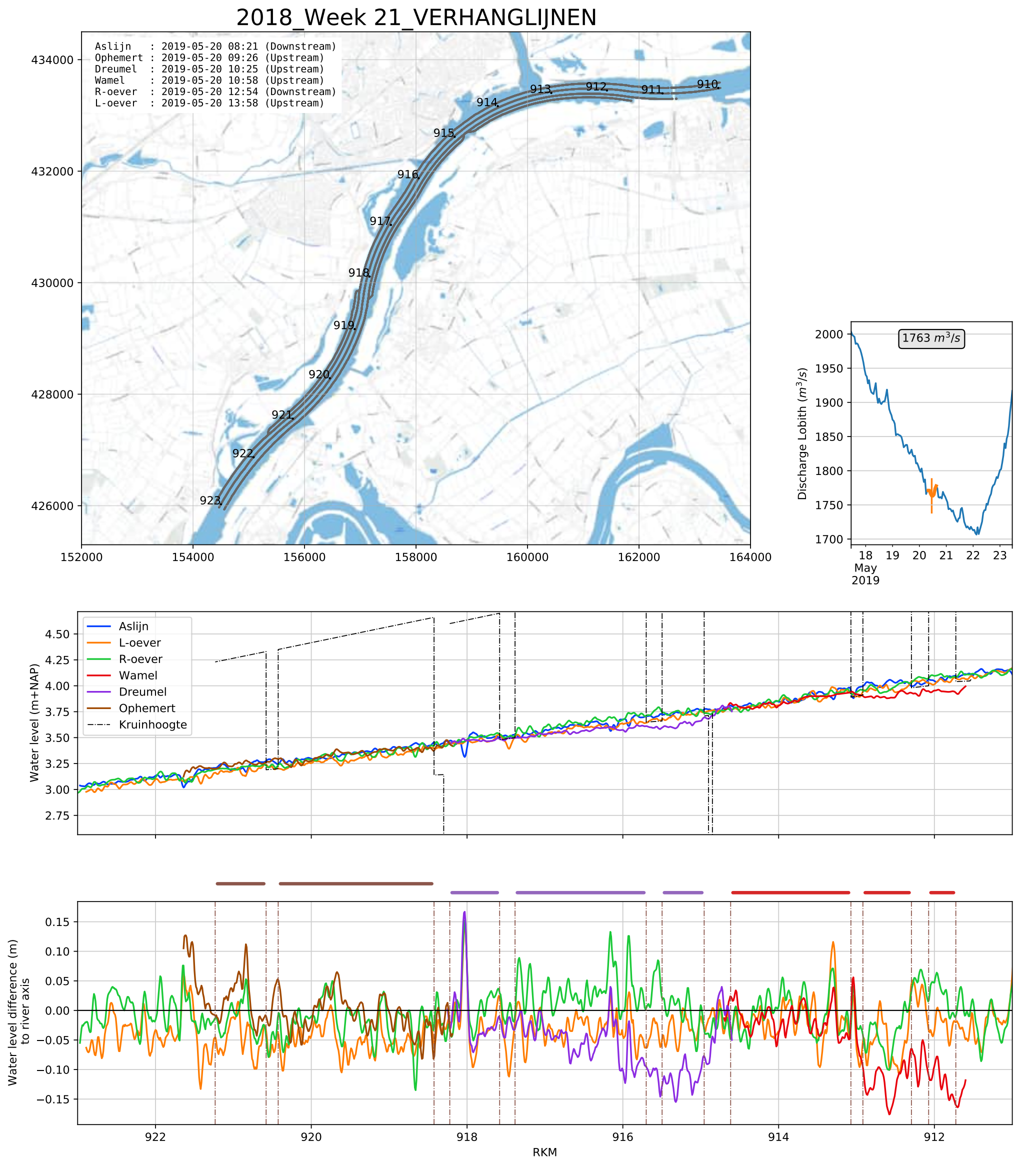

Figure B.63 Verhanglijnmeting van 2019-05-20 (afvoer Lobith: 1763 m^3/s)

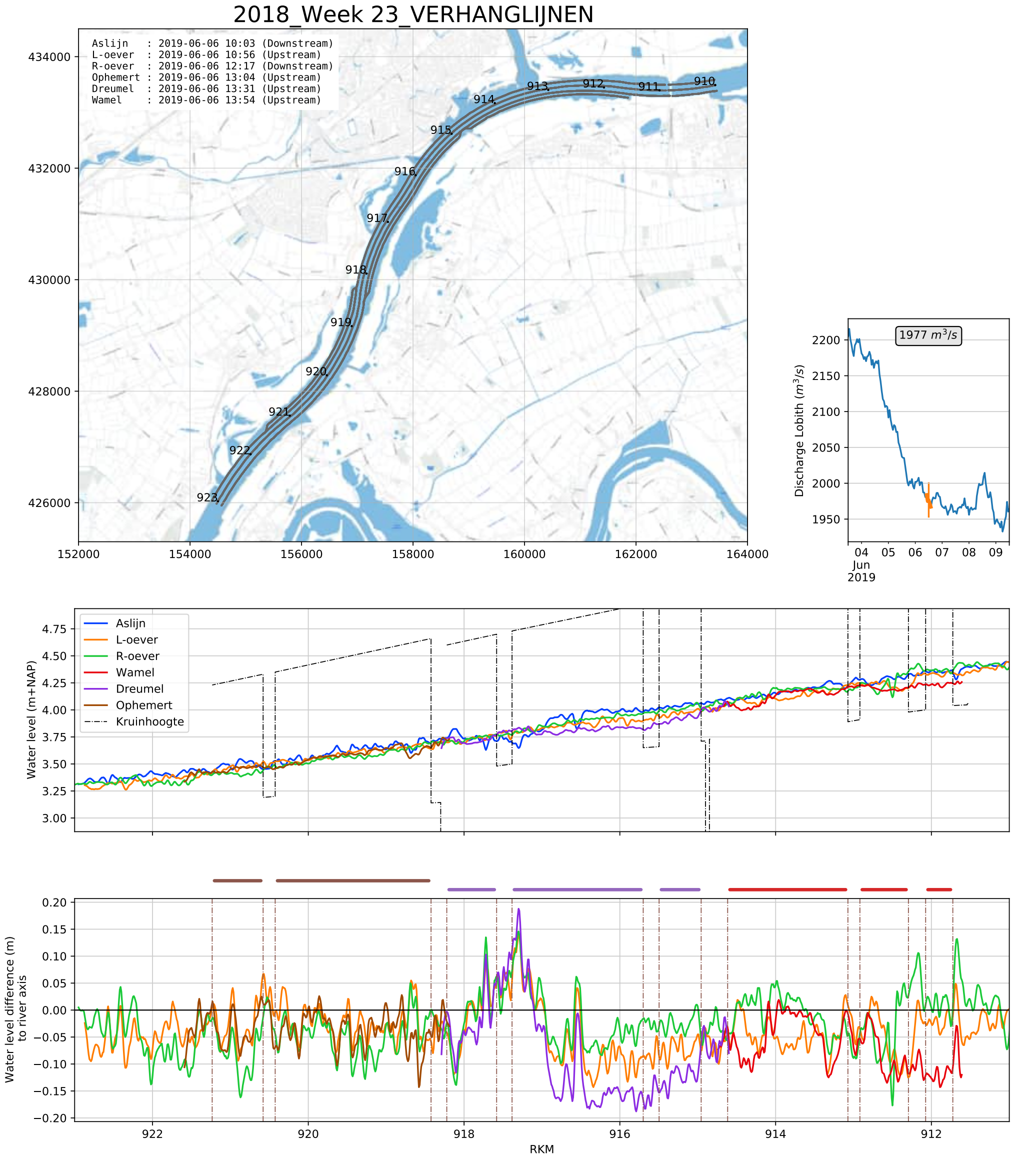

Figure B.64 Verhanglijnmeting van 2019-06-06 (afvoer Lobith: 1977 m^3/s)

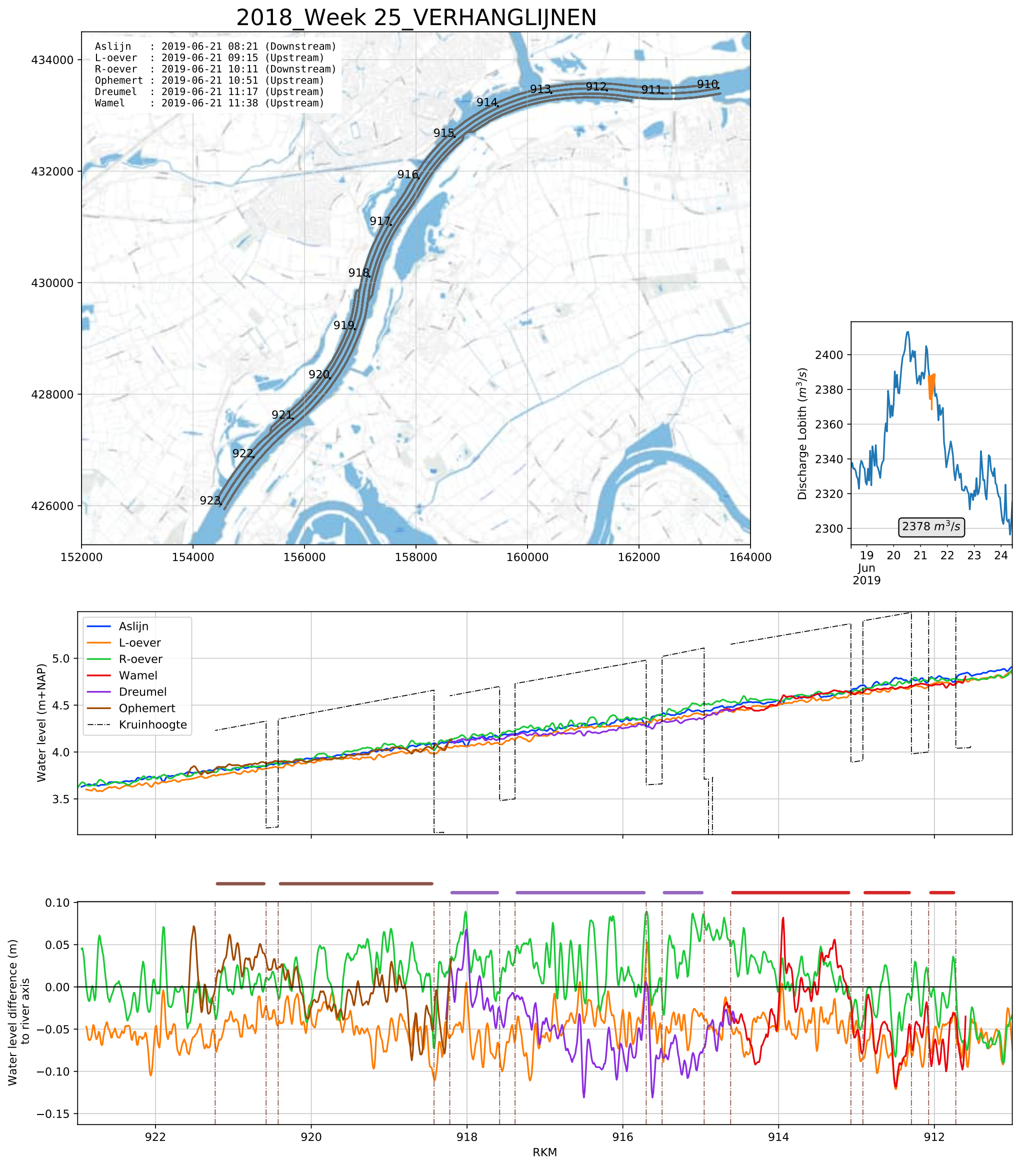

Figure B.65 Verhanglijnmeting van 2019-06-21 (afvoer Lobith: 2378 m^3/s)

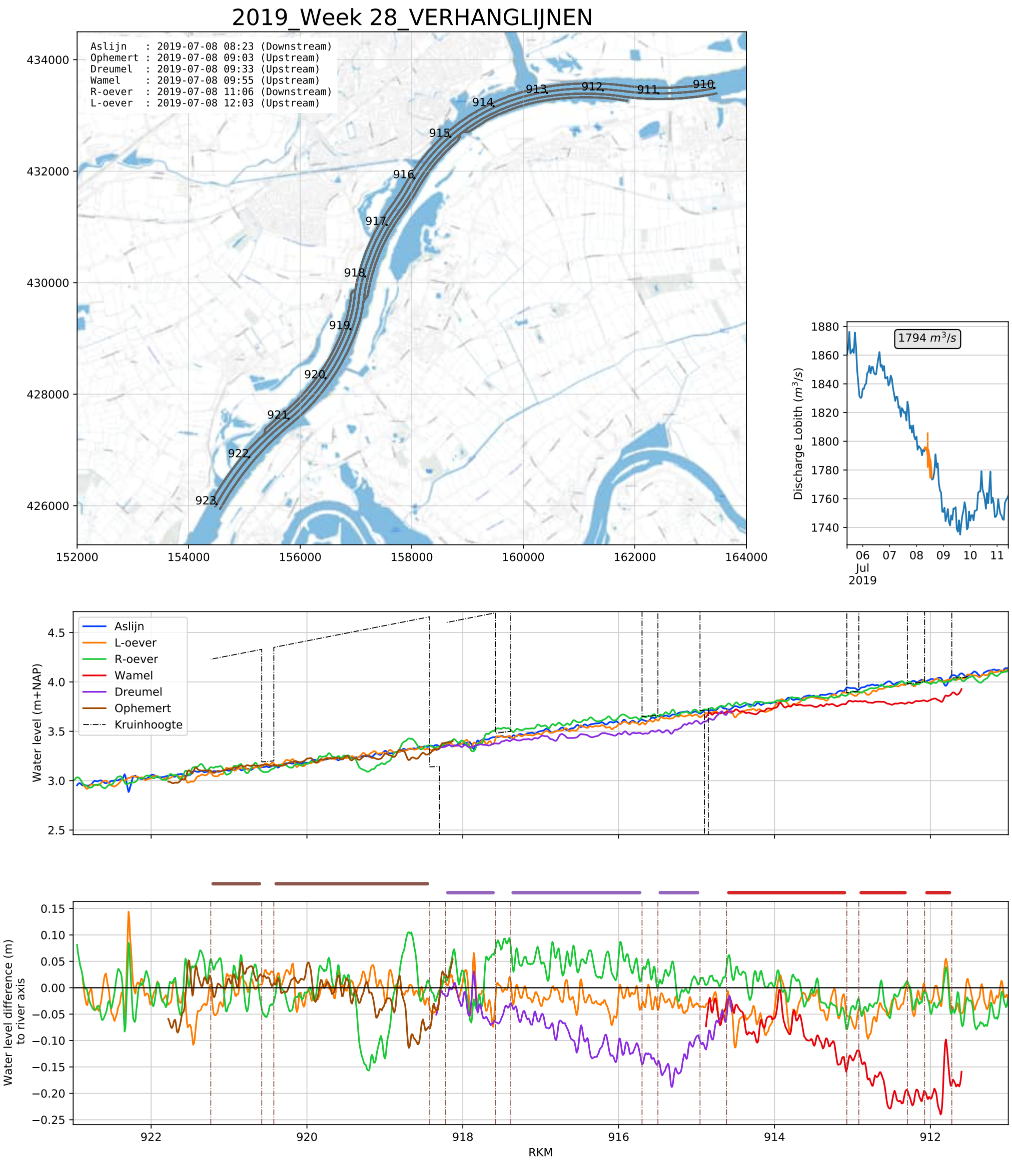

Figure B.66 Verhanglijnmeting van 2019-07-08 (afvoer Lobith: 1794 m^3/s)

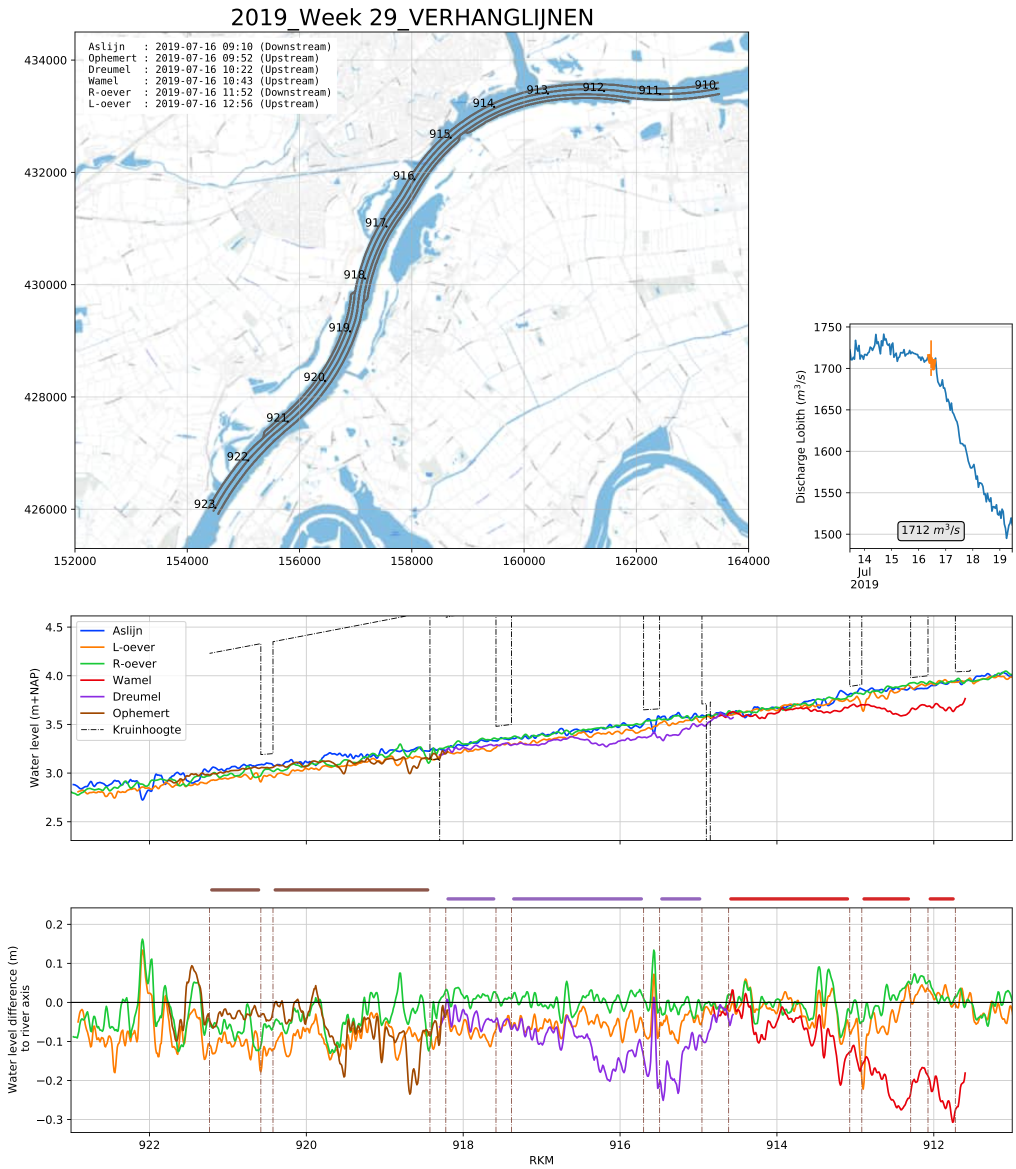

Figure B.67 Verhanglijnmeting van 2019-07-16 (afvoer Lobith: 1712 m^3/s)

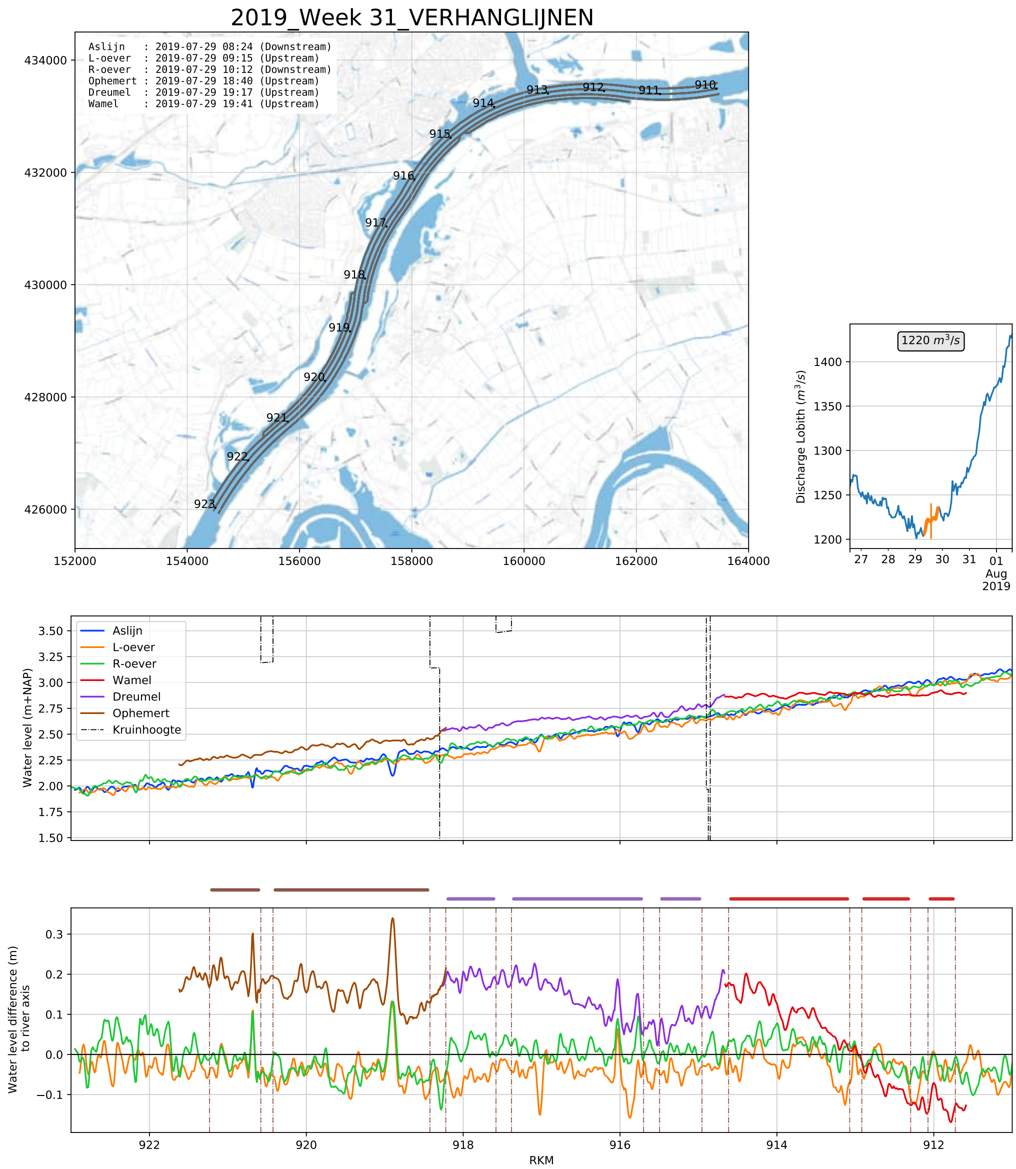

Figure B.68 Verhanglijnmeting van 2019-07-29 (afvoer Lobith: 1220 m^3/s)

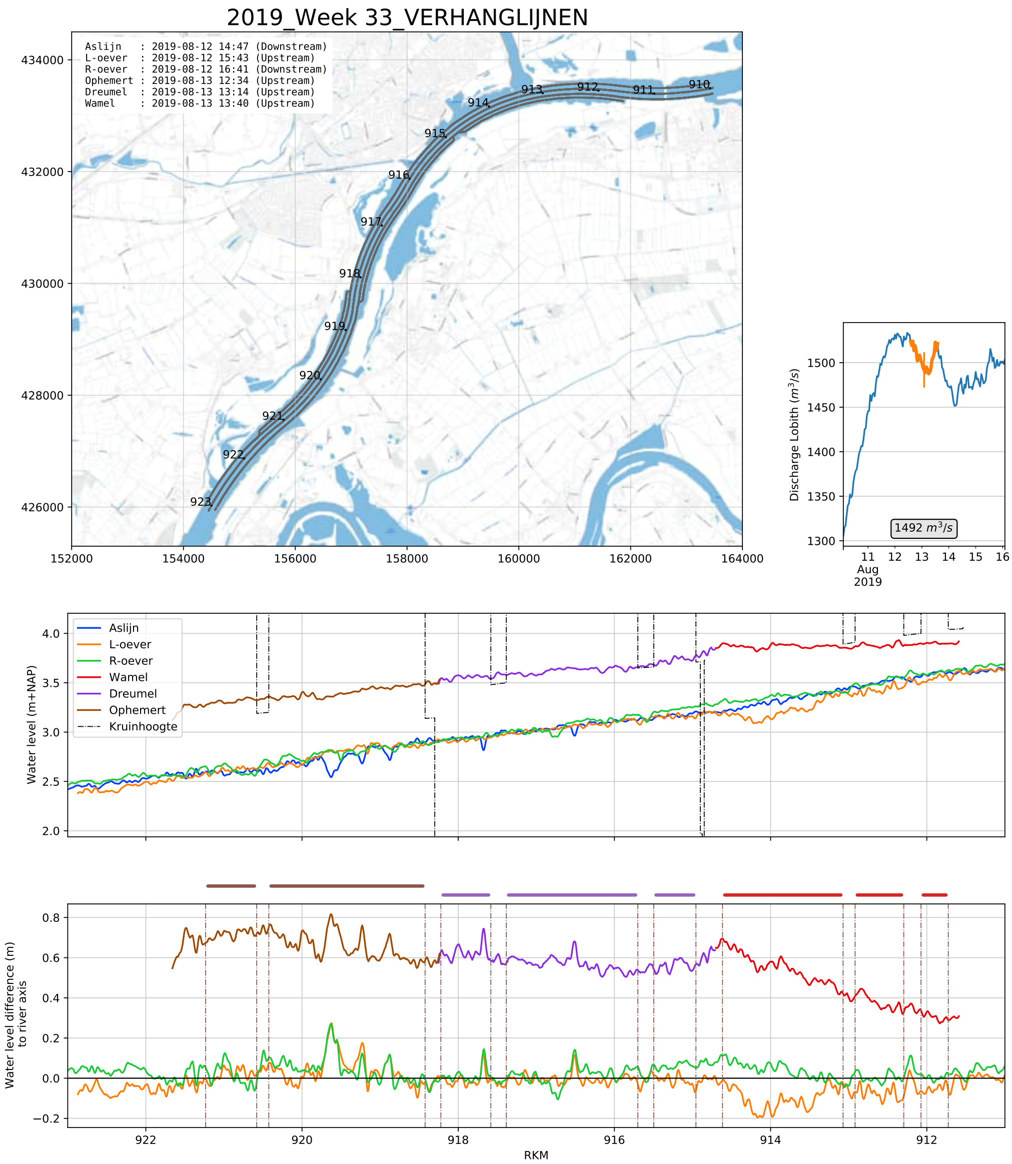

Figure B.69 Verhanglijnmeting van 2019-08-13 (afvoer Lobith: 1492 m^3/s)

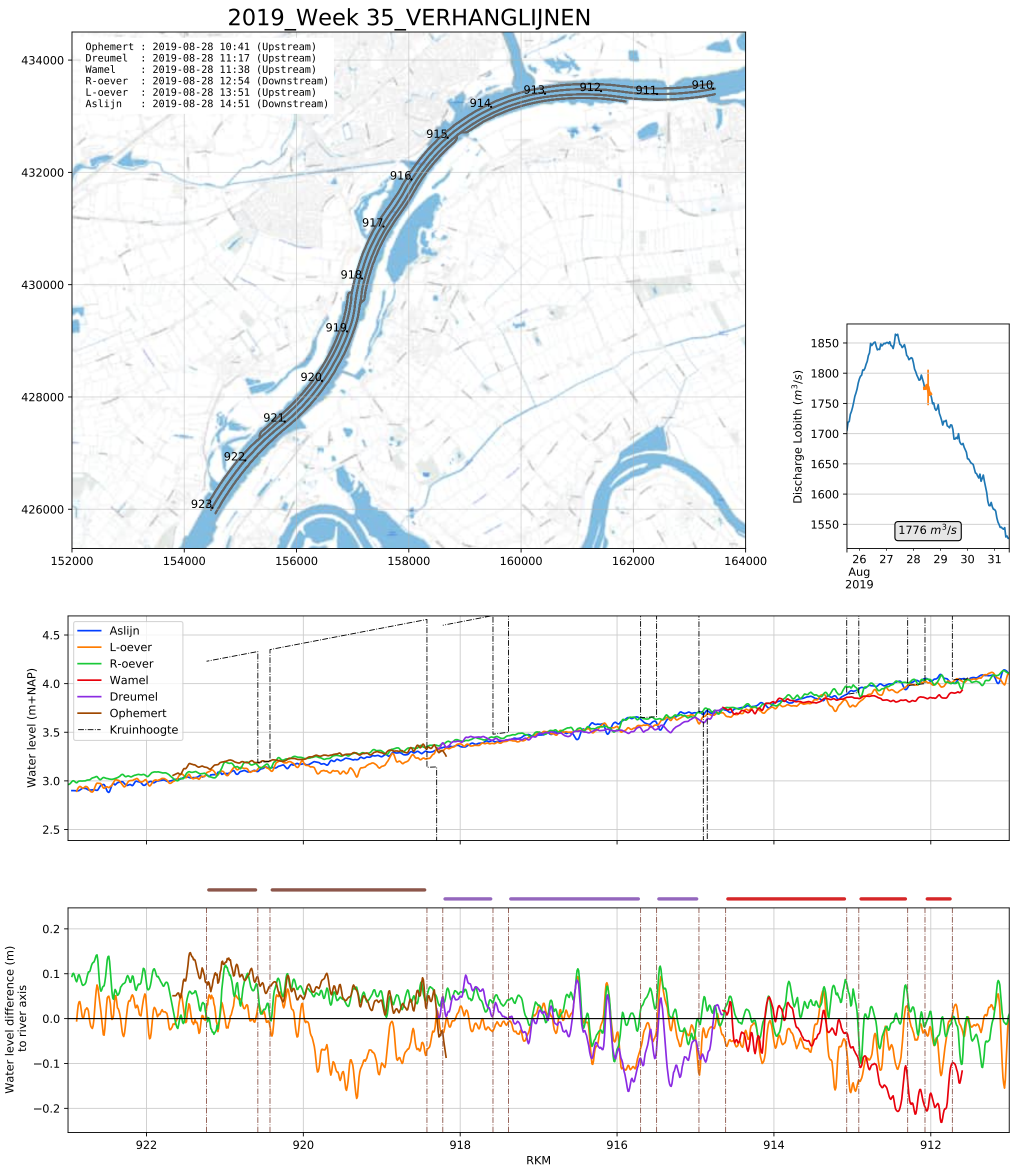

Figure B.70 Verhanglijnmeting van 2019-08-28 (afvoer Lobith: 1776 m^3/s)

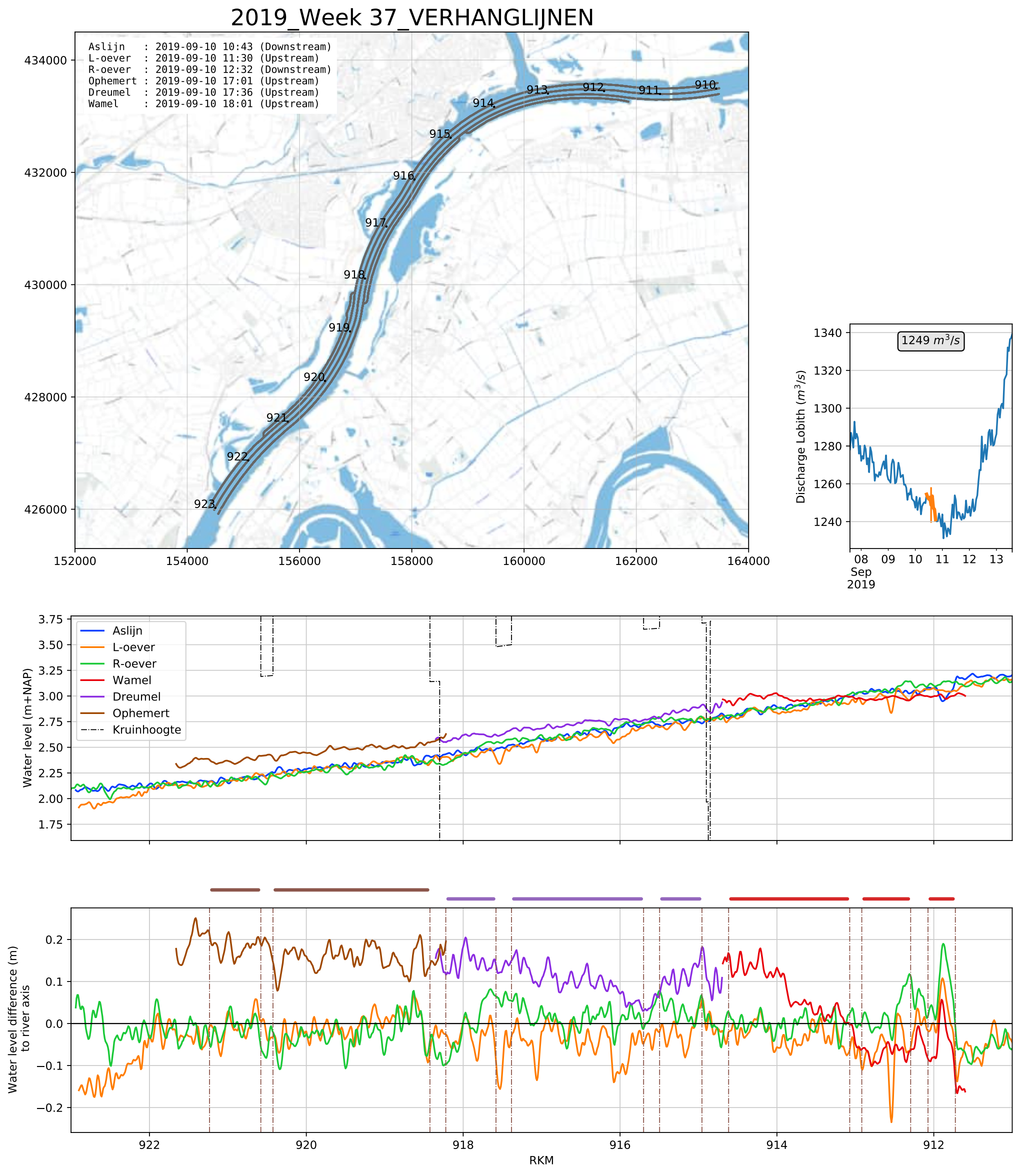

Figure B.71 Verhanglijnmeting van 2019-09-10 (afvoer Lobith: 1249 m^3/s)

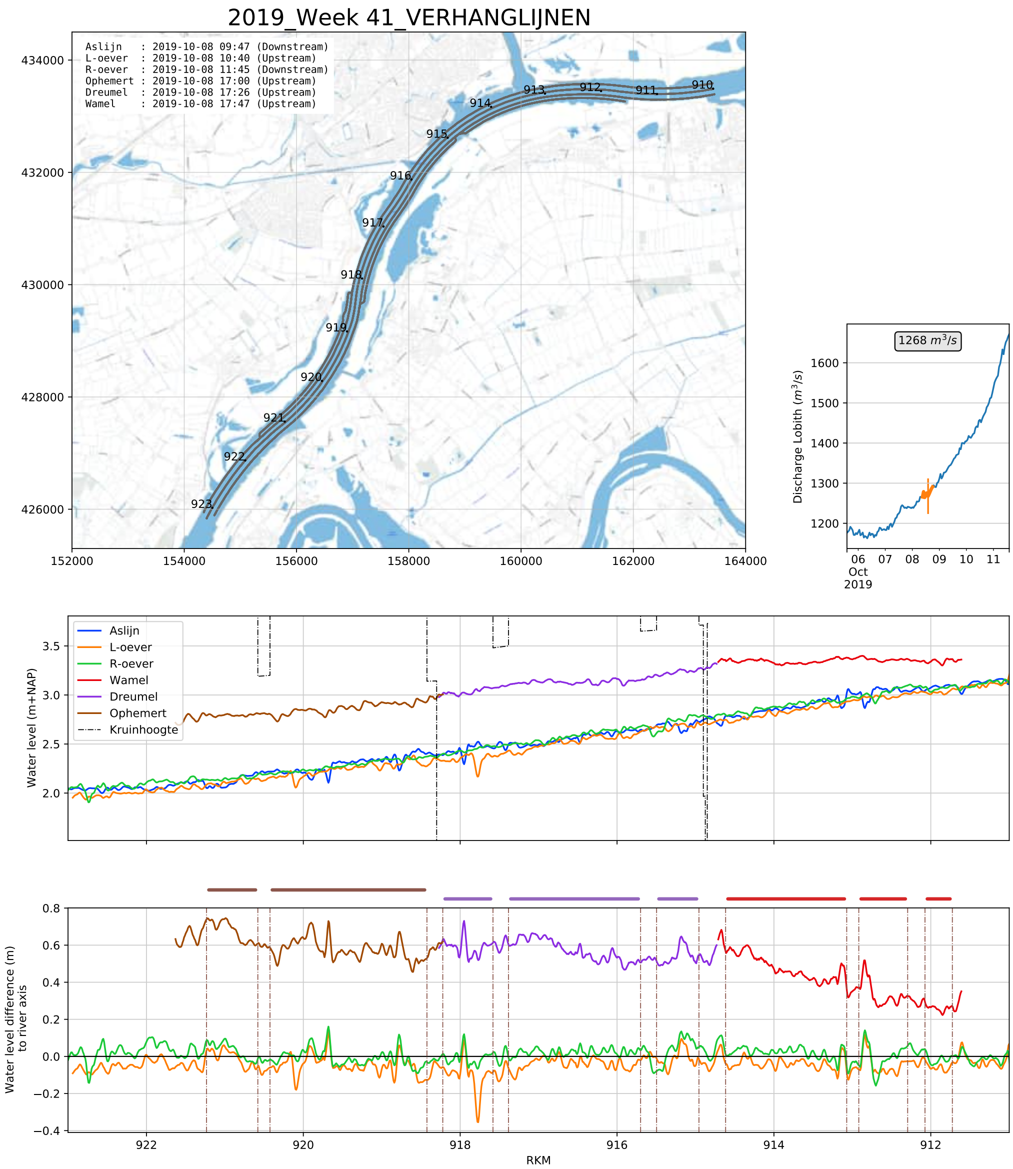

Figure B.72 Verhanglijnmeting van 2019-10-08 (afvoer Lobith: 1268 m^3/s)

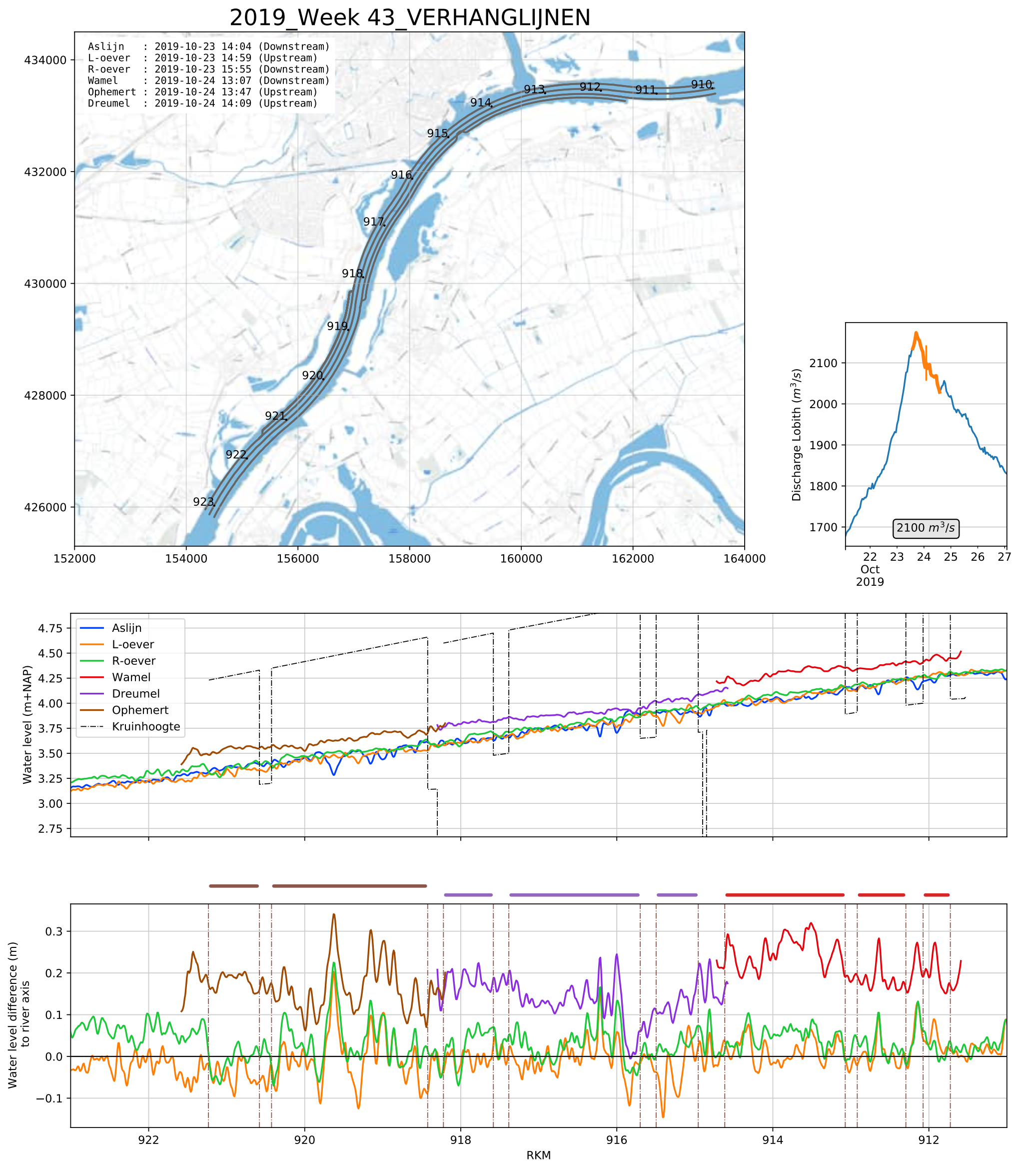

Figure B.73 Verhanglijnmeting van 2019-10-24 (afvoer Lobith: 2100 m^3/s)

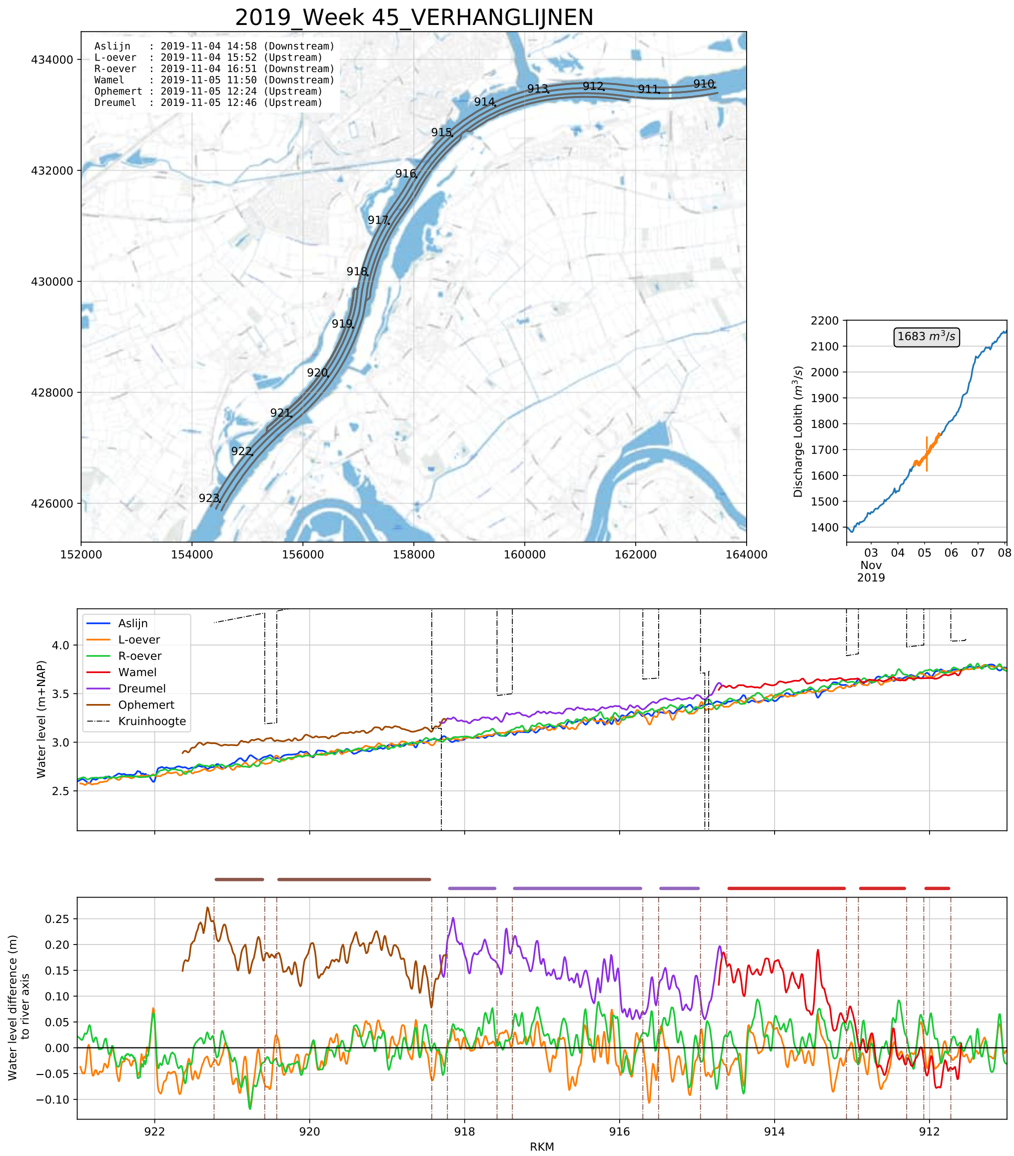

Figure B.74 Verhanglijnmeting van 2019-11-05 (afvoer Lobith: 1683 m^3/s)

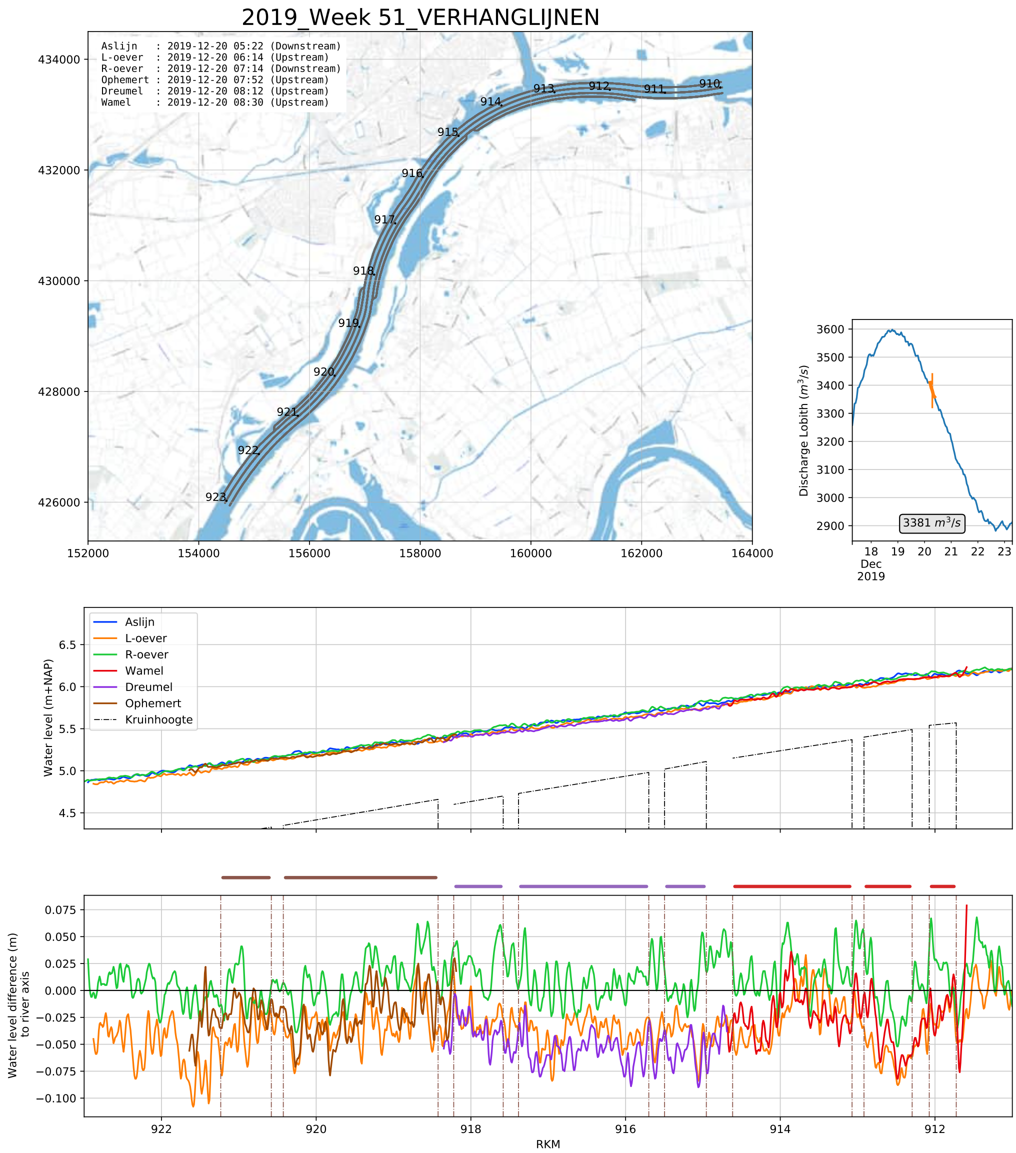

Figure B.75 Verhanglijnmeting van 2019-12-20 (afvoer Lobith: 3381 m^3/s)

Deltares

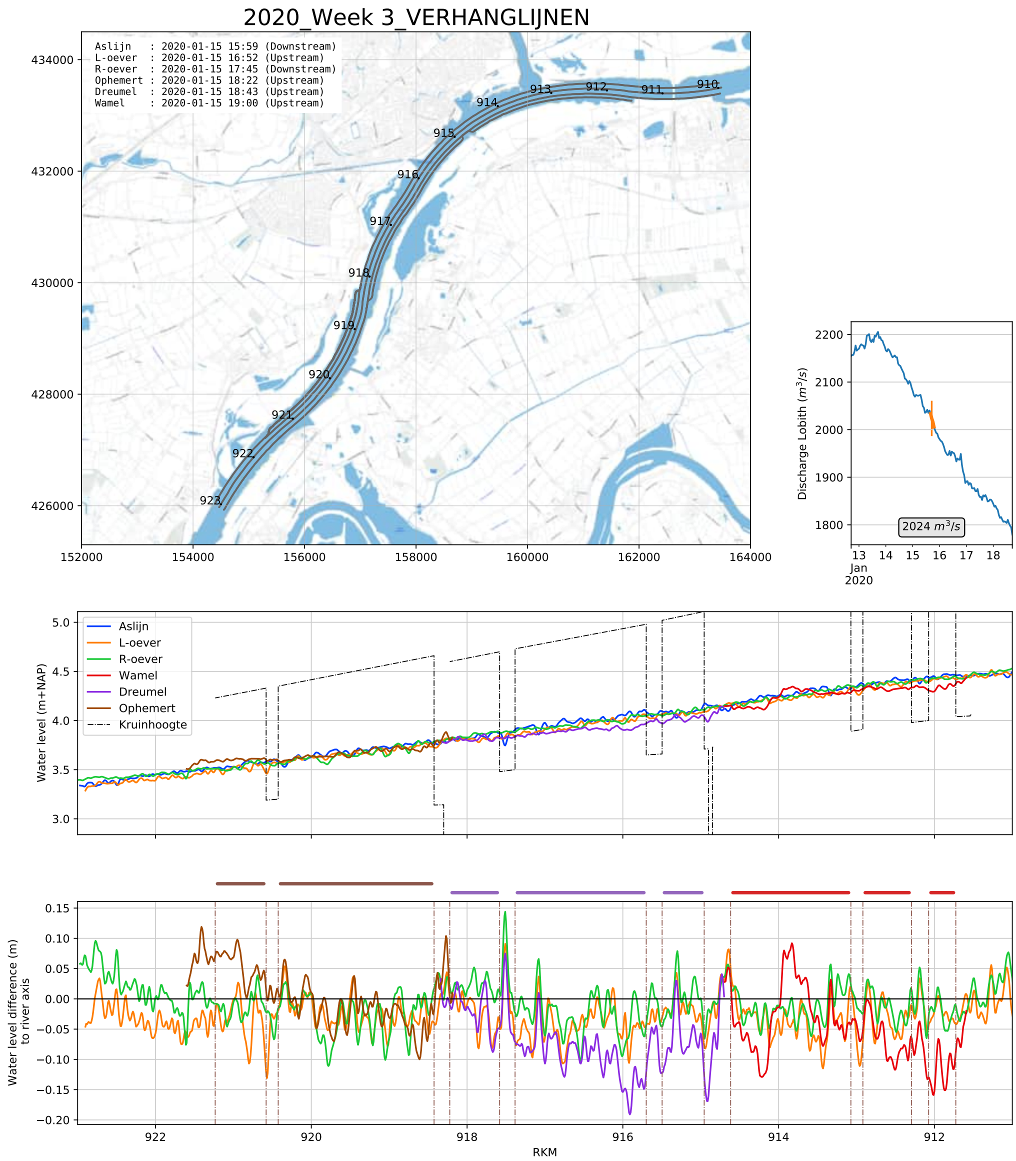

Figure B.76 Verhanglijnmeting van 2020-01-15 (afvoer Lobith: 2024 m^3/s)

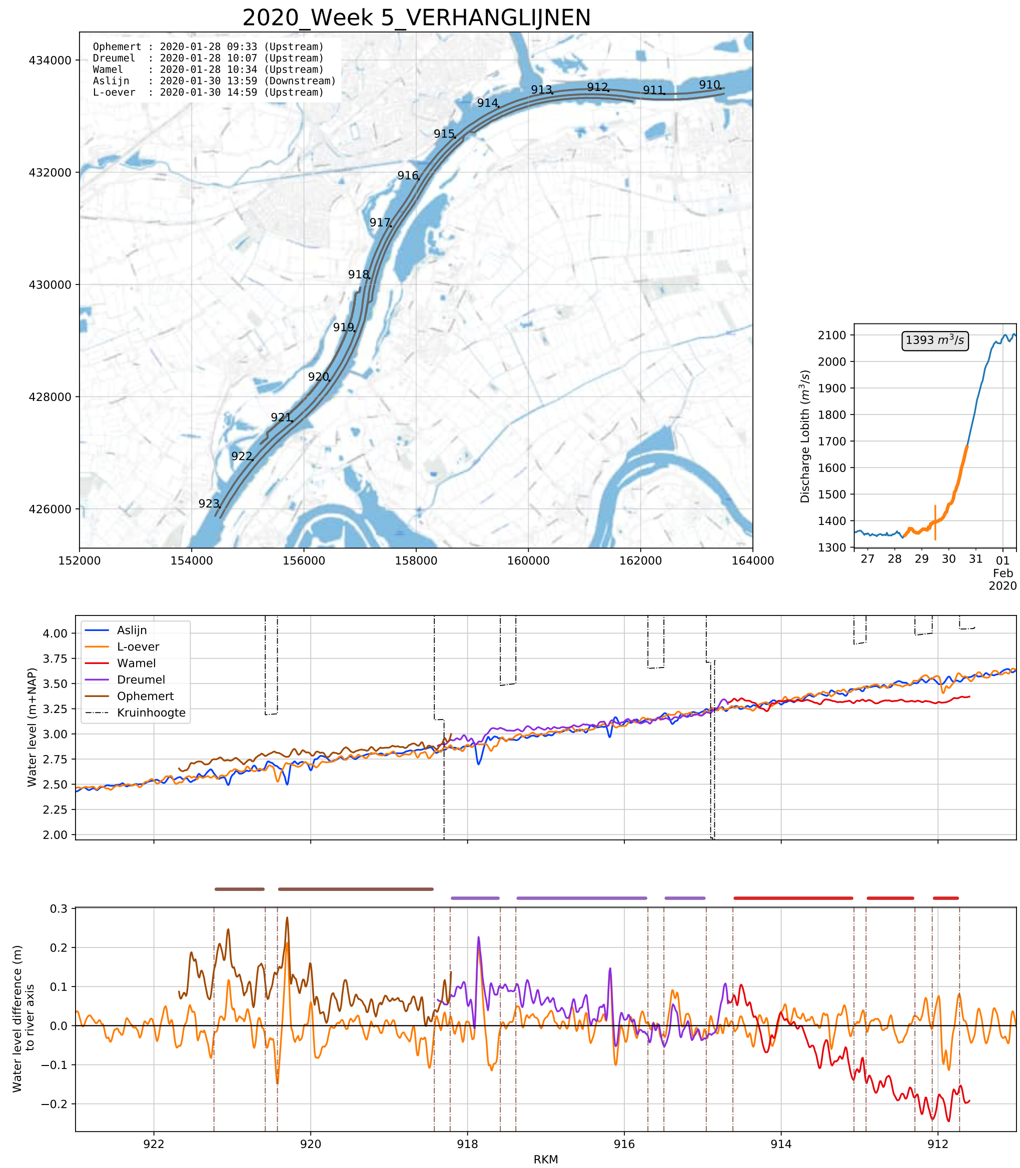

Figure B.77 Verhanglijnmeting van 2020-01-29 (afvoer Lobith: 1393 m^3/s)

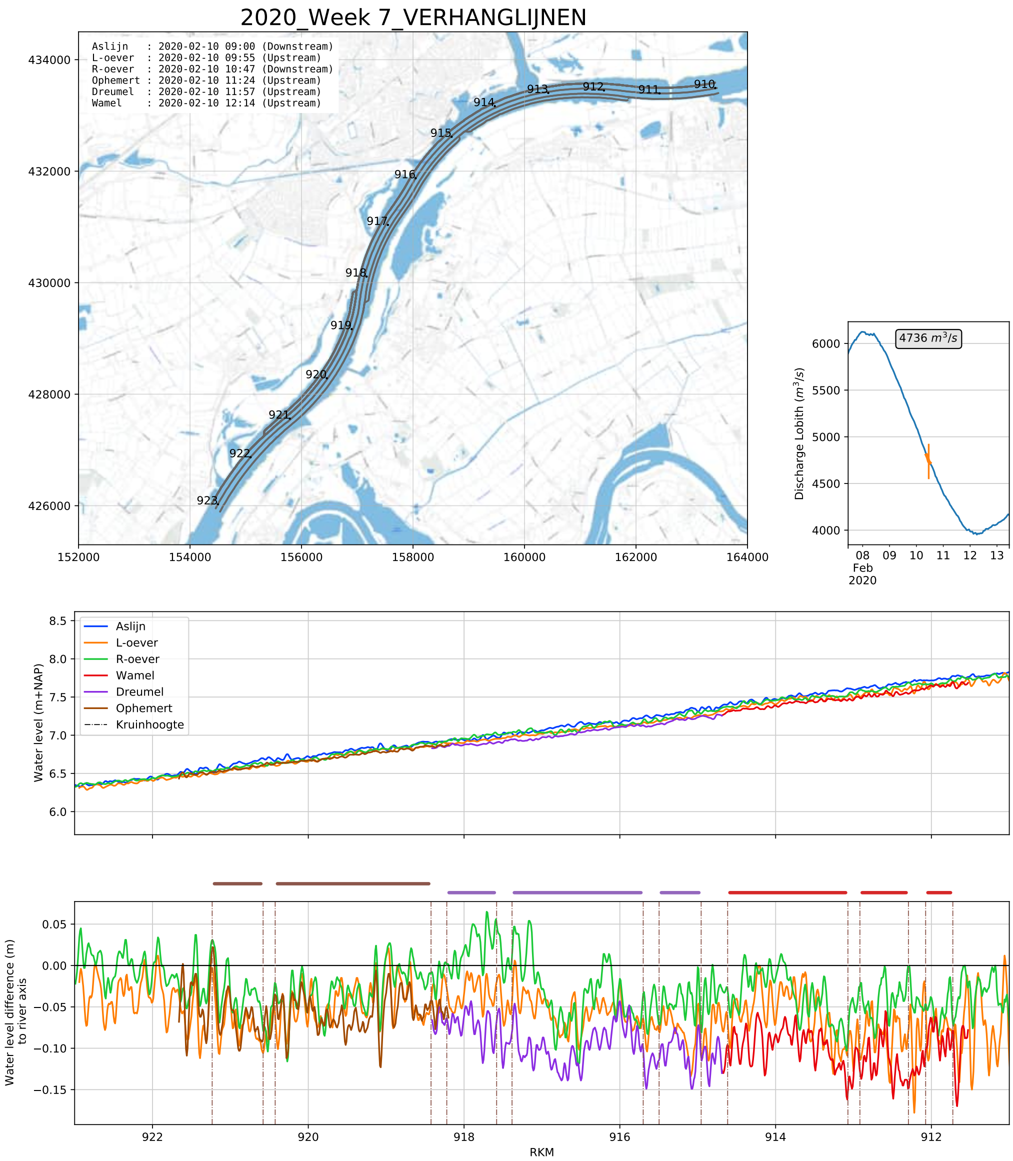

Figure B.78 Verhanglijnmeting van 2020-02-10 (afvoer Lobith: 4736 m^3/s)

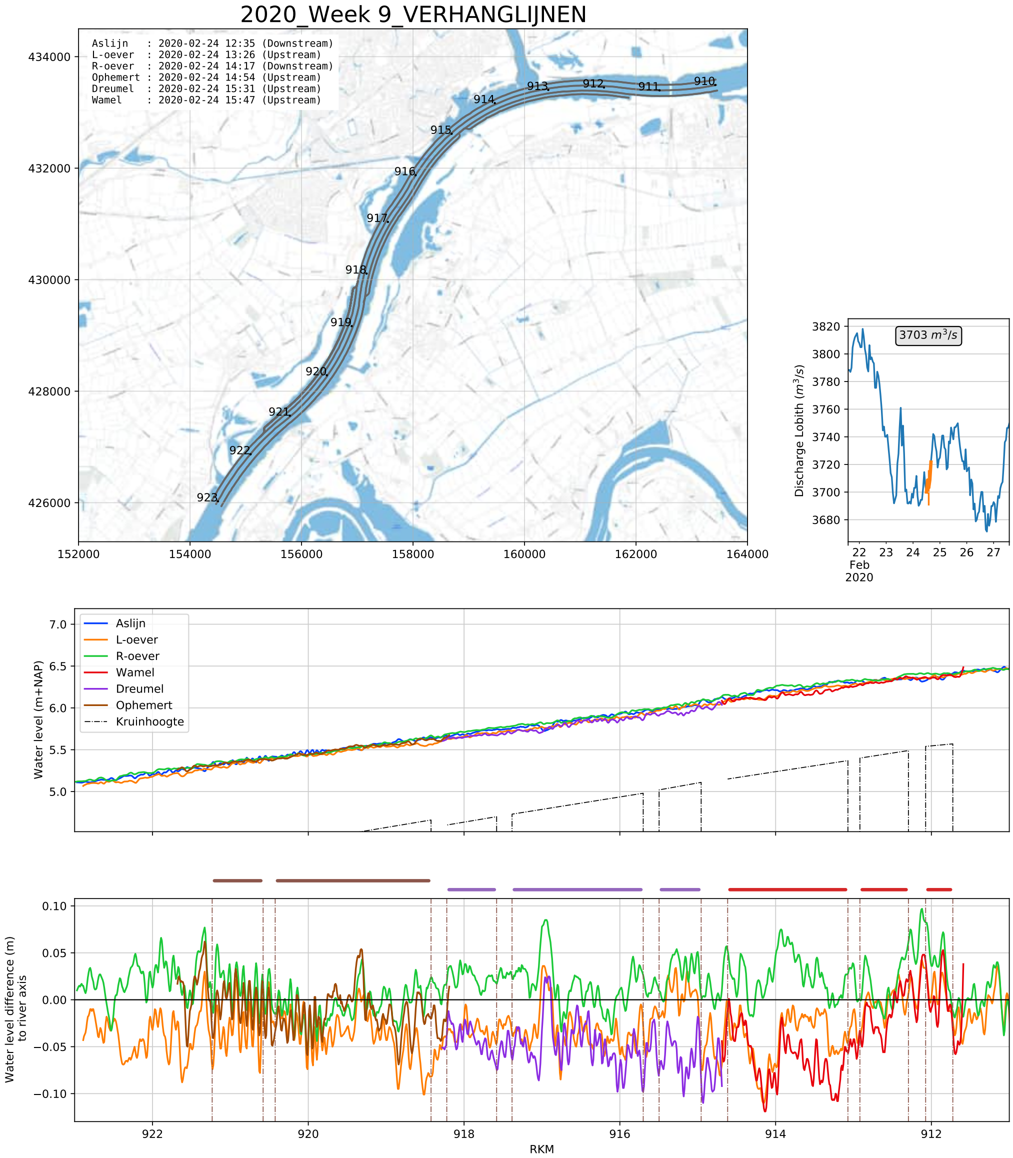

Figure B.79 Verhanglijnmeting van 2020-02-24 (afvoer Lobith: 3703 m^3/s)

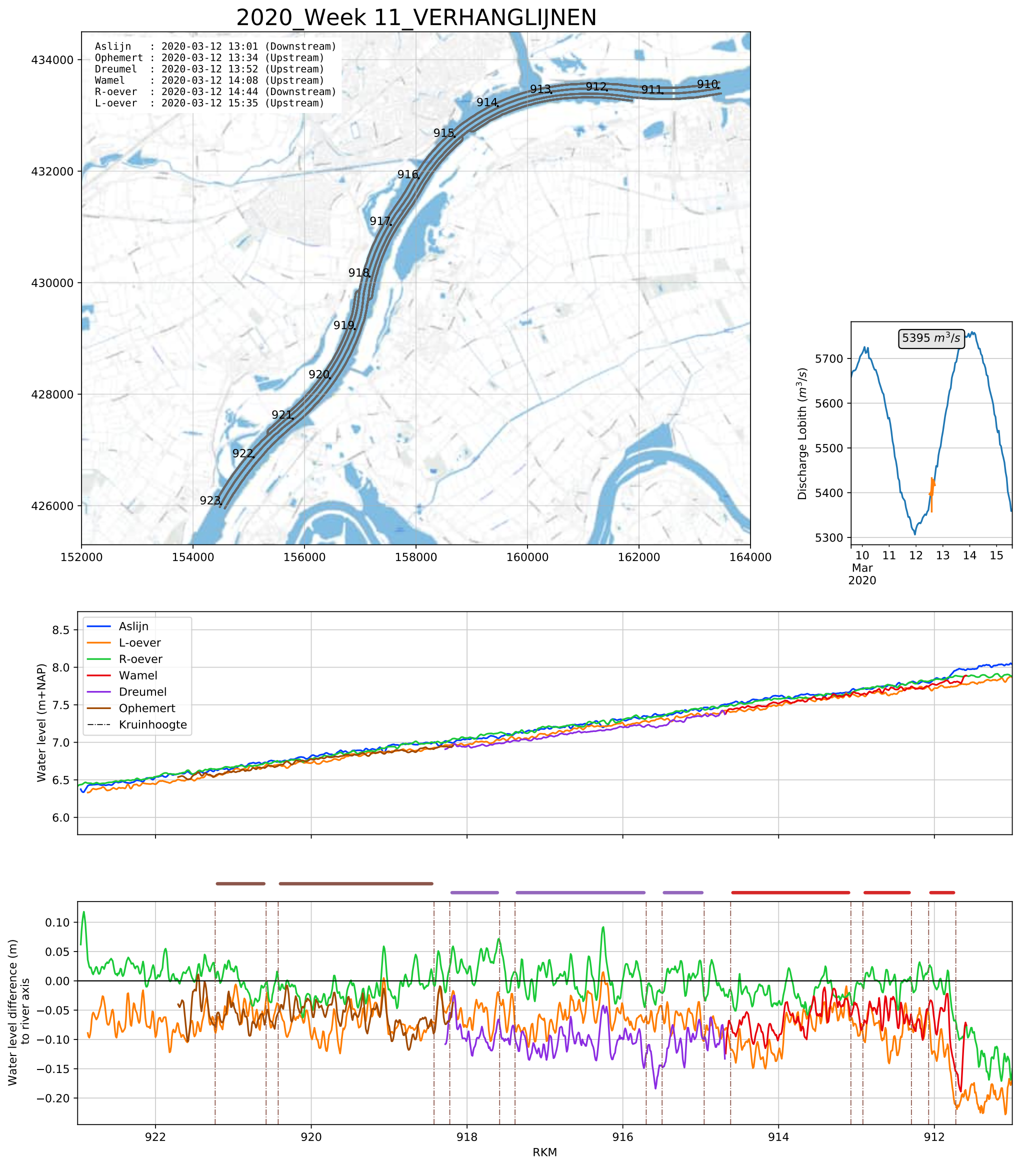

Figure B.80 Verhanglijnmeting van 2020-03-12 (afvoer Lobith: 5395 m^3/s)

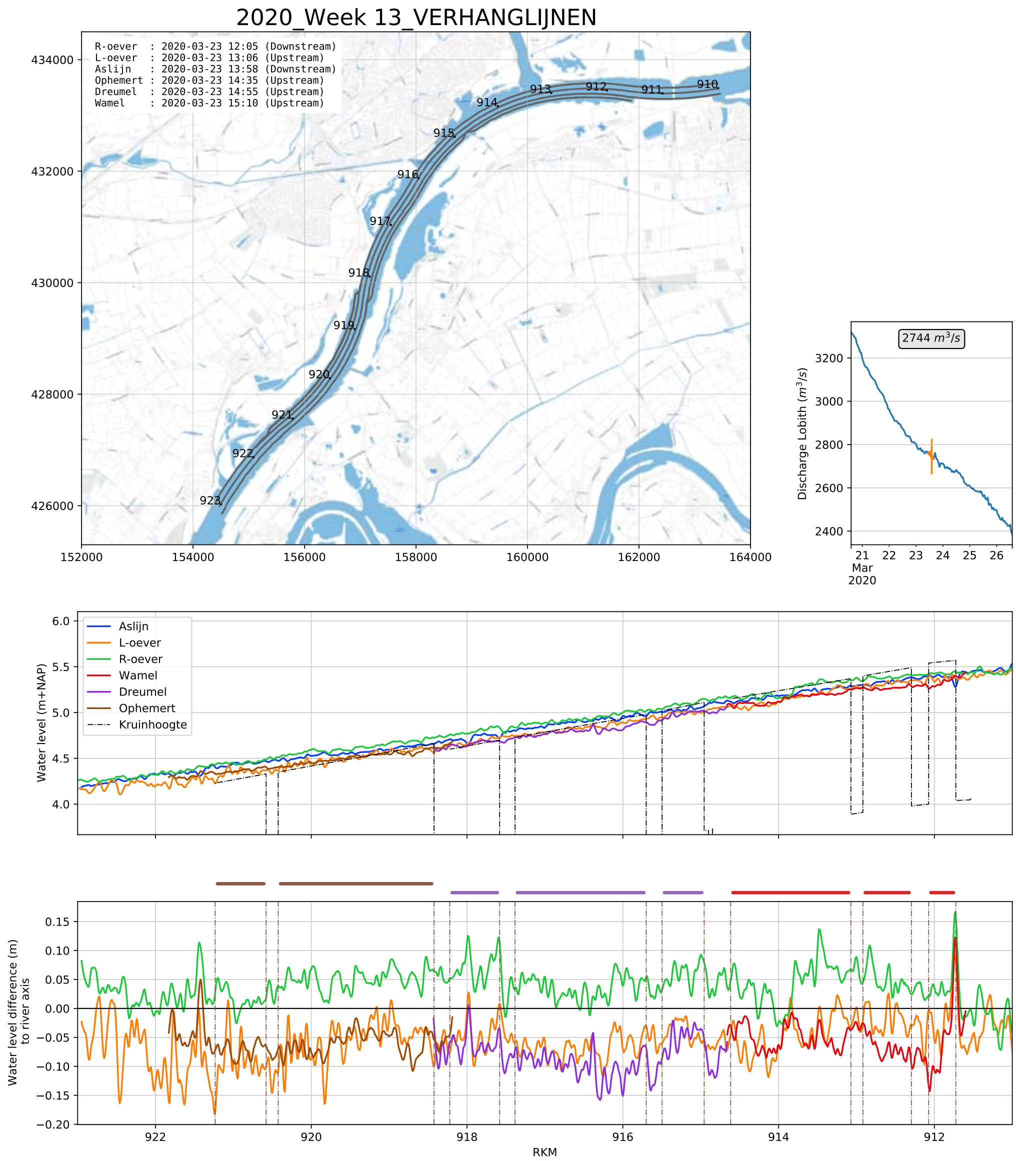

Figure B.81 Verhanglijnmeting van 2020-03-23 (afvoer Lobith: 2744 m^3/s)

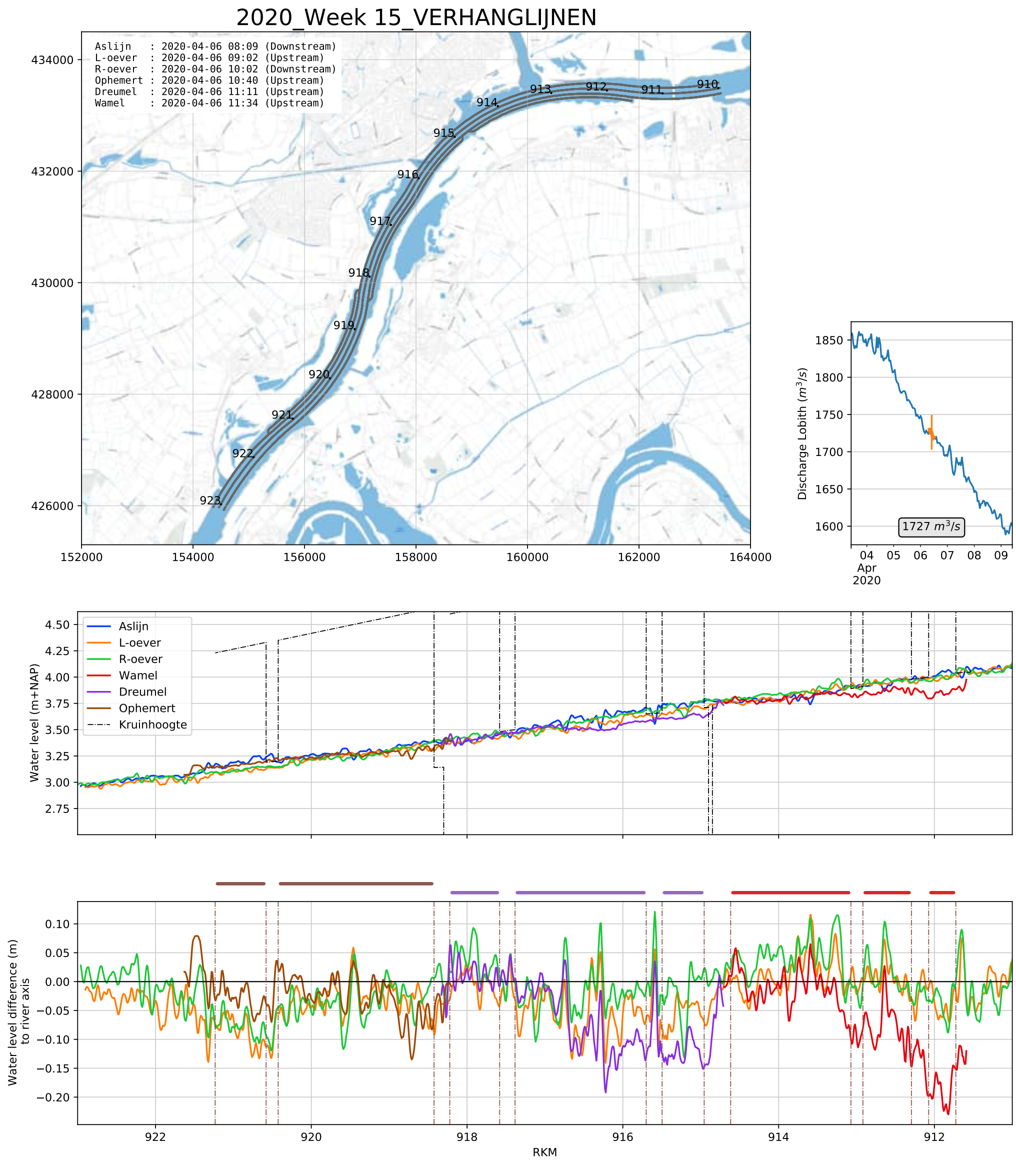

Figure B.82 Verhanglijnmeting van 2020-04-06 (afvoer Lobith: 1727 m^3/s)

Deltares

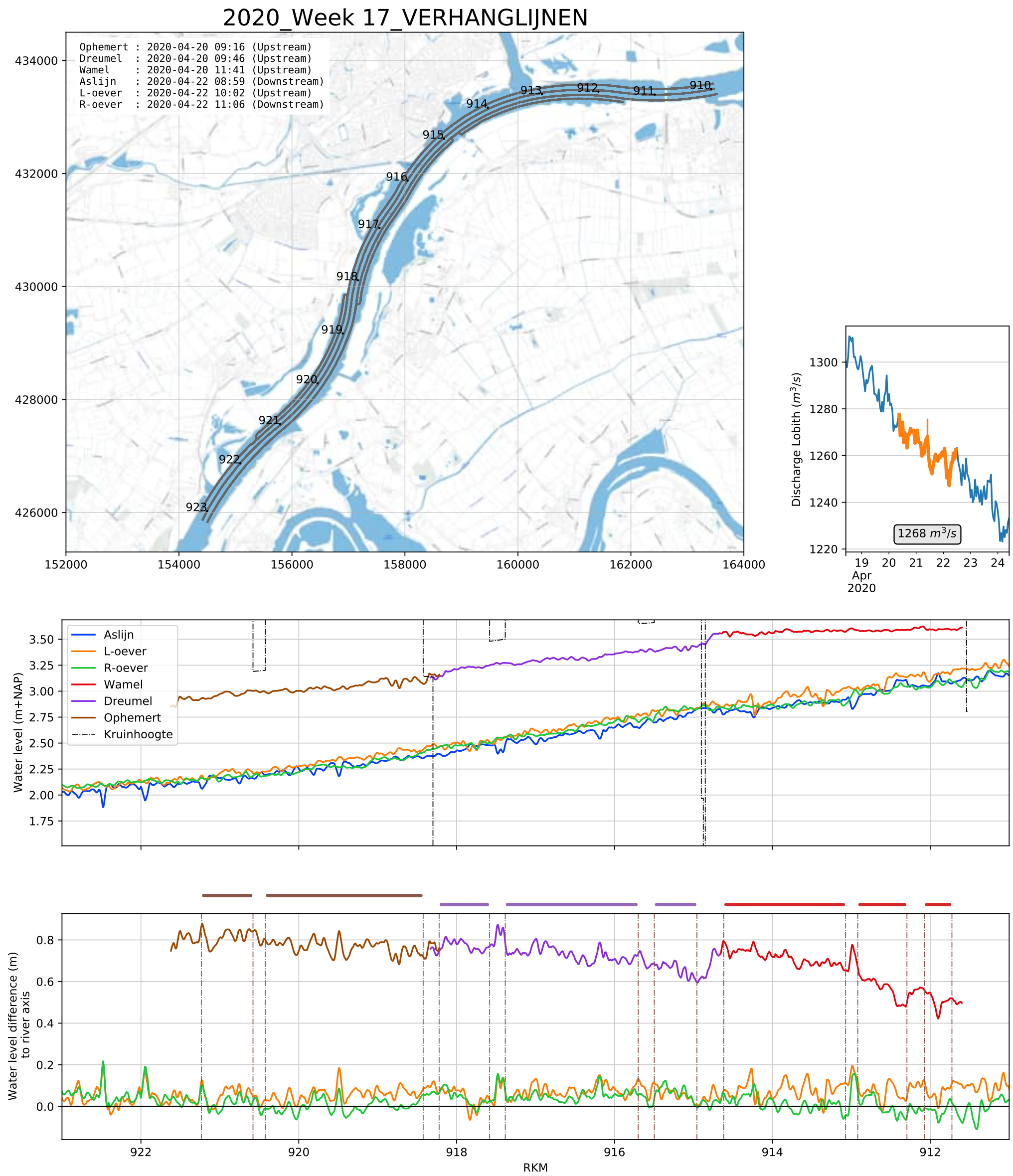

Figure B.83 Verhanglijnmeting van 2020-04-21 (afvoer Lobith: 1268 m^3/s)

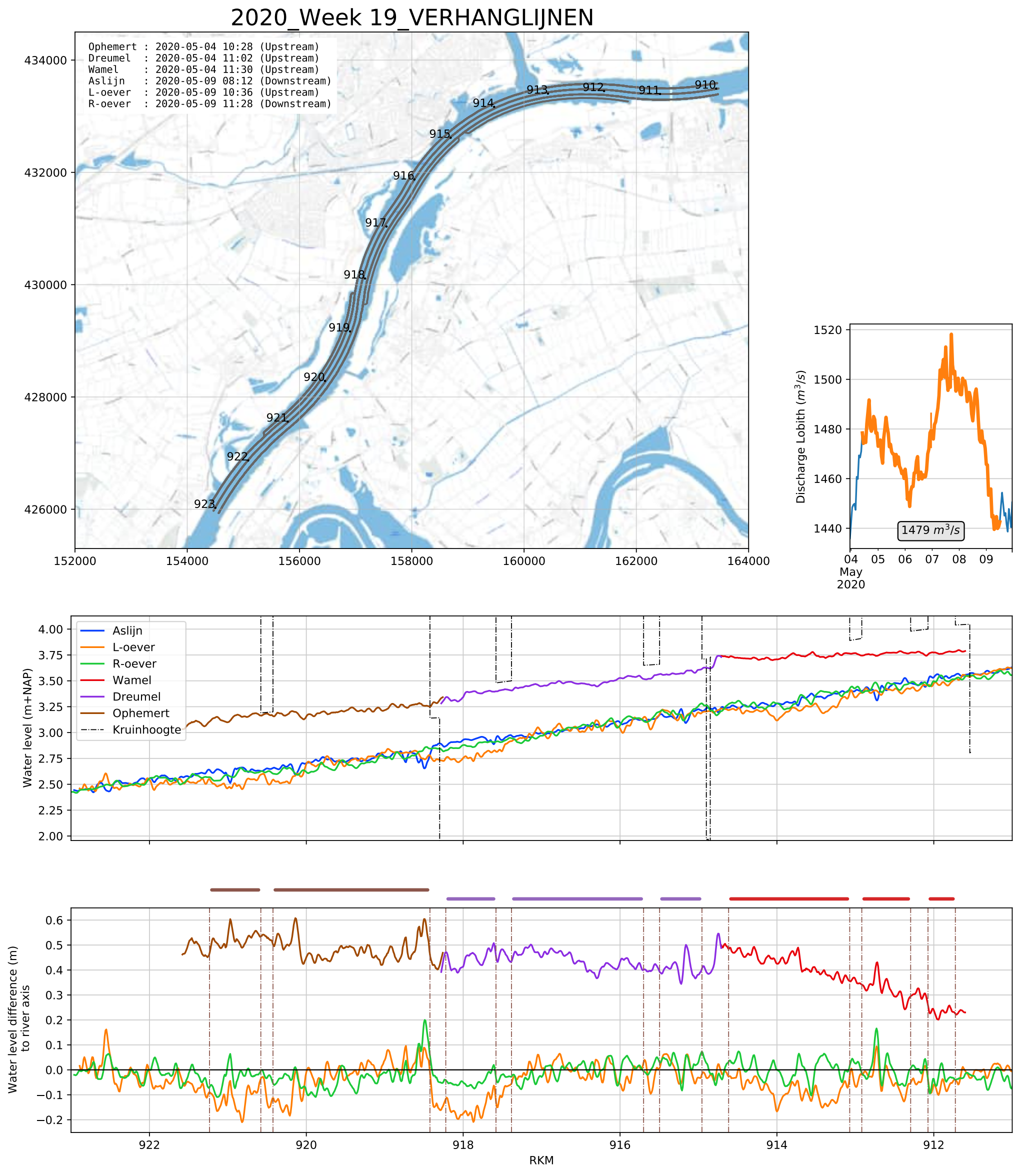

Figure B.84 Verhanglijnmeting van 2020-05-06 (afvoer Lobith: 1479 m^3/s)

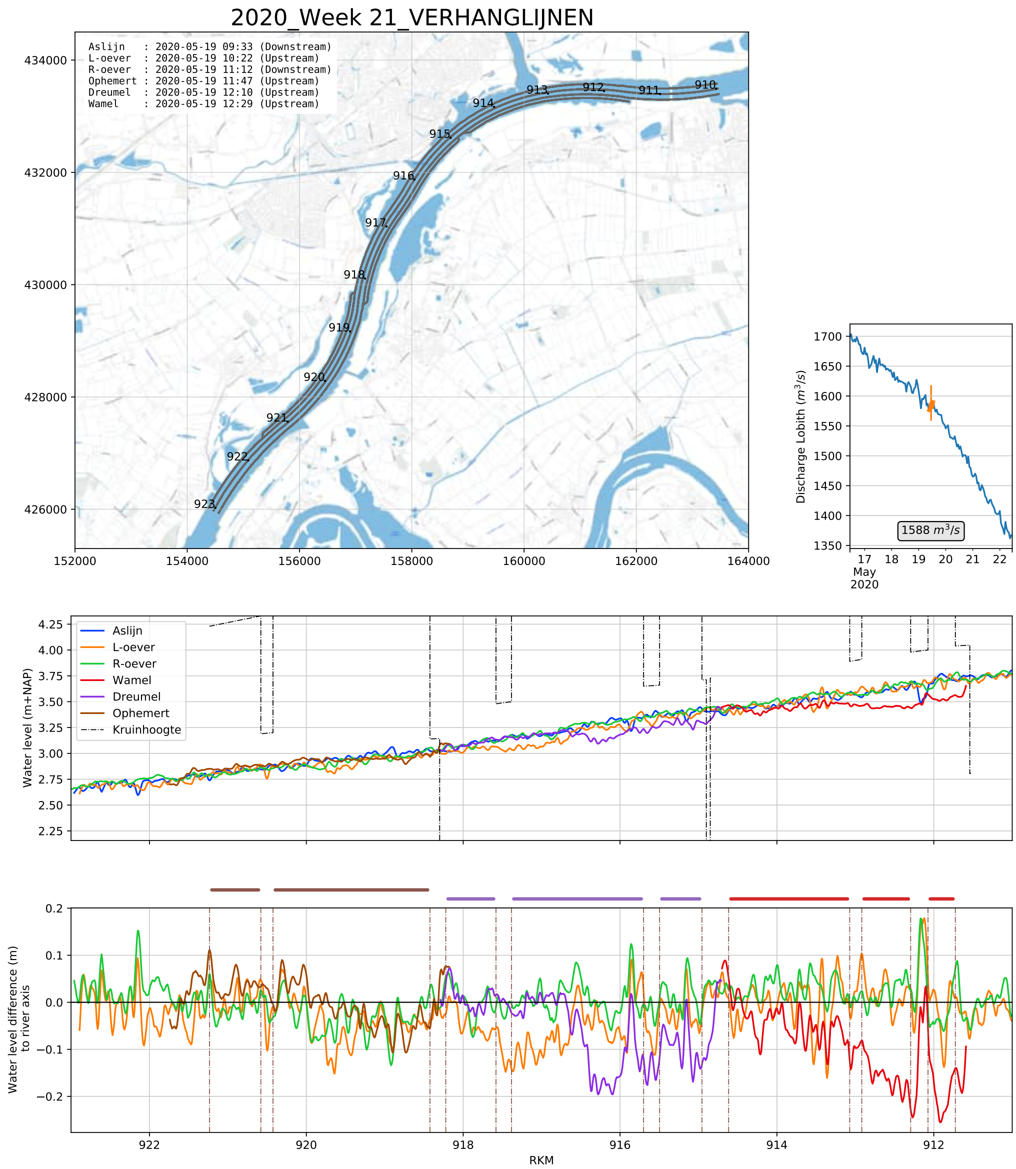

Figure B.85 Verhanglijnmeting van 2020-05-19 (afvoer Lobith: 1588 m^3/s)

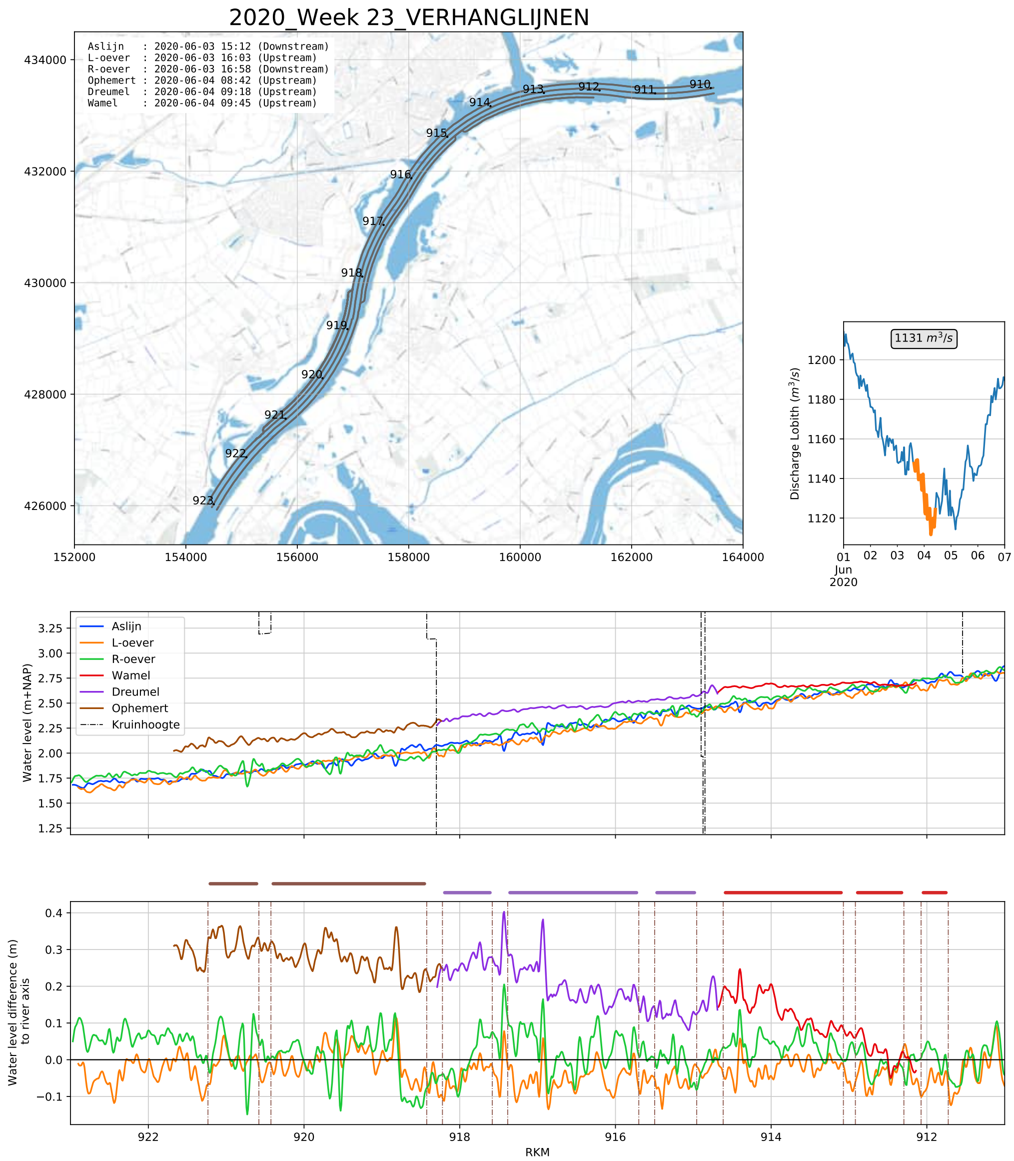

Figure B.86 Verhanglijnmeting van 2020-06-04 (afvoer Lobith: 1131 m^3/s)

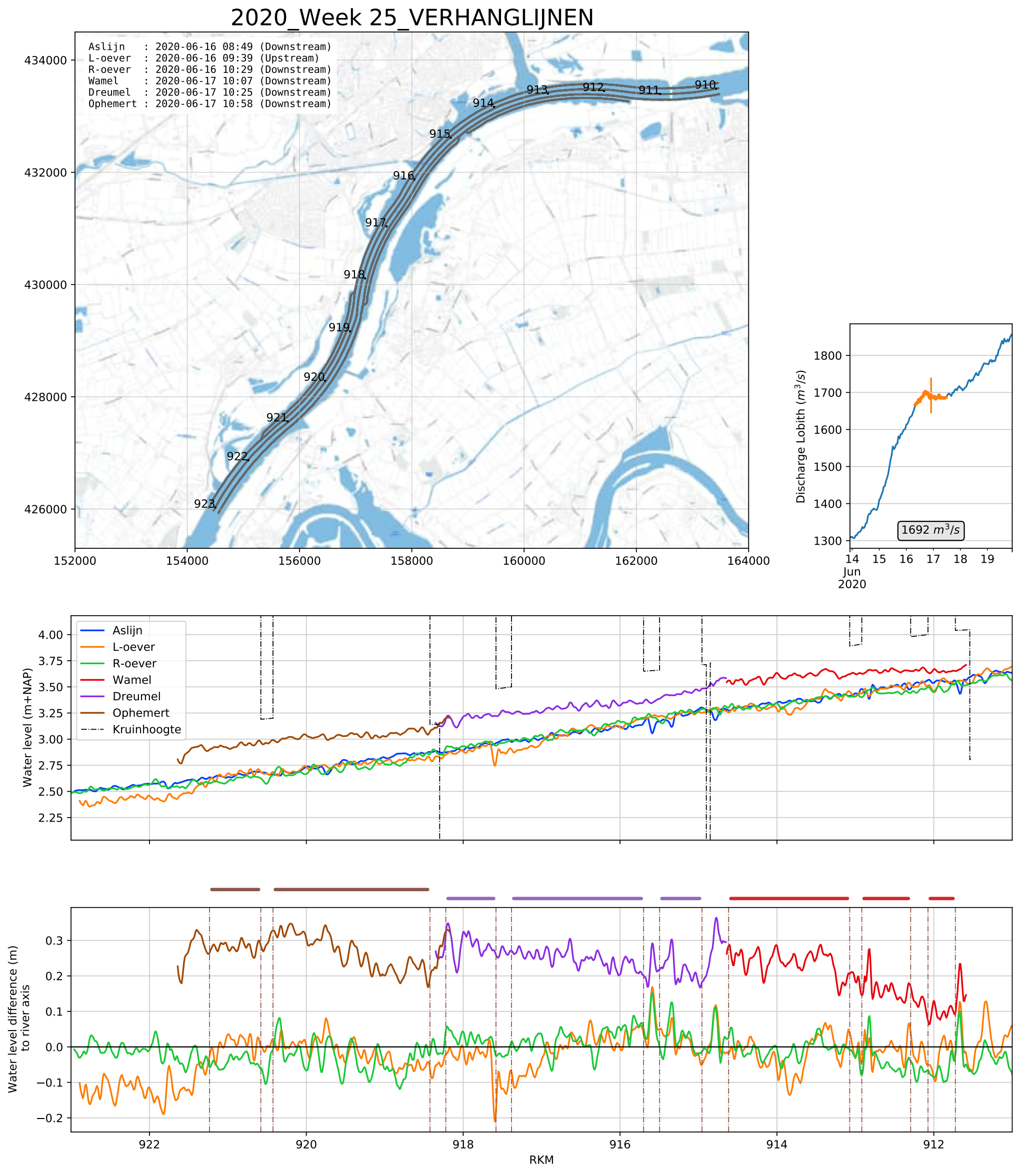

Figure B.87 Verhanglijnmeting van 2020-06-16 (afvoer Lobith: 1692 m^3/s)

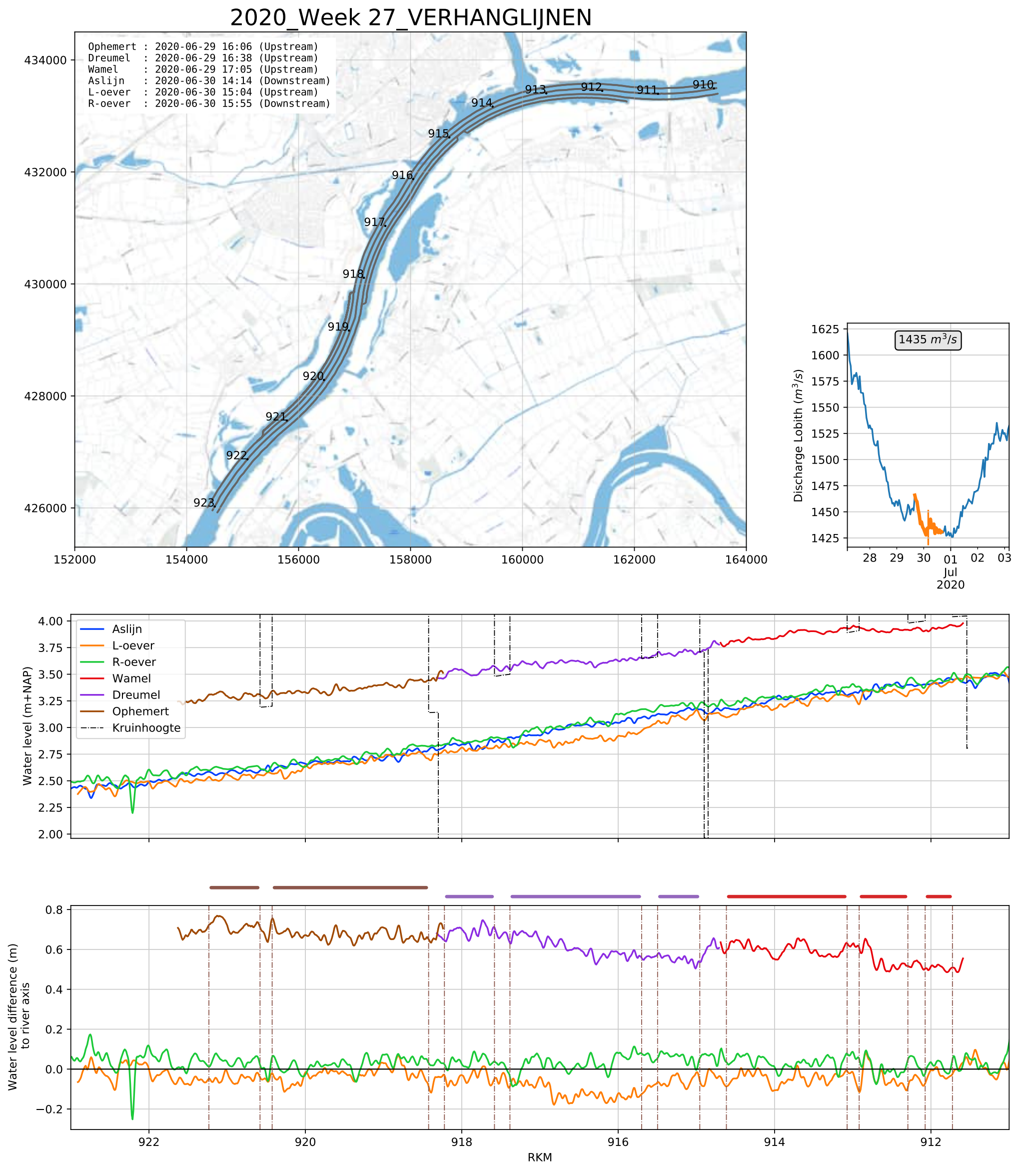

Figure B.88 Verhanglijnmeting van 2020-06-30 (afvoer Lobith: 1435 m^3/s)

B.4 Average of longitudinal measurements

This appendix shows all longitudinal measurements at the Aslijn and the three auxiliary channels. Each plot contains the water levels with Savitsky-Golay filtering for a range of discharge. The linestyle indicates different moments in time (dotted: oldest, solid, dash-dot: most recent). For the Aslijn plot this results in before construction (dotted), during construction (solid) and after construction (dash-dot). For the auxiliary channels this results in after construction (dotted), before the first change in inlet (solid) and after the first change in inlet (dash-dot).

B.4.1 Aslijn

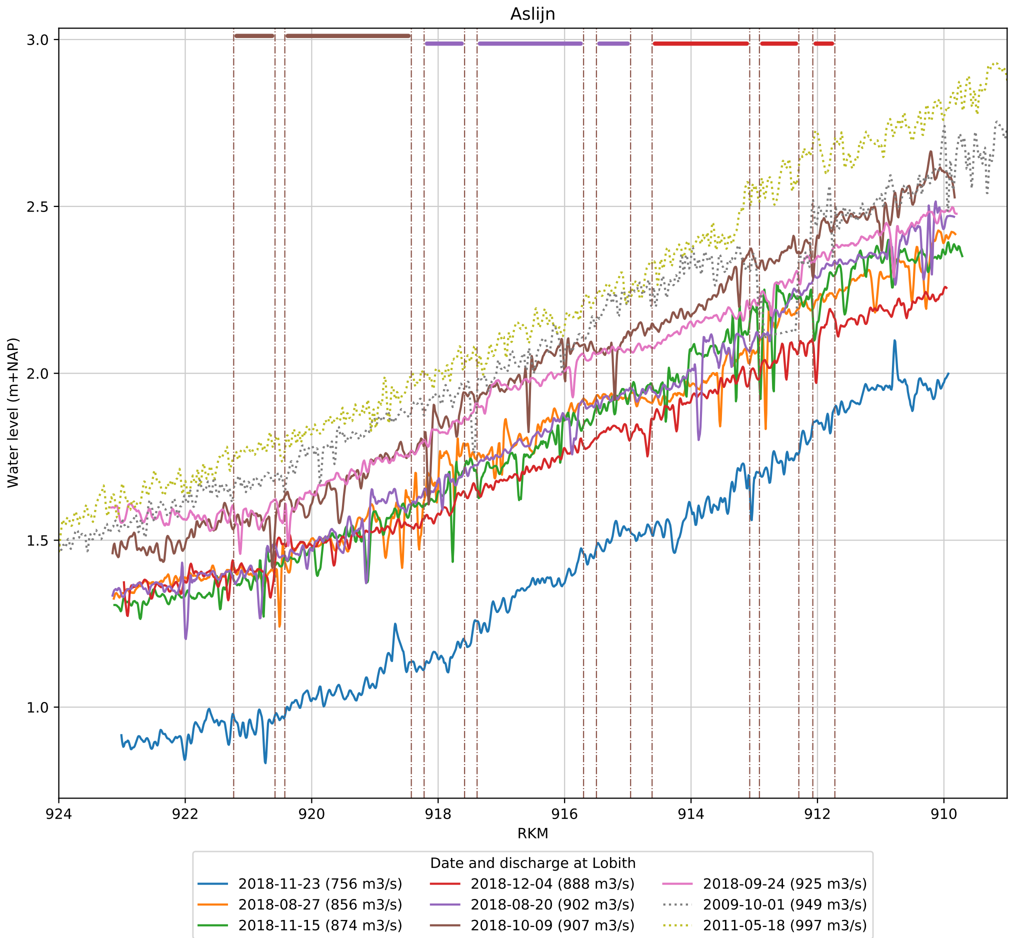

Figure B.89 Longitudinal water level measurements for discharges up to 1000 m^3/s in the main channel (Aslijn) using the Savitsky-Golay filter.

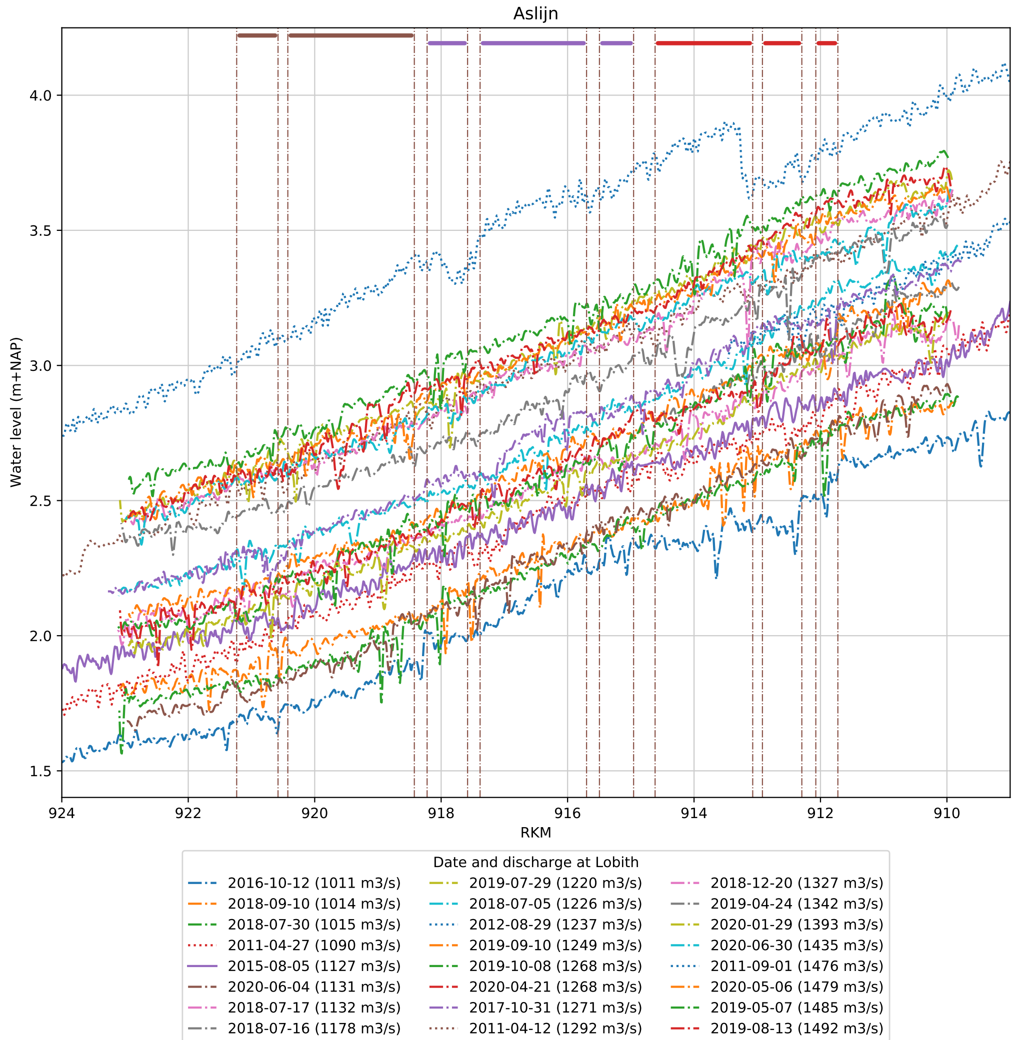

Figure B.90 Longitudinal water level measurements for discharges between 1000 and 1500 m^3/s in the main channel (Aslijn) using the Savitsky-Golay filter.

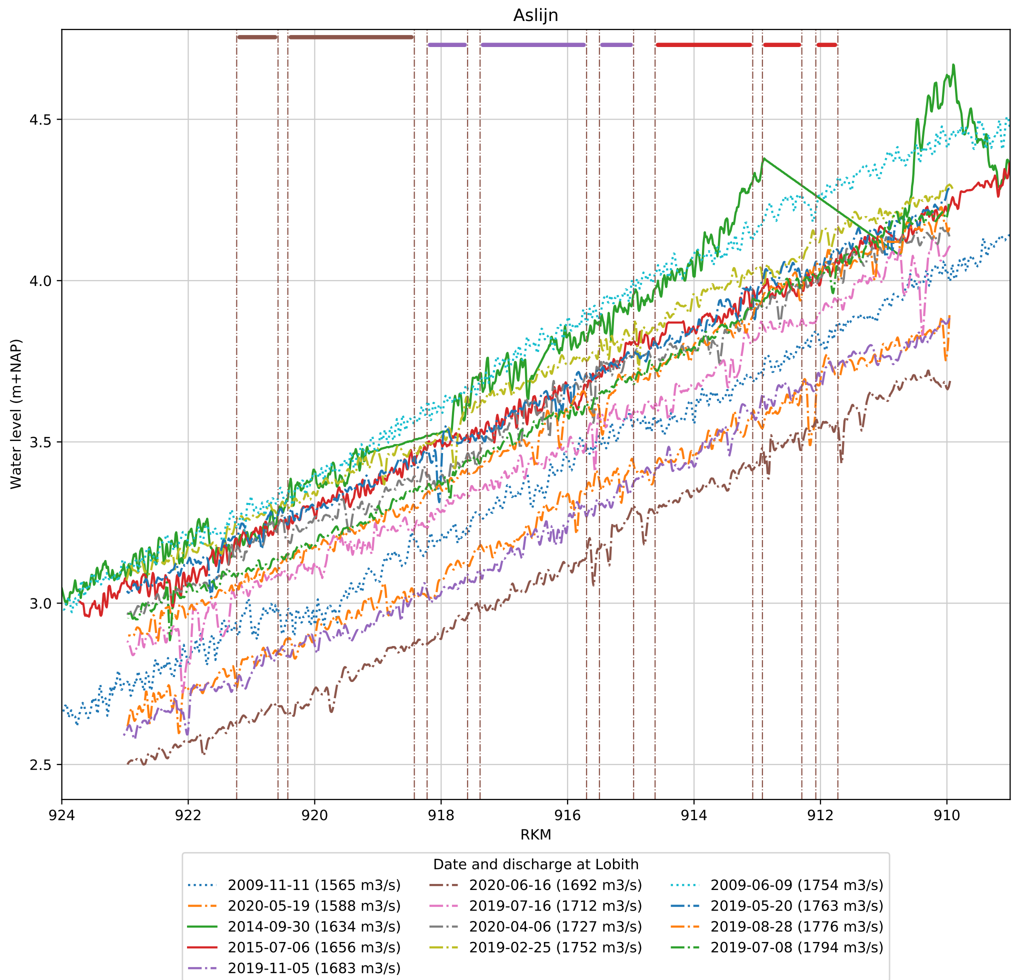

Figure B.91 Longitudinal water level measurements for discharges between 1500 and 1800 m^3/s in the main channel (Aslijn) using the Savitsky-Golay filter.

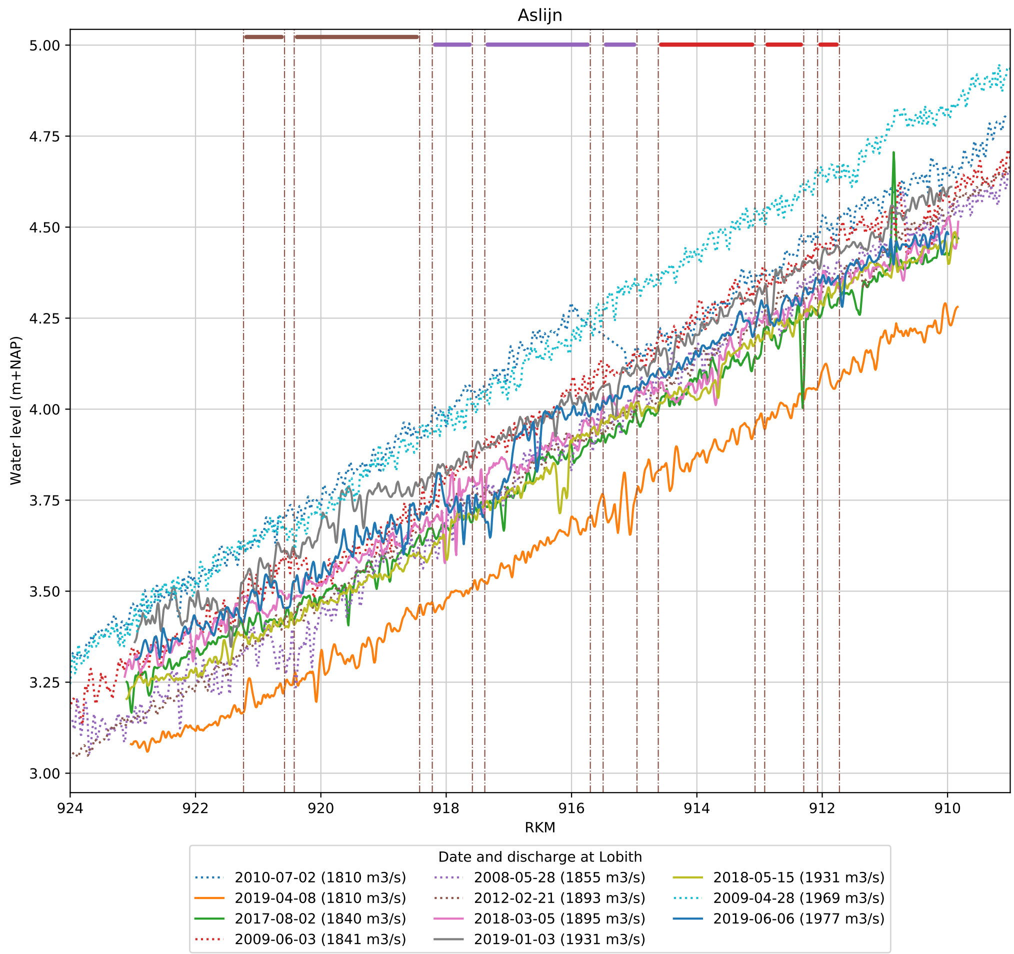

Figure B.92 Longitudinal water level measurements for discharges between 1800 and 2000 m^3/s in the main channel (Aslijn) using the Savitsky-Golay filter.

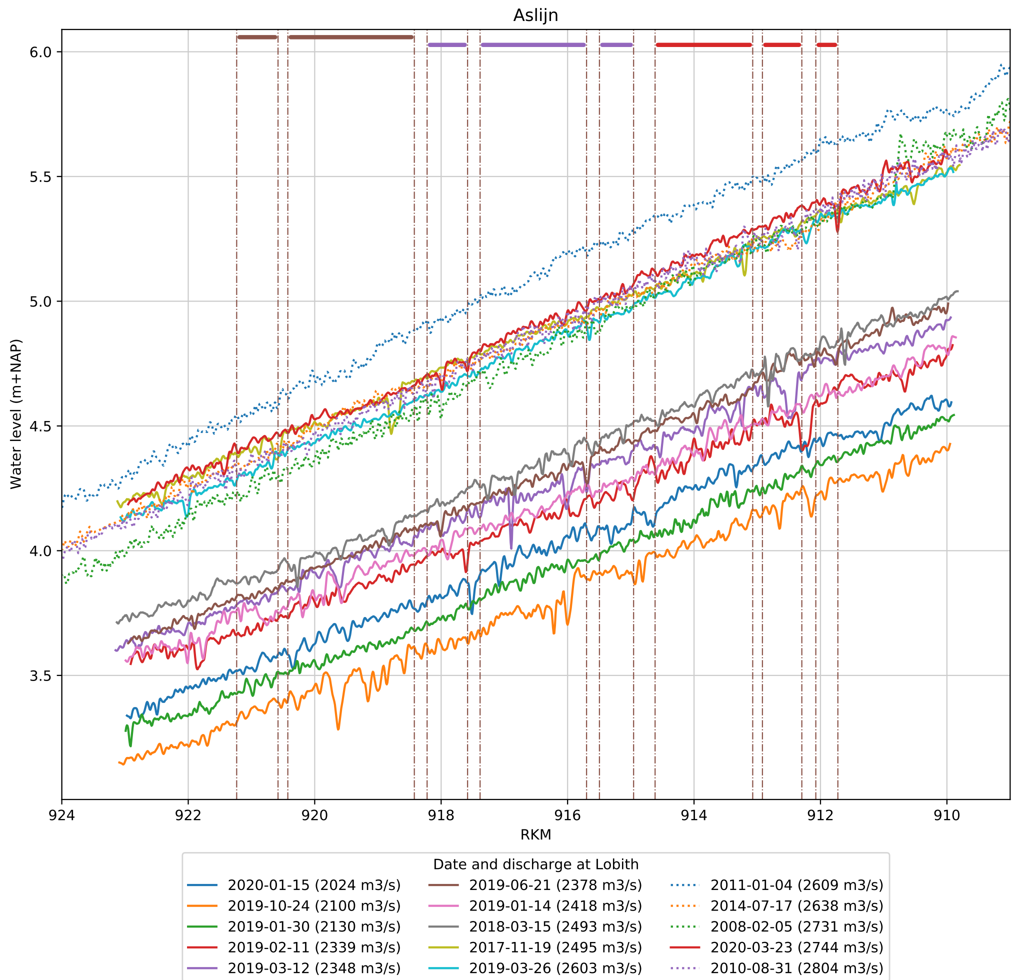

Figure B.93 Longitudinal water level measurements for discharges between 2000 and 3000 m^3/s in the main channel (Aslijn) using the Savitsky-Golay filter.

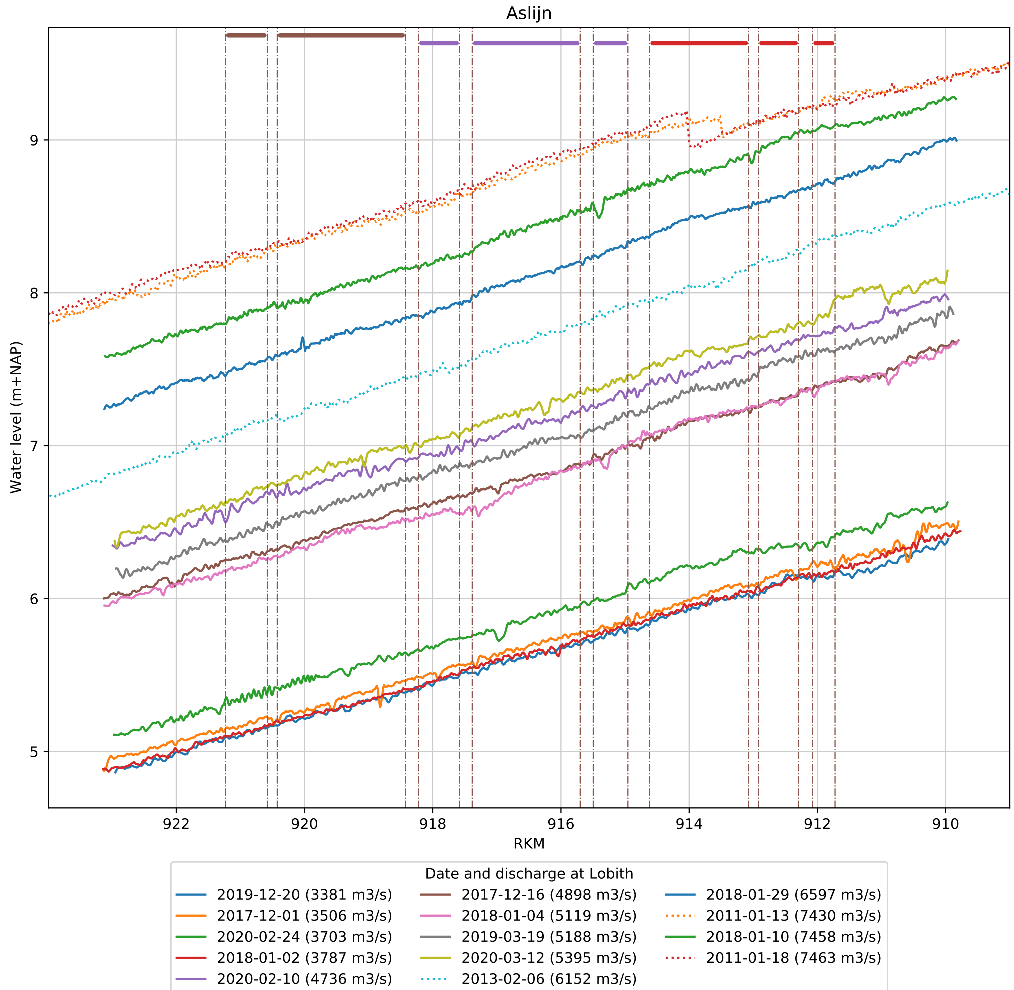

Figure B.94 Longitudinal water level measurements for discharges larger than 3000 m^3/s in the main channel (Aslijn) using the Savitsky-Golay filter.

B.4.2 Wamel

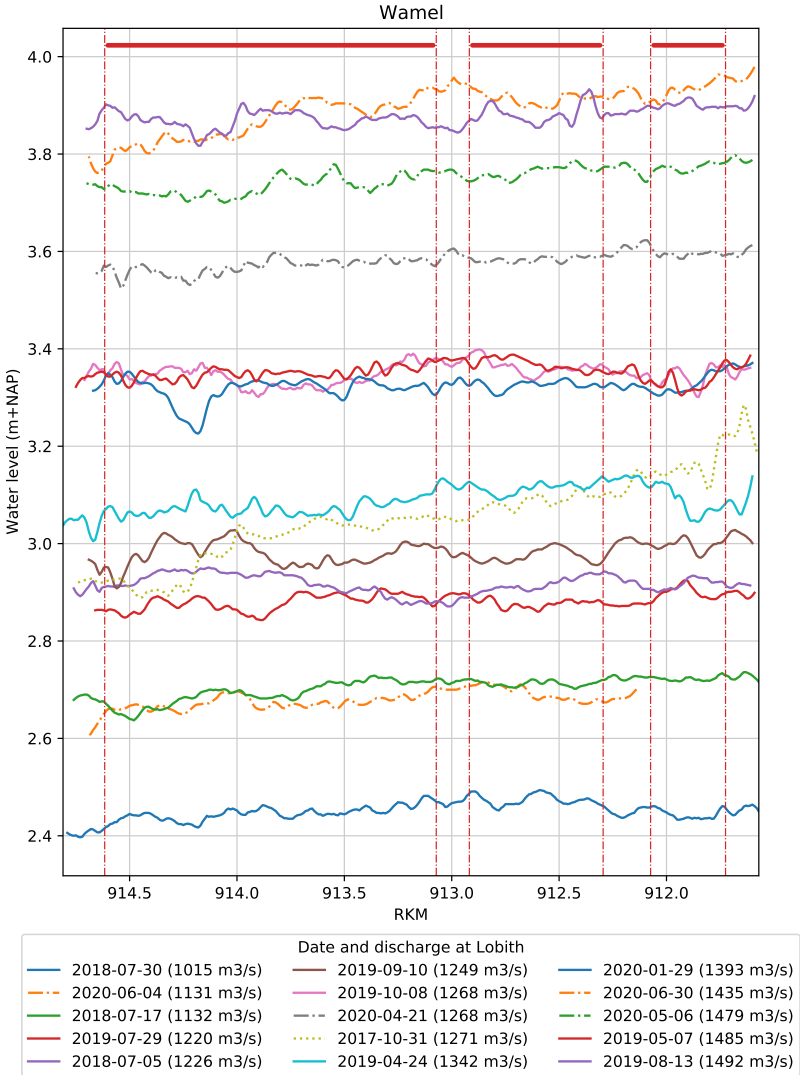

Figure B.95 Longitudinal water level measurements for discharges up to 1500 m^3/s in the auxiliary channel Wamel using the Savitsky-Golay filter.

Deltares

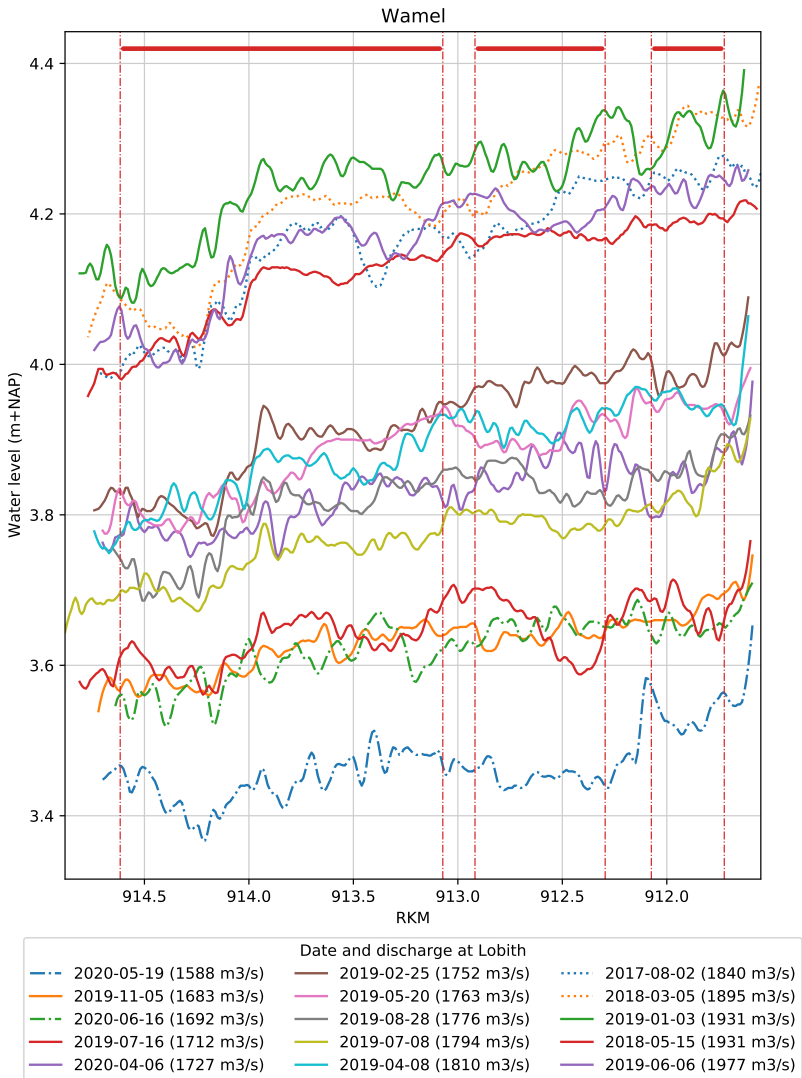

Figure B.96 Longitudinal water level measurements for discharges between 1500 and 2000 m^3/s in the auxiliary channel Wamel using the Savitsky-Golay filter.

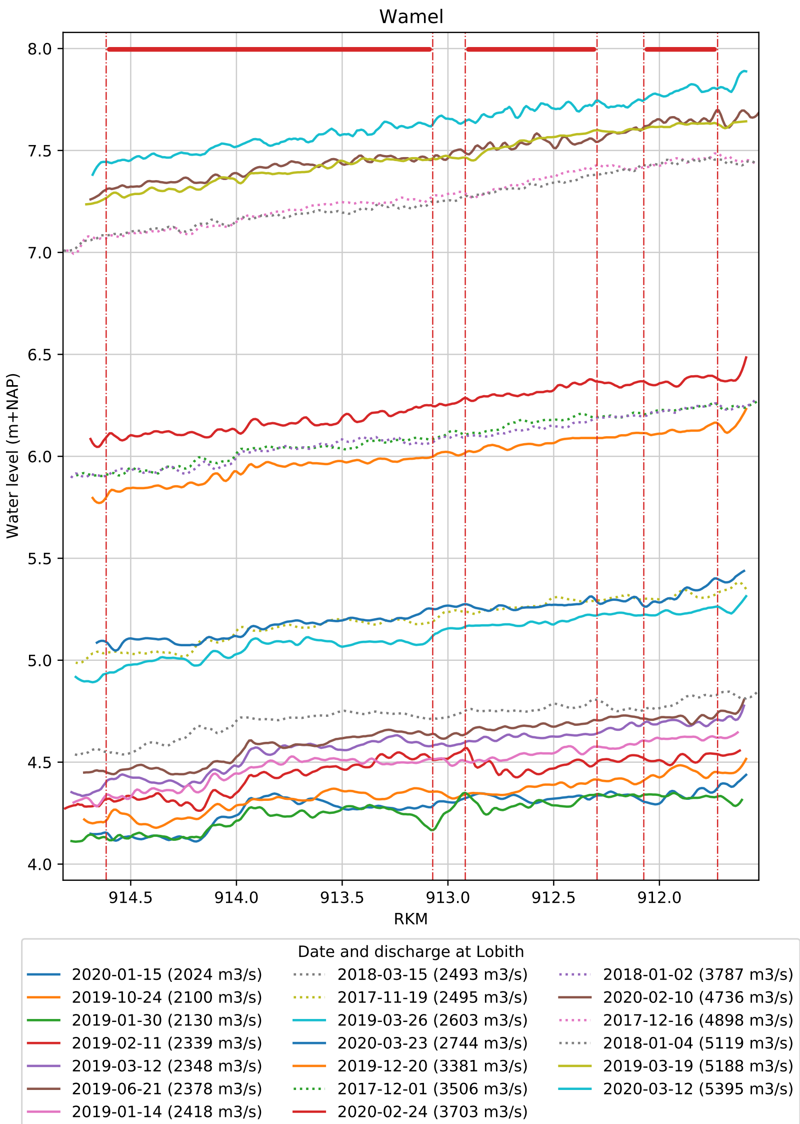

Figure B.97 Longitudinal water level measurements for discharges larger than 2000 m^3/s in the auxiliary channel Wamel using the Savitsky-Golay filter.

B.4.3 Dreumel

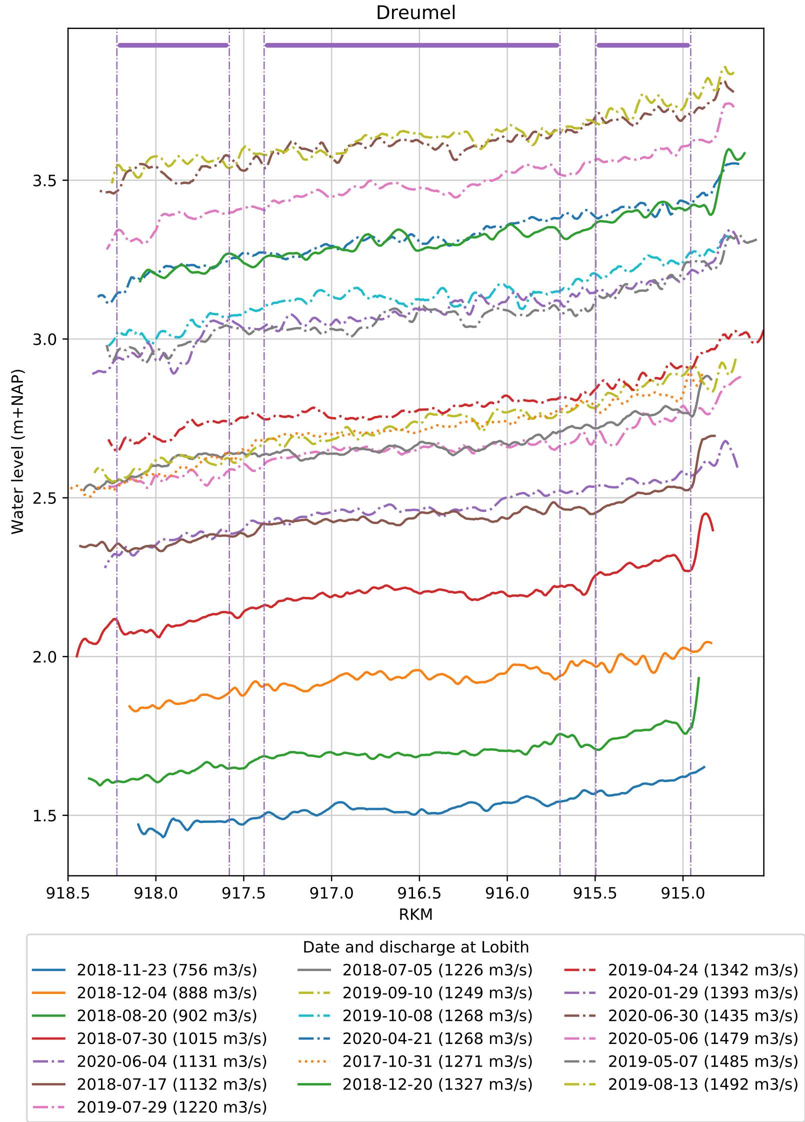

Figure B.98 Longitudinal water level measurements for discharges up to 1500 m^3/s in the auxiliary channel Dreumel using the Savitsky-Golay filter.

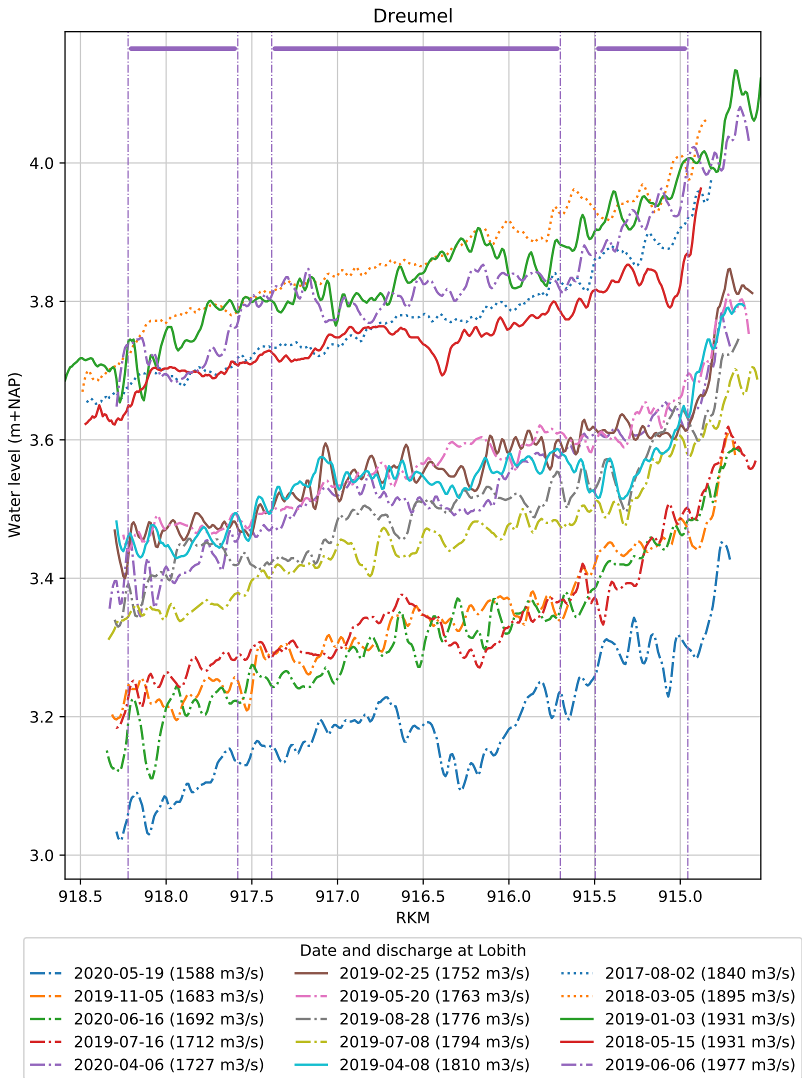

Figure B.99 Longitudinal water level measurements for discharges between 1500 and 2000 m^3/s in the auxiliary channel Dreumel using the Savitsky-Golay filter.

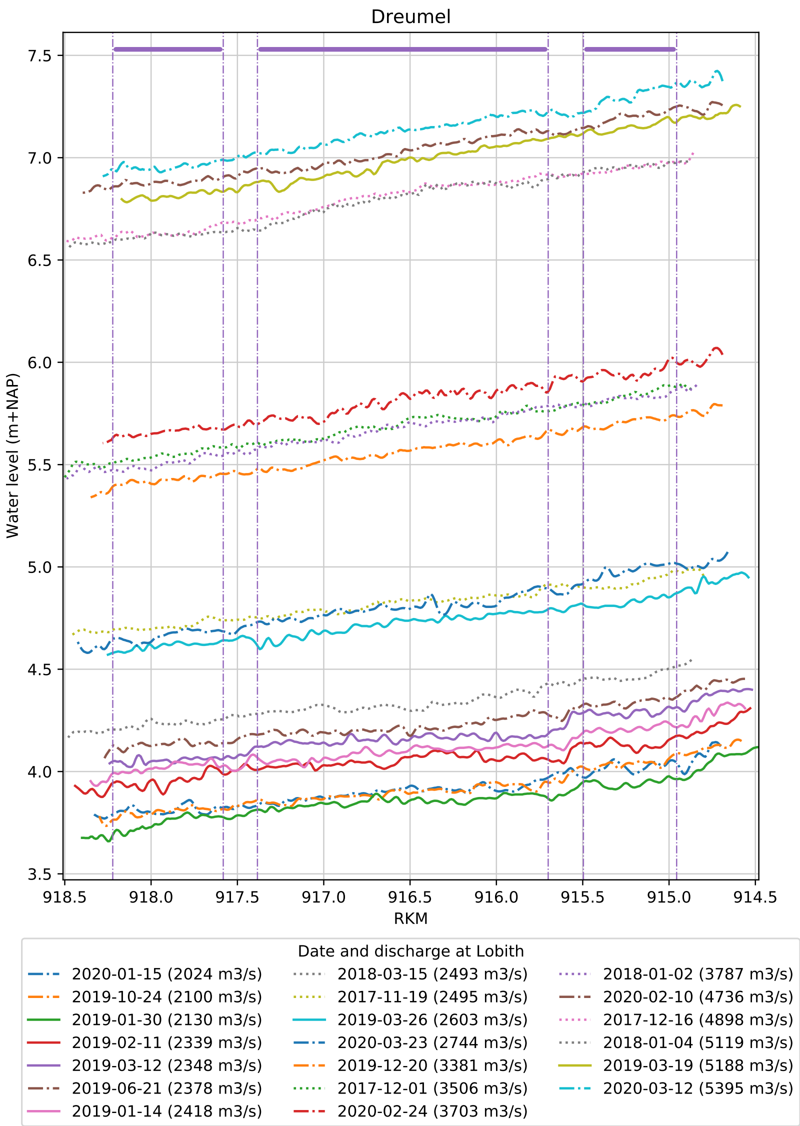

Figure B.100 Longitudinal water level measurements for discharges larger than 2000 m^3/s in the auxiliary channel Dreumel using the Savitsky-Golay filter.

B.4.4 Ophemert

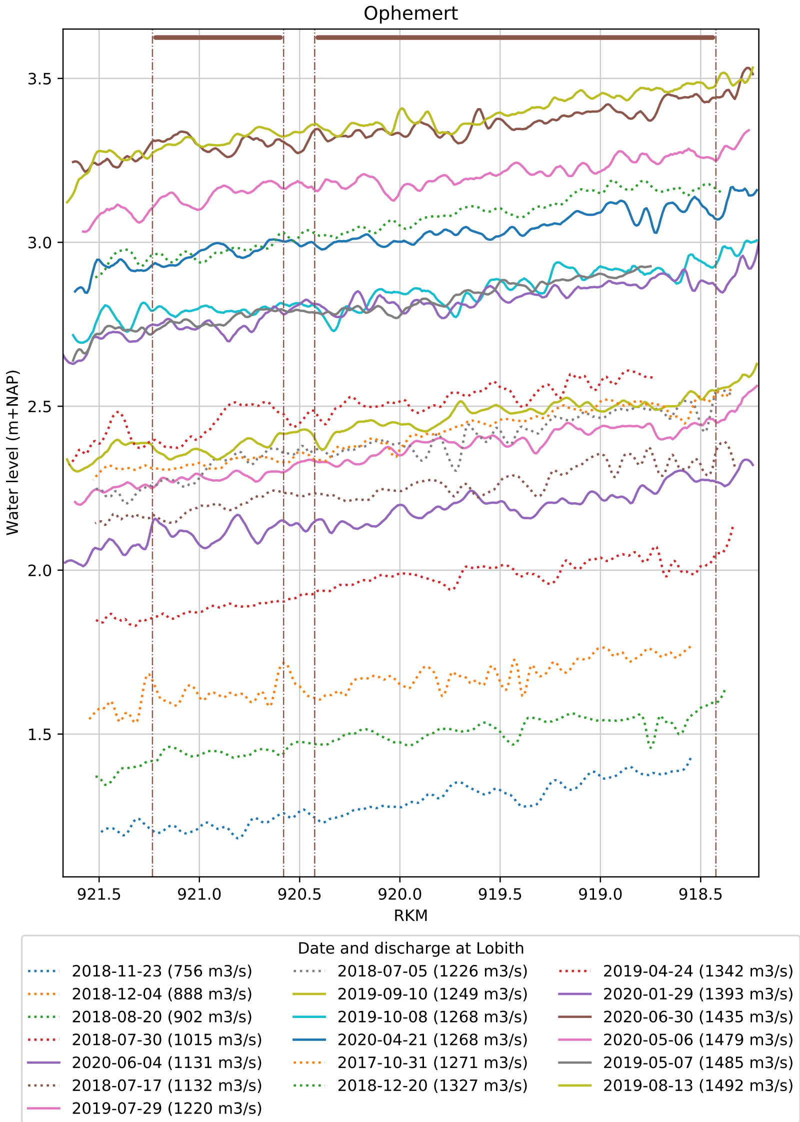

Figure B.101 Longitudinal water level measurements for discharges up to 1500 m^3/s in the auxiliary channel Ophemert using the Savitsky-Golay filter.

Deltares

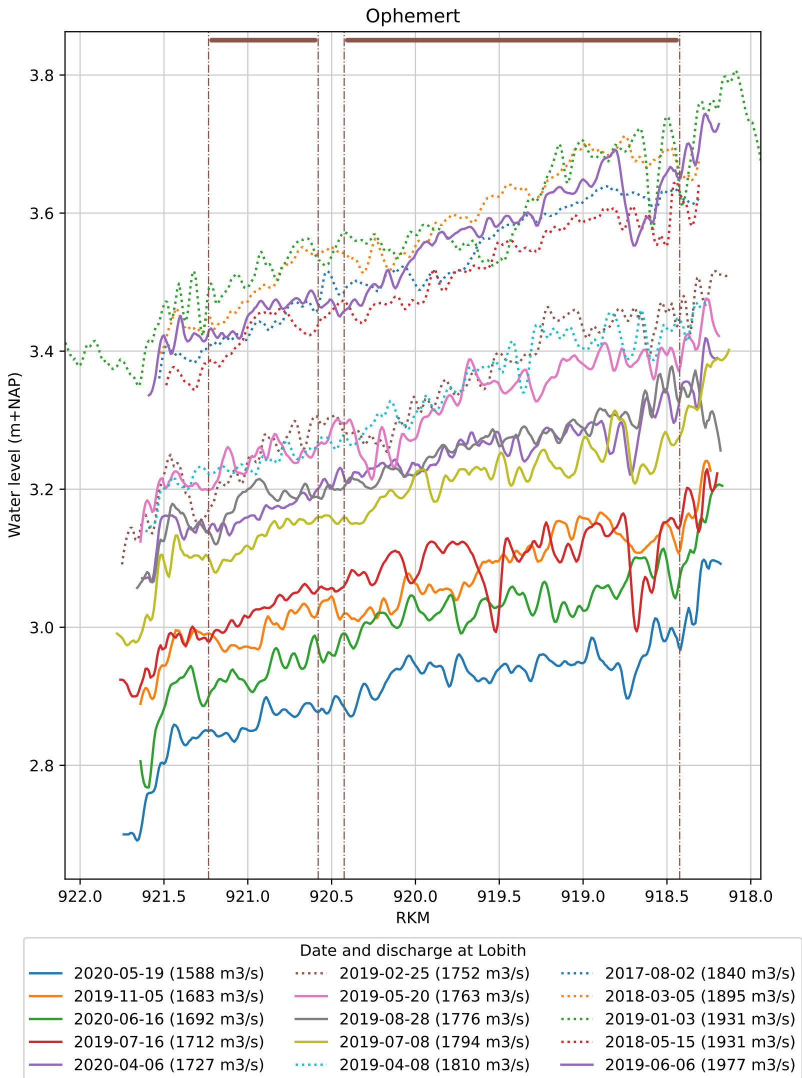

Figure B.102 Longitudinal water level measurements for discharges between 1500 and 2000m^3/s in the auxiliary channel Ophemert using the Savitsky-Golay filter.

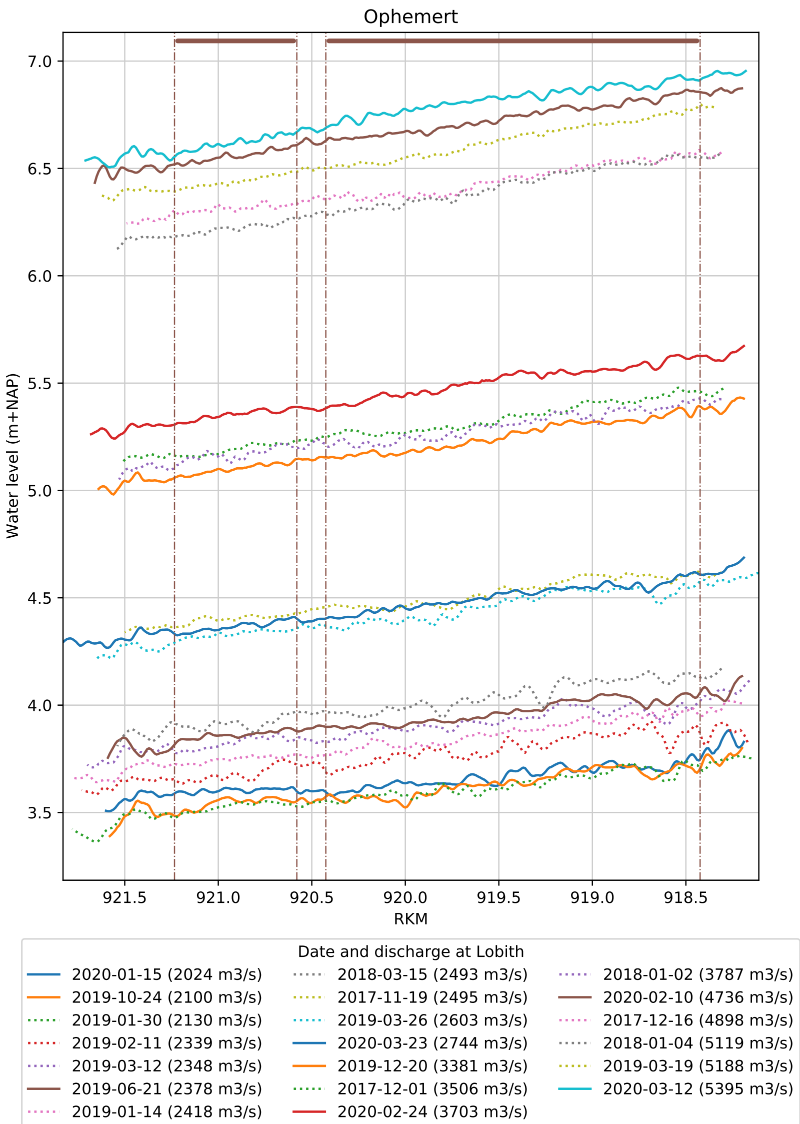

Figure B.103 Longitudinal water level measurements for discharges larger than 2000 m^3/s in the auxiliary channel Ophemert using the Savitsky-Golay filter.

B.5 Head difference to main channel

In the appendix the difference between the main channel ('Aslijn') and the auxiliary channel are analysed. For these plots the data with rolling average is used, as the smaller scale, but relatively large, variations in the measurements (and the Savitsky-Golay filtering) make it hard to conclude anything. The rolling average, however, can sometimes also introduce effects due to the filtering technique.

B.5.1 Wamel

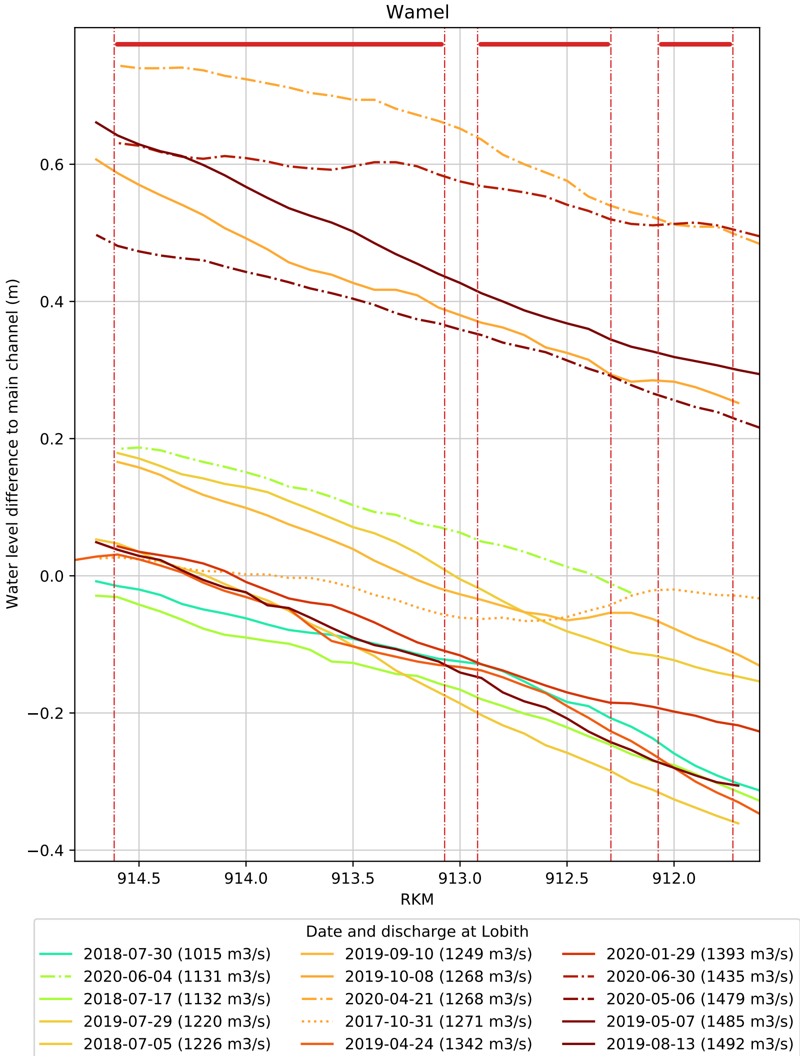

Figure B.104 Water level difference to the river axis to discharges up to 1500 m^3/s in the auxiliary channel Wamel using the Rolling average.

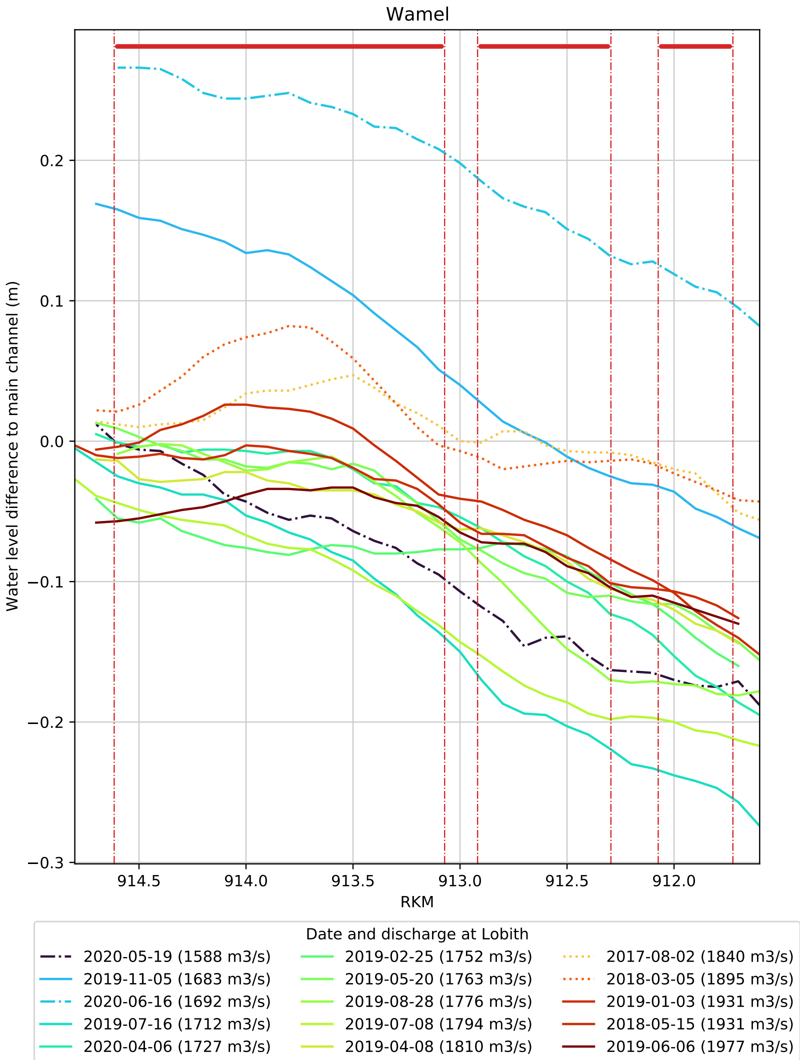

Figure B.105 Water level difference to the river axis to discharges between 1500 and 2000 m^3/s in the auxiliary channel Wamel using the Rolling average.

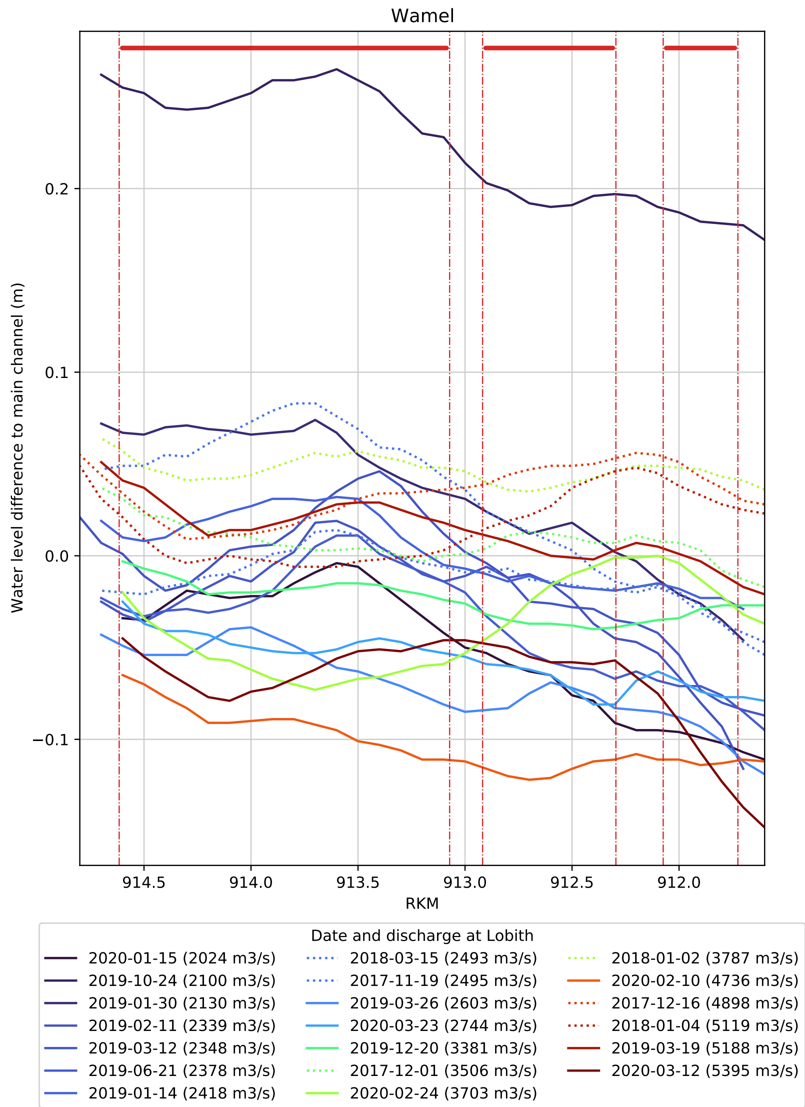

Figure B.106 Water level difference to the river axis to discharges larger than 2000 m^3/s in the auxiliary channel Wamel using the Rolling average.

B.5.2 Dreumel

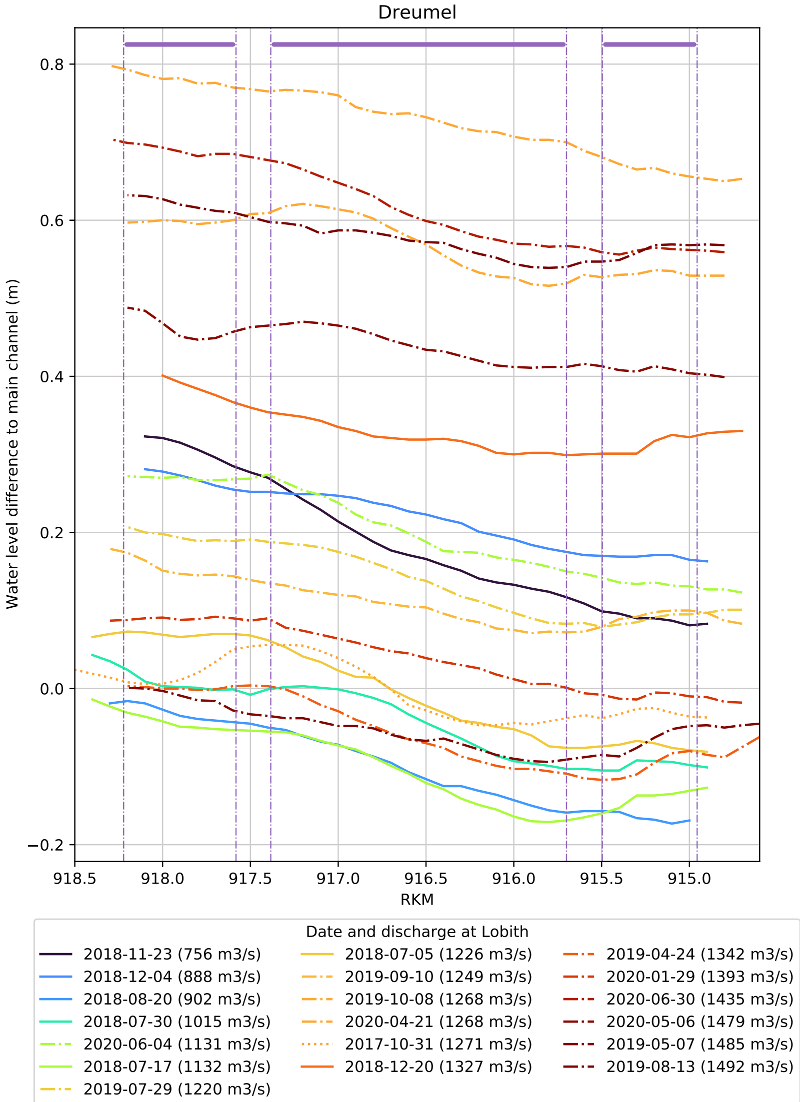

Figure B.107 Water level difference to the river axis to discharges up to 1500 m^3/s in the auxiliary channel Dreumel using the Rolling average.

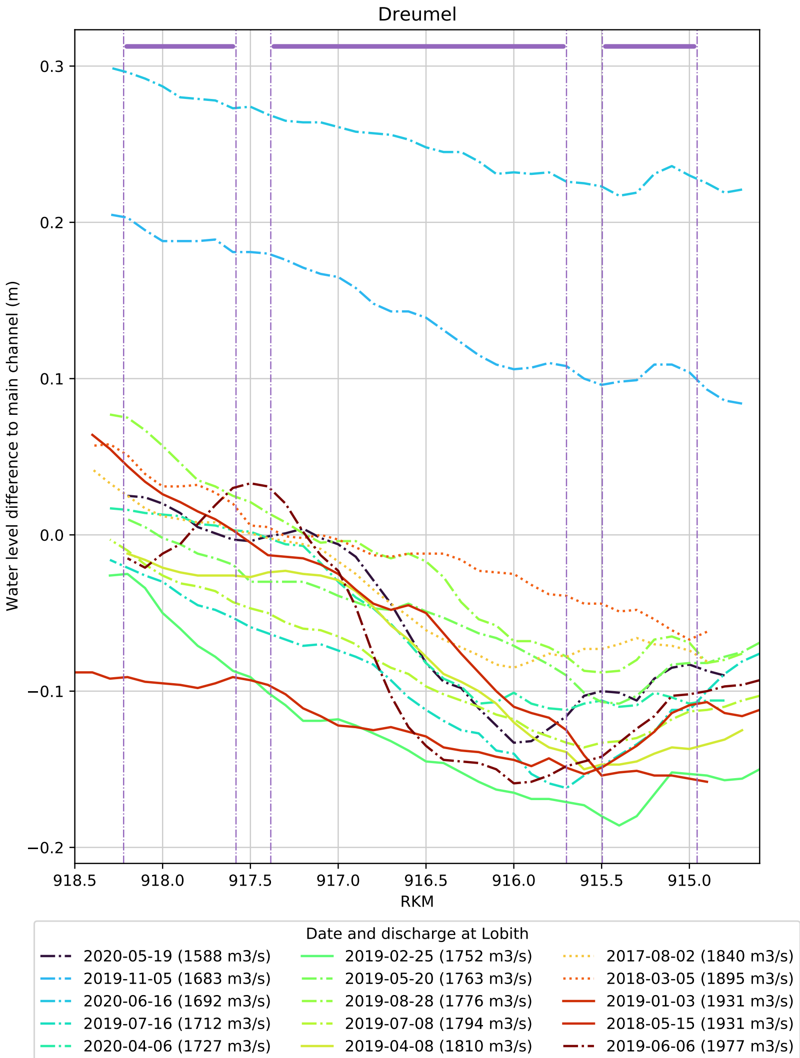

Figure B.108 Water level difference to the river axis to discharges between 1500 and 2000 m^3/s in the auxiliary channel Dreumel using the Rolling average.

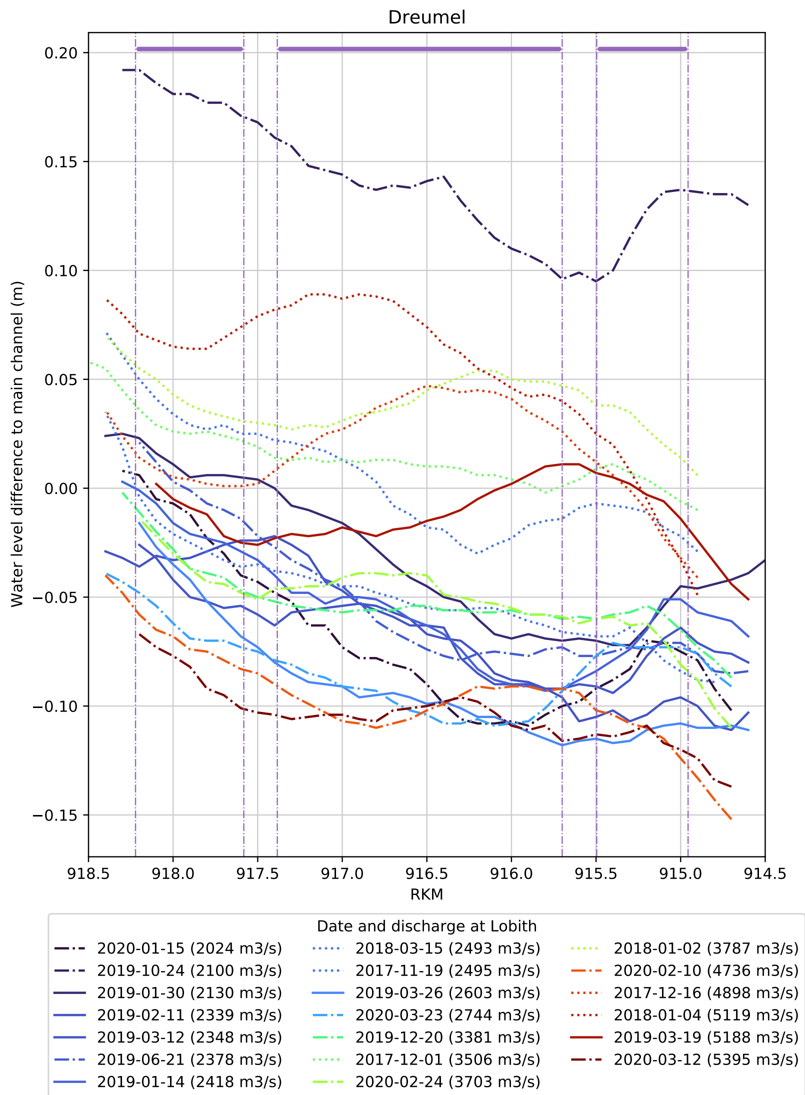

Figure B.109 Water level difference to the river axis to discharges larger than 2000 m^3/s in the auxiliary channel Dreumel using the Rolling average.

B.5.3 Ophemert

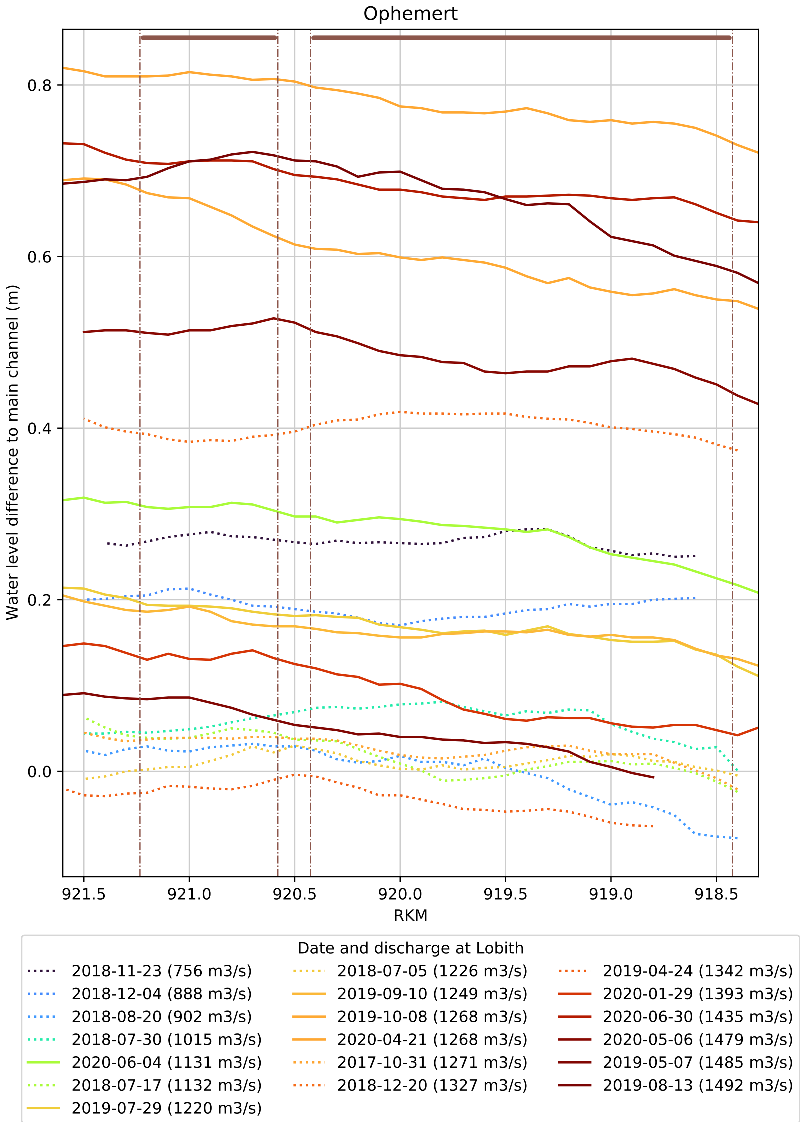

Figure B.110 Water level difference to the river axis to discharges up to 1500 m^3/s in the auxiliary channel Ophemert using the Rolling average.

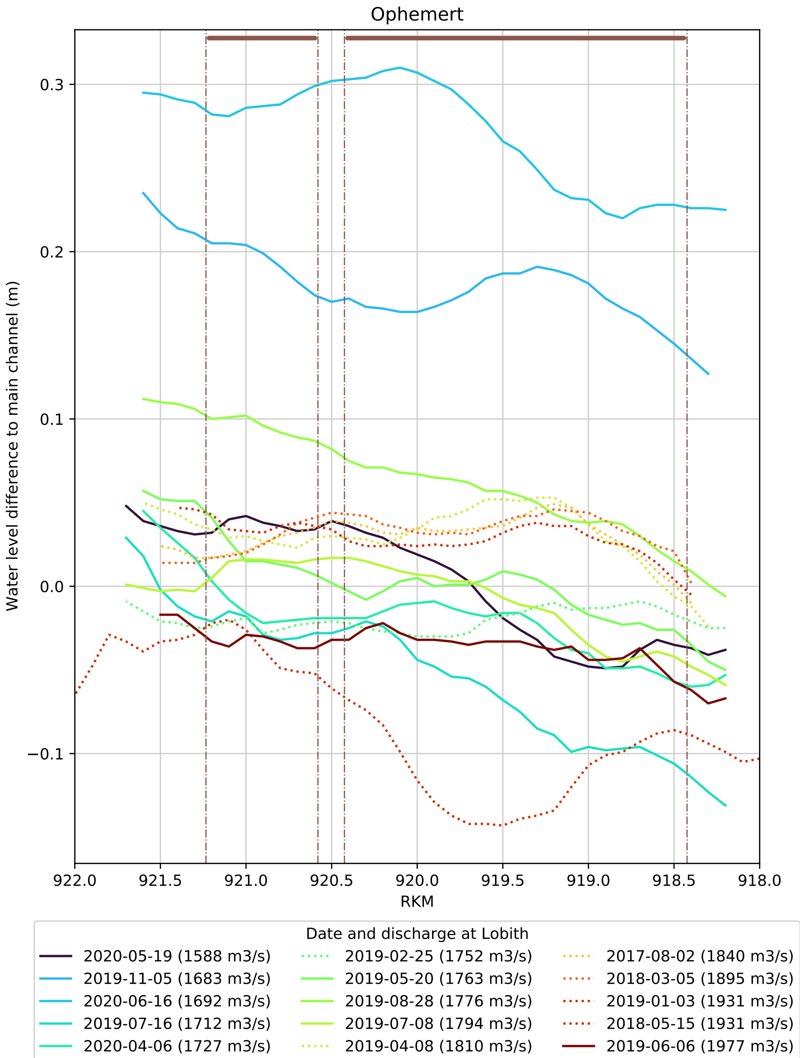

Figure B.111 Water level difference to the river axis to discharges between 1500 and 2000m^3/s in the auxiliary channel Ophemert using the Rolling average.

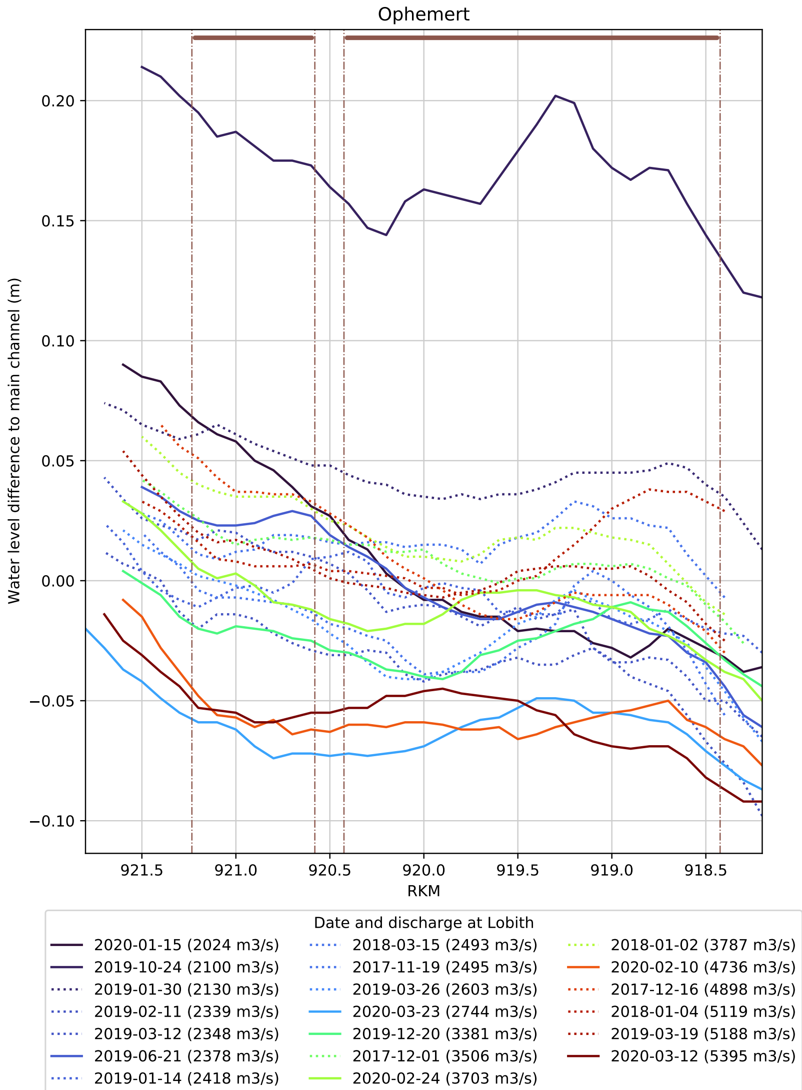

Figure B.112 Water level difference to the river axis to discharges larger than 2000 m^3/s in the auxiliary channel Ophemert using the Rolling average.

B.6 Effect on curvature

In all recent measurement campaigns the upstream water level in the main channel was measured over three parallel tracks: left, center and right of the fairway. In this section the value of these parallel tracks is investigated. As the slope in water level is of a much lower order than the waves in the measured water levels, the Savitsky-Golay filtered results are used.

As a first comparison the cross slope is plotted against the curvature of the river. In Figure B.113 both parameters are given in longitudinal direction and as a scatter plot. The spatial lag between curvature and slope has not been included in this plot. The results show no a very slight dependency between water level and curvature, but again the effect of local variations greatly disturb the image.

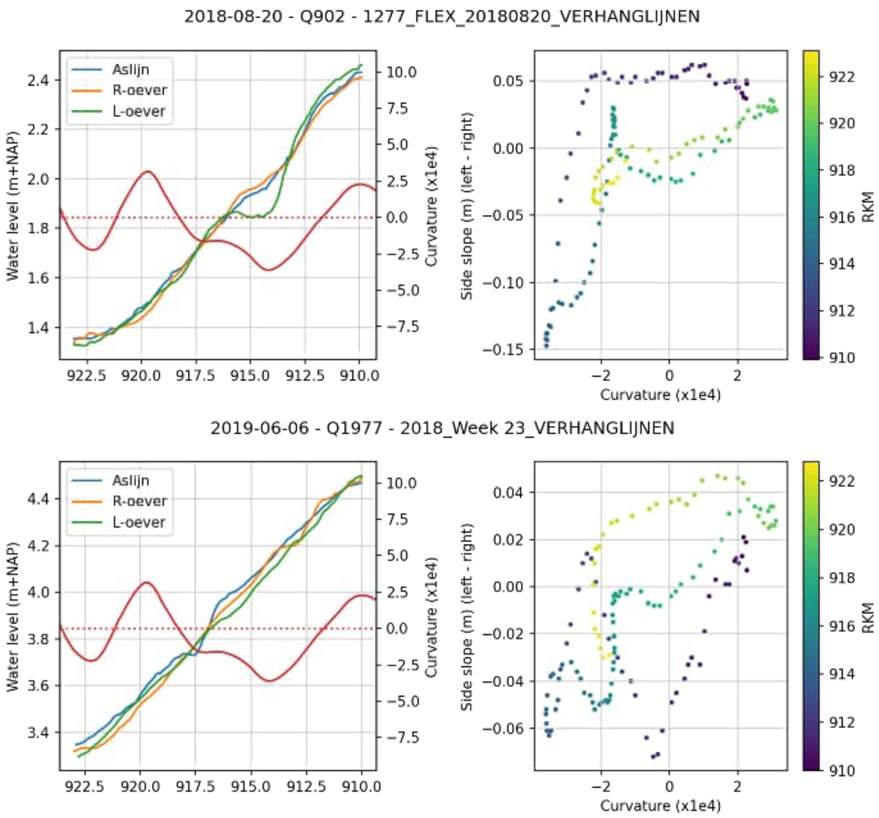

Figure B.113 Comparing curvature to the slope in perpendicular direction for the longitudinal measurements on 20-08-2018 (902 m^3/s) and 06-06-2019 (1977 m^3/s)

C Water level measurements at stations

This appendix describes the processing of the water level measurements at stations. It describes both the measurement of the LMW ('Landelijk Meetnet Water', also sometimes referred to as 'Monitoring Waterstaatkundige Toestand des Lands' or MWTL) (section C.1.1) and measurement of 'divers' placed at the LTW(section C.1.5).

C.1 LMW-measurements

C.1.1 Processing

An overview of all LMW measurements considered in the report is given in figure C.1. Data from January 2008 up to July 2020 is analysed. Not all measurements cover the entire period. The discharge measurements on the Rhine are not directly measured, but approximated based on the water level.

Using these measurements the following analyses are included in the appendix:

- Construction of a rating curve (the relation between water level and discharge) for each station. The data-set is separated in before construction and after construction (section C.1.2).
- Using a similar analyses, but the water level for each (Lobith) discharge per year (section C.1.3).
- Analyses of peaks and troughs for each wave (section C.1.2).

As all analyses uses a relation to the discharge at Lobith, a time shift is applied to correct for both the hysteresis between discharge and waterlevel, and for the wave runtime between Lobith and each station. The optimal time shift is found to compute the standard deviation for discharge bins up to 2000 m^3/s (as visualised in C.2) and apply a time shift until the standard deviation is at it's lowest. This results in Lobith (5 hours), Nijmegen haven (9 hours), Dodewaard (13 hours), Tiel Waal (17 hours), Sint Andries Waal (21 hours), Zaltbommel (22 hours), Vuren (23 hours).

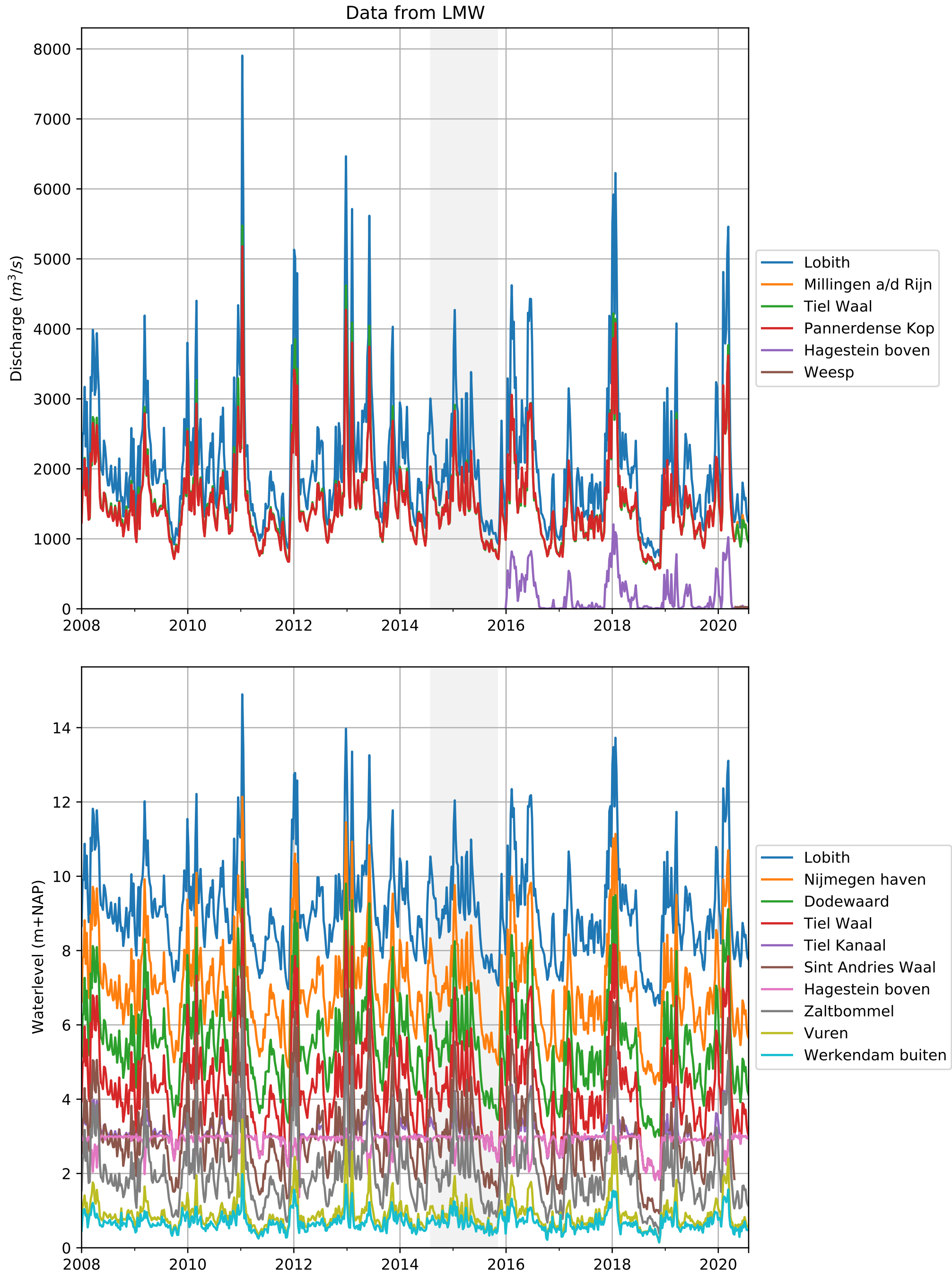

Figure C.1 Discharge and water level measurements from LMW, downloaded from Waterinfo. The years influenced by construction are marked in grey. The data in the plot is averaged per 7 days to make the figure better readable.

C.1.2 Rating curves

Similar to the analyses in WP10 of this evaluation (Chavarrías *et al.* (2021)), the discharge at Lobith is binned in containers of 200 m^3/s and for each bin the statistics are computed for the water level stations. In figure C.2 a rating curve is constructed, split for the situation before and after construction. In figure C.3 the change to the situation before construction is plotted.

It is chosen not to plot to the discharge at Tiel (or Pannerdensche Kop) due to the error in these measurements as concluded by Sieben (2020). An analysis in Chavarrías *et al.* (2021) using these discharge gave very different result for low discharges and were not trusted. As an alternative, a test was done using the water level at Zaltbommel (instead of discharge at Lobith), which gave similar conclusions as the figures below. These figures are not included in this report.

Some limitations on this processing technique:

- A bin can have a positive bias if more samples exists for the higher discharges in a bin. This happens most apparent in the lowest bin.
- There is not corrected for the time offset between the discharge at Lobith and at the given stations. Although this might average out in the mean of most discharge, this does increase the standard deviation and might introduce a positive bias for the lower discharge bins.
- There is not corrected for hysteresis in the water levels. This also introduces a larger standard deviation and a positive bias for the lower discharge bins.
- For equal discharge at Lobith, the more recent measurements are expected to have a higher discharge on the Waal as a result of the bed erosion on the upper section of the Waal. Without this change in discharge distribution, the water levels would have been lower.
- Operation of structures (both Prins Bernhardsluis and at Driel) might influence the results and are not explicitly included or excluded.

After performing this analyses also ADCP-measurements at Tiel were delivered by Rijkswaterstaat. These measurements are frequently carried out to validate the rating curve at Tiel. In figure C.4 a similar result as the previous analyses is given, but now using this new dataset (see also Chavarrías *et al.* (2021)). As the results are now plotted to the discharge at Tiel, changes in discharge distribution do not influence the results. From this data an even larger lowering in the water levels at Tiel is concluded, ranging from 0.2 to 0.4 m. From this it can be concluded that in the earlier plots (figure C.3) a fraction of the lowering has been compensated by an increase in discharge to the Waal.

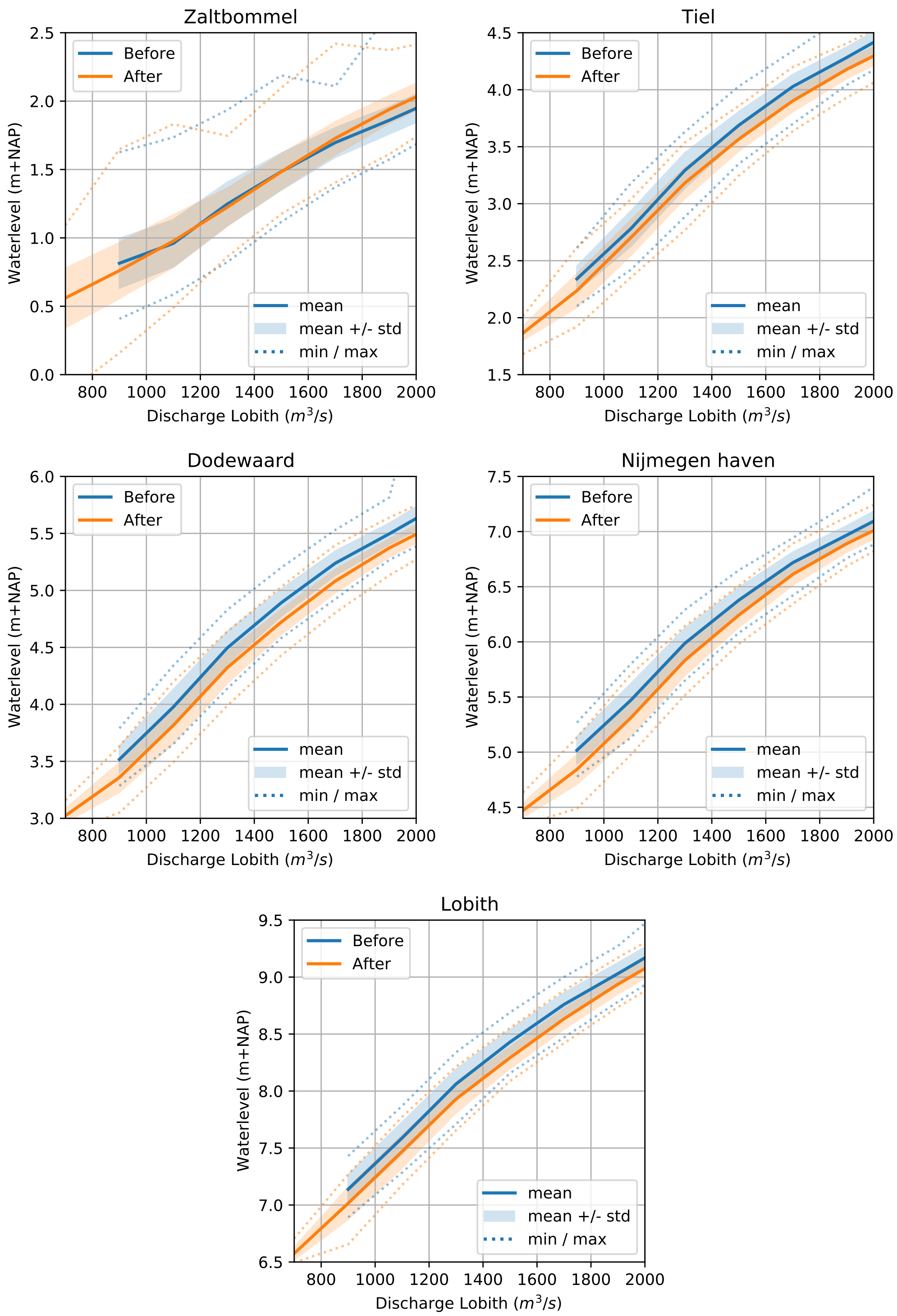

Figure C.2 Rating curves for the situation before construction (up to July 2014) and after construction (from November 2015).

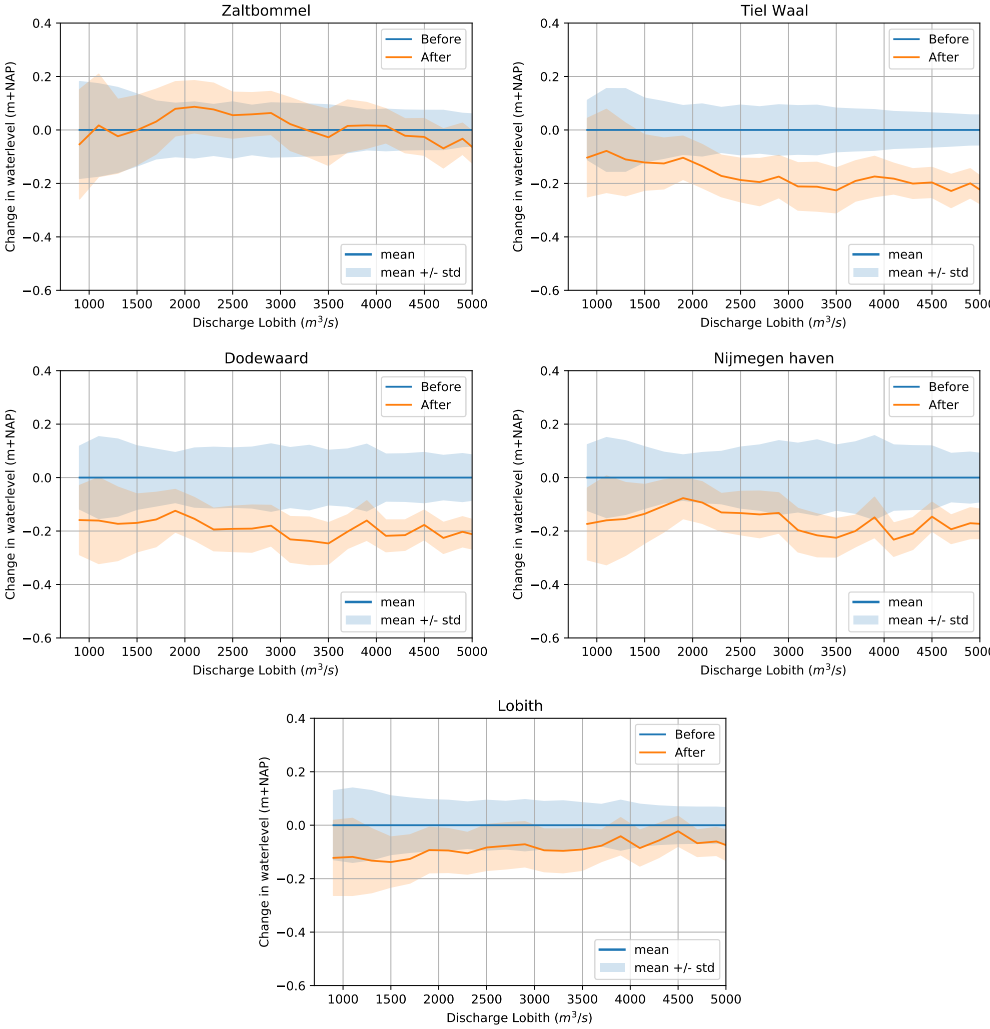

Figure C.3 Change in rating curves of the situation before construction (up to July 2014) to the situation after construction (from November 2015).

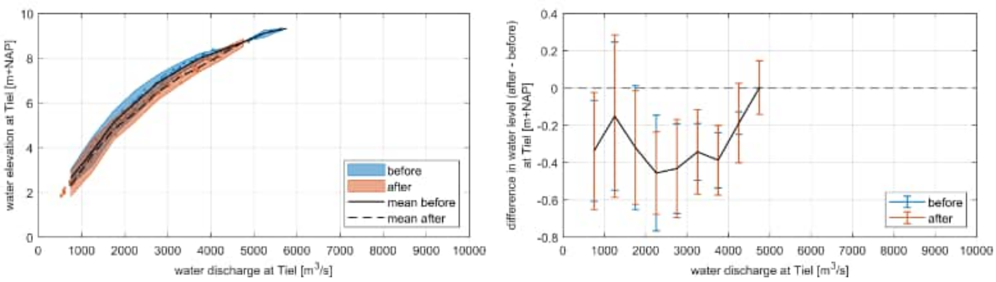

Figure C.4 Rating curve at Tiel based on ADCP-measurements before and after construction (left) and the change in values (right)

C.1.3 Water level trends

In this section a similar analyses to the previous section is applied, but data is split per year. Data of 2020 was only half of the year, and therefore excluded from the analyses. For each station the left subplot contains data up to 2400 m^3/s and in the right subplot up to 5000 m^3/s. For the lower and higher discharges the number of data samples can be very low, thereby easily introducing some error in these averages.

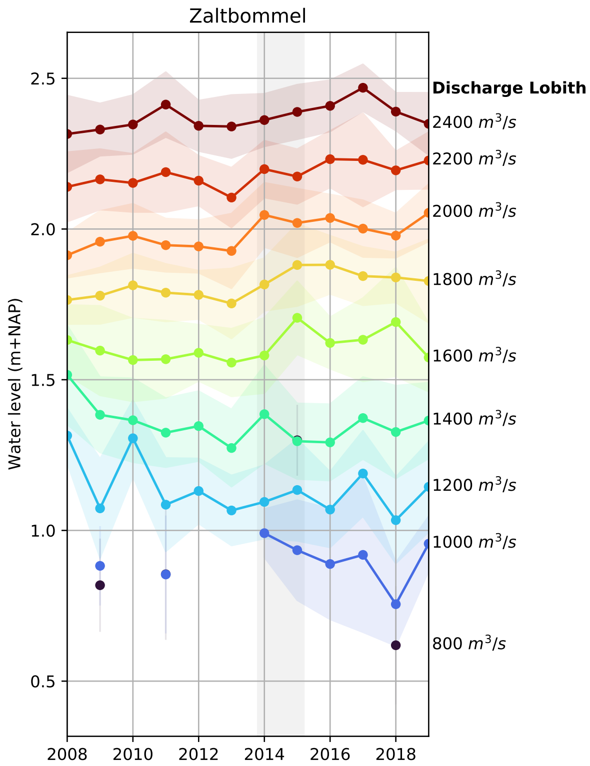

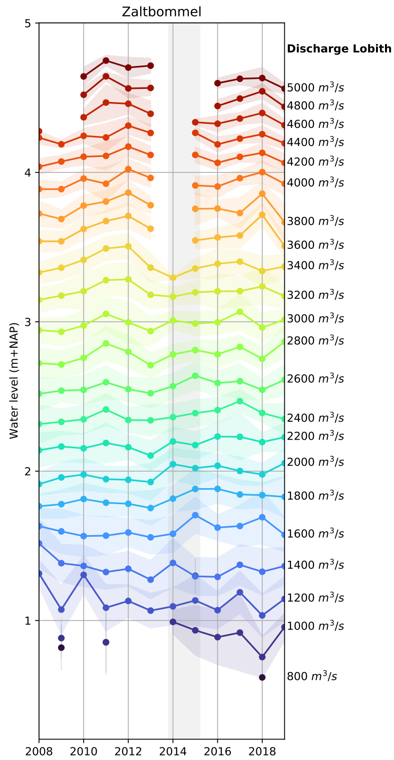

Figure C.5 Trends in water level at Zaltbommel, showing the mean and standard-deviation per discharge bin (+/- 100 m^3/s)

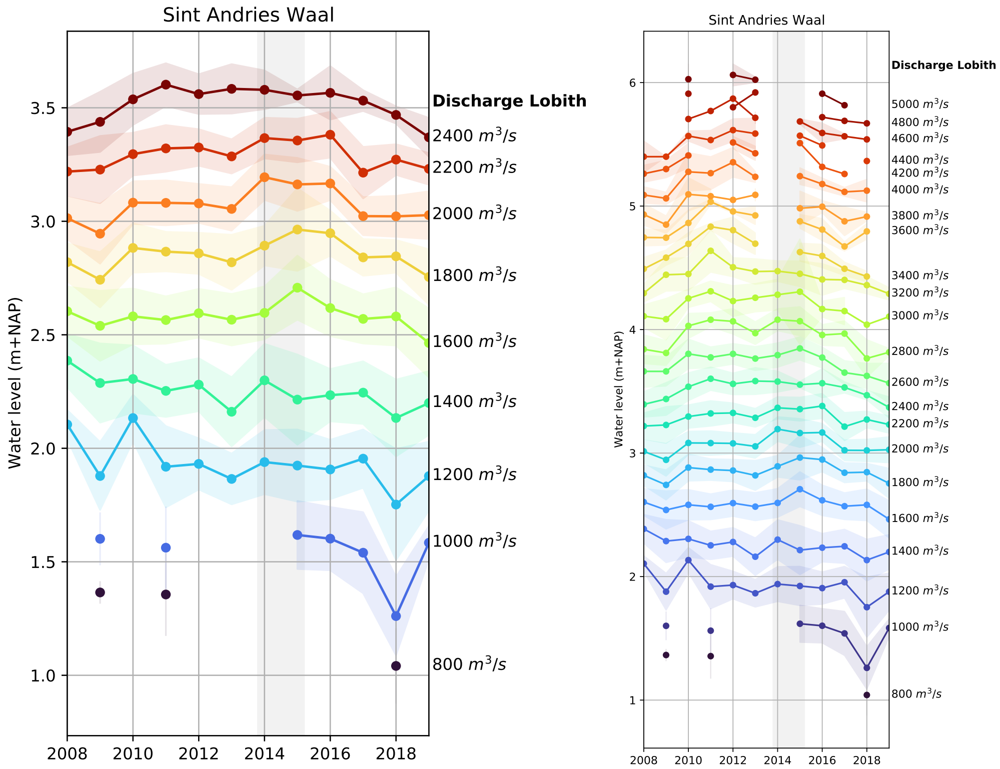

Figure C.6 Trends in water level at St. Andries, showing the mean and standard-deviation per discharge bin (+/- 100 m^3/s)

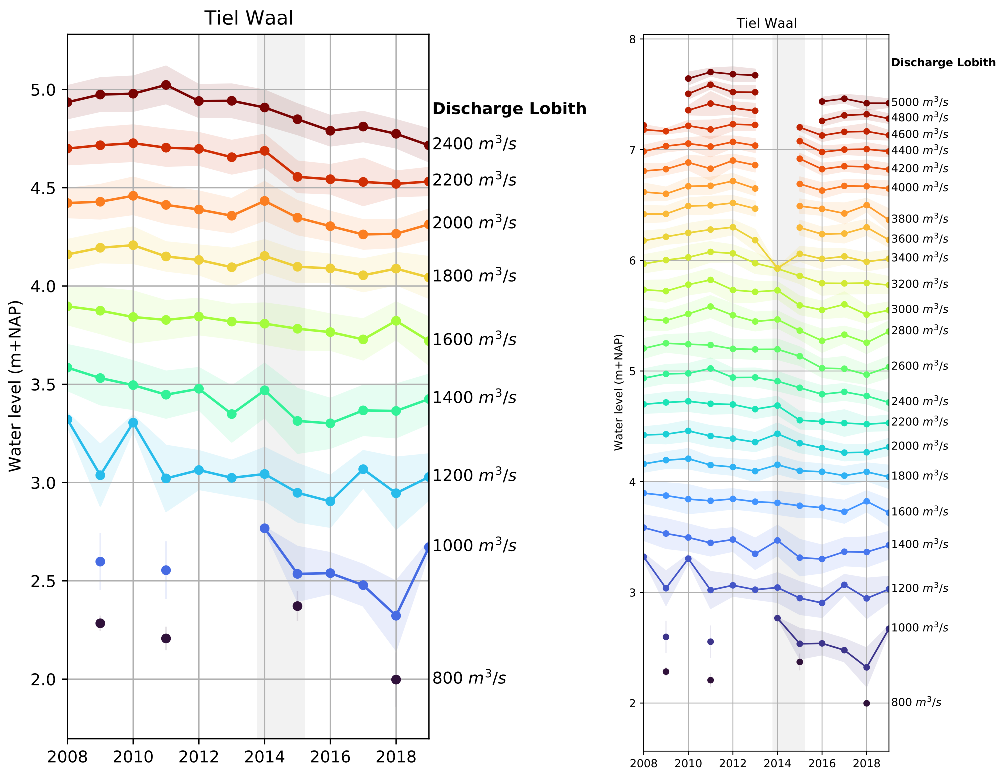

Figure C.7 Trends in water level at Tiel, showing the mean and standard-deviation per discharge bin (+/- 100 m^3/s)

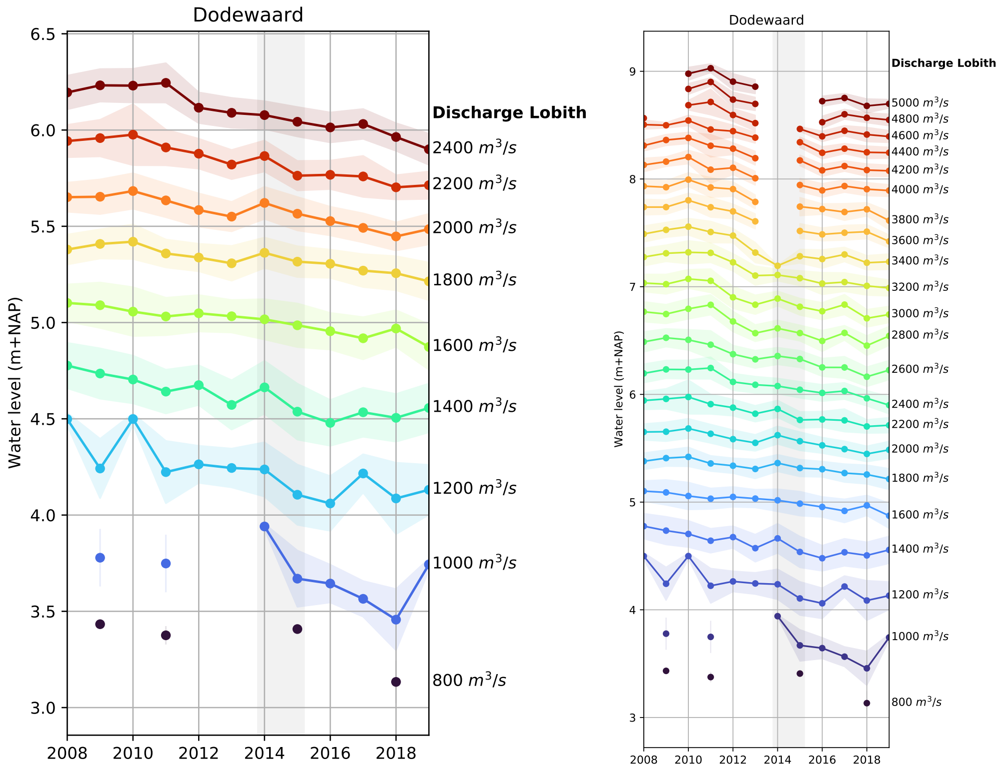

Figure C.8 Trends in water level at Dodewaard, showing the mean and standard-deviation per discharge bin (+/- 100 m^3/s)

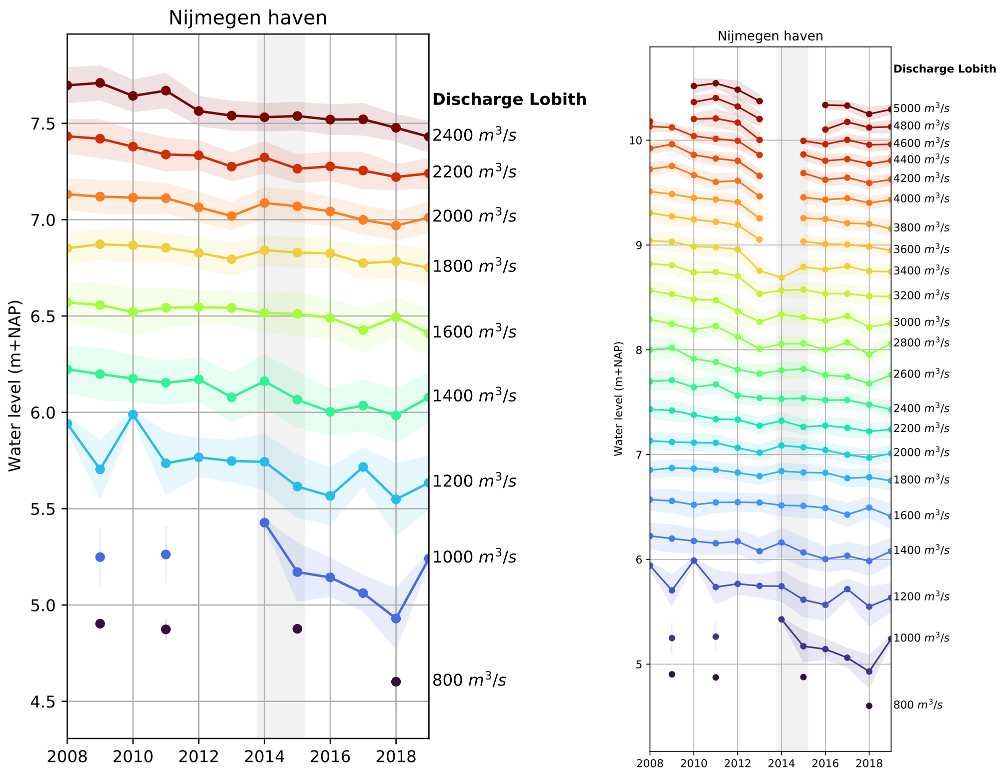

Figure C.9 Trends in water level at Nijmegen, showing the mean and standard-deviation per discharge bin (+/- 100 m^3/s)

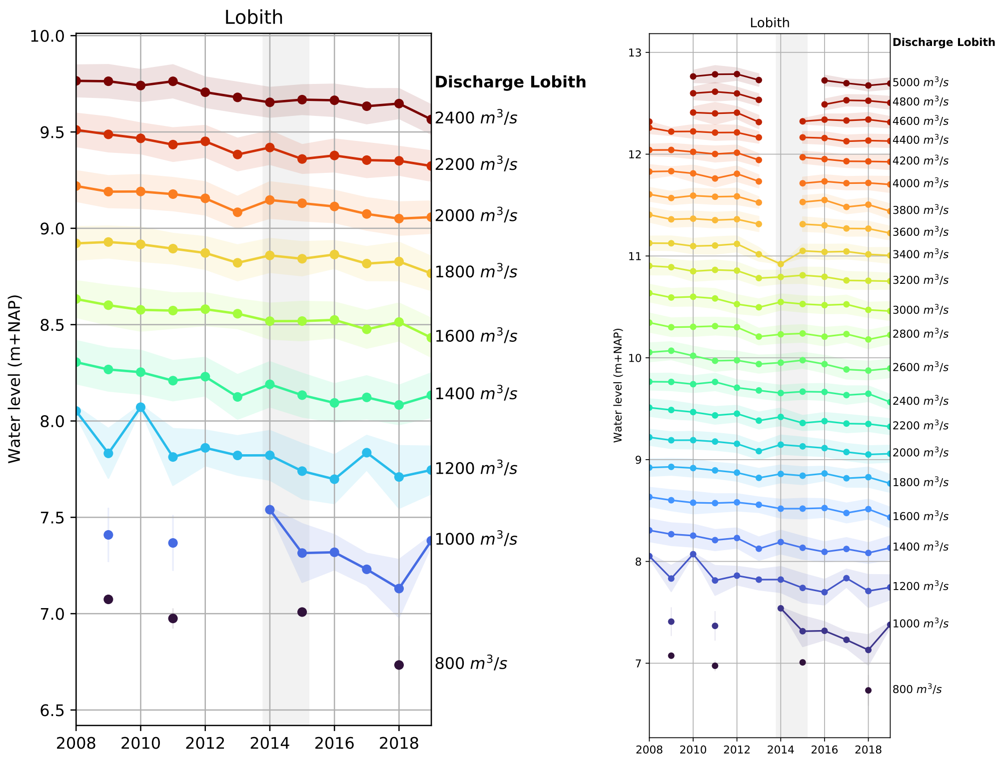

Figure C.10 Trends in water level at Lobith, showing the mean and standard-deviation per discharge bin (+/- 100 m^3/s)

C.1.4 Head Difference trends

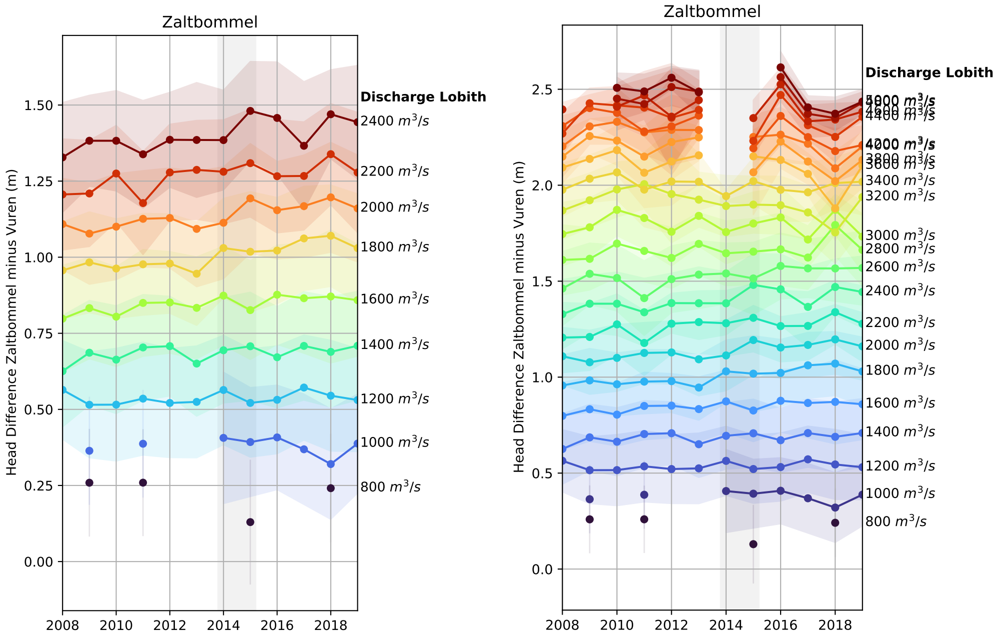

Figure C.11 Trends in water level difference Zaltbommel minus Vuren, showing the mean and standard-deviation per discharge bin (+/- 100 m^3/s)

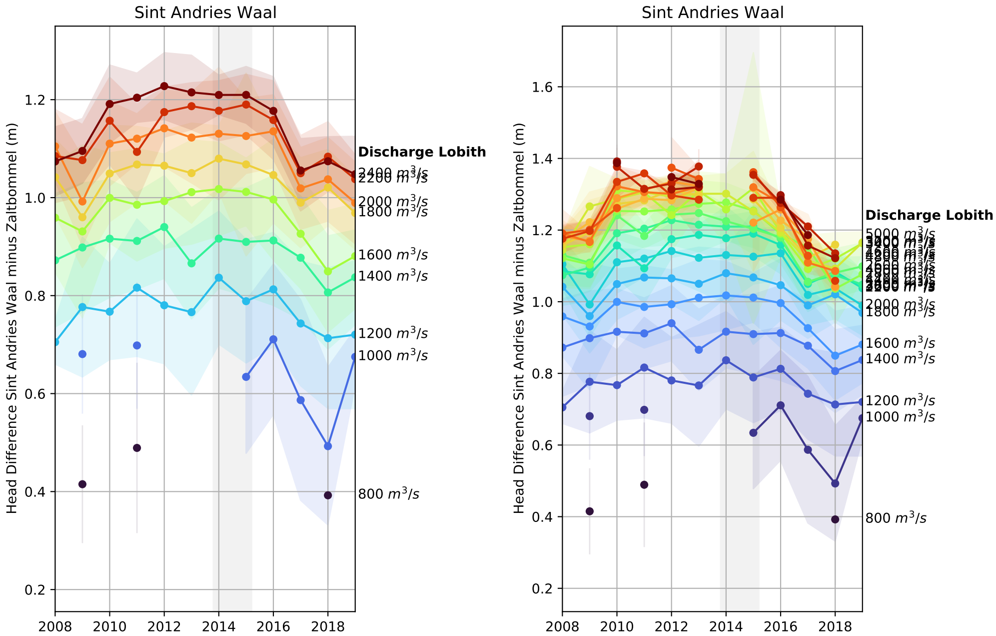

Figure C.12 Trends in water level difference Sint Andries minus Zaltbommel, showing the mean and standard-deviation per discharge bin (+/- 100 m^3/s)

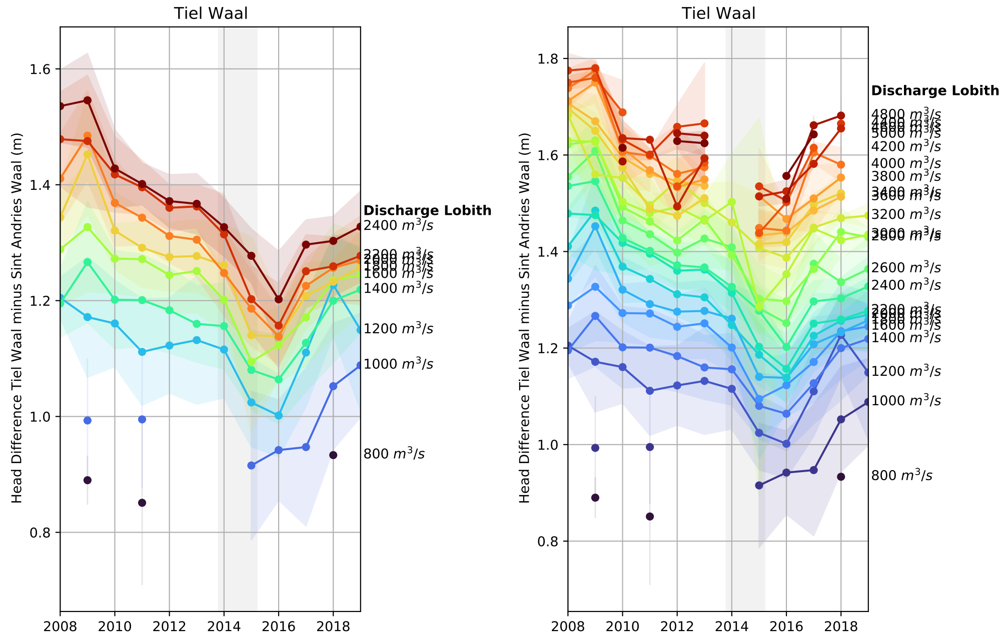

Figure C.13 Trends in water level difference Tiel minus Sint Andries, showing the mean and standard-deviation per discharge bin (+/- 100 m^3/s)

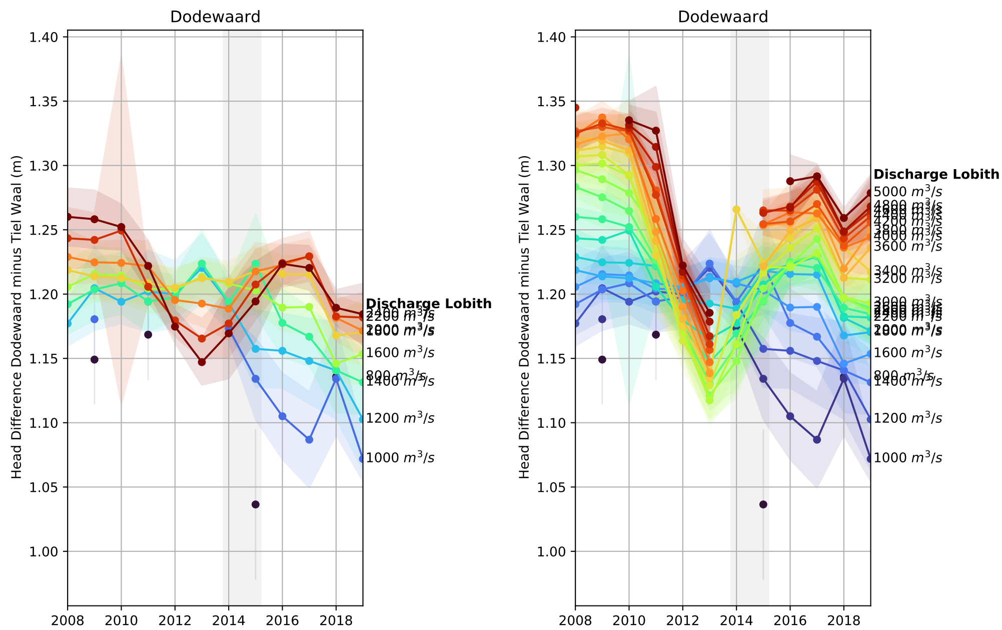

Figure C.14 Trends in water level difference Dodewaard minus Tiel, showing the mean and standard-deviation per discharge bin (+/- 100 m^3/s)

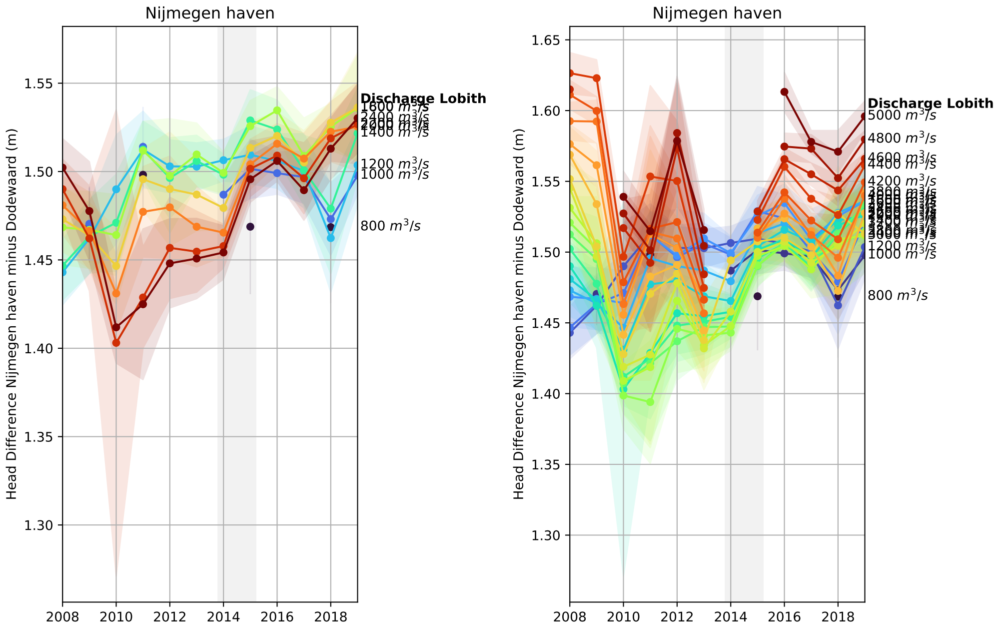

Figure C.15 Trends in water level difference Nijmegen minus Dodewaard, showing the mean and standard-deviation per discharge bin (+/- 100 m^3/s)

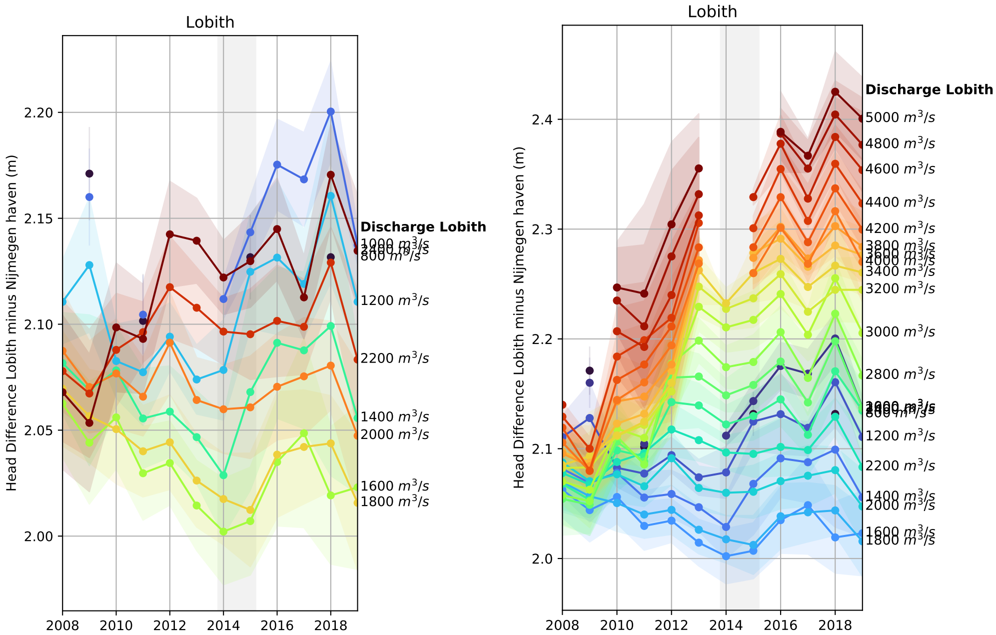

Figure C.16 Trends in water level difference Lobith minus Nijmegen, showing the mean and standard-deviation per discharge bin (+/- 100 m^3/s)

C.1.5 Peaks and troughs

In this section an analyses of peaks and troughs is included. This analyses was inspired by the figure on the blog of Alphons van Winden[1]

All peaks and troughs are analysed from the daily average discharge and water levels. At first all local maxima and minima are determined from the discharge at Lobith. For each subsequent peaks it is analysed if in-between the peaks the discharge went at least 100 m^3/s lower than the lowest peak. If this was not the case, the lowest peak was removed. For troughs the discharge should have been at least 100 m^3/s higher than the highest trough. For each peak the maximum water level is taken during the period around the peak discharge (-0.5 to +2 days, including the time correction as mentioned before) from the peak and for each trough the minimum during this period around the lowest discharge.

In the plots (figures C.17 to C.22) only troughs lower than 2000 m^3/s and peaks higher than 2000 m^3/s are shown. A least squares second order polynomial fit is added to offer a bit of guidance to the conclusions. It should be noted that there is a large scatter around this line.

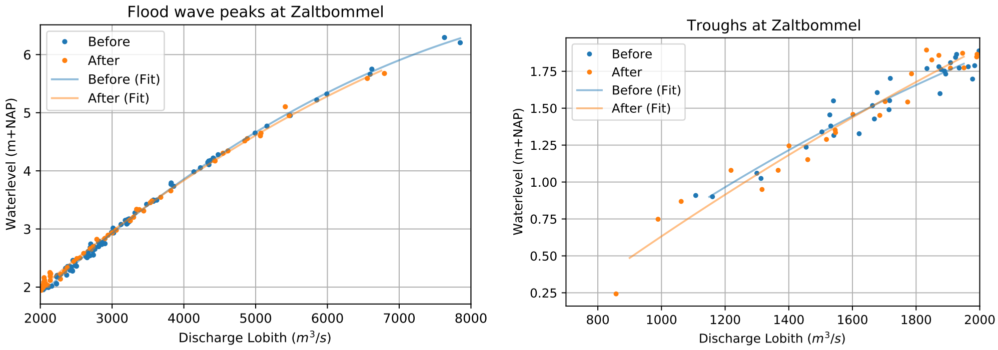

Figure C.17 Peaks and troughs at Zaltbommel

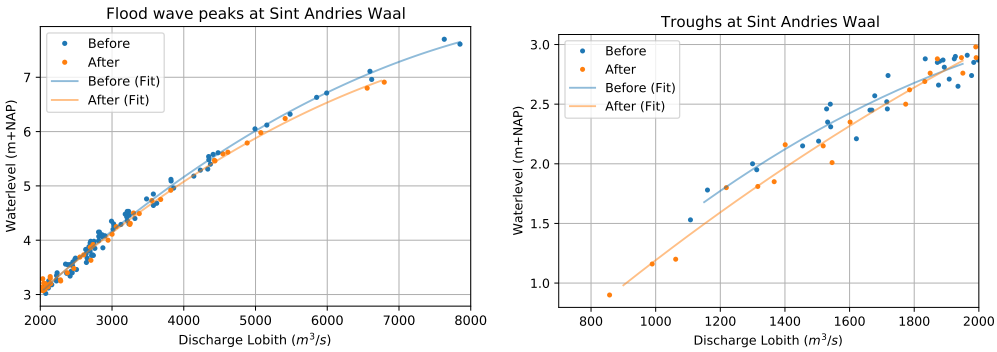

Figure C.18 Peaks and troughs at Sint Andries Waal

[1] Blog Alfons van Winden:
https://www.waterpeilen.nl/berichten/weinig-neerslag-de-stroomgebieden-en-dalende-waterstanden

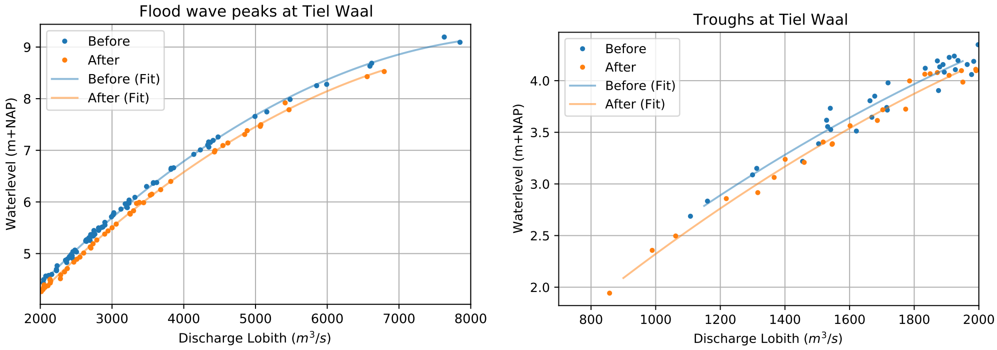

Figure C.19 Peaks and troughs at Tiel Waal

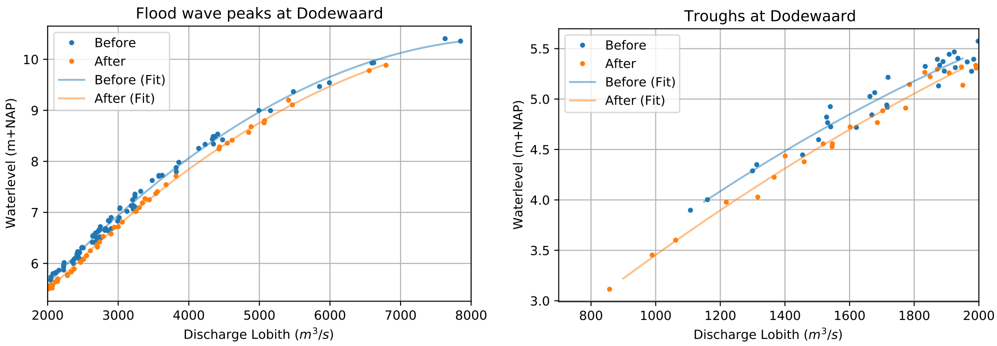

Figure C.20 Peaks and troughs at Dodewaard

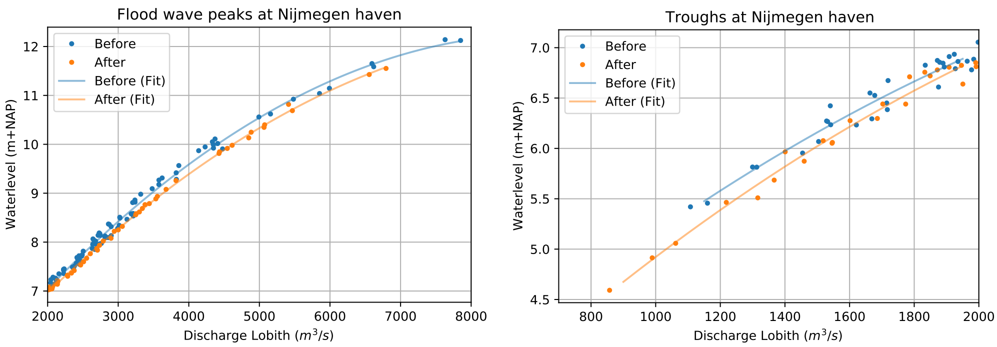

Figure C.21 Peaks and troughs at Nijmegen haven

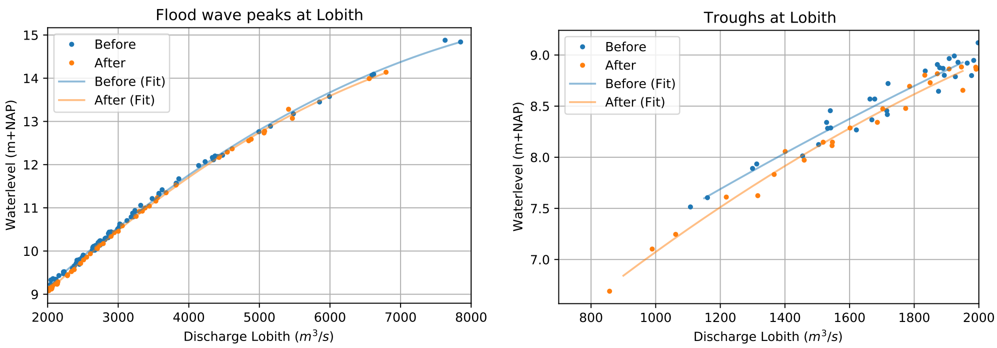

Figure C.22 Peaks and troughs at Lobith

C.1.6 Peak water level trends

The previous plot might be subjected to a trend within the period 'Before' or 'After'. Similar to the water level analyses, the analyses is repeated for each single year and given in the left plot of figure C.23 to C.27. As the water levels in a rating curve mostly follow the diagonal of the figure, the trends over the years is not clearly visible. To better use the entire axes of the plot, the right plots include the water level difference between the peak water level and a temporary polynomial fit. This second order polynomial fit is applied on all data of the station. The figure can be interpreted as a rotation ver 45 degree of the plots to the left. The horizontal grid lines of the left plots (the water levels) are added as diagonal lines in the right plot and labelled at the top of the figure.

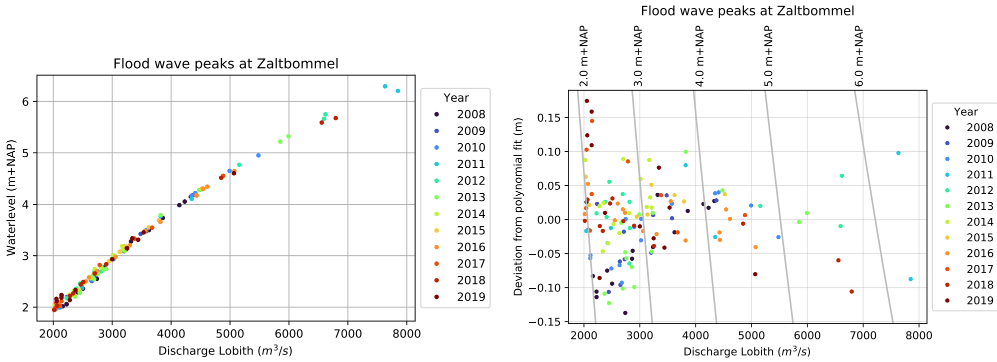

Figure C.23 Trend in flood peaks per year at Zaltbommel. Left: Absolute water level; right: Water level after subtracting a polynomial fit for increased readability.

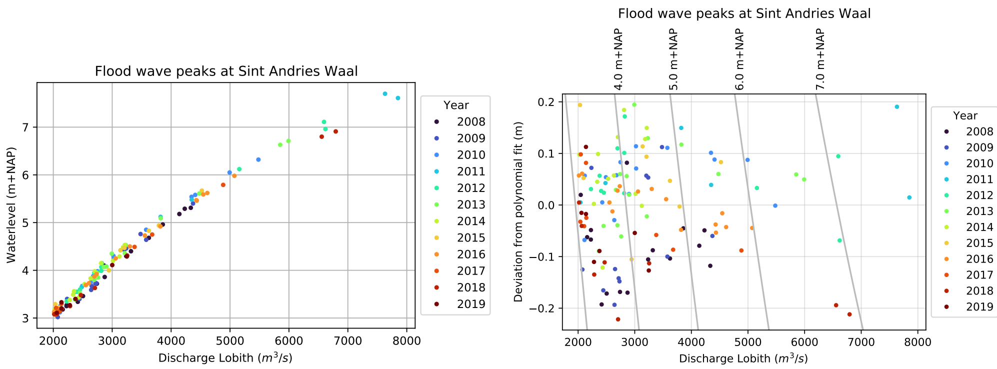

Figure C.24 Trend in flood peaks per year at Sint Andries Waal. Left: Absolute water level; right: Water level after subtracting a polynomial fit for increased readability.

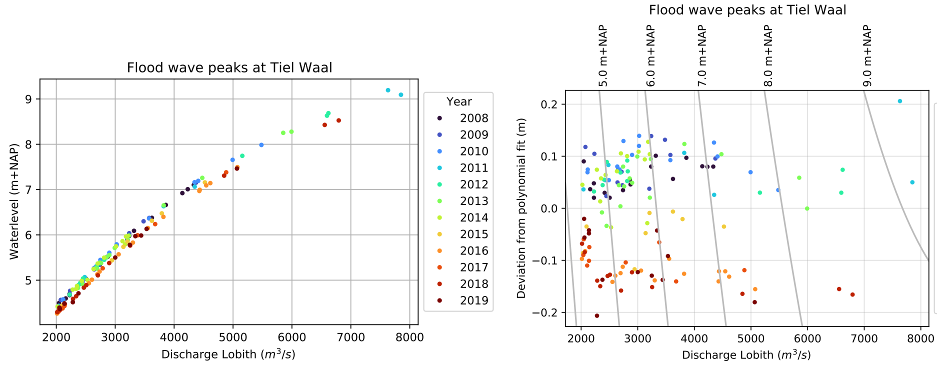

Figure C.25 Trend in flood peaks per year at Tiel Waal. Left: Absolute water level; right: Water level after subtracting a polynomial fit for increased readability.

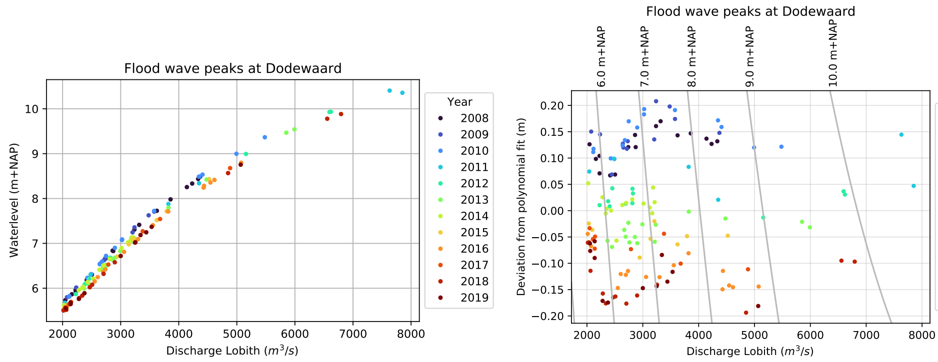

Figure C.26 Trend in flood peaks per year at Dodewaard. Left: Absolute water level; right: Water level after subtracting a polynomial fit for increased readability.

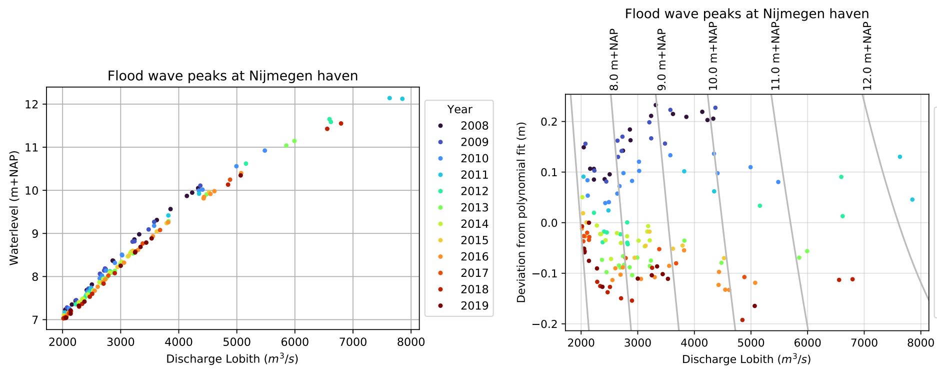

Figure C.27 Trend in flood peaks per year at Nijmegen haven. Left: Absolute water level; right: Water level after subtracting a polynomial fit for increased readability.

Deltares

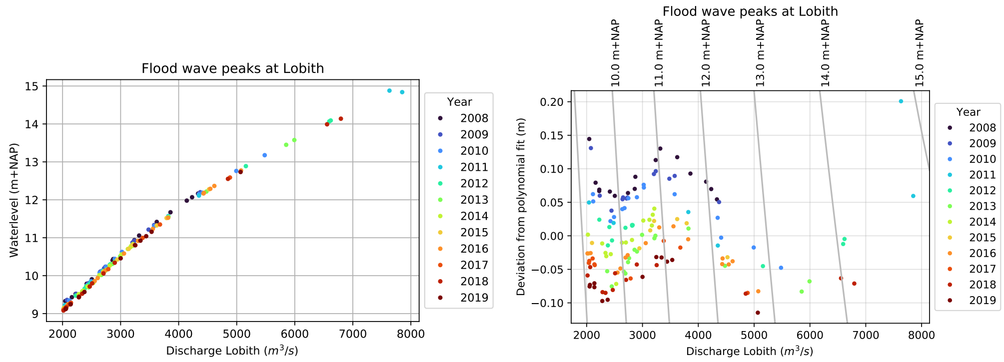

Figure C.28 Trend in flood peaks per year at Lobith. Left: Absolute water level; right: Water level after subtracting a polynomial fit for increased readability.

C.1.7 Trough water level trends

Similar to the previous section, the troughs have been analysed per year

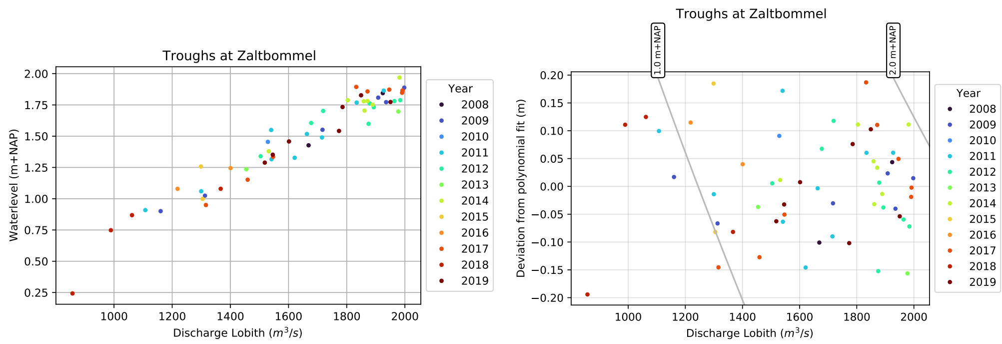

Figure C.29 Trend in troughs per year at Zaltbommel. Left: Absolute water level; right: Water level after subtracting a polynomial fit for increased readability.

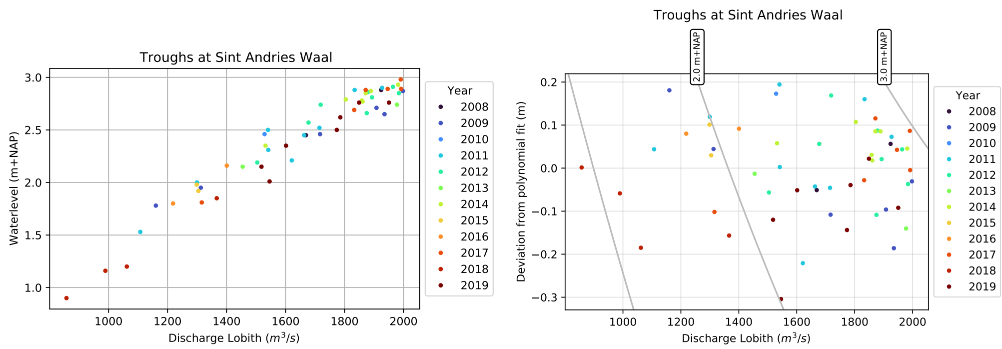

Figure C.30 Trend in troughs per year at Sint Andries Waal. Left: Absolute water level; right: Water level after subtracting a polynomial fit for increased readability.

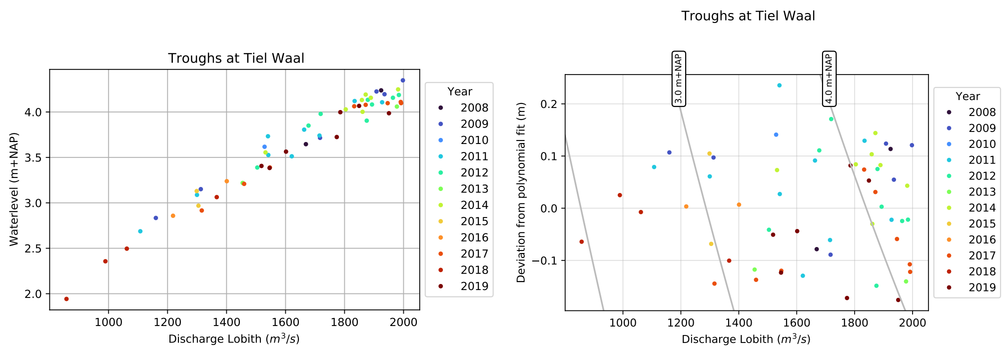

Figure C.31 Trend in troughs per year at Tiel Waal. Left: Absolute water level; right: Water level after subtracting a polynomial fit for increased readability.

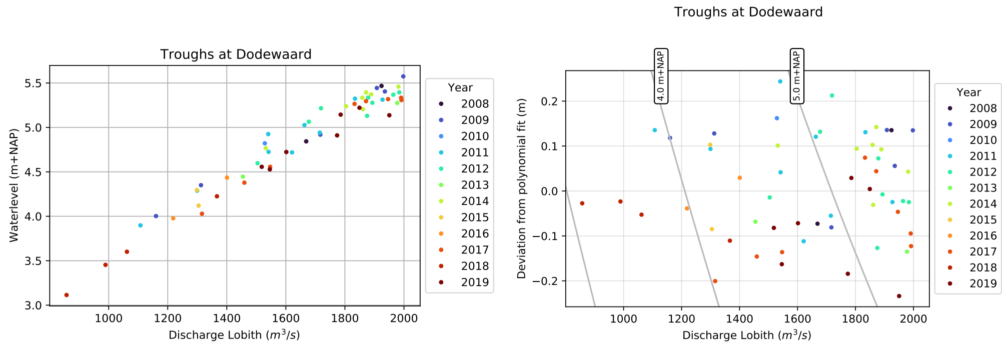

Figure C.32 Trend in troughs per year at Dodewaard. Left: Absolute water level; right: Water level after subtracting a polynomial fit for increased readability.

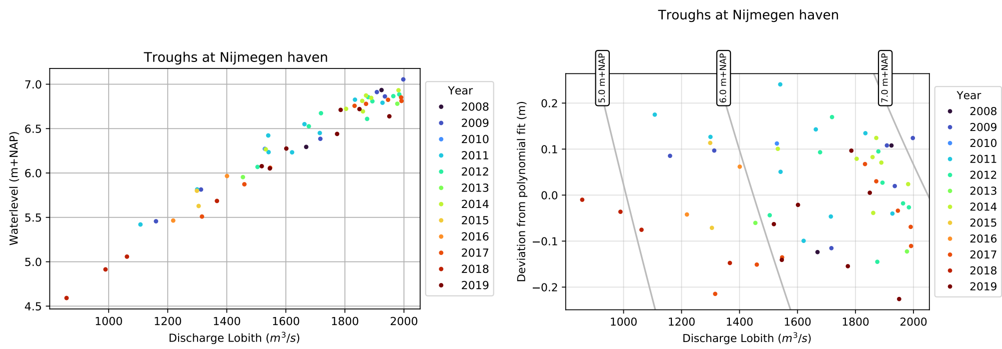

Figure C.33 Trend in troughs per year at Nijmegen haven. Left: Absolute water level; right: Water level after subtracting a polynomial fit for increased readability.

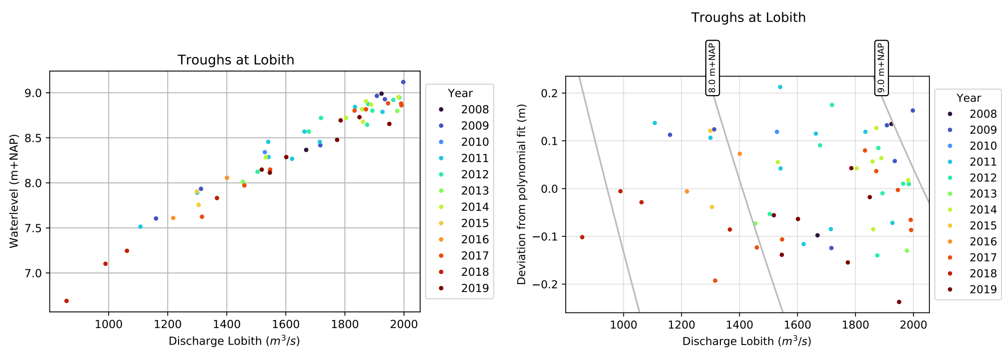

Figure C.34 Trend in troughs per year at Lobith. Left: Absolute water level; right: Water level after subtracting a polynomial fit for increased readability.

C.1.8 Discharge Amsterdam-Rijnkanaal

No full time series exist of the discharge through the Betuwepand of the Amsterdam-Rijnkanaal (in short: ARK). Occasional ADCP-measurements are available, as well as water levels directly upstream and downstream of the locks.

At first the entire time series is analysed and at all moments that the head difference over the locks is less than 3 cm it is assumed that the locks are opened. The results are given in figure C.35. This method appears to be a good approximation. It results in over 140 days of open locks in 2018, and 0 days in 2008 and 2010.

As a second step the scarce ADCP measurements in the ARK (11 measurements in total) are plotted to the head difference at the lock to see if any correlation exists in figure C.36. In this figure the long 'wiskers' of all measurements indicate the variation in head difference over the day (between the 10% and 90% percentile). If we try to look for a trend, there appears to be a slight increase in the head difference for increasing discharge. However, this correlation is not strong enough to be applicable on the entire waterlevel-timeseries.

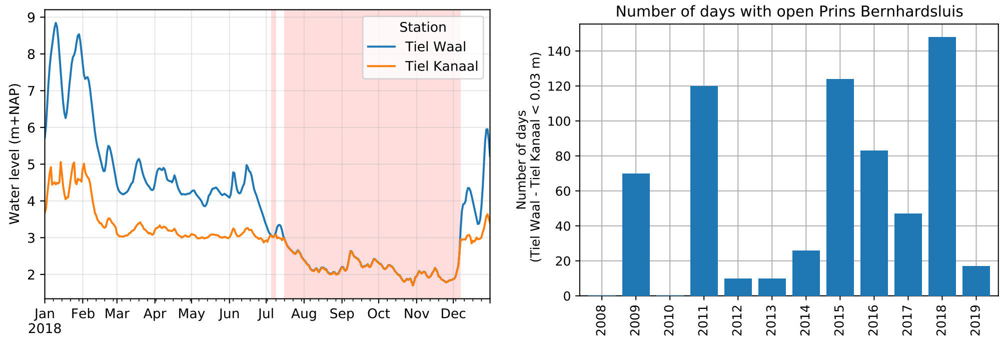

Figure C.35 Days that the Prins Bernhardsluizen are opened. Left: an example of 2018 where the days that the head difference is smaller than 3 cm and thus assumed open are marked, right: the total number of days in all years

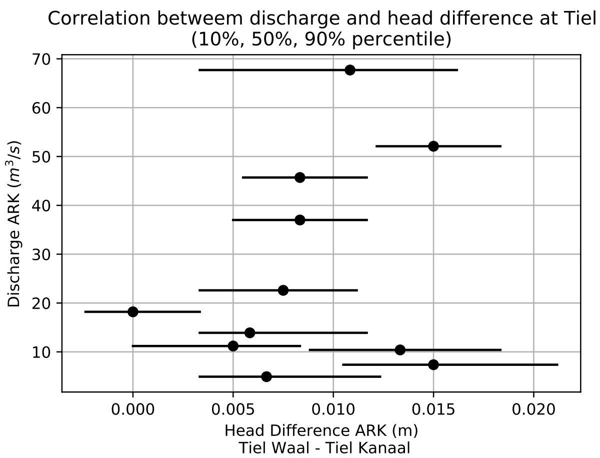

Figure C.36 Analyses of the possible correlation between the ADCP-measured discharge to the ARK and the head difference between Tiel Waal and Tiel Kanaal

C.2 Diver measurements

Although plans were initially made to install divers at many locations, in the final plans only at two locations divers were placed (rkm 911.5 and rkm 922). At both locations two divers were placed (labelled with -1 and -2), but it is not known what the difference of both divers is.

The data set for these divers is far from complete: data after November 2016 could not be found by Rijkswaterstaat, the diver 911.5-2 was only available for the first year (2014), for low discharges none of the divers gave valid results (invalid measurements were marked as ’Onbetrouwbare waarde’ or ’Hiaat waarde’ in the delivered data). An overview of all measurements is given in figure C.37. In this figure the construction period is marked in grey, showing that this covers a large part of the available measurements.

In the second stage of the project additional time series data was retrieved for divers placed at the head of all three longitudinal training walls. Unfortunately this data was only available for the period October 2020 to December 2020 (see C.38). The measurements are registered with steps of 10 cm. For the figure the moving average (over 12 hour) is added to show the general trend. The data from these divers is not used in any of the further analyses.

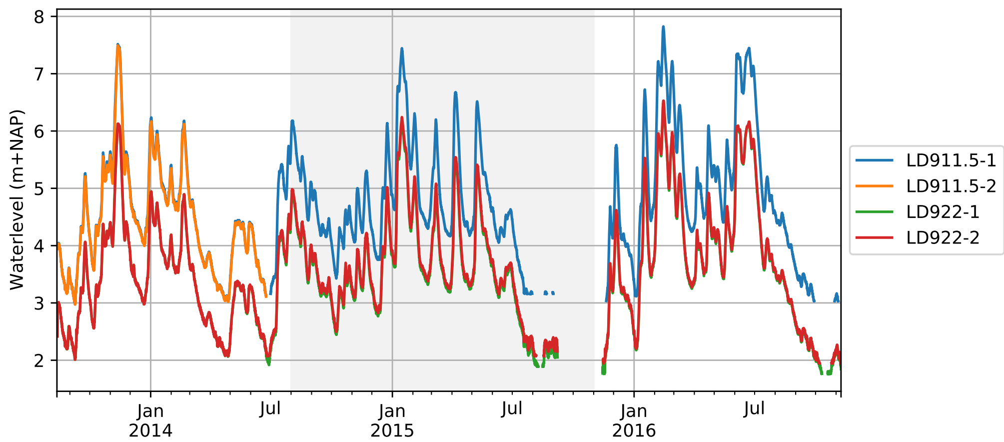

Figure C.37 Time series of the measurement data from diversat rkm 911.5 and rkm 922

To analyse effects of the longitudinal training walls at low discharges, the measurements are plotted to the discharge at Lobith (from LMW measurements) in figure C.39. For further analyses the data at the upstream diver (rkm 911.5) is split in before construction (up to July 2014) and after construction (from November 2015) and given in figure C.42. From this figure there appears no effect of the construction of the LTW, but this could also be caused by the limited available data.

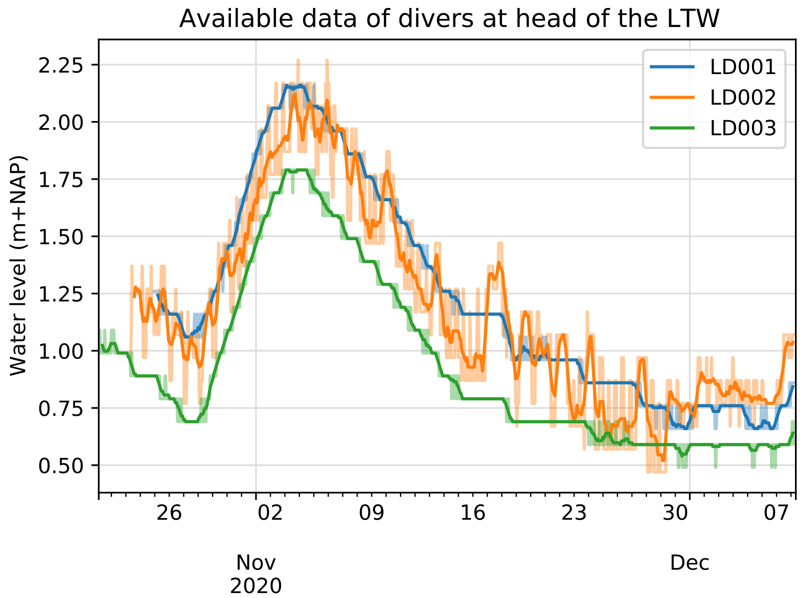

Figure C.38 Time series of the measurement data from divers at the head of the longitudinal training walls. Shown are the raw data (every hour) and the moving average over 12 hours.

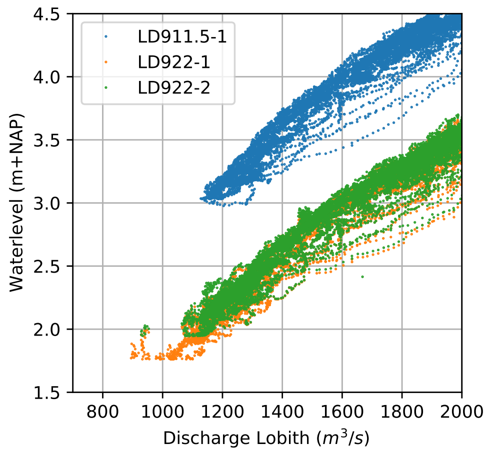

Figure C.39 Scatter plot of diver measurements at low discharge

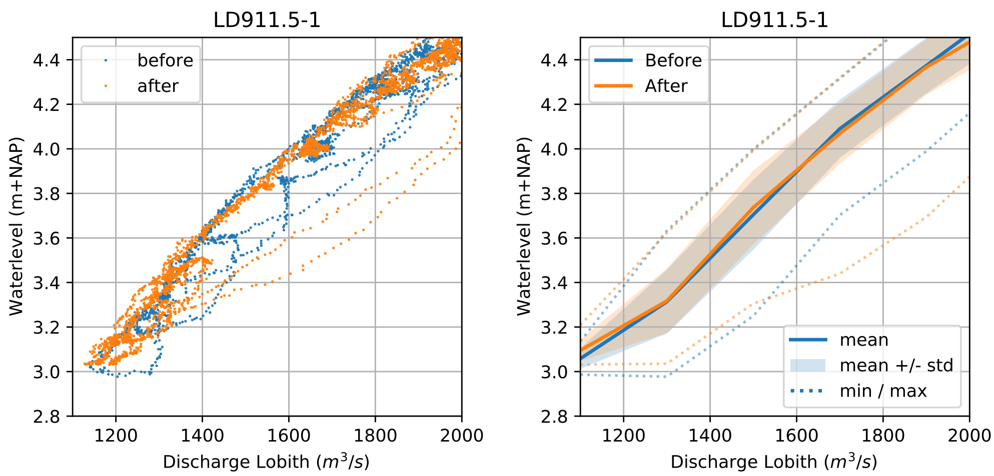

Figure C.40 Rating curve at diver LD911.5-1

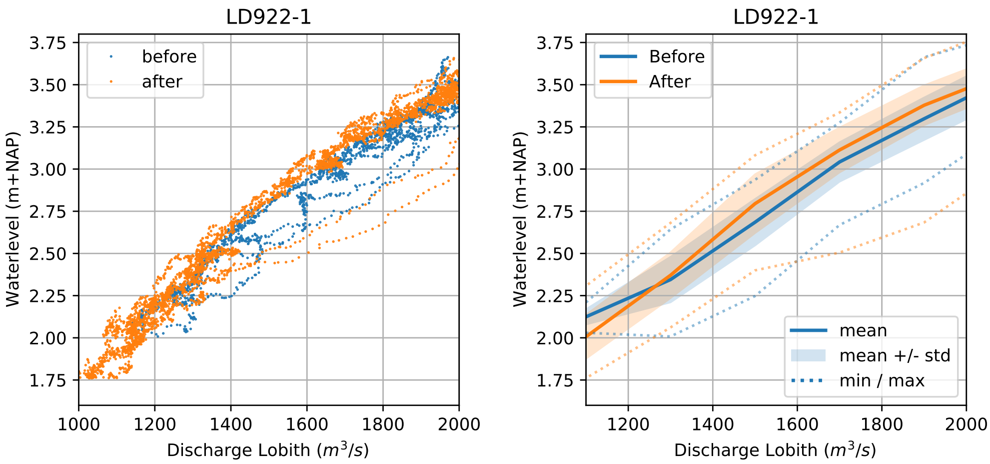

Figure C.41 Rating curve at diver LD922-1

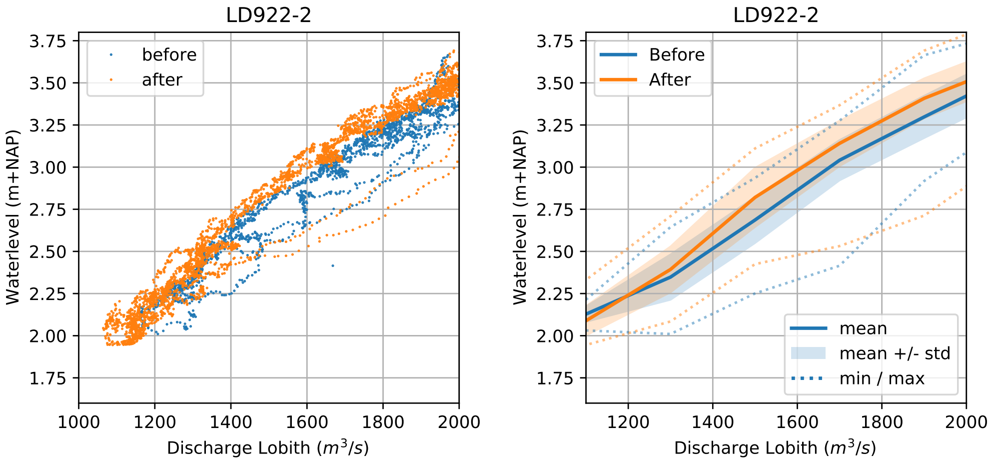

Figure C.42 Rating curve at diver LD922-2

D ADCP

D.1 Summary of all ADCP profiles along the Waal River.

river km	date	water discharge at Lobith [m^3/s]
915.553	14-Nov-2011 15:25	938
915.553	17-Nov-2011 15:08	922
922.171	01-Feb-2013 09:02	3329
911.463	01-Feb-2013 09:17	3329
921.771	01-Feb-2013 09:57	3352
911.920	01-Feb-2013 10:00	3352
921.782	01-Feb-2013 10:31	3375
911.931	01-Feb-2013 10:31	3375
921.571	01-Feb-2013 10:45	3368
912.452	01-Feb-2013 10:50	3368
912.453	01-Feb-2013 11:01	3376
920.625	01-Feb-2013 11:24	3413
913.069	01-Feb-2013 11:29	3413
913.081	01-Feb-2013 11:47	3444
913.078	01-Feb-2013 11:56	3436
914.554	01-Feb-2013 12:20	3467
918.485	01-Feb-2013 12:22	3467
915.181	01-Feb-2013 13:08	3475
917.858	01-Feb-2013 13:09	3475
915.191	01-Feb-2013 13:10	3475
915.950	01-Feb-2013 13:41	3498
911.388	02-Feb-2013 09:05	4102
922.078	02-Feb-2013 09:11	4102
922.089	02-Feb-2013 09:38	4103
911.829	02-Feb-2013 09:52	4121
921.844	02-Feb-2013 10:16	4122
921.859	02-Feb-2013 10:31	4141
912.539	02-Feb-2013 10:51	4150
921.439	02-Feb-2013 10:58	4123
921.458	02-Feb-2013 11:13	4160
913.130	02-Feb-2013 11:49	4161
920.515	02-Feb-2013 11:56	4170
913.140	02-Feb-2013 11:57	4170
914.908	02-Feb-2013 12:40	4162
918.586	02-Feb-2013 12:54	4162
914.919	02-Feb-2013 13:04	4172
918.631	02-Feb-2013 13:26	4200
915.265	02-Feb-2013 13:33	4200

river km	date	water discharge at Lobith [m^3/s]
915.293	02-Feb-2013 13:37	4182
917.773	02-Feb-2013 14:03	4201
915.958	02-Feb-2013 14:10	4229
911.385	04-Feb-2013 09:26	5000
911.397	04-Feb-2013 09:30	5000
922.068	04-Feb-2013 09:34	5000
911.408	04-Feb-2013 09:45	5011
921.853	04-Feb-2013 10:18	5033
911.832	04-Feb-2013 10:26	5022
921.866	04-Feb-2013 10:40	5022
921.460	04-Feb-2013 11:03	5033
912.537	04-Feb-2013 11:25	5055
920.533	04-Feb-2013 11:51	5066
913.121	04-Feb-2013 12:20	5055
918.594	04-Feb-2013 12:49	5066
914.900	04-Feb-2013 13:17	5066
914.918	04-Feb-2013 13:43	5077
917.786	04-Feb-2013 13:45	5077
917.796	04-Feb-2013 13:49	5077
915.266	04-Feb-2013 14:18	5088
915.948	04-Feb-2013 14:42	5088
915.964	04-Feb-2013 14:47	5099
614.100	18-Mar-2014 09:56	1497
915.555	20-Mar-2014 09:49	1450
925.008	10-Aug-2015 08:43	1060
923.998	10-Aug-2015 10:03	1056
923.016	10-Aug-2015 11:05	1046
922.005	10-Aug-2015 11:56	1047
920.991	10-Aug-2015 12:51	1042
920.006	11-Aug-2015 09:56	1057
918.999	11-Aug-2015 10:42	1075
918.521	11-Aug-2015 11:34	1066
917.690	11-Aug-2015 12:26	1065
919.974	12-Aug-2015 07:51	1123
915.794	12-Aug-2015 09:58	1140
915.092	12-Aug-2015 10:46	1140
914.005	12-Aug-2015 11:41	1122
913.095	12-Aug-2015 12:42	1118
912.321	13-Aug-2015 08:08	1079
911.749	13-Aug-2015 09:29	1084
910.993	13-Aug-2015 10:54	1084
910.239	13-Aug-2015 11:54	1093
909.003	13-Aug-2015 13:01	1089
908.305	14-Aug-2015 07:42	1072

river km	date	water discharge at Lobith [m^3/s]
908.318	14-Aug-2015 08:12	1094
907.083	14-Aug-2015 08:51	1081
906.315	14-Aug-2015 10:17	1077
905.246	14-Aug-2015 11:37	1086
924.846	17-Aug-2015 08:08	1187
924.078	17-Aug-2015 09:20	1186
923.139	17-Aug-2015 10:13	1191
921.877	17-Aug-2015 11:02	1196
920.709	17-Aug-2015 11:46	1191
911.001	07-Jun-2016 09:36	4509
911.013	07-Jun-2016 09:39	4509
911.759	07-Jun-2016 10:34	4509
911.770	07-Jun-2016 10:41	4509
912.316	07-Jun-2016 11:30	4509
912.332	07-Jun-2016 11:48	4509
913.096	07-Jun-2016 12:28	4509
914.018	07-Jun-2016 13:41	4529
915.082	07-Jun-2016 14:39	4529
915.100	07-Jun-2016 14:42	4529
913.088	29-Jun-2016 08:41	4250
916.659	29-Jun-2016 09:05	4260
919.742	29-Jun-2016 09:34	4260
911.000	29-Jun-2016 11:59	4230
910.997	30-Jun-2016 10:06	4057
914.732	30-Jun-2016 11:47	4029
919.666	30-Jun-2016 13:09	4029
921.850	30-Jun-2016 13:49	4011
921.861	30-Jun-2016 13:52	4011
921.989	11-Oct-2016 08:34	1020
918.516	11-Oct-2016 09:37	1025
918.536	11-Oct-2016 09:42	1025
918.398	11-Oct-2016 10:43	1025
614.100	17-Oct-2016 15:32	965
614.100	18-Oct-2016 08:34	974
906.974	14-Nov-2016 09:09	1505
908.015	14-Nov-2016 09:43	1505
908.937	14-Nov-2016 10:15	1506
909.932	14-Nov-2016 10:53	1501
911.050	14-Nov-2016 11:32	1523
911.697	14-Nov-2016 12:09	1551
911.735	14-Nov-2016 12:43	1535
912.376	14-Nov-2016 13:16	1530
912.387	14-Nov-2016 13:37	1536
913.090	14-Nov-2016 13:51	1542

river km	date	water discharge at Lobith [m³/s]
913.931	14-Nov-2016 14:24	1542
914.844	14-Nov-2016 14:55	1565
915.173	14-Nov-2016 15:28	1554
915.731	15-Nov-2016 08:17	1762
915.746	15-Nov-2016 08:27	1774
916.978	15-Nov-2016 08:58	1775
917.688	15-Nov-2016 09:38	1794
917.699	15-Nov-2016 09:50	1788
918.407	15-Nov-2016 10:09	1794
918.298	15-Nov-2016 10:40	1776
918.522	15-Nov-2016 11:11	1789
918.538	15-Nov-2016 11:19	1807
918.989	15-Nov-2016 11:46	1808
919.000	15-Nov-2016 12:00	1808
920.048	15-Nov-2016 12:20	1820
920.758	15-Nov-2016 12:49	1827
920.951	15-Nov-2016 13:28	1840
920.963	15-Nov-2016 13:30	1840
921.368	15-Nov-2016 14:03	1835
921.999	16-Nov-2016 10:43	1894
922.011	16-Nov-2016 10:58	1888
922.030	16-Nov-2016 11:04	1888
923.000	16-Nov-2016 11:35	1883
924.008	16-Nov-2016 12:13	1895
925.084	16-Nov-2016 12:53	1889
925.097	16-Nov-2016 12:56	1889
909.946	11-Sep-2017 09:37	1734
909.973	11-Sep-2017 09:40	1734
911.058	11-Sep-2017 10:22	1734
911.732	11-Sep-2017 10:50	1728
911.745	11-Sep-2017 10:54	1728
911.762	11-Sep-2017 10:57	1728
912.359	11-Sep-2017 11:19	1728
913.088	11-Sep-2017 11:49	1728
913.098	11-Sep-2017 11:55	1728
914.554	11-Sep-2017 12:19	1728
914.566	11-Sep-2017 12:23	1728
915.043	11-Sep-2017 12:47	1710
915.745	11-Sep-2017 13:15	1721
917.721	11-Sep-2017 13:45	1739
917.734	11-Sep-2017 13:51	1739
918.262	12-Sep-2017 08:38	1668
918.522	12-Sep-2017 09:06	1668
918.537	12-Sep-2017 09:13	1668

river km	date	water discharge at Lobith [m^3/s]
920.730	12-Sep-2017 09:42	1663
921.350	12-Sep-2017 10:16	1686
922.008	12-Sep-2017 10:48	1662
923.007	12-Sep-2017 11:16	1645
918.570	12-Sep-2017 12:33	1644
918.587	12-Sep-2017 12:42	1650
918.463	12-Sep-2017 12:50	1656
918.277	12-Sep-2017 14:54	1656
917.693	15-Sep-2017 08:51	1592
917.715	15-Sep-2017 08:55	1602
915.830	15-Sep-2017 09:16	1608
915.078	15-Sep-2017 09:32	1608
914.872	15-Sep-2017 09:49	1620
914.932	15-Sep-2017 11:04	1615
914.559	15-Sep-2017 11:48	1609
913.123	15-Sep-2017 12:06	1615
913.135	15-Sep-2017 12:13	1615
912.388	15-Sep-2017 12:25	1621
911.824	15-Sep-2017 12:44	1621
911.633	15-Sep-2017 13:01	1621
911.657	15-Sep-2017 13:50	1622
911.672	15-Sep-2017 14:06	1633
909.937	23-Oct-2017 09:53	1291
911.034	23-Oct-2017 10:35	1281
911.050	23-Oct-2017 10:37	1281
911.744	23-Oct-2017 11:11	1272
911.757	23-Oct-2017 11:30	1276
912.348	23-Oct-2017 11:53	1282
913.085	23-Oct-2017 12:31	1277
913.097	23-Oct-2017 12:41	1277
914.534	23-Oct-2017 13:16	1296
915.017	23-Oct-2017 13:50	1281
915.731	23-Oct-2017 14:17	1287
915.742	23-Oct-2017 14:26	1282
917.705	23-Oct-2017 14:54	1287
917.717	23-Oct-2017 15:06	1292
918.259	24-Oct-2017 08:49	1288
918.521	24-Oct-2017 09:21	1273
920.713	24-Oct-2017 10:03	1259
920.726	24-Oct-2017 10:06	1273
921.345	24-Oct-2017 10:34	1273
921.991	24-Oct-2017 11:04	1268
923.001	24-Oct-2017 11:37	1278
918.425	24-Oct-2017 14:15	1283

river km	date	water discharge at Lobith [m³/s]
914.882	24-Oct-2017 15:36	1264
911.634	25-Oct-2017 08:14	1259
914.664	25-Oct-2017 09:36	1284
915.713	17-Nov-2017 12:24	3096
917.334	17-Nov-2017 12:31	3104
918.254	17-Nov-2017 12:36	3089
919.041	17-Nov-2017 13:58	3096
920.506	17-Nov-2017 14:05	3089
921.325	17-Nov-2017 14:10	3089
918.392	22-Nov-2017 09:31	2152
918.408	22-Nov-2017 09:41	2146
918.435	22-Nov-2017 12:05	2146
918.448	22-Nov-2017 12:36	2153
918.505	22-Nov-2017 14:17	2160
918.519	22-Nov-2017 14:19	2160
918.557	22-Nov-2017 14:53	2152
918.535	24-Nov-2017 10:54	2271
918.556	24-Nov-2017 11:00	2271
920.767	24-Nov-2017 11:26	2277
920.779	24-Nov-2017 11:47	2284
921.352	24-Nov-2017 11:58	2284
918.584	24-Nov-2017 13:05	2271
911.631	01-Dec-2017 09:47	3518
911.651	01-Dec-2017 09:50	3518
911.667	01-Dec-2017 10:01	3510
911.693	01-Dec-2017 10:12	3510
911.735	01-Dec-2017 10:37	3502
911.747	01-Dec-2017 10:45	3502
911.758	01-Dec-2017 11:00	3510
911.768	01-Dec-2017 11:06	3502
911.787	01-Dec-2017 11:20	3502
911.813	01-Dec-2017 11:49	3502
914.882	01-Dec-2017 12:02	3502
914.952	01-Dec-2017 12:12	3494
914.970	01-Dec-2017 13:59	3494
918.437	01-Dec-2017 14:35	3494
918.455	01-Dec-2017 15:10	3494
918.522	01-Dec-2017 15:24	3494
918.537	01-Dec-2017 15:55	3510
918.565	01-Dec-2017 16:13	3494
918.581	01-Dec-2017 16:18	3486
911.644	05-Dec-2017 09:37	2702
911.674	05-Dec-2017 10:24	2709
911.687	05-Dec-2017 10:36	2723

river km	date	water discharge at Lobith [m^3/s]
911.702	05-Dec-2017 10:40	2723
911.716	05-Dec-2017 11:03	2702
914.882	05-Dec-2017 11:31	2681
918.411	05-Dec-2017 13:13	2681
918.434	05-Dec-2017 13:20	2702
918.444	05-Dec-2017 13:53	2675
918.456	05-Dec-2017 14:26	2668
918.535	05-Dec-2017 15:03	2675
918.549	05-Dec-2017 15:15	2675
918.561	05-Dec-2017 15:27	2682
909.941	06-Dec-2017 09:31	2500
911.040	06-Dec-2017 10:14	2494
911.054	06-Dec-2017 10:17	2487
911.748	06-Dec-2017 11:02	2487
912.347	06-Dec-2017 11:40	2494
913.100	06-Dec-2017 12:12	2500
914.551	06-Dec-2017 12:52	2487
915.032	06-Dec-2017 13:22	2494
915.047	06-Dec-2017 13:27	2480
915.734	06-Dec-2017 13:58	2500
915.746	06-Dec-2017 14:02	2500
917.710	06-Dec-2017 14:36	2474
918.254	06-Dec-2017 15:09	2487
912.183	07-Dec-2017 09:20	2367
912.199	07-Dec-2017 09:28	2373
912.994	07-Dec-2017 13:03	2350
913.012	07-Dec-2017 13:40	2350
911.735	07-Dec-2017 14:10	2336
911.752	07-Dec-2017 14:19	2350
911.822	07-Dec-2017 14:38	2330
911.042	07-Dec-2017 14:55	2336
911.626	08-Dec-2017 09:26	2301
911.636	08-Dec-2017 09:47	2287
911.656	08-Dec-2017 10:15	2287
911.675	08-Dec-2017 10:17	2287
911.685	08-Dec-2017 10:27	2287
911.698	08-Dec-2017 11:03	2301
911.822	08-Dec-2017 11:51	2301
912.380	08-Dec-2017 12:10	2308
913.126	08-Dec-2017 12:34	2301
914.555	08-Dec-2017 13:06	2301
913.101	08-Dec-2017 13:38	2295
913.115	08-Dec-2017 13:42	2295
912.355	08-Dec-2017 14:25	2287

river km	date	water discharge at Lobith [m^3/s]
911.736	08-Dec-2017 14:56	2295
911.049	08-Dec-2017 15:18	2281
911.746	12-Dec-2017 09:11	2540
912.350	12-Dec-2017 09:30	2527
913.087	12-Dec-2017 09:57	2534
914.629	12-Dec-2017 10:16	2554
915.040	12-Dec-2017 10:30	2547
915.767	12-Dec-2017 10:44	2547
917.696	12-Dec-2017 11:03	2560
918.278	12-Dec-2017 11:22	2547
923.007	12-Dec-2017 12:32	2547
923.018	12-Dec-2017 12:54	2547
922.013	12-Dec-2017 13:04	2547
921.352	12-Dec-2017 13:31	2560
920.733	12-Dec-2017 13:53	2554
916.512	13-Dec-2017 09:47	3038
916.546	13-Dec-2017 10:10	3052
915.040	13-Dec-2017 13:47	3264
915.746	13-Dec-2017 14:11	3294
915.757	13-Dec-2017 14:20	3272
917.708	13-Dec-2017 14:40	3317
917.727	13-Dec-2017 14:42	3317
917.748	13-Dec-2017 14:50	3324
918.255	13-Dec-2017 15:08	3354
918.272	13-Dec-2017 15:13	3354
910.066	18-Dec-2017 10:43	5035
911.133	18-Dec-2017 11:41	5002
911.150	18-Dec-2017 12:17	5024
911.854	18-Dec-2017 12:35	5013
911.869	18-Dec-2017 12:45	5035
912.371	18-Dec-2017 13:20	5013
912.384	18-Dec-2017 13:33	5013
913.144	18-Dec-2017 14:02	5013
913.160	18-Dec-2017 14:08	5013
914.488	18-Dec-2017 14:34	5013
914.508	18-Dec-2017 14:37	5013
915.150	18-Dec-2017 15:28	5013
915.897	19-Dec-2017 09:15	4916
915.862	19-Dec-2017 09:17	4916
917.733	19-Dec-2017 10:07	4894
917.753	19-Dec-2017 10:15	4894
918.123	19-Dec-2017 10:55	4905
918.134	19-Dec-2017 10:57	4905
918.145	19-Dec-2017 11:12	4905

river km	date	water discharge at Lobith [m^3/s]
918.638	19-Dec-2017 11:47	4916
918.650	19-Dec-2017 12:16	4883
920.855	19-Dec-2017 12:51	4894
920.867	19-Dec-2017 12:54	4894
920.879	19-Dec-2017 13:17	4873
921.301	19-Dec-2017 13:27	4873
921.318	19-Dec-2017 13:30	4873
921.328	19-Dec-2017 13:56	4905
921.880	19-Dec-2017 14:08	4905
921.890	19-Dec-2017 14:10	4905
921.901	19-Dec-2017 14:14	4905
922.900	19-Dec-2017 14:51	4862
922.910	19-Dec-2017 15:08	4862
911.842	20-Dec-2017 09:11	4630
911.855	20-Dec-2017 09:18	4641
912.372	20-Dec-2017 09:41	4610
913.152	20-Dec-2017 10:11	4599
914.484	20-Dec-2017 10:37	4610
915.093	20-Dec-2017 10:58	4599
915.104	20-Dec-2017 11:00	4599
911.842	04-Jan-2018 08:46	5054
911.857	04-Jan-2018 08:48	5054
912.382	04-Jan-2018 09:05	5065
913.155	04-Jan-2018 09:22	5065
914.470	04-Jan-2018 09:42	5076
915.094	04-Jan-2018 09:58	5087
915.122	04-Jan-2018 10:00	5087
915.892	04-Jan-2018 10:12	5109
915.903	04-Jan-2018 10:13	5109
917.739	04-Jan-2018 10:35	5088
917.756	04-Jan-2018 10:39	5088
918.111	04-Jan-2018 10:52	5109
918.138	04-Jan-2018 10:54	5109
920.841	04-Jan-2018 11:50	5121
920.869	04-Jan-2018 11:53	5121
921.325	04-Jan-2018 12:31	5154
921.882	04-Jan-2018 13:08	5176
921.893	04-Jan-2018 13:19	5154
921.905	04-Jan-2018 13:33	5165
922.914	04-Jan-2018 13:52	5177
922.938	04-Jan-2018 14:09	5166
918.665	04-Jan-2018 14:48	5199
918.679	04-Jan-2018 15:04	5199
913.137	16-Jan-2018 10:59	3763

river km	date	water discharge at Lobith [m^3/s]
913.150	16-Jan-2018 11:04	3763
913.160	16-Jan-2018 11:10	3763
911.844	17-Jan-2018 09:48	3555
911.866	17-Jan-2018 09:49	3555
912.384	17-Jan-2018 10:06	3538
914.456	17-Jan-2018 10:31	3554
914.469	17-Jan-2018 10:34	3554
915.114	17-Jan-2018 10:51	3538
915.894	17-Jan-2018 11:10	3546
917.737	17-Jan-2018 11:42	3546
917.750	17-Jan-2018 11:46	3529
918.122	17-Jan-2018 12:02	3538
918.143	17-Jan-2018 12:04	3538
918.608	17-Jan-2018 12:28	3538
922.889	17-Jan-2018 13:34	3529
922.901	17-Jan-2018 13:40	3521
921.897	17-Jan-2018 14:08	3537
921.304	17-Jan-2018 14:39	3521
920.867	17-Jan-2018 15:08	3537
910.025	01-Feb-2018 09:21	5036
910.042	01-Feb-2018 09:31	5036
910.055	01-Feb-2018 09:39	5036
911.159	01-Feb-2018 10:03	5025
911.866	01-Feb-2018 10:40	5014
911.898	01-Feb-2018 10:43	5014
912.366	01-Feb-2018 11:14	5003
912.392	01-Feb-2018 11:23	5003
913.150	01-Feb-2018 11:41	5015
914.480	01-Feb-2018 12:17	4982
914.495	01-Feb-2018 12:20	4982
915.148	01-Feb-2018 12:49	4993
915.158	01-Feb-2018 12:52	4993
915.866	01-Feb-2018 13:23	4982
915.885	01-Feb-2018 13:47	4960
917.745	01-Feb-2018 14:01	4971
917.758	01-Feb-2018 14:17	4949
918.157	01-Feb-2018 14:33	4949
918.176	01-Feb-2018 14:40	4960
911.634	02-Feb-2018 09:11	4736
911.657	02-Feb-2018 09:49	4736
911.681	02-Feb-2018 09:52	4736
911.695	02-Feb-2018 10:28	4726
914.857	02-Feb-2018 11:10	4705
914.868	02-Feb-2018 11:14	4705

river km	date	water discharge at Lobith [m^3/s]
914.902	02-Feb-2018 11:46	4715
918.430	02-Feb-2018 14:16	4715
918.457	02-Feb-2018 14:29	4705
910.013	09-Feb-2018 09:35	3624
910.033	09-Feb-2018 09:45	3624
911.158	09-Feb-2018 10:28	3606
911.852	09-Feb-2018 10:57	3606
911.873	09-Feb-2018 11:00	3606
911.885	09-Feb-2018 11:07	3615
912.373	09-Feb-2018 11:20	3589
913.149	09-Feb-2018 11:46	3598
914.496	09-Feb-2018 12:09	3581
914.509	09-Feb-2018 12:26	3581
915.149	09-Feb-2018 12:39	3598
915.845	09-Feb-2018 13:04	3572
915.855	09-Feb-2018 13:07	3581
917.734	09-Feb-2018 13:34	3572
918.140	09-Feb-2018 13:54	3581
918.647	09-Feb-2018 14:13	3581
918.663	09-Feb-2018 14:22	3572
911.823	15-Feb-2018 08:48	2663
912.346	15-Feb-2018 09:00	2643
913.085	15-Feb-2018 09:15	2657
914.593	15-Feb-2018 09:29	2657
915.077	15-Feb-2018 09:41	2670
915.806	15-Feb-2018 09:55	2663
917.736	15-Feb-2018 10:15	2670
917.754	15-Feb-2018 10:17	2670
918.559	15-Feb-2018 10:50	2657
918.585	15-Feb-2018 10:54	2657
922.011	15-Feb-2018 11:42	2657
922.022	15-Feb-2018 11:49	2650
923.028	15-Feb-2018 12:15	2650
921.353	15-Feb-2018 12:41	2643
920.724	15-Feb-2018 13:05	2629
920.735	15-Feb-2018 13:14	2629
918.542	15-Feb-2018 13:42	2629
918.258	15-Feb-2018 14:04	2636
918.273	15-Feb-2018 14:10	2629
917.708	15-Feb-2018 14:34	2643
917.722	15-Feb-2018 14:39	2643
915.741	15-Feb-2018 14:56	2629
915.026	15-Feb-2018 15:16	2629
914.534	15-Feb-2018 15:38	2616

river km	date	water discharge at Lobith [m^3/s]
914.553	15-Feb-2018 15:40	2616
913.110	16-Feb-2018 08:42	2549
913.123	16-Feb-2018 08:47	2549
912.348	16-Feb-2018 09:01	2549
912.360	16-Feb-2018 09:07	2549
911.749	16-Feb-2018 09:27	2549
911.031	16-Feb-2018 09:48	2542
911.049	16-Feb-2018 10:01	2556
909.959	16-Feb-2018 10:09	2556
910.000	16-Feb-2018 10:13	2556
911.646	16-Feb-2018 10:43	2556
911.693	16-Feb-2018 10:45	2556
914.855	16-Feb-2018 12:17	2522
914.869	16-Feb-2018 12:49	2536
914.888	16-Feb-2018 13:42	2536
918.418	16-Feb-2018 13:53	2542
918.431	16-Feb-2018 14:16	2536
918.442	16-Feb-2018 14:25	2529
918.460	16-Feb-2018 14:47	2522
918.470	16-Feb-2018 14:53	2522
911.821	06-Mar-2018 08:51	1896
912.341	06-Mar-2018 09:09	1889
913.087	06-Mar-2018 09:29	1914
914.625	06-Mar-2018 09:49	1895
915.065	06-Mar-2018 10:03	1902
915.782	06-Mar-2018 10:19	1896
918.588	06-Mar-2018 11:15	1908
918.600	06-Mar-2018 11:19	1908
922.015	06-Mar-2018 12:11	1909
922.037	06-Mar-2018 12:20	1909
923.020	06-Mar-2018 12:42	1902
923.035	06-Mar-2018 12:44	1902
921.346	06-Mar-2018 13:16	1914
920.726	06-Mar-2018 13:39	1909
918.539	06-Mar-2018 14:07	1921
918.256	06-Mar-2018 14:30	1921
917.703	06-Mar-2018 14:56	1909
917.720	06-Mar-2018 15:10	1896
915.735	06-Mar-2018 15:31	1921
915.043	06-Mar-2018 15:51	1903
914.549	07-Mar-2018 08:39	1935
913.118	07-Mar-2018 09:08	1922
912.364	07-Mar-2018 09:31	1935
911.732	07-Mar-2018 10:03	1916

river km	date	water discharge at Lobith [m^3/s]
911.034	07-Mar-2018 10:32	1916
909.943	07-Mar-2018 10:58	1916
911.627	07-Mar-2018 11:25	1942
911.650	07-Mar-2018 11:35	1916
911.662	07-Mar-2018 12:06	1923
911.682	07-Mar-2018 12:14	1923
911.692	07-Mar-2018 12:16	1916
911.709	07-Mar-2018 12:28	1923
918.405	07-Mar-2018 13:08	1929
918.419	07-Mar-2018 13:16	1923
918.446	07-Mar-2018 13:57	1929
918.464	07-Mar-2018 14:09	1923
918.479	07-Mar-2018 14:38	1923
914.843	07-Mar-2018 14:54	1923
914.855	07-Mar-2018 15:20	1936
914.880	07-Mar-2018 16:25	1949
914.483	14-May-2018 10:25	1845
914.499	14-May-2018 10:52	1845
913.142	14-May-2018 11:12	1858
912.379	14-May-2018 11:45	1847
911.862	14-May-2018 12:17	1859
911.885	14-May-2018 12:32	1847
911.134	14-May-2018 12:54	1853
911.131	15-May-2018 08:30	1924
915.145	15-May-2018 09:13	1937
915.875	15-May-2018 09:49	1924
917.733	15-May-2018 10:42	1937
918.134	15-May-2018 11:11	1918
918.145	15-May-2018 11:39	1925
915.889	15-May-2018 12:20	1931
915.907	15-May-2018 12:33	1931
918.638	25-Jun-2018 08:59	1671
918.651	25-Jun-2018 09:17	1688
918.415	25-Jun-2018 10:02	1688
918.426	25-Jun-2018 11:07	1664
918.460	25-Jun-2018 11:13	1664
918.471	25-Jun-2018 11:35	1670
918.487	25-Jun-2018 11:45	1652
915.037	25-Jun-2018 12:23	1664
915.091	25-Jun-2018 12:56	1658
914.847	25-Jun-2018 13:12	1658
914.873	25-Jun-2018 13:53	1652
914.886	25-Jun-2018 14:18	1646
914.919	25-Jun-2018 14:55	1657

river km	date	water discharge at Lobith [m^3/s]
914.496	25-Jun-2018 15:27	1652
914.507	25-Jun-2018 15:35	1640
911.088	05-Jul-2018 08:35	1243
911.916	05-Jul-2018 09:23	1239
911.931	05-Jul-2018 09:42	1229
912.371	05-Jul-2018 09:53	1224
912.389	05-Jul-2018 09:59	1234
913.153	05-Jul-2018 10:31	1234
914.545	05-Jul-2018 11:13	1224
915.184	05-Jul-2018 11:37	1219
915.956	05-Jul-2018 12:14	1224
915.967	05-Jul-2018 12:29	1229
917.746	05-Jul-2018 12:42	1224
914.585	05-Jul-2018 13:12	1224
918.145	05-Jul-2018 13:27	1229
911.858	06-Jul-2018 09:13	1231
912.384	06-Jul-2018 09:51	1221
921.258	06-Jul-2018 09:52	1221
920.813	06-Jul-2018 10:31	1231
913.112	06-Jul-2018 10:33	1231
918.740	06-Jul-2018 11:26	1226
914.451	06-Jul-2018 11:44	1226
915.145	06-Jul-2018 12:31	1226
918.111	06-Jul-2018 12:35	1235
917.730	06-Jul-2018 12:56	1240
915.804	06-Jul-2018 13:07	1235
911.929	16-Jul-2018 09:34	1173
911.824	16-Jul-2018 09:48	1174
914.520	16-Jul-2018 10:11	1178
914.475	16-Jul-2018 10:26	1169
915.145	16-Jul-2018 10:43	1169
915.171	16-Jul-2018 10:58	1169
918.129	16-Jul-2018 11:15	1183
918.139	16-Jul-2018 11:18	1183
918.150	16-Jul-2018 11:26	1178
918.647	16-Jul-2018 11:36	1188
918.134	16-Jul-2018 11:45	1174
921.315	16-Jul-2018 12:08	1165
922.886	16-Jul-2018 12:34	1174
918.938	16-Jul-2018 12:50	1165
921.859	16-Jul-2018 13:02	1174
921.880	16-Jul-2018 13:08	1165
921.214	16-Jul-2018 13:31	1174
920.871	16-Jul-2018 13:40	1160

river km	date	water discharge at Lobith [m^3/s]
920.885	16-Jul-2018 13:46	1160
917.720	16-Jul-2018 14:18	1160
915.887	20-Jul-2018 08:08	1092
913.135	20-Jul-2018 08:43	1092
913.158	20-Jul-2018 08:45	1074
912.362	20-Jul-2018 09:04	1088
912.372	20-Jul-2018 09:09	1083
911.077	20-Jul-2018 09:37	1088
911.094	20-Jul-2018 09:45	1083
909.988	20-Jul-2018 10:10	1078
911.619	20-Jul-2018 10:48	1079
911.634	20-Jul-2018 10:54	1079
914.850	20-Jul-2018 11:44	1083
911.937	30-Jul-2018 09:46	1028
914.491	30-Jul-2018 10:14	1010
914.538	30-Jul-2018 10:15	1014
915.145	30-Jul-2018 10:39	1014
915.226	30-Jul-2018 10:55	1028
918.128	30-Jul-2018 11:11	1014
918.142	30-Jul-2018 11:27	1018
918.643	30-Jul-2018 11:31	1018
918.654	30-Jul-2018 11:43	1014
921.301	30-Jul-2018 11:55	1014
921.312	30-Jul-2018 12:00	1014
918.914	30-Jul-2018 12:33	1019
918.939	30-Jul-2018 12:36	1010
911.070	03-Aug-2018 08:44	965
914.160	03-Aug-2018 09:34	951
915.170	20-Aug-2018 10:49	906
918.170	20-Aug-2018 11:30	902
911.922	20-Aug-2018 11:38	902
918.658	20-Aug-2018 12:21	906
914.521	20-Aug-2018 12:31	906
915.139	20-Aug-2018 12:56	894
918.130	20-Aug-2018 13:37	907
918.637	20-Aug-2018 14:05	897
921.314	20-Aug-2018 14:58	897
911.914	27-Aug-2018 10:03	870
914.480	27-Aug-2018 11:19	861
915.171	27-Aug-2018 11:20	861
915.119	27-Aug-2018 11:52	853
915.131	27-Aug-2018 11:57	856
918.159	27-Aug-2018 12:10	852
918.136	27-Aug-2018 12:35	856

river km	date	water discharge at Lobith [m^3/s]
918.685	27-Aug-2018 12:48	861
918.146	27-Aug-2018 12:55	856
918.641	27-Aug-2018 13:05	852
921.305	27-Aug-2018 13:38	848
911.919	10-Sep-2018 10:04	1012
915.171	10-Sep-2018 10:19	1021
914.491	10-Sep-2018 10:55	1030
914.501	10-Sep-2018 10:56	1030
915.138	10-Sep-2018 11:20	1021
915.149	10-Sep-2018 11:48	1017
915.158	24-Sep-2018 10:40	925
918.633	24-Sep-2018 15:11	932
918.647	24-Sep-2018 15:13	932
911.834	08-Oct-2018 09:23	920
915.168	08-Oct-2018 10:16	920
914.482	08-Oct-2018 11:02	919
918.740	08-Oct-2018 11:19	898
915.129	08-Oct-2018 11:32	919
915.140	08-Oct-2018 11:45	919
918.137	08-Oct-2018 12:09	911
918.629	08-Oct-2018 12:35	915
918.649	08-Oct-2018 12:40	915
921.306	08-Oct-2018 13:08	924
918.307	11-Oct-2018 08:22	867
918.344	11-Oct-2018 08:38	880
918.226	11-Oct-2018 08:51	880
918.377	11-Oct-2018 10:33	889
918.395	11-Oct-2018 10:47	893
918.620	11-Oct-2018 11:51	893
918.658	11-Oct-2018 12:16	885
918.711	11-Oct-2018 12:40	889
918.482	11-Oct-2018 12:43	889
918.775	11-Oct-2018 12:55	893
918.534	11-Oct-2018 13:31	884
918.546	11-Oct-2018 13:50	889
918.594	11-Oct-2018 14:04	875
918.183	21-Nov-2018 08:09	762
915.061	21-Nov-2018 09:09	771
921.332	21-Nov-2018 10:28	780
911.753	22-Nov-2018 16:32	756
914.542	22-Nov-2018 17:32	756
914.555	22-Nov-2018 17:42	752
915.028	23-Nov-2018 10:17	752
915.042	23-Nov-2018 10:23	752

river km	date	water discharge at Lobith [m^3/s]
918.267	23-Nov-2018 10:47	770
918.511	23-Nov-2018 11:43	770
918.528	23-Nov-2018 11:45	765
921.359	23-Nov-2018 12:23	757
921.347	03-Dec-2018 08:23	818
918.519	03-Dec-2018 09:36	818
918.263	03-Dec-2018 10:33	823
918.274	03-Dec-2018 10:46	823
915.014	03-Dec-2018 11:52	817
915.038	03-Dec-2018 12:00	830
914.541	03-Dec-2018 12:43	826
914.553	03-Dec-2018 12:50	839
911.739	03-Dec-2018 13:54	859
915.074	05-Dec-2018 10:00	981
918.251	05-Dec-2018 10:49	1012
918.573	05-Dec-2018 12:19	1015
921.335	05-Dec-2018 12:59	1019
915.551	06-Dec-2018 08:24	1270
915.562	06-Dec-2018 14:15	1372
915.138	19-Dec-2018 09:37	1443
918.037	19-Dec-2018 11:57	1442
918.714	19-Dec-2018 12:35	1436
921.320	19-Dec-2018 13:41	1414
921.346	20-Dec-2018 08:25	1344
921.358	20-Dec-2018 08:32	1344
918.518	20-Dec-2018 11:13	1325
918.528	20-Dec-2018 11:30	1325
918.273	20-Dec-2018 12:16	1334
915.001	20-Dec-2018 13:20	1315
915.037	20-Dec-2018 13:28	1315
914.545	20-Dec-2018 14:14	1315
911.715	20-Dec-2018 15:11	1311
921.352	02-Jan-2019 10:41	2088
918.524	02-Jan-2019 11:38	2094
921.312	02-Jan-2019 12:32	2081
918.660	02-Jan-2019 13:12	2055
918.178	02-Jan-2019 13:53	2061
918.275	02-Jan-2019 15:22	2047
915.086	02-Jan-2019 16:10	2054
914.549	02-Jan-2019 16:42	2040
914.556	03-Jan-2019 08:52	1973
911.808	03-Jan-2019 09:23	1955
915.033	03-Jan-2019 12:38	1935
915.045	03-Jan-2019 12:58	1922

river km	date	water discharge at Lobith [m^3/s]
911.719	03-Jan-2019 13:36	1928
911.684	04-Jan-2019 08:56	1866
911.619	04-Jan-2019 12:47	1865
911.633	04-Jan-2019 12:57	1865
914.856	04-Jan-2019 13:25	1877
914.871	04-Jan-2019 13:44	1840
914.884	04-Jan-2019 14:04	1840
914.901	04-Jan-2019 14:24	1852
918.396	05-Jan-2019 08:28	1830
918.421	05-Jan-2019 08:59	1825
918.438	05-Jan-2019 11:08	1849
918.455	05-Jan-2019 11:20	1849
914.949	05-Jan-2019 13:28	1849
915.088	05-Jan-2019 13:45	1824
921.354	15-Jan-2019 09:35	2563
918.523	15-Jan-2019 12:09	2591
918.262	15-Jan-2019 13:09	2597
918.272	15-Jan-2019 13:36	2597
915.041	15-Jan-2019 17:24	2665
911.736	16-Jan-2019 07:45	2915
911.747	16-Jan-2019 08:18	2915
914.554	16-Jan-2019 08:59	2929
914.553	28-Jan-2019 08:53	1844
923.004	28-Jan-2019 09:38	1850
923.020	28-Jan-2019 09:48	1850
922.006	28-Jan-2019 10:14	1850
921.347	28-Jan-2019 10:45	1850
921.371	28-Jan-2019 10:46	1850
920.721	28-Jan-2019 11:14	1844
920.737	28-Jan-2019 11:15	1857
918.520	28-Jan-2019 11:49	1839
918.263	28-Jan-2019 12:23	1844
917.694	28-Jan-2019 13:04	1857
915.733	28-Jan-2019 13:47	1844
915.033	28-Jan-2019 14:20	1875
915.051	28-Jan-2019 14:39	1832
914.548	28-Jan-2019 14:51	1857
913.084	28-Jan-2019 15:29	1844
913.096	28-Jan-2019 15:48	1844
912.347	28-Jan-2019 16:13	1857
911.709	28-Jan-2019 16:51	1857
911.745	28-Jan-2019 16:56	1851
921.312	29-Jan-2019 08:20	1935
921.310	29-Jan-2019 08:28	1897

river km	date	water discharge at Lobith [m^3/s]
920.721	29-Jan-2019 08:57	1935
920.733	29-Jan-2019 08:59	1935
918.655	29-Jan-2019 09:30	1935
918.327	29-Jan-2019 09:58	1935
918.154	29-Jan-2019 10:02	1935
917.678	29-Jan-2019 11:08	1936
915.827	29-Jan-2019 11:40	1943
915.086	29-Jan-2019 12:05	1956
914.625	29-Jan-2019 12:24	1963
914.555	29-Jan-2019 12:27	1980
913.222	29-Jan-2019 13:04	1950
912.552	29-Jan-2019 13:29	1963
912.385	29-Jan-2019 13:31	1963
911.971	29-Jan-2019 14:02	1975
911.810	29-Jan-2019 14:09	1975
911.053	29-Jan-2019 15:07	1970
911.064	29-Jan-2019 15:12	1970
910.161	29-Jan-2019 15:49	1984
921.349	12-Feb-2019 08:29	2638
921.359	12-Feb-2019 08:39	2651
918.524	12-Feb-2019 10:07	2659
918.261	12-Feb-2019 11:14	2713
918.272	12-Feb-2019 11:41	2720
915.037	12-Feb-2019 14:08	2795
914.549	12-Feb-2019 14:45	2816
914.566	12-Feb-2019 14:57	2823
911.730	12-Feb-2019 15:48	2844
911.743	12-Feb-2019 16:14	2851
921.361	26-Feb-2019 08:06	1690
918.266	26-Feb-2019 11:21	1714
918.524	26-Feb-2019 12:24	1744
915.035	27-Feb-2019 07:33	1687
914.538	27-Feb-2019 08:16	1664
914.549	27-Feb-2019 08:48	1676
911.743	27-Feb-2019 09:24	1676
914.864	27-Feb-2019 10:23	1682
914.874	27-Feb-2019 10:47	1694
915.017	27-Feb-2019 13:14	1687
915.038	27-Feb-2019 14:00	1658
909.940	13-Mar-2019 07:14	2506
911.041	13-Mar-2019 07:57	2519
911.736	13-Mar-2019 08:45	2545
912.351	13-Mar-2019 09:30	2545
913.097	13-Mar-2019 10:20	2546

river km	date	water discharge at Lobith [m^3/s]
911.743	13-Mar-2019 11:22	2572
912.372	13-Mar-2019 11:49	2585
912.382	13-Mar-2019 11:52	2585
913.220	13-Mar-2019 12:15	2579
914.554	13-Mar-2019 12:41	2592
914.554	13-Mar-2019 13:12	2572
915.033	13-Mar-2019 13:50	2612
915.044	13-Mar-2019 13:52	2612
915.729	13-Mar-2019 15:00	2612
915.744	13-Mar-2019 15:10	2612
915.760	13-Mar-2019 15:22	2606
915.070	13-Mar-2019 15:43	2613
915.828	13-Mar-2019 16:10	2606
917.678	13-Mar-2019 16:45	2626
917.690	14-Mar-2019 07:26	2770
918.265	14-Mar-2019 08:04	2756
918.156	14-Mar-2019 08:41	2770
918.522	14-Mar-2019 09:21	2784
918.653	14-Mar-2019 10:00	2791
920.723	14-Mar-2019 10:38	2812
921.310	14-Mar-2019 11:22	2805
920.725	14-Mar-2019 12:05	2819
921.354	14-Mar-2019 12:47	2833
922.962	14-Mar-2019 13:56	2847
922.973	14-Mar-2019 14:07	2854
921.997	14-Mar-2019 14:33	2854
922.966	18-Mar-2019 12:58	4808
922.080	18-Mar-2019 13:53	4819
921.307	18-Mar-2019 14:56	4851
920.727	18-Mar-2019 15:56	4862
917.695	18-Mar-2019 17:49	4916
918.263	19-Mar-2019 06:59	5170
915.869	19-Mar-2019 08:04	5170
915.881	19-Mar-2019 08:31	5181
918.604	19-Mar-2019 08:38	5181
920.725	19-Mar-2019 09:10	5171
920.736	19-Mar-2019 09:12	5171
915.096	19-Mar-2019 09:27	5192
921.322	19-Mar-2019 09:34	5192
914.574	19-Mar-2019 11:12	5182
914.588	19-Mar-2019 12:02	5193
913.092	19-Mar-2019 12:28	5182
912.350	19-Mar-2019 13:23	5204
911.783	19-Mar-2019 14:54	5193

river km	date	water discharge at Lobith [m^3/s]
910.998	19-Mar-2019 16:14	5182
911.010	19-Mar-2019 16:22	5205
910.009	19-Mar-2019 17:31	5205
914.862	20-Mar-2019 08:20	5116
914.872	20-Mar-2019 10:09	5116
911.667	20-Mar-2019 12:45	5061
918.394	21-Mar-2019 10:07	4666
918.413	21-Mar-2019 10:23	4676
918.423	21-Mar-2019 11:55	4635
918.440	21-Mar-2019 11:59	4635
918.452	21-Mar-2019 13:06	4604
921.347	25-Mar-2019 10:04	2825
921.357	25-Mar-2019 10:12	2803
921.311	25-Mar-2019 10:48	2811
918.658	25-Mar-2019 11:42	2797
918.525	25-Mar-2019 12:14	2797
918.263	25-Mar-2019 12:46	2797
918.164	25-Mar-2019 13:35	2762
915.084	25-Mar-2019 14:19	2762
915.033	25-Mar-2019 14:45	2762
914.544	25-Mar-2019 15:24	2776
914.554	26-Mar-2019 07:30	2626
911.745	26-Mar-2019 08:01	2619
911.737	26-Mar-2019 08:53	2613
911.678	26-Mar-2019 13:54	2586
918.415	27-Mar-2019 06:19	2453
918.426	27-Mar-2019 07:31	2433
918.444	27-Mar-2019 08:24	2447
915.016	27-Mar-2019 09:54	2433
915.033	27-Mar-2019 10:25	2427
921.346	08-Apr-2019 07:59	1781
918.857	08-Apr-2019 08:48	1781
918.522	08-Apr-2019 10:52	1793
918.868	08-Apr-2019 11:21	1805
918.262	08-Apr-2019 11:38	1799
918.883	08-Apr-2019 13:08	1806
915.035	08-Apr-2019 13:40	1799
920.462	08-Apr-2019 13:41	1799
914.547	08-Apr-2019 14:28	1811
911.734	08-Apr-2019 16:23	1806
916.651	09-Apr-2019 07:23	1789
916.684	09-Apr-2019 09:20	1807
916.733	09-Apr-2019 10:16	1819
916.912	09-Apr-2019 11:59	1807

river km	date	water discharge at Lobith [m^3/s]
917.083	09-Apr-2019 12:41	1801
917.943	09-Apr-2019 13:09	1801
913.060	10-Apr-2019 06:30	1807
913.096	10-Apr-2019 07:20	1782
913.536	10-Apr-2019 11:09	1782
921.349	23-Apr-2019 07:53	1342
921.359	23-Apr-2019 07:55	1332
918.521	23-Apr-2019 09:49	1337
918.262	23-Apr-2019 10:25	1337
915.027	23-Apr-2019 13:19	1348
914.547	23-Apr-2019 15:16	1347
911.735	23-Apr-2019 16:07	1342
914.937	24-Apr-2019 14:25	1329
915.004	24-Apr-2019 14:33	1329
915.021	24-Apr-2019 14:53	1324
918.344	24-Apr-2019 15:55	1324
921.353	06-May-2019 06:55	1499
918.523	06-May-2019 09:16	1499
918.262	06-May-2019 10:35	1487
915.028	06-May-2019 12:57	1487
914.546	06-May-2019 13:43	1481
911.727	06-May-2019 14:50	1481
914.782	07-May-2019 11:24	1485
911.739	20-May-2019 13:55	1763
914.541	20-May-2019 14:41	1775
915.033	20-May-2019 16:51	1780
918.265	20-May-2019 17:31	1763
918.524	20-May-2019 18:14	1768
921.351	20-May-2019 18:55	1757
921.352	04-Jun-2019 07:56	2177
921.323	04-Jun-2019 08:47	2171
918.750	04-Jun-2019 09:30	2164
915.074	04-Jun-2019 10:17	2177
911.737	04-Jun-2019 10:56	2185
918.524	04-Jun-2019 12:49	2164
918.262	04-Jun-2019 13:29	2170
918.155	04-Jun-2019 14:10	2164
915.032	04-Jun-2019 14:52	2164
914.545	04-Jun-2019 15:36	2170
914.555	06-Jun-2019 06:54	1993
911.744	06-Jun-2019 07:30	1980
921.351	20-Jun-2019 06:44	2387
918.525	20-Jun-2019 08:43	2401
918.263	20-Jun-2019 09:29	2409

river km	date	water discharge at Lobith [m^3/s]
915.028	20-Jun-2019 11:25	2402
914.544	20-Jun-2019 12:20	2417
911.736	20-Jun-2019 14:08	2417
916.777	04-Jul-2019 09:34	1882
918.418	04-Jul-2019 14:24	1876
918.434	04-Jul-2019 14:36	1869
918.843	05-Jul-2019 07:07	1844
918.857	05-Jul-2019 07:44	1850
918.877	05-Jul-2019 09:38	1880
918.404	05-Jul-2019 10:37	1856
921.347	08-Jul-2019 13:33	1777
921.323	08-Jul-2019 14:33	1771
918.751	08-Jul-2019 15:12	1771
918.526	08-Jul-2019 16:01	1784
918.263	09-Jul-2019 05:56	1744
918.158	09-Jul-2019 07:44	1756
915.147	09-Jul-2019 08:42	1744
915.029	09-Jul-2019 09:02	1756
914.544	09-Jul-2019 09:47	1750
911.733	09-Jul-2019 11:26	1762
914.553	09-Jul-2019 12:25	1738
911.743	09-Jul-2019 13:09	1732
921.348	15-Jul-2019 08:31	1724
918.524	15-Jul-2019 10:33	1718
918.261	15-Jul-2019 11:15	1718
915.031	15-Jul-2019 14:37	1718
914.544	15-Jul-2019 15:15	1718
911.735	15-Jul-2019 16:03	1718
921.347	29-Jul-2019 10:56	1235
918.523	29-Jul-2019 11:45	1226
918.263	29-Jul-2019 12:29	1211
915.028	29-Jul-2019 14:50	1220
914.542	29-Jul-2019 15:39	1230
911.732	29-Jul-2019 16:23	1216
921.320	31-Jul-2019 10:48	1347
918.823	31-Jul-2019 11:17	1338
918.157	31-Jul-2019 11:51	1352
915.026	31-Jul-2019 12:45	1356
921.347	12-Aug-2019 08:16	1519
918.522	12-Aug-2019 09:06	1525
918.262	12-Aug-2019 09:49	1519
915.029	12-Aug-2019 10:47	1536
914.543	12-Aug-2019 11:30	1536
911.731	12-Aug-2019 12:32	1531

river km	date	water discharge at Lobith [m^3/s]
915.159	13-Aug-2019 10:01	1501
918.154	13-Aug-2019 10:29	1506
919.004	13-Aug-2019 11:01	1522
921.324	13-Aug-2019 11:35	1506
921.348	28-Aug-2019 08:47	1791
921.323	29-Aug-2019 07:50	1708
918.750	29-Aug-2019 08:36	1720
918.523	29-Aug-2019 09:15	1708
918.263	29-Aug-2019 09:57	1713
918.155	29-Aug-2019 10:34	1713
915.148	29-Aug-2019 11:47	1695
915.029	29-Aug-2019 12:26	1700
914.552	29-Aug-2019 13:14	1689
914.547	29-Aug-2019 13:43	1695
911.736	29-Aug-2019 14:32	1683
911.743	29-Aug-2019 15:32	1695
921.348	10-Sep-2019 13:06	1256
918.523	10-Sep-2019 13:52	1246
918.262	10-Sep-2019 14:26	1246
915.028	10-Sep-2019 15:27	1251
914.548	10-Sep-2019 16:24	1242
911.737	10-Sep-2019 17:15	1242
921.323	23-Sep-2019 11:57	1084
920.726	23-Sep-2019 12:18	1075
918.499	23-Sep-2019 12:46	1084
918.246	23-Sep-2019 13:12	1075
917.682	23-Sep-2019 13:28	1084
915.825	23-Sep-2019 13:51	1079
915.160	23-Sep-2019 14:15	1079
923.005	24-Sep-2019 07:44	1067
921.995	24-Sep-2019 08:29	1072
921.346	24-Sep-2019 09:11	1076
920.729	24-Sep-2019 09:57	1062
918.521	24-Sep-2019 10:57	1080
918.263	24-Sep-2019 11:38	1076
917.709	24-Sep-2019 12:26	1076
915.733	24-Sep-2019 13:17	1080
915.029	24-Sep-2019 14:03	1085
914.543	24-Sep-2019 15:30	1075
913.095	24-Sep-2019 16:07	1062
912.349	24-Sep-2019 16:52	1080
911.737	24-Sep-2019 17:37	1061
913.400	25-Sep-2019 07:24	1063
911.046	25-Sep-2019 08:08	1063

river km	date	water discharge at Lobith [m^3/s]
909.940	25-Sep-2019 08:53	1058
911.624	25-Sep-2019 09:43	1073
911.638	25-Sep-2019 10:11	1063
918.400	26-Sep-2019 07:43	1054
918.414	26-Sep-2019 07:53	1054
918.454	26-Sep-2019 09:06	1059
914.864	26-Sep-2019 13:00	1086
914.875	26-Sep-2019 13:51	1080
915.007	26-Sep-2019 15:34	1094
921.347	07-Oct-2019 10:15	1201
918.522	07-Oct-2019 11:21	1224
918.266	07-Oct-2019 12:09	1219
911.738	07-Oct-2019 14:10	1237
915.032	08-Oct-2019 07:31	1267
914.545	08-Oct-2019 08:22	1271
915.158	08-Oct-2019 14:31	1270
918.157	08-Oct-2019 15:00	1280
918.498	08-Oct-2019 15:38	1275
921.324	08-Oct-2019 16:07	1279
921.351	23-Oct-2019 08:28	2078
918.524	23-Oct-2019 09:27	2072
918.263	23-Oct-2019 10:25	2099
915.030	23-Oct-2019 11:20	2107
914.545	23-Oct-2019 11:59	2121
911.735	23-Oct-2019 12:57	2115
921.324	24-Oct-2019 08:33	2075
918.598	24-Oct-2019 09:21	2062
918.158	24-Oct-2019 10:13	2068
915.160	24-Oct-2019 11:06	2061
914.637	24-Oct-2019 11:36	2067
911.741	24-Oct-2019 12:20	2048
921.347	04-Nov-2019 08:06	1591
918.525	04-Nov-2019 08:58	1586
918.262	04-Nov-2019 09:32	1592
915.029	04-Nov-2019 10:32	1610
914.544	04-Nov-2019 11:16	1655
911.740	04-Nov-2019 13:40	1634
921.323	05-Nov-2019 07:37	1717
918.598	05-Nov-2019 08:41	1712
918.157	05-Nov-2019 09:09	1718
915.160	05-Nov-2019 10:02	1725
914.638	05-Nov-2019 10:27	1731
911.732	05-Nov-2019 11:11	1748
921.348	21-Nov-2019 08:09	1853

river km	date	water discharge at Lobith [m^3/s]
918.522	21-Nov-2019 10:37	1859
918.263	21-Nov-2019 11:16	1859
915.029	21-Nov-2019 13:12	1846
914.543	21-Nov-2019 14:12	1853
911.732	21-Nov-2019 15:53	1829
921.343	09-Dec-2019 09:37	1847
918.521	09-Dec-2019 10:35	1852
918.263	09-Dec-2019 11:46	1859
915.030	09-Dec-2019 13:38	1884
914.543	09-Dec-2019 14:27	1866
911.734	09-Dec-2019 16:43	1879
918.404	18-Dec-2019 08:43	3548
922.984	18-Dec-2019 08:55	3557
922.124	18-Dec-2019 09:50	3573
921.300	18-Dec-2019 10:45	3582
918.426	18-Dec-2019 11:20	3574
920.726	18-Dec-2019 11:29	3582
921.314	18-Dec-2019 12:06	3565
918.440	18-Dec-2019 12:15	3582
920.676	18-Dec-2019 12:46	3582
918.595	18-Dec-2019 14:04	3574
918.456	18-Dec-2019 14:14	3591
918.545	18-Dec-2019 14:32	3591
918.263	18-Dec-2019 15:18	3599
917.683	18-Dec-2019 15:56	3599
918.155	18-Dec-2019 16:33	3599
917.682	18-Dec-2019 17:02	3591
915.824	18-Dec-2019 17:35	3591
915.075	19-Dec-2019 08:32	3549
914.929	19-Dec-2019 08:46	3558
914.940	19-Dec-2019 08:53	3558
915.867	19-Dec-2019 08:56	3566
915.090	19-Dec-2019 09:36	3549
914.571	19-Dec-2019 10:17	3533
913.096	19-Dec-2019 11:15	3549
914.957	19-Dec-2019 11:53	3558
914.555	19-Dec-2019 12:00	3549
914.969	19-Dec-2019 12:07	3541
915.012	19-Dec-2019 12:42	3549
913.127	19-Dec-2019 12:46	3549
912.381	19-Dec-2019 14:06	3541
911.628	19-Dec-2019 14:12	3541
911.732	19-Dec-2019 14:32	3524
910.971	19-Dec-2019 15:02	3524

river km	date	water discharge at Lobith [m^3/s]
909.864	19-Dec-2019 15:52	3516
911.665	19-Dec-2019 15:58	3507
911.774	19-Dec-2019 16:49	3507
912.351	19-Dec-2019 17:34	3516
921.347	16-Jan-2020 07:48	1945
918.156	28-Jan-2020 13:09	1368
918.812	28-Jan-2020 14:00	1362
921.323	29-Jan-2020 08:59	1376
914.772	29-Jan-2020 09:11	1386
914.786	29-Jan-2020 09:40	1391
915.161	29-Jan-2020 09:57	1402
921.348	30-Jan-2020 08:08	1536
918.523	30-Jan-2020 08:52	1537
918.264	30-Jan-2020 09:33	1549
915.029	30-Jan-2020 10:23	1560
914.544	30-Jan-2020 10:58	1589
911.734	30-Jan-2020 12:49	1619
918.419	05-Feb-2020 08:23	3536
911.623	05-Feb-2020 08:41	3537
918.435	05-Feb-2020 10:00	3579
911.668	05-Feb-2020 10:54	3629
914.991	05-Feb-2020 12:00	3647
915.002	05-Feb-2020 12:06	3664
911.682	05-Feb-2020 12:09	3664
918.407	06-Feb-2020 12:36	4929
914.856	06-Feb-2020 12:39	4929
918.418	06-Feb-2020 13:10	4961
914.868	06-Feb-2020 13:30	4983
918.434	06-Feb-2020 14:02	4995
911.597	06-Feb-2020 16:04	5126
914.964	06-Feb-2020 16:06	5127
911.627	06-Feb-2020 16:09	5127
914.977	06-Feb-2020 16:50	5161
911.642	06-Feb-2020 16:56	5172
911.666	06-Feb-2020 17:35	5205
921.297	14-Feb-2020 07:44	4156
921.311	14-Feb-2020 08:38	4165
918.546	14-Feb-2020 09:50	4175
918.262	14-Feb-2020 10:50	4156
915.090	14-Feb-2020 12:43	4156
914.575	14-Feb-2020 13:26	4175
911.769	14-Feb-2020 15:26	4156
922.983	19-Feb-2020 15:35	3777
922.124	19-Feb-2020 16:24	3786

river km	date	water discharge at Lobith [m^3/s]
921.299	20-Feb-2020 08:19	3741
920.725	20-Feb-2020 09:04	3767
920.725	20-Feb-2020 09:48	3750
918.594	20-Feb-2020 10:31	3759
918.540	20-Feb-2020 11:01	3750
918.264	20-Feb-2020 11:43	3759
918.158	20-Feb-2020 12:22	3732
917.682	20-Feb-2020 13:05	3759
917.683	20-Feb-2020 13:34	3724
915.822	20-Feb-2020 14:14	3741
915.069	20-Feb-2020 14:39	3741
915.869	20-Feb-2020 15:05	3759
915.087	20-Feb-2020 15:41	3732
914.573	20-Feb-2020 16:28	3732
914.555	21-Feb-2020 07:30	3776
913.127	21-Feb-2020 07:54	3768
912.384	21-Feb-2020 08:27	3776
911.733	21-Feb-2020 08:53	3776
909.867	21-Feb-2020 09:25	3794
910.970	21-Feb-2020 10:24	3785
911.775	21-Feb-2020 11:11	3785
912.351	21-Feb-2020 11:58	3803
913.096	21-Feb-2020 12:39	3803
911.733	24-Feb-2020 16:01	3714
911.774	24-Feb-2020 16:24	3732
921.301	25-Feb-2020 07:43	3732
921.313	25-Feb-2020 08:25	3741
918.544	25-Feb-2020 08:54	3732
918.261	25-Feb-2020 09:44	3741
918.593	25-Feb-2020 10:24	3758
918.155	25-Feb-2020 10:53	3741
915.069	25-Feb-2020 11:29	3741
915.092	25-Feb-2020 11:49	3758
914.571	25-Feb-2020 12:35	3732
914.554	25-Feb-2020 13:25	3750
909.860	03-Mar-2020 16:28	4770
910.968	04-Mar-2020 07:55	4898
911.773	04-Mar-2020 09:11	4909
912.350	04-Mar-2020 11:02	4963
913.095	04-Mar-2020 12:29	4952
914.574	04-Mar-2020 13:30	4931
911.733	04-Mar-2020 14:49	4942
912.384	04-Mar-2020 15:13	4963
913.127	04-Mar-2020 15:39	4963

river km	date	water discharge at Lobith [m^3/s]
914.493	04-Mar-2020 16:11	4953
915.090	04-Mar-2020 16:39	4953
915.875	04-Mar-2020 17:29	4974
917.683	05-Mar-2020 07:07	5040
918.263	05-Mar-2020 07:45	5029
920.725	05-Mar-2020 08:34	5029
921.299	05-Mar-2020 09:20	5050
922.126	05-Mar-2020 10:15	5018
922.959	05-Mar-2020 11:12	5040
921.313	05-Mar-2020 12:15	5050
920.728	05-Mar-2020 12:42	5040
918.594	05-Mar-2020 13:16	5029
918.542	05-Mar-2020 13:51	5029
918.206	05-Mar-2020 14:39	5029
917.763	05-Mar-2020 15:11	5029
915.825	05-Mar-2020 15:50	5040
915.069	05-Mar-2020 16:14	5029
921.303	12-Mar-2020 07:43	5340
921.314	12-Mar-2020 08:20	5363
918.592	12-Mar-2020 09:03	5352
918.546	12-Mar-2020 09:36	5363
918.202	12-Mar-2020 10:37	5363
918.207	12-Mar-2020 11:13	5363
915.068	12-Mar-2020 11:54	5386
915.091	13-Mar-2020 07:46	5628
914.575	13-Mar-2020 08:44	5663
914.492	13-Mar-2020 09:39	5675
911.736	13-Mar-2020 10:15	5663
911.771	13-Mar-2020 10:43	5675
918.435	02-Apr-2020 07:01	1879
911.678	02-Apr-2020 12:34	1897
915.014	03-Apr-2020 06:32	1851
923.002	06-Apr-2020 12:47	1725
921.995	06-Apr-2020 13:24	1719
921.347	06-Apr-2020 14:08	1719
920.725	06-Apr-2020 14:52	1719
918.520	06-Apr-2020 15:42	1718
915.030	07-Apr-2020 06:13	1670
918.262	07-Apr-2020 07:40	1687
917.682	07-Apr-2020 08:28	1693
915.869	07-Apr-2020 09:20	1698
914.544	07-Apr-2020 10:03	1686
921.323	07-Apr-2020 10:17	1686
920.727	07-Apr-2020 10:53	1675

river km	date	water discharge at Lobith [m^3/s]
913.094	07-Apr-2020 11:38	1681
918.598	07-Apr-2020 11:49	1675
912.350	07-Apr-2020 12:44	1681
918.156	07-Apr-2020 12:49	1698
917.681	07-Apr-2020 13:30	1692
911.733	07-Apr-2020 13:31	1692
915.824	07-Apr-2020 14:14	1686
911.044	07-Apr-2020 14:24	1686
915.160	07-Apr-2020 14:51	1680
909.938	07-Apr-2020 15:10	1663
914.641	08-Apr-2020 07:59	1630
913.126	08-Apr-2020 08:50	1637
912.380	08-Apr-2020 09:57	1630
911.734	08-Apr-2020 11:05	1630
911.678	22-Apr-2020 08:17	1256
911.769	22-Apr-2020 09:02	1256
911.734	22-Apr-2020 10:41	1256
914.638	22-Apr-2020 11:25	1265
909.945	22-Apr-2020 14:26	1256
912.380	22-Apr-2020 15:07	1261
911.042	22-Apr-2020 15:16	1260
911.058	22-Apr-2020 15:30	1260
913.126	22-Apr-2020 15:42	1241
915.159	22-Apr-2020 16:13	1241
911.733	23-Apr-2020 07:00	1237
912.350	23-Apr-2020 07:49	1247
914.859	23-Apr-2020 08:29	1232
913.093	23-Apr-2020 08:56	1256
914.882	23-Apr-2020 09:40	1247
914.543	23-Apr-2020 09:47	1232
913.400	23-Apr-2020 10:49	1232
914.951	23-Apr-2020 11:02	1242
914.962	23-Apr-2020 11:13	1247
915.005	23-Apr-2020 11:31	1237
915.016	23-Apr-2020 11:53	1247
915.821	23-Apr-2020 12:39	1237
915.029	23-Apr-2020 12:39	1237
917.682	23-Apr-2020 13:35	1247
915.863	23-Apr-2020 13:38	1247
918.154	23-Apr-2020 14:11	1237
917.681	23-Apr-2020 14:28	1242
918.594	23-Apr-2020 14:50	1242
918.261	23-Apr-2020 15:18	1247
918.523	24-Apr-2020 06:28	1224

river km	date	water discharge at Lobith [m^3/s]
920.725	24-Apr-2020 07:14	1234
921.349	24-Apr-2020 07:56	1224
921.996	24-Apr-2020 08:46	1224
922.999	24-Apr-2020 09:37	1234
918.405	24-Apr-2020 09:39	1234
918.426	24-Apr-2020 11:24	1239
918.445	24-Apr-2020 12:21	1248
920.724	24-Apr-2020 13:11	1239
921.321	24-Apr-2020 13:41	1224
914.636	04-May-2020 14:22	1477
911.733	04-May-2020 15:23	1499
921.321	05-May-2020 08:14	1483
918.810	05-May-2020 09:16	1477
918.155	05-May-2020 10:01	1477
915.159	05-May-2020 10:59	1466
921.349	08-May-2020 11:53	1484
918.519	08-May-2020 12:54	1479
918.262	08-May-2020 13:32	1495
915.027	08-May-2020 14:24	1495
914.543	08-May-2020 15:03	1495
911.729	08-May-2020 15:57	1501
921.349	18-May-2020 07:39	1625
921.313	18-May-2020 08:20	1613
918.585	18-May-2020 08:59	1625
918.523	18-May-2020 09:27	1625
918.263	18-May-2020 10:09	1625
918.156	18-May-2020 10:47	1619
915.068	18-May-2020 11:46	1619
915.029	18-May-2020 13:31	1619
914.544	18-May-2020 14:13	1619
911.736	18-May-2020 15:04	1619
914.554	19-May-2020 07:22	1594
911.730	19-May-2020 11:50	1582
921.347	03-Jun-2020 08:30	1144
918.521	03-Jun-2020 09:22	1144
918.262	03-Jun-2020 10:12	1139
915.027	03-Jun-2020 11:21	1163
914.544	03-Jun-2020 11:59	1164
911.735	03-Jun-2020 13:02	1177
921.349	16-Jun-2020 10:04	1672
921.312	16-Jun-2020 10:51	1684
918.586	16-Jun-2020 12:14	1685
918.522	16-Jun-2020 12:47	1668
918.262	16-Jun-2020 13:28	1674

river km	date	water discharge at Lobith [m^3/s]
918.157	16-Jun-2020 14:26	1686
915.069	16-Jun-2020 15:33	1692
915.029	17-Jun-2020 06:24	1694
914.544	17-Jun-2020 07:03	1688
914.639	17-Jun-2020 07:57	1688
911.732	17-Jun-2020 08:38	1676
911.735	17-Jun-2020 10:53	1694

Table D.12 Summary of all ADCP profiles along the Waal River.

D.2 Summary of ADCP profiles used in the analysis of conditions prior/post intervention.

condition	location	river km	date	water level at Tiel at 00:00 [cm]
1	1	916	17-11-2011	238
1	1	916	06-12-2018	234
2	1	912	01-02-2013	496
2	1	912	16-01-2019	494
2	2	912	01-02-2013	496
2	2	912	16-01-2019	494
2	3	912	01-02-2013	496
2	3	912	16-01-2019	494
2	4	913	01-02-2013	496
2	4	912	16-01-2019	494
2	5	915	01-02-2013	496
2	5	915	16-01-2019	494
2	6	915	01-02-2013	496
2	6	915	15-01-2019	464
2	7	916	01-02-2013	496
2	7	915	15-01-2019	464
2	8	918	01-02-2013	496
2	8	918	15-01-2019	464
2	9	919	01-02-2013	496
2	9	919	15-01-2019	464
2	10	921	01-02-2013	496
2	10	921	15-01-2019	464
2	11	922	01-02-2013	496
2	11	921	15-01-2019	464
2	12	922	01-02-2013	496
2	12	921	15-01-2019	464
2	13	922	01-02-2013	496

condition	location	river km	date	water level at Tiel at 00:00 [cm]
2	13	921	15-01-2019	464
3	1	912	02-02-2013	609
3	1	912	19-12-2019	618
3	2	912	02-02-2013	609
3	2	912	19-12-2019	618
3	3	912	02-02-2013	609
3	3	912	19-12-2019	618
3	4	913	02-02-2013	609
3	4	912	19-12-2019	618
3	5	915	02-02-2013	609
3	5	915	19-12-2019	618
3	6	915	02-02-2013	609
3	6	915	19-12-2019	618
3	7	916	02-02-2013	609
3	7	915	19-12-2019	618
3	8	918	02-02-2013	609
3	8	918	18-12-2019	590
3	9	919	02-02-2013	609
3	9	919	18-12-2019	590
3	10	921	02-02-2013	609
3	10	921	18-12-2019	590
3	11	922	02-02-2013	609
3	11	921	18-12-2019	590
3	12	922	02-02-2013	609
3	12	921	18-12-2019	590
3	13	922	02-02-2013	609
3	13	921	18-12-2019	590
4	1	912	04-02-2013	728
4	1	912	18-12-2017	747
4	2	912	04-02-2013	728
4	2	912	18-12-2017	747
4	3	912	04-02-2013	728
4	3	912	18-12-2017	747
4	4	913	04-02-2013	728
4	4	913	18-12-2017	747
4	5	915	04-02-2013	728
4	5	915	18-12-2017	747
4	6	915	04-02-2013	728
4	6	915	18-12-2017	747
4	7	916	04-02-2013	728
4	7	916	19-12-2017	750
4	8	918	04-02-2013	728
4	8	918	19-12-2017	750

condition	location	river km	date	water level at Tiel at 00:00 [cm]
4	9	919	04-02-2013	728
4	9	919	19-12-2017	750
4	10	921	04-02-2013	728
4	10	921	19-12-2017	750
4	11	922	04-02-2013	728
4	11	921	19-12-2017	750
4	12	922	04-02-2013	728
4	12	922	19-12-2017	750
4	13	922	04-02-2013	728
4	13	922	19-12-2017	750

Table D.13 ADCP profiles used in the analysis of conditions prior/post intervention.

D.3 Comparison of the flow pattern before and after intervention

D.3.1 Condition 1

D.3.1.1 Location 1

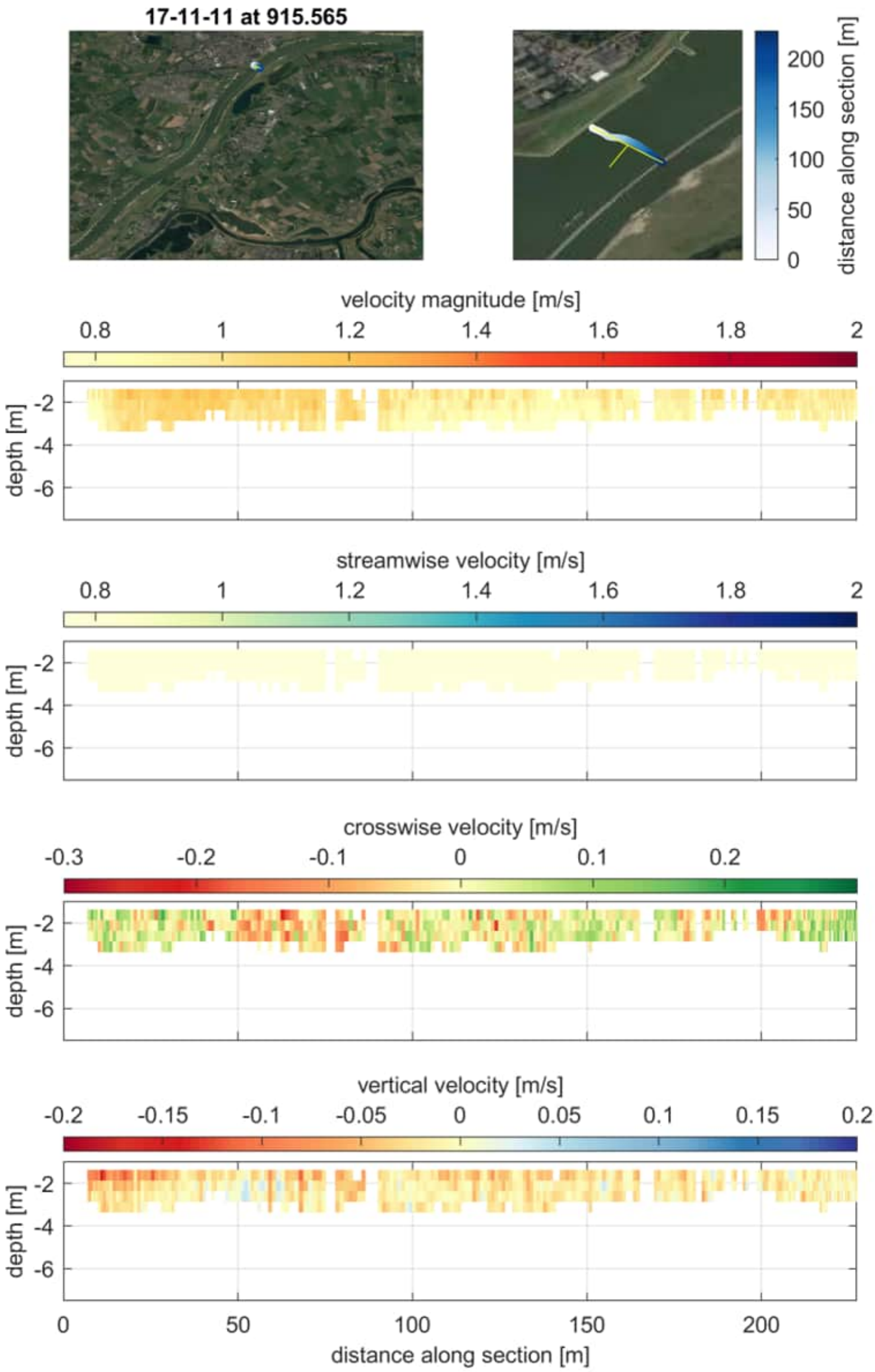

Figure D.1 Cross-sectional measurements on 17-11-11 (discharge at Lobith at 12:00 equal to 922 m^3/s) at rkm 915.565 projected on measurement plane.

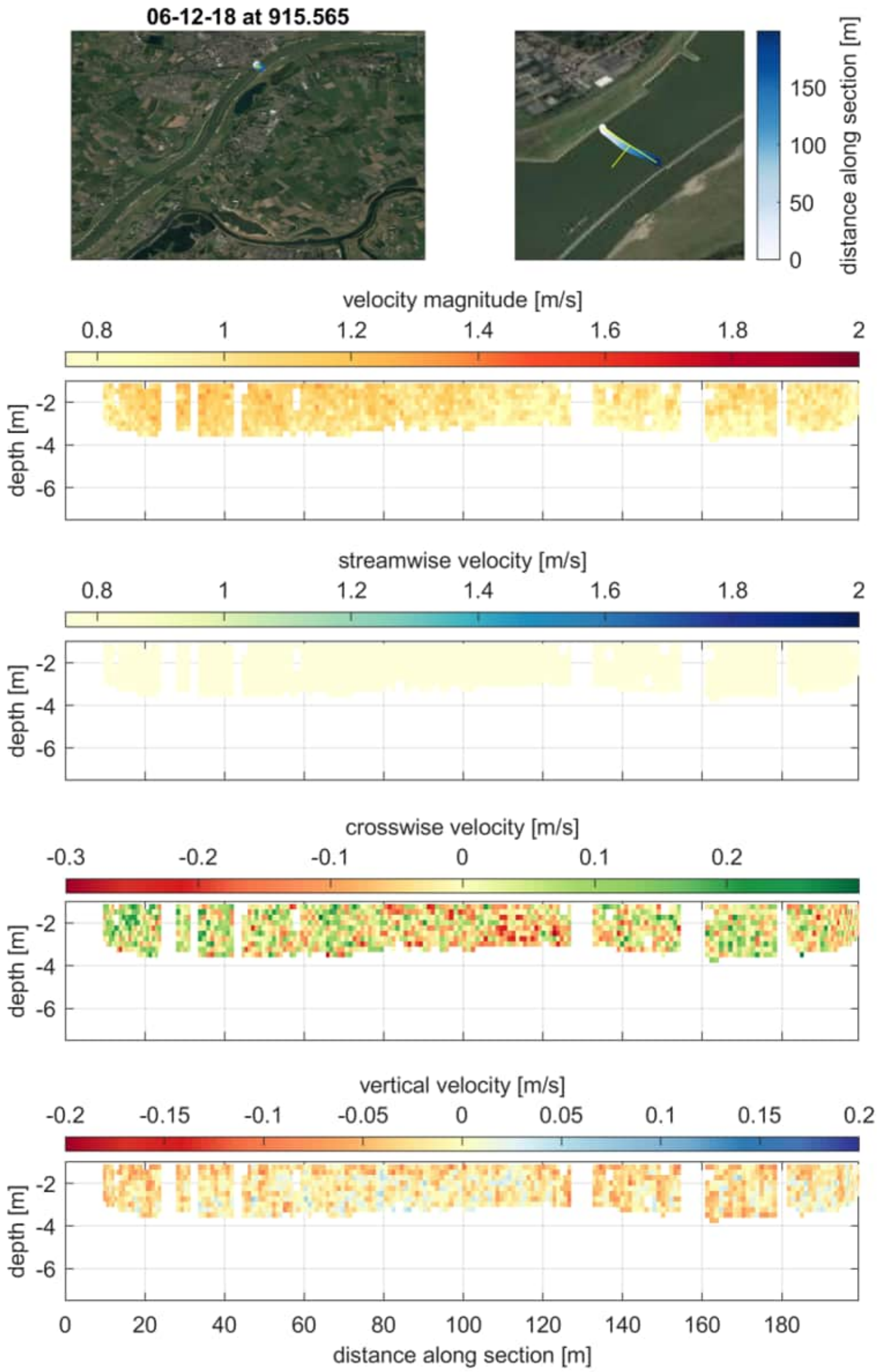

Figure D.2 Cross-sectional measurements on 06-12-18 (discharge at Lobith at 12:00 equal to 1341 m^3/s) at rkm 915.565 projected on measurement plane.

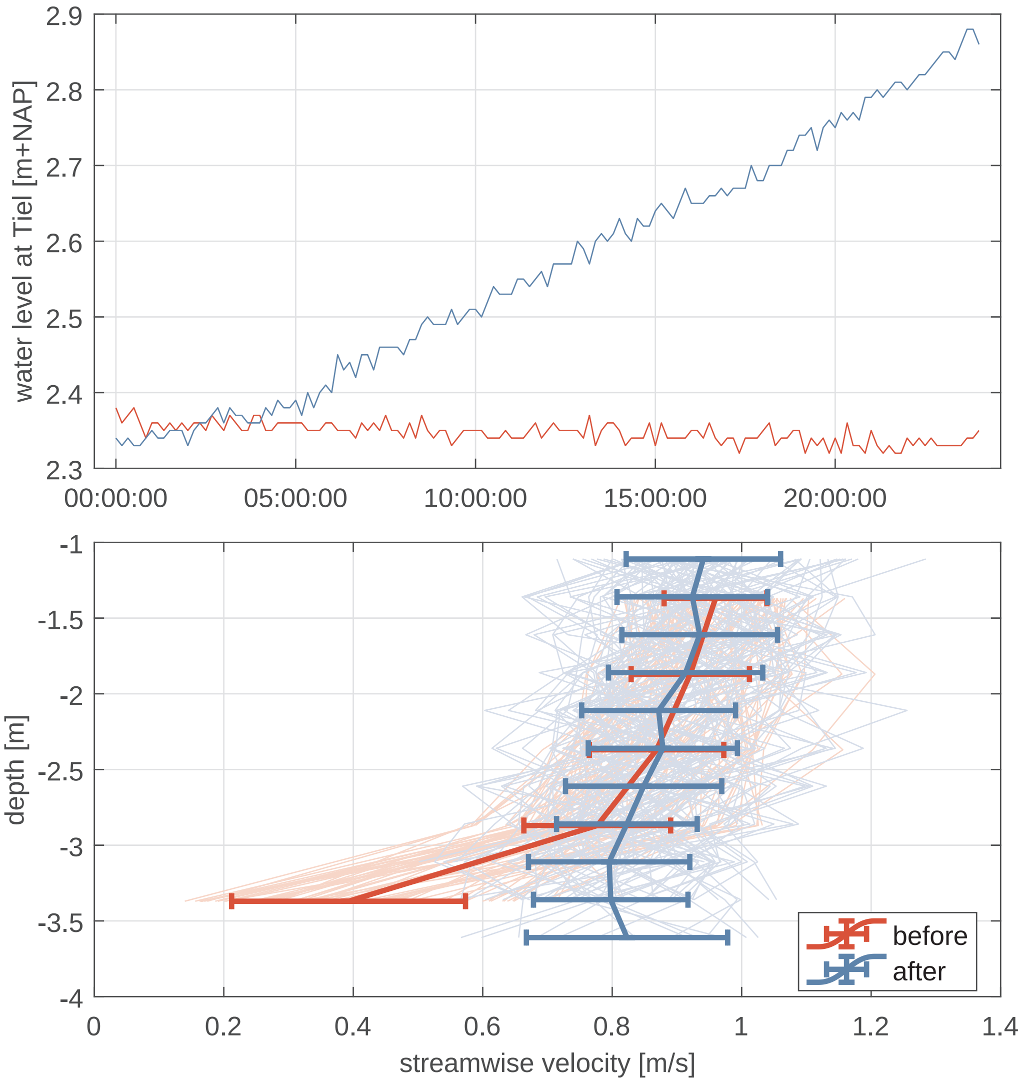

Figure D.3 Streamwise velocity at the central 100 m of channel before (17-11-11, discharge at Lobith at 12:00 equal to 922 m^3/s, rkm 915.565) and after (06-12-18, discharge at Lobith at 12:00 equal to 1341 m^3/s, rkm 915.565)

D.3.2 Condition 2

D.3.2.1 Location 1

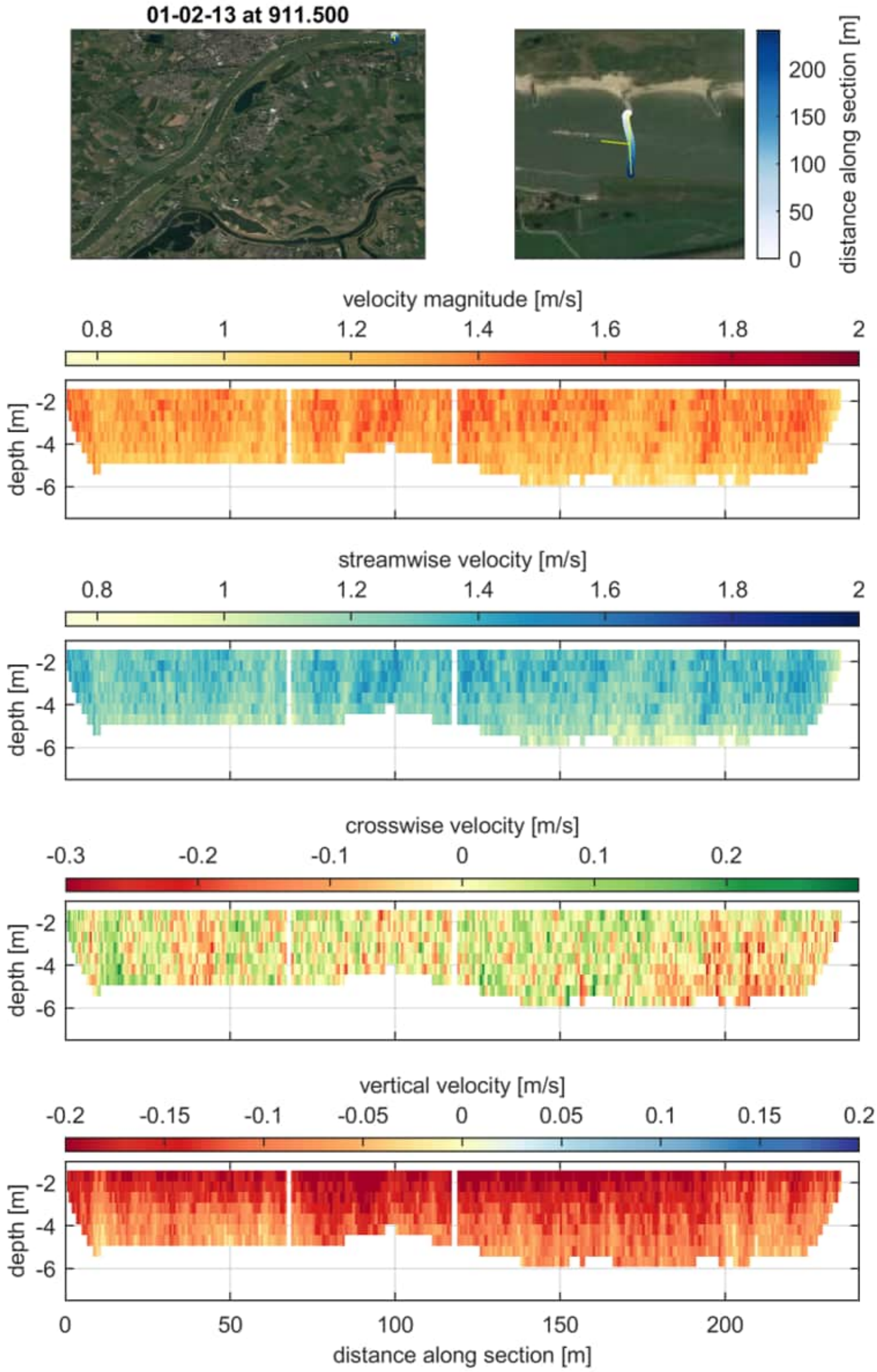

Figure D.4 Cross-sectional measurements on 01-02-13 (discharge at Lobith at 12:00 equal to 3436 m^3/s) at rkm 911.500 projected on measurement plane.

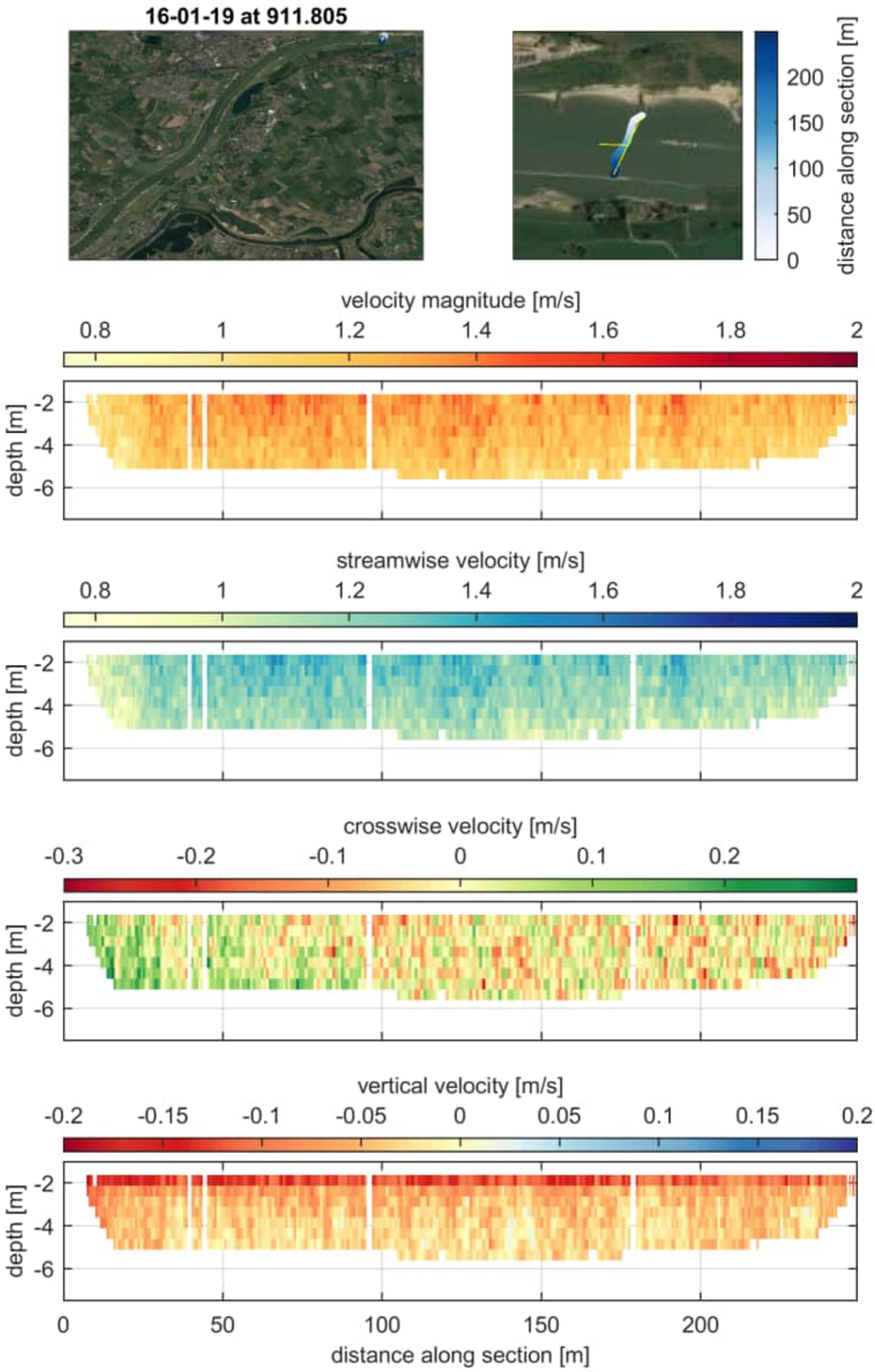

Figure D.5 Cross-sectional measurements on 16-01-19 (discharge at Lobith at 12:00 equal to 3022 m^3/s) at rkm 911.805 projected on measurement plane.

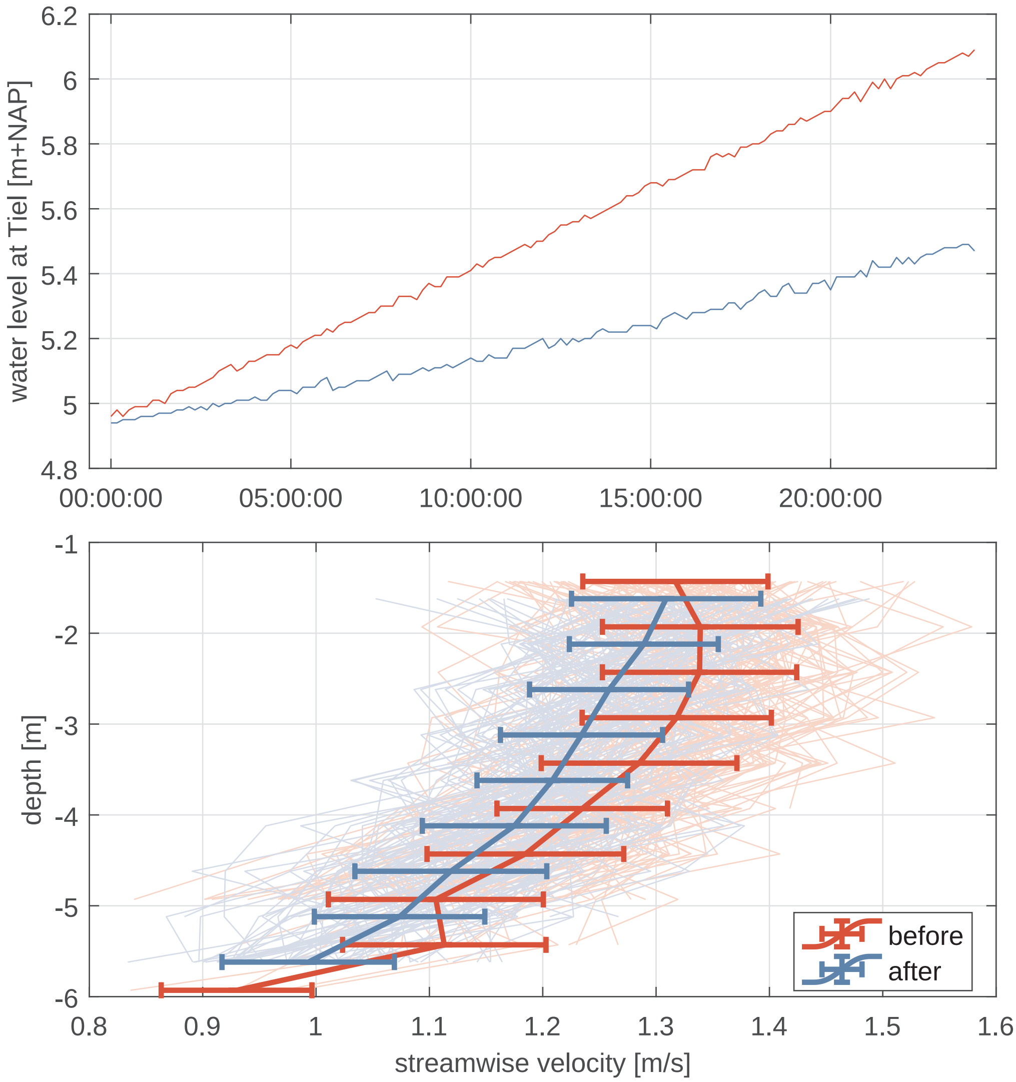

Figure D.6 Streamwise velocity at the central 100 m of channel before (01-02-13, discharge at Lobith at 12:00 equal to 3436 m^3/s, rkm 911.500) and after (16-01-19, discharge at Lobith at 12:00 equal to 3022 m^3/s, rkm 911.805)

D.3.2.2 Location 2

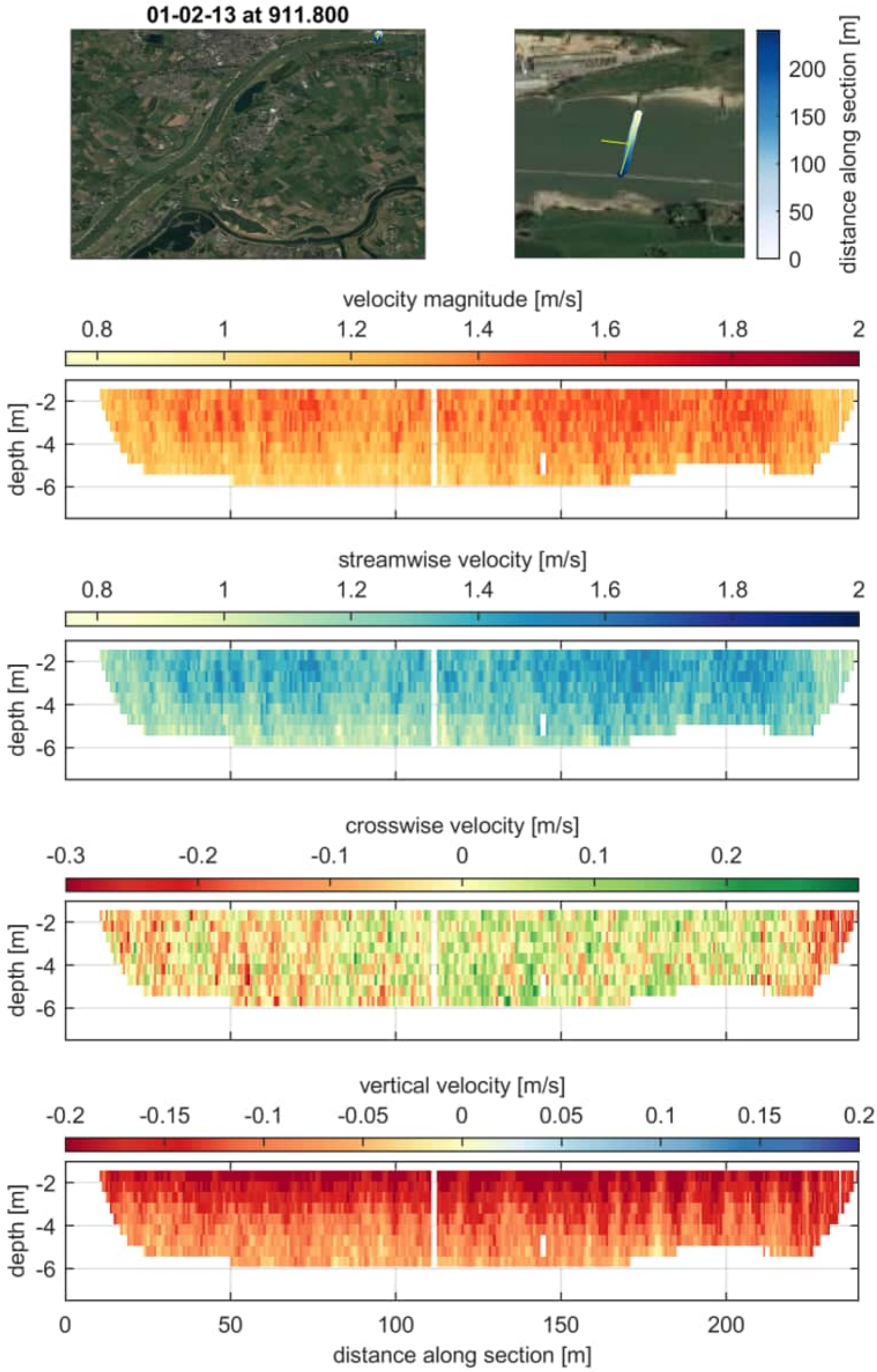

Figure D.7 Cross-sectional measurements on 01-02-13 (discharge at Lobith at 12:00 equal to 3436 m^3/s) at rkm 911.800 projected on measurement plane.

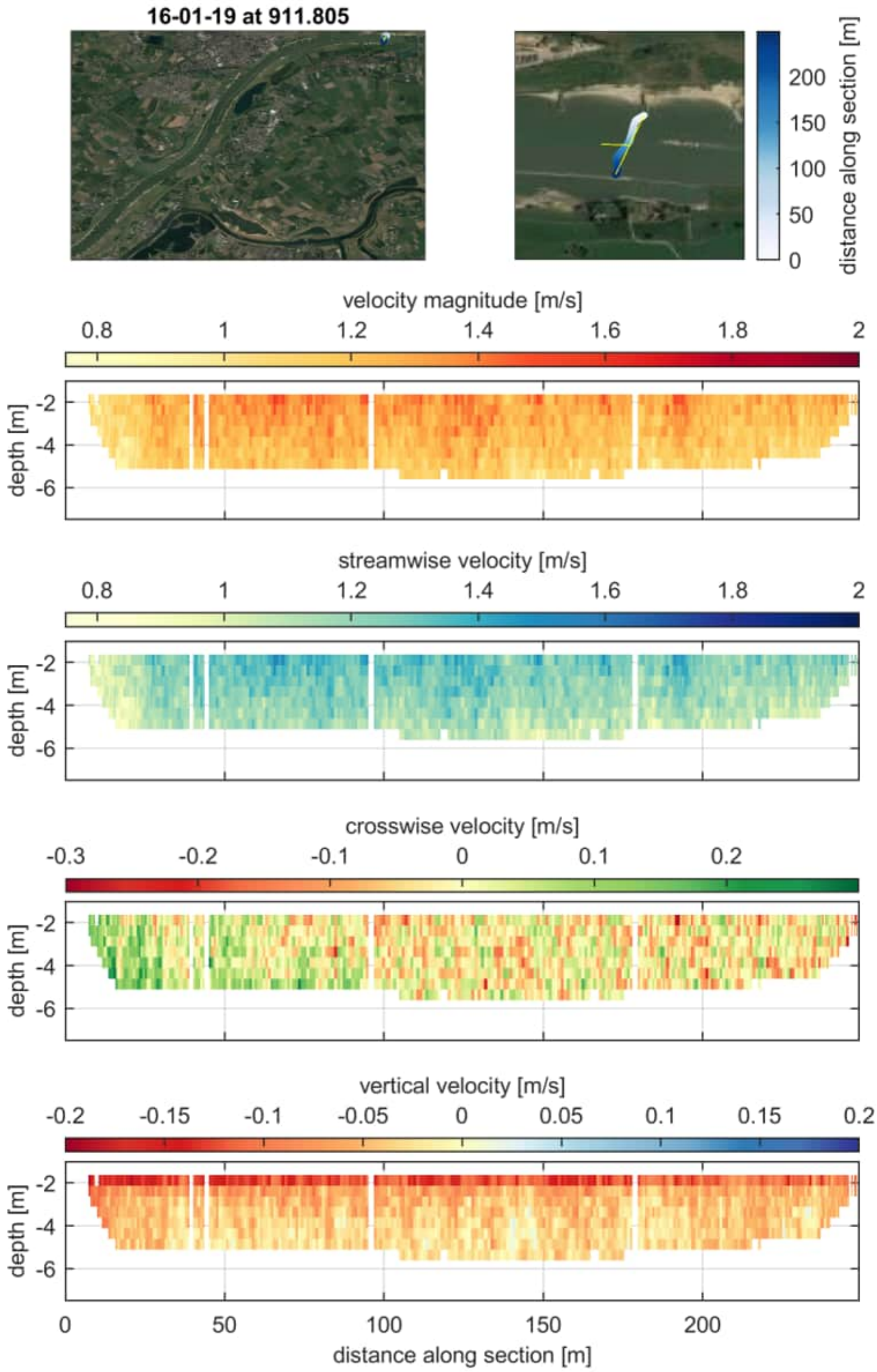

Figure D.8 Cross-sectional measurements on 16-01-19 (discharge at Lobith at 12:00 equal to 3022 m^3/s) at rkm 911.805 projected on measurement plane.

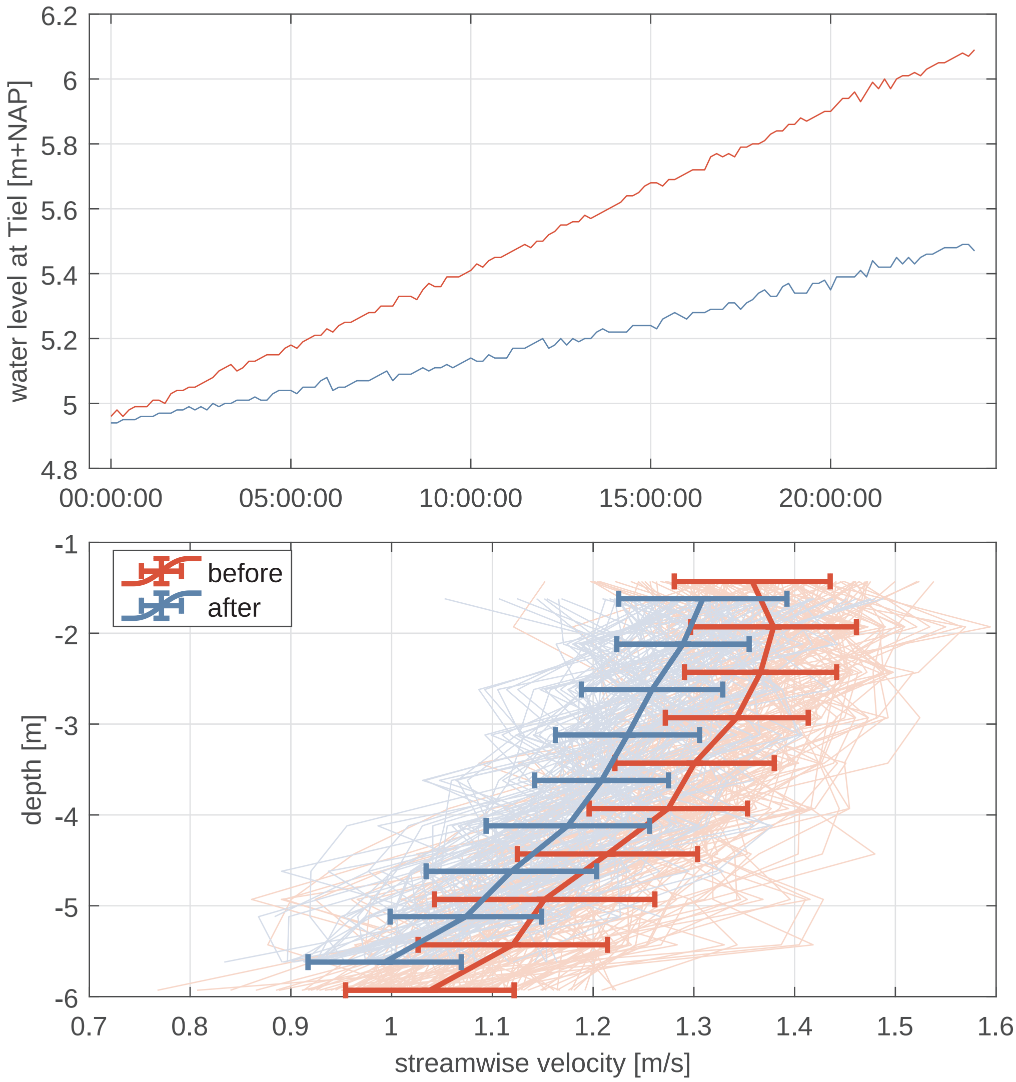

Figure D.9 Streamwise velocity at the central 100 m of channel before (01-02-13, discharge at Lobith at 12:00 equal to 3436 m^3/s, rkm 911.800) and after (16-01-19, discharge at Lobith at 12:00 equal to 3022 m^3/s, rkm 911.805)

D.3.2.3 Location 3

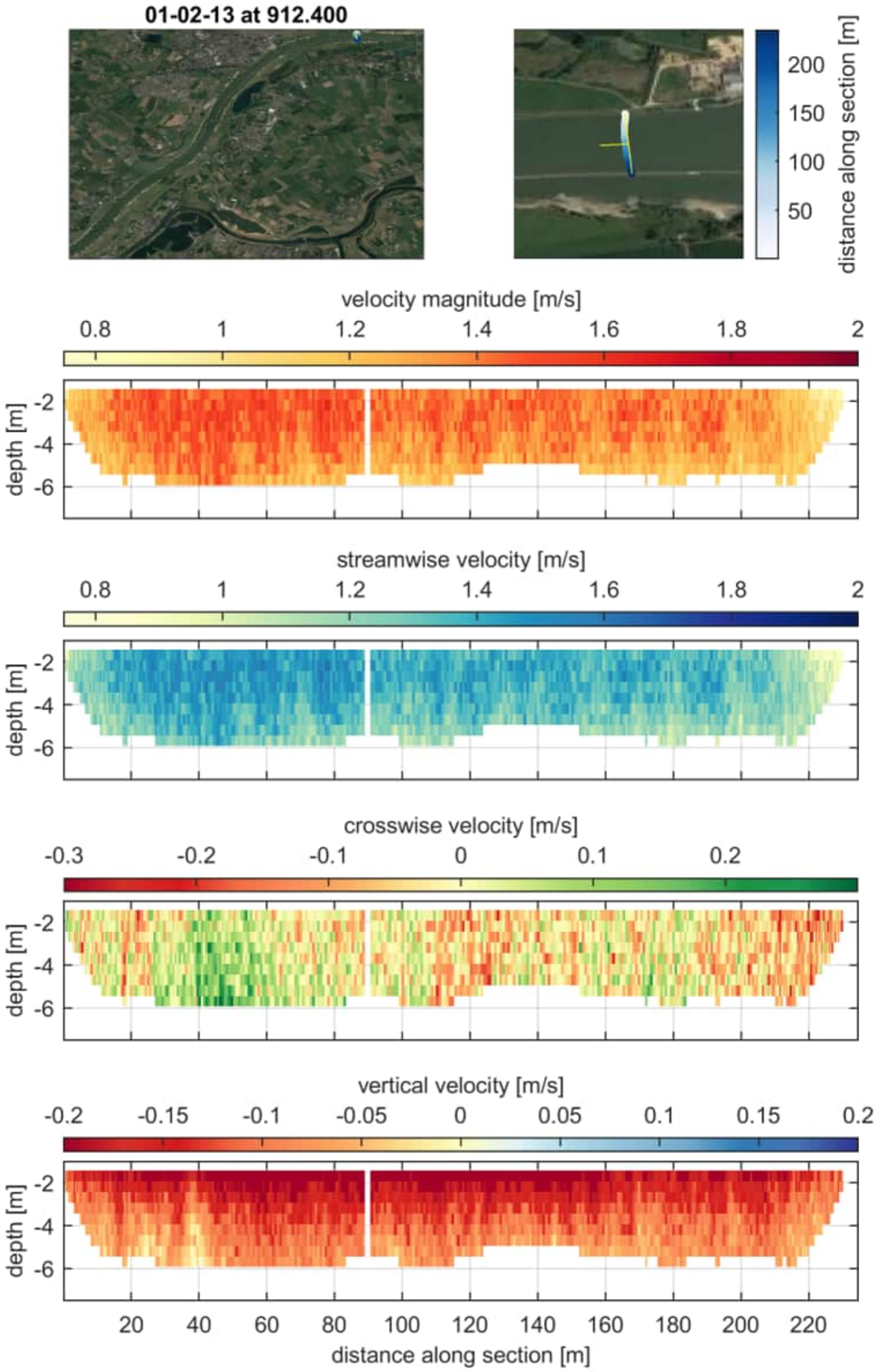

Figure D.10 Cross-sectional measurements on 01-02-13 (discharge at Lobith at 12:00 equal to 3436 m^3/s) at rkm 912.400 projected on measurement plane.

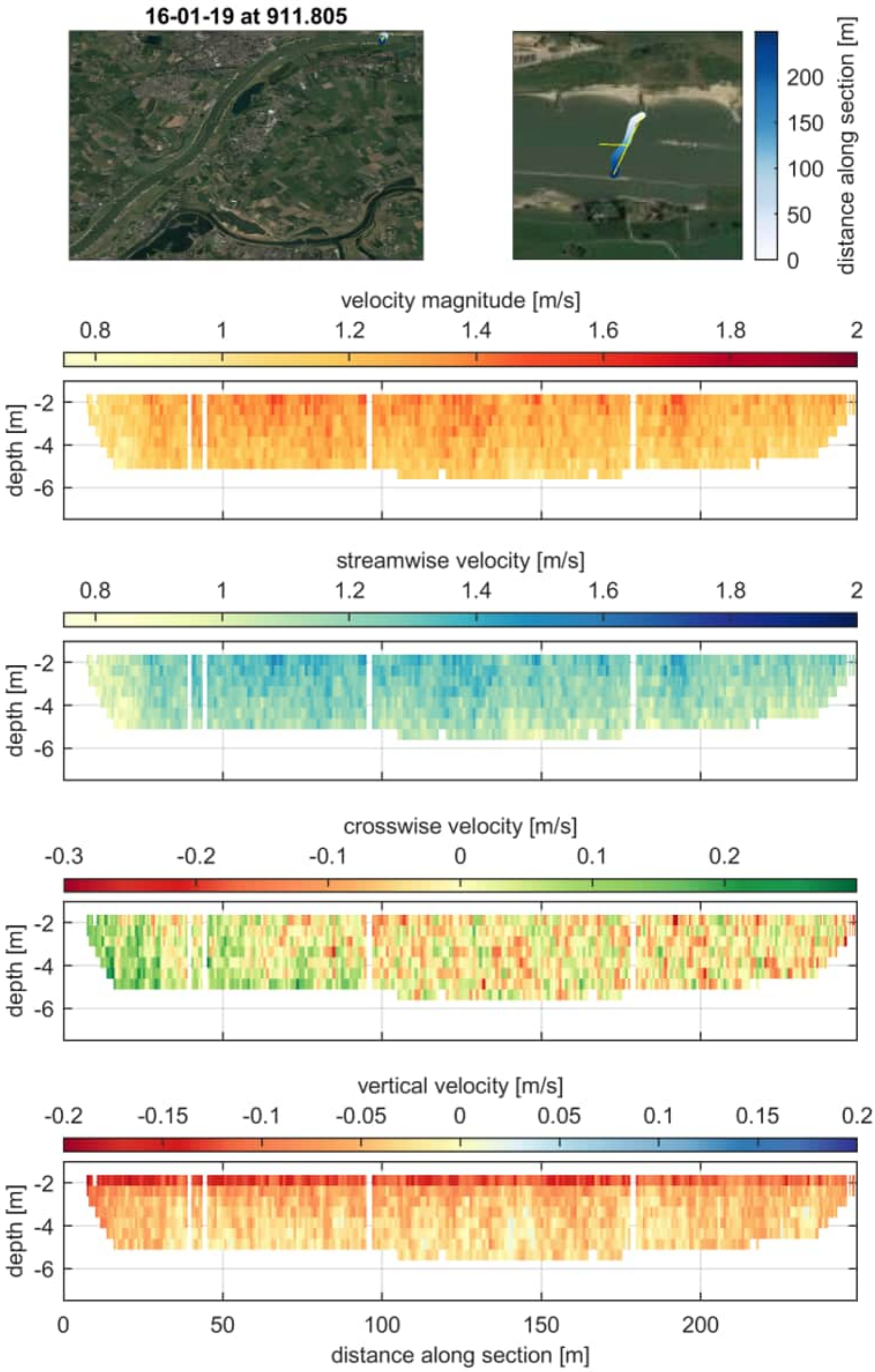

Figure D.11 Cross-sectional measurements on 16-01-19 (discharge at Lobith at 12:00 equal to 3022 m^3/s) at rkm 911.805 projected on measurement plane.

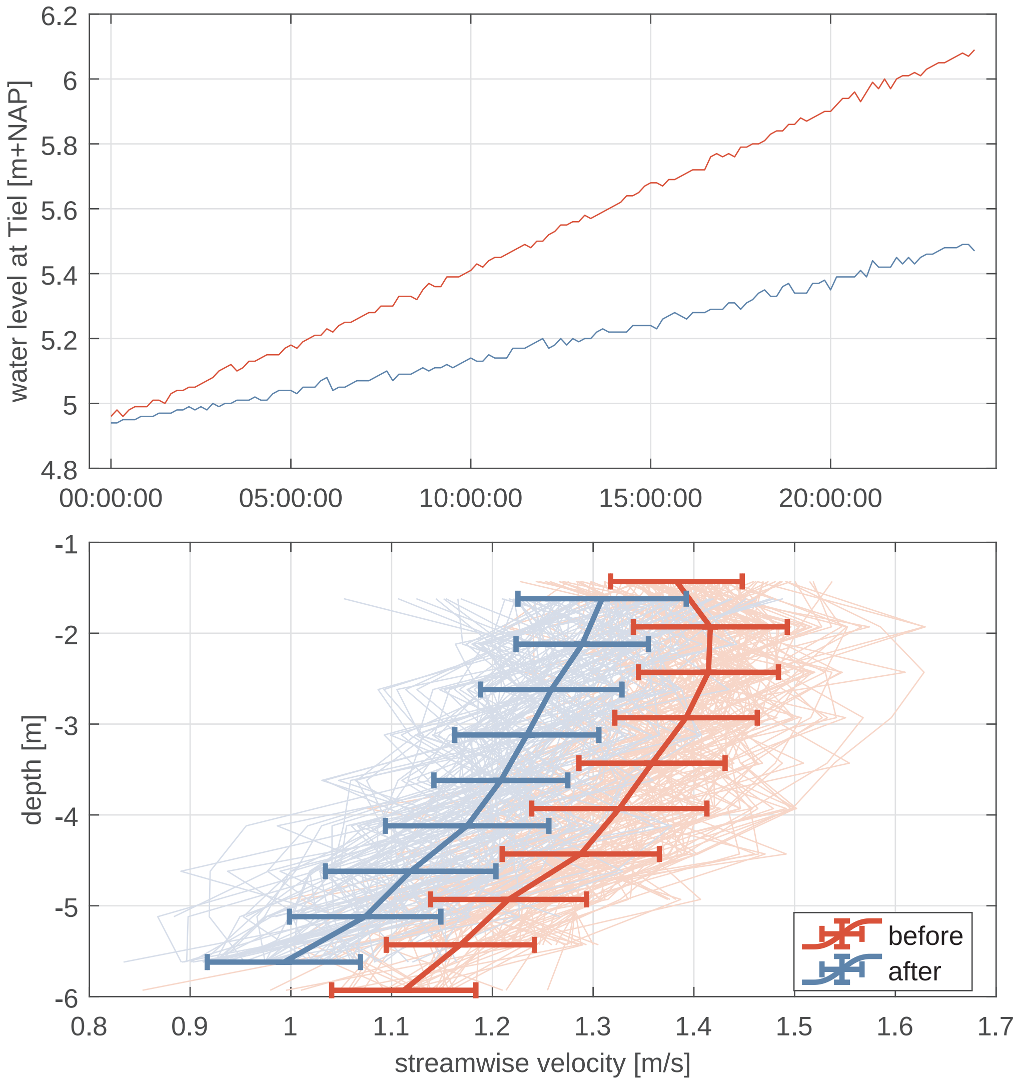

Figure D.12 Streamwise velocity at the central 100 m of channel before (01-02-13, discharge at Lobith at 12:00 equal to 3436 m^3/s, rkm 912.400) and after (16-01-19, discharge at Lobith at 12:00 equal to 3022 m^3/s, rkm 911.805)

D.3.2.4 Location 4

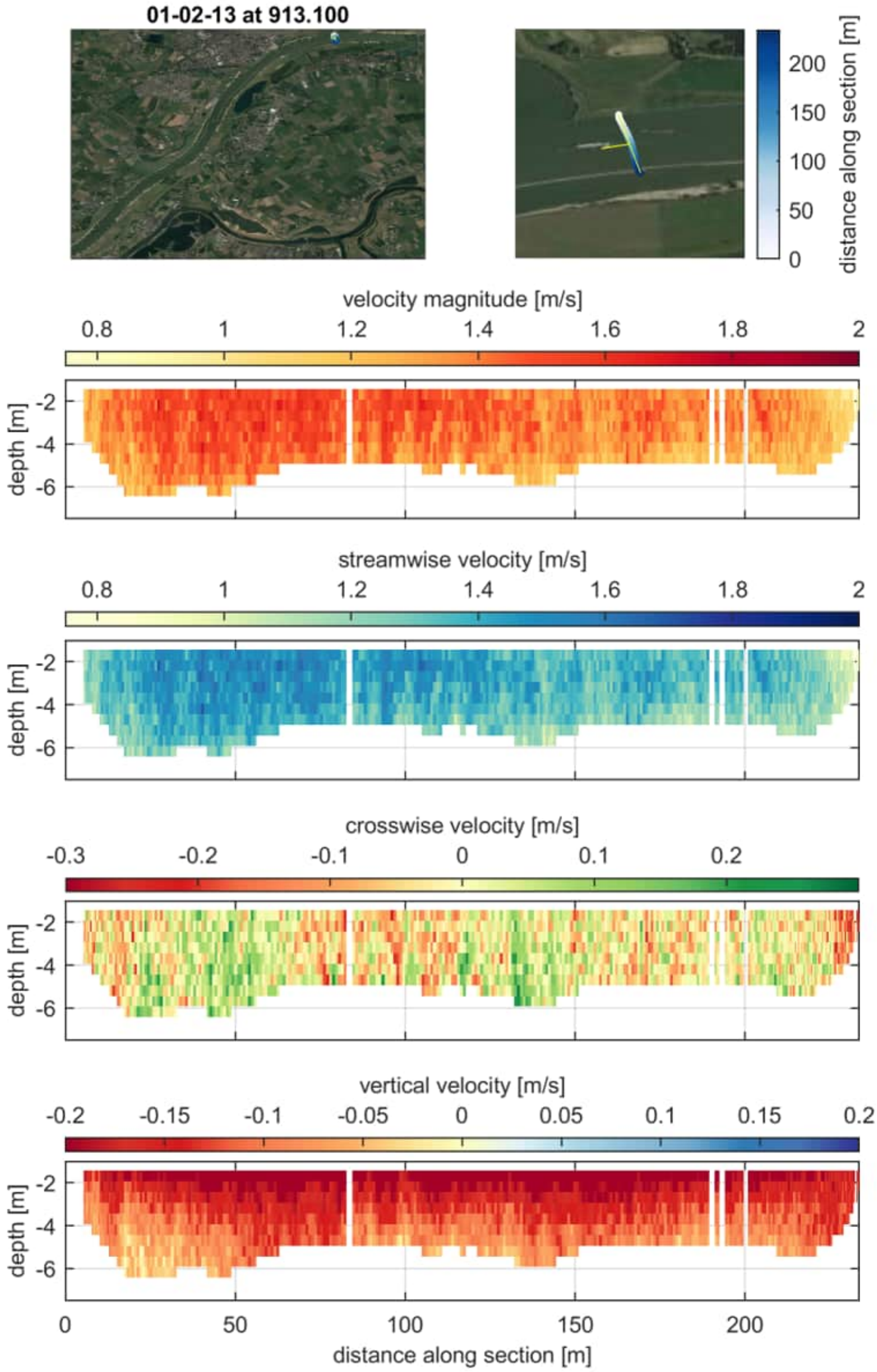

Figure D.13 Cross-sectional measurements on 01-02-13 (discharge at Lobith at 12:00 equal to 3436 m^3/s) at rkm 913.100 projected on measurement plane.

Deltares

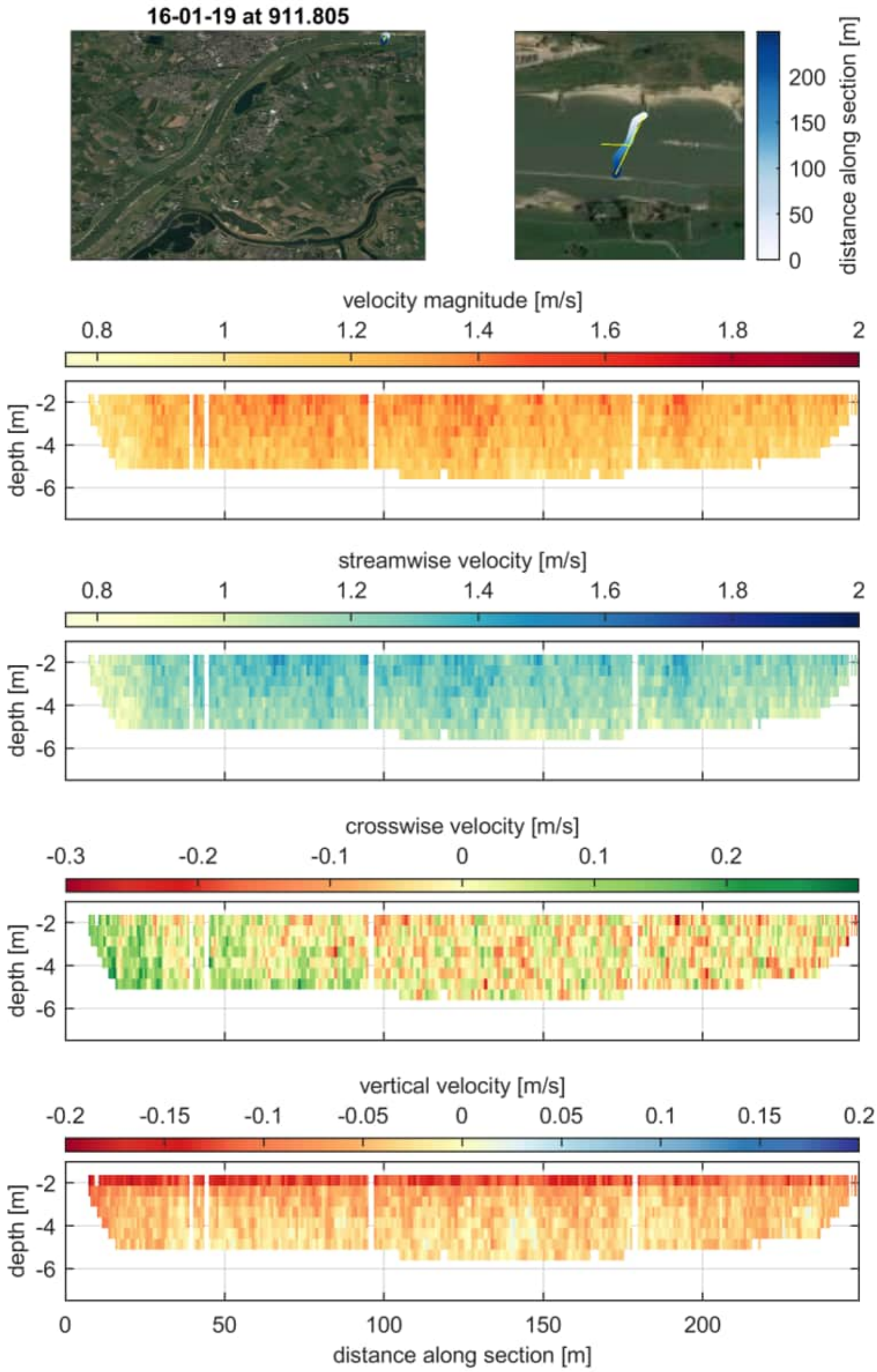

Figure D.14 Cross-sectional measurements on 16-01-19 (discharge at Lobith at 12:00 equal to 3022 m^3/s) at rkm 911.805 projected on measurement plane.

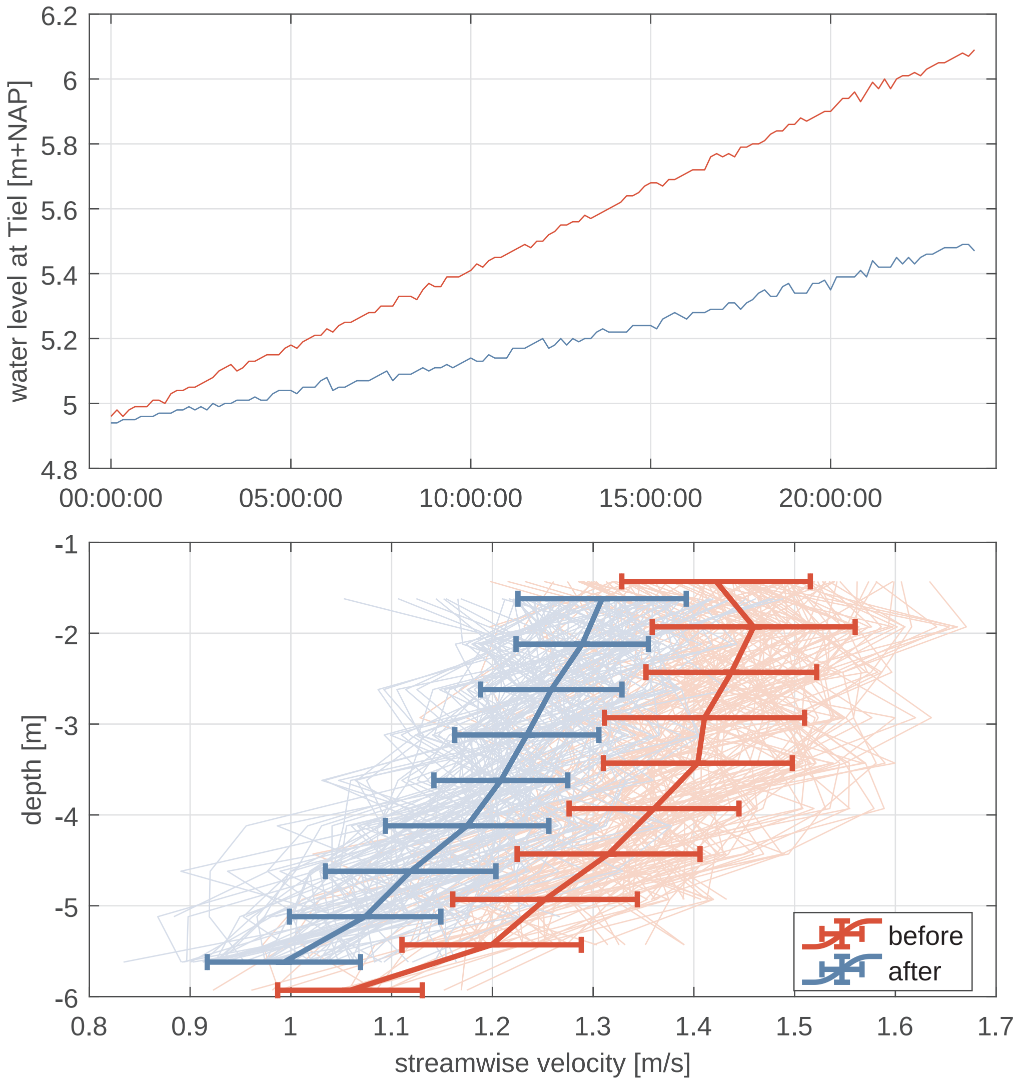

Figure D.15 Streamwise velocity at the central 100 m of channel before (01-02-13, discharge at Lobith at 12:00 equal to 3436 m^3/s, rkm 913.100) and after (16-01-19, discharge at Lobith at 12:00 equal to 3022 m^3/s, rkm 911.805)

D.3.2.5 Location 5

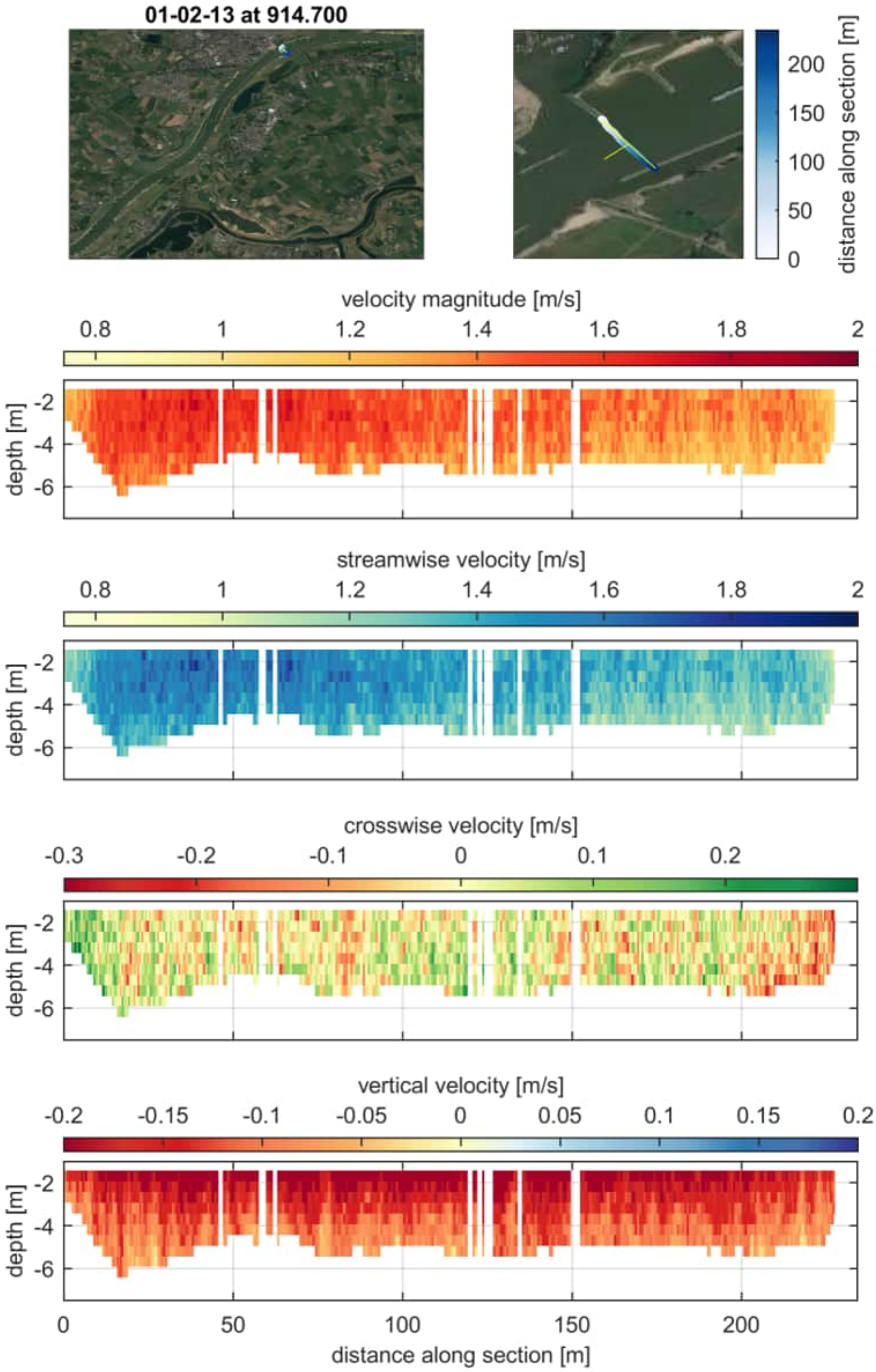

Figure D.16 Cross-sectional measurements on 01-02-13 (discharge at Lobith at 12:00 equal to 3436 m^3/s) at rkm 914.700 projected on measurement plane.

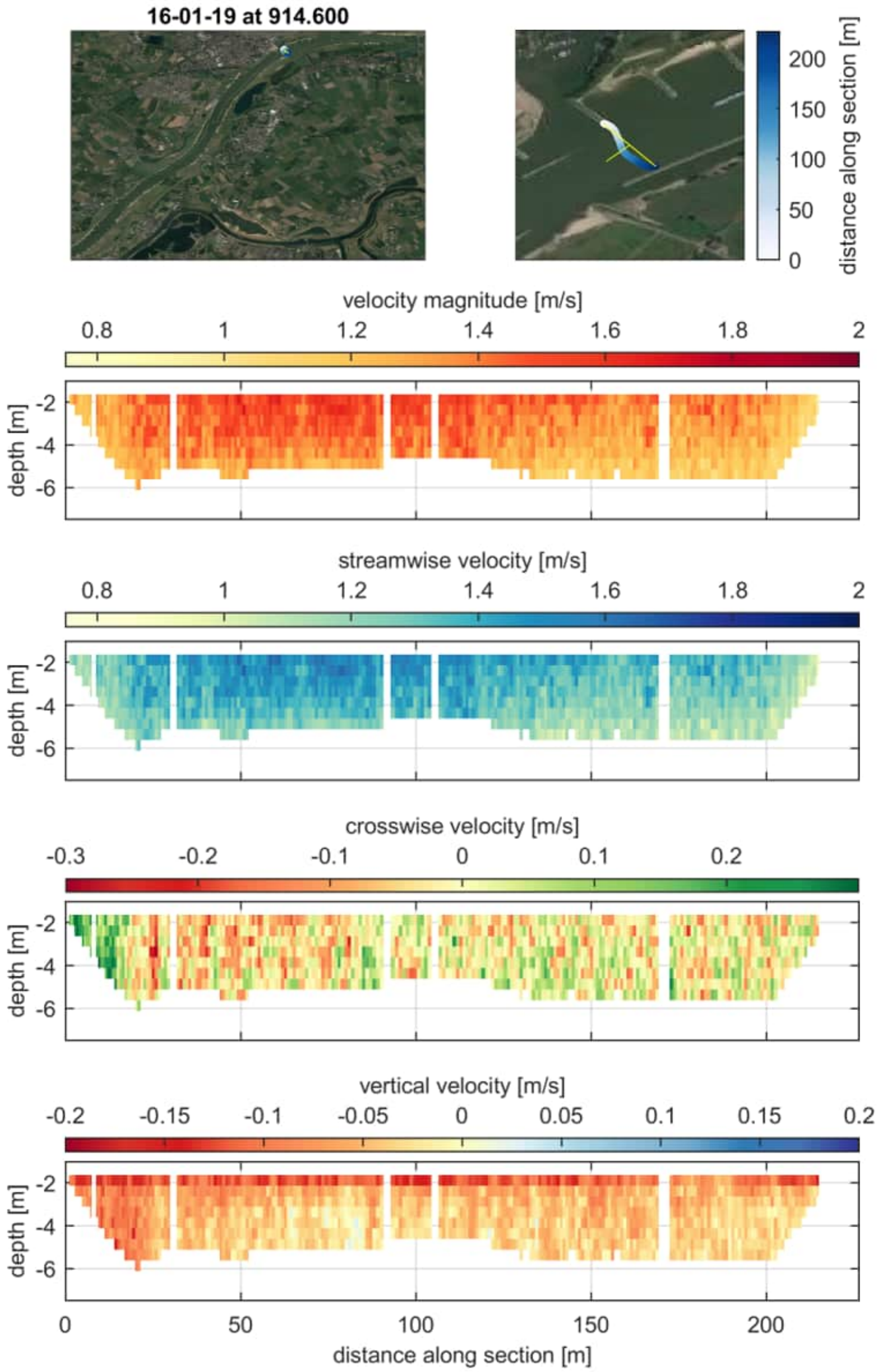

Figure D.17 Cross-sectional measurements on 16-01-19 (discharge at Lobith at 12:00 equal to 3022 m^3/s) at rkm 914.600 projected on measurement plane.

Deltares

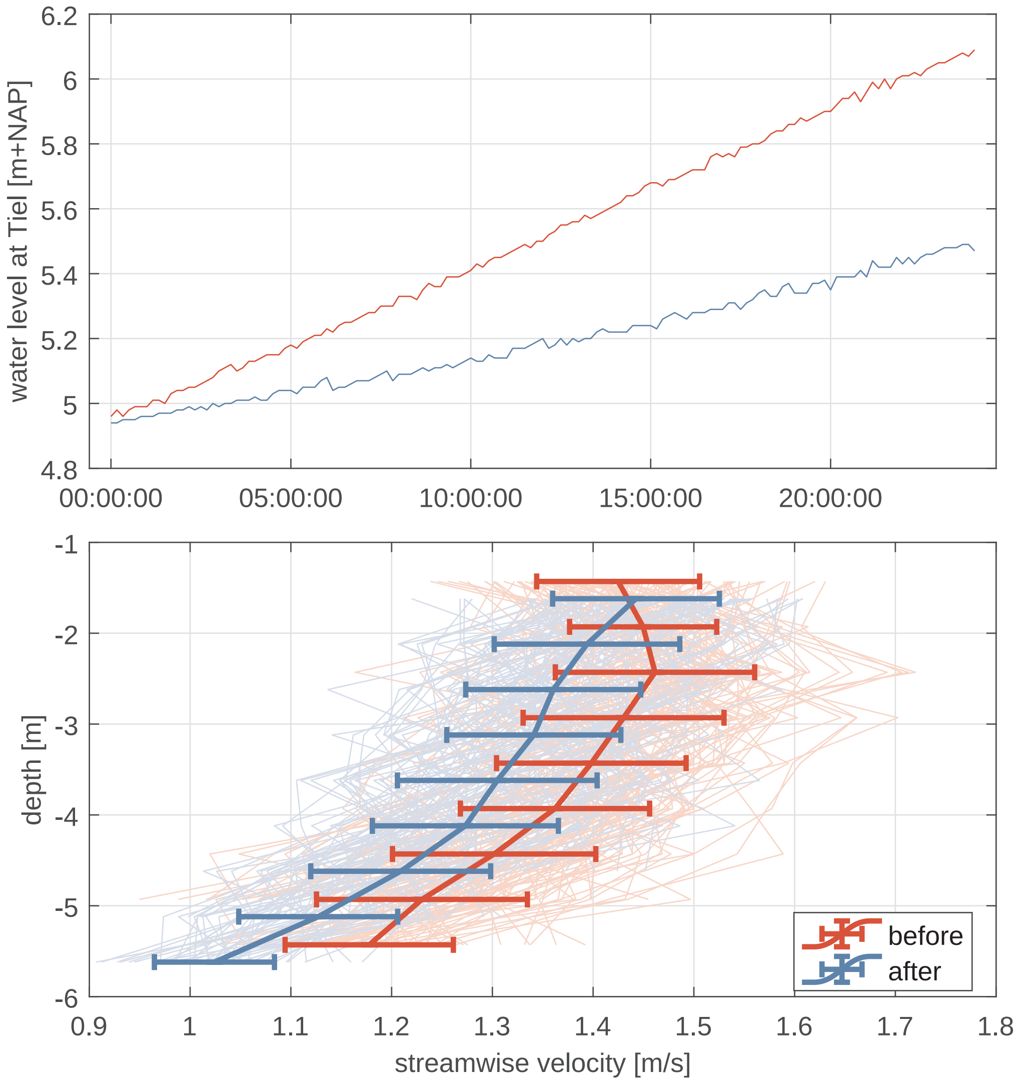

Figure D.18 Streamwise velocity at the central 100 m of channel before (01-02-13, discharge at Lobith at 12:00 equal to 3436 m^3/s, rkm 914.700) and after (16-01-19, discharge at Lobith at 12:00 equal to 3022 m^3/s, rkm 914.600)

D.3.2.6 Location 6

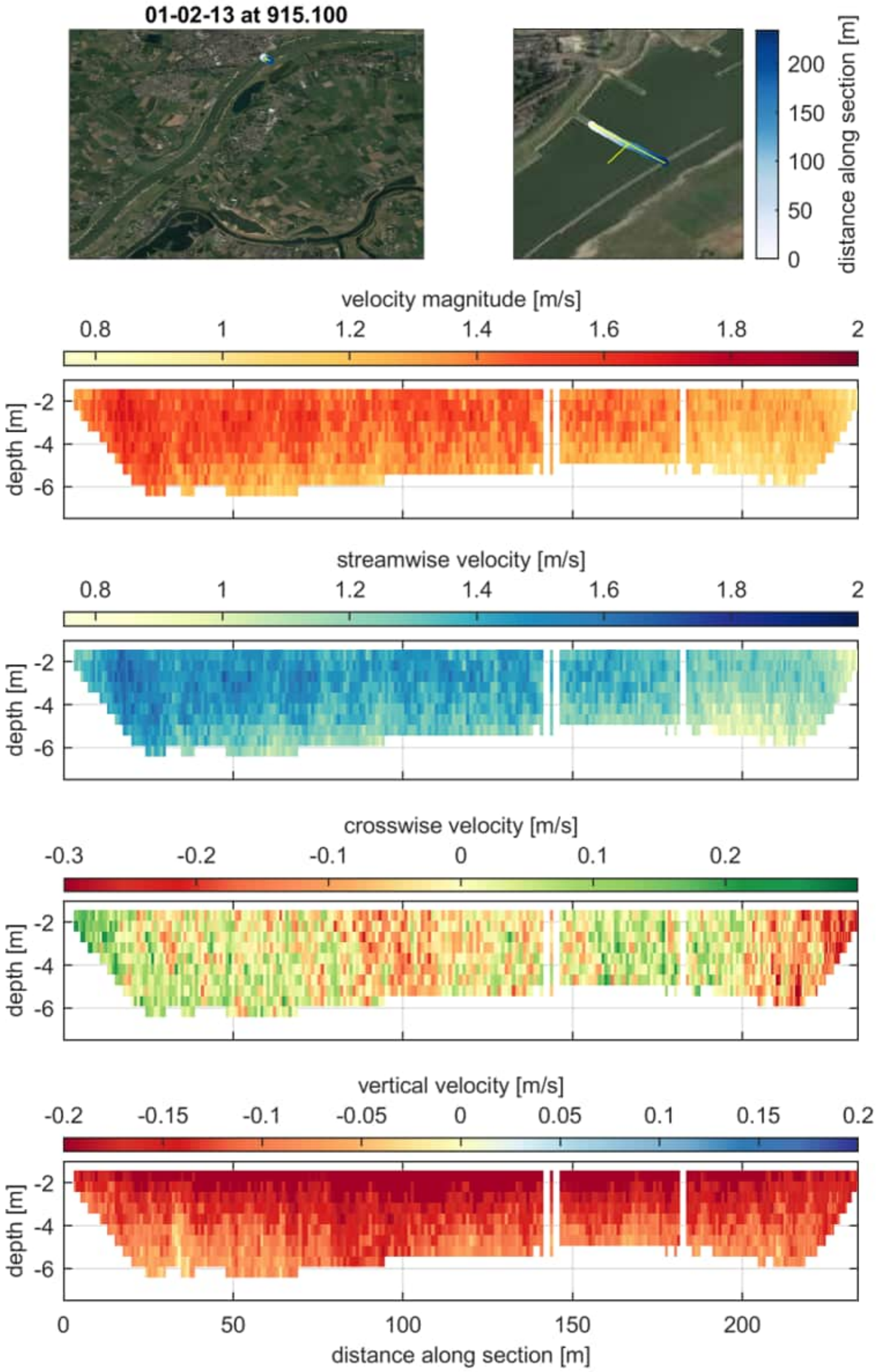

Figure D.19 Cross-sectional measurements on 01-02-13 (discharge at Lobith at 12:00 equal to 3436 m^3/s) at rkm 915.100 projected on measurement plane.

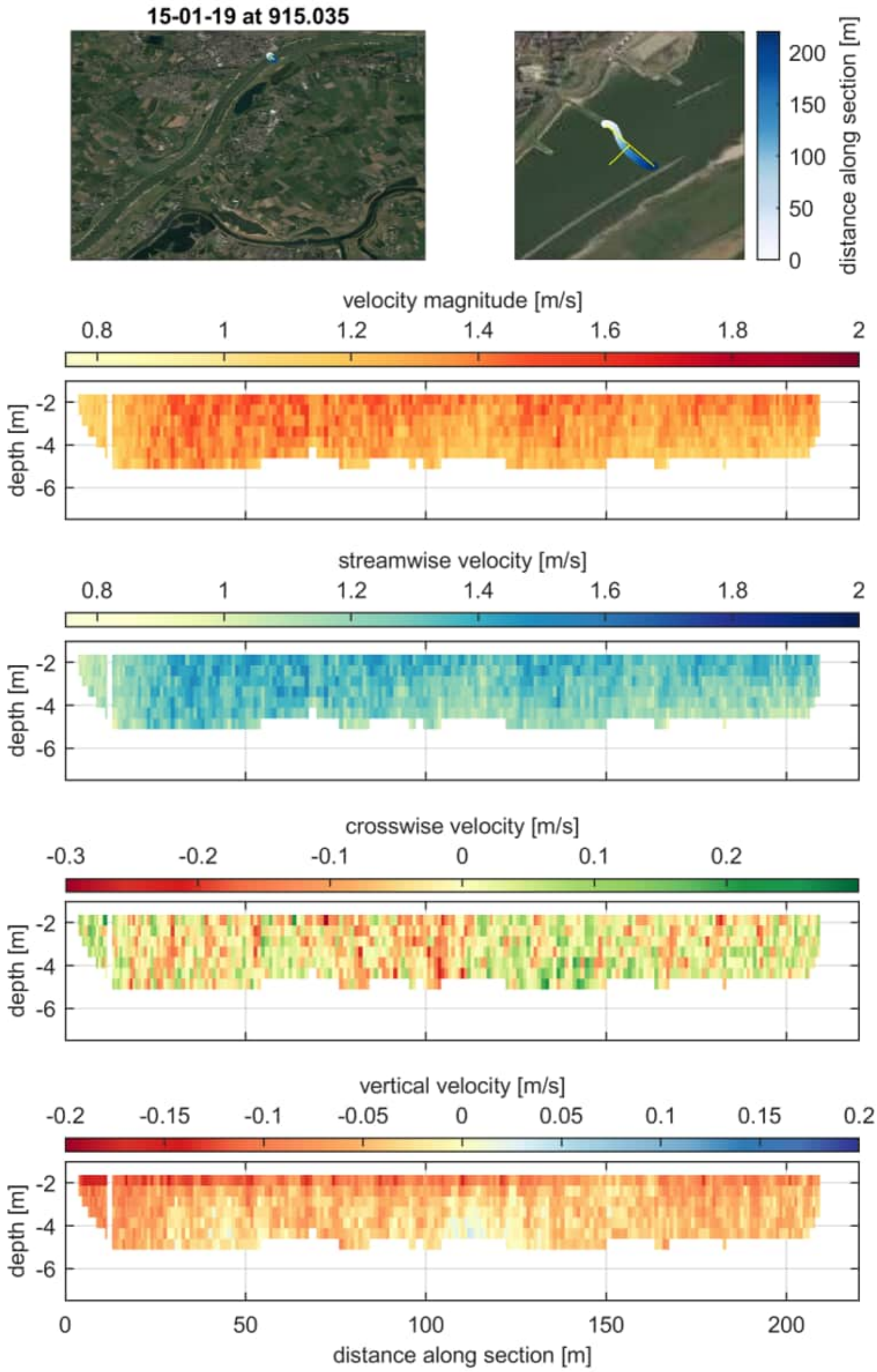

Figure D.20 Cross-sectional measurements on 15-01-19 (discharge at Lobith at 12:00 equal to 2590 m^3/s) at rkm 918.035 projected on measurement plane.

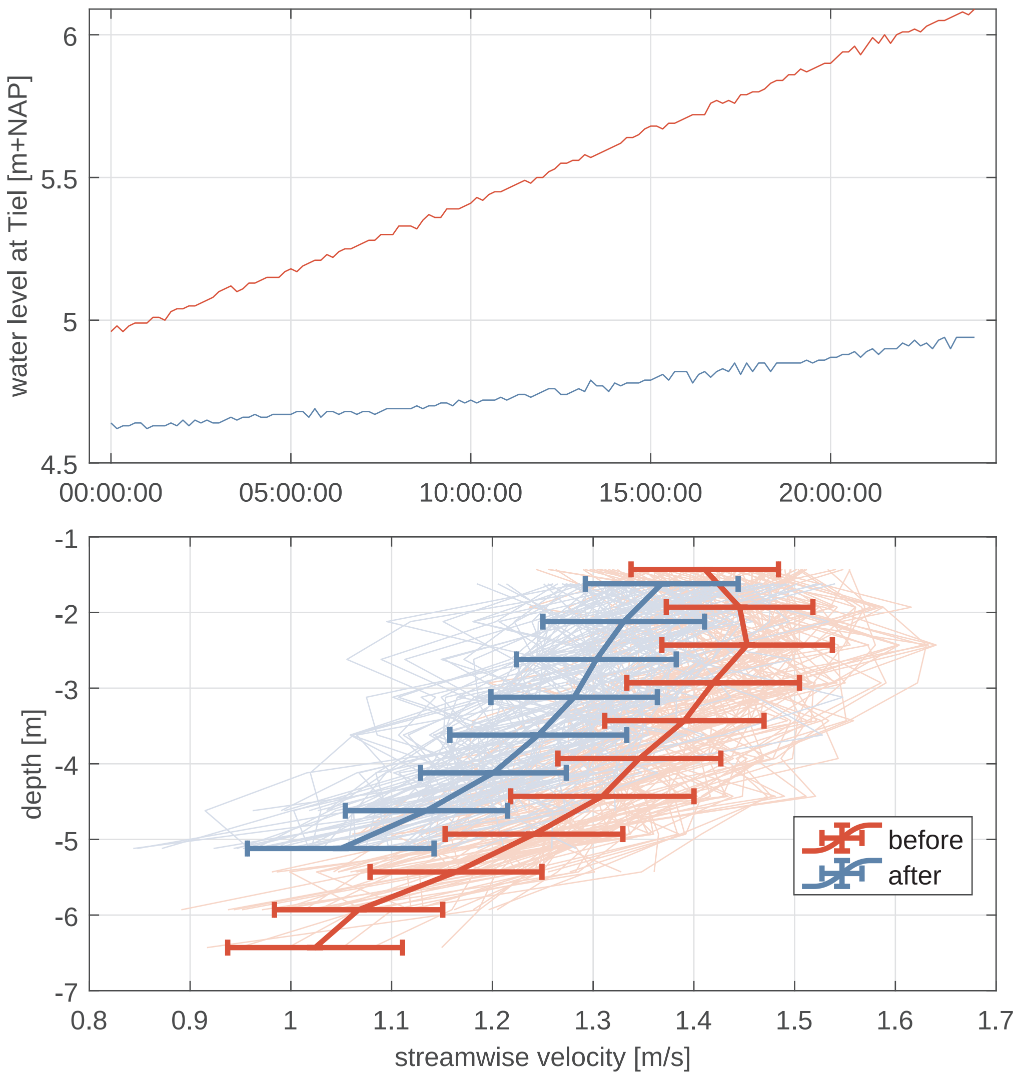

Figure D.21 Streamwise velocity at the central 100 m of channel before (01-02-13, discharge at Lobith at 12:00 equal to 3436 m^3/s, rkm 915.100) and after (15-01-19, discharge at Lobith at 12:00 equal to 2590 m^3/s, rkm 918.035)

D.3.2.7 Location 7

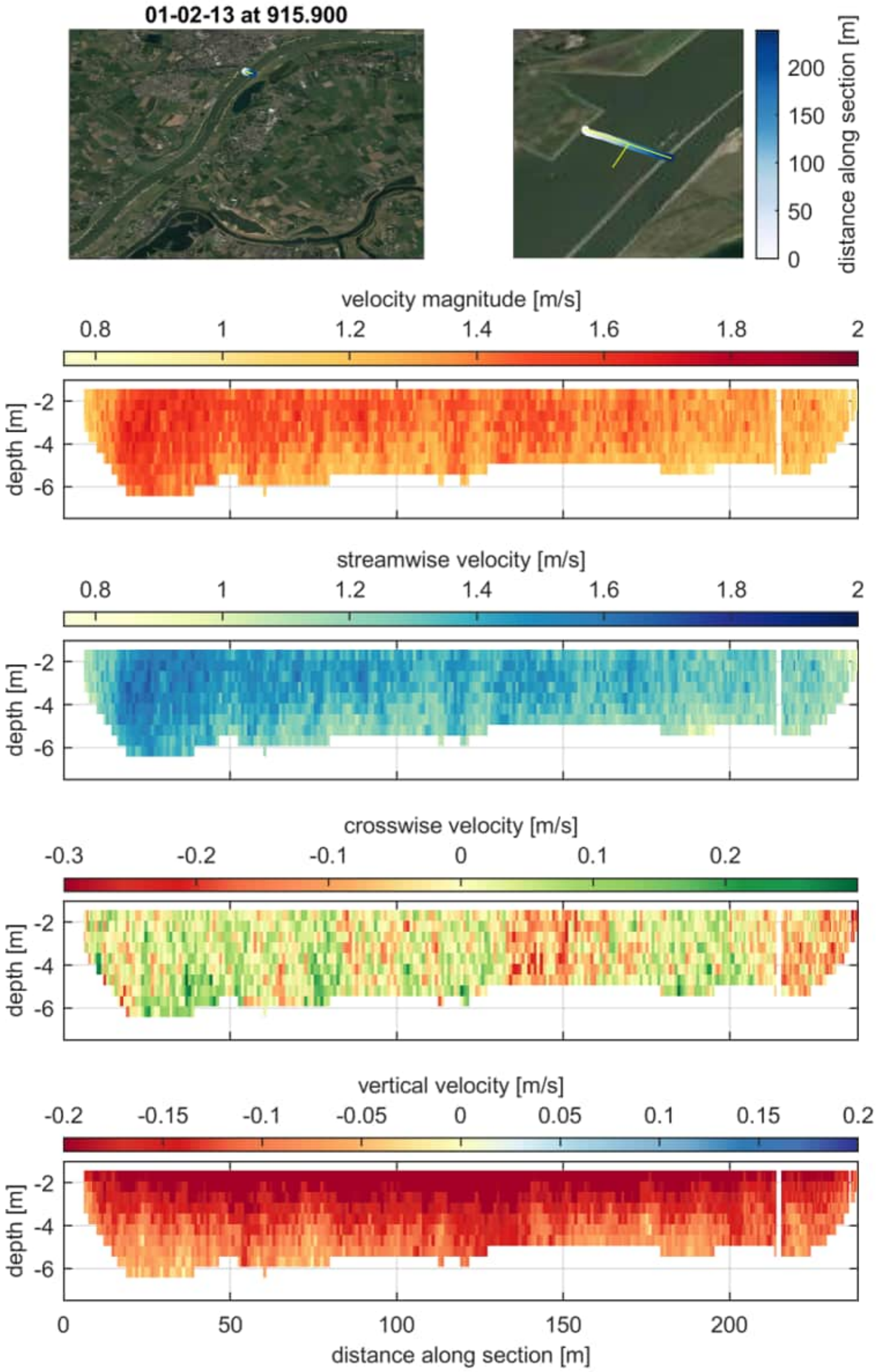

Figure D.22 Cross-sectional measurements on 01-02-13 (discharge at Lobith at 12:00 equal to 3436 m^3/s) at rkm 915.900 projected on measurement plane.

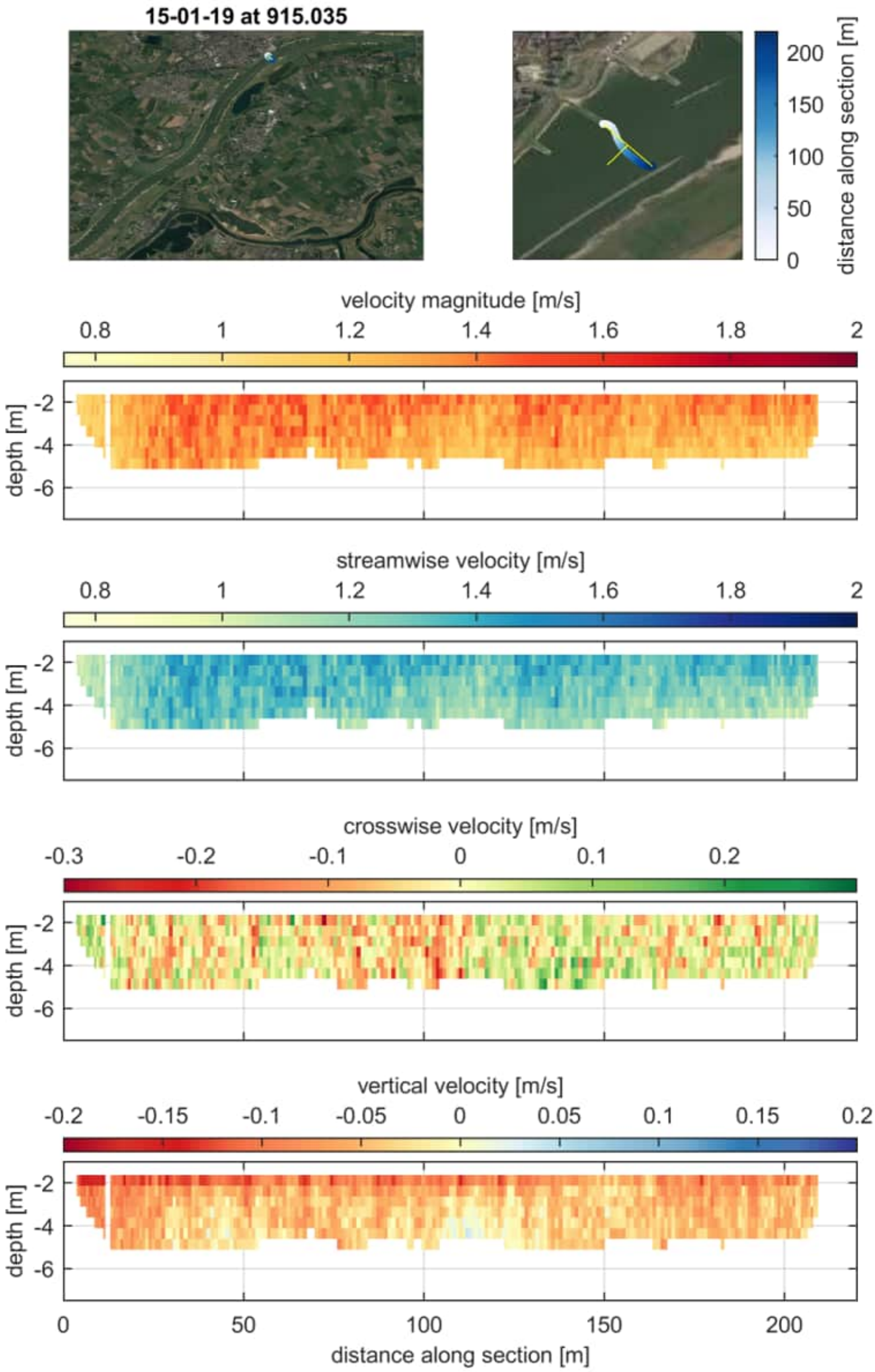

Figure D.23 Cross-sectional measurements on 15-01-19 (discharge at Lobith at 12:00 equal to 2590 m^3/s) at rkm 918.035 projected on measurement plane.

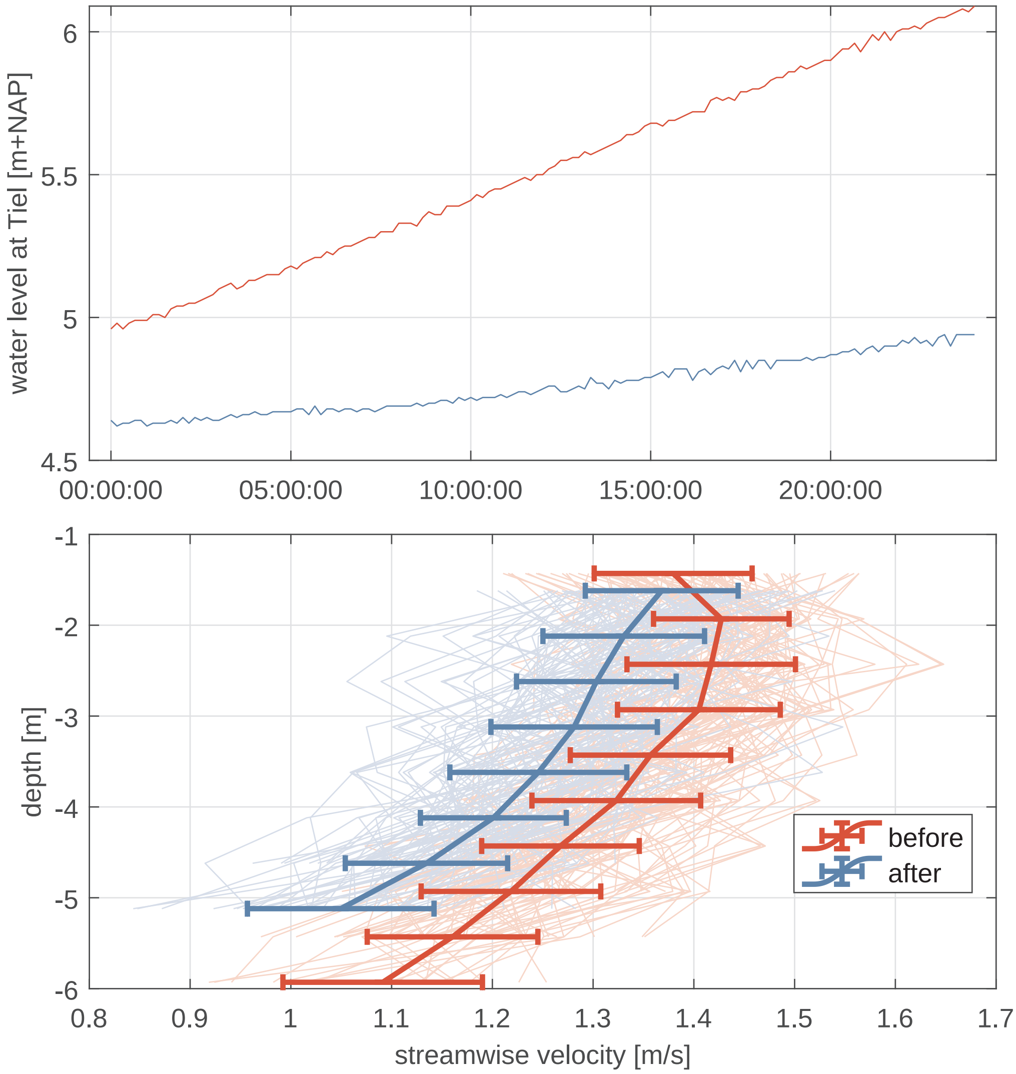

Figure D.24 Streamwise velocity at the central 100 m of channel before (01-02-13, discharge at Lobith at 12:00 equal to 3436 m^3/s, rkm 915.900) and after (15-01-19, discharge at Lobith at 12:00 equal to 2590 m^3/s, rkm 918.035)

D.3.2.8 Location 8

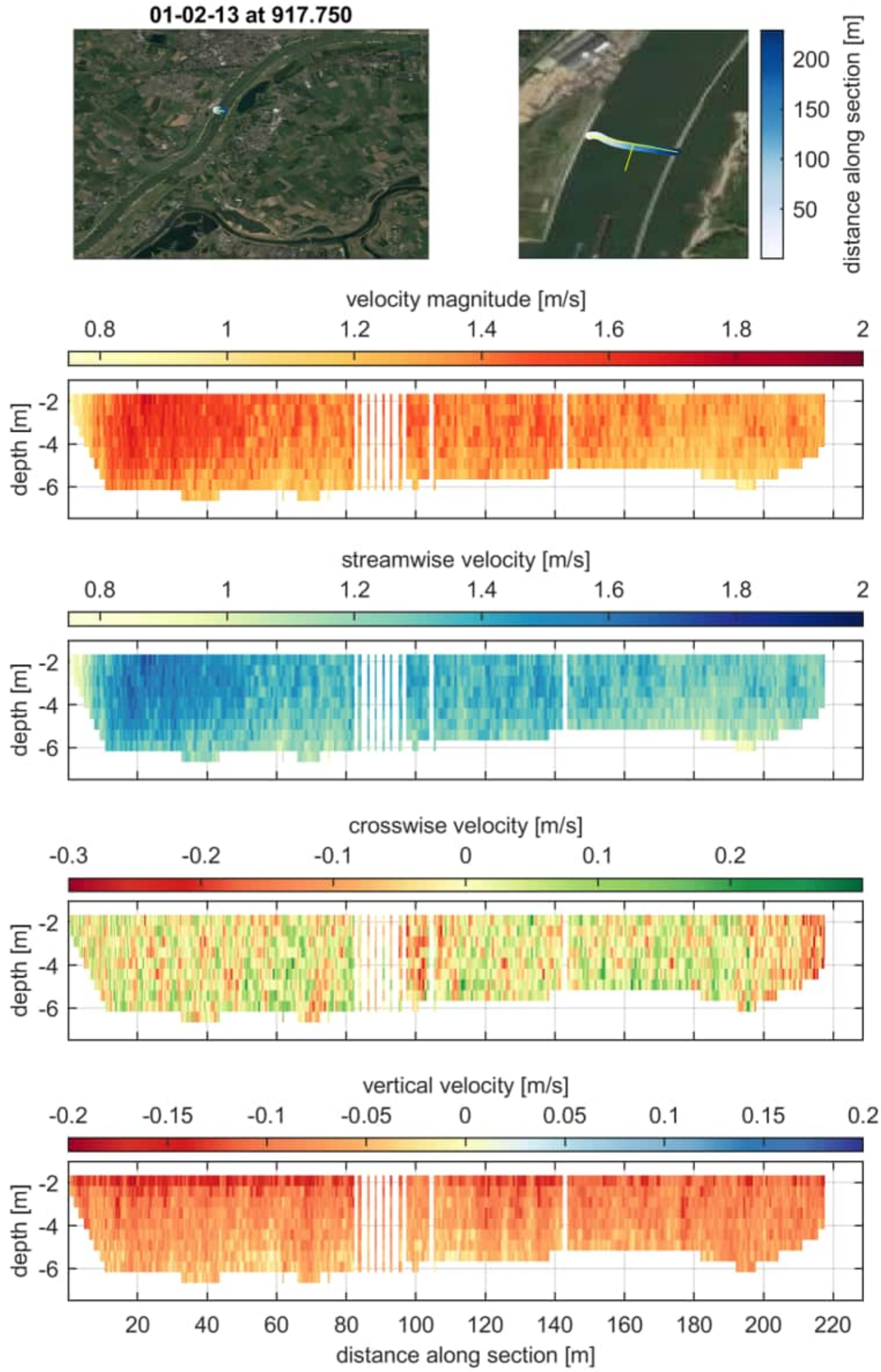

Figure D.25 Cross-sectional measurements on 01-02-13 (discharge at Lobith at 12:00 equal to 3436 m^3/s) at rkm 917.750 projected on measurement plane.

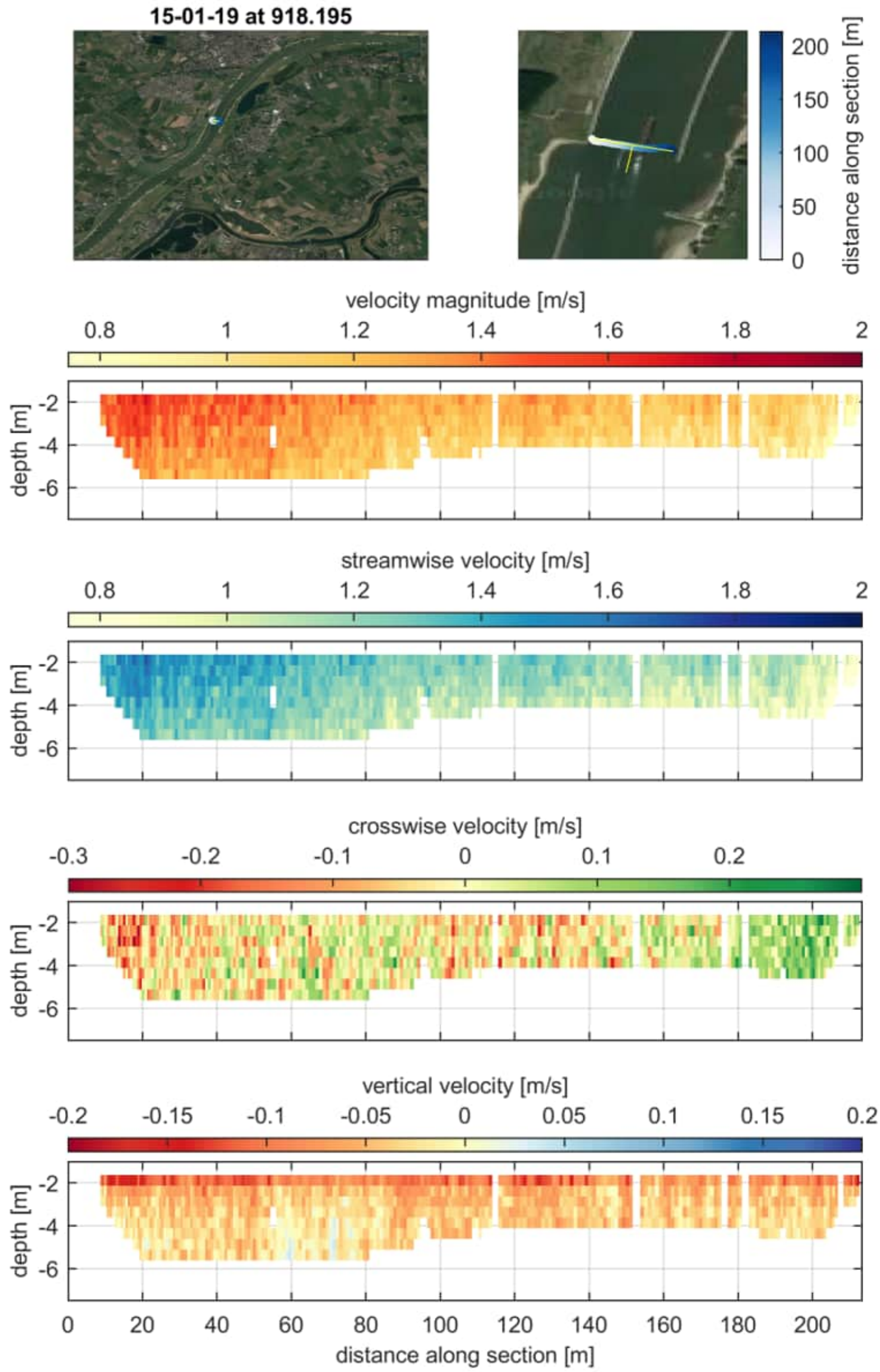

Figure D.26 Cross-sectional measurements on 15-01-19 (discharge at Lobith at 12:00 equal to 2590 m^3/s) at rkm 918.195 projected on measurement plane.

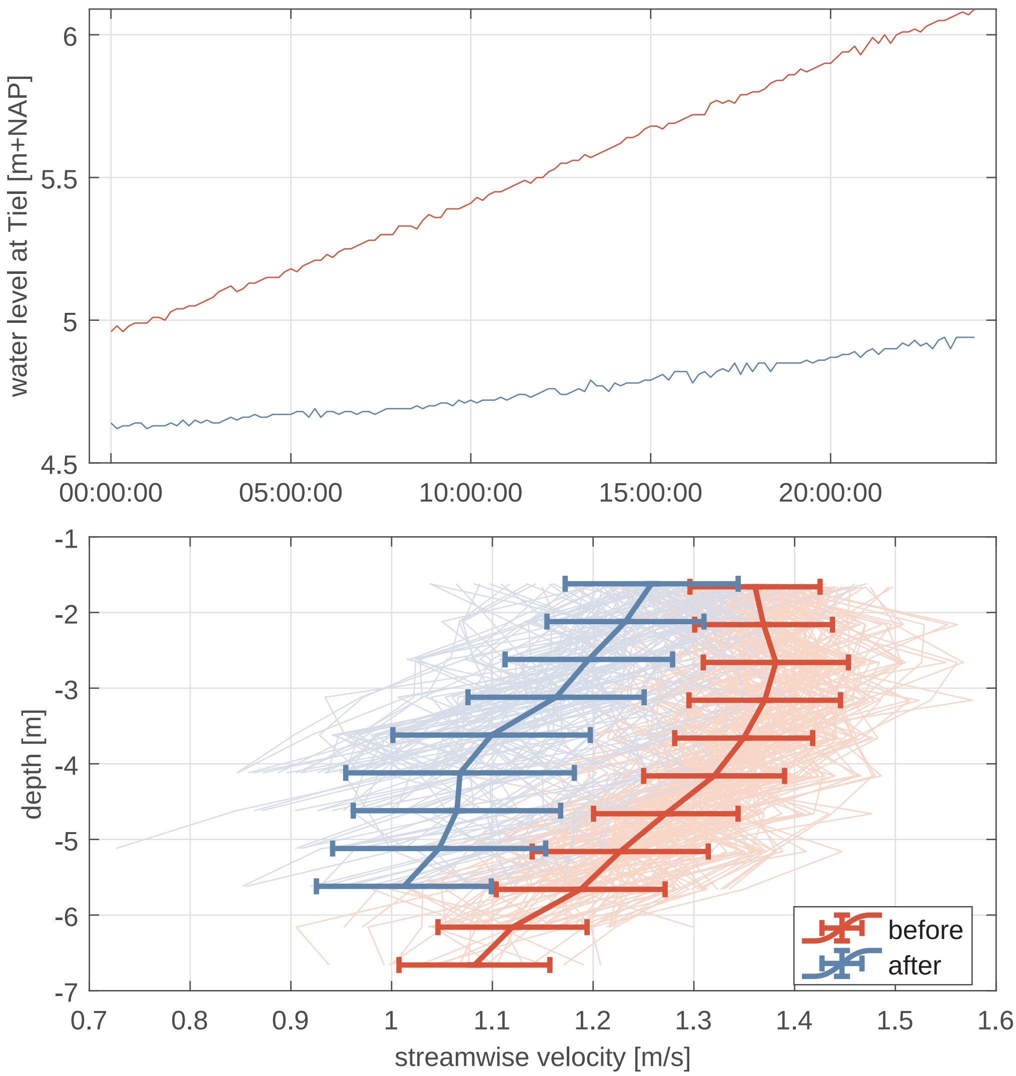

Figure D.27 Streamwise velocity at the central 100 m of channel before (01-02-13, discharge at Lobith at 12:00 equal to 3436 m^3/s, rkm 917.750) and after (15-01-19, discharge at Lobith at 12:00 equal to 2590 m^3/s, rkm 918.195)

D.3.2.9 Location 9

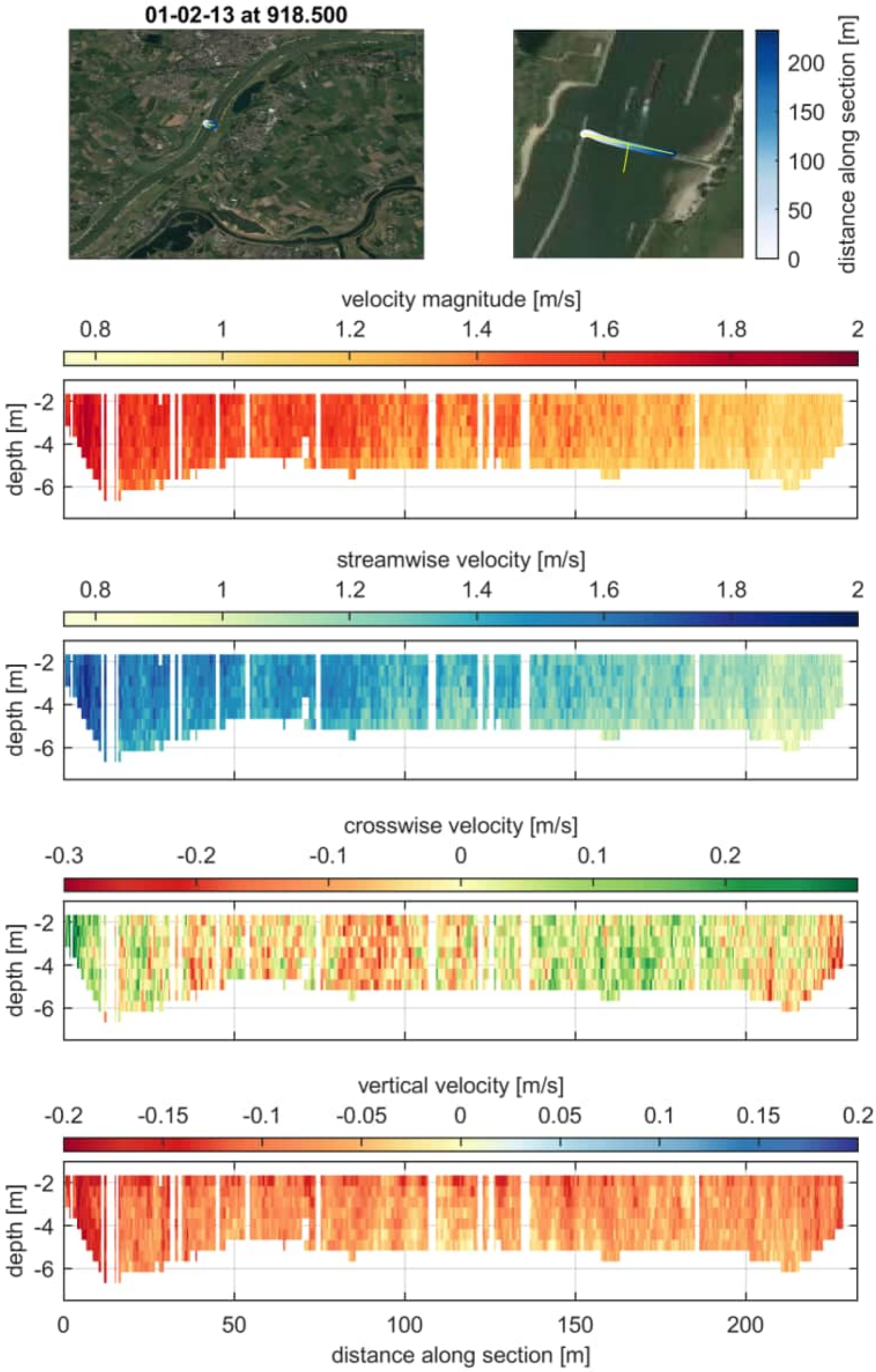

Figure D.28 Cross-sectional measurements on 01-02-13 (discharge at Lobith at 12:00 equal to 3436 m^3/s) at rkm 918.500 projected on measurement plane.

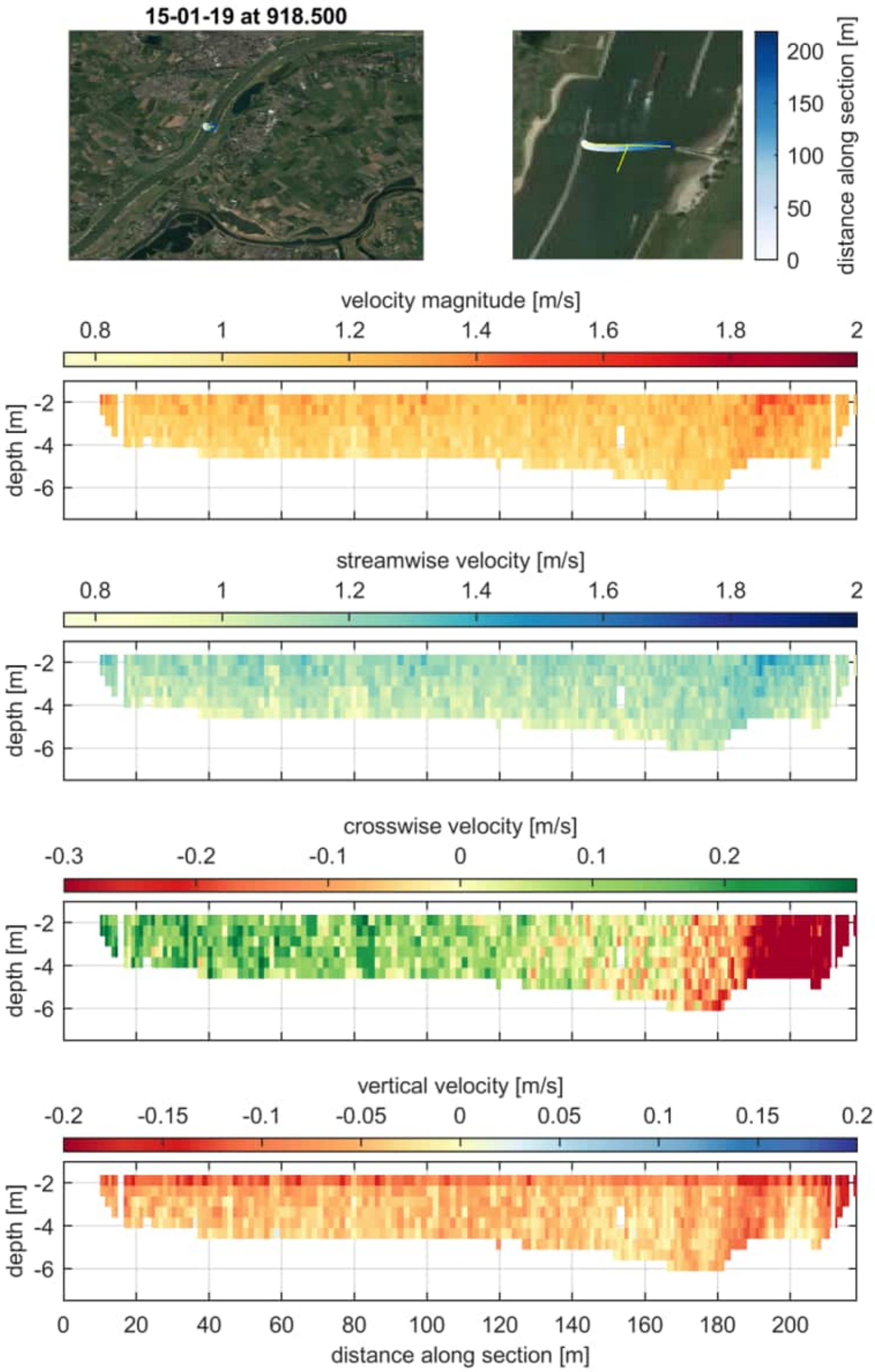

Figure D.29 Cross-sectional measurements on 15-01-19 (discharge at Lobith at 12:00 equal to 2590 m^3/s) at rkm 918.500 projected on measurement plane.

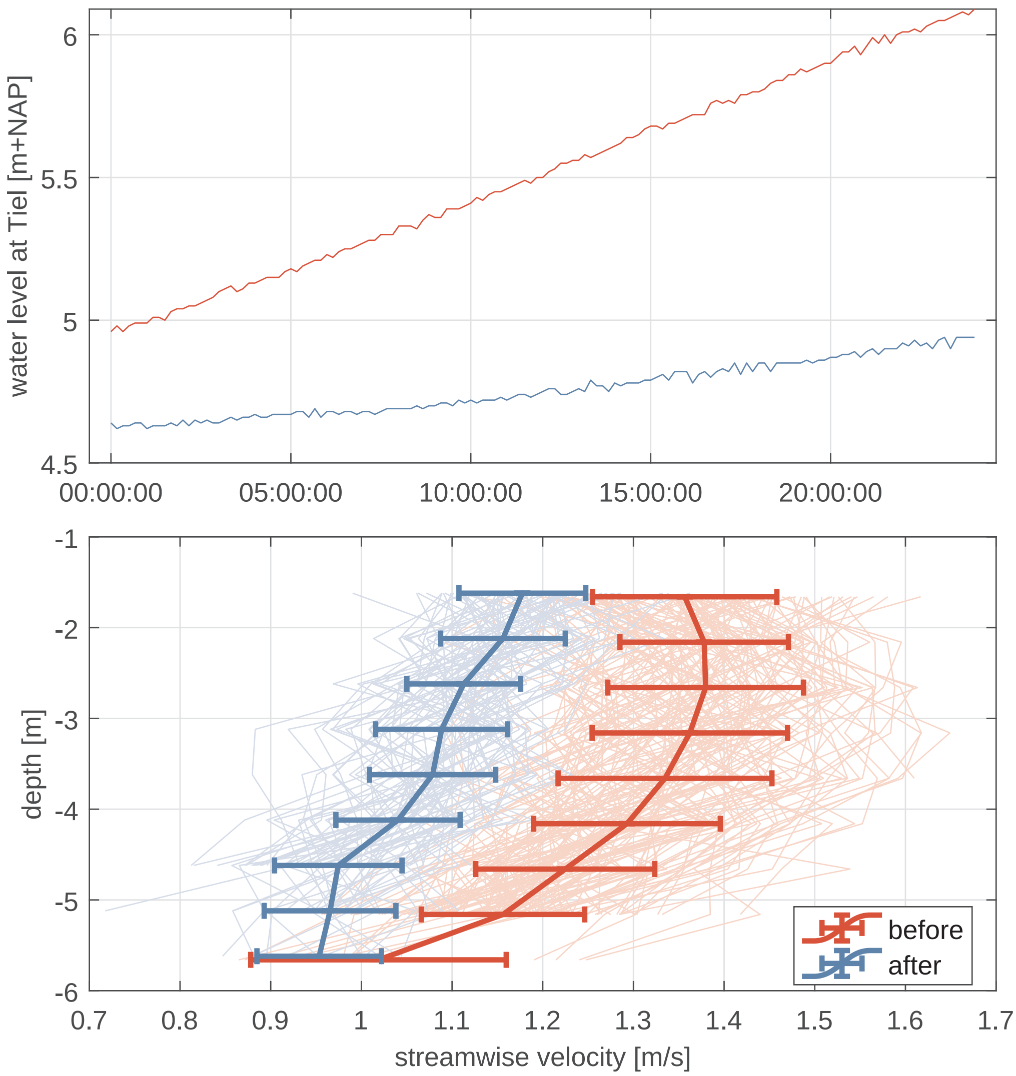

Figure D.30 Streamwise velocity at the central 100 m of channel before (01-02-13, discharge at Lobith at 12:00 equal to 3436 m^3/s, rkm 918.500) and after (15-01-19, discharge at Lobith at 12:00 equal to 2590 m^3/s, rkm 918.500)

D.3.2.10 Location 10

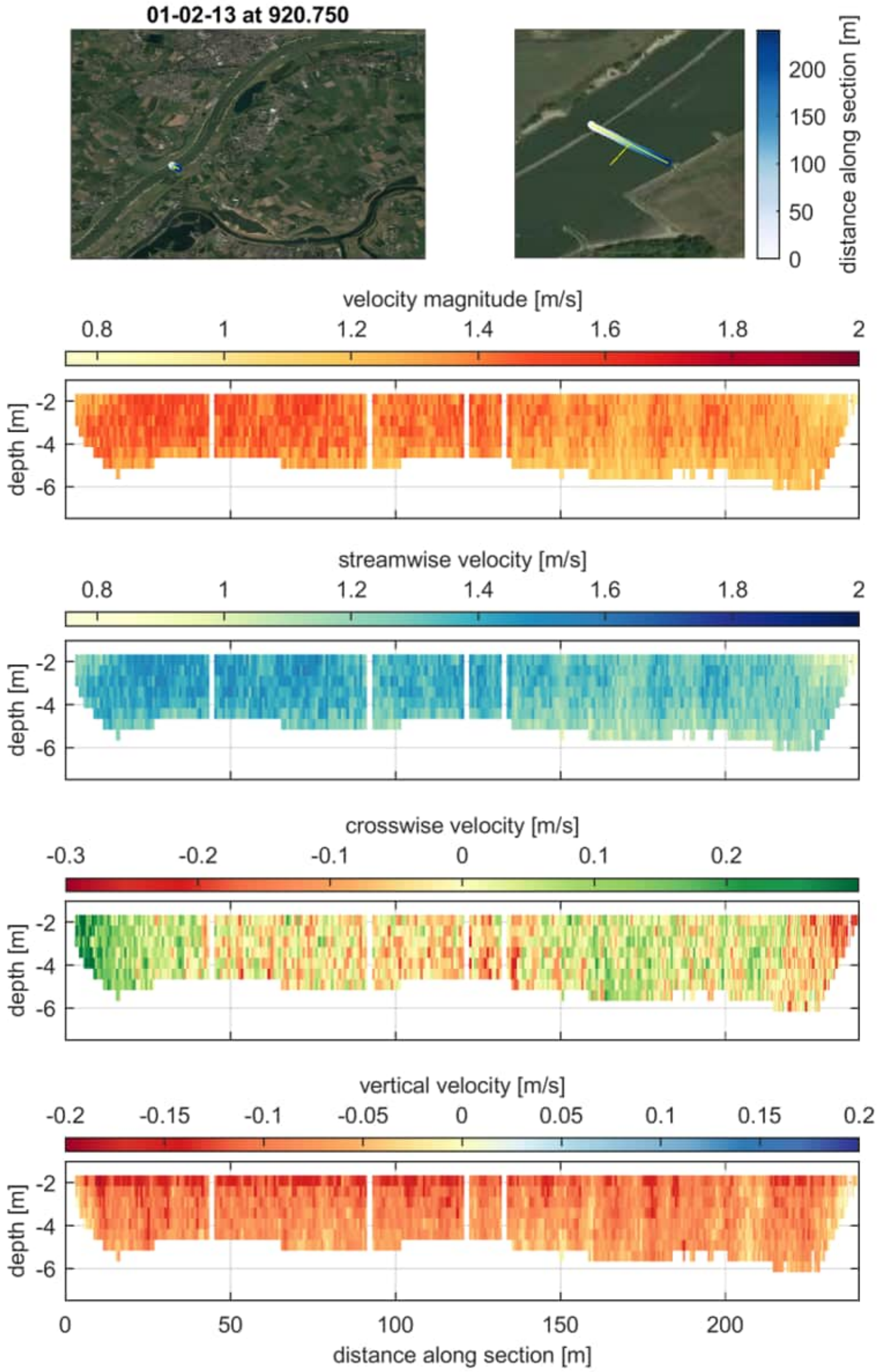

Figure D.31 Cross-sectional measurements on 01-02-13 (discharge at Lobith at 12:00 equal to 3436 m^3/s) at rkm 920.750 projected on measurement plane.

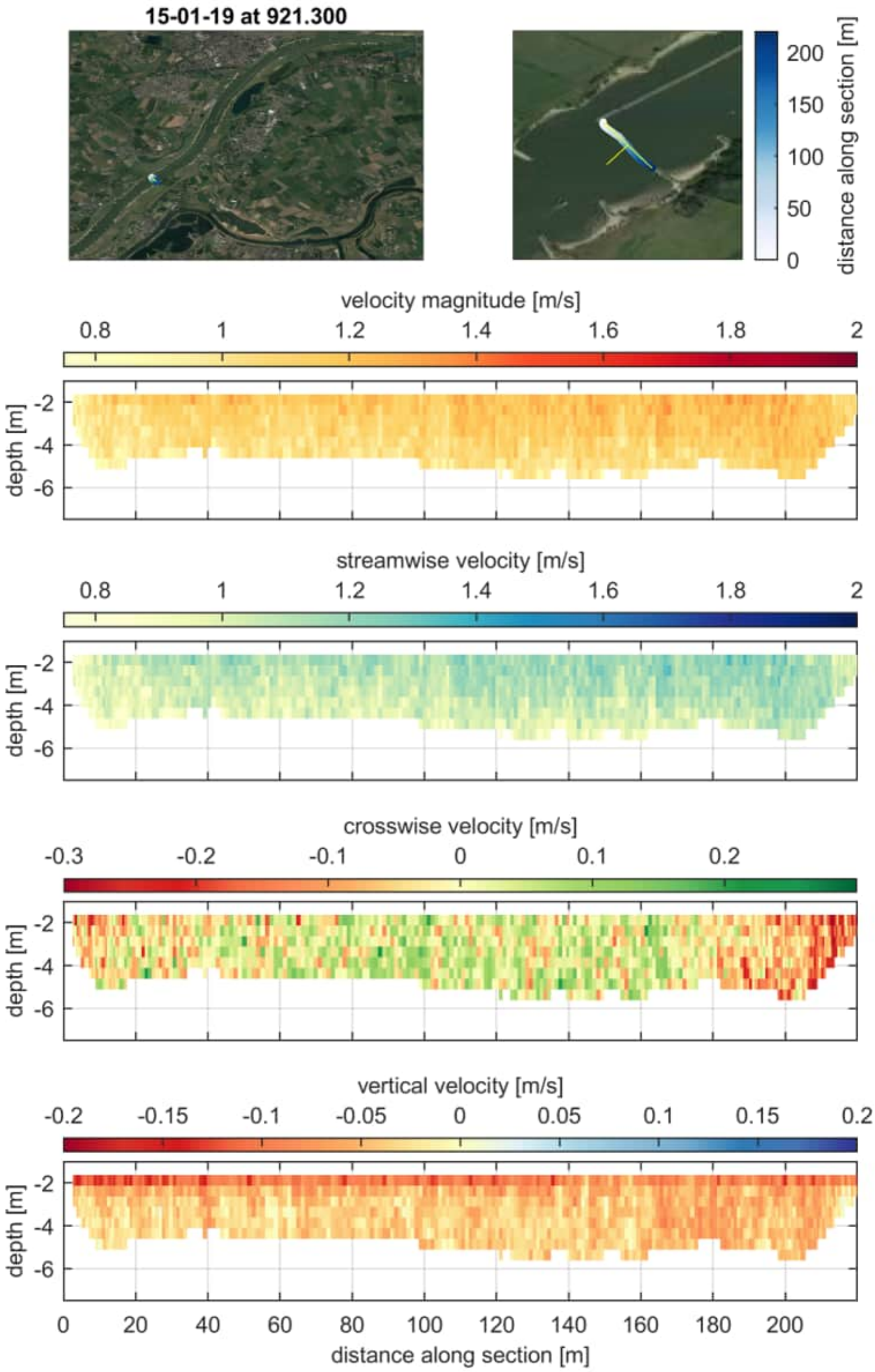

Figure D.32 Cross-sectional measurements on 15-01-19 (discharge at Lobith at 12:00 equal to 2590 m^3/s) at rkm 921.300 projected on measurement plane.

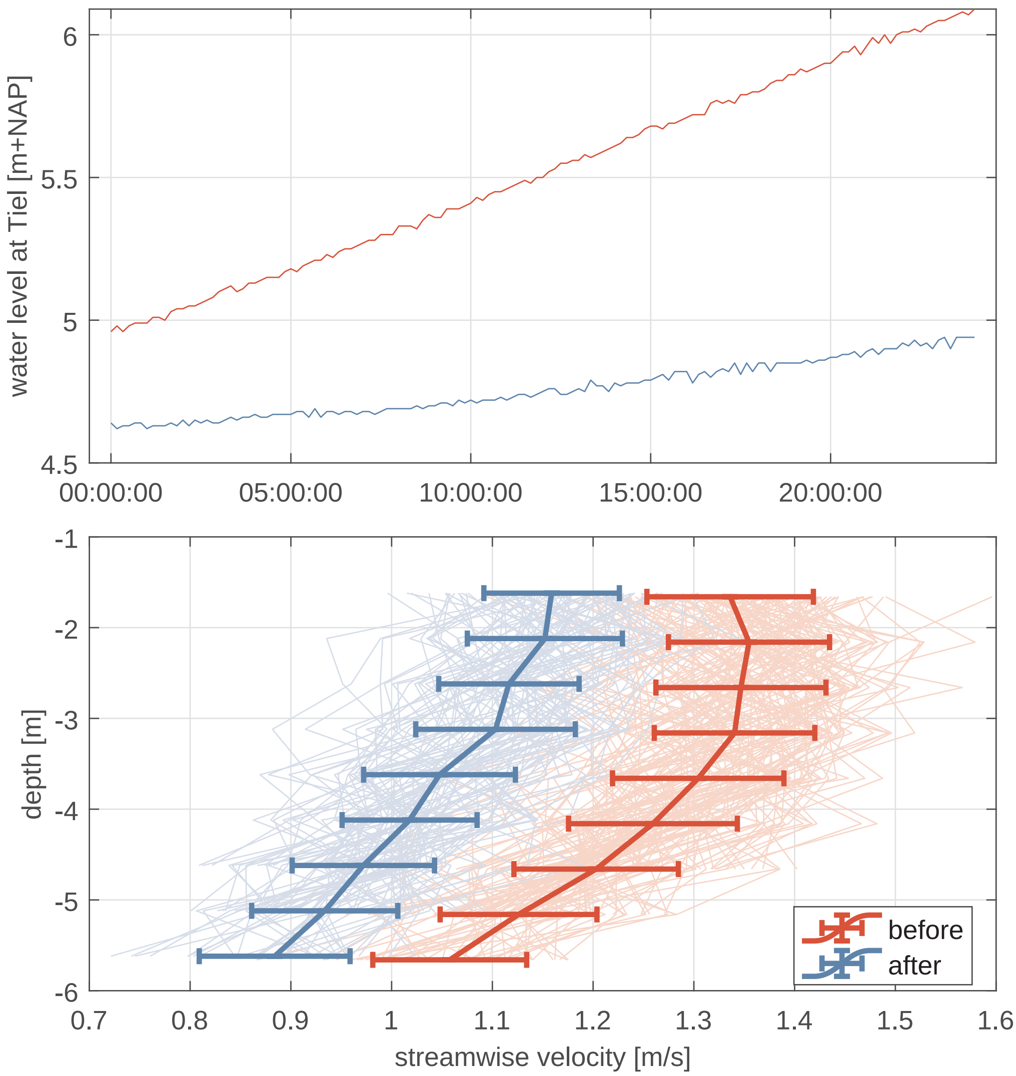

Figure D.33 Streamwise velocity at the central 100 m of channel before (01-02-13, discharge at Lobith at 12:00 equal to 3436 m^3/s, rkm 920.750) and after (15-01-19, discharge at Lobith at 12:00 equal to 2590 m^3/s, rkm 921.300)

D.3.2.11 Location 11

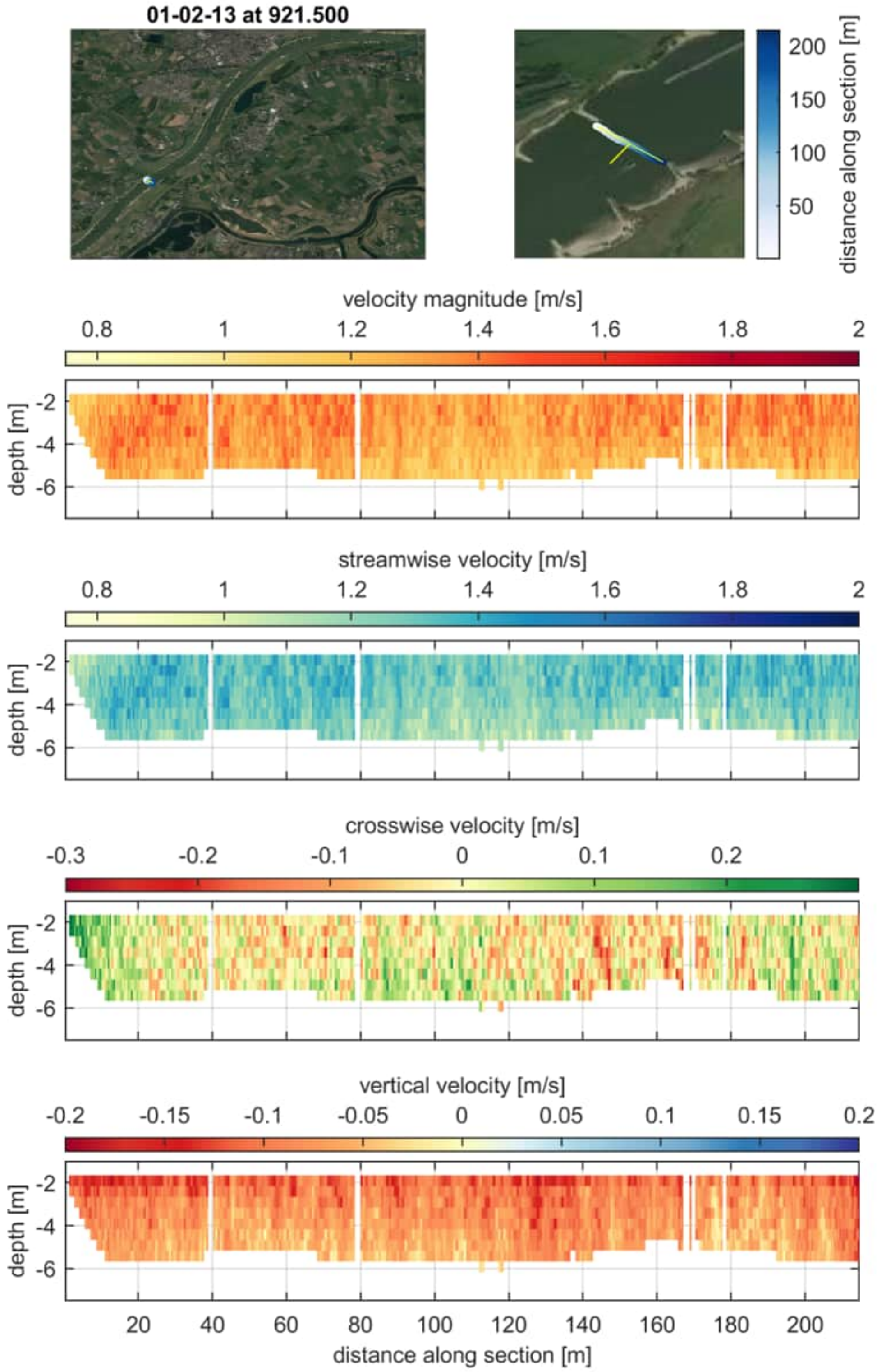

Figure D.34 Cross-sectional measurements on 01-02-13 (discharge at Lobith at 12:00 equal to 3436 m^3/s) at rkm 921.500 projected on measurement plane.

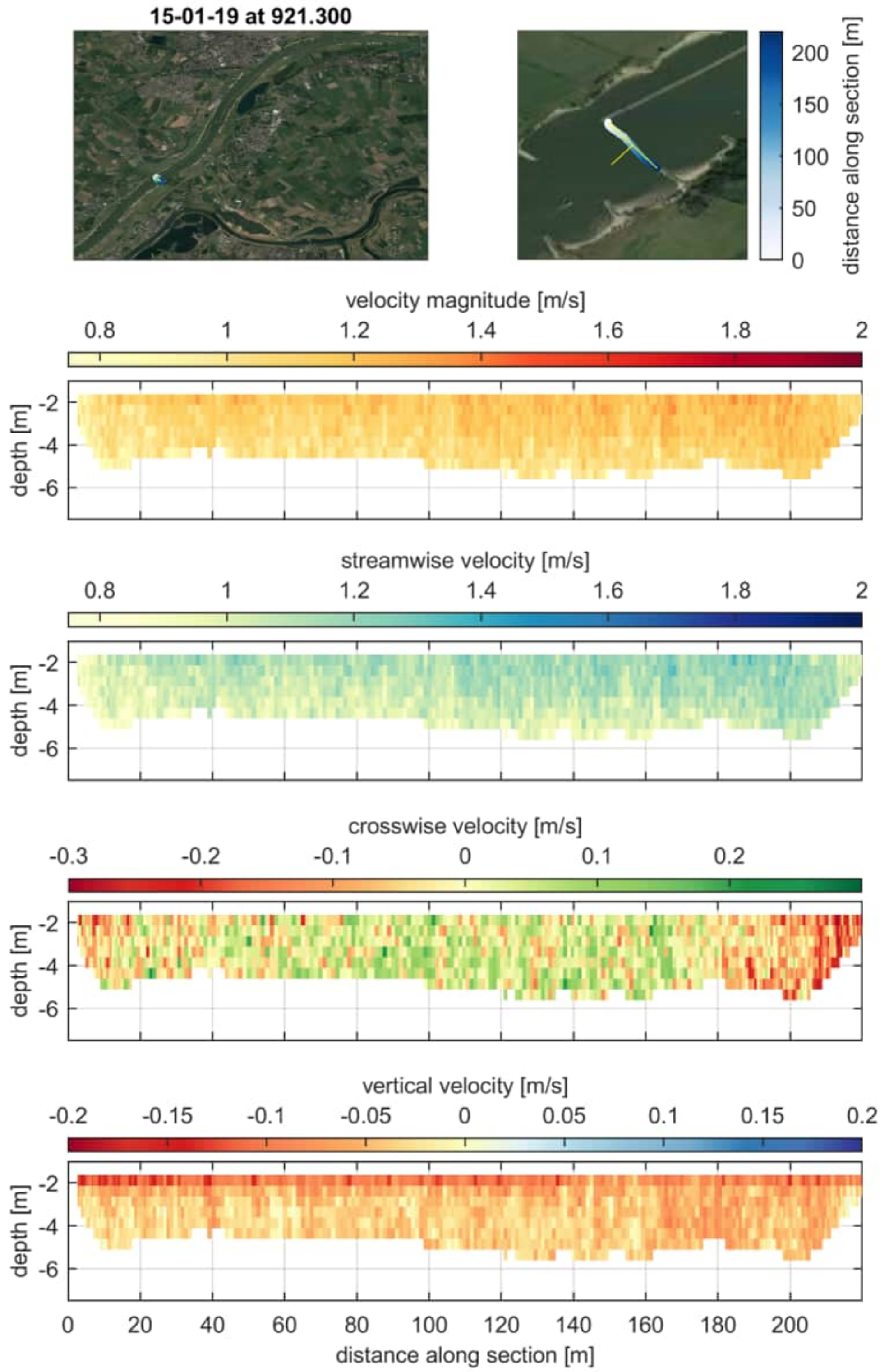

Figure D.35 Cross-sectional measurements on 15-01-19 (discharge at Lobith at 12:00 equal to 2590 m^3/s) at rkm 921.300 projected on measurement plane.

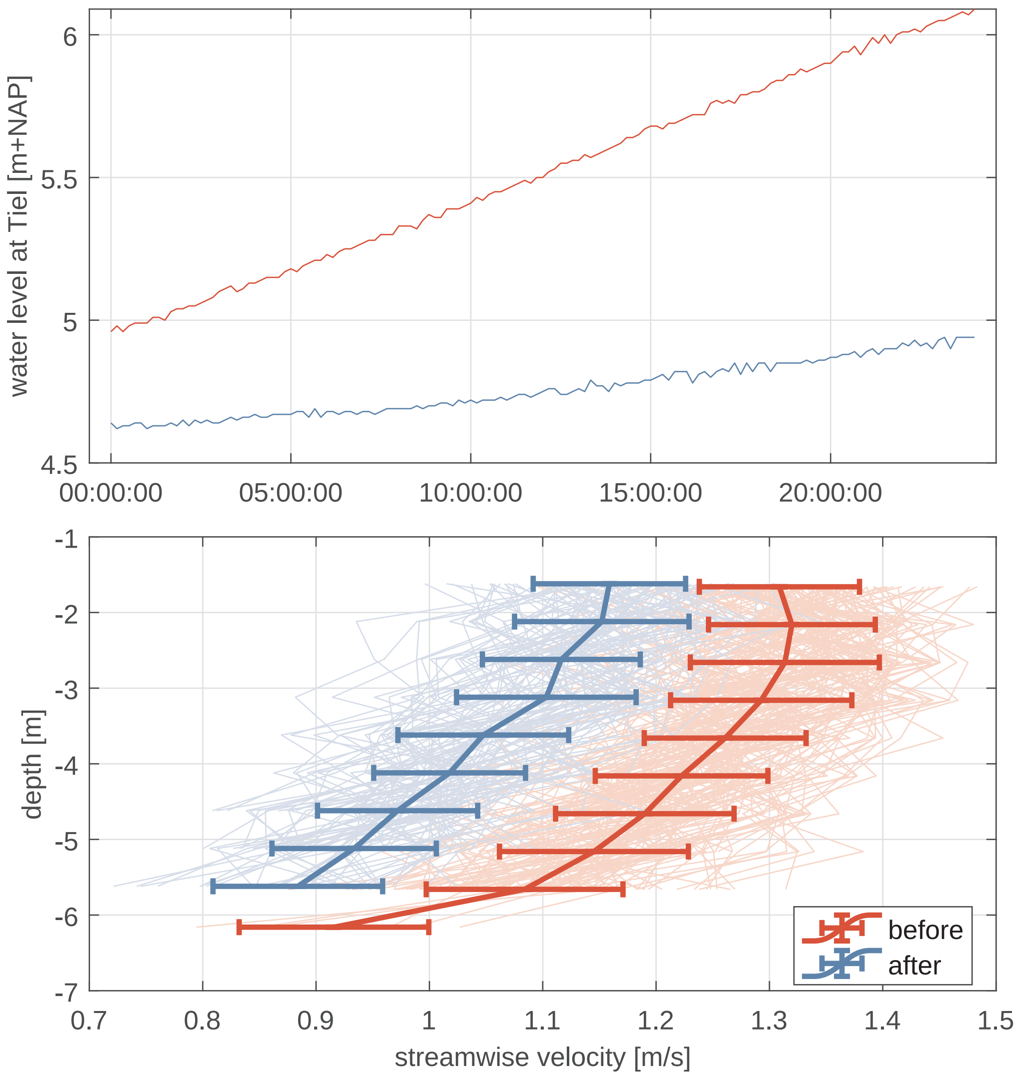

Figure D.36 Streamwise velocity at the central 100 m of channel before (01-02-13, discharge at Lobith at 12:00 equal to 3436 m^3/s, rkm 921.500) and after (15-01-19, discharge at Lobith at 12:00 equal to 2590 m^3/s, rkm 921.300)

D.3.2.12 Location 12

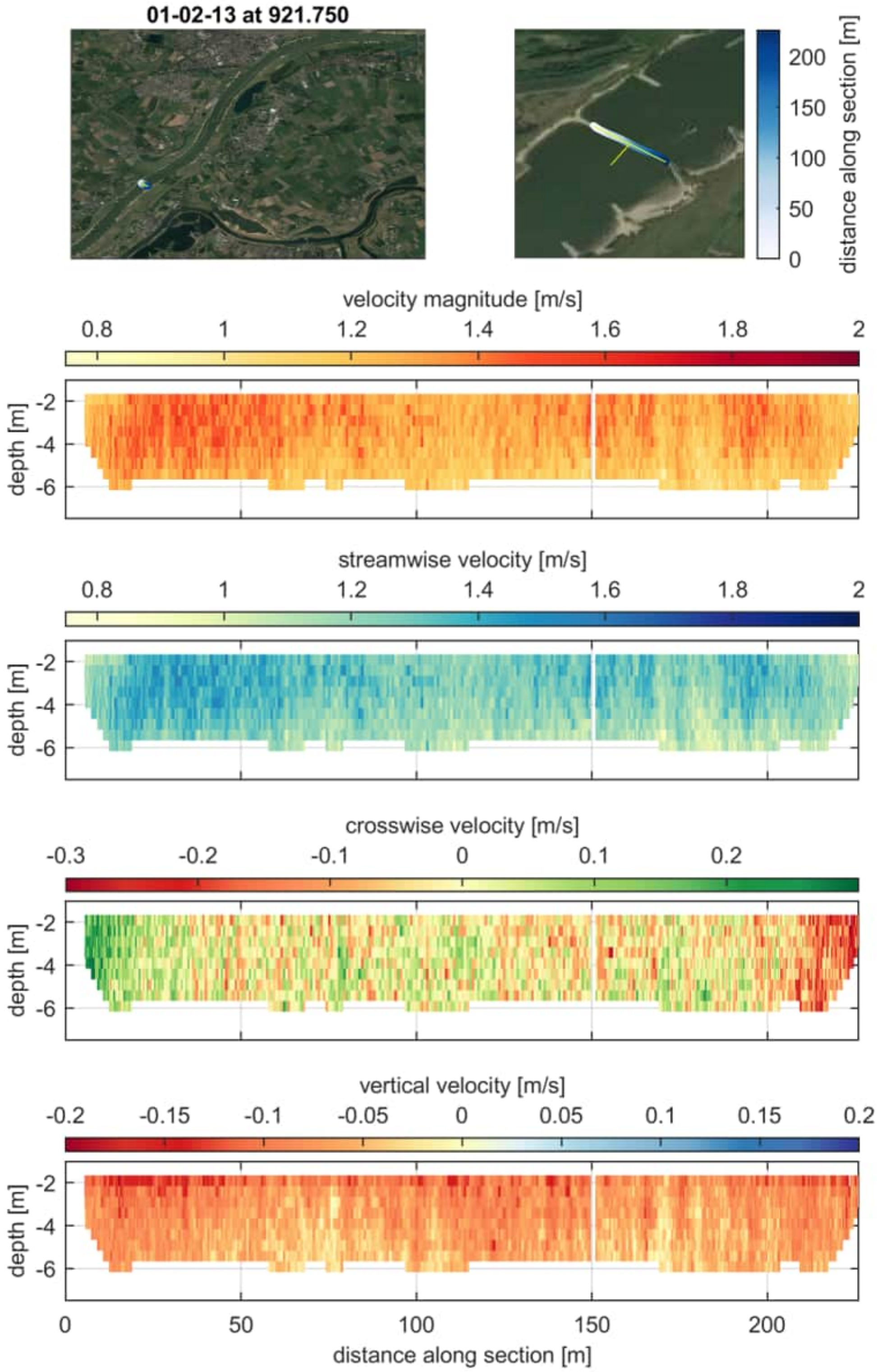

Figure D.37 Cross-sectional measurements on 01-02-13 (discharge at Lobith at 12:00 equal to 3436 m^3/s) at rkm 921.750 projected on measurement plane.

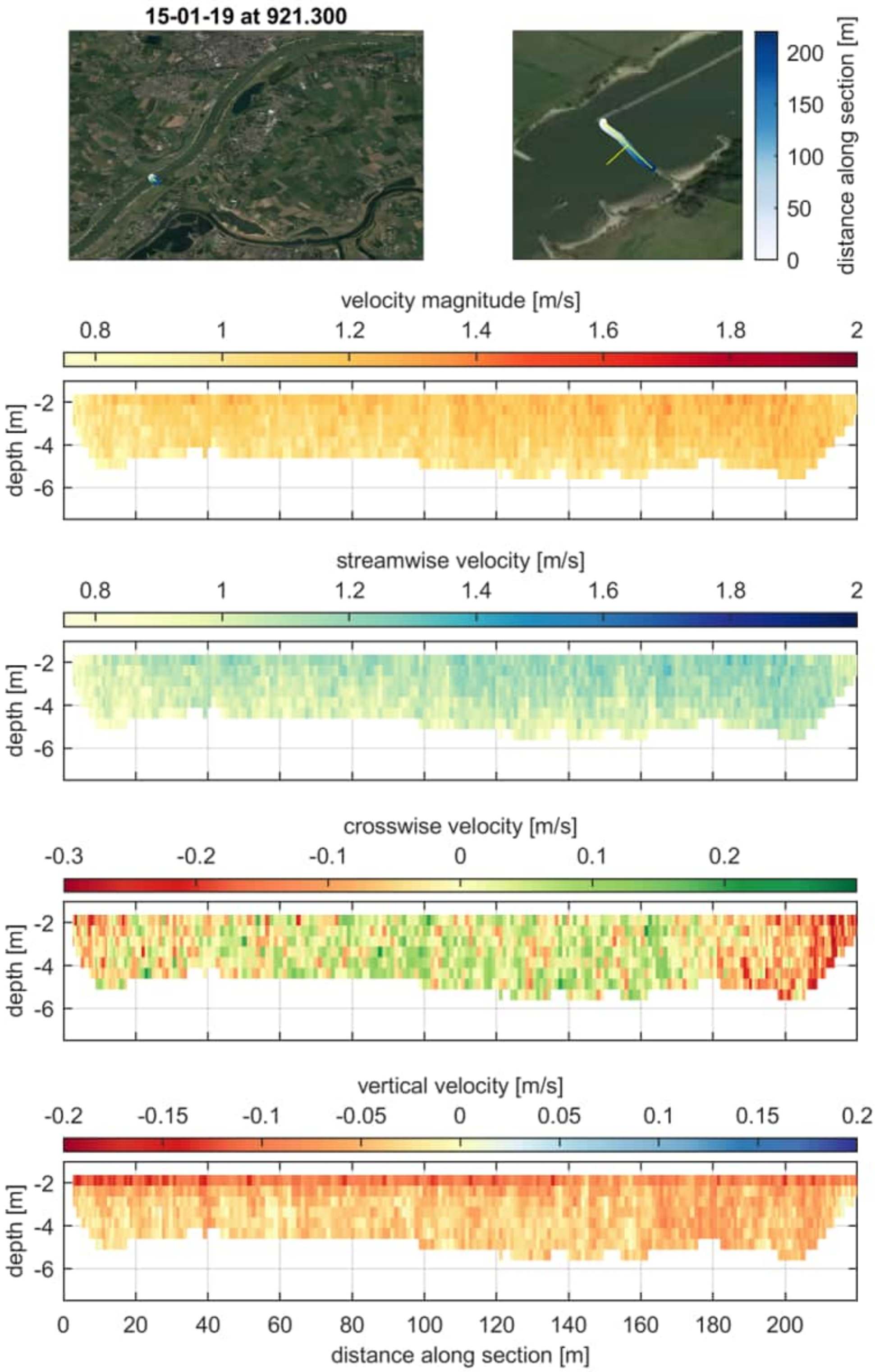

Figure D.38 Cross-sectional measurements on 15-01-19 (discharge at Lobith at 12:00 equal to 2590 m^3/s) at rkm 921.300 projected on measurement plane.

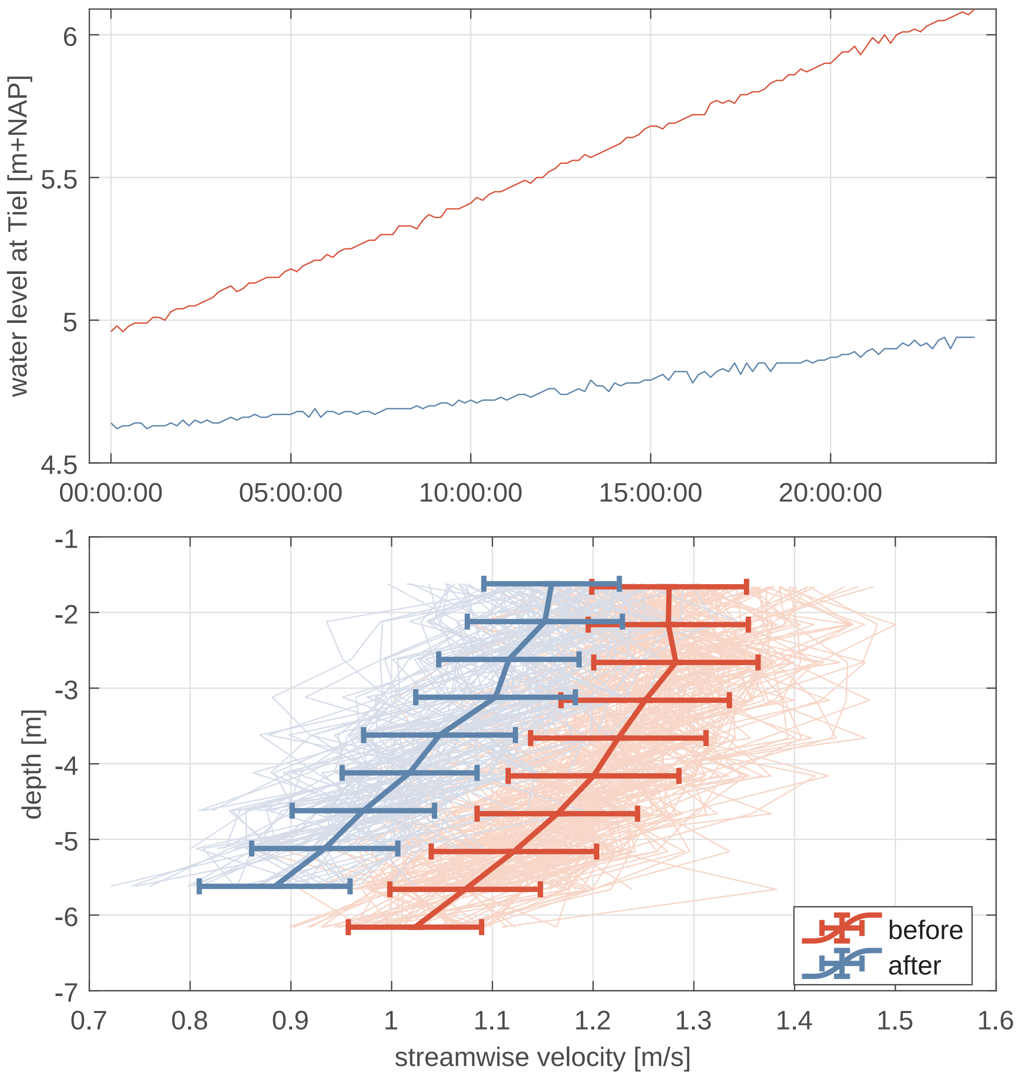

Figure D.39 Streamwise velocity at the central 100 m of channel before (01-02-13, discharge at Lobith at 12:00 equal to 3436 m^3/s, rkm 921.750) and after (15-01-19, discharge at Lobith at 12:00 equal to 2590 m^3/s, rkm 921.300)

D.3.2.13 Location 13

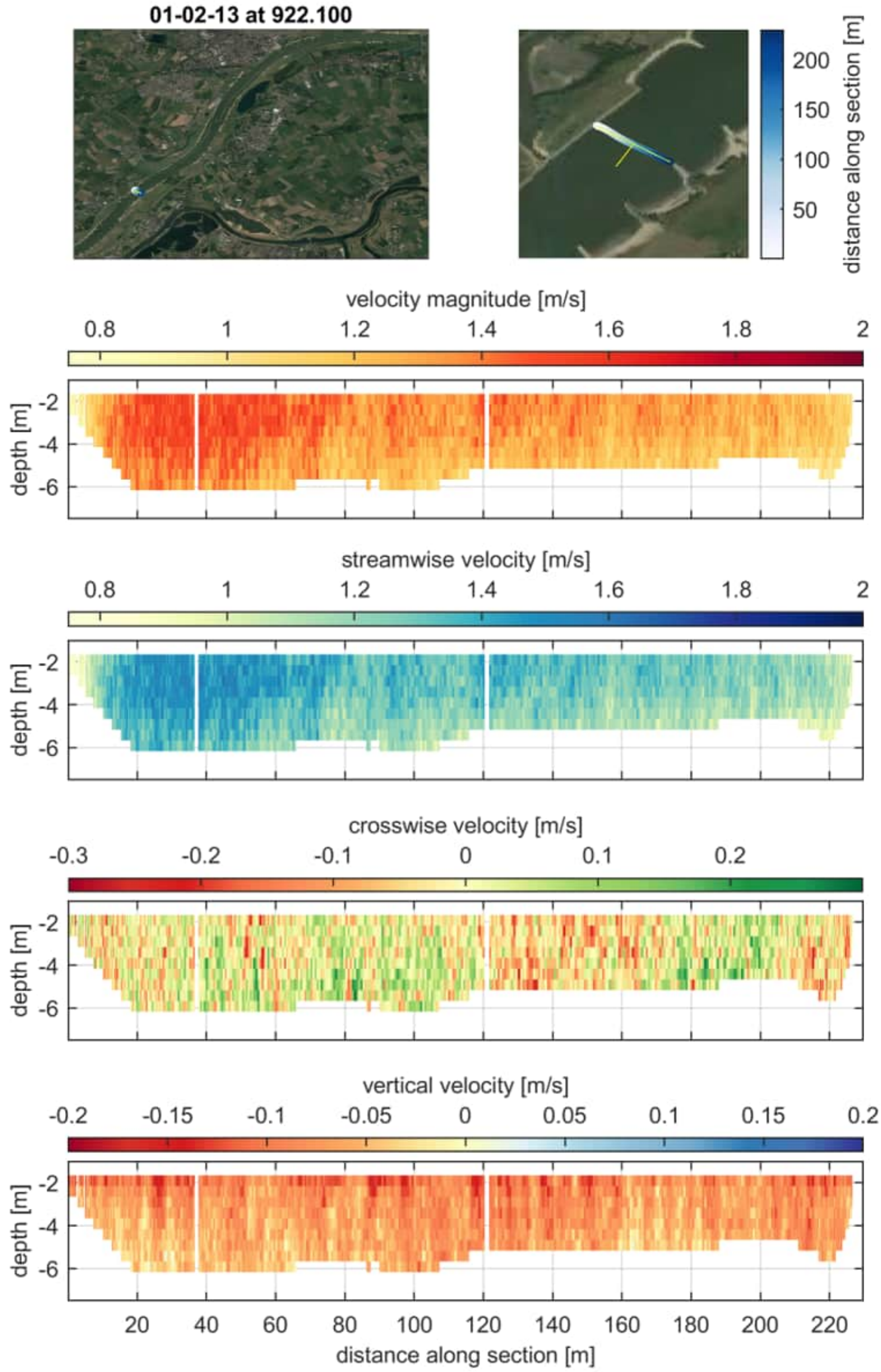

Figure D.40 Cross-sectional measurements on 01-02-13 (discharge at Lobith at 12:00 equal to 3436 m^3/s) at rkm 922.100 projected on measurement plane.

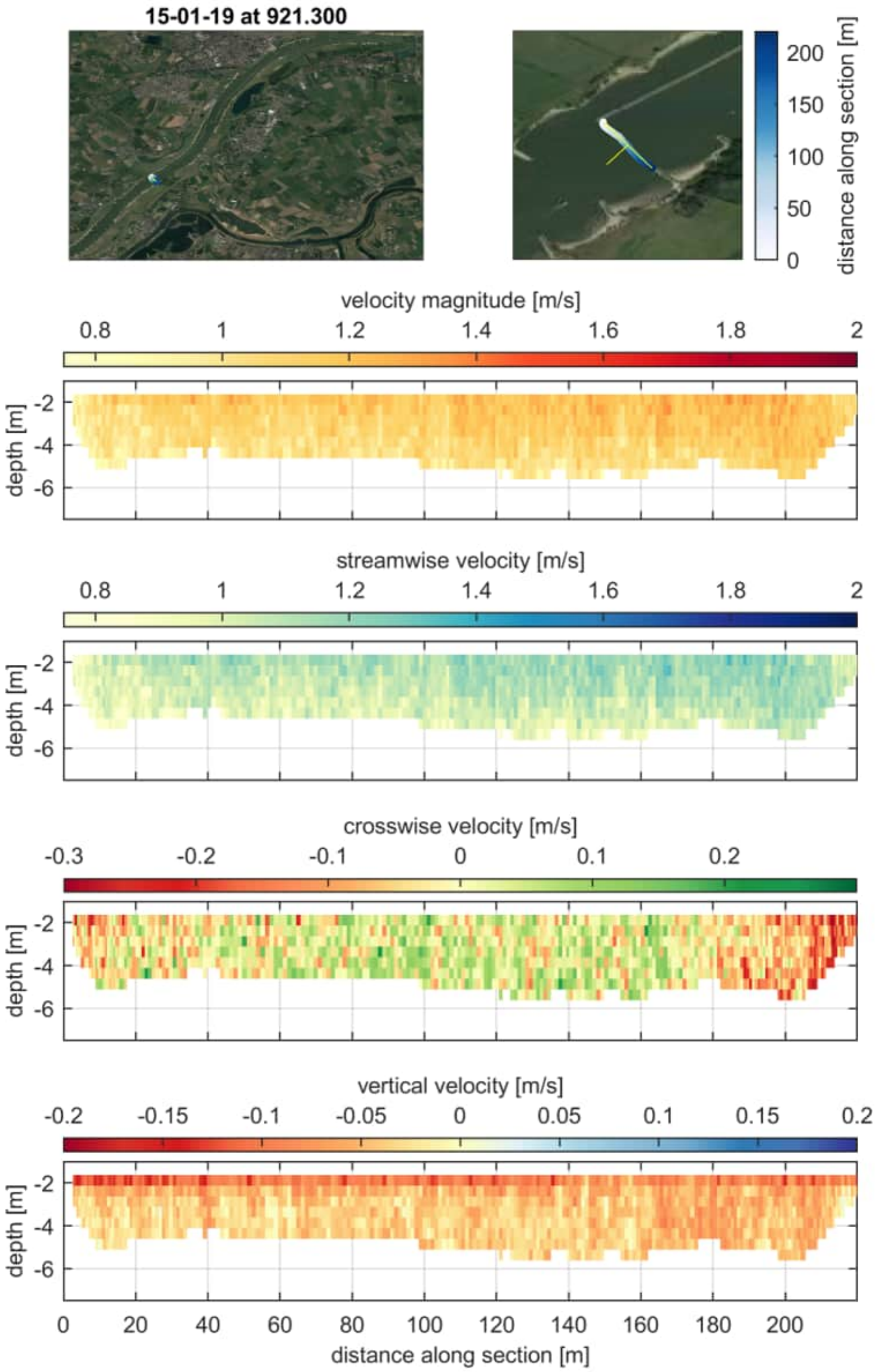

Figure D.41 Cross-sectional measurements on 15-01-19 (discharge at Lobith at 12:00 equal to 2590 m^3/s) at rkm 921.300 projected on measurement plane.

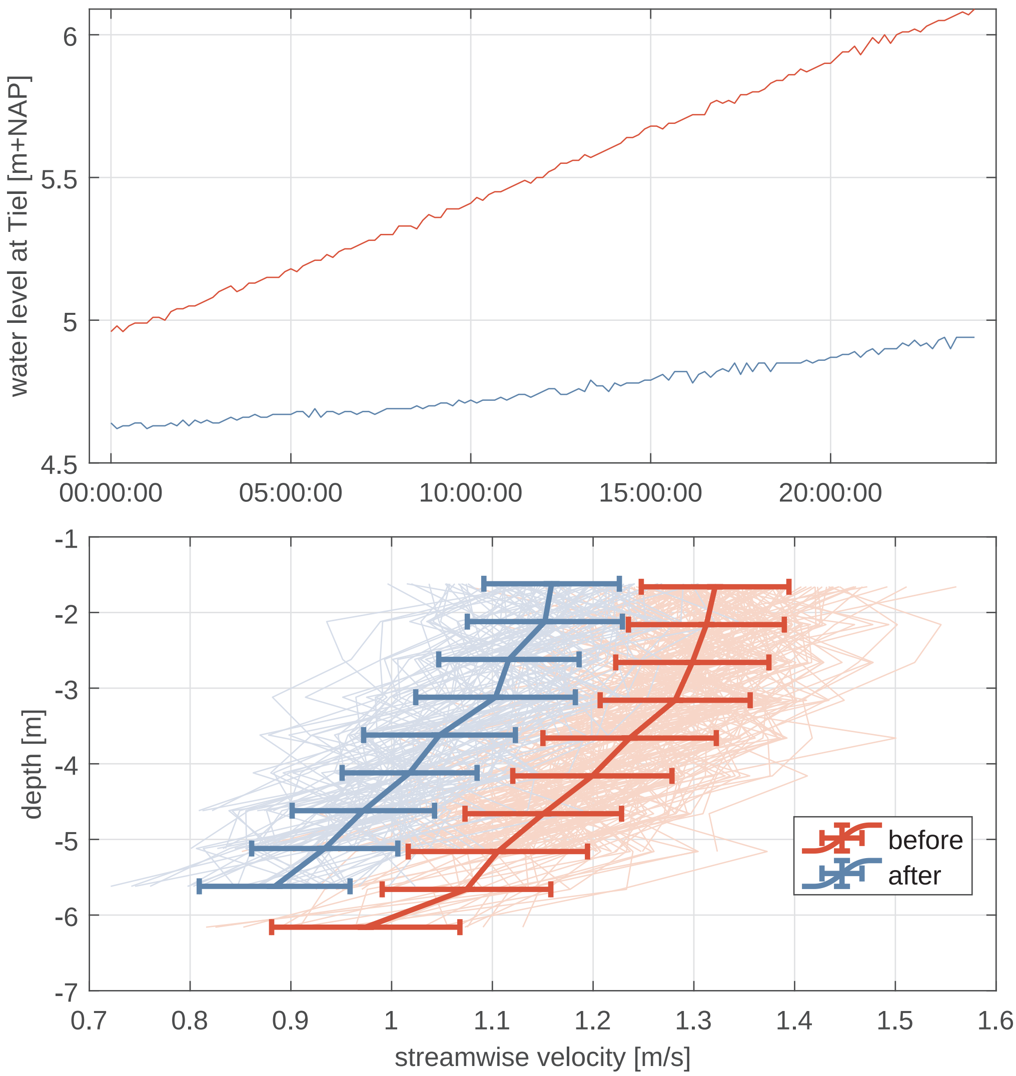

Figure D.42 Streamwise velocity at the central 100 m of channel before (01-02-13, discharge at Lobith at 12:00 equal to 3436 m^3/s, rkm 922.100) and after (15-01-19, discharge at Lobith at 12:00 equal to 2590 m^3/s, rkm 921.300)

D.3.3 Condition 3

D.3.3.1 Location 1

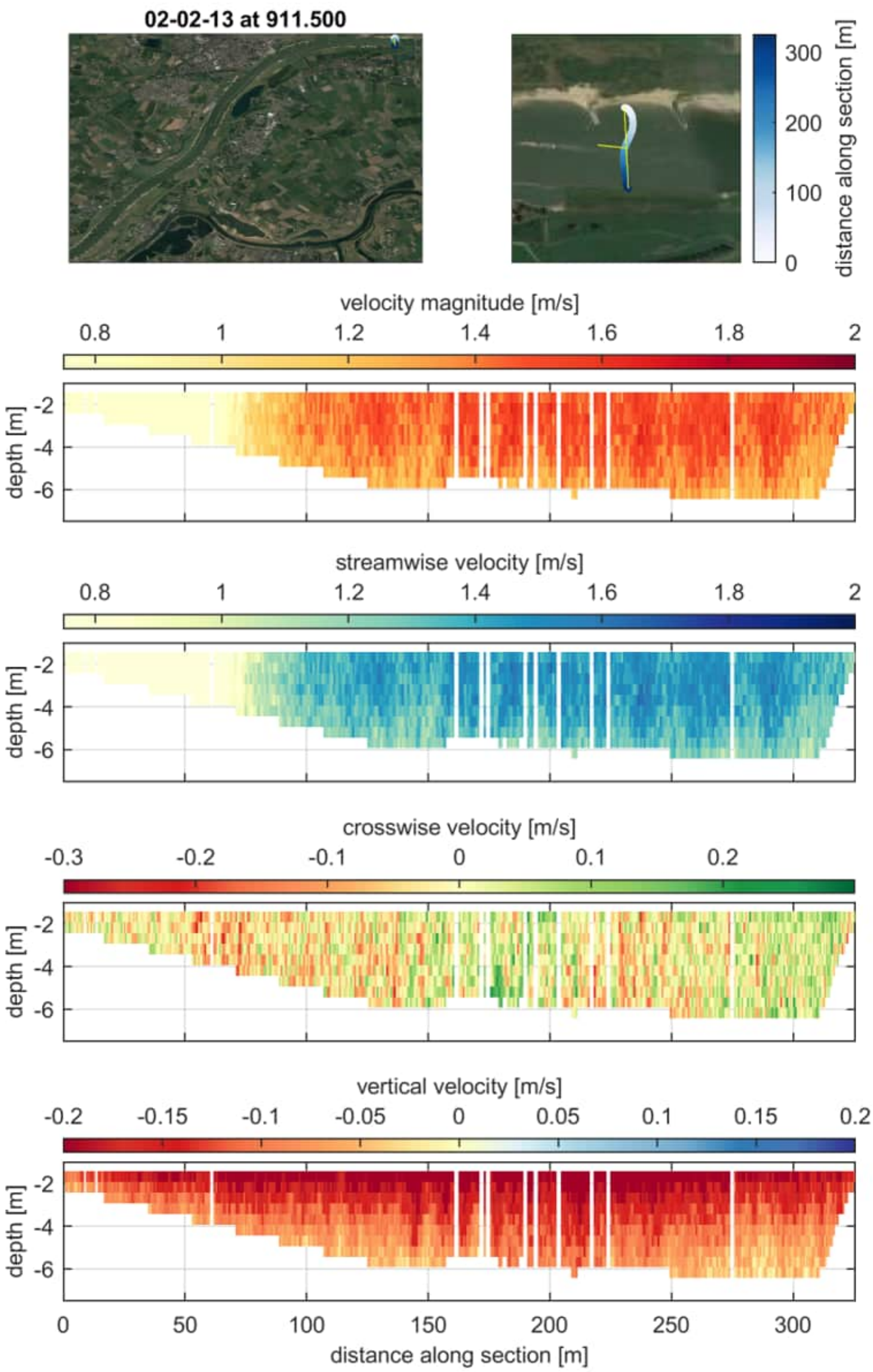

Figure D.43 Cross-sectional measurements on 02-02-13 (discharge at Lobith at 12:00 equal to 4170 m^3/s) at rkm 911.500 projected on measurement plane.

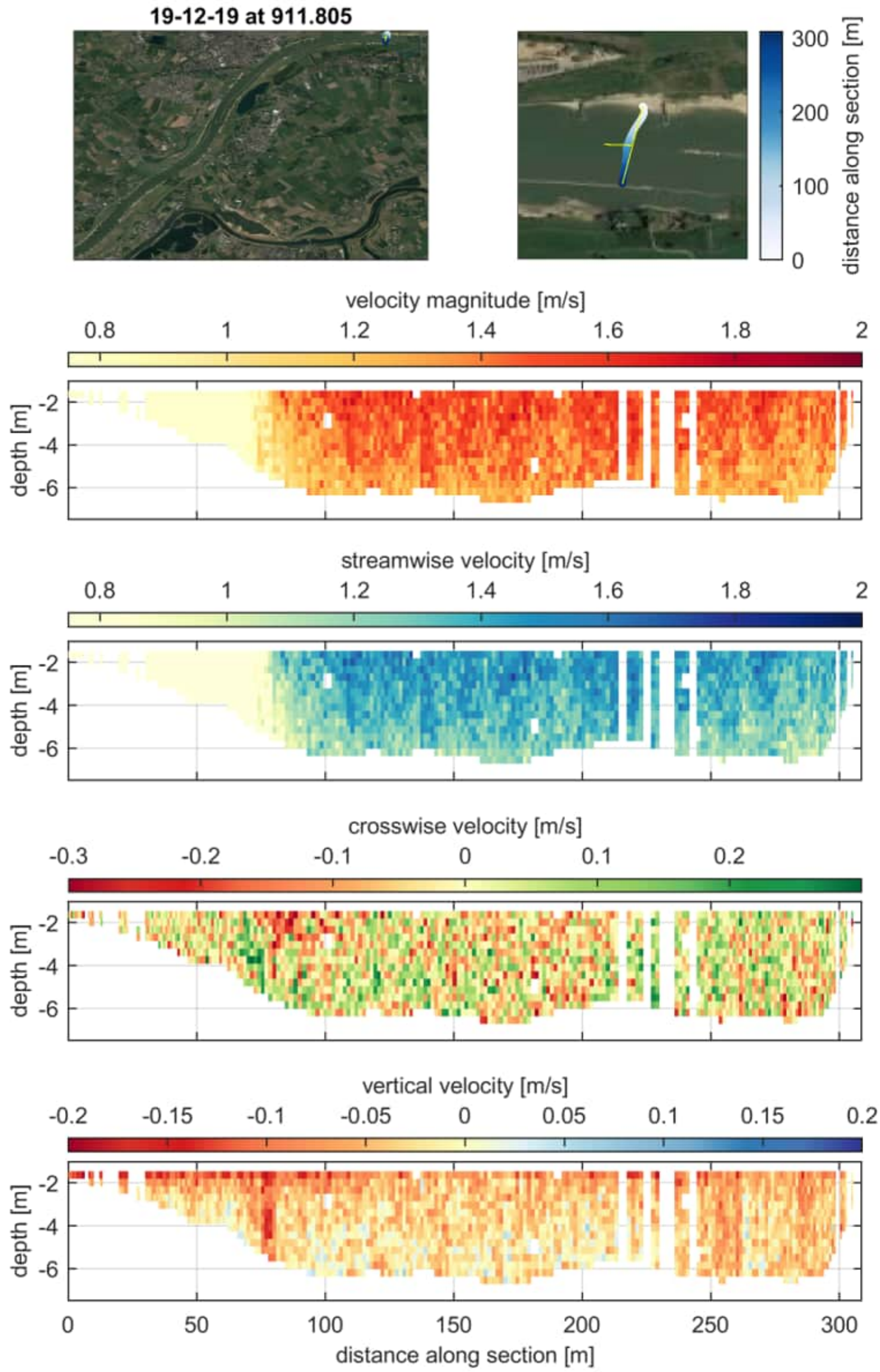

Figure D.44 Cross-sectional measurements on 19-12-19 (discharge at Lobith at 12:00 equal to 3549 m^3/s) at rkm 911.805 projected on measurement plane.

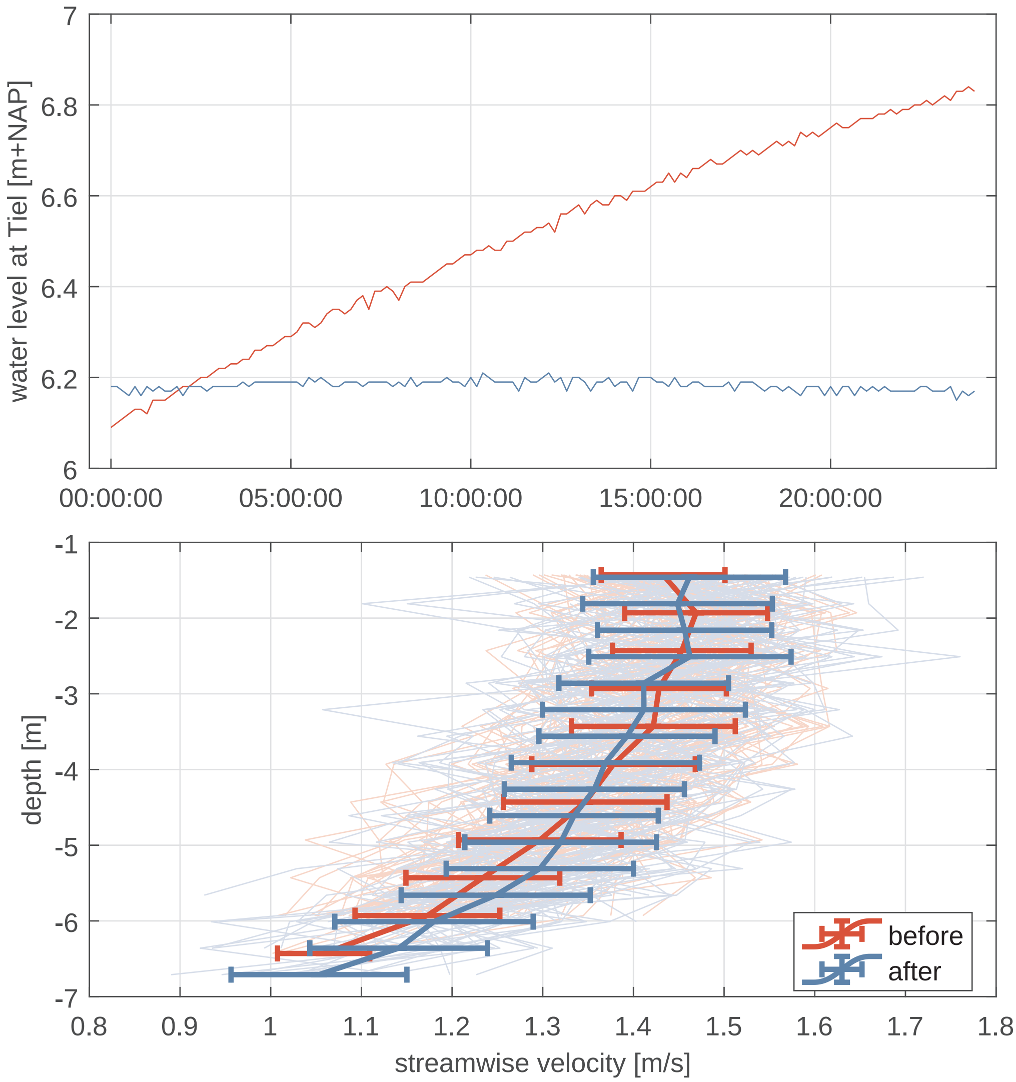

Figure D.45 Streamwise velocity at the central 100 m of channel before (02-02-13, discharge at Lobith at 12:00 equal to 4170 m^3/s, rkm 911.500) and after (19-12-19, discharge at Lobith at 12:00 equal to 3549 m^3/s, rkm 911.805)

D.3.3.2 Location 2

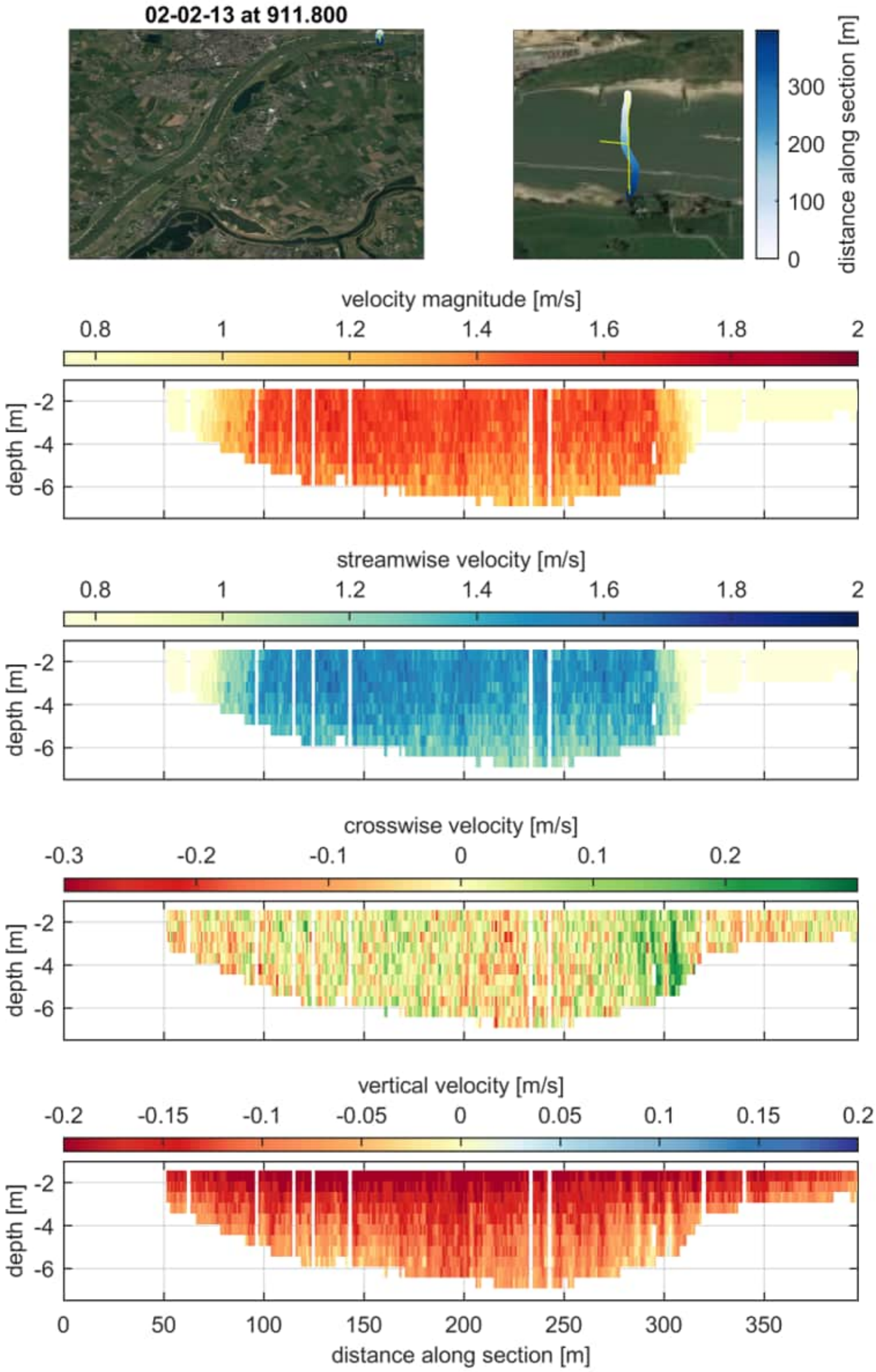

Figure D.46 Cross-sectional measurements on 02-02-13 (discharge at Lobith at 12:00 equal to 4170 m^3/s) at rkm 911.800 projected on measurement plane.

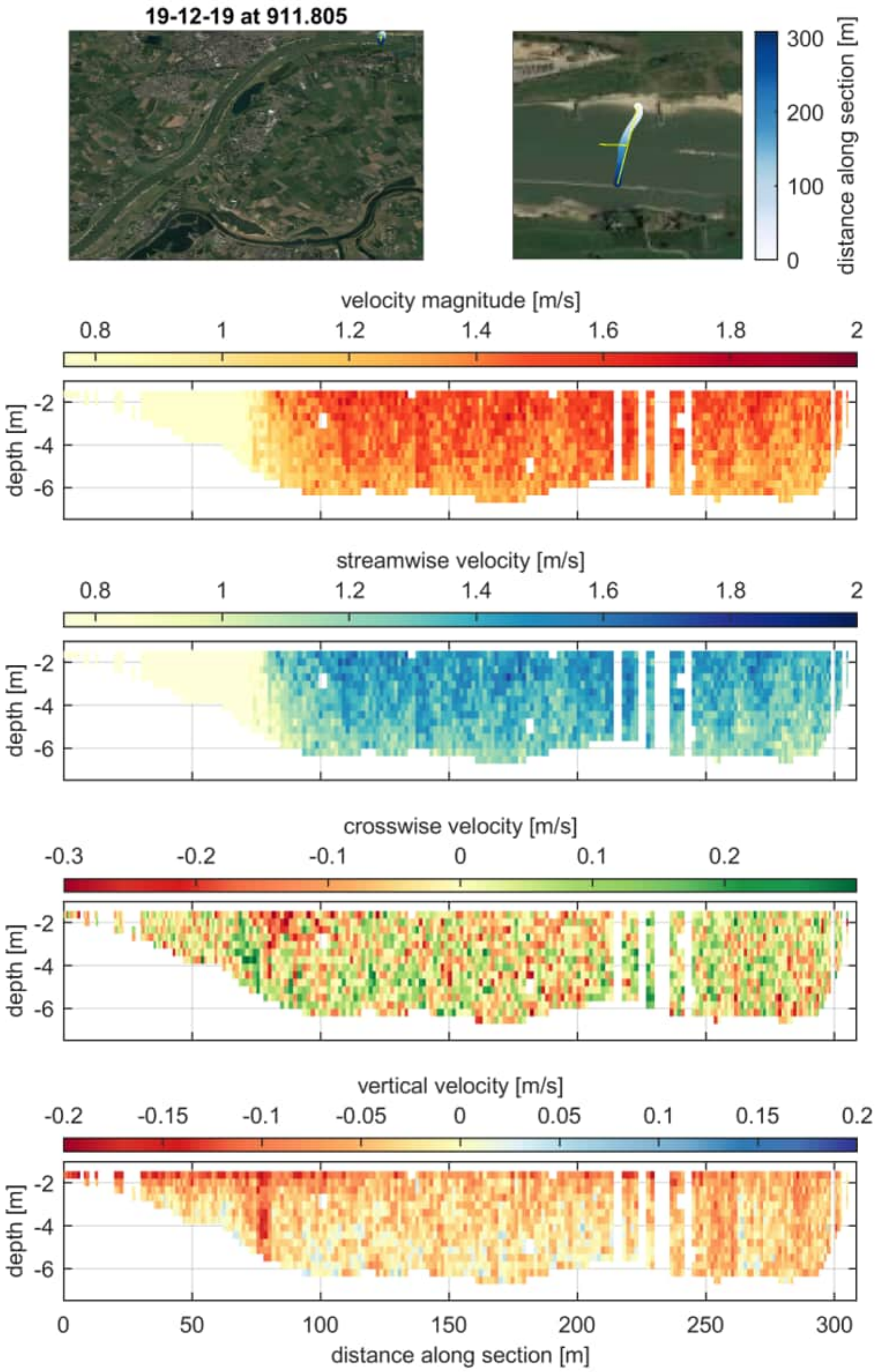

Figure D.47 Cross-sectional measurements on 19-12-19 (discharge at Lobith at 12:00 equal to 3549 m^3/s) at rkm 911.805 projected on measurement plane.

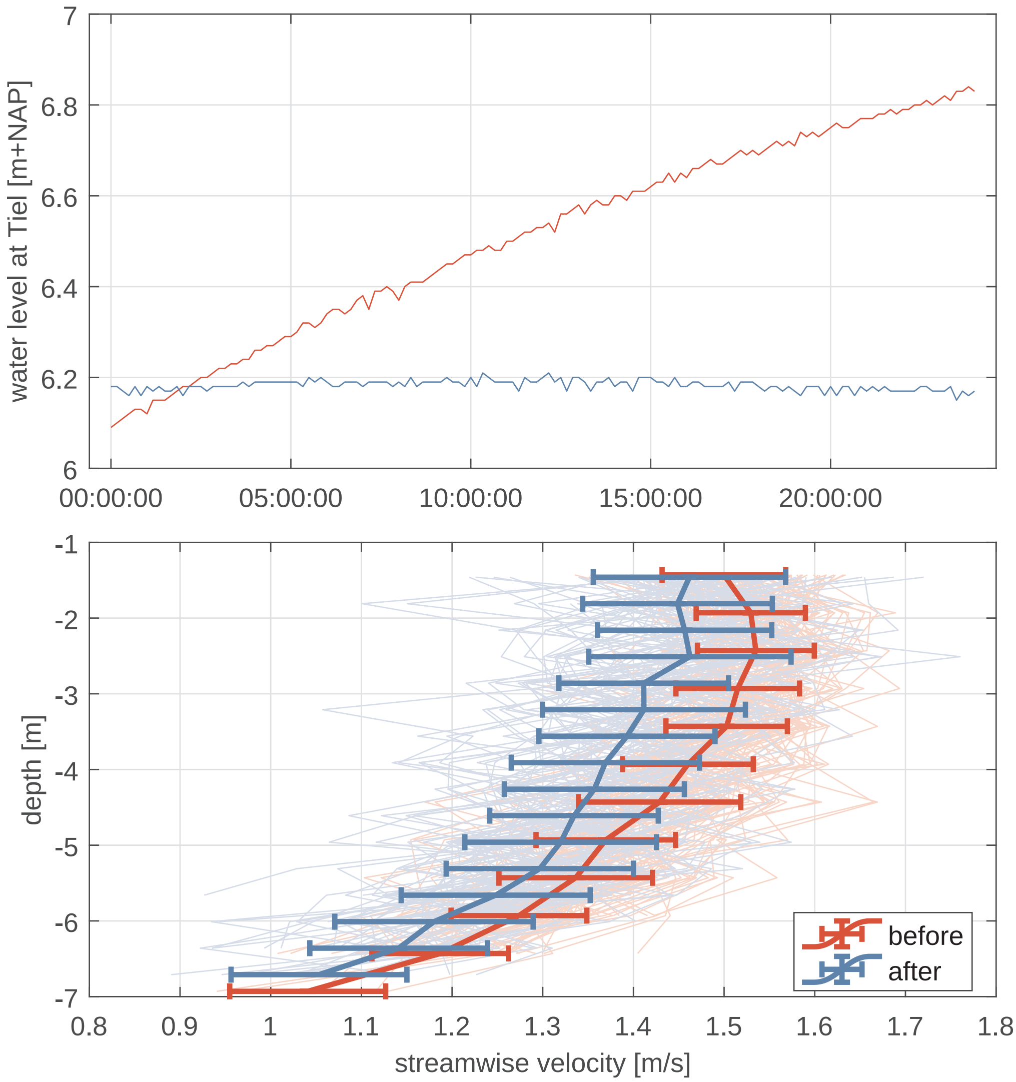

Figure D.48 Streamwise velocity at the central 100 m of channel before (02-02-13, discharge at Lobith at 12:00 equal to 4170 m^3/s, rkm 911.800) and after (19-12-19, discharge at Lobith at 12:00 equal to 3549 m^3/s, rkm 911.805)

D.3.3.3 Location 3

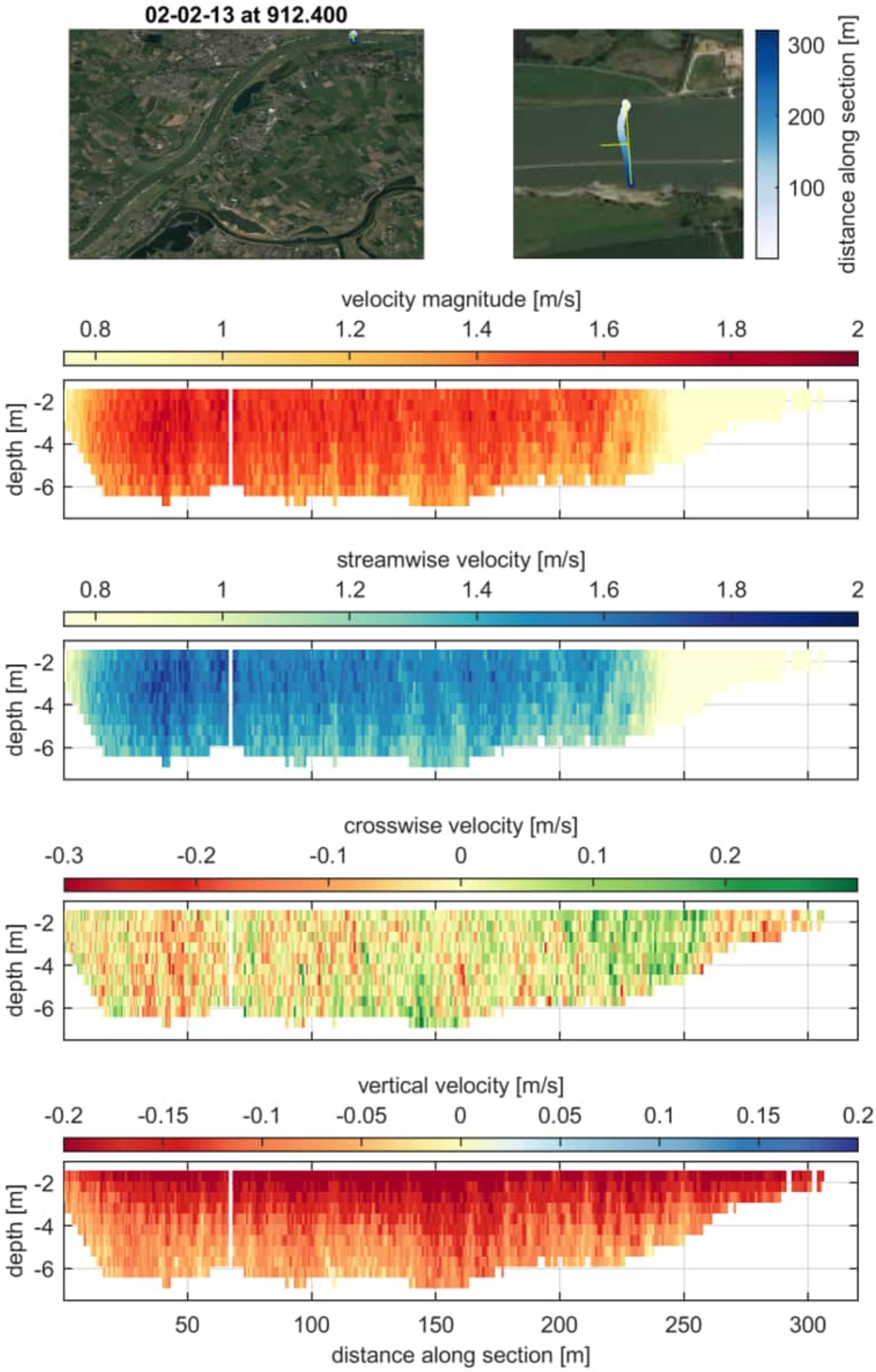

Figure D.49 Cross-sectional measurements on 02-02-13 (discharge at Lobith at 12:00 equal to 4170 m^3/s) at rkm 912.400 projected on measurement plane.

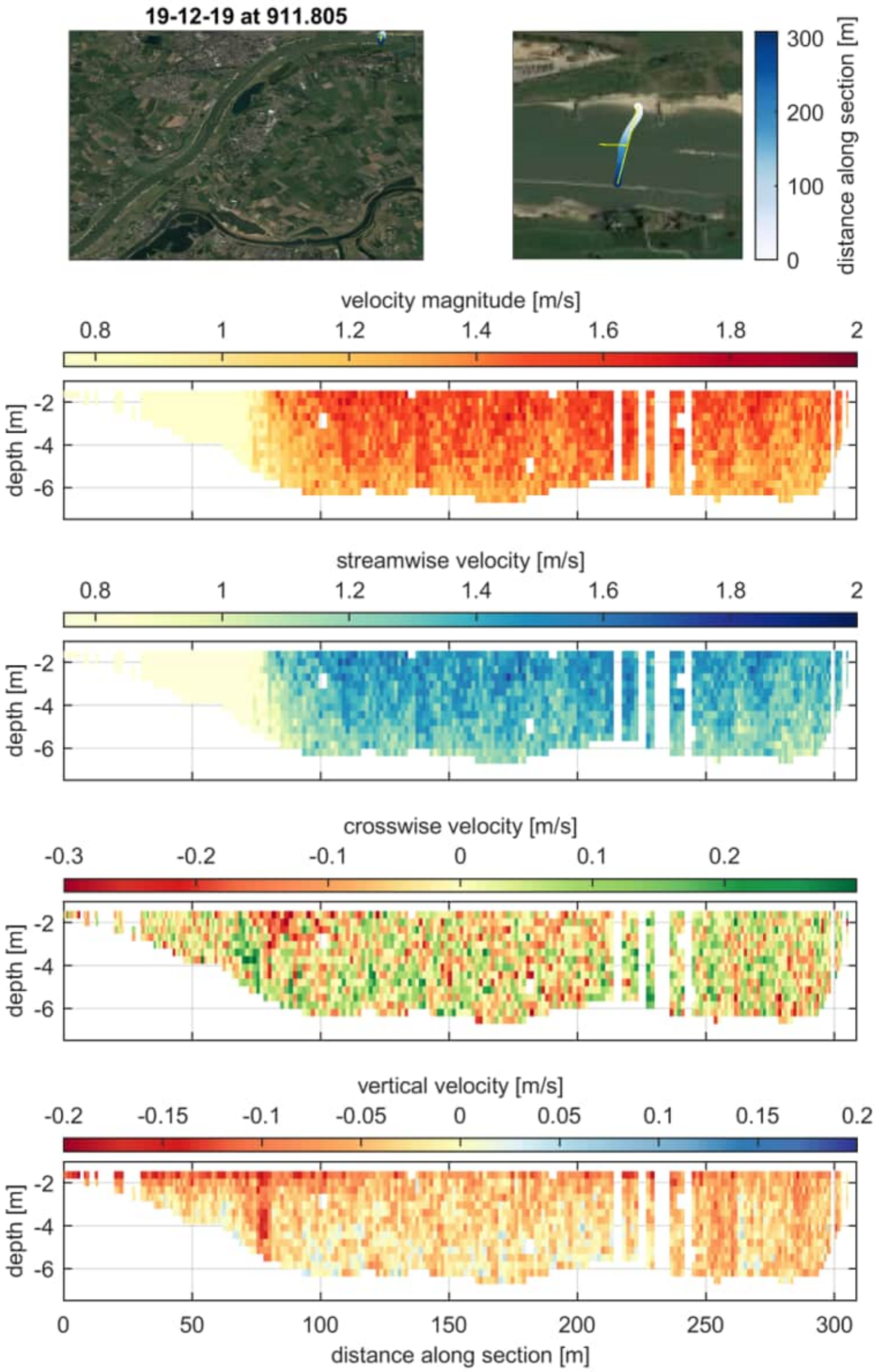

Figure D.50 Cross-sectional measurements on 19-12-19 (discharge at Lobith at 12:00 equal to 3549 m^3/s) at rkm 911.805 projected on measurement plane.

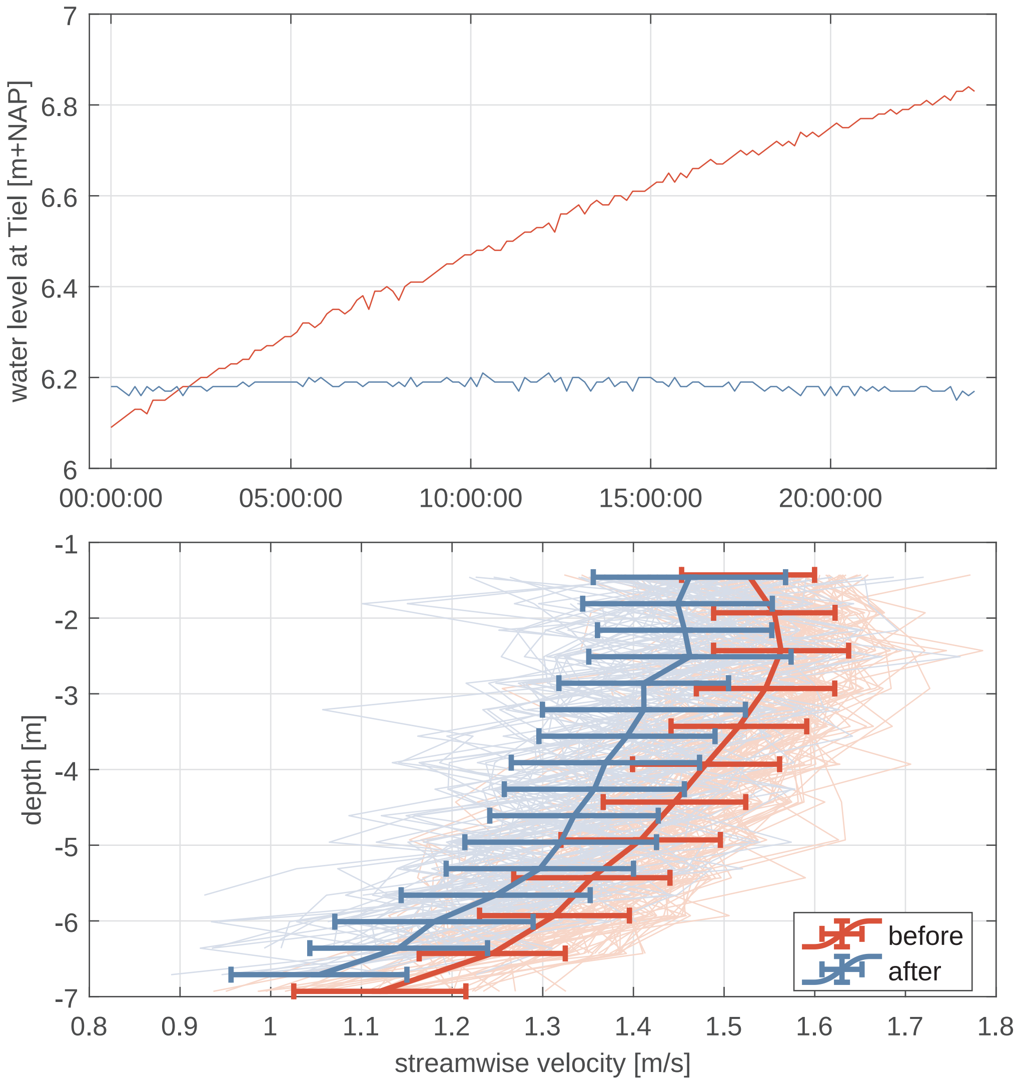

Figure D.51 Streamwise velocity at the central 100 m of channel before (02-02-13, discharge at Lobith at 12:00 equal to 4170 m^3/s, rkm 912.400) and after (19-12-19, discharge at Lobith at 12:00 equal to 3549 m^3/s, rkm 911.805)

Deltares

D.3.3.4 Location 4

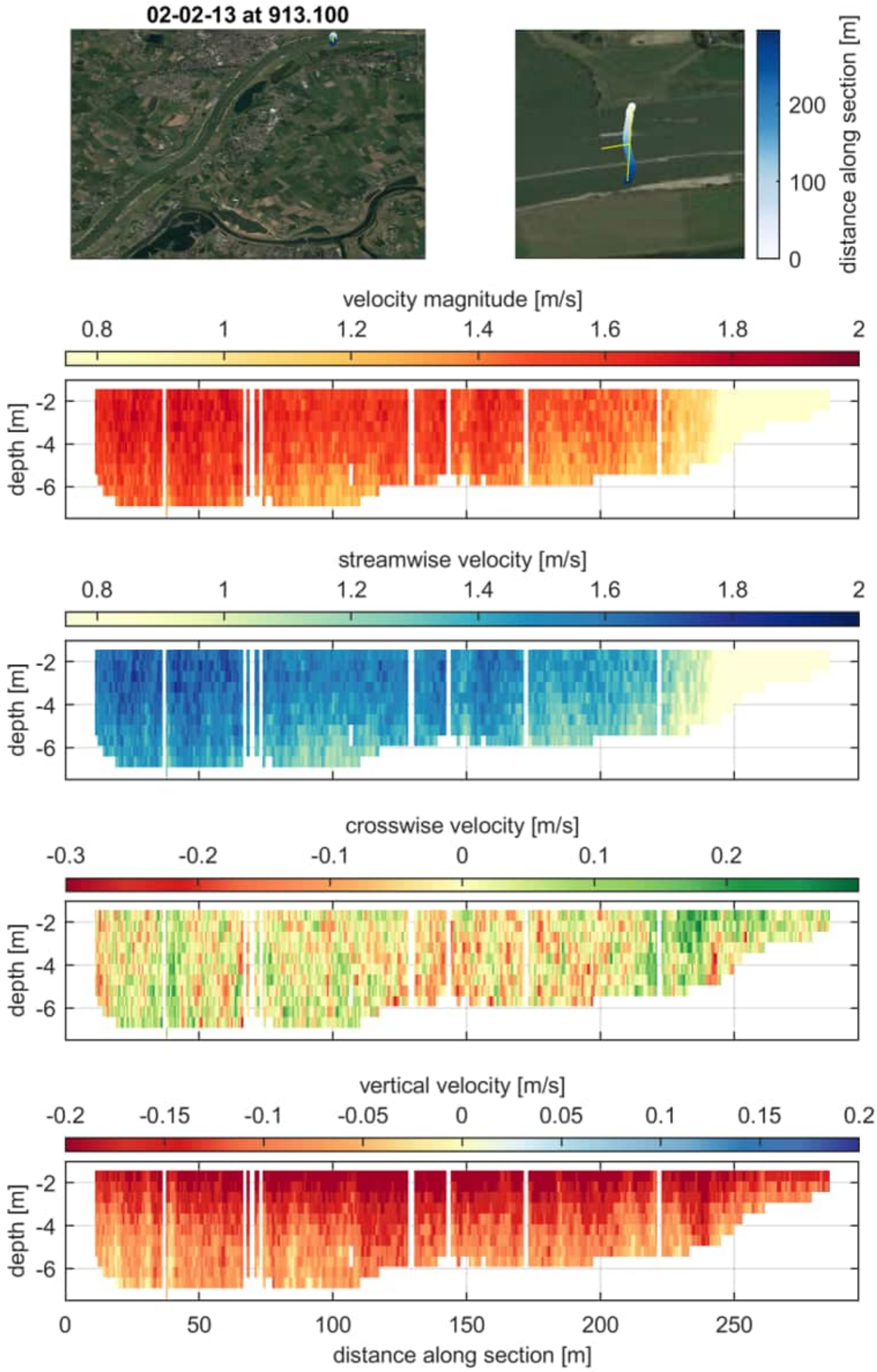

Figure D.52 Cross-sectional measurements on 02-02-13 (discharge at Lobith at 12:00 equal to 4170 m^3/s) at rkm 913.100 projected on measurement plane.

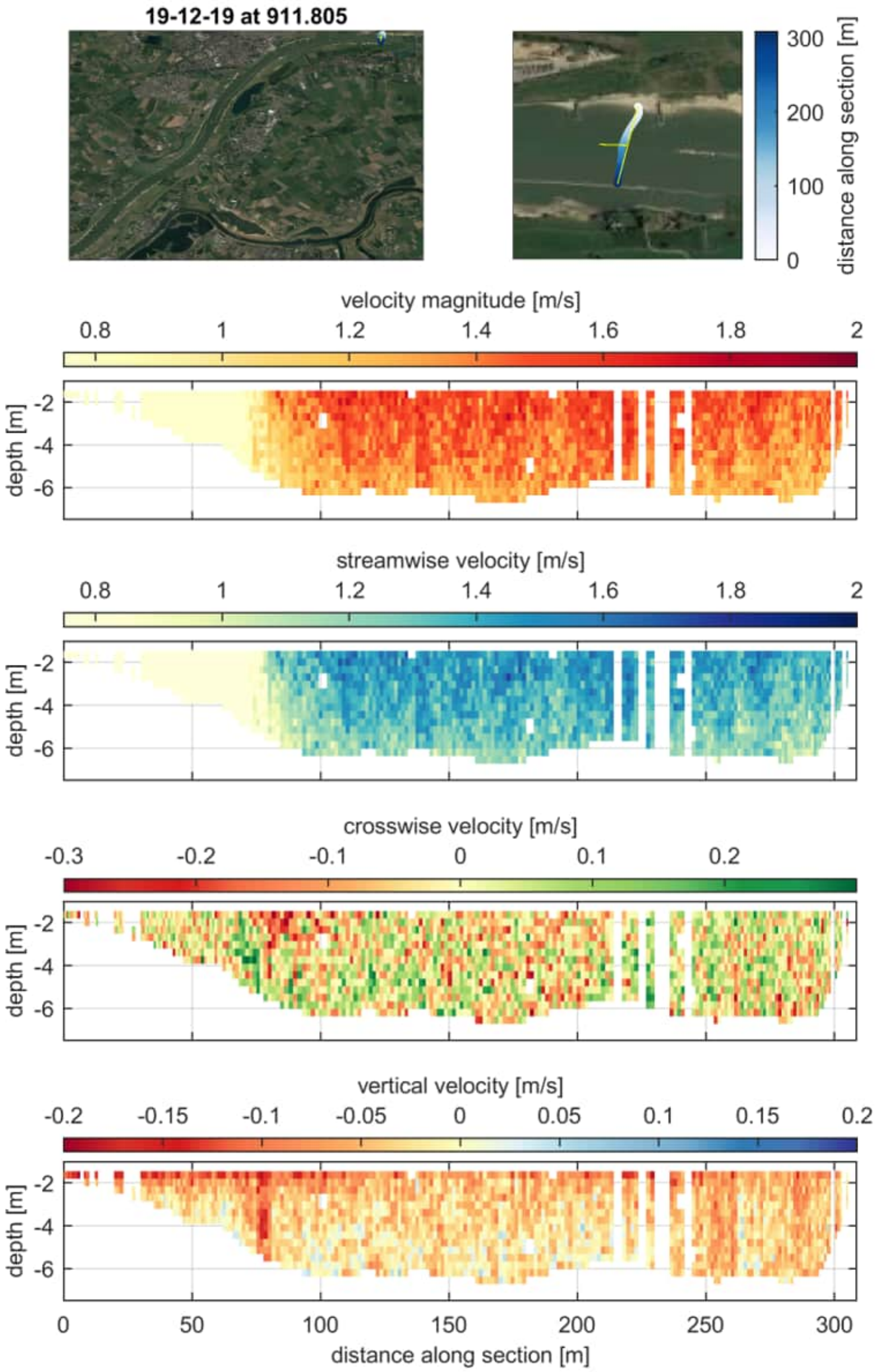

Figure D.53 Cross-sectional measurements on 19-12-19 (discharge at Lobith at 12:00 equal to 3549 m^3/s) at rkm 911.805 projected on measurement plane.

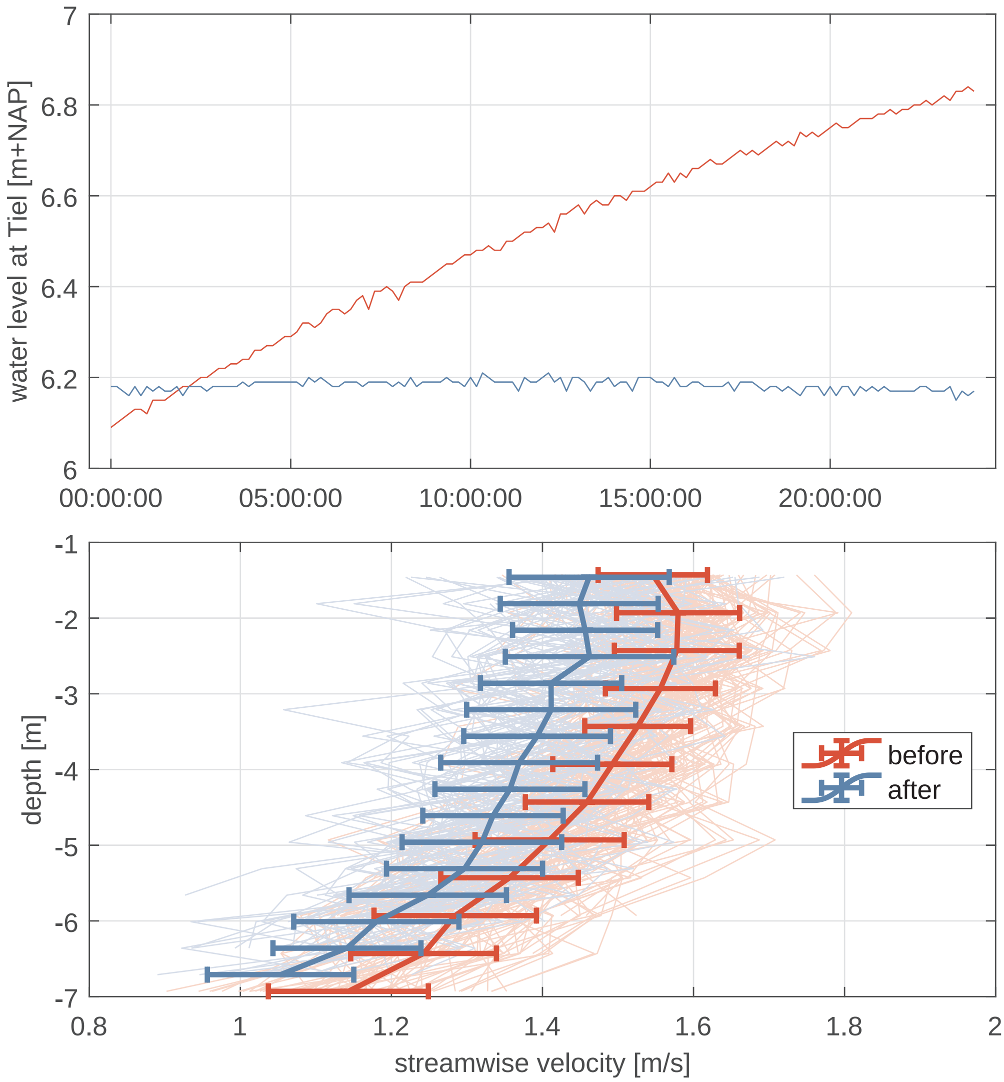

Figure D.54 Streamwise velocity at the central 100 m of channel before (02-02-13, discharge at Lobith at 12:00 equal to 4170 m^3/s, rkm 913.100) and after (19-12-19, discharge at Lobith at 12:00 equal to 3549 m^3/s, rkm 911.805)

D.3.3.5 Location 5

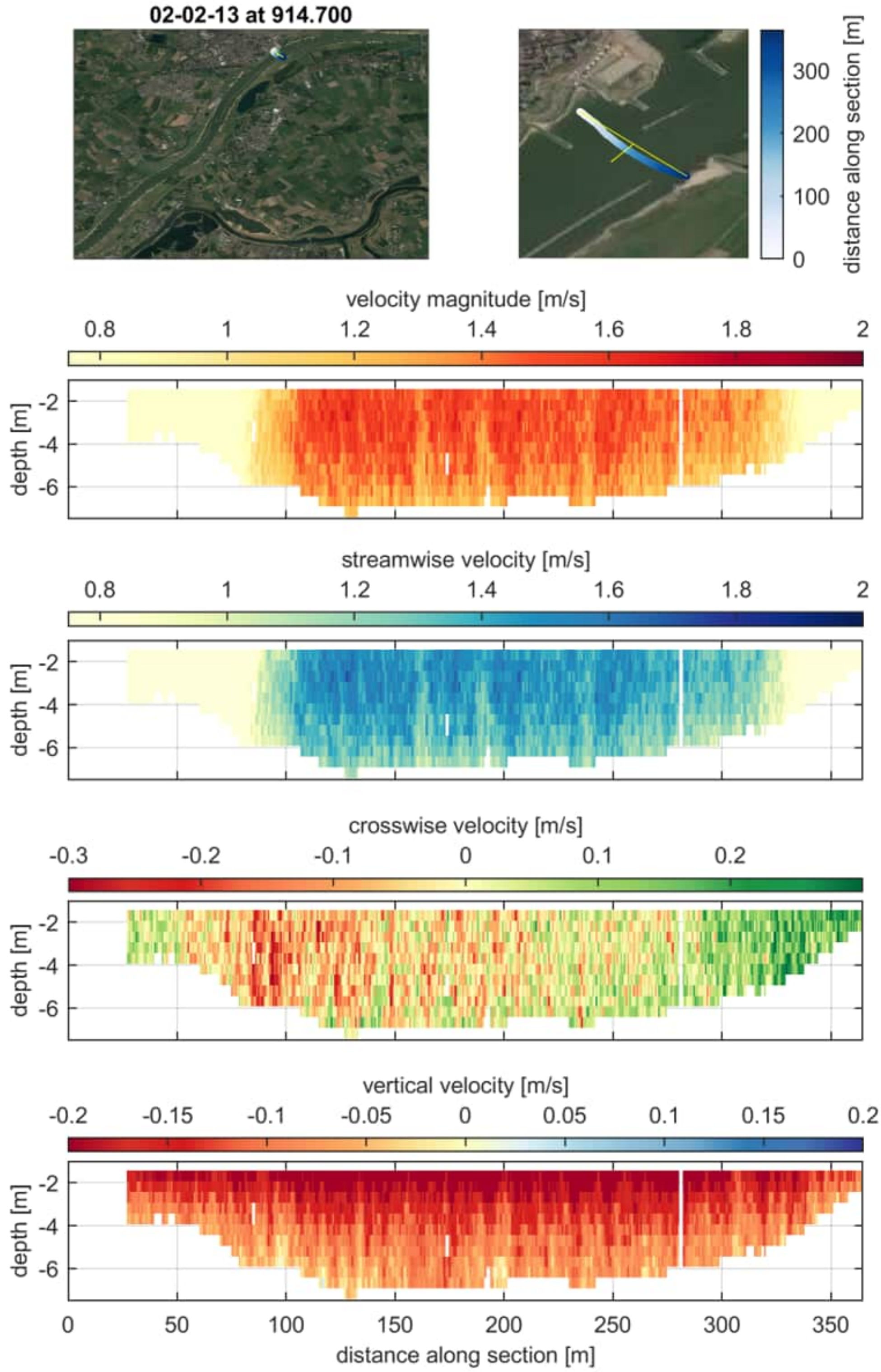

Figure D.55 Cross-sectional measurements on 02-02-13 (discharge at Lobith at 12:00 equal to 4170 m^3/s) at rkm 914.700 projected on measurement plane.

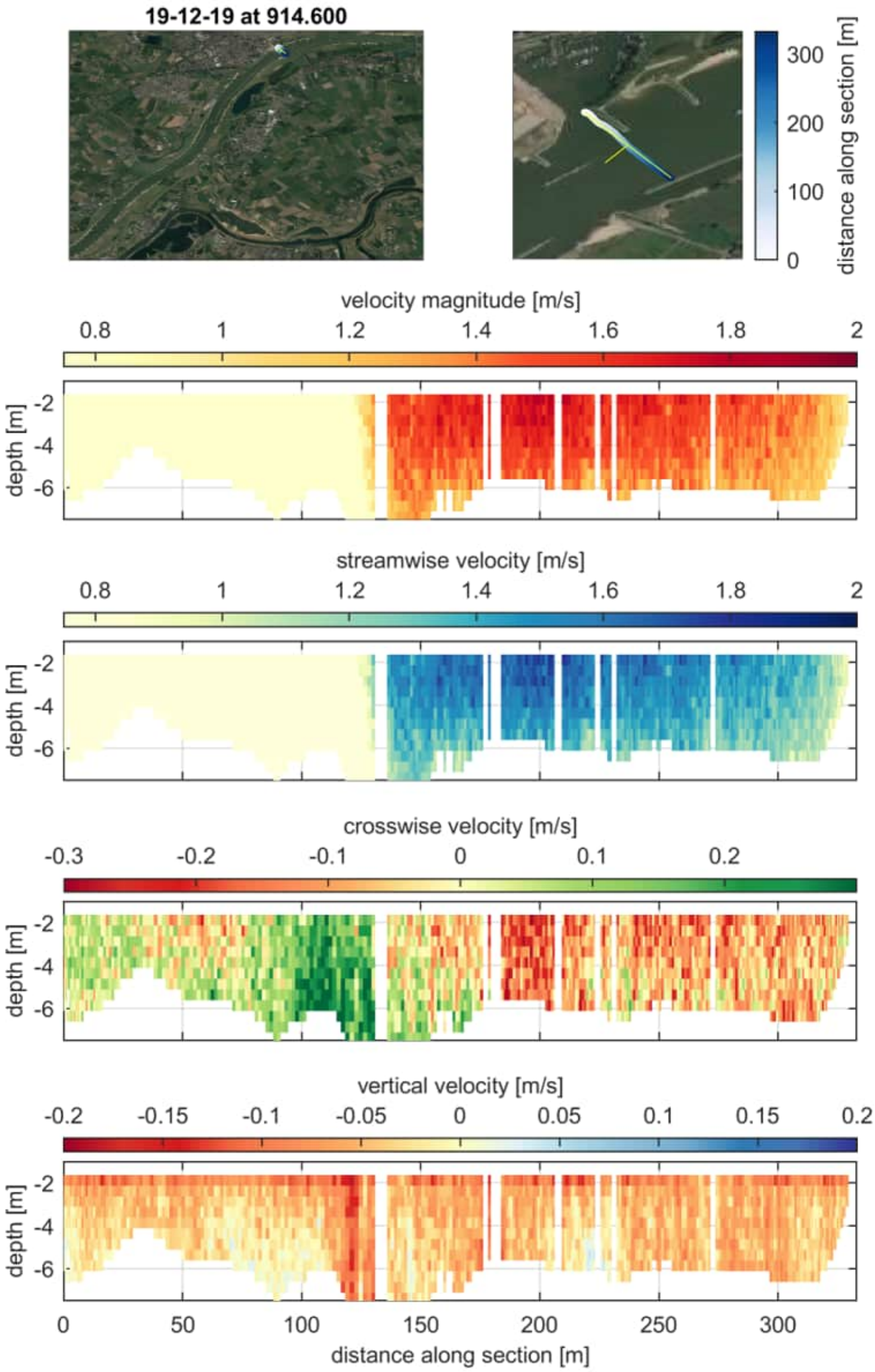

Figure D.56 Cross-sectional measurements on 19-12-19 (discharge at Lobith at 12:00 equal to 3549 m^3/s) at rkm 914.600 projected on measurement plane.

Deltares

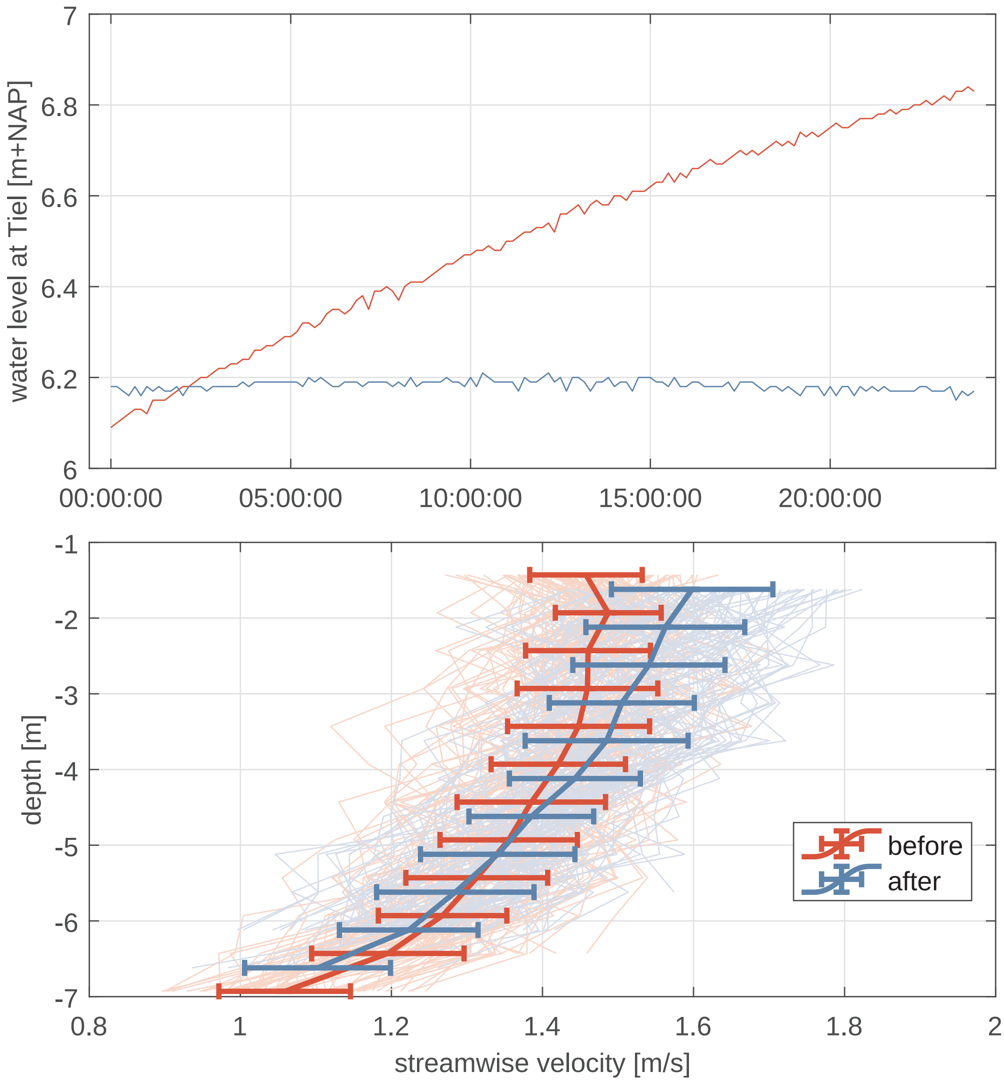

Figure D.57 Streamwise velocity at the central 100 m of channel before (02-02-13, discharge at Lobith at 12:00 equal to 4170 m^3/s, rkm 914.700) and after (19-12-19, discharge at Lobith at 12:00 equal to 3549 m^3/s, rkm 914.600)

D.3.3.6 Location 6

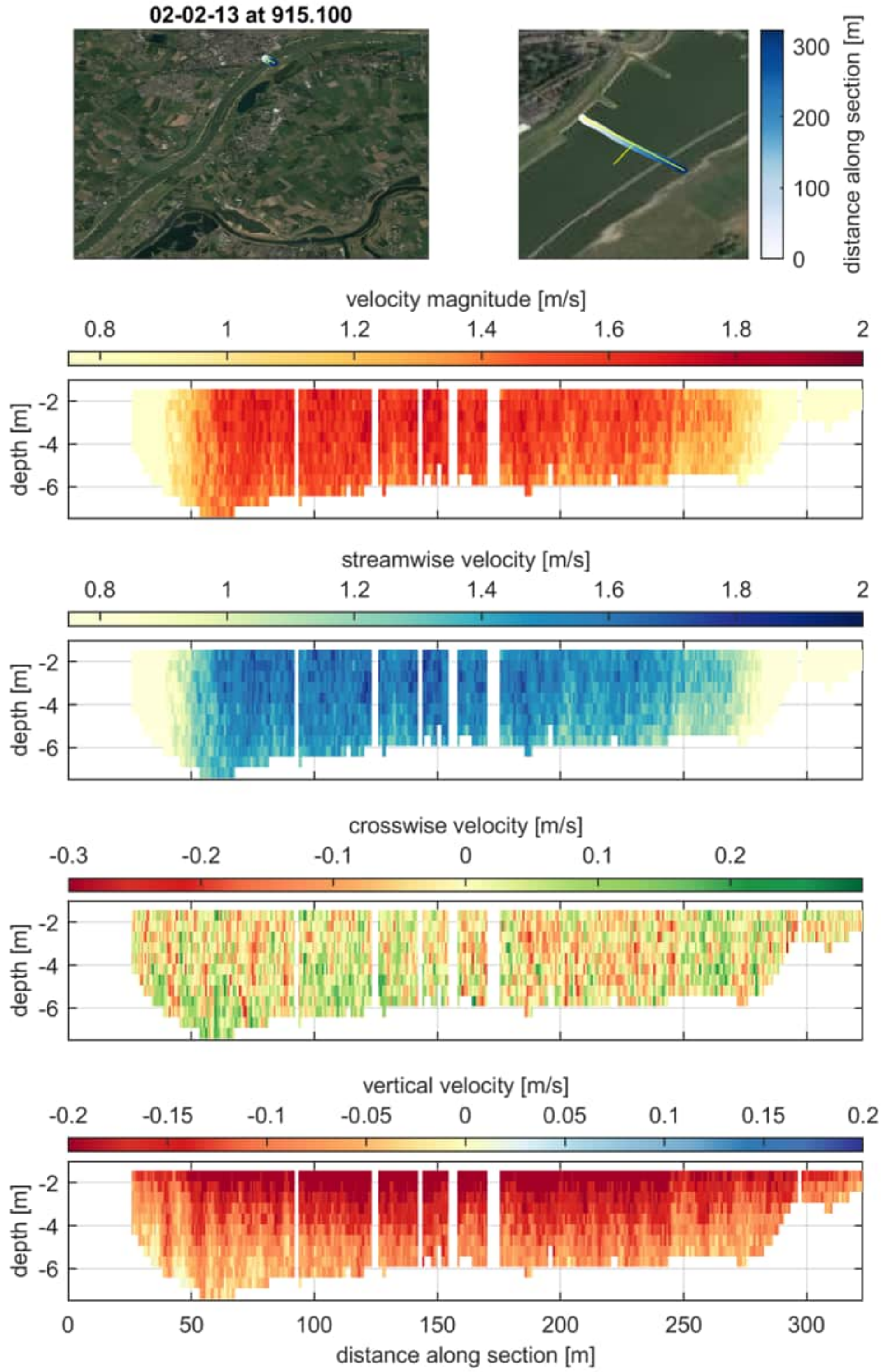

Figure D.58 Cross-sectional measurements on 02-02-13 (discharge at Lobith at 12:00 equal to 4170 m^3/s) at rkm 915.100 projected on measurement plane.

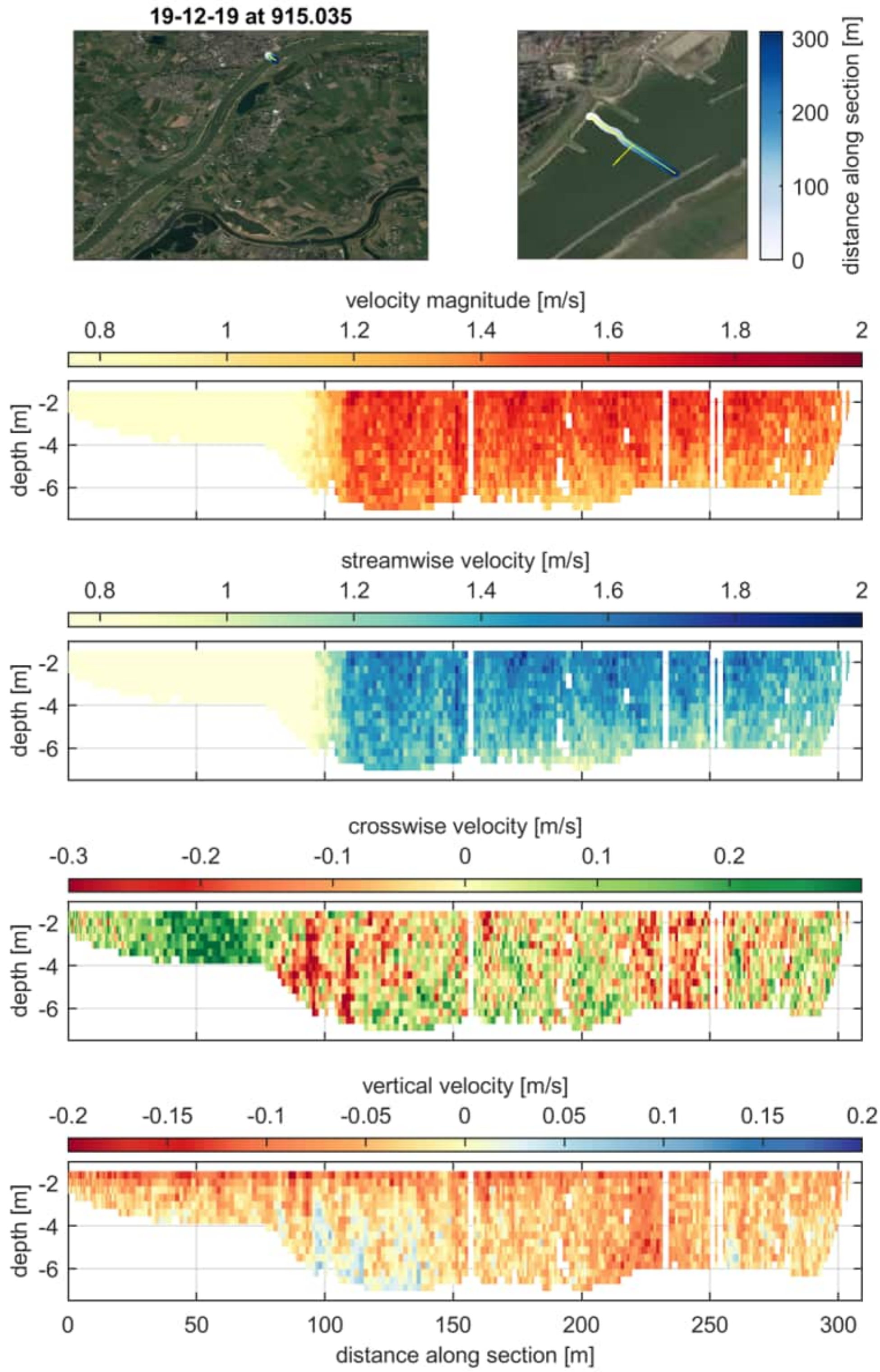

Figure D.59 Cross-sectional measurements on 19-12-19 (discharge at Lobith at 12:00 equal to 3549 m^3/s) at rkm 915.035 projected on measurement plane.

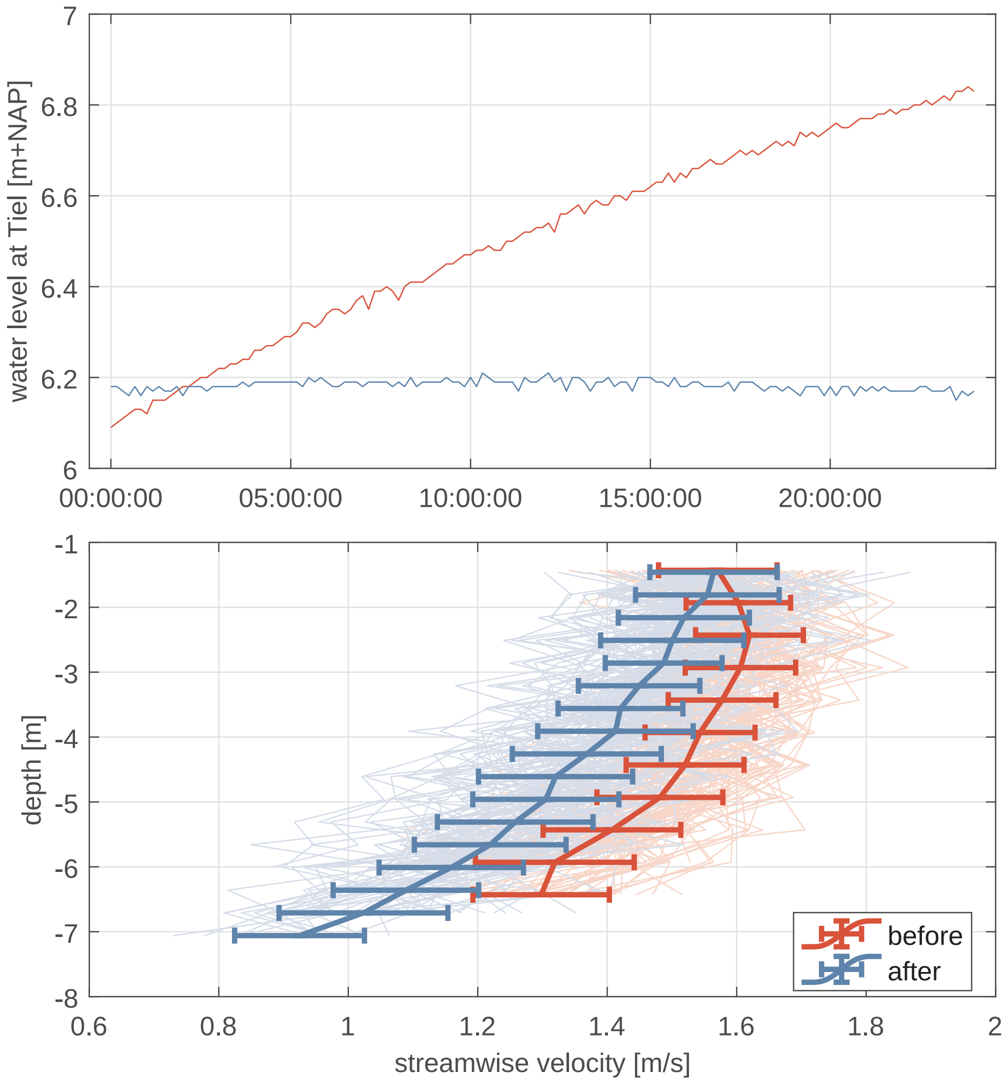

Figure D.60 Streamwise velocity at the central 100 m of channel before (02-02-13, discharge at Lobith at 12:00 equal to 4170 m^3/s, rkm 915.100) and after (19-12-19, discharge at Lobith at 12:00 equal to 3549 m^3/s, rkm 915.035)

D.3.3.7 Location 7

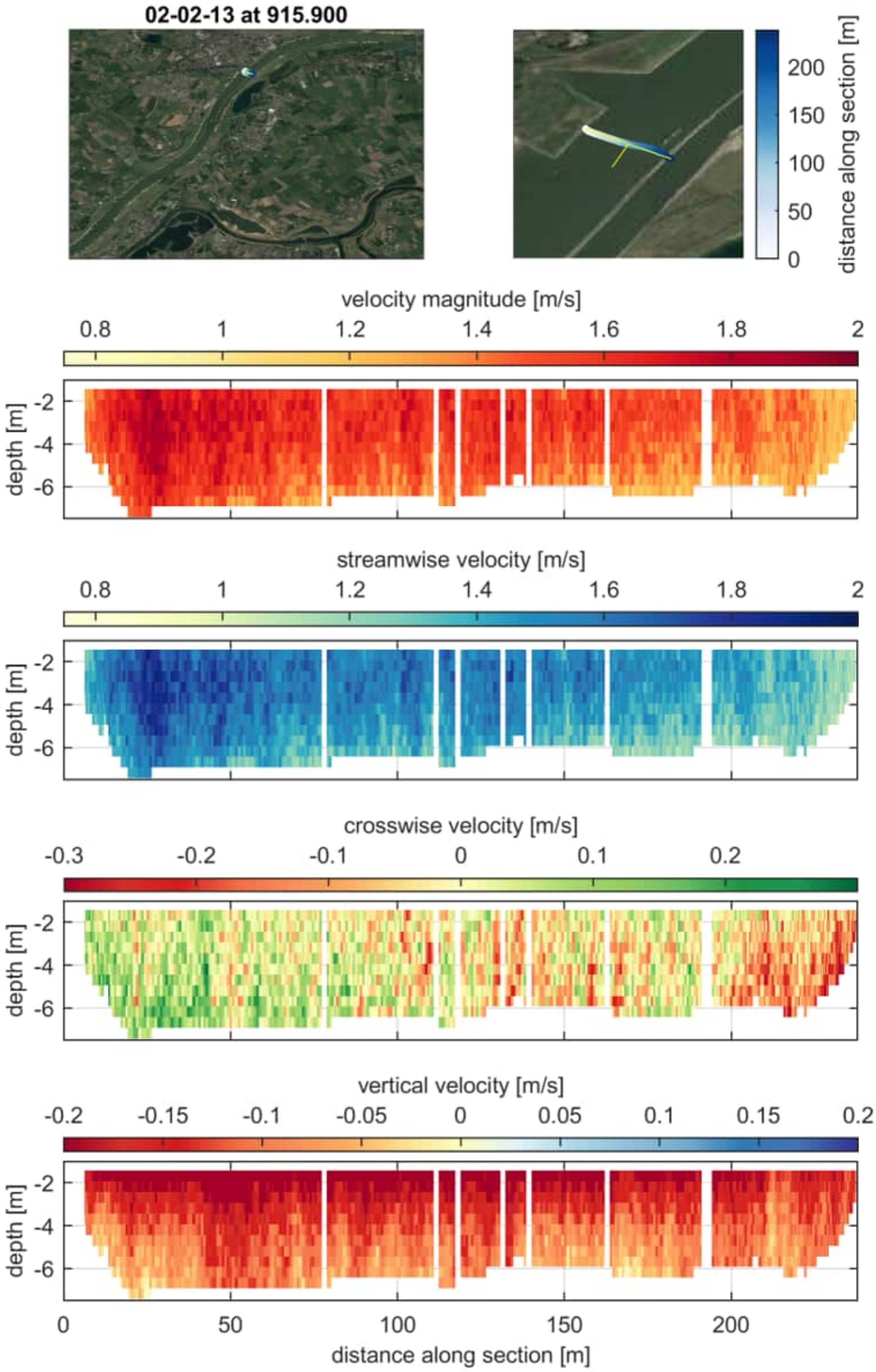

Figure D.61 Cross-sectional measurements on 02-02-13 (discharge at Lobith at 12:00 equal to 4170 m^3/s) at rkm 915.900 projected on measurement plane.

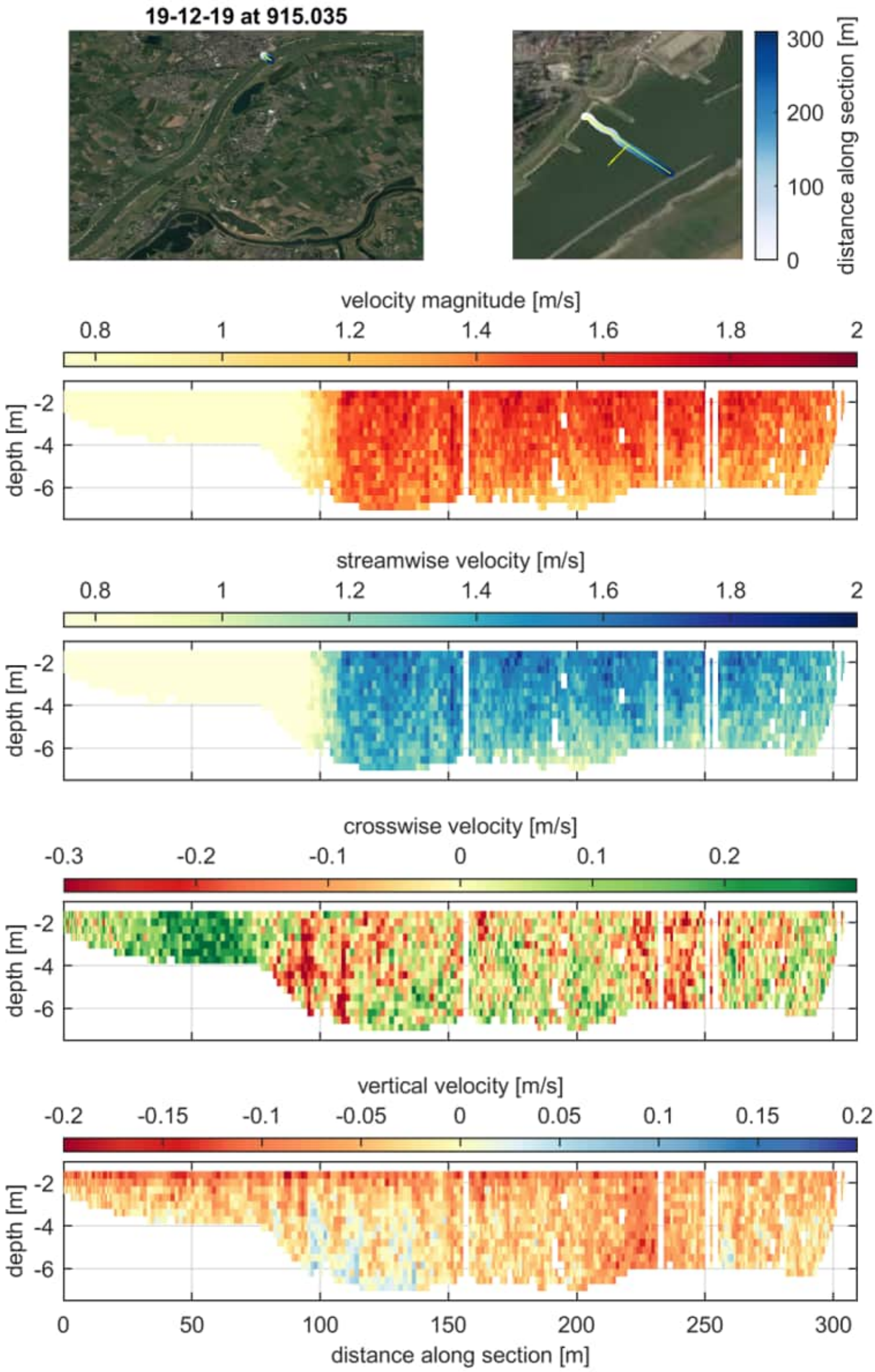

Figure D.62 Cross-sectional measurements on 19-12-19 (discharge at Lobith at 12:00 equal to 3549 m^3/s) at rkm 915.035 projected on measurement plane.

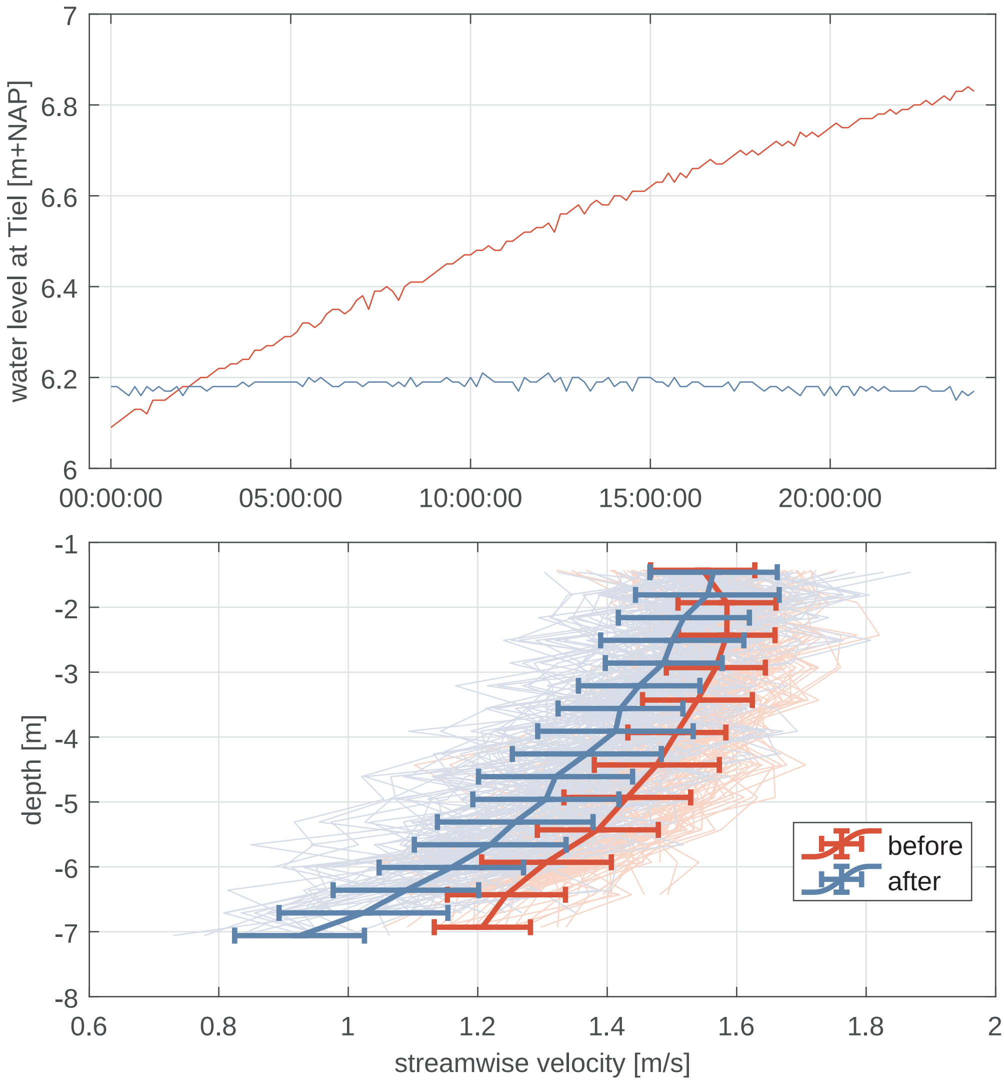

Figure D.63 Streamwise velocity at the central 100 m of channel before (02-02-13, discharge at Lobith at 12:00 equal to 4170 m^3/s, rkm 915.900) and after (19-12-19, discharge at Lobith at 12:00 equal to 3549 m^3/s, rkm 915.035)

D.3.3.8 Location 8

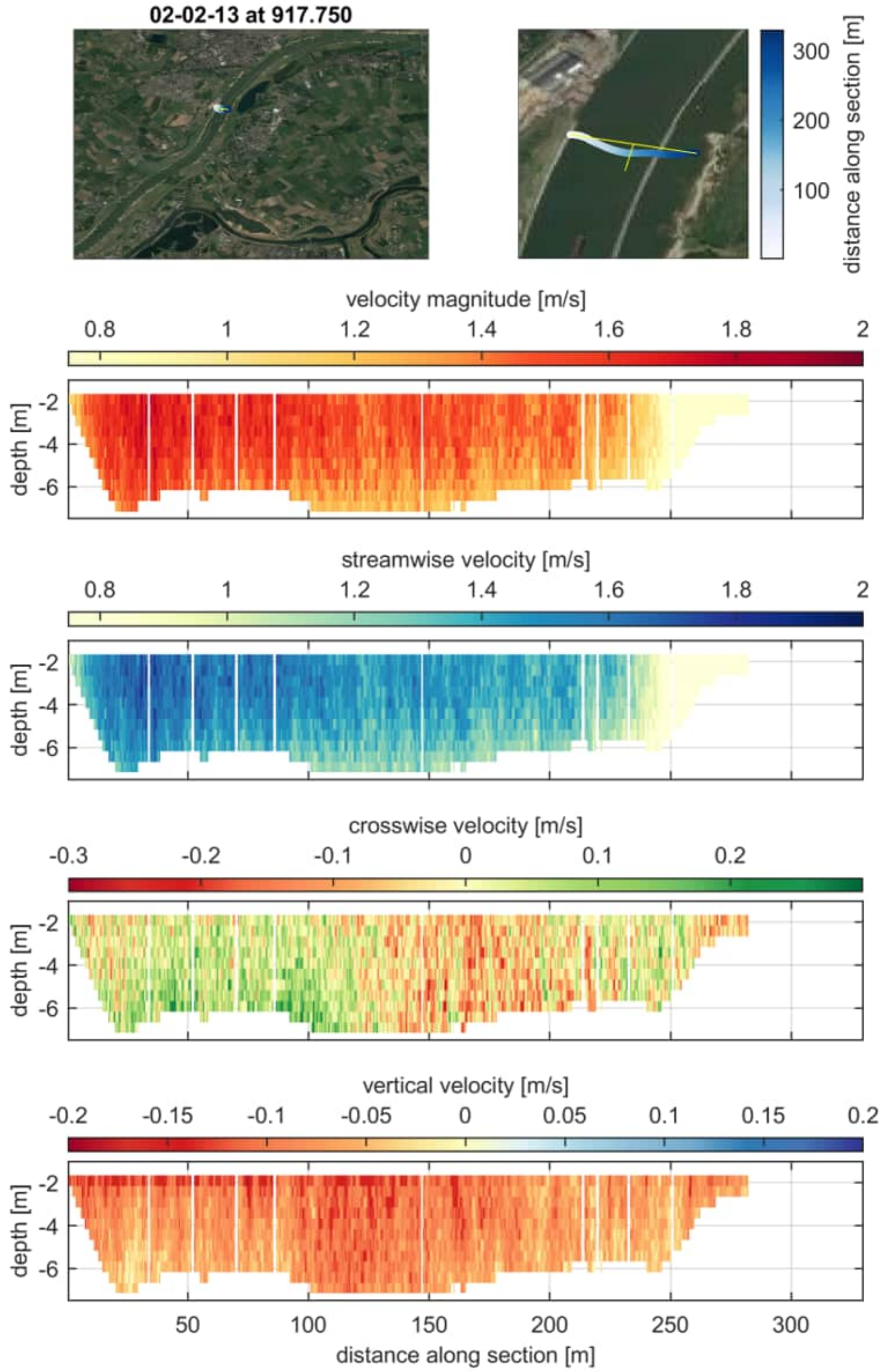

Figure D.64 Cross-sectional measurements on 02-02-13 (discharge at Lobith at 12:00 equal to 4170 m^3/s) at rkm 917.750 projected on measurement plane.

Deltares

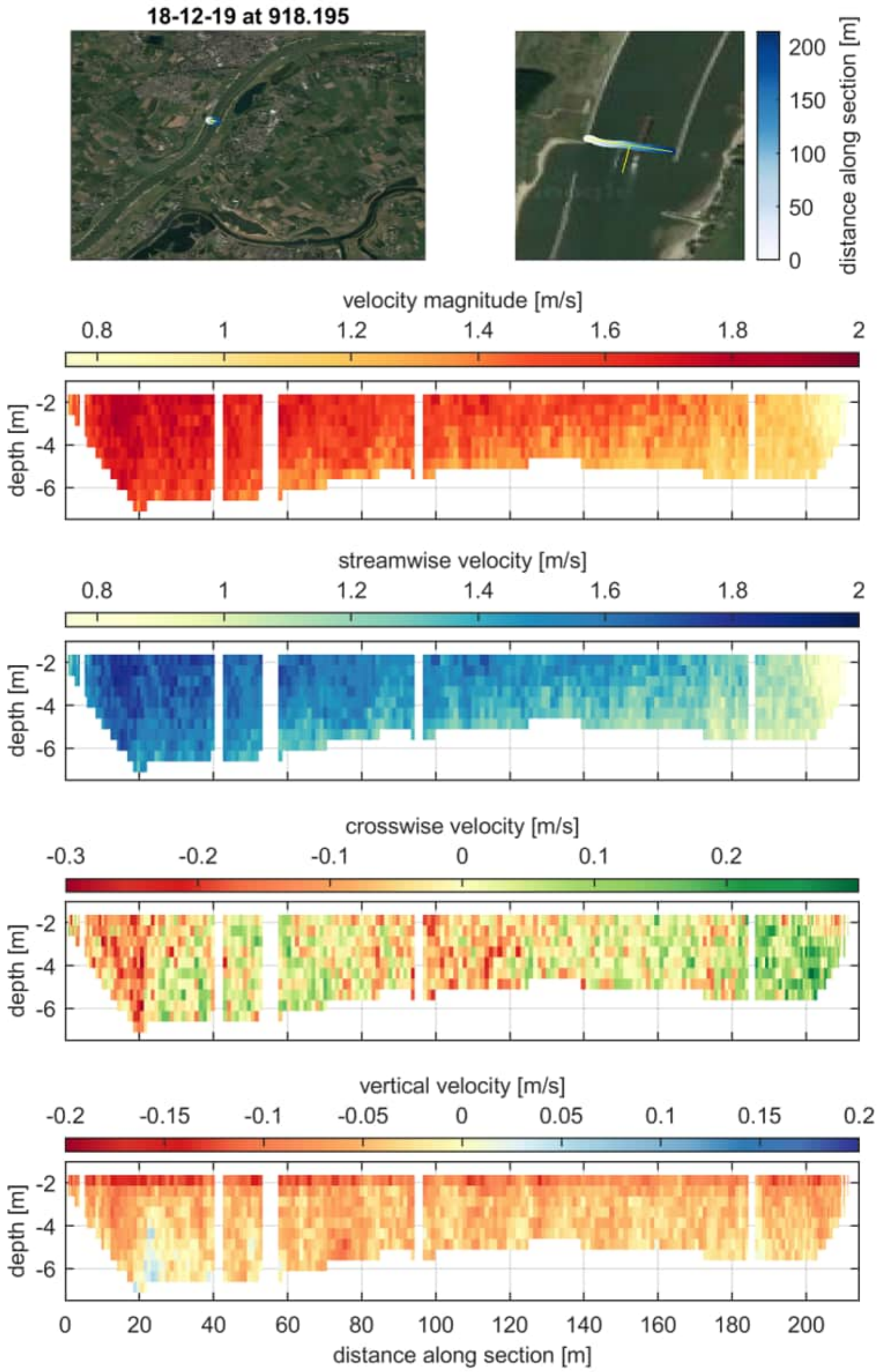

Figure D.65 Cross-sectional measurements on 18-12-19 (discharge at Lobith at 12:00 equal to 3565 m^3/s) at rkm 918.195 projected on measurement plane.

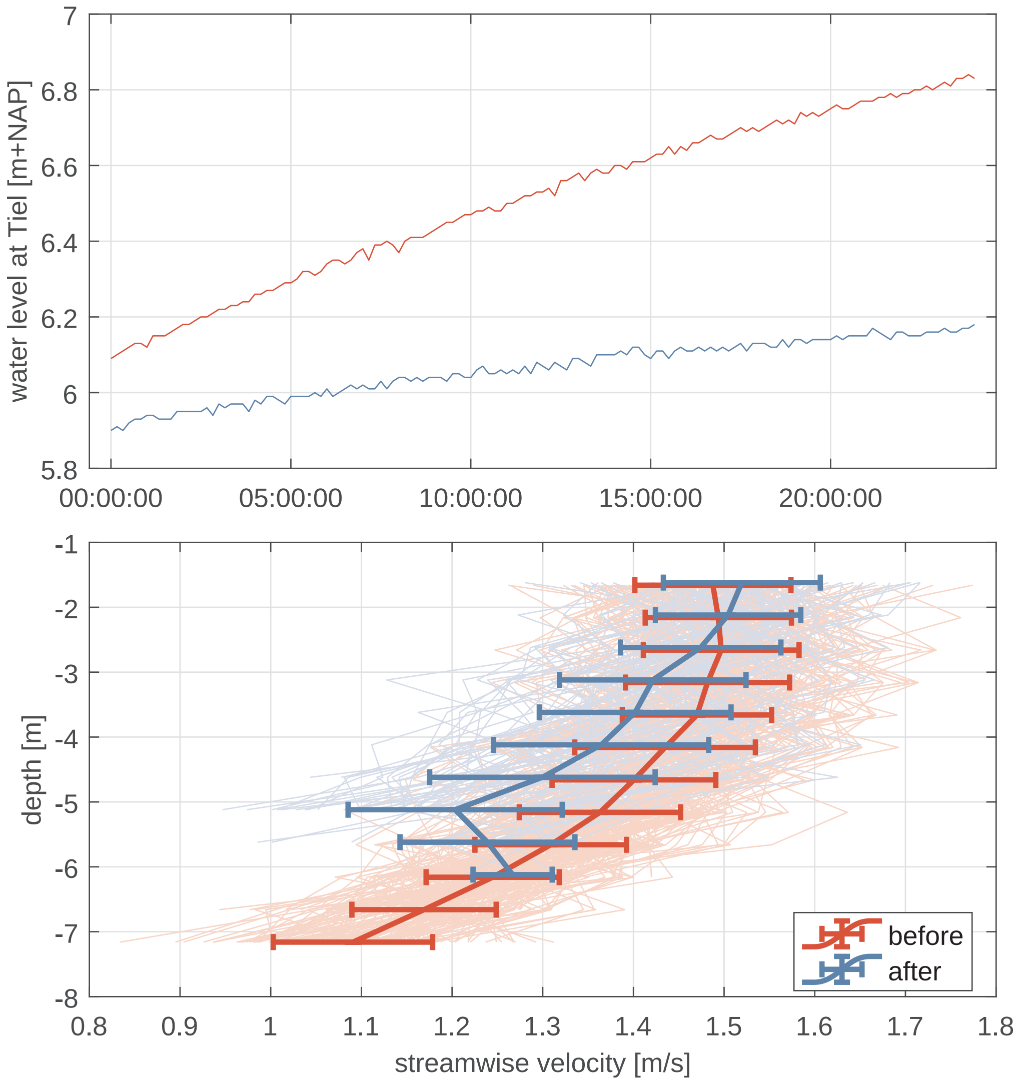

Figure D.66 Streamwise velocity at the central 100 m of channel before (02-02-13, discharge at Lobith at 12:00 equal to 4170 m^3/s, rkm 917.750) and after (18-12-19, discharge at Lobith at 12:00 equal to 3565 m^3/s, rkm 918.195)

D.3.3.9 Location 9

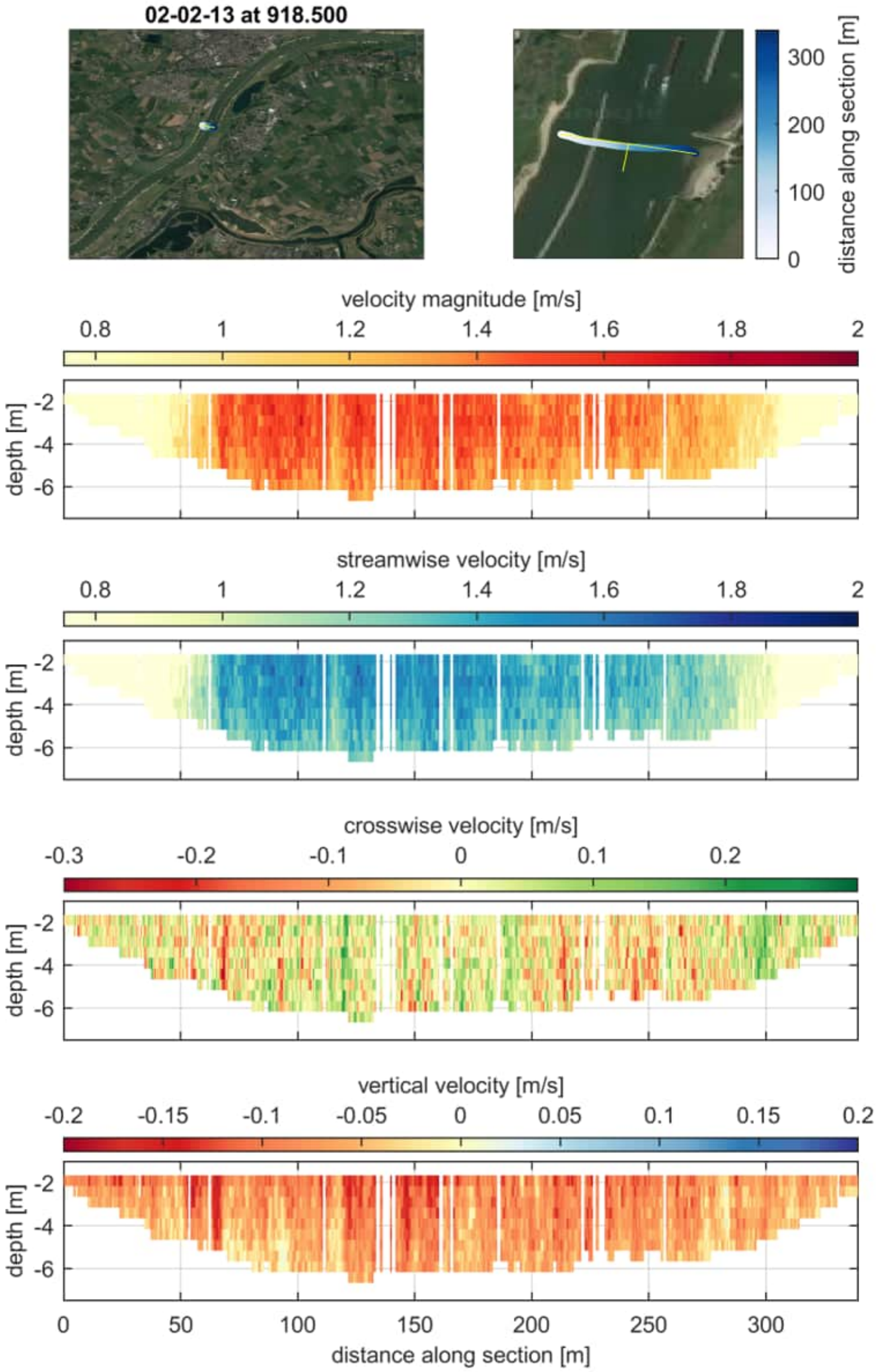

Figure D.67 Cross-sectional measurements on 02-02-13 (discharge at Lobith at 12:00 equal to 4170 m^3/s) at rkm 918.500 projected on measurement plane.

Deltares

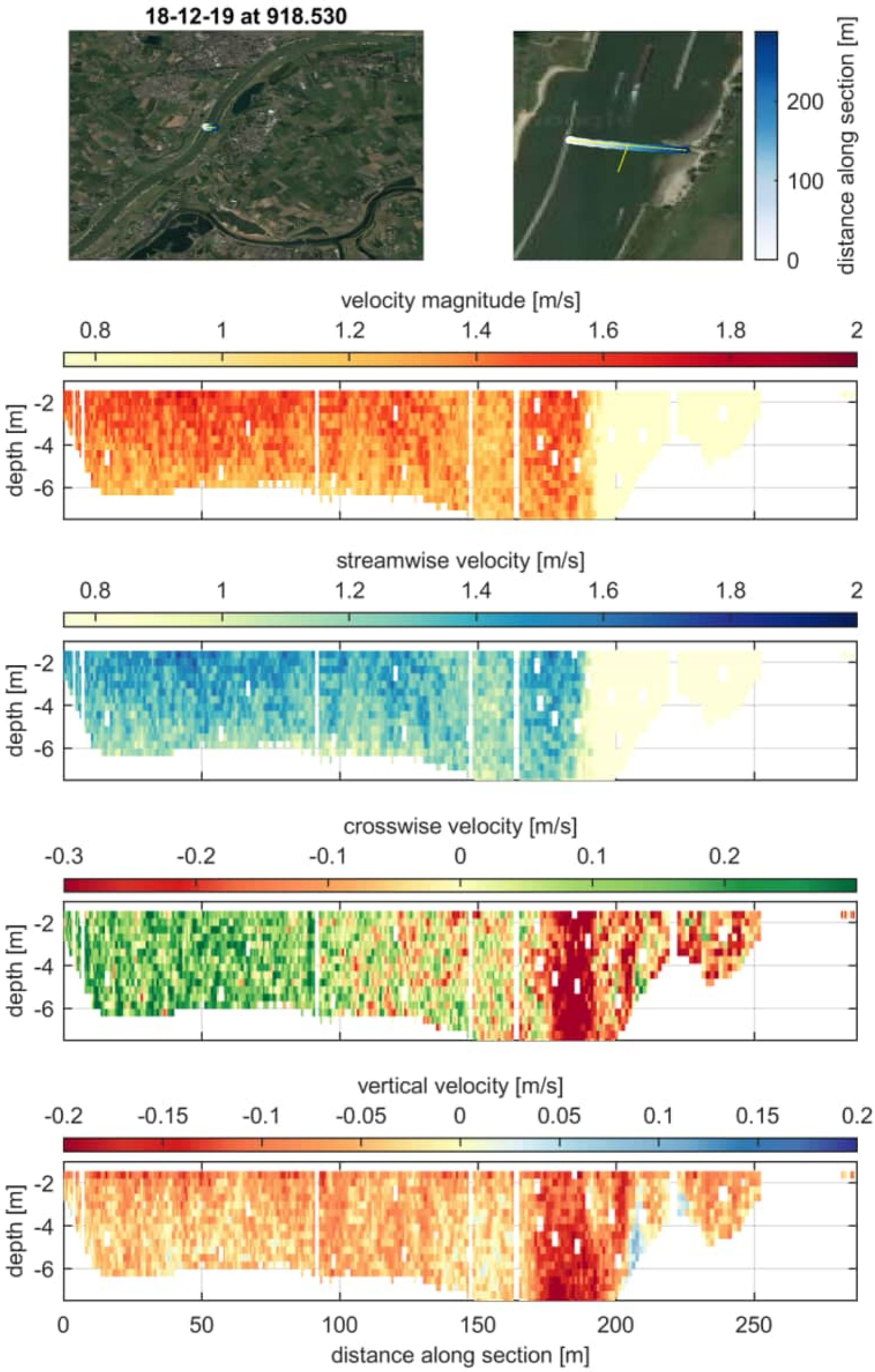

Figure D.68 Cross-sectional measurements on 18-12-19 (discharge at Lobith at 12:00 equal to 3565 m^3/s) at rkm 918.530 projected on measurement plane.

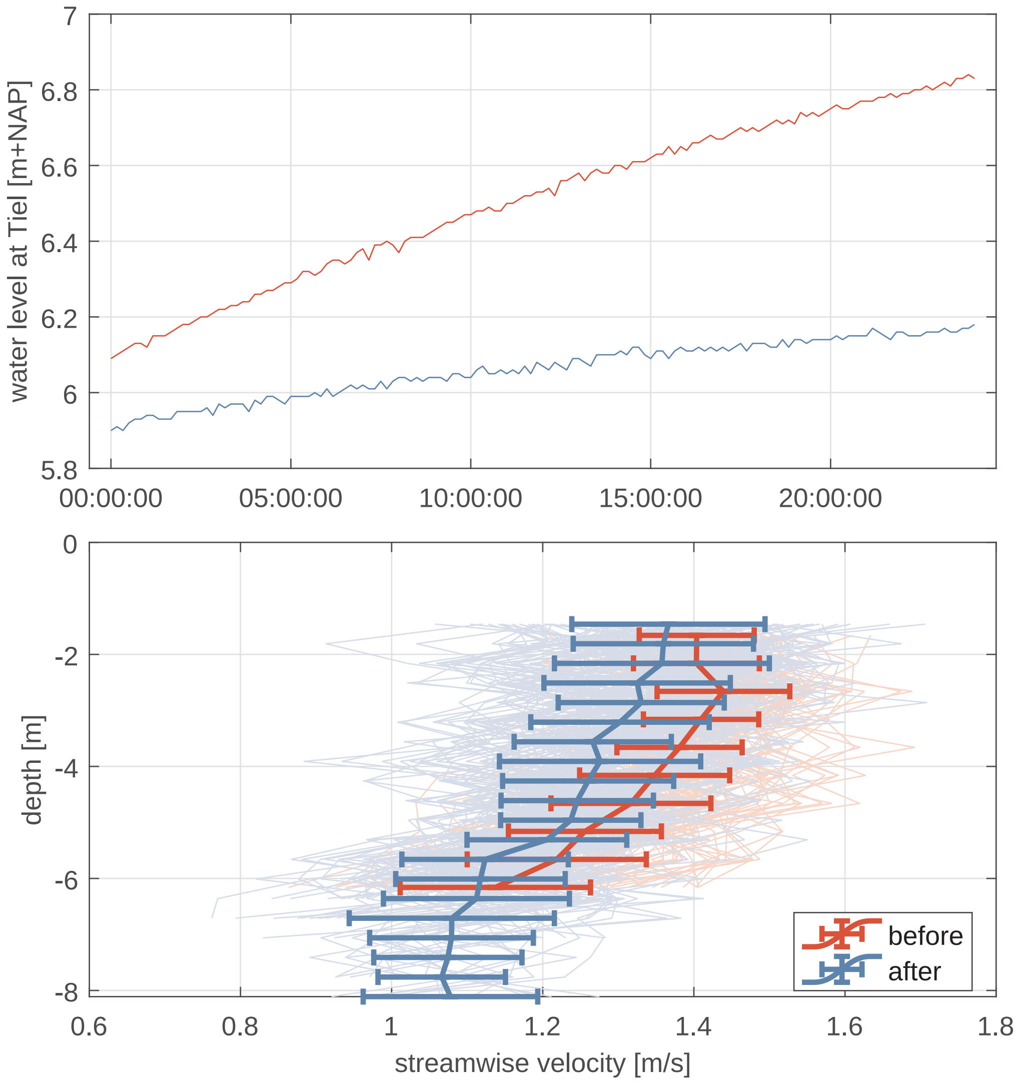

Figure D.69 Streamwise velocity at the central 100 m of channel before (02-02-13, discharge at Lobith at 12:00 equal to 4170 m^3/s, rkm 918.500) and after (18-12-19, discharge at Lobith at 12:00 equal to 3565 m^3/s, rkm 918.530)

D.3.3.10 Location 10

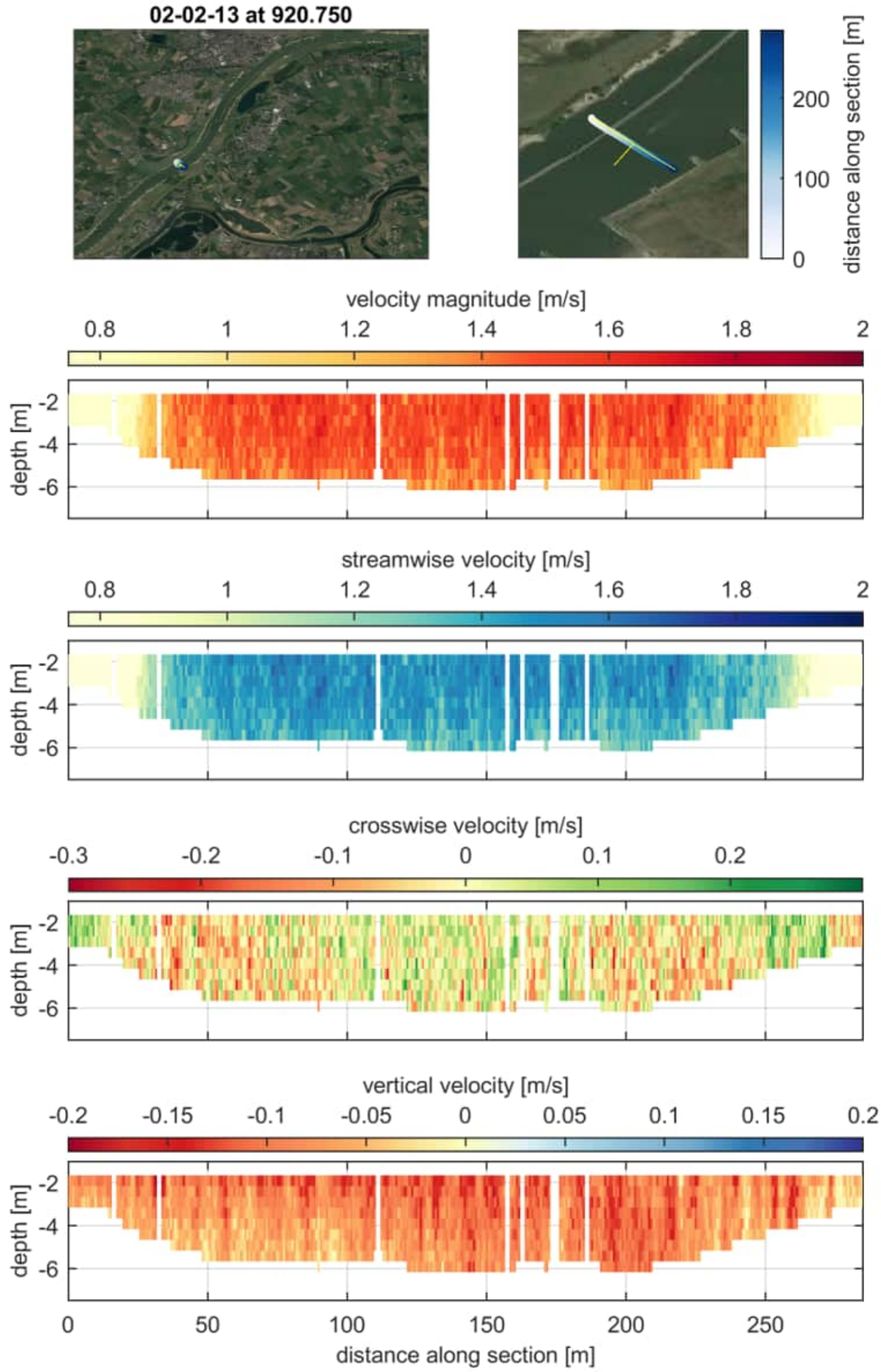

Figure D.70 Cross-sectional measurements on 02-02-13 (discharge at Lobith at 12:00 equal to 4170 m^3/s) at rkm 920.750 projected on measurement plane.

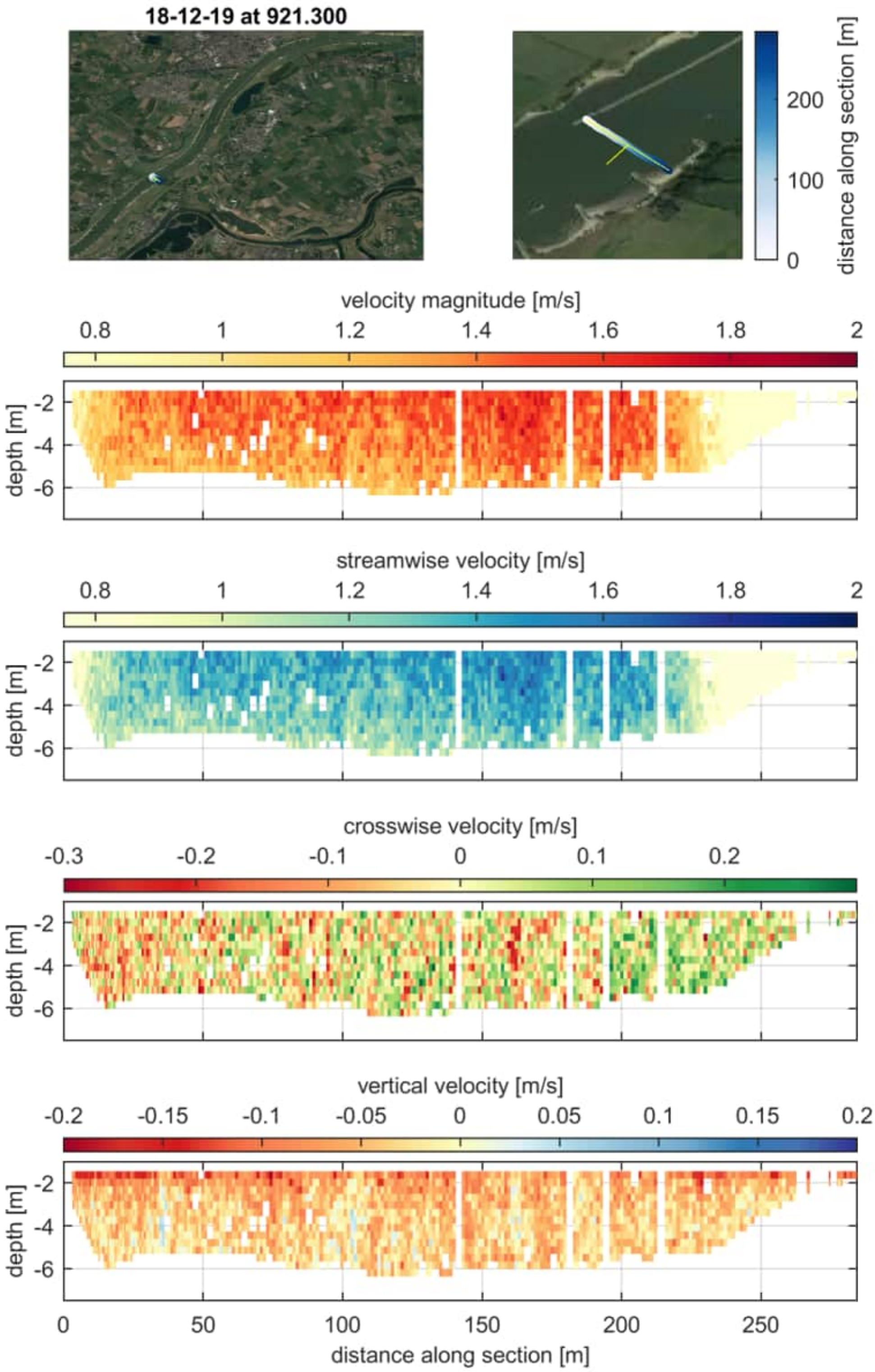

Figure D.71 Cross-sectional measurements on 18-12-19 (discharge at Lobith at 12:00 equal to 3565 m^3/s) at rkm 921.300 projected on measurement plane.

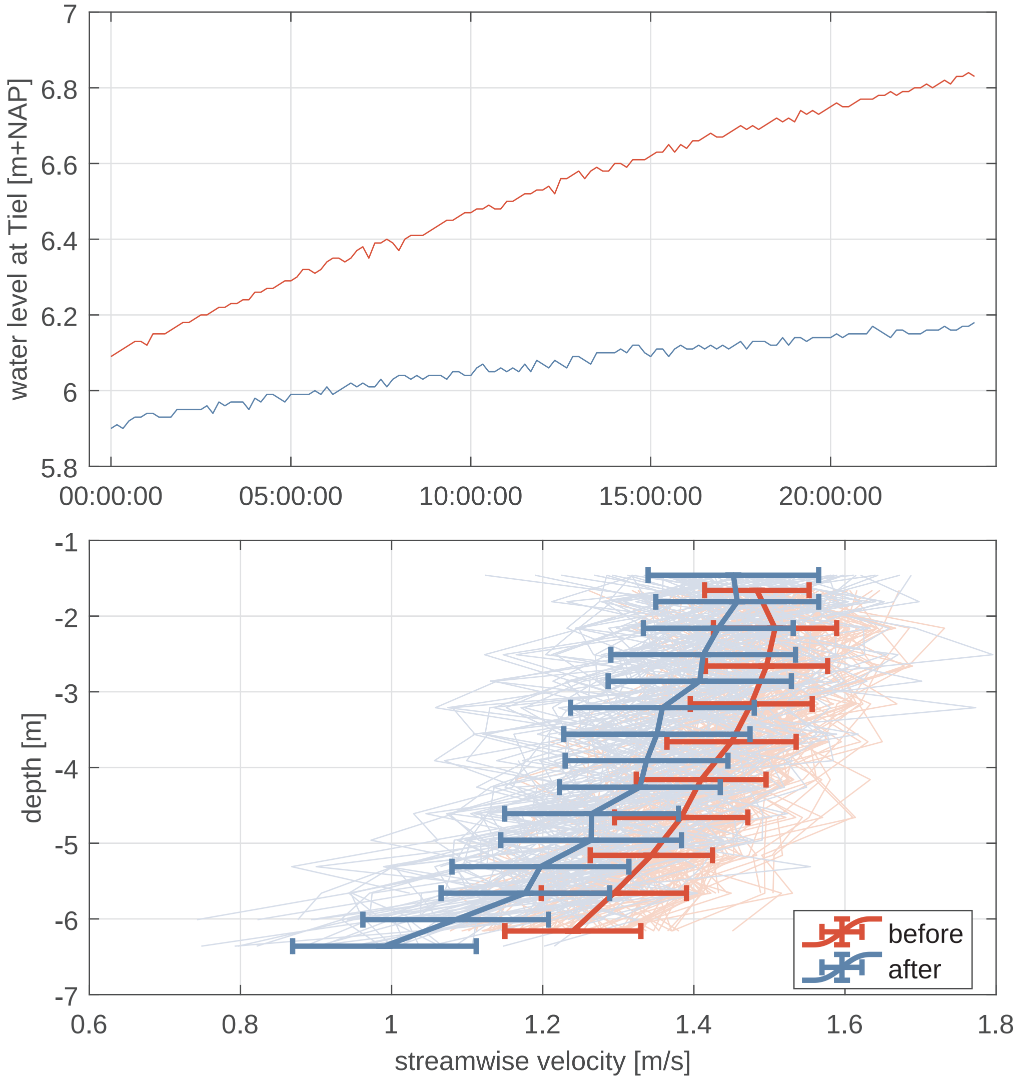

Figure D.72 Streamwise velocity at the central 100 m of channel before (02-02-13, discharge at Lobith at 12:00 equal to 4170 m^3/s, rkm 920.750) and after (18-12-19, discharge at Lobith at 12:00 equal to 3565 m^3/s, rkm 921.300)

D.3.3.11 Location 11

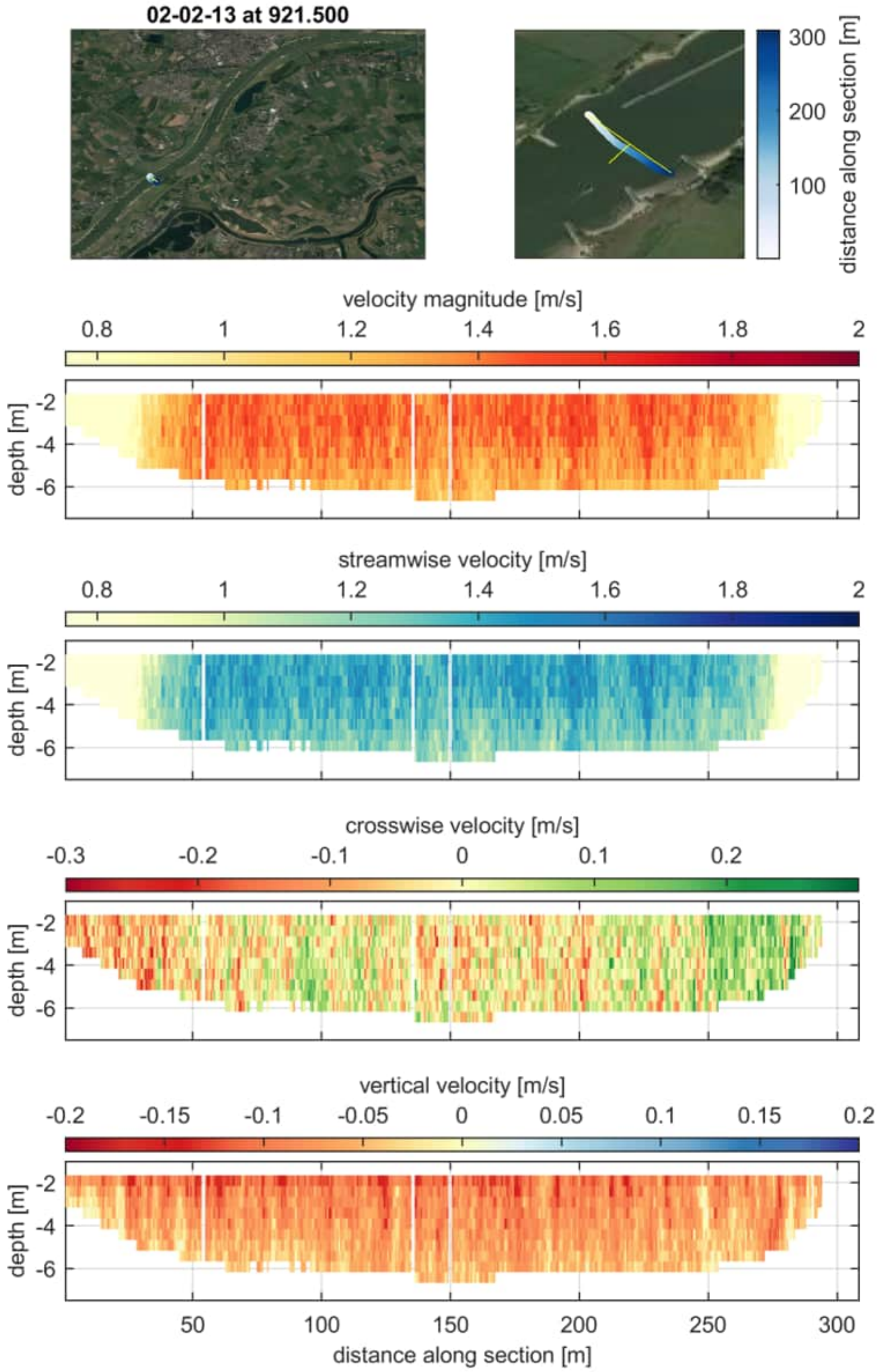

Figure D.73 Cross-sectional measurements on 02-02-13 (discharge at Lobith at 12:00 equal to 4170 m^3/s) at rkm 921.500 projected on measurement plane.

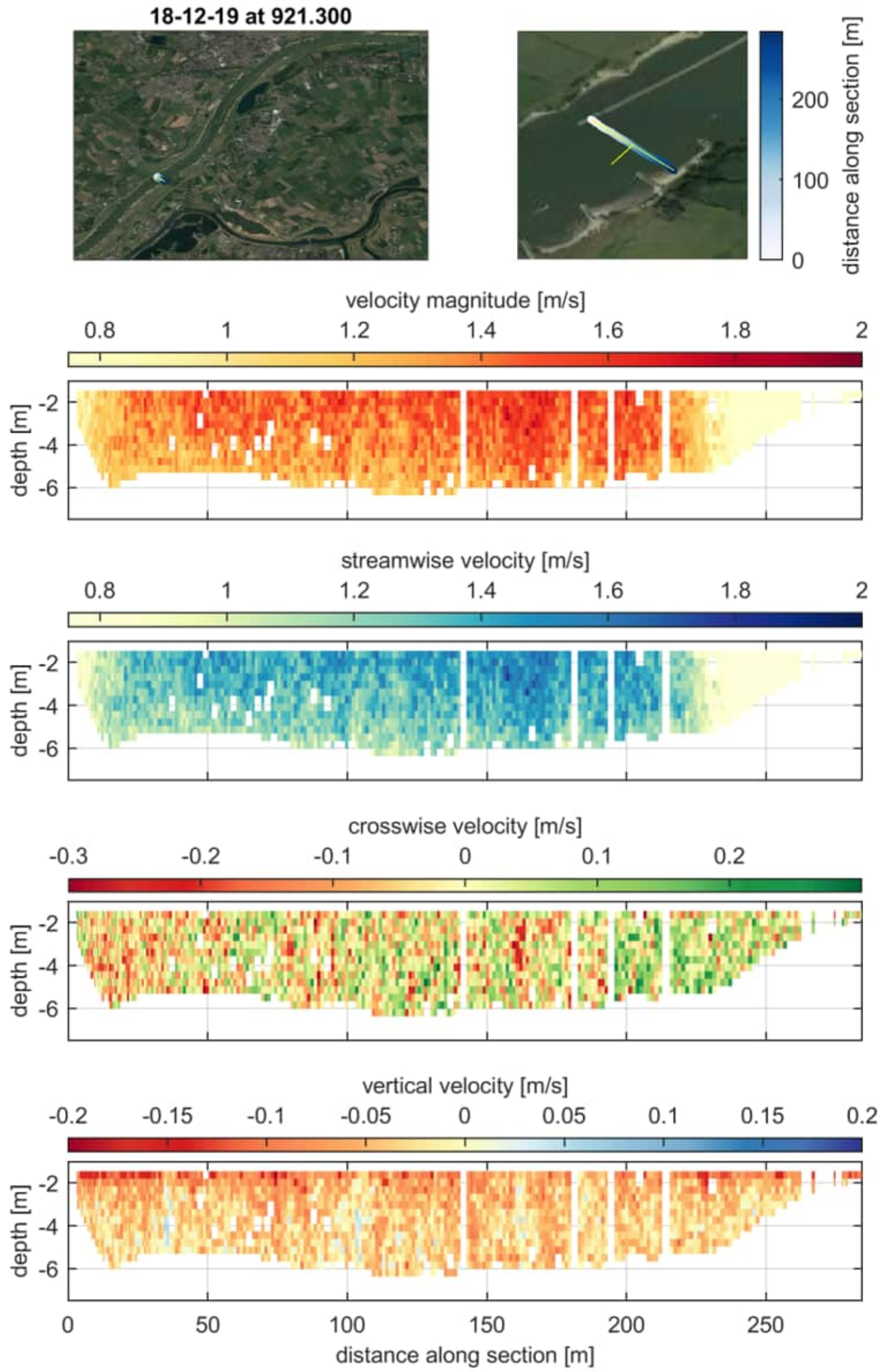

Figure D.74 Cross-sectional measurements on 18-12-19 (discharge at Lobith at 12:00 equal to 3565 m^3/s) at rkm 921.300 projected on measurement plane.

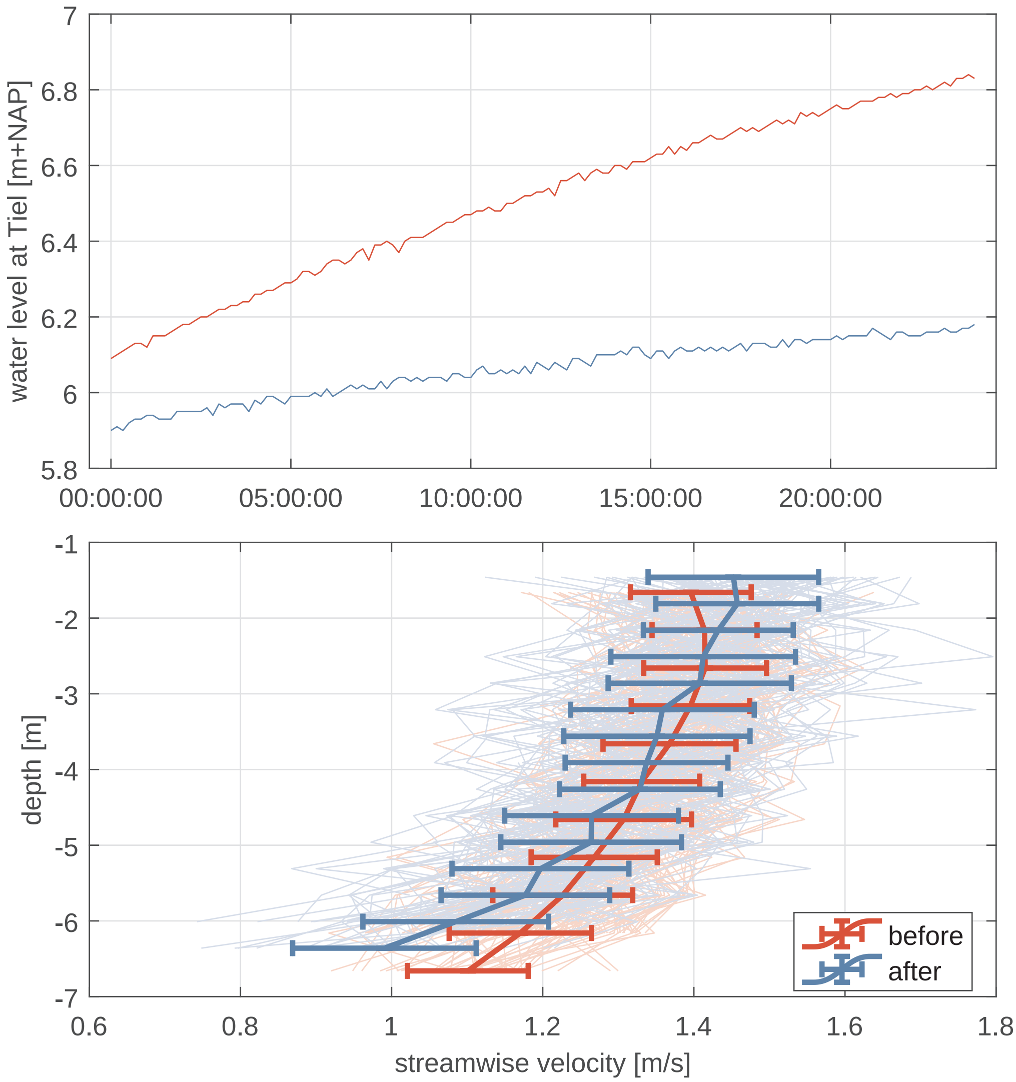

Figure D.75 Streamwise velocity at the central 100 m of channel before (02-02-13, discharge at Lobith at 12:00 equal to 4170 m^3/s, rkm 921.500) and after (18-12-19, discharge at Lobith at 12:00 equal to 3565 m^3/s, rkm 921.300)

Deltares

D.3.3.12 Location 12

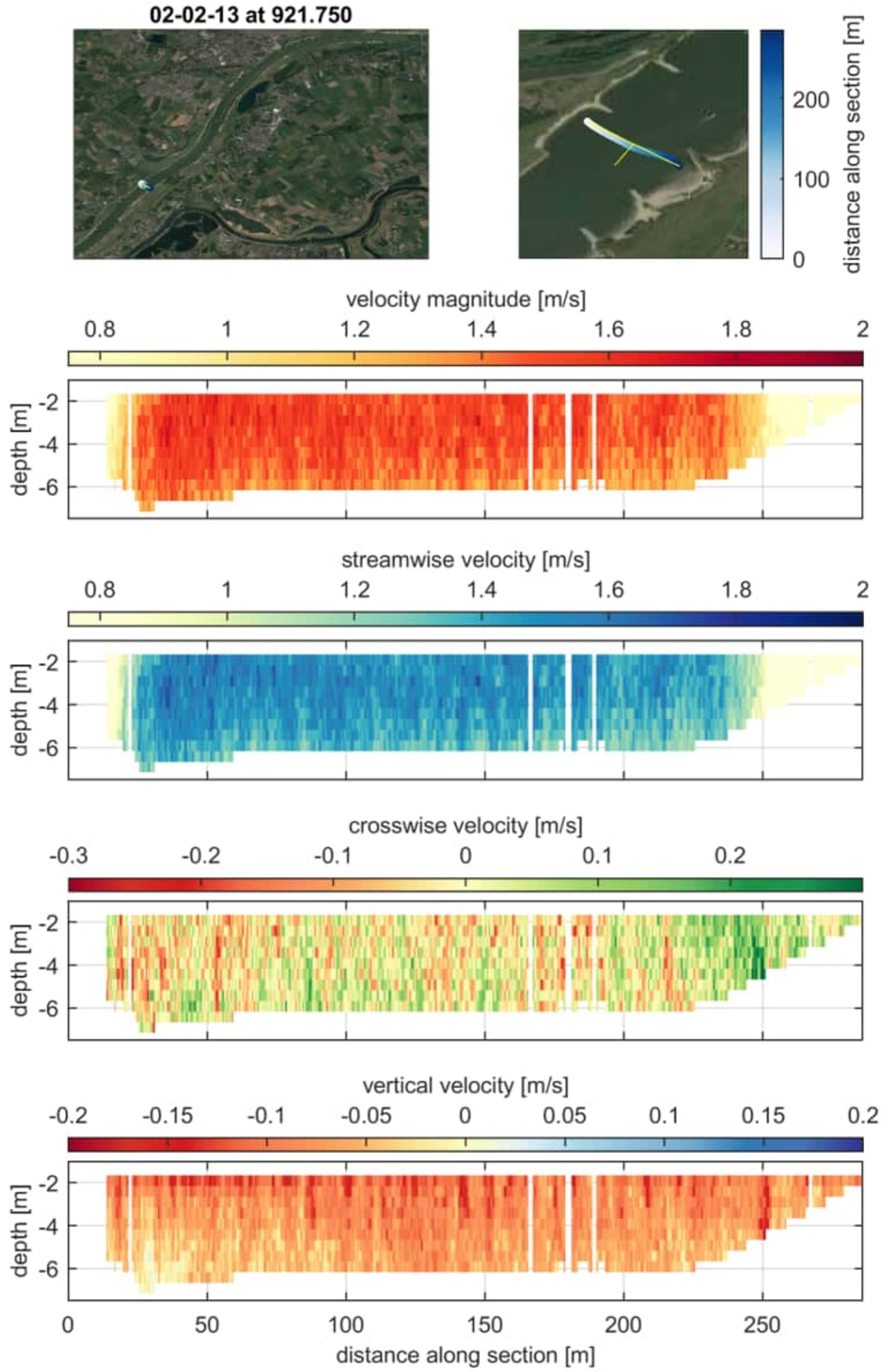

Figure D.76 Cross-sectional measurements on 02-02-13 (discharge at Lobith at 12:00 equal to 4170 m^3/s) at rkm 921.750 projected on measurement plane.

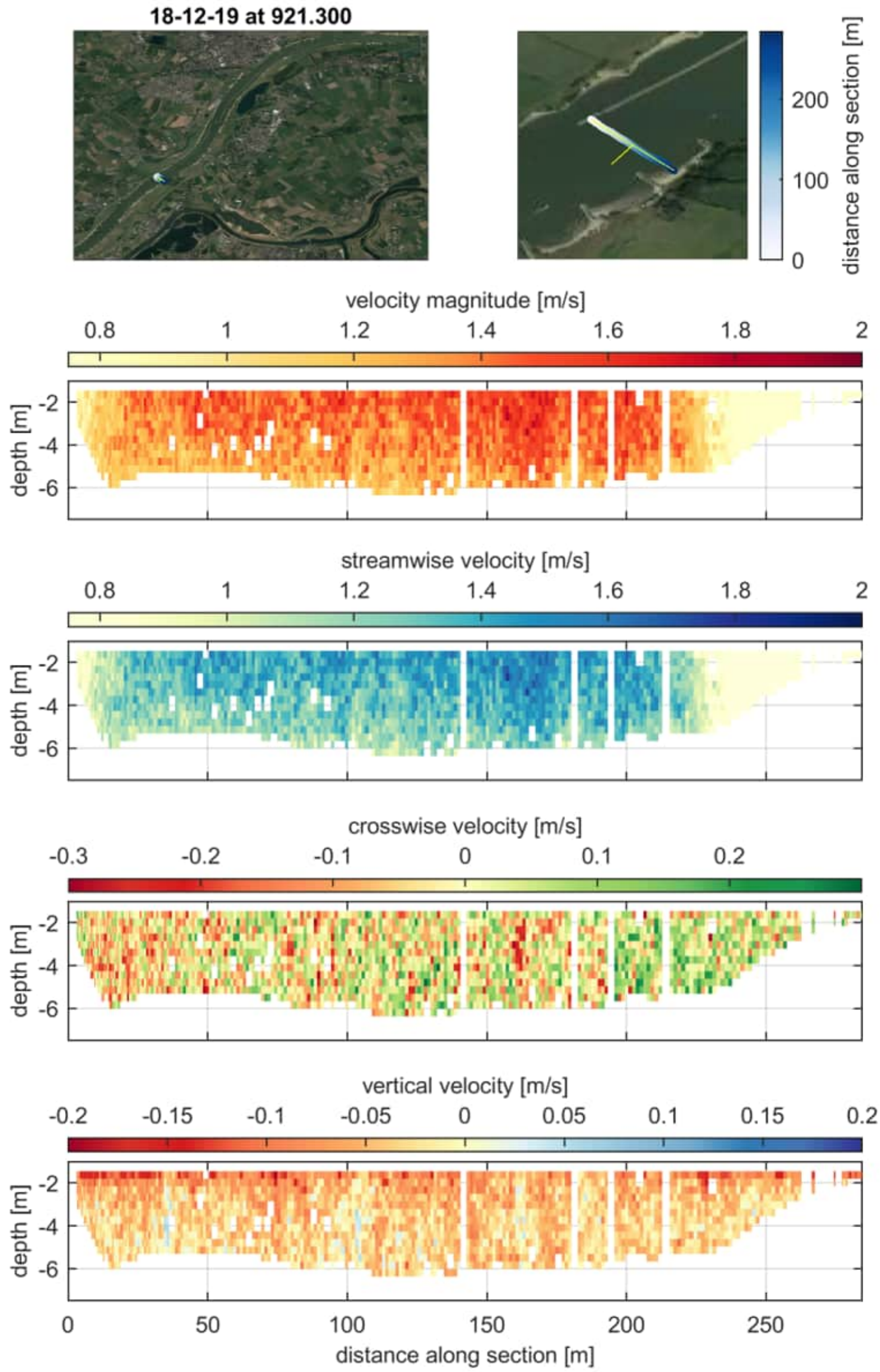

Figure D.77 Cross-sectional measurements on 18-12-19 (discharge at Lobith at 12:00 equal to 3565 m^3/s) at rkm 921.300 projected on measurement plane.

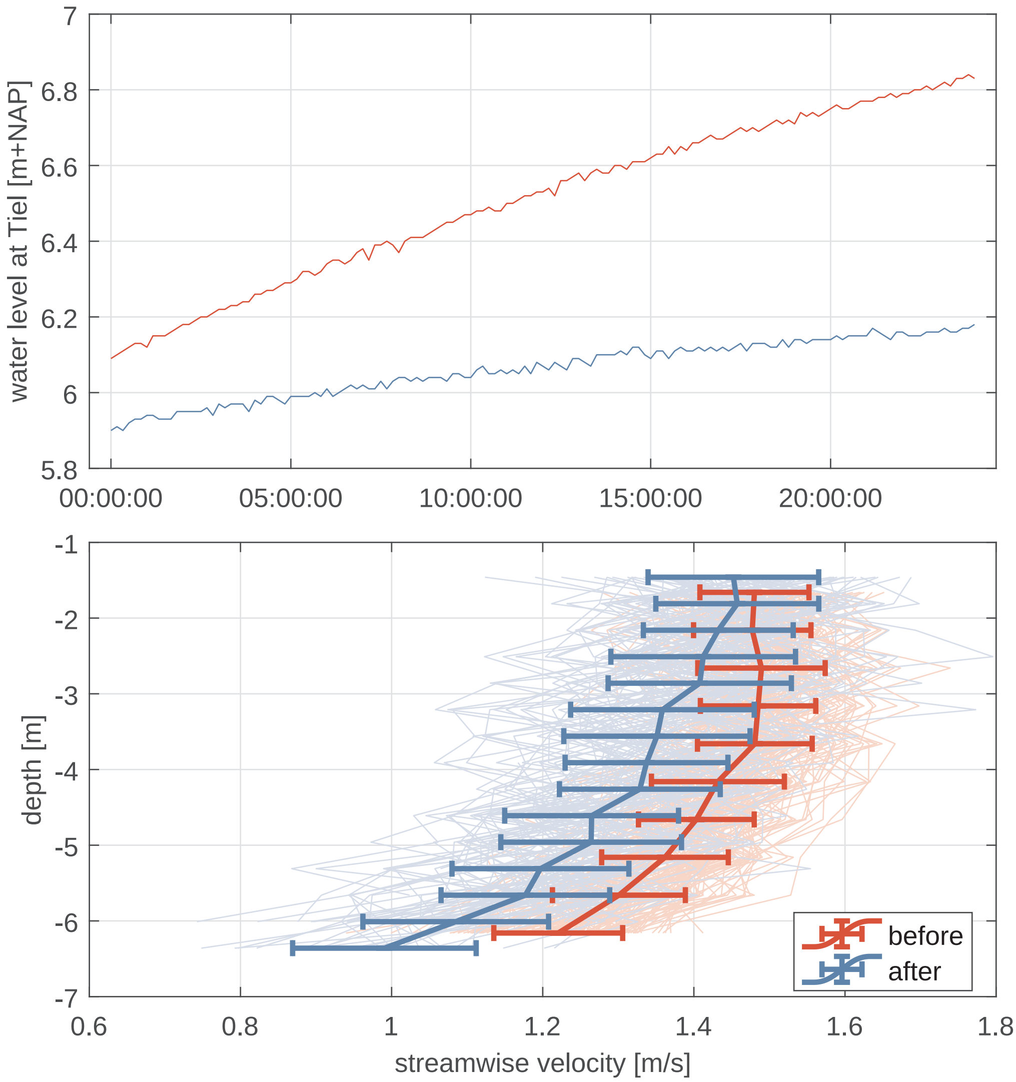

Figure D.78 Streamwise velocity at the central 100 m of channel before (02-02-13, discharge at Lobith at 12:00 equal to 4170 m^3/s, rkm 921.750) and after (18-12-19, discharge at Lobith at 12:00 equal to 3565 m^3/s, rkm 921.300)

D.3.3.13 Location 13

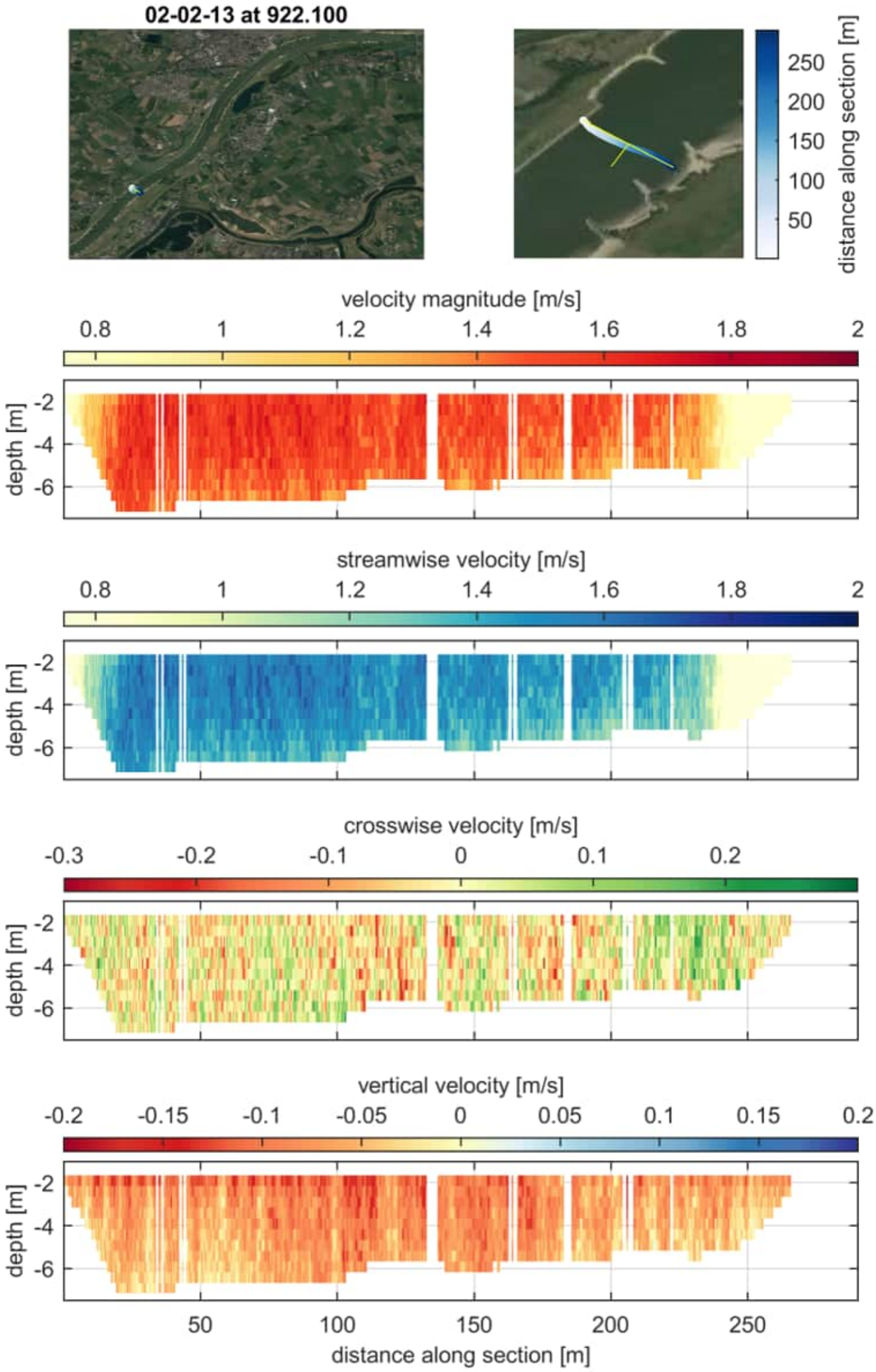

Figure D.79 Cross-sectional measurements on 02-02-13 (discharge at Lobith at 12:00 equal to 4170 m^3/s) at rkm 922.100 projected on measurement plane.

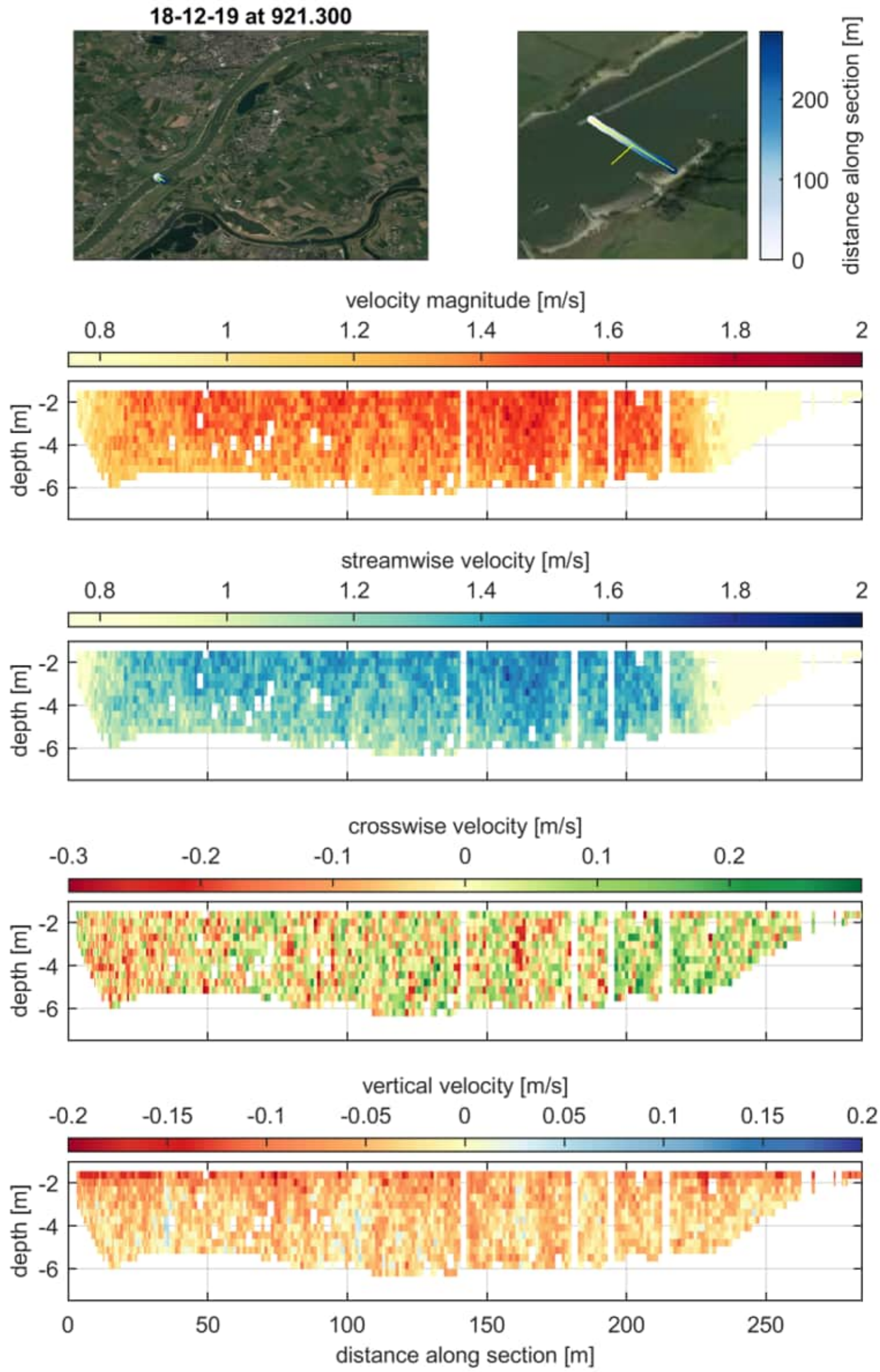

Figure D.80 Cross-sectional measurements on 18-12-19 (discharge at Lobith at 12:00 equal to 3565 m^3/s) at rkm 921.300 projected on measurement plane.

Deltares

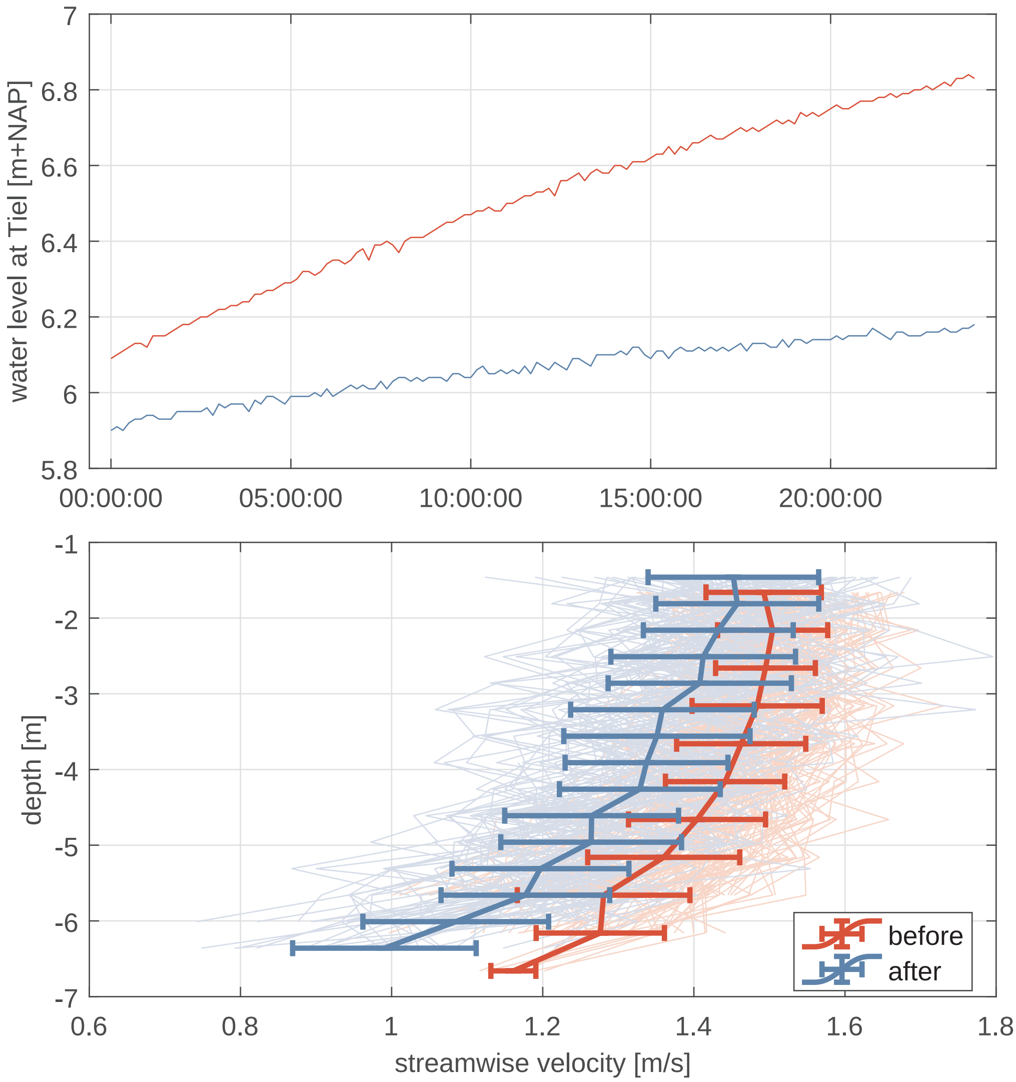

Figure D.81 Streamwise velocity at the central 100 m of channel before (02-02-13, discharge at Lobith at 12:00 equal to 4170 m^3/s, rkm 922.100) and after (18-12-19, discharge at Lobith at 12:00 equal to 3565 m^3/s, rkm 921.300)

D.3.4 Condition 4

D.3.4.1 Location 1

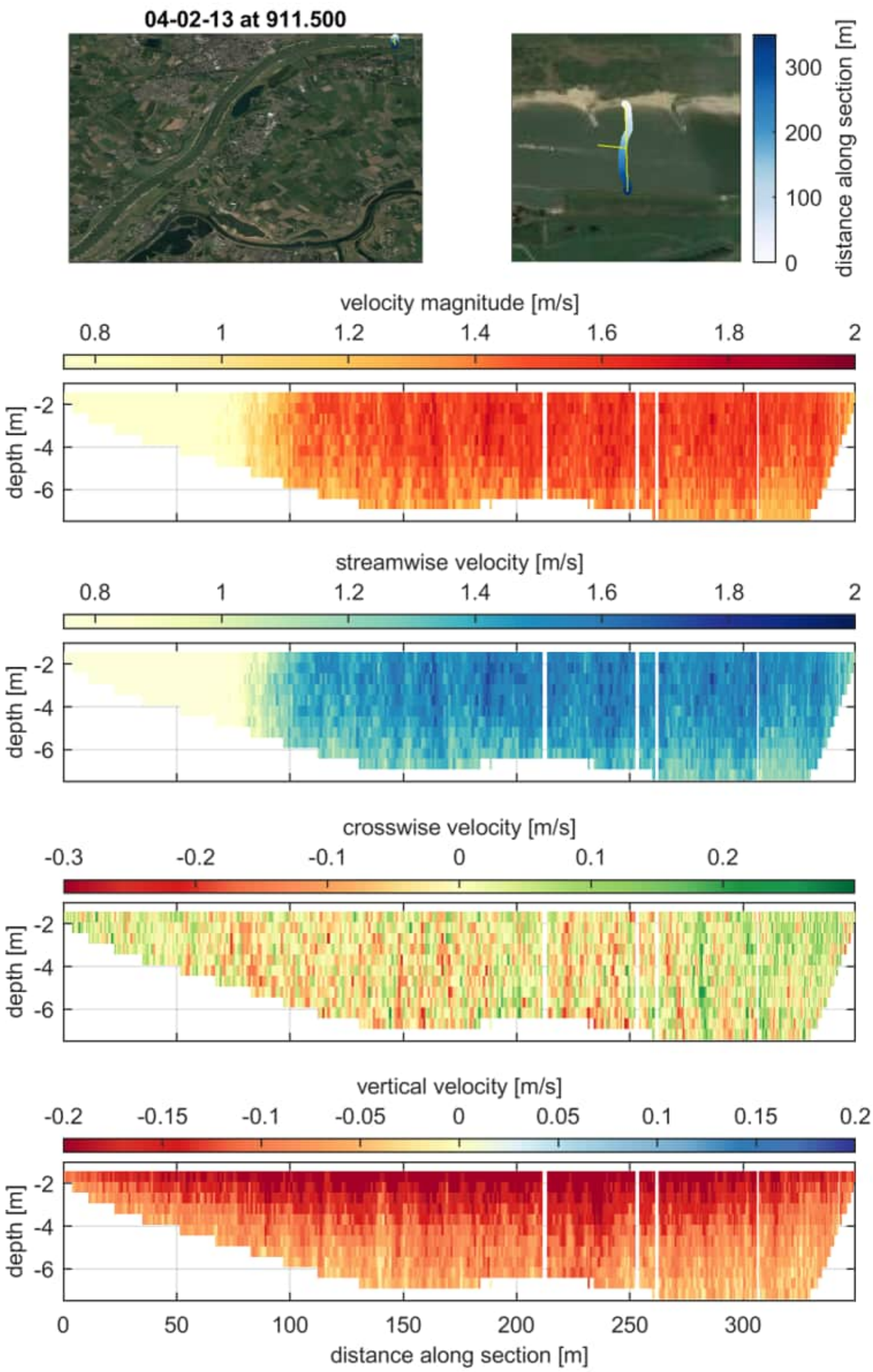

Figure D.82 Cross-sectional measurements on 04-02-13 (discharge at Lobith at 12:00 equal to 5087 m^3/s) at rkm 911.500 projected on measurement plane.

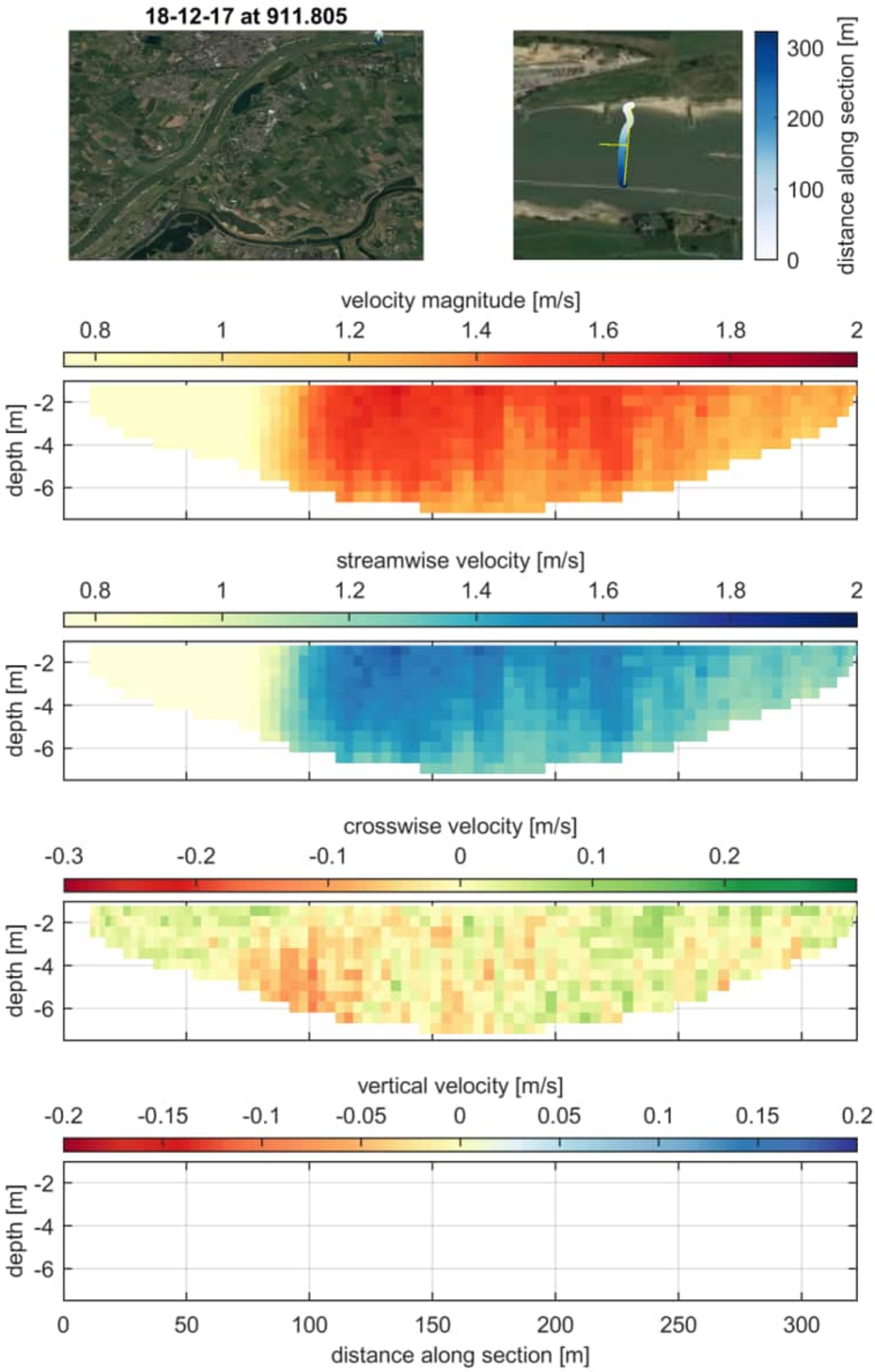

Figure D.83 Cross-sectional measurements on 18-12-17 (discharge at Lobith at 12:00 equal to 5013 m^3/s) at rkm 911.805 projected on measurement plane.

Deltares

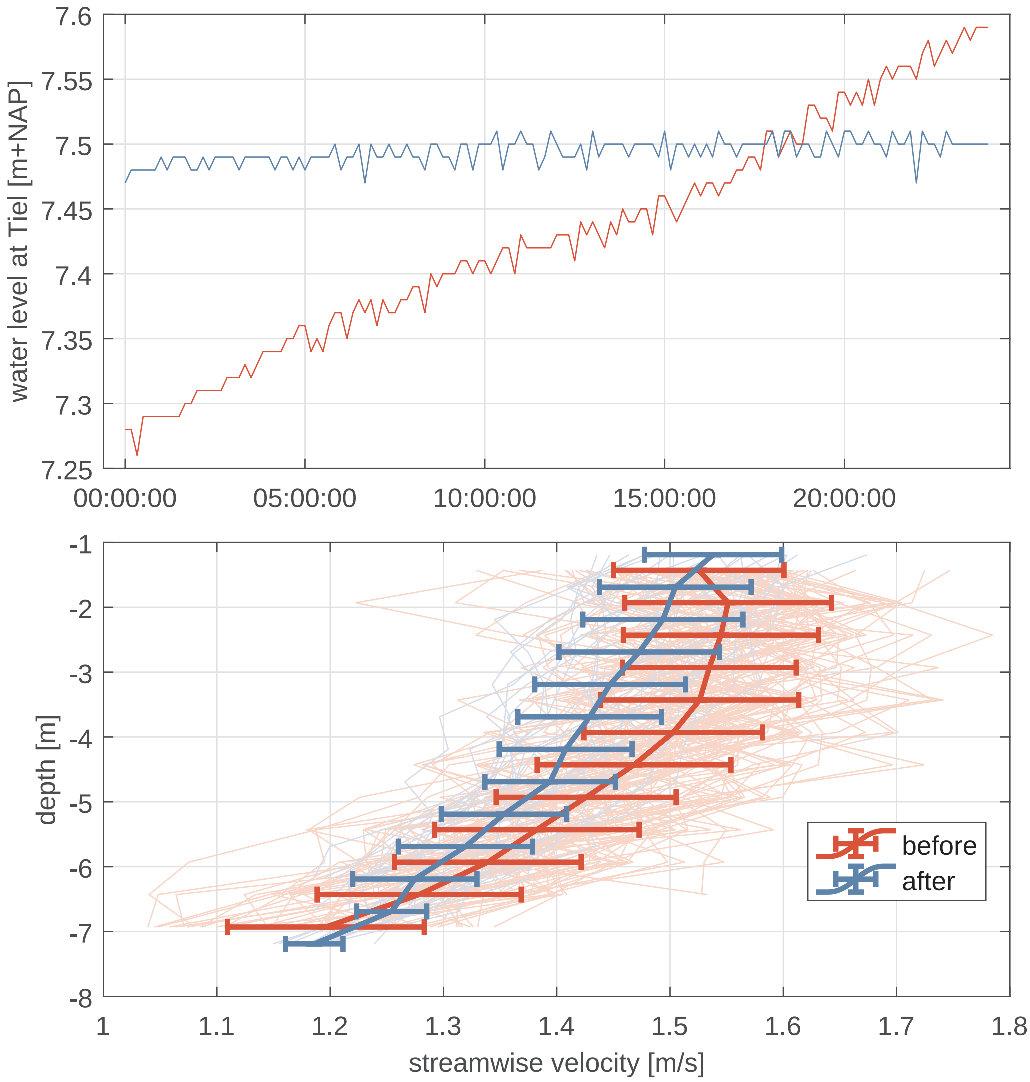

Figure D.84 Streamwise velocity at the central 100 m of channel before (04-02-13, discharge at Lobith at 12:00 equal to 5087 m^3/s, rkm 911.500) and after (18-12-17, discharge at Lobith at 12:00 equal to 5013 m^3/s, rkm 911.805)

D.3.4.2 Location 2

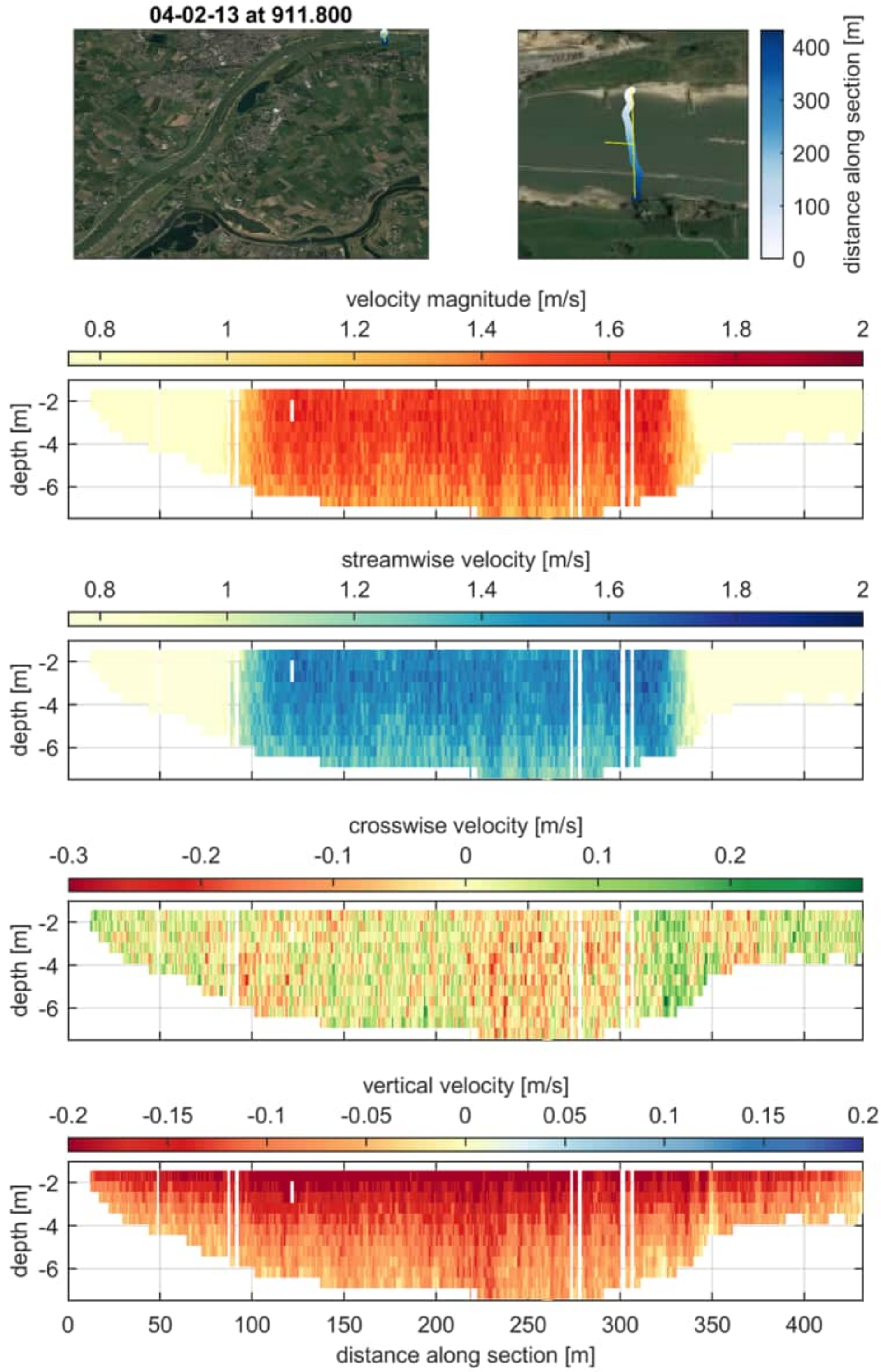

Figure D.85 Cross-sectional measurements on 04-02-13 (discharge at Lobith at 12:00 equal to 5087 m^3/s) at rkm 911.800 projected on measurement plane.

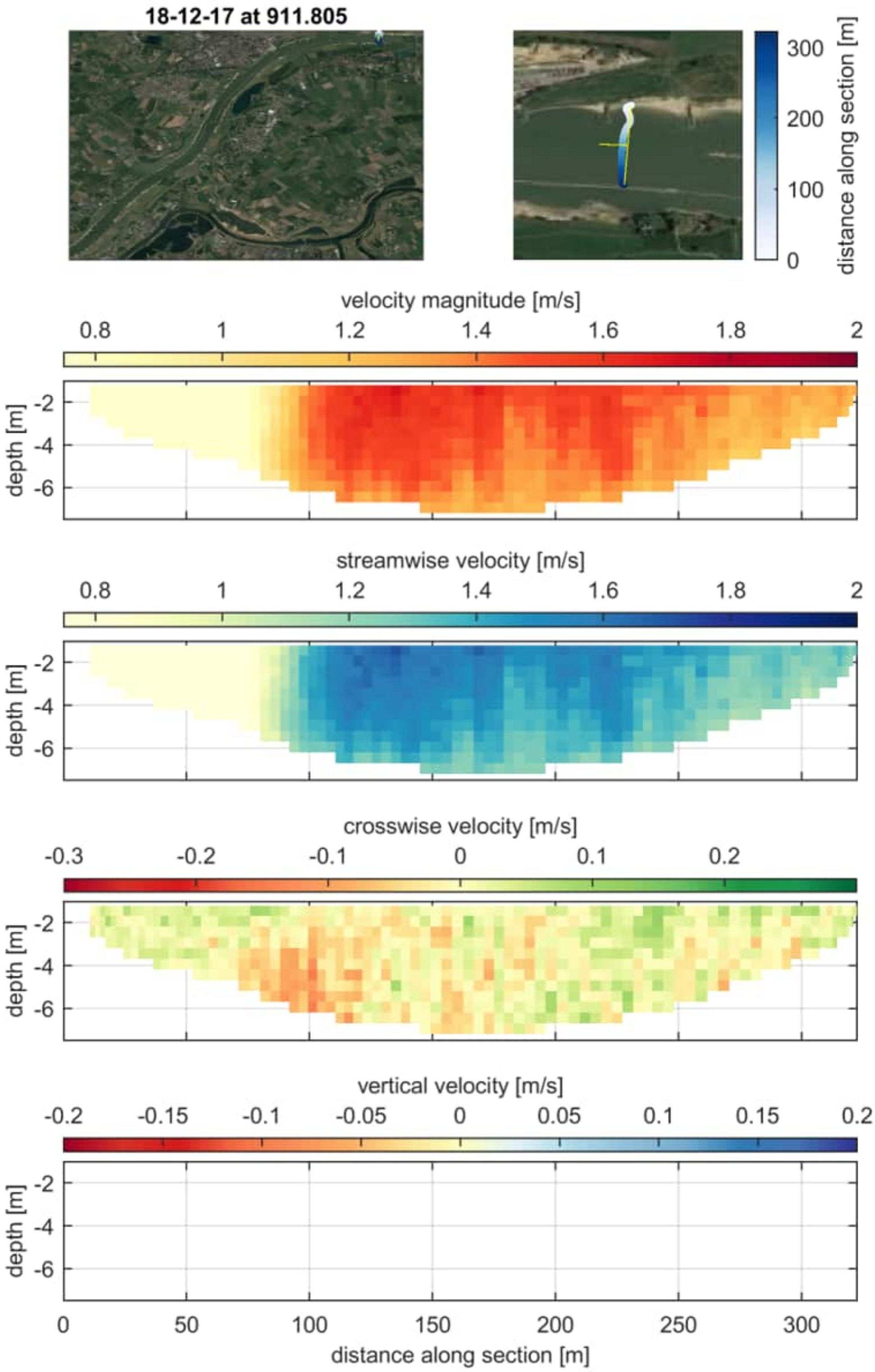

Figure D.86 Cross-sectional measurements on 18-12-17 (discharge at Lobith at 12:00 equal to 5013 m^3/s) at rkm 911.805 projected on measurement plane.

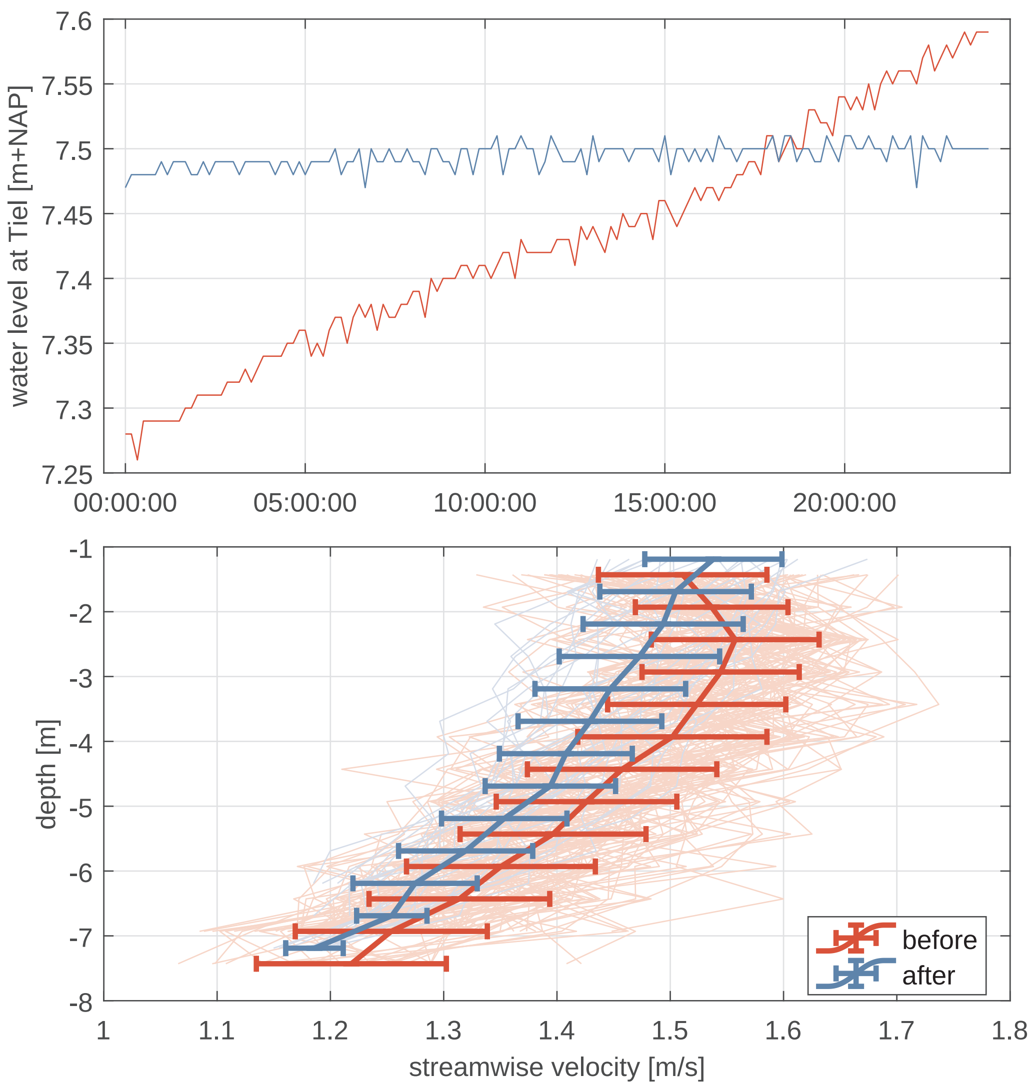

Figure D.87 Streamwise velocity at the central 100 m of channel before (04-02-13, discharge at Lobith at 12:00 equal to 5087 m^3/s, rkm 911.800) and after (18-12-17, discharge at Lobith at 12:00 equal to 5013 m^3/s, rkm 911.805)

D.3.4.3 Location 3

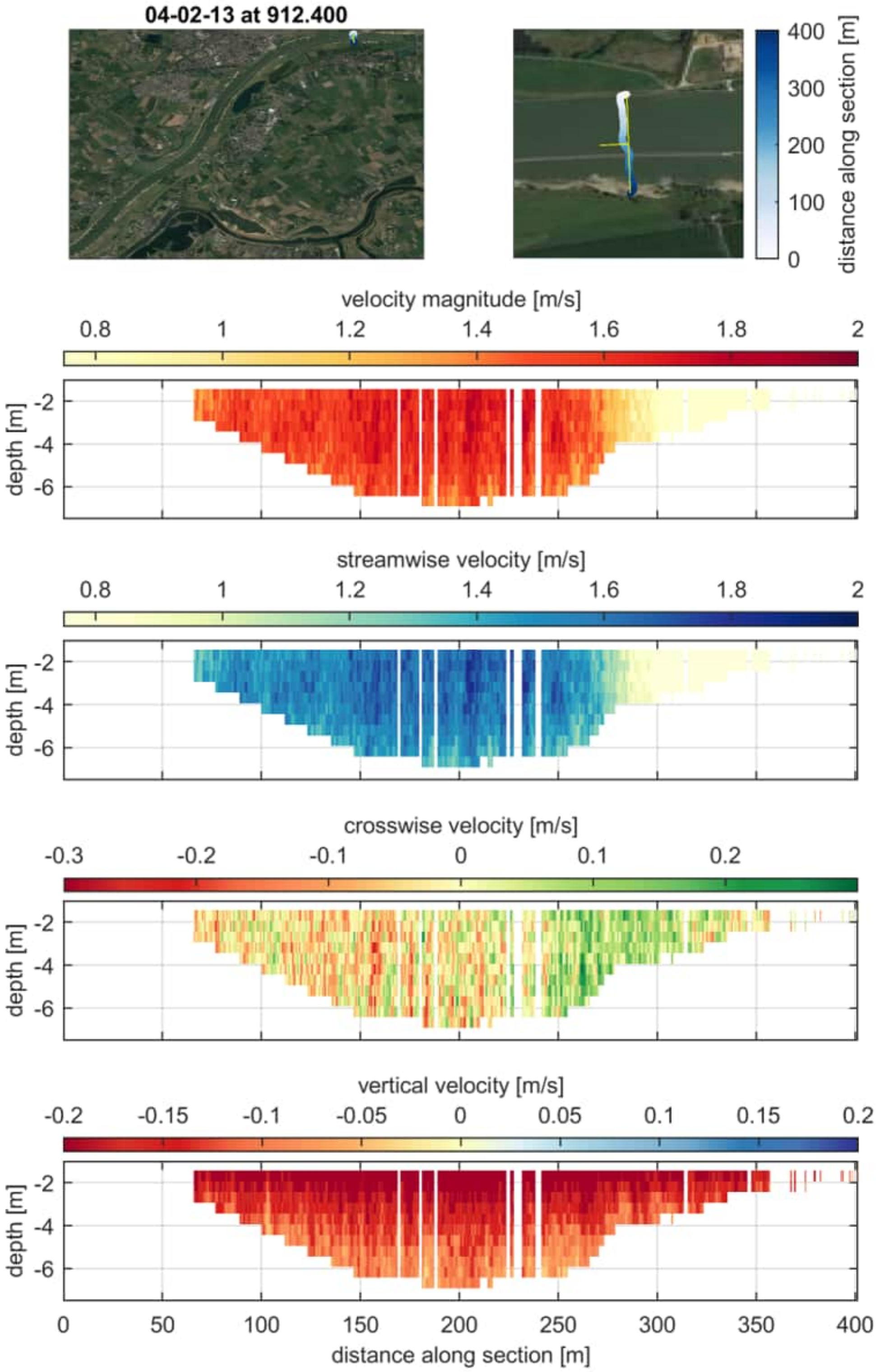

Figure D.88 Cross-sectional measurements on 04-02-13 (discharge at Lobith at 12:00 equal to 5087 m^3/s) at rkm 912.400 projected on measurement plane.

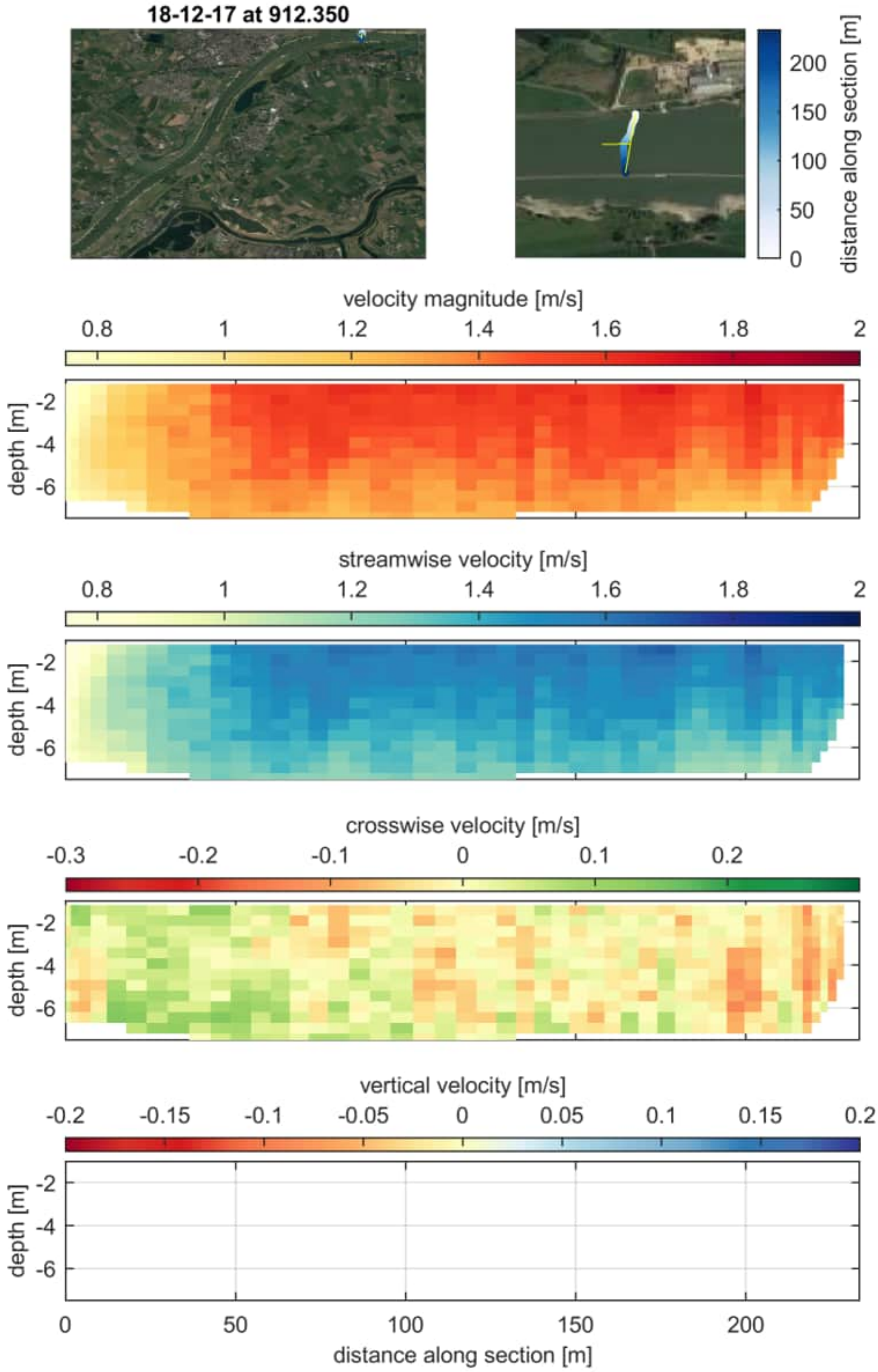

Figure D.89 Cross-sectional measurements on 18-12-17 (discharge at Lobith at 12:00 equal to 5013 m^3/s) at rkm 912.350 projected on measurement plane.

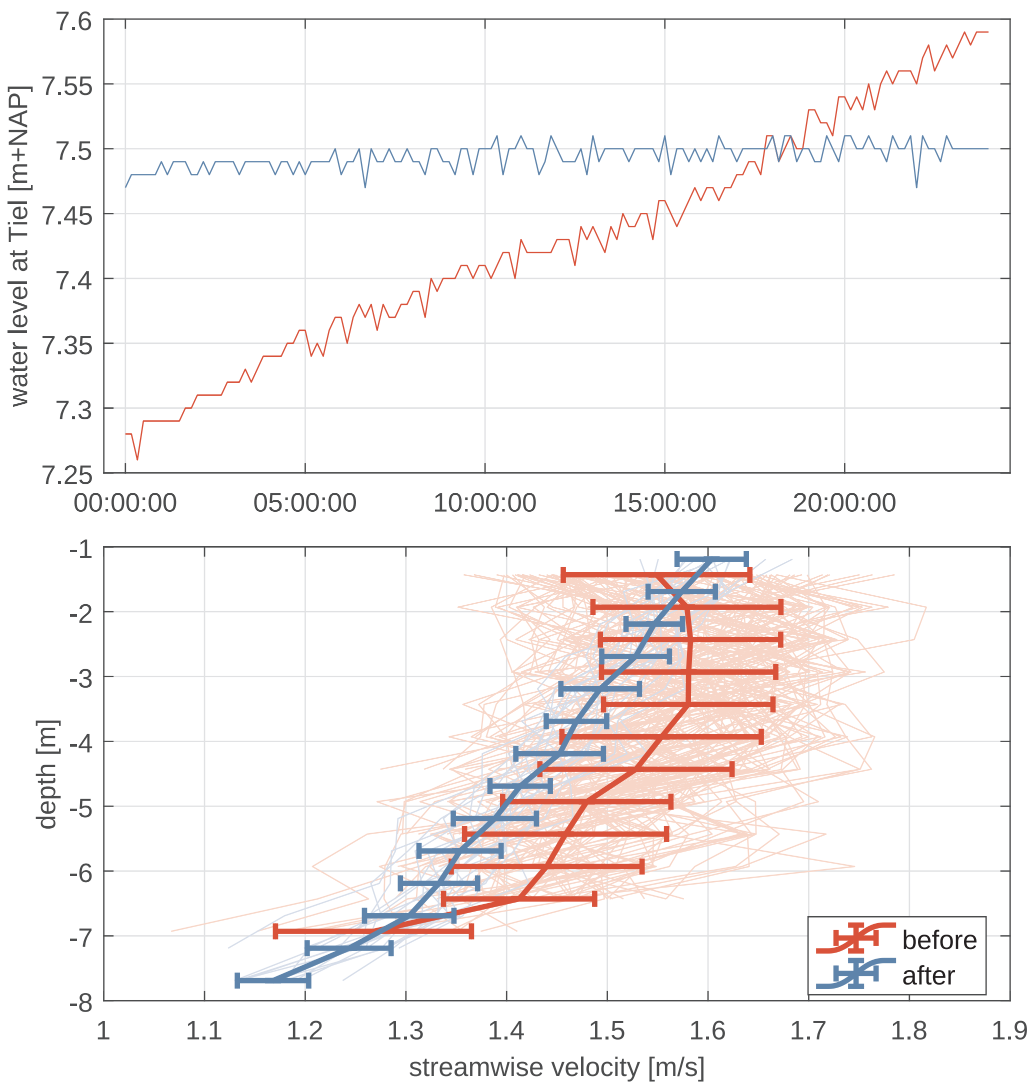

Figure D.90 Streamwise velocity at the central 100 m of channel before (04-02-13, discharge at Lobith at 12:00 equal to 5087 m^3/s, rkm 912.400) and after (18-12-17, discharge at Lobith at 12:00 equal to 5013 m^3/s, rkm 912.350)

D.3.4.4 Location 4

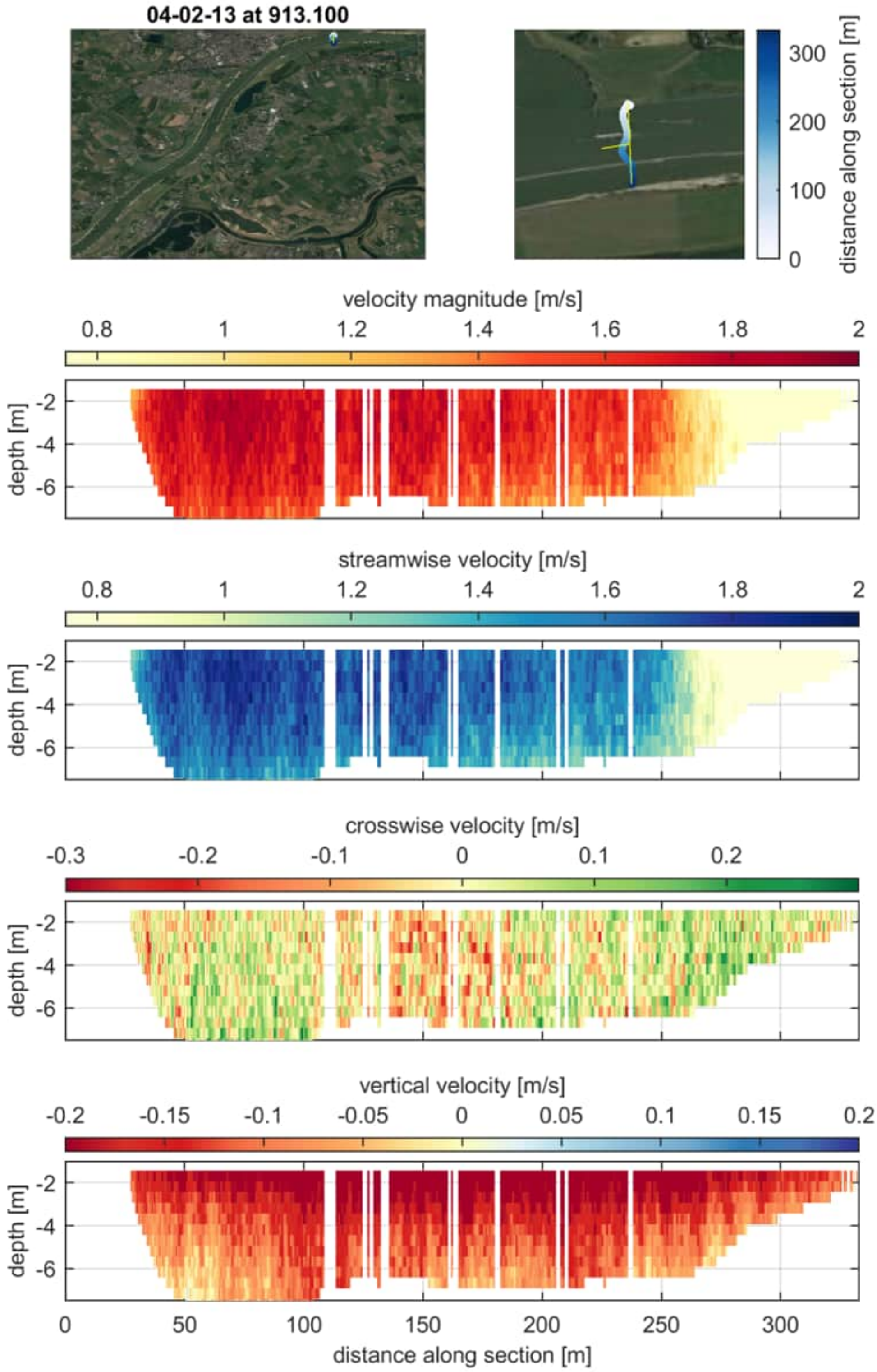

Figure D.91 Cross-sectional measurements on 04-02-13 (discharge at Lobith at 12:00 equal to 5087 m^3/s) at rkm 913.100 projected on measurement plane.

Deltares

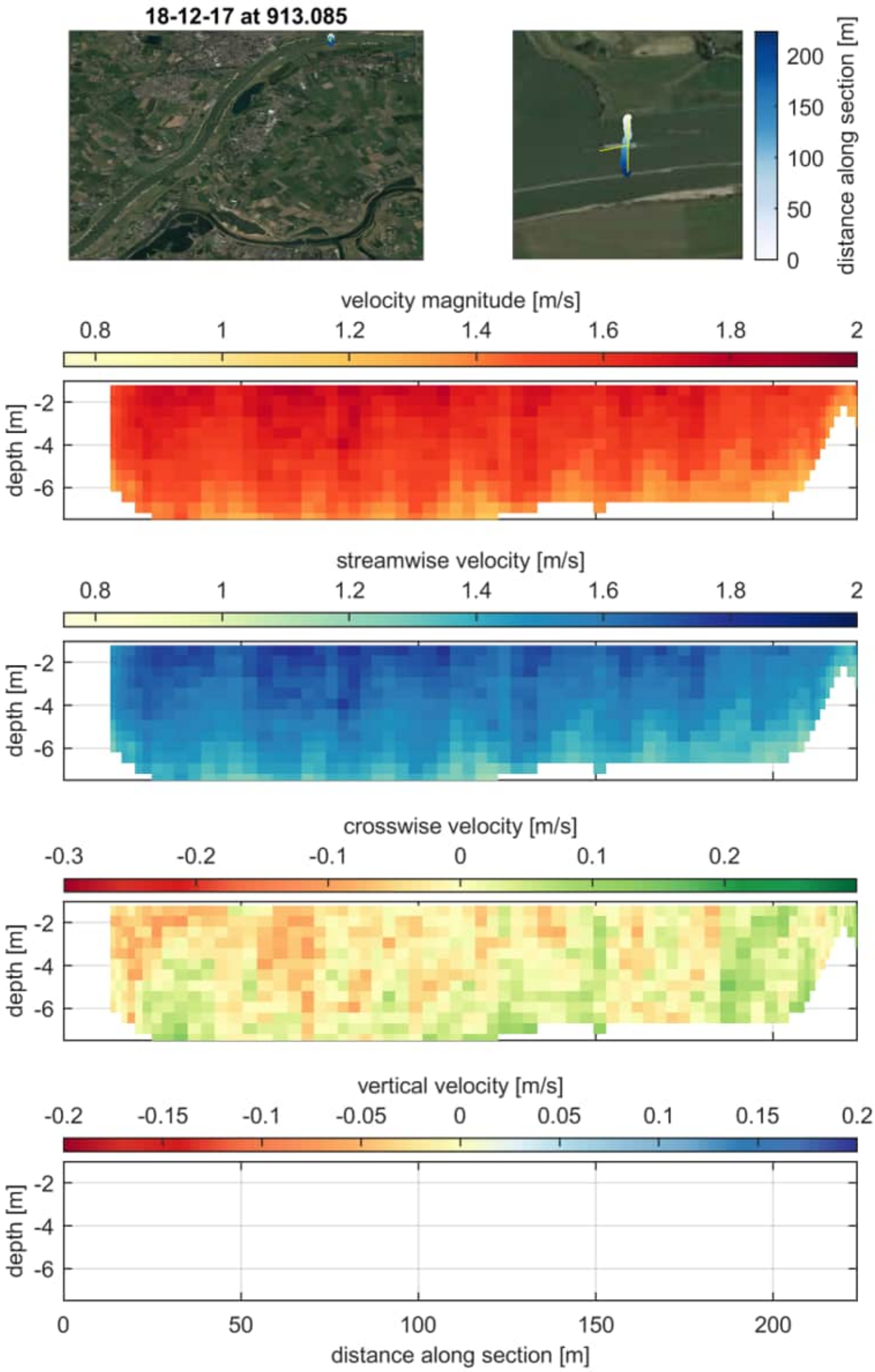

Figure D.92 Cross-sectional measurements on 18-12-17 (discharge at Lobith at 12:00 equal to 5013 m^3/s) at rkm 913.085 projected on measurement plane.

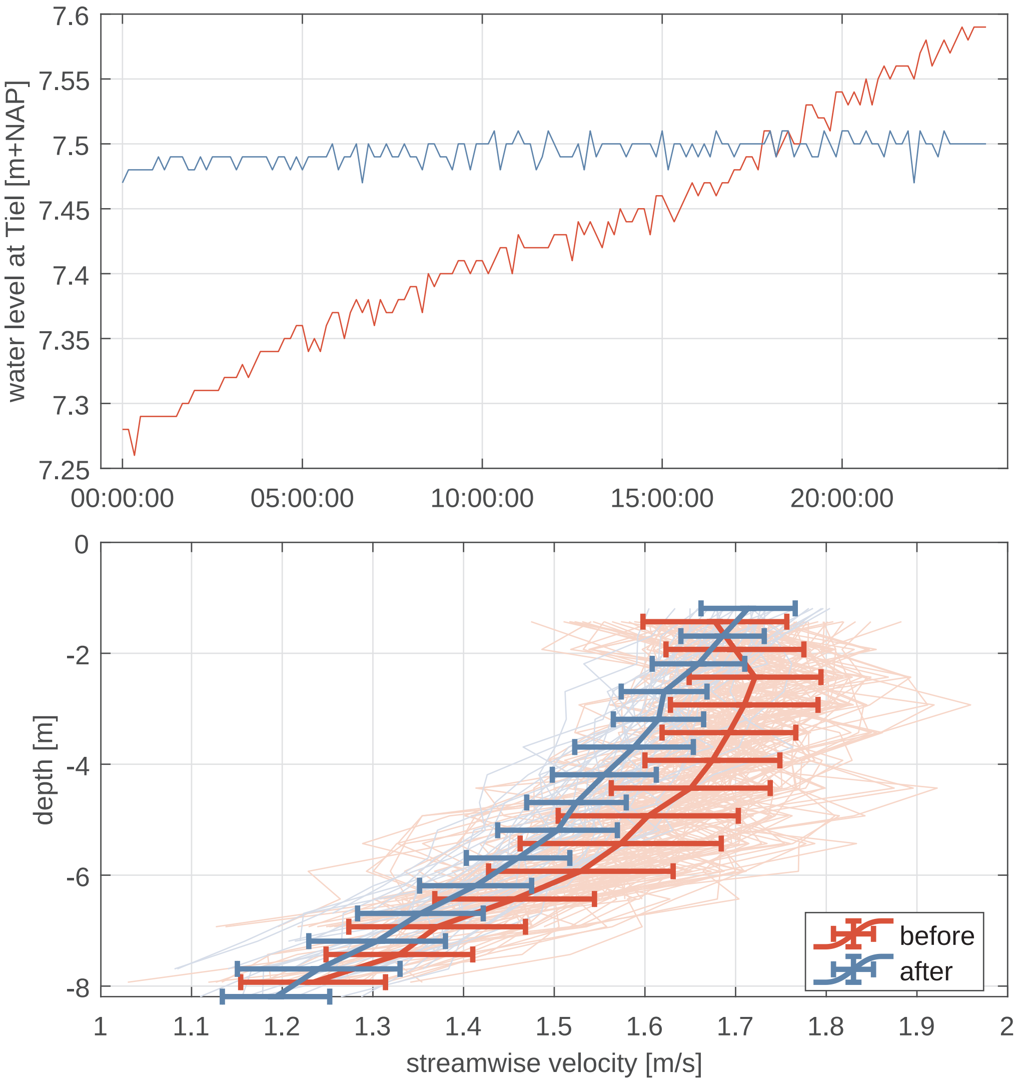

Figure D.93 Streamwise velocity at the central 100 m of channel before (04-02-13, discharge at Lobith at 12:00 equal to 5087 m^3/s, rkm 913.100) and after (18-12-17, discharge at Lobith at 12:00 equal to 5013 m^3/s, rkm 913.085)

D.3.4.5 Location 5

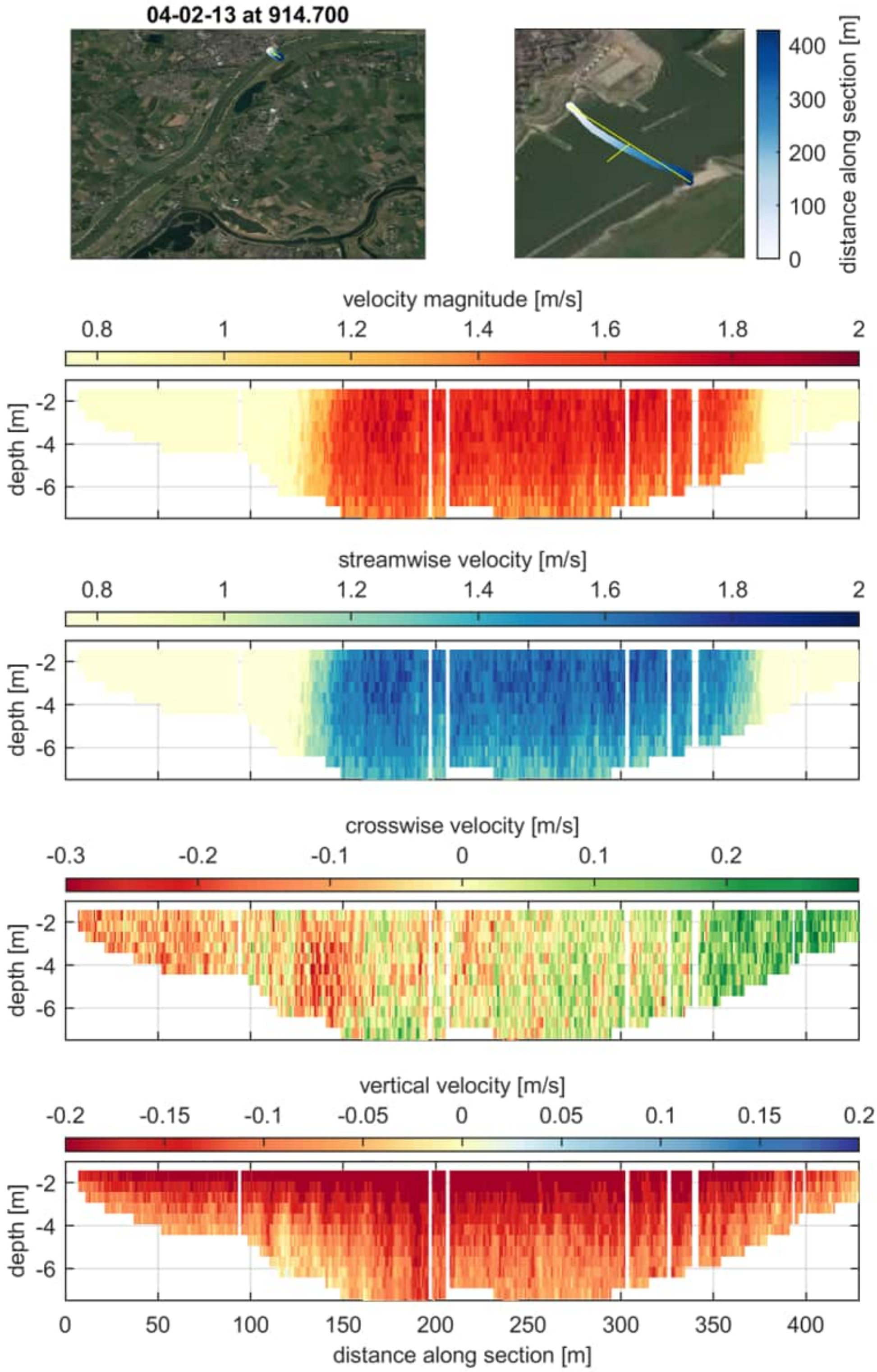

Figure D.94 Cross-sectional measurements on 04-02-13 (discharge at Lobith at 12:00 equal to 5087 m^3/s) at rkm 914.700 projected on measurement plane.

Deltares

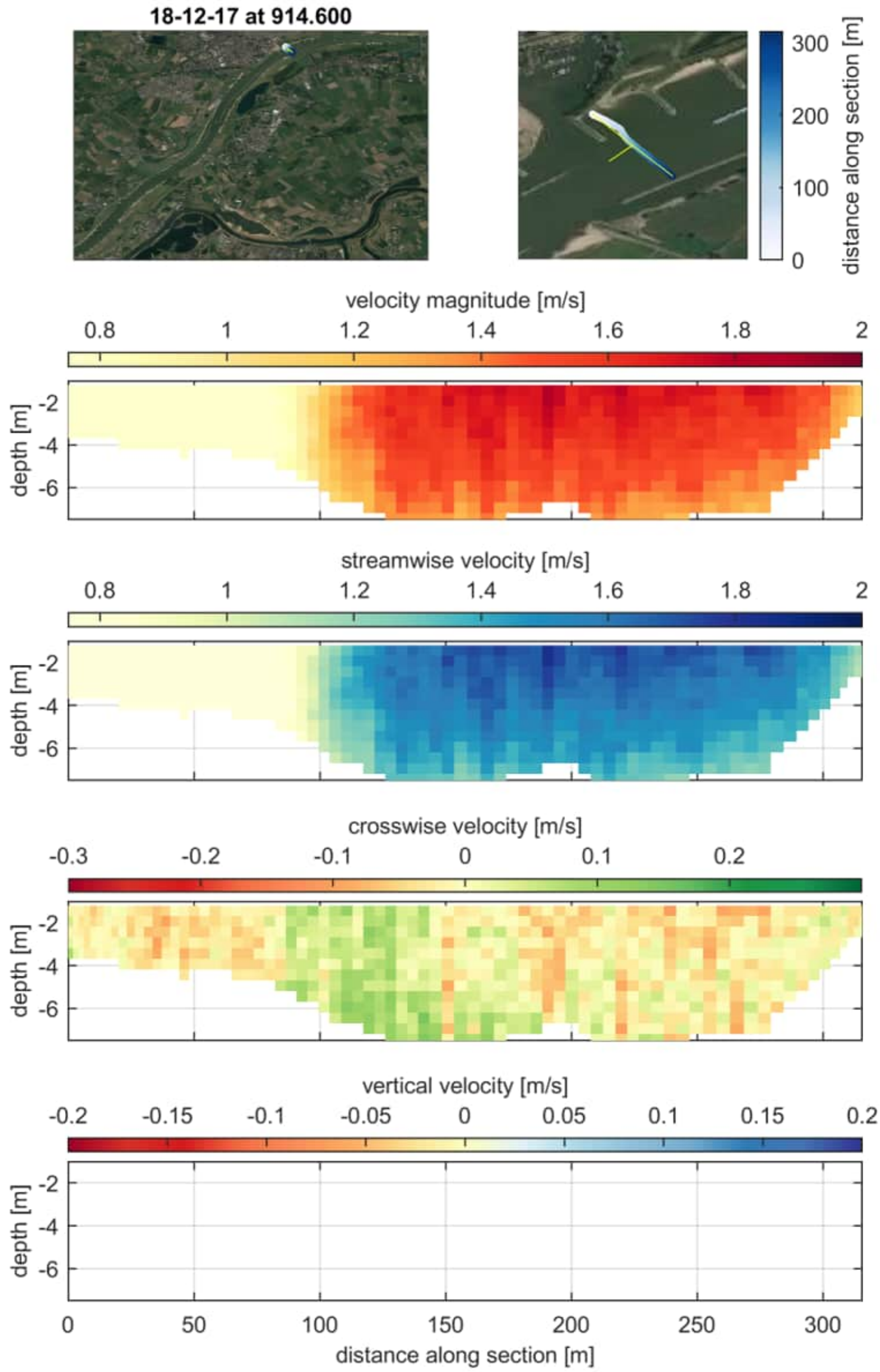

Figure D.95 Cross-sectional measurements on 18-12-17 (discharge at Lobith at 12:00 equal to 5013 m^3/s) at rkm 914.600 projected on measurement plane.

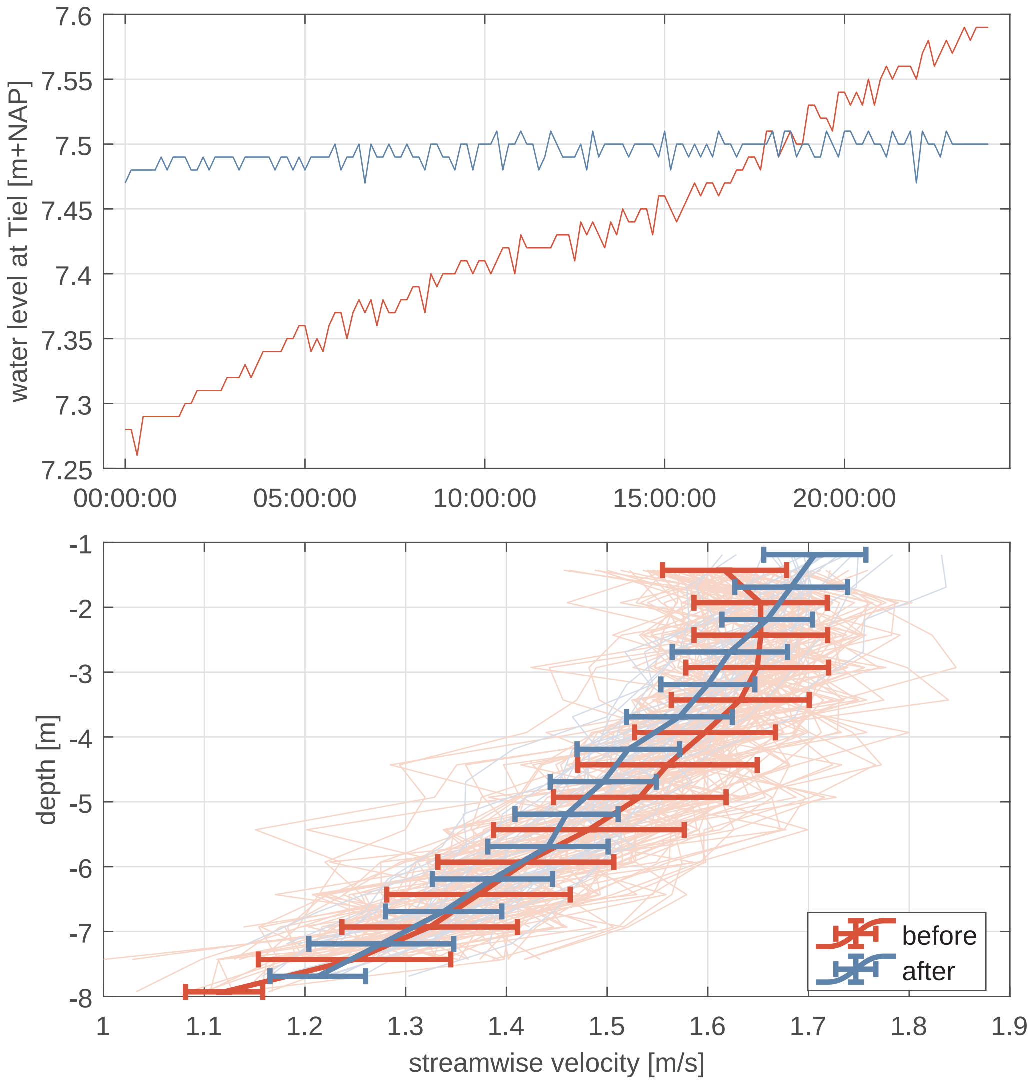

Figure D.96 Streamwise velocity at the central 100 m of channel before (04-02-13, discharge at Lobith at 12:00 equal to 5087 m^3/s, rkm 914.700) and after (18-12-17, discharge at Lobith at 12:00 equal to 5013 m^3/s, rkm 914.600)

D.3.4.6 Location 6

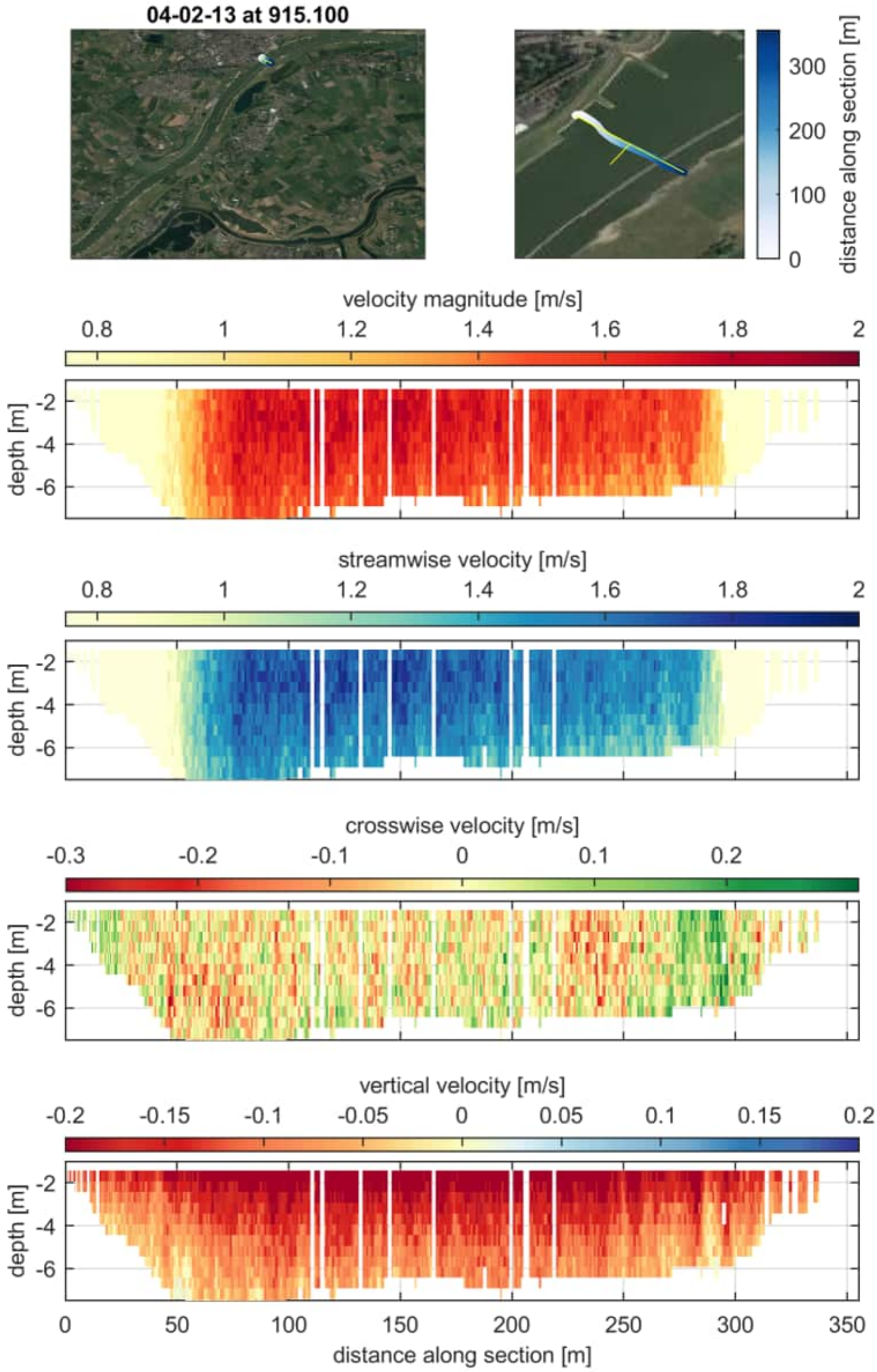

Figure D.97 Cross-sectional measurements on 04-02-13 (discharge at Lobith at 12:00 equal to 5087 m^3/s) at rkm 915.100 projected on measurement plane.

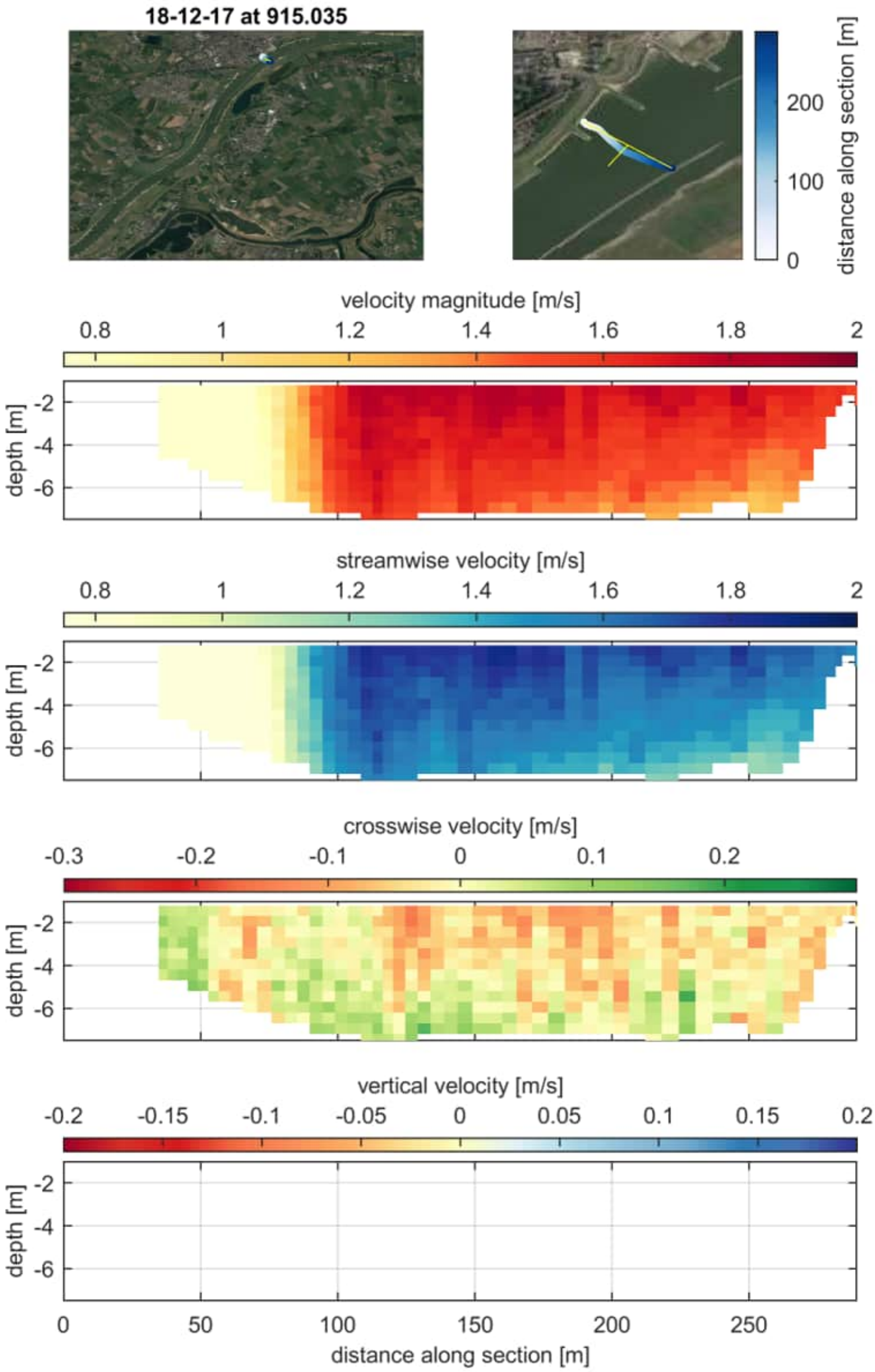

Figure D.98 Cross-sectional measurements on 18-12-17 (discharge at Lobith at 12:00 equal to 5013 m^3/s) at rkm 915.035 projected on measurement plane.

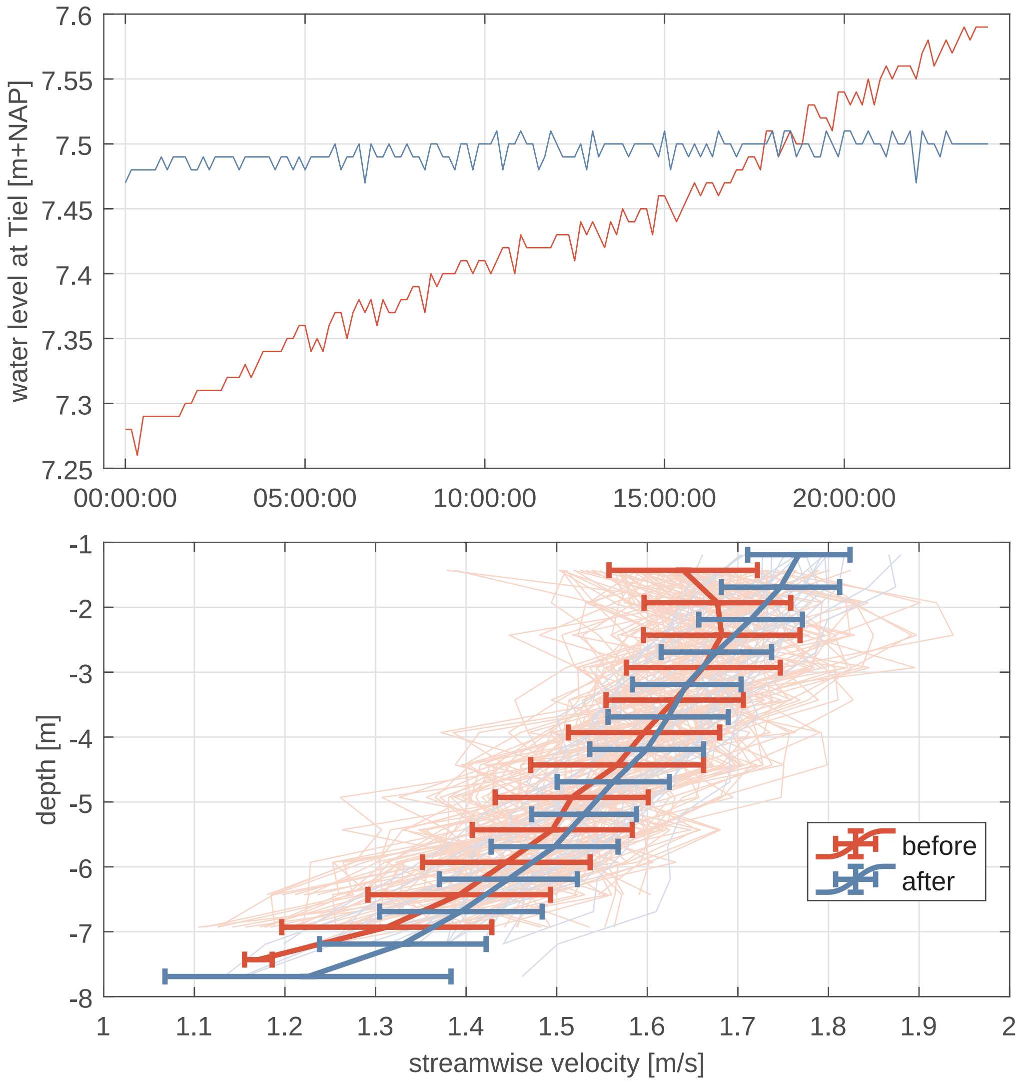

Figure D.99 Streamwise velocity at the central 100 m of channel before (04-02-13, discharge at Lobith at 12:00 equal to 5087 m^3/s, rkm 915.100) and after (18-12-17, discharge at Lobith at 12:00 equal to 5013 m^3/s, rkm 915.035)

D.3.4.7 Location 7

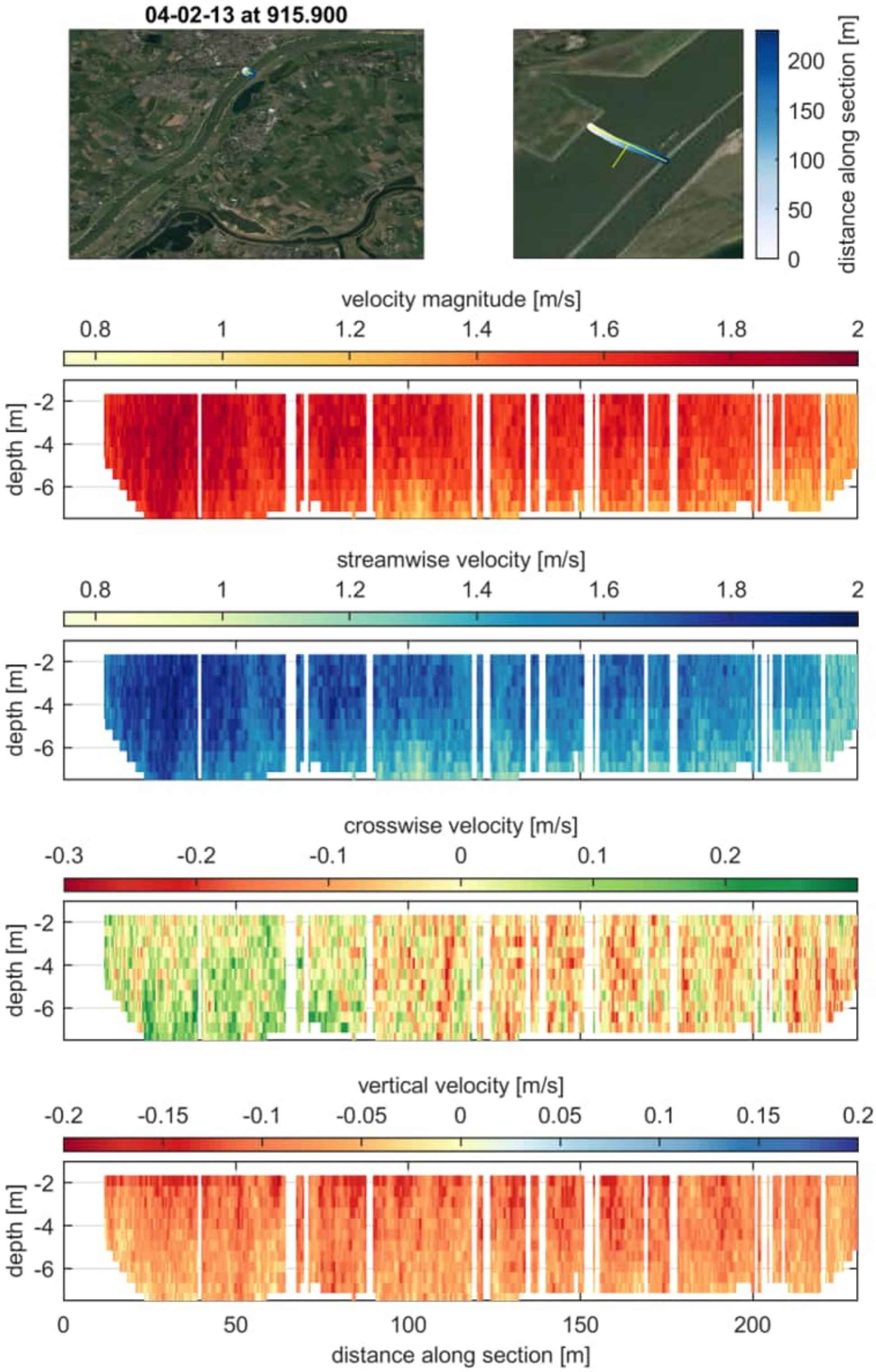

Figure D.100 Cross-sectional measurements on 04-02-13 (discharge at Lobith at 12:00 equal to 5087 m^3/s) at rkm 915.900 projected on measurement plane.

Deltares

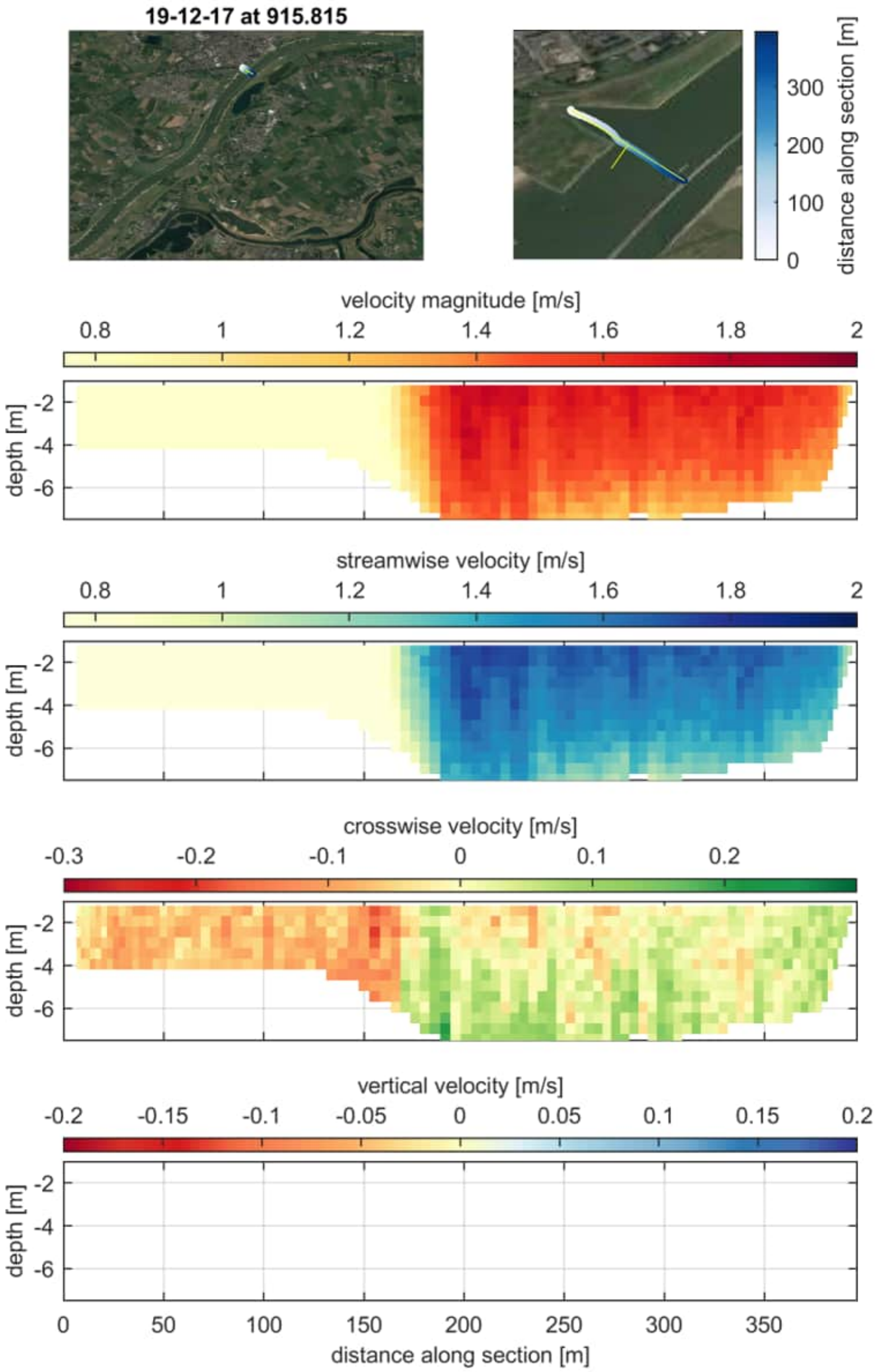

Figure D.101 Cross-sectional measurements on 19-12-17 (discharge at Lobith at 12:00 equal to 4905 m^3/s) at rkm 915.815 projected on measurement plane.

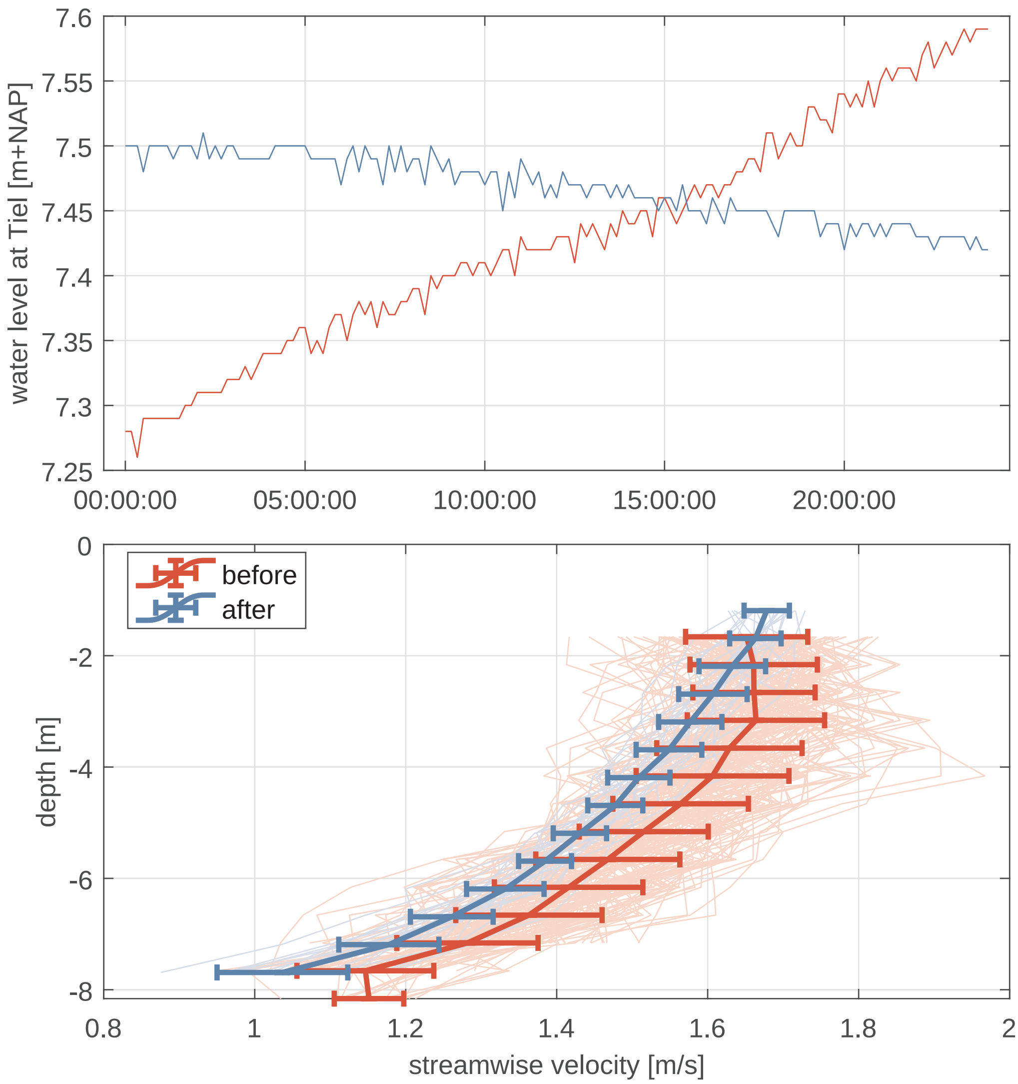

Figure D.102 Streamwise velocity at the central 100 m of channel before (04-02-13, discharge at Lobith at 12:00 equal to 5087 m^3/s, rkm 915.900) and after (19-12-17, discharge at Lobith at 12:00 equal to 4905 m^3/s, rkm 915.815)

D.3.4.8 Location 8

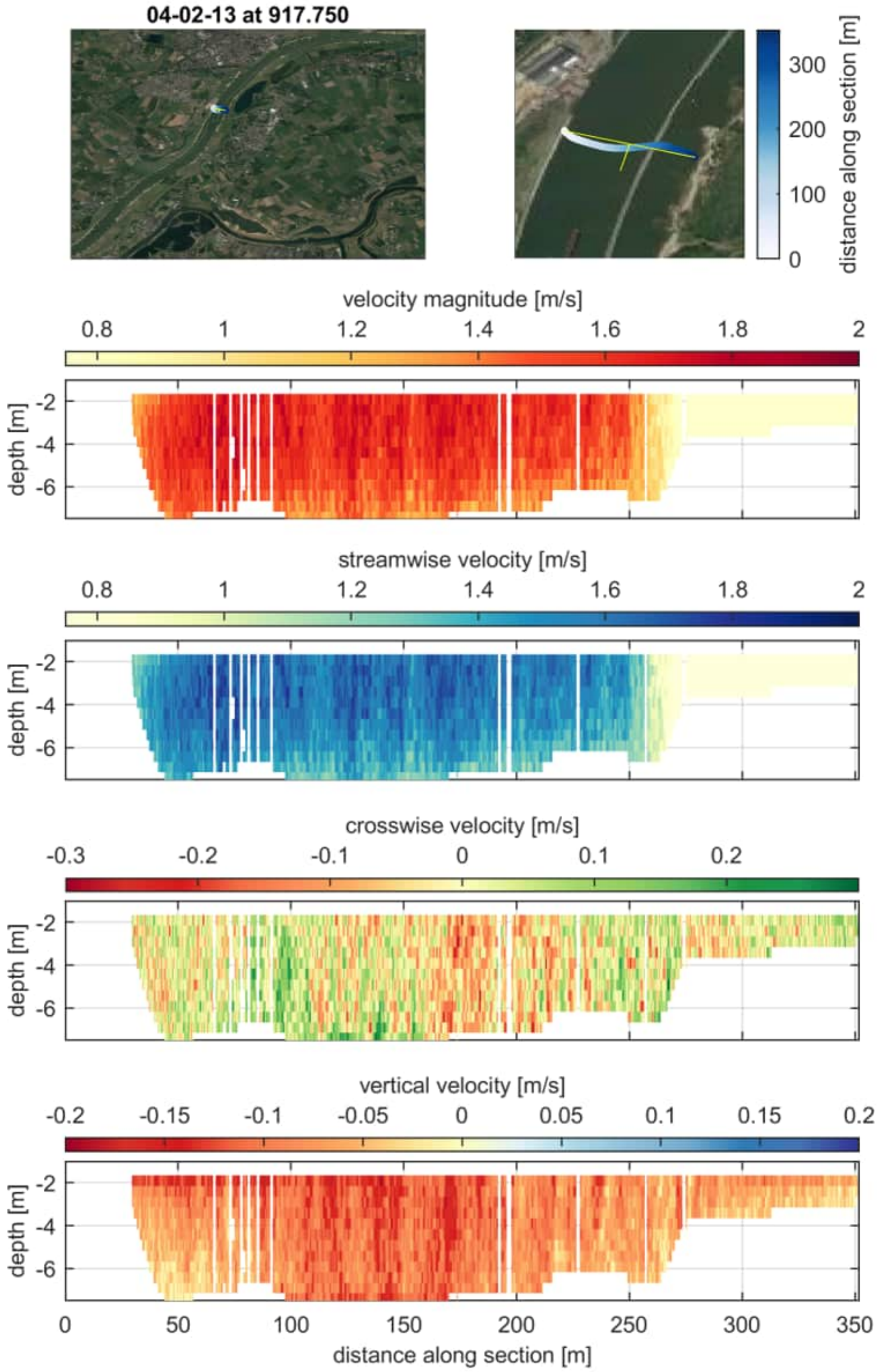

Figure D.103 Cross-sectional measurements on 04-02-13 (discharge at Lobith at 12:00 equal to 5087 m^3/s) at rkm 917.750 projected on measurement plane.

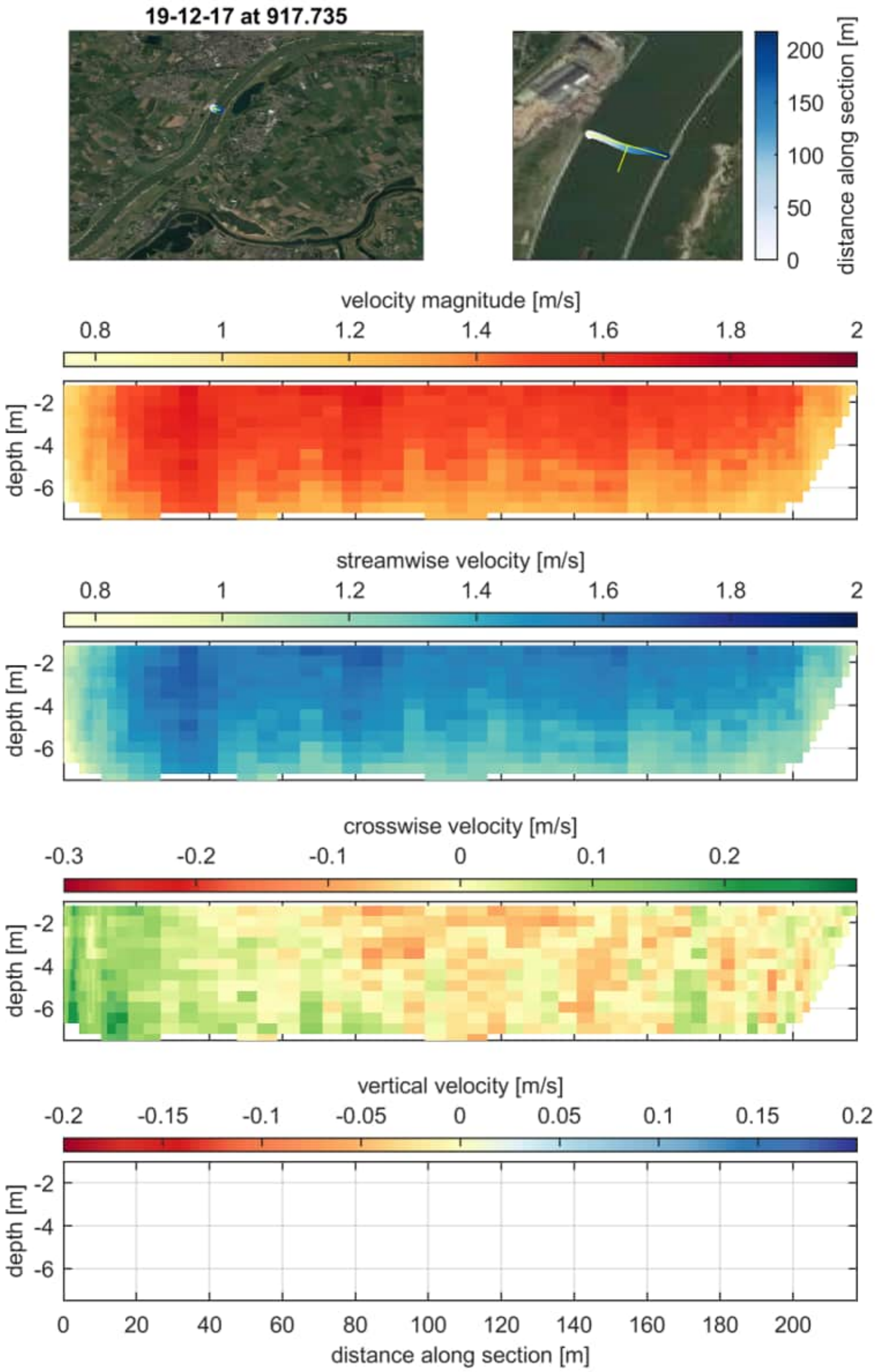

Figure D.104 Cross-sectional measurements on 19-12-17 (discharge at Lobith at 12:00 equal to 4905 m^3/s) at rkm 917.735 projected on measurement plane.

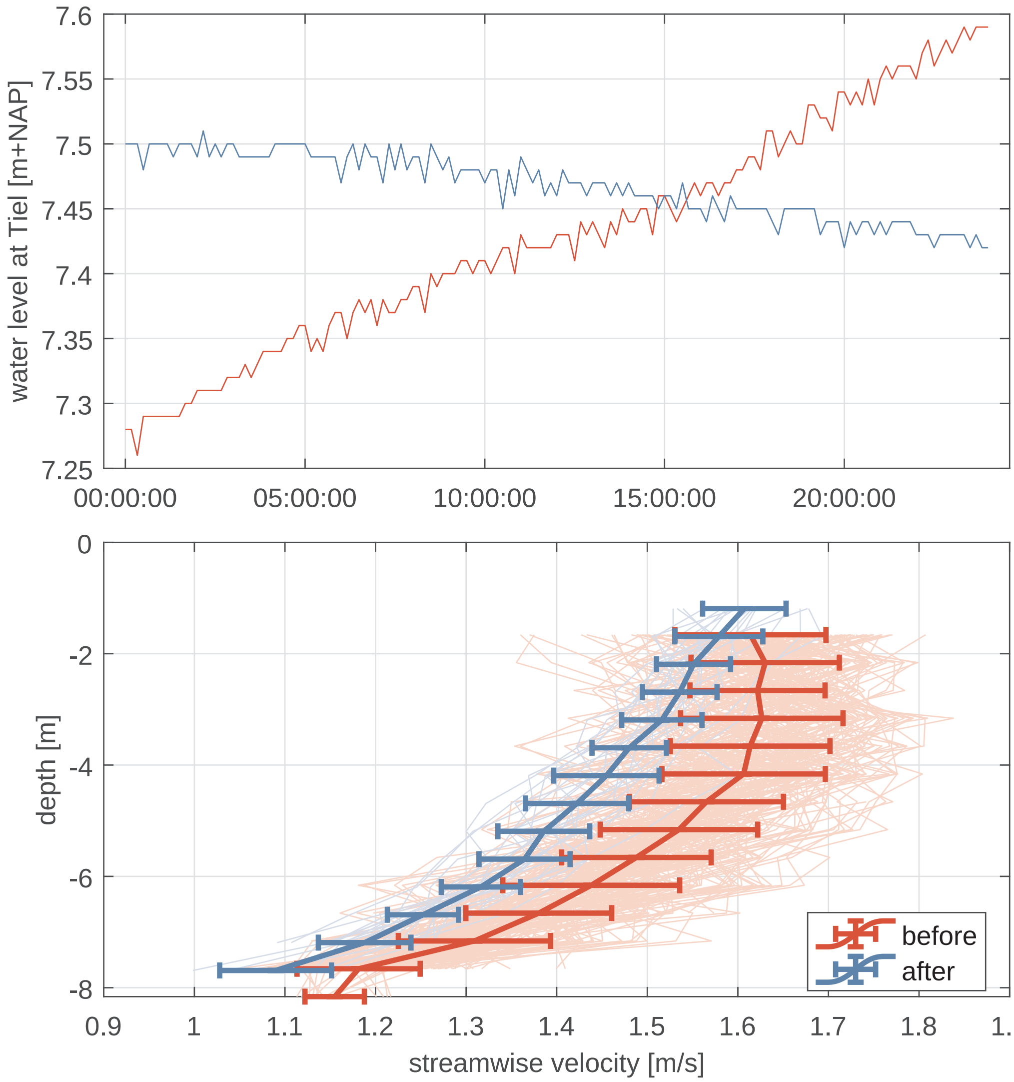

Figure D.105 Streamwise velocity at the central 100 m of channel before (04-02-13, discharge at Lobith at 12:00 equal to 5087 m^3/s, rkm 917.750) and after (19-12-17, discharge at Lobith at 12:00 equal to 4905 m^3/s, rkm 917.735)

D.3.4.9 Location 9

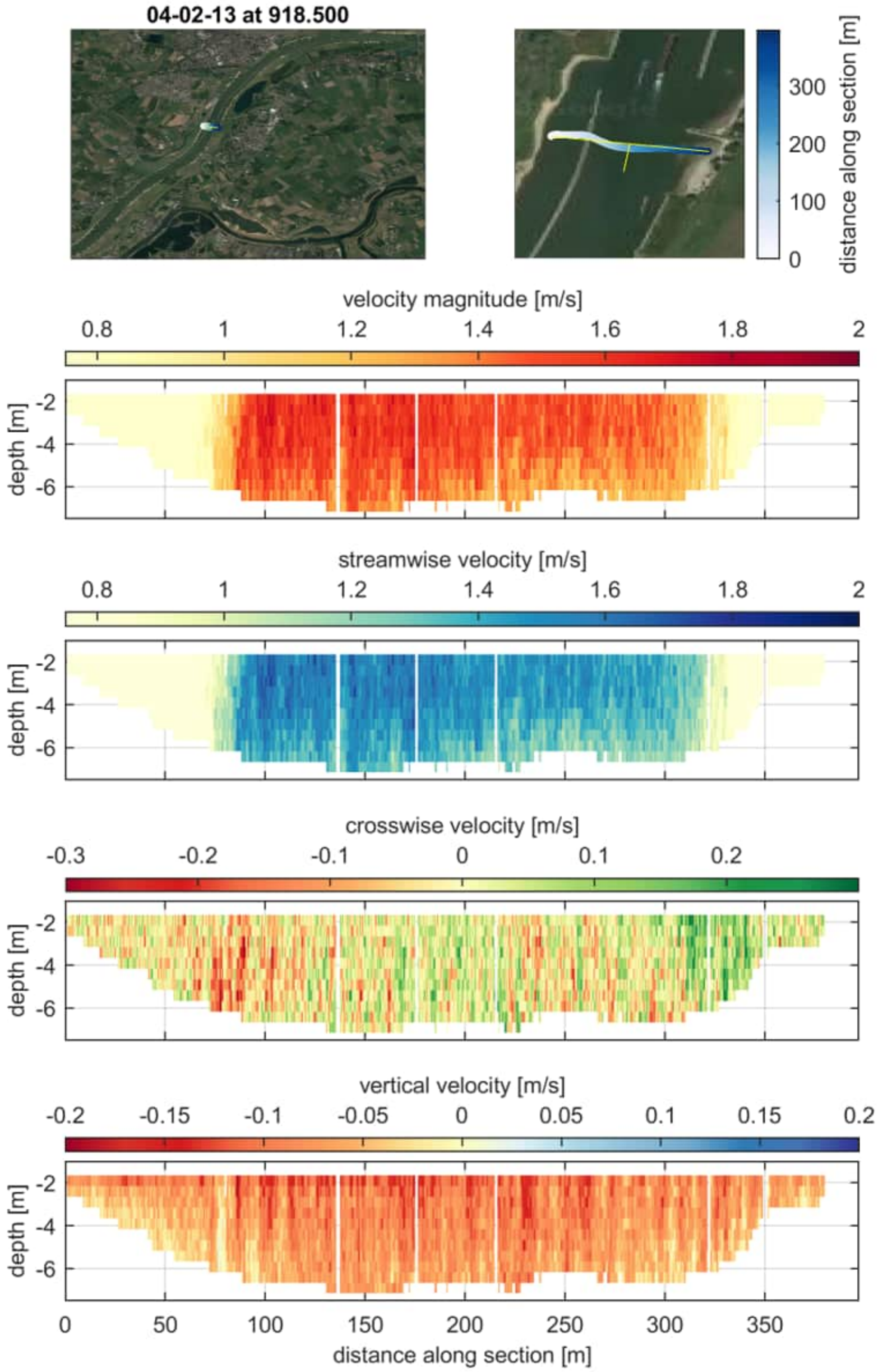

Figure D.106 Cross-sectional measurements on 04-02-13 (discharge at Lobith at 12:00 equal to 5087 m^3/s) at rkm 918.500 projected on measurement plane.

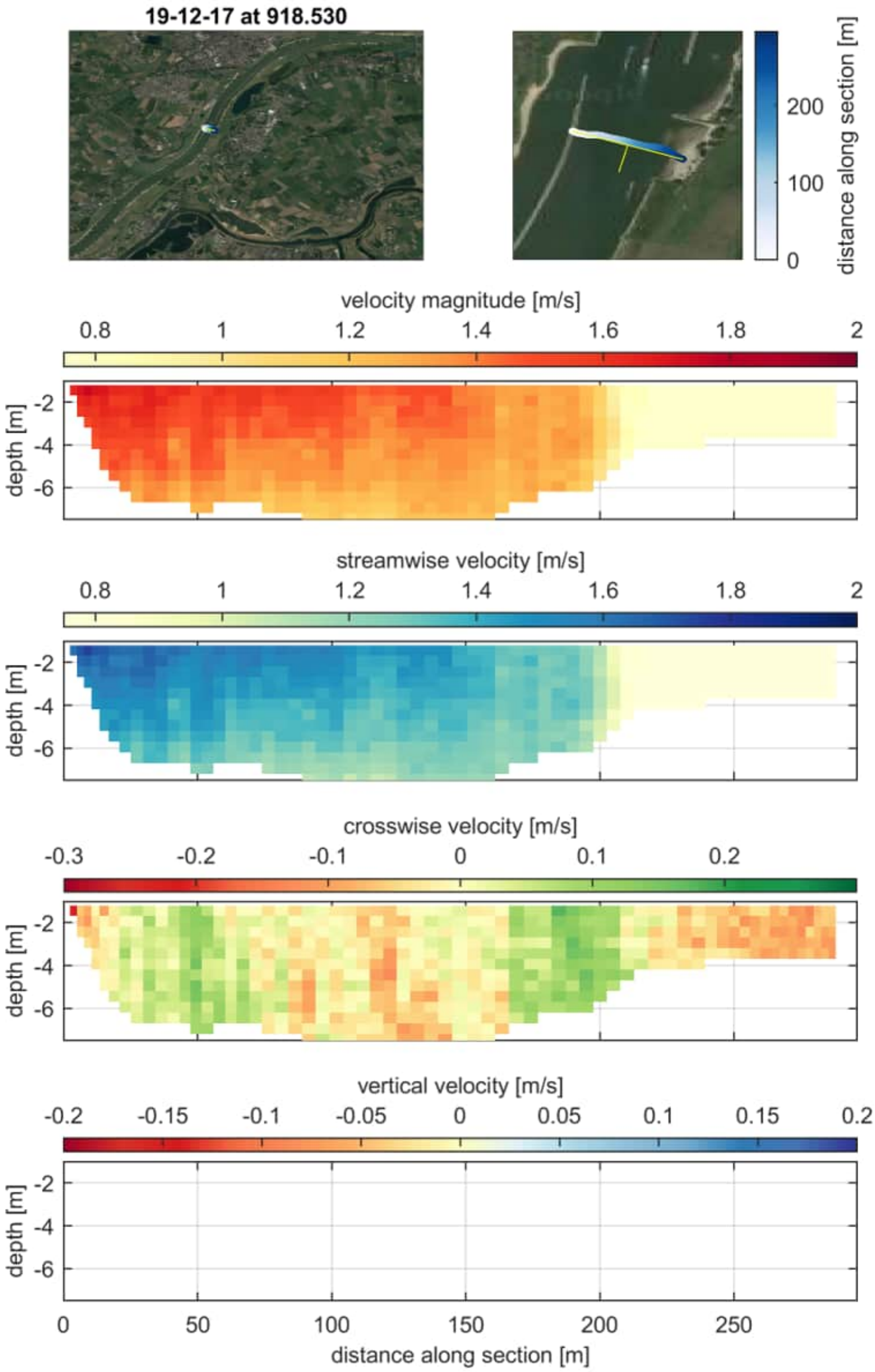

Figure D.107 Cross-sectional measurements on 19-12-17 (discharge at Lobith at 12:00 equal to 4905 m^3/s) at rkm 918.530 projected on measurement plane.

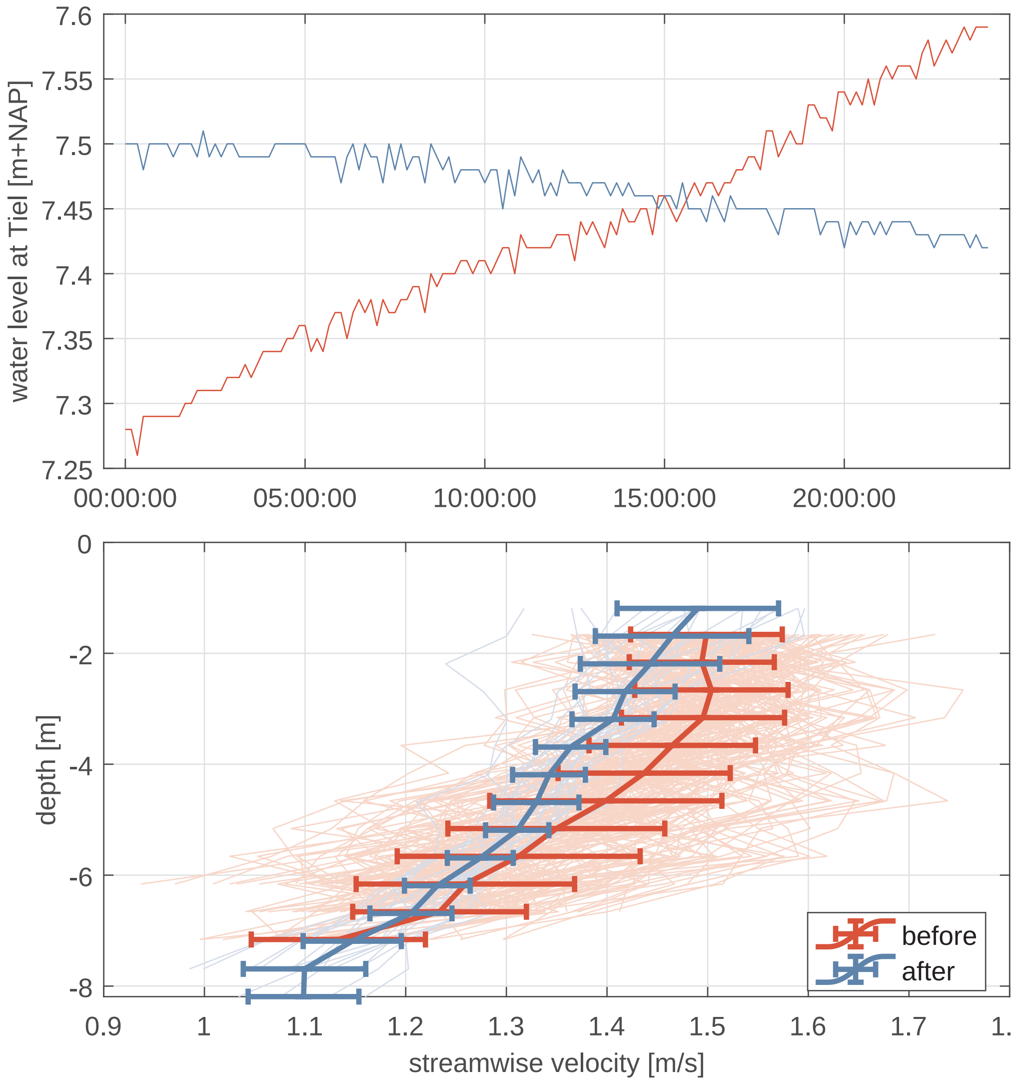

Figure D.108 Streamwise velocity at the central 100 m of channel before (04-02-13, discharge at Lobith at 12:00 equal to 5087 m^3/s, rkm 918.500) and after (19-12-17, discharge at Lobith at 12:00 equal to 4905 m^3/s, rkm 918.530)

D.3.4.10 Location 10

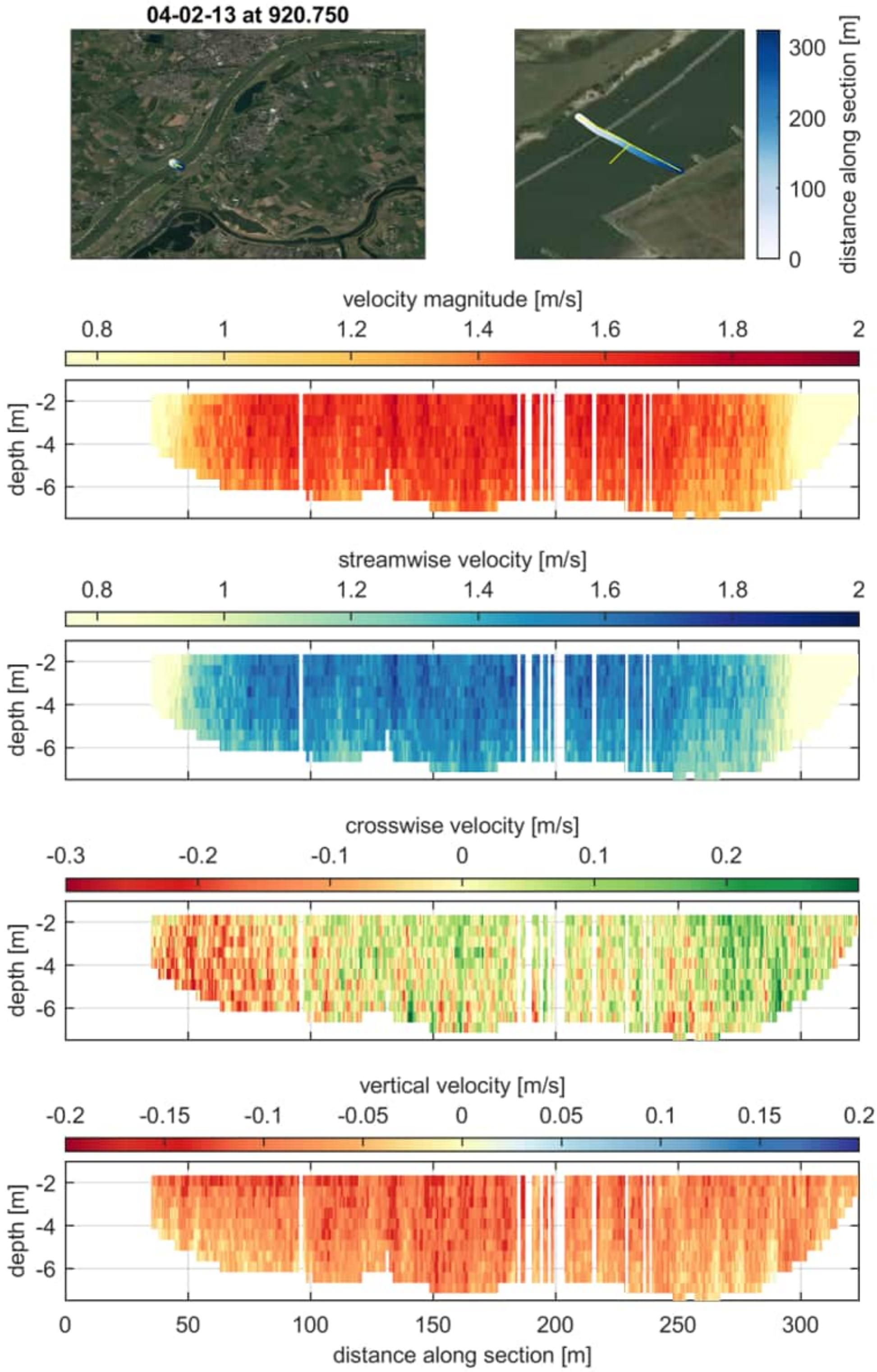

Figure D.109 Cross-sectional measurements on 04-02-13 (discharge at Lobith at 12:00 equal to 5087 m^3/s) at rkm 920.750 projected on measurement plane.

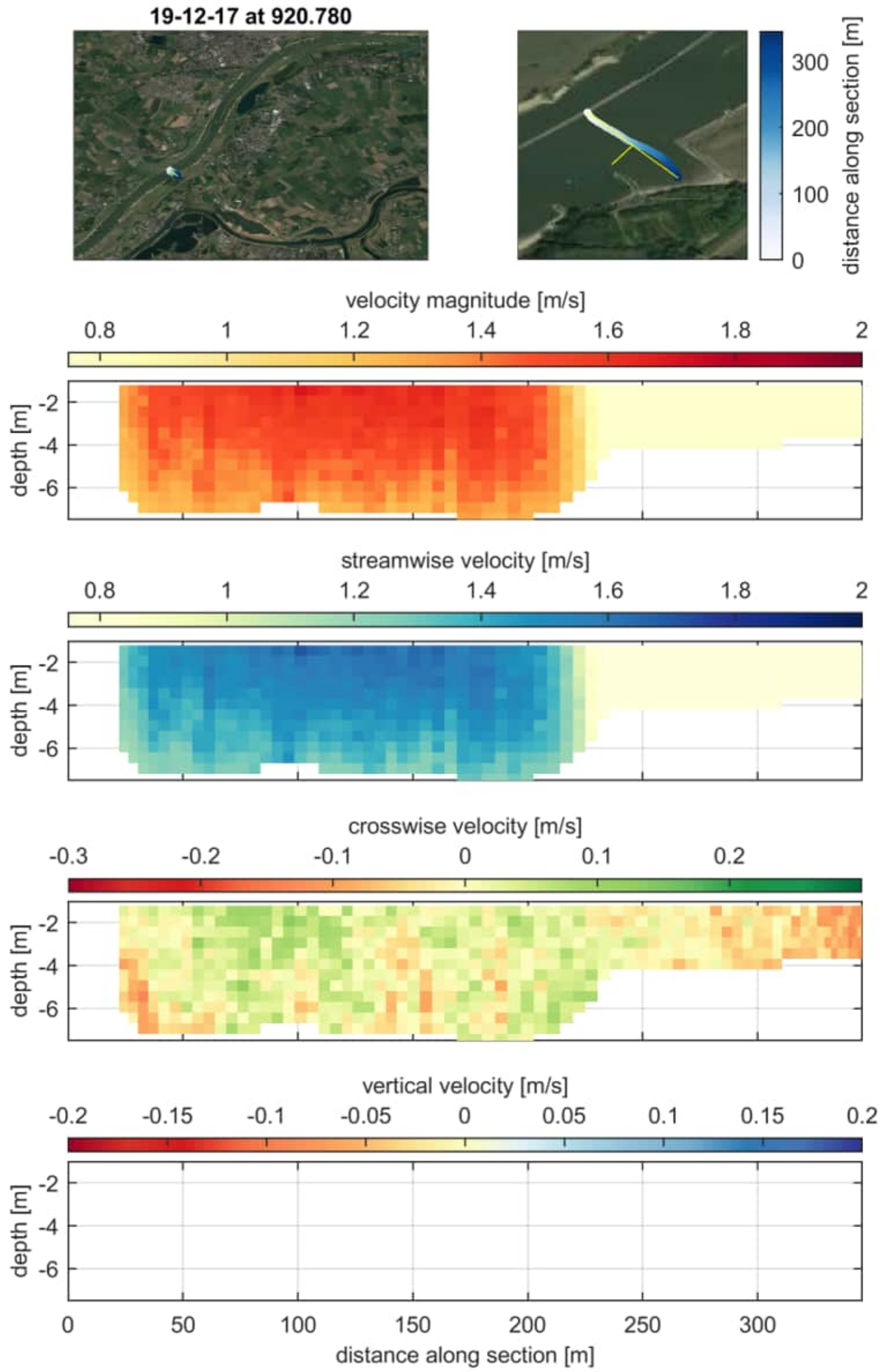

Figure D.110 Cross-sectional measurements on 19-12-17 (discharge at Lobith at 12:00 equal to 4905 m^3/s) at rkm 920.780 projected on measurement plane.

Deltares

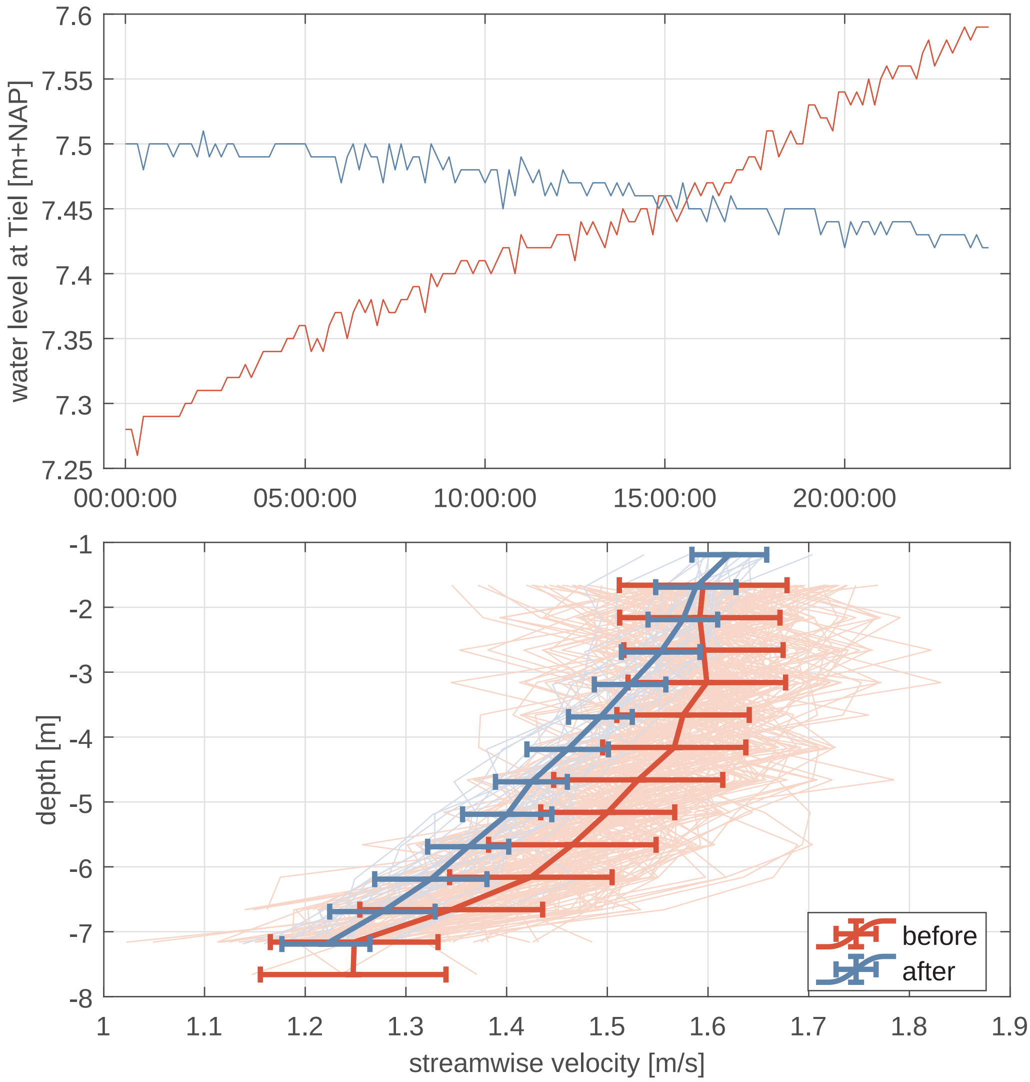

Figure D.111 Streamwise velocity at the central 100 m of channel before (04-02-13, discharge at Lobith at 12:00 equal to 5087 m^3/s, rkm 920.750) and after (19-12-17, discharge at Lobith at 12:00 equal to 4905 m^3/s, rkm 920.780)

D.3.4.11 Location 11

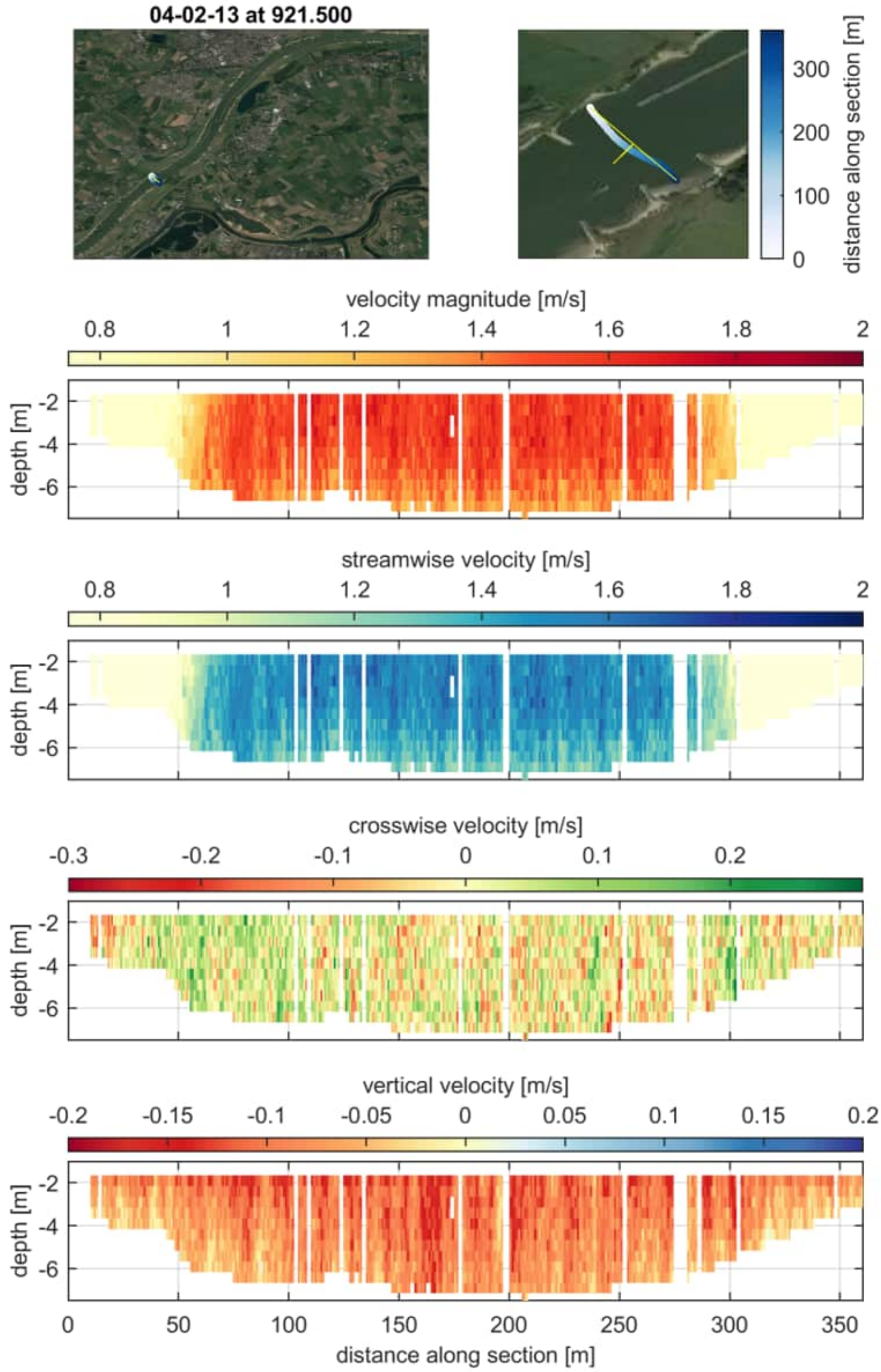

Figure D.112 Cross-sectional measurements on 04-02-13 (discharge at Lobith at 12:00 equal to 5087 m^3/s) at rkm 921.500 projected on measurement plane.

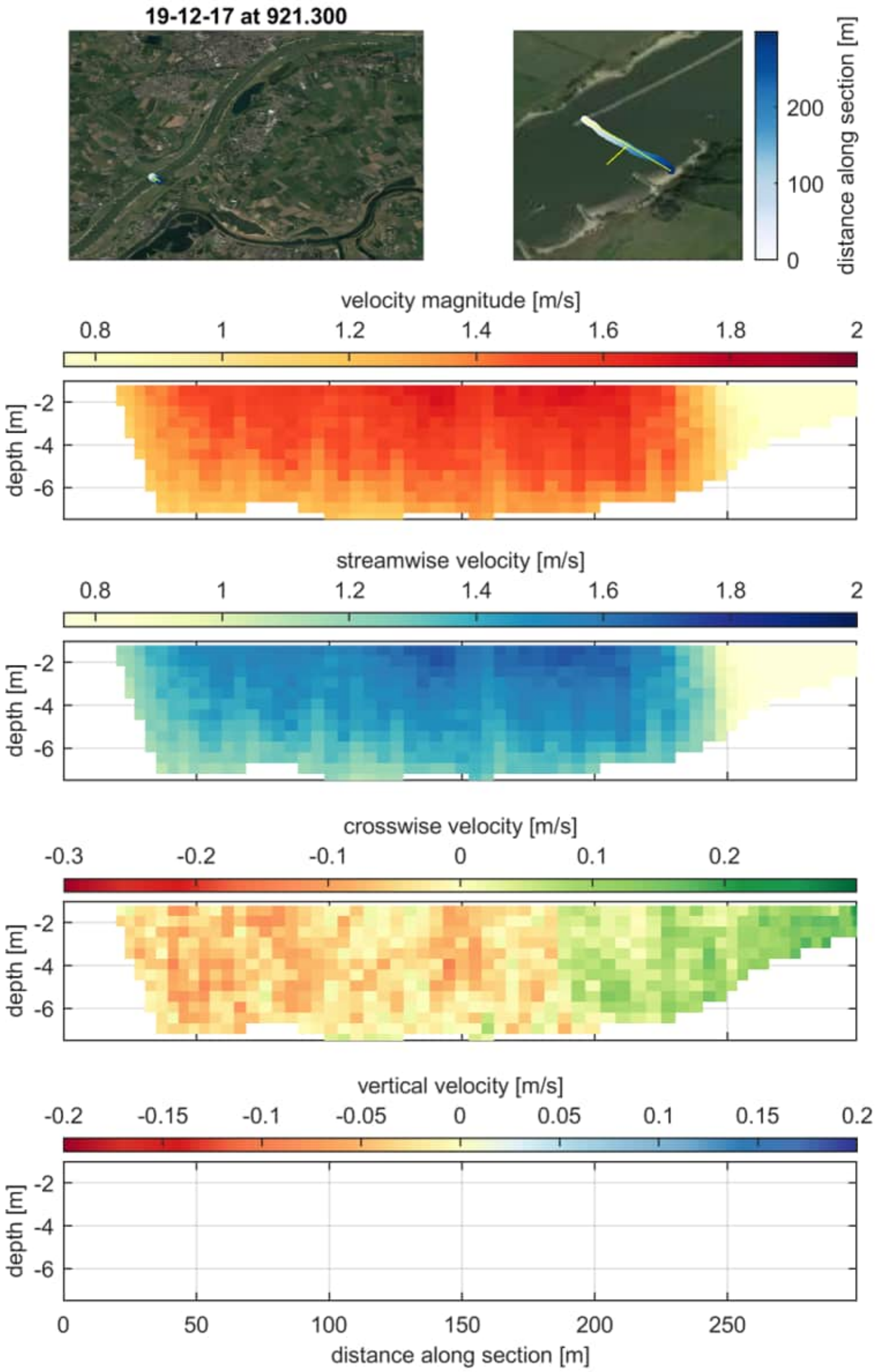

Figure D.113 Cross-sectional measurements on 19-12-17 (discharge at Lobith at 12:00 equal to 4905 m^3/s) at rkm 921.300 projected on measurement plane.

Deltares

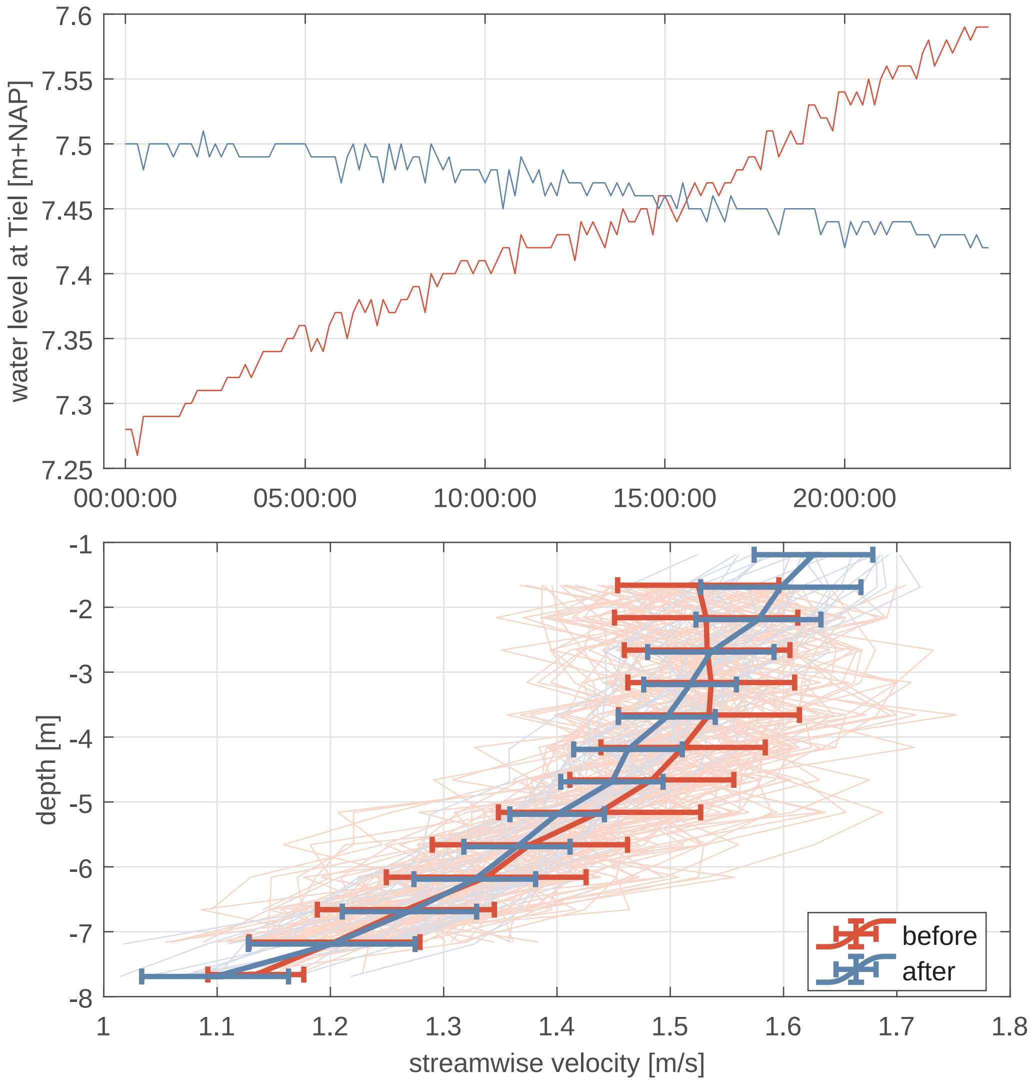

Figure D.114 Streamwise velocity at the central 100 m of channel before (04-02-13, discharge at Lobith at 12:00 equal to 5087 m^3/s, rkm 921.500) and after (19-12-17, discharge at Lobith at 12:00 equal to 4905 m^3/s, rkm 921.300)

D.3.4.12 Location 12

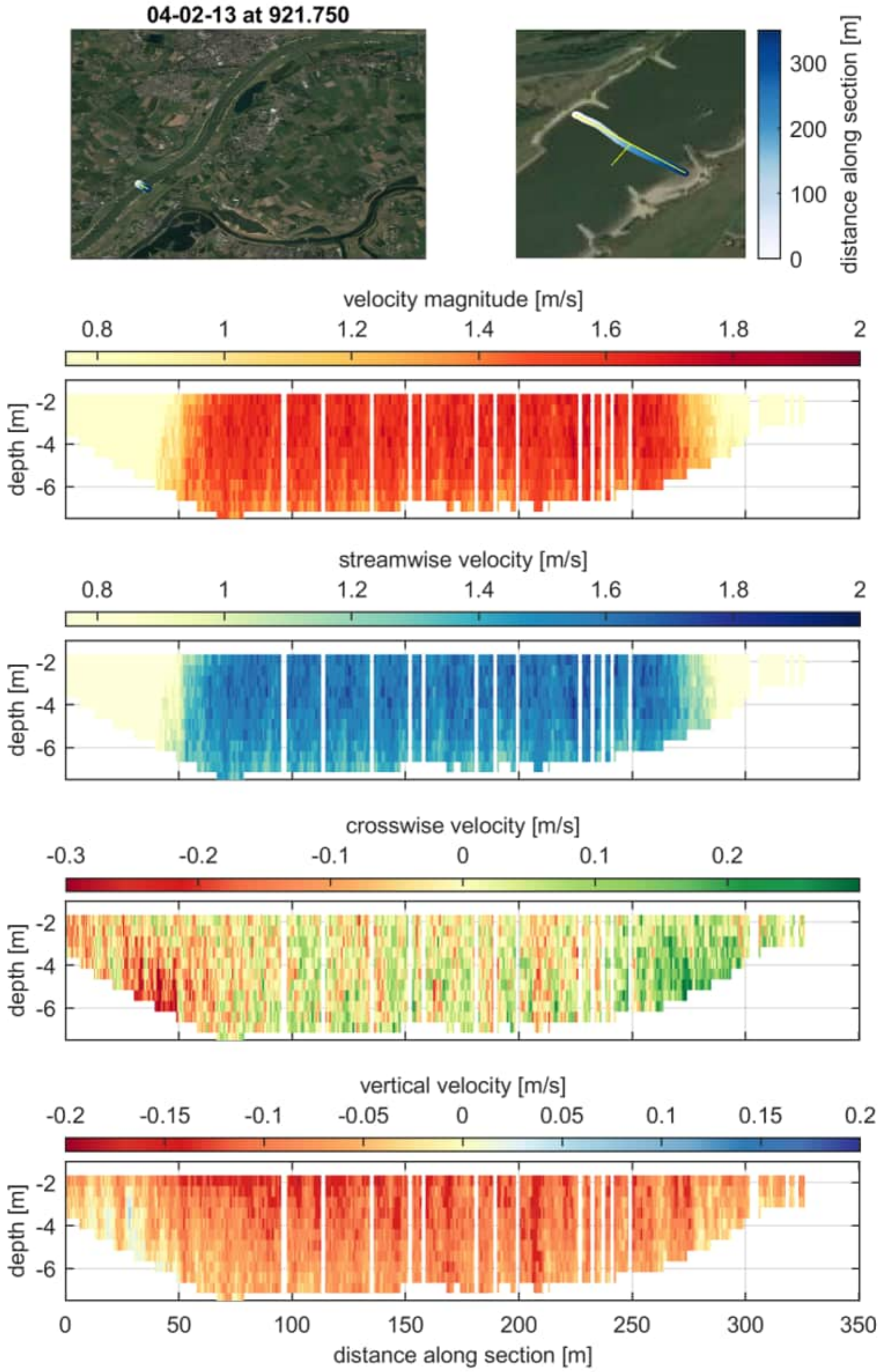

Figure D.115 Cross-sectional measurements on 04-02-13 (discharge at Lobith at 12:00 equal to 5087 m^3/s) at rkm 921.750 projected on measurement plane.

Deltares

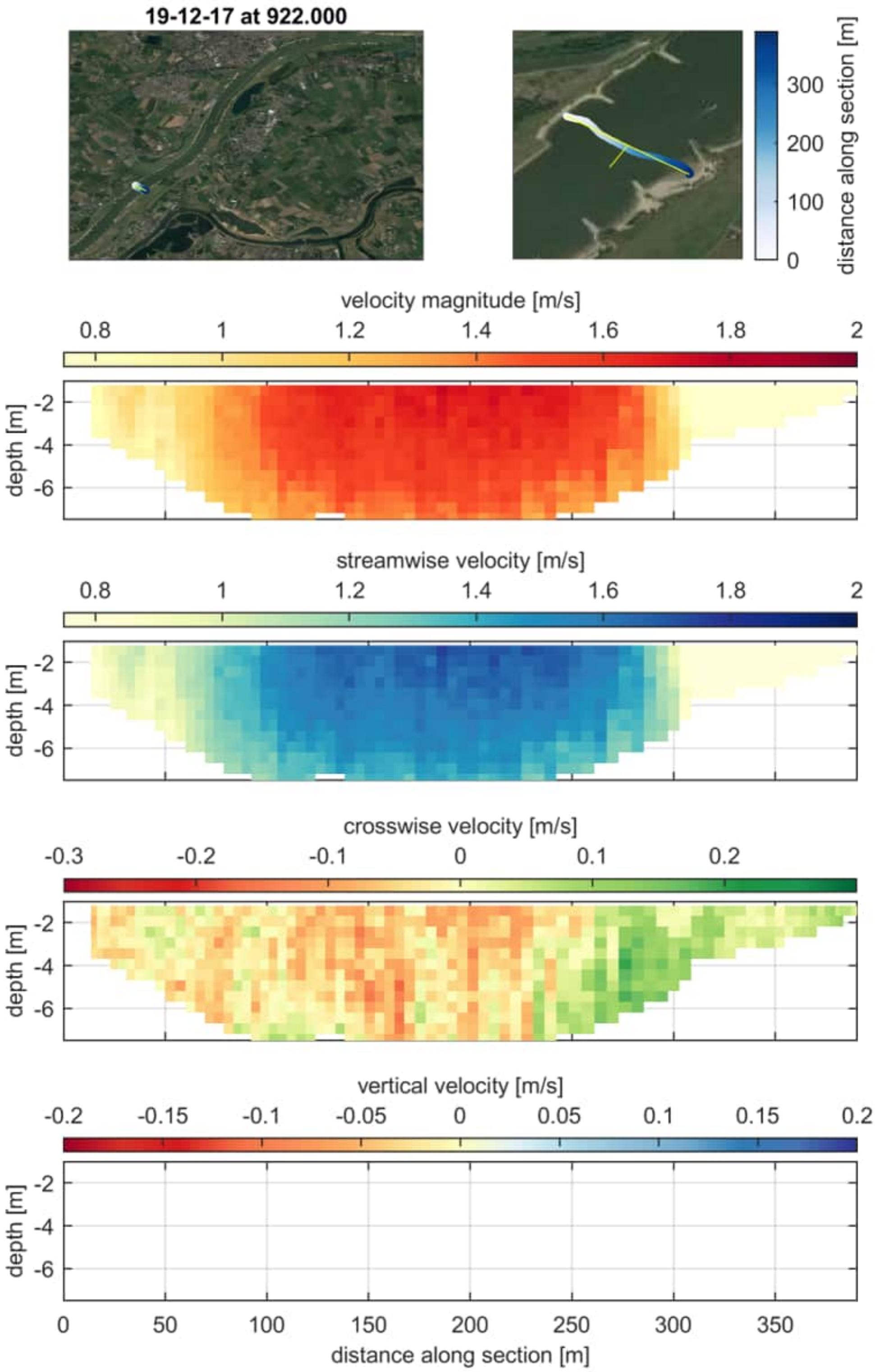

Figure D.116 Cross-sectional measurements on 19-12-17 (discharge at Lobith at 12:00 equal to 4905 m^3/s) at rkm 922.000 projected on measurement plane.

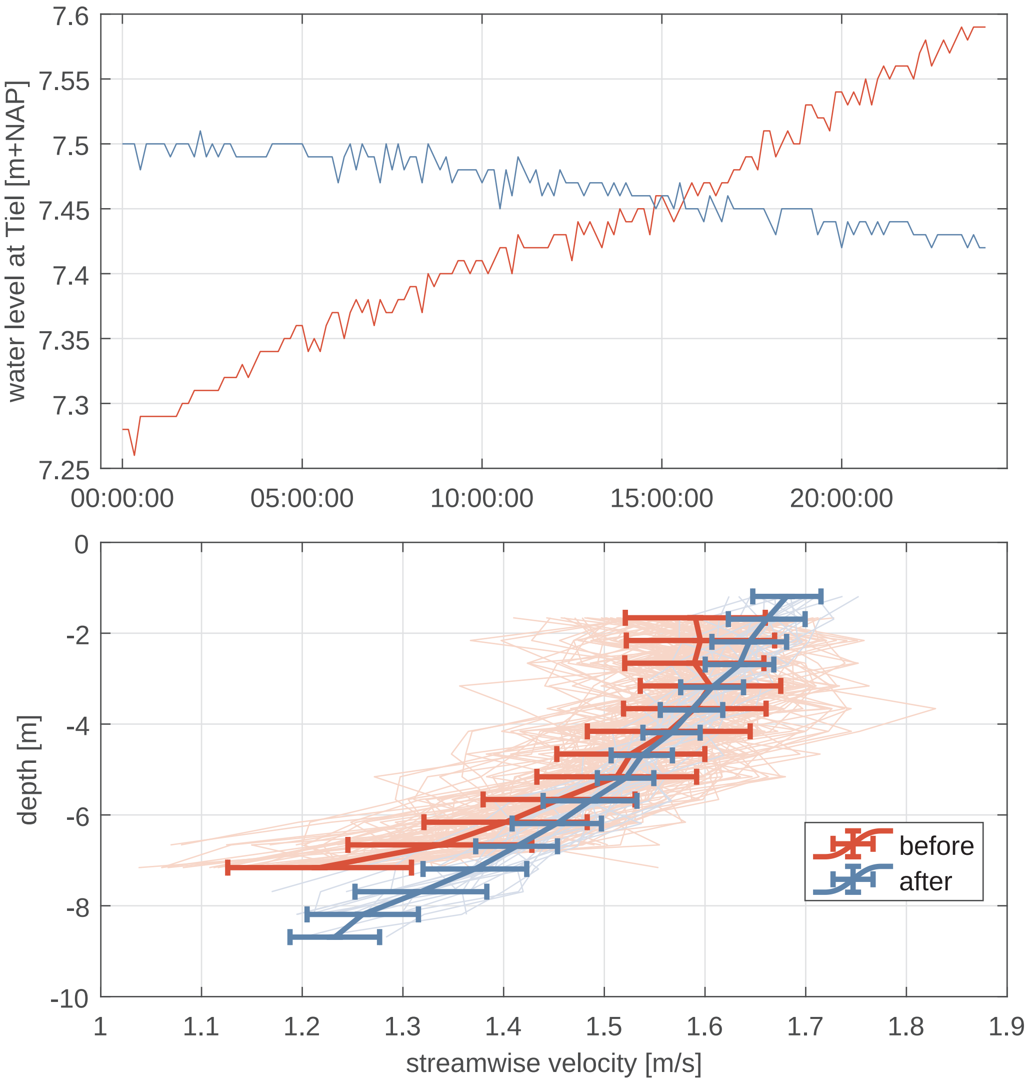

Figure D.117 Streamwise velocity at the central 100 m of channel before (04-02-13, discharge at Lobith at 12:00 equal to 5087 m^3/s, rkm 921.750) and after (19-12-17, discharge at Lobith at 12:00 equal to 4905 m^3/s, rkm 922.000)

D.3.4.13 Location 13

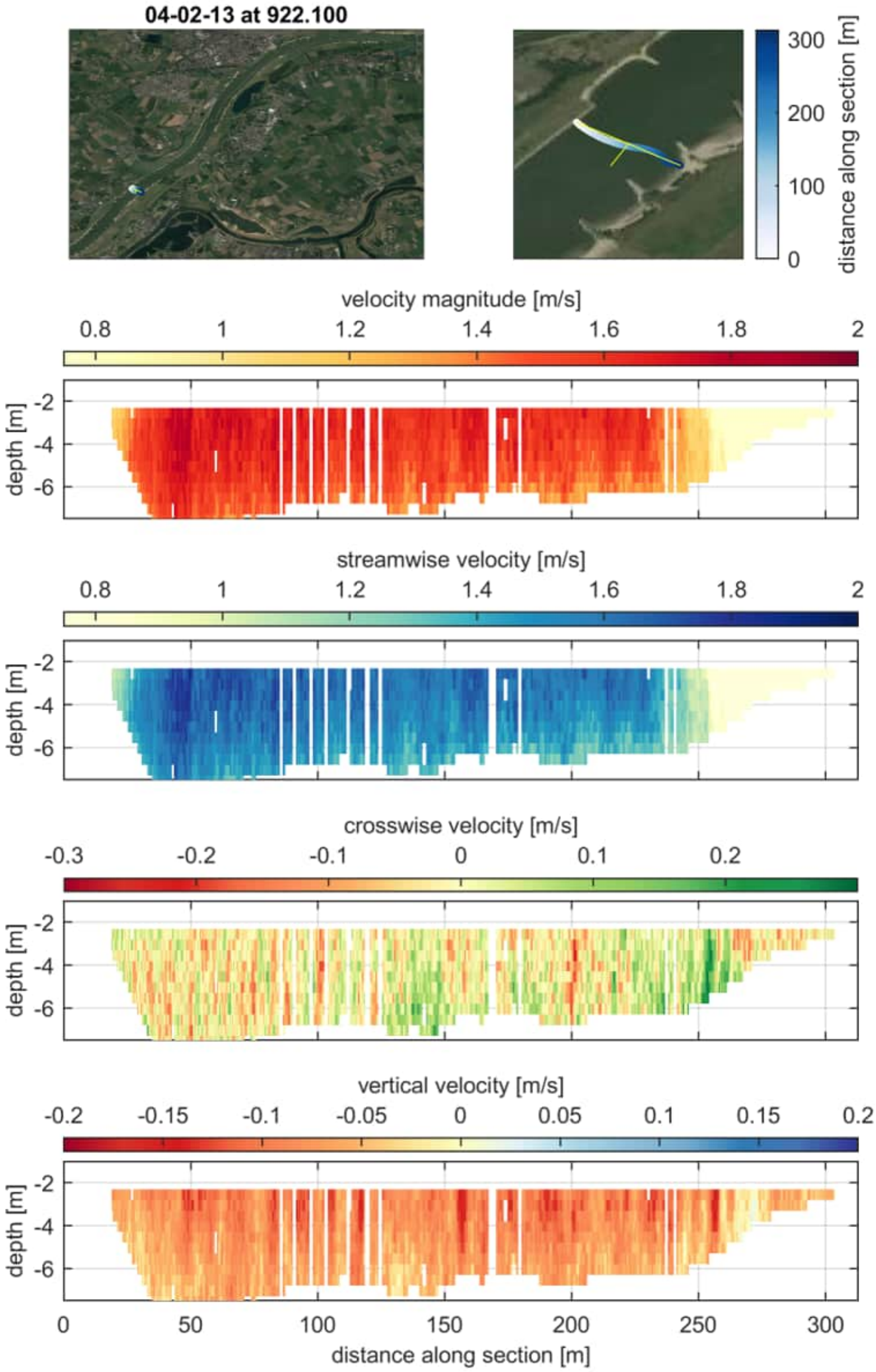

Figure D.118 Cross-sectional measurements on 04-02-13 (discharge at Lobith at 12:00 equal to 5087 m^3/s) at rkm 922.100 projected on measurement plane.

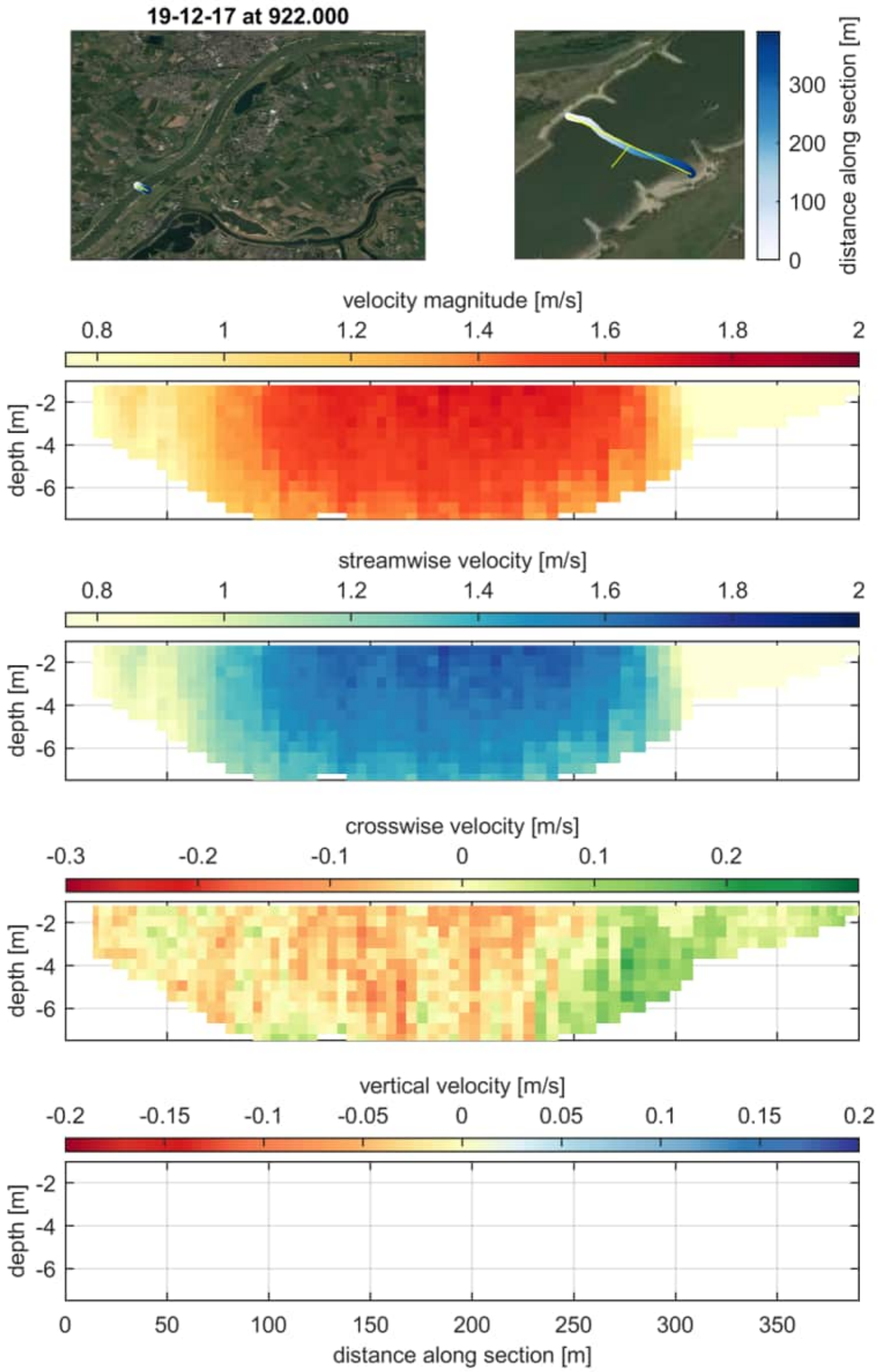

Figure D.119 Cross-sectional measurements on 19-12-17 (discharge at Lobith at 12:00 equal to 4905 m^3/s) at rkm 922.000 projected on measurement plane.

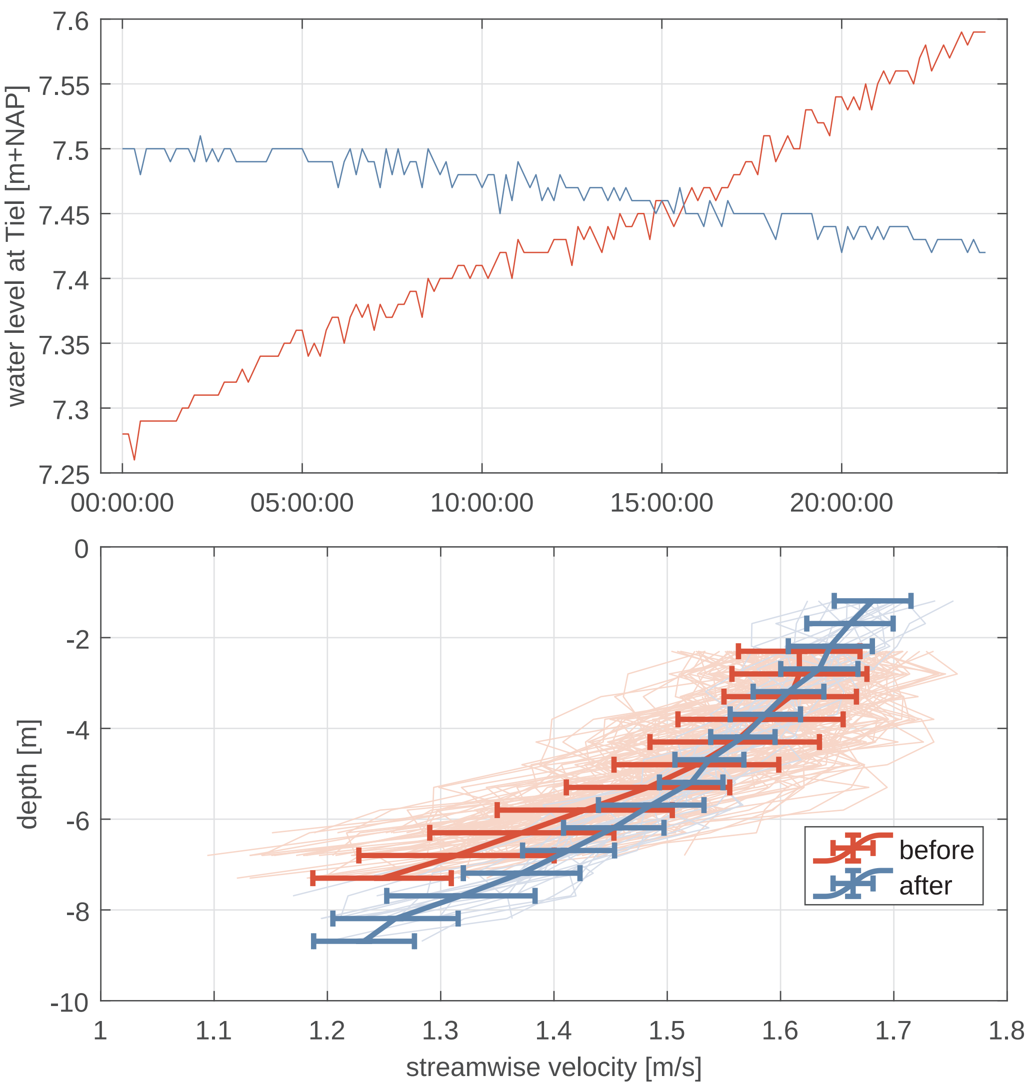

Figure D.120 Streamwise velocity at the central 100 m of channel before (04-02-13, discharge at Lobith at 12:00 equal to 5087 m^3/s, rkm 922.100) and after (19-12-17, discharge at Lobith at 12:00 equal to 4905 m^3/s, rkm 922.000)

D.4 Summary of ADCP profiles used in analysis of velocity at entrances.

number	location	date
01	Wamel upstream	19-Dec-2019
02	Wamel-Dreumel	19-Dec-2019
03	Ophemert upstream	18-Dec-2019
04	Wamel upstream	20-Mar-2019
05	Wamel-Dreumel	20-Mar-2019
06	Ophemert upstream	21-Mar-2019
07	Wamel upstream	25-Sep-2019
08	Wamel-Dreumel	26-Sep-2019
09	Ophemert upstream	26-Sep-2019
10	Wamel upstream	04-Mar-2019
11	Wamel upstream	04-Jan-2019
12	Wamel-Dreumel	04-Jan-2019
13	Wamel-Dreumel	09-Jan-2019
14	Ophemert upstream	05-Jan-2019
15	Wamel-Dreumel	27-Feb-2019
16	Wamel upstream	26-Mar-2019
17	Wamel-Dreumel	27-Mar-2019
18	Ophemert upstream	27-Mar-2019
19	Wamel upstream	05-Feb-2020
20	Wamel-Dreumel	05-Feb-2020
21	Ophemert upstream	05-Feb-2020
22	Wamel upstream	06-Feb-2020
23	Wamel-Dreumel	06-Feb-2020
24	Ophemert upstream	06-Feb-2020
25	Wamel upstream	21-Apr-2020
26	Wamel-Dreumel	23-Apr-2020
27	Ophemert upstream	24-Apr-2020
28	Wamel upstream	02-Apr-2020
29	Wamel-Dreumel	03-Apr-2020
30	Ophemert upstream	02-Apr-2020
31	Wamel inlet 2	07-Dec-2017
32	Wamel inlet 2	07-Dec-2017
33	Wamel inlet 1	07-Dec-2017
34	Wamel inlet 1	07-Dec-2017
35	Wamel upstream	01-Dec-2017
36	Wamel-Dreumel	01-Dec-2017
37	Ophemert upstream	01-Dec-2017
38	Ophemert upstream	11-Oct-2016
39	Wamel upstream	20-Jul-2018
40	Wamel-Dreumel	20-Jul-2018
41	Wamel upstream	07-Mar-2018
42	Wamel-Dreumel	07-Mar-2018
43	Ophemert upstream	07-Mar-2018

number	location	date
44	Wamel upstream	16-Feb-2018
45	Wamel-Dreumel	16-Feb-2018
46	Ophemert upstream	16-Feb-2018
47	Wamel upstream	02-Feb-2018
48	Wamel-Dreumel	02-Feb-2018
49	Ophemert upstream	02-Feb-2018

Table D.14 Inlet locations analysed.

D.5 Transverse velocity near inlets

D.5.1 Ophemert upstream

D.5.1.1 11-10-16

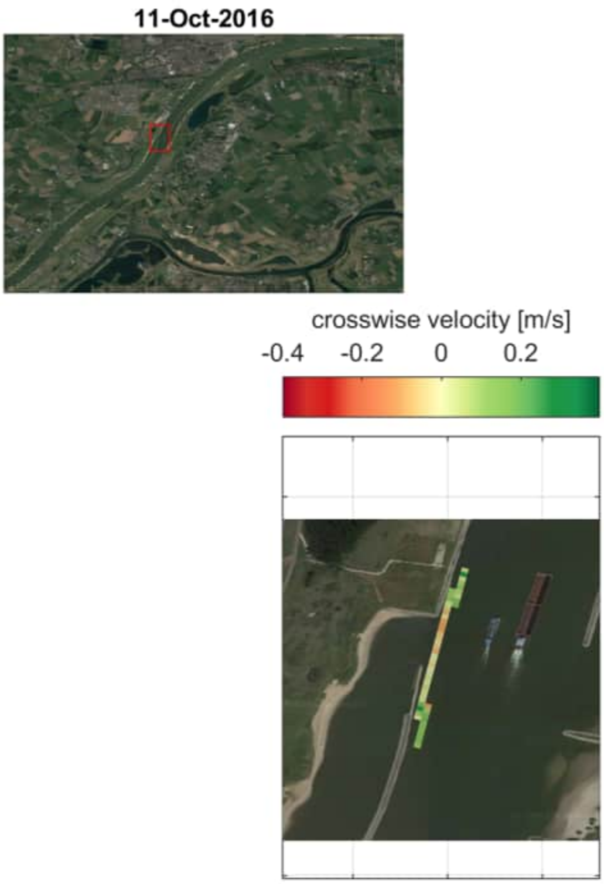

Figure D.121 Depth-averaged velocity field considering the full water column on 11-10-16 (discharge at Lobith at 12:00 equal to 1025 m^3/s).

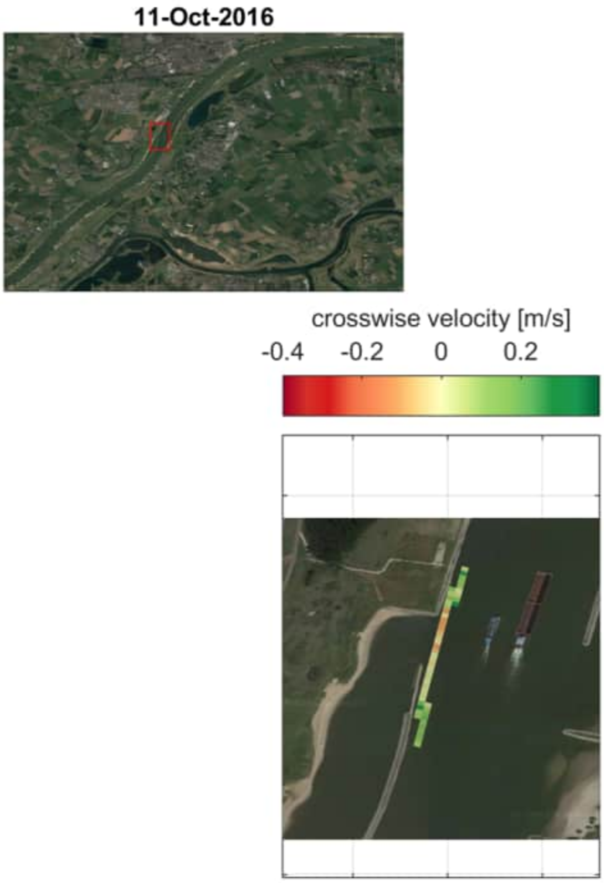

Figure D.122 Depth-averaged velocity field considering the top 2 m on 11-10-16 (discharge at Lobith at 12:00 equal to 1025 m^3/s).

D.5.1.2 05-01-19

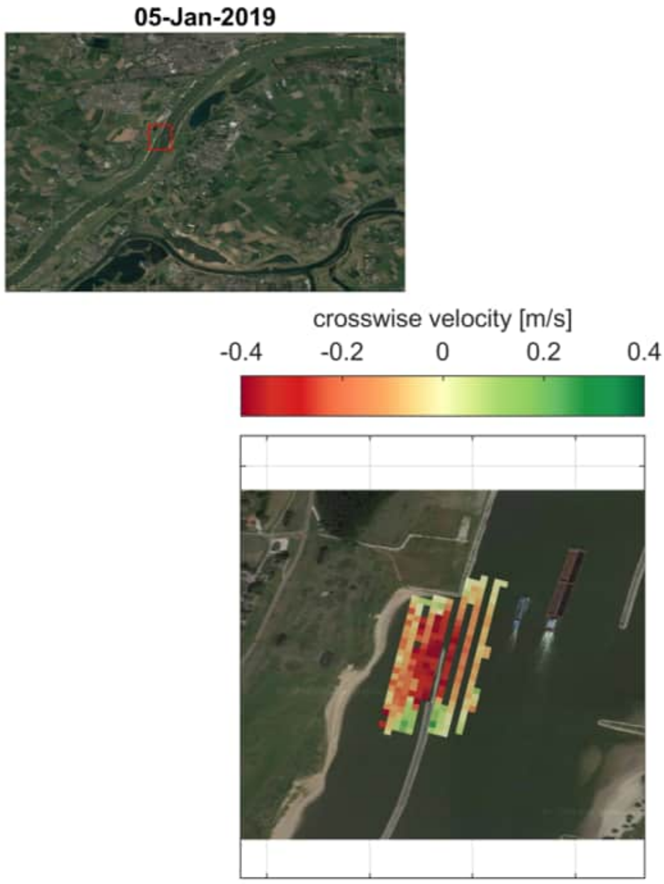

Figure D.123 Depth-averaged velocity field considering the full water column on 05-01-19 (discharge at Lobith at 12:00 equal to 1843 m^3/s).

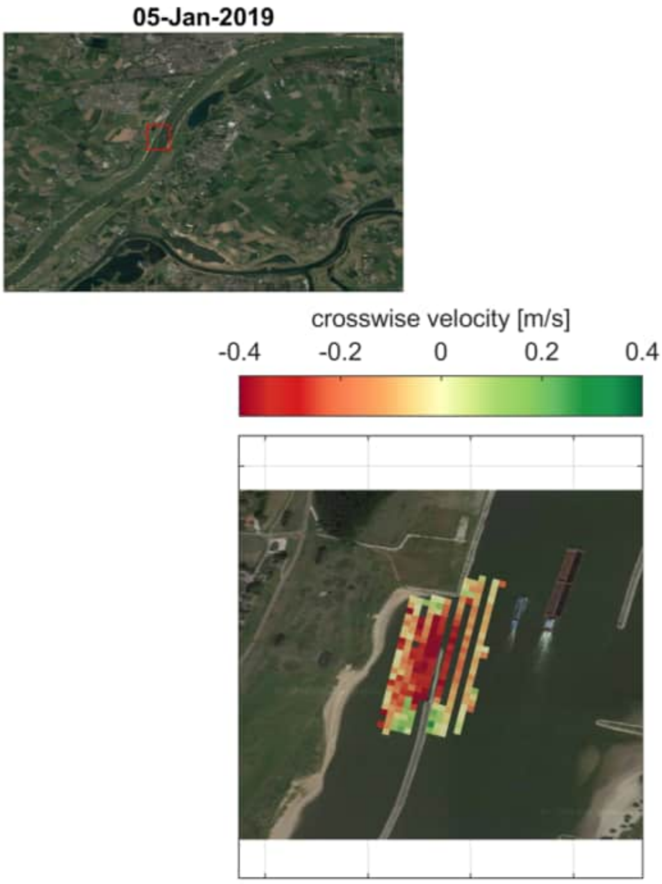

Figure D.124 Depth-averaged velocity field considering the top 2 m on 05-01-19 (discharge at Lobith at 12:00 equal to 1843 m^3/s).

D.5.1.3 21-03-19

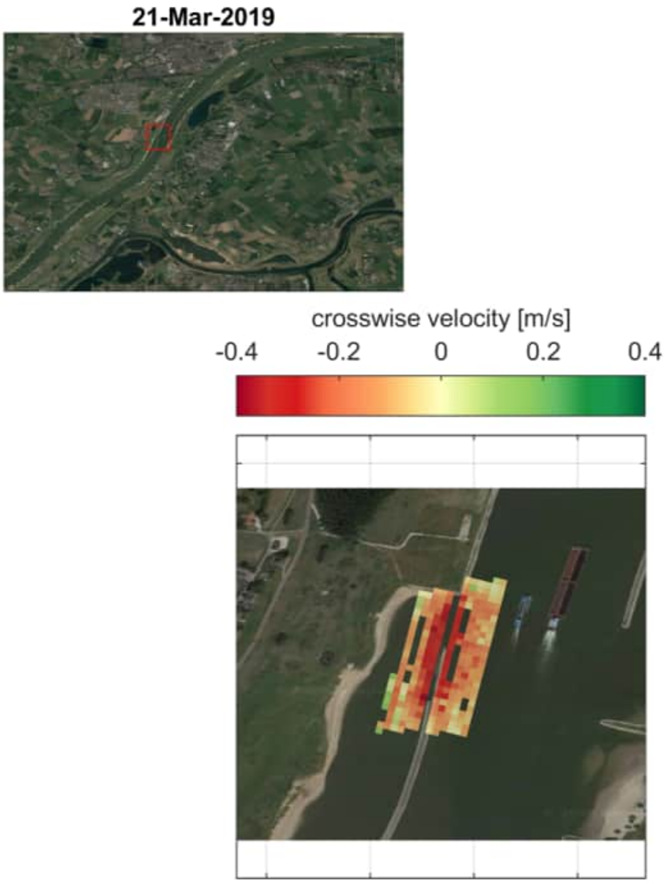

Figure D.125 Depth-averaged velocity field considering the full water column on 21-03-19 (discharge at Lobith at 12:00 equal to 4635 m^3/s).

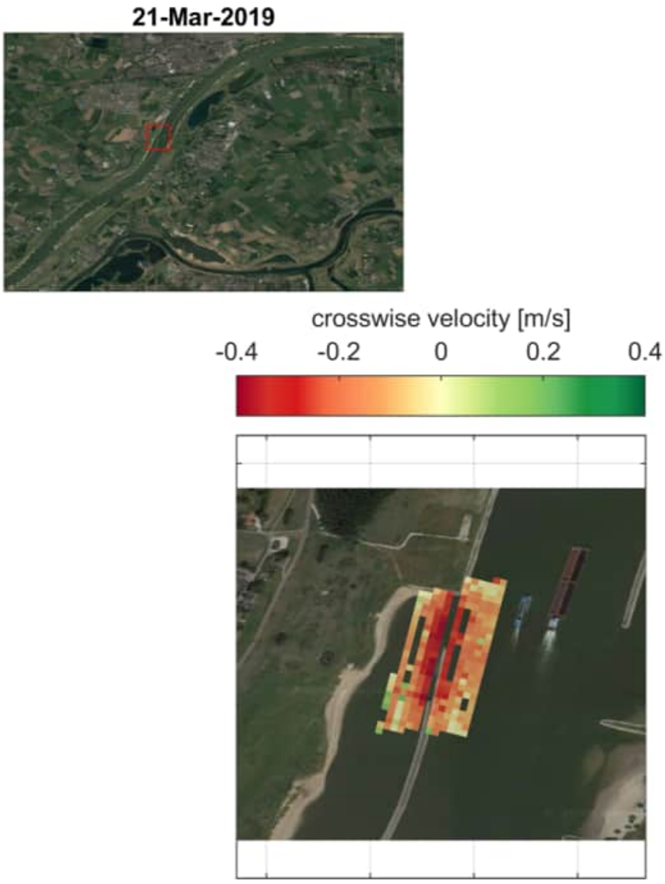

Figure D.126 Depth-averaged velocity field considering the top 2 m on 21-03-19 (discharge at Lobith at 12:00 equal to 4635 m^3/s).

D.5.1.4 27-03-19

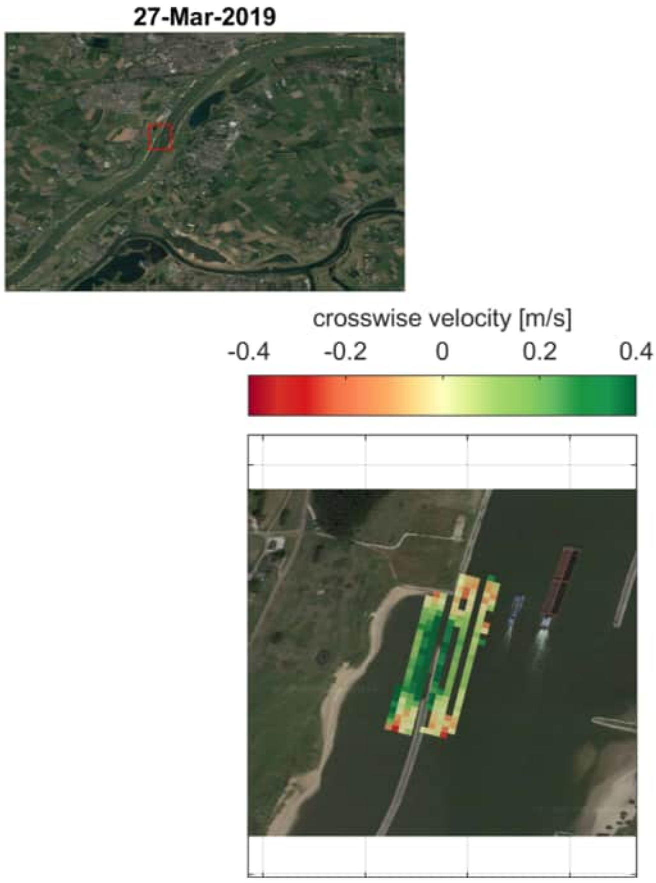

Figure D.127 Depth-averaged velocity field considering the full water column on 27-03-19 (discharge at Lobith at 12:00 equal to 2434 m^3/s).

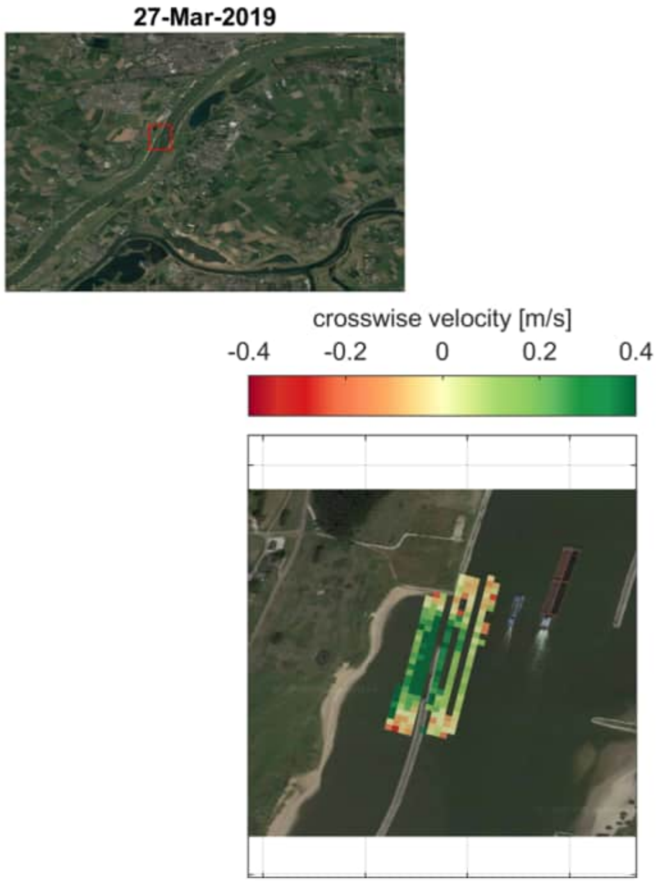

Figure D.128 Depth-averaged velocity field considering the top 2 m on 27-03-19 (discharge at Lobith at 12:00 equal to 2434 m^3/s).

D.5.1.5 26-09-19

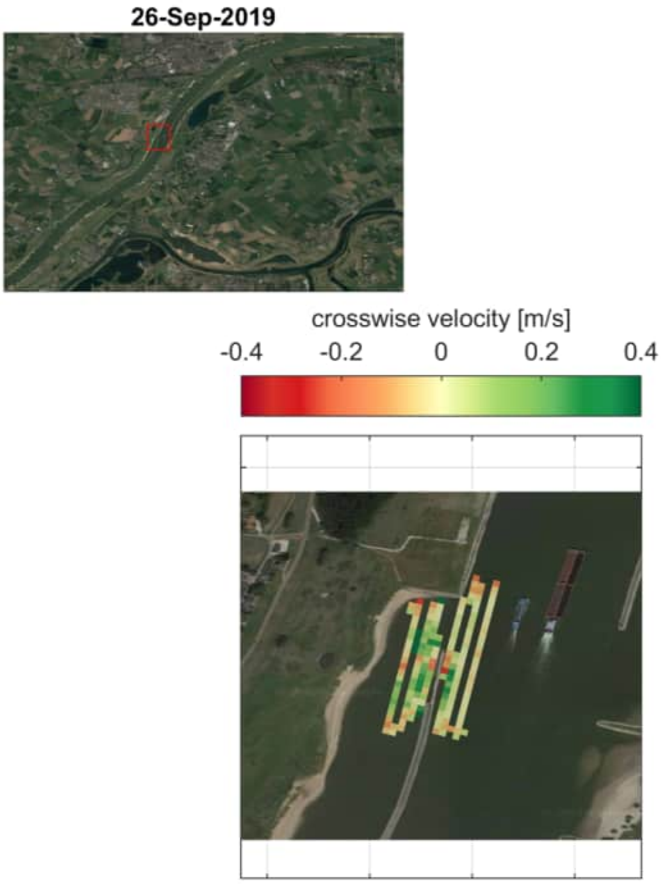

Figure D.129 Depth-averaged velocity field considering the full water column on 26-09-19 (discharge at Lobith at 12:00 equal to 1077 m^3/s).

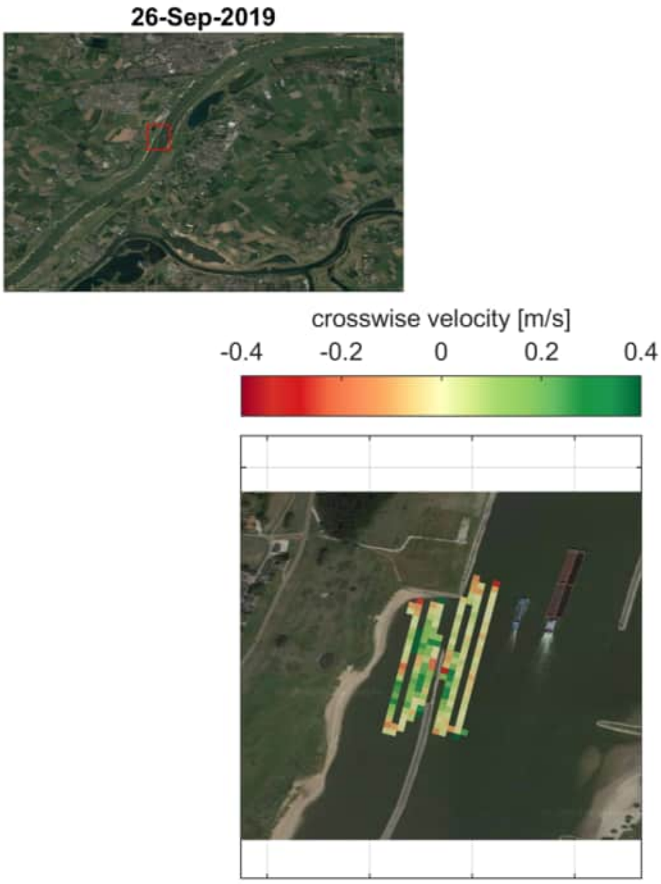

Figure D.130 Depth-averaged velocity field considering the top 2 m on 26-09-19 (discharge at Lobith at 12:00 equal to 1077 m^3/s).

D.5.1.6 18-12-19

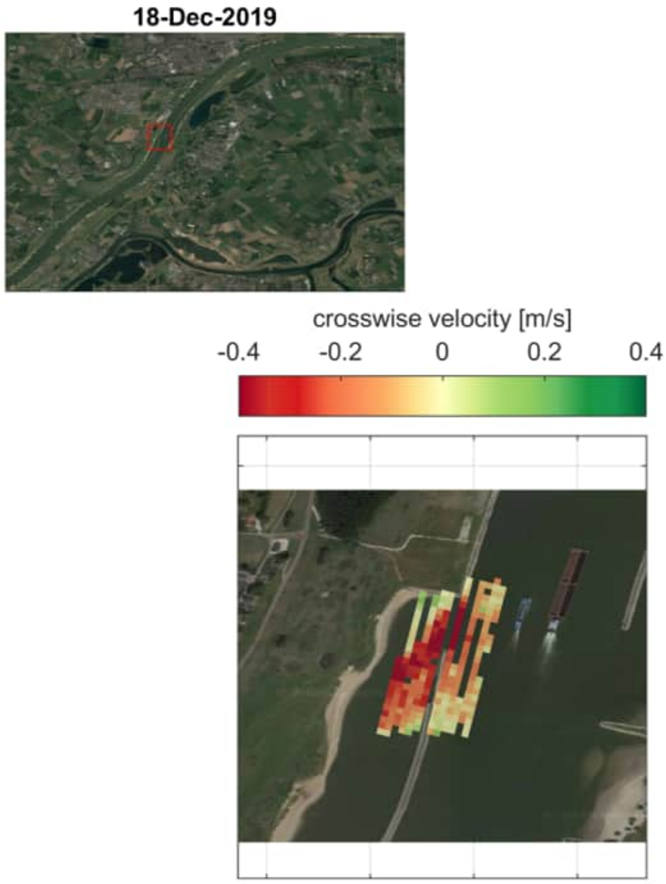

Figure D.131 Depth-averaged velocity field considering the full water column on 18-12-19 (discharge at Lobith at 12:00 equal to 3565 m^3/s).

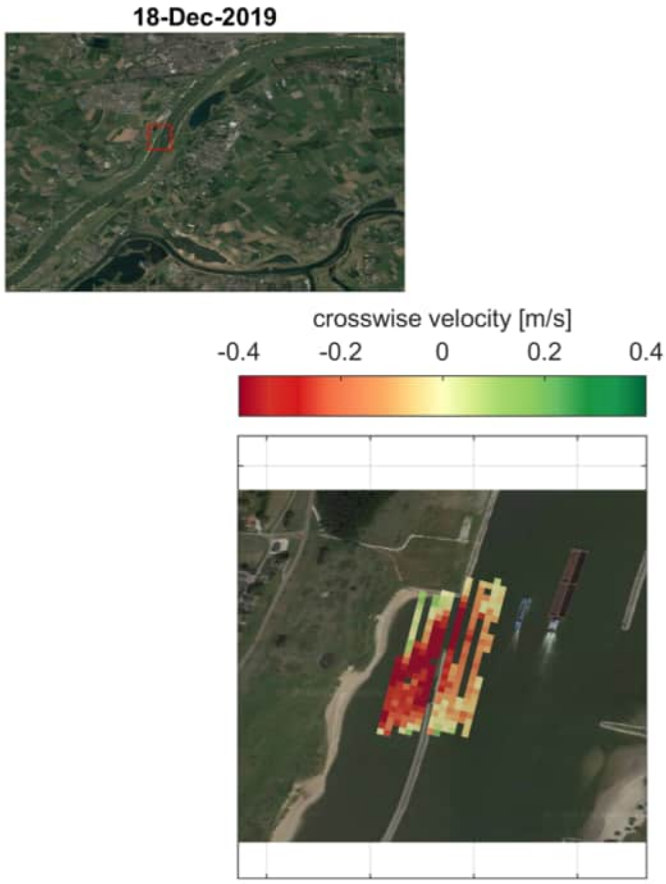

Figure D.132 Depth-averaged velocity field considering the top 2 m on 18-12-19 (discharge at Lobith at 12:00 equal to 3565 m^3/s).

D.5.1.7 05-02-20

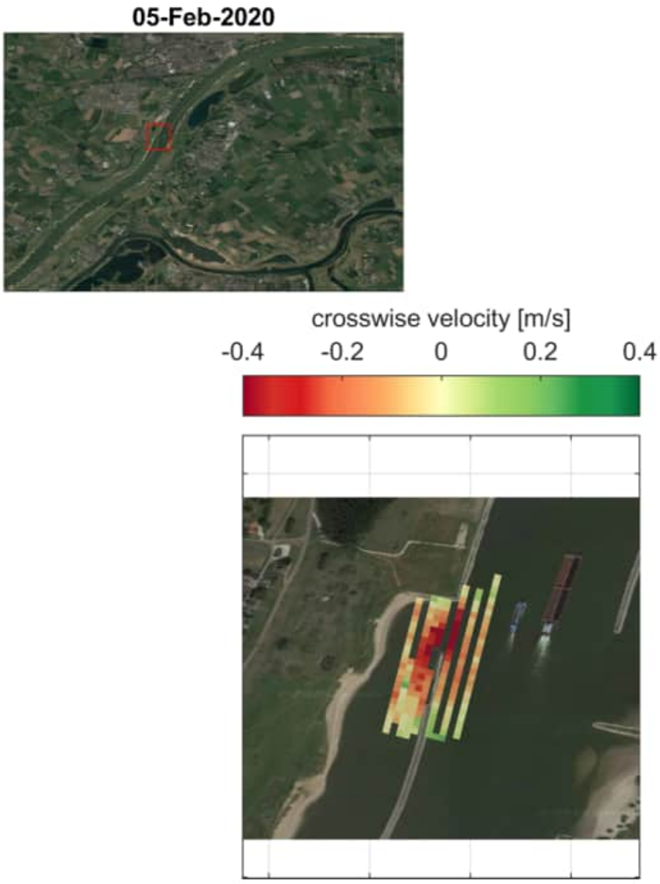

Figure D.133 Depth-averaged velocity field considering the full water column on 05-02-20 (discharge at Lobith at 12:00 equal to 3647 m^3/s).

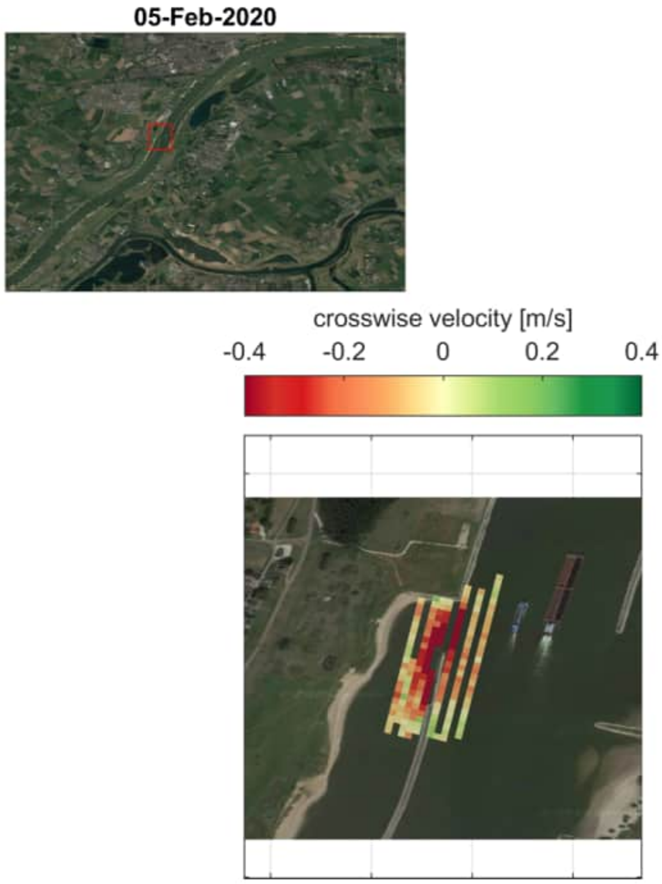

Figure D.134 Depth-averaged velocity field considering the top 2 m on 05-02-20 (discharge at Lobith at 12:00 equal to 3647 m^3/s).

D.5.1.8 06-02-20

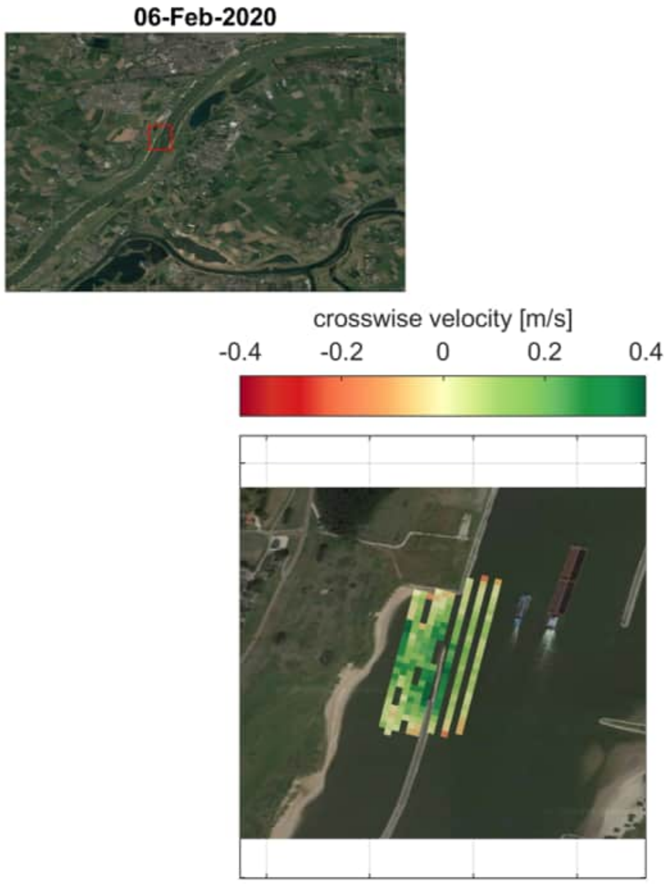

Figure D.135 Depth-averaged velocity field considering the full water column on 06-02-20 (discharge at Lobith at 12:00 equal to 4885 m^3/s).

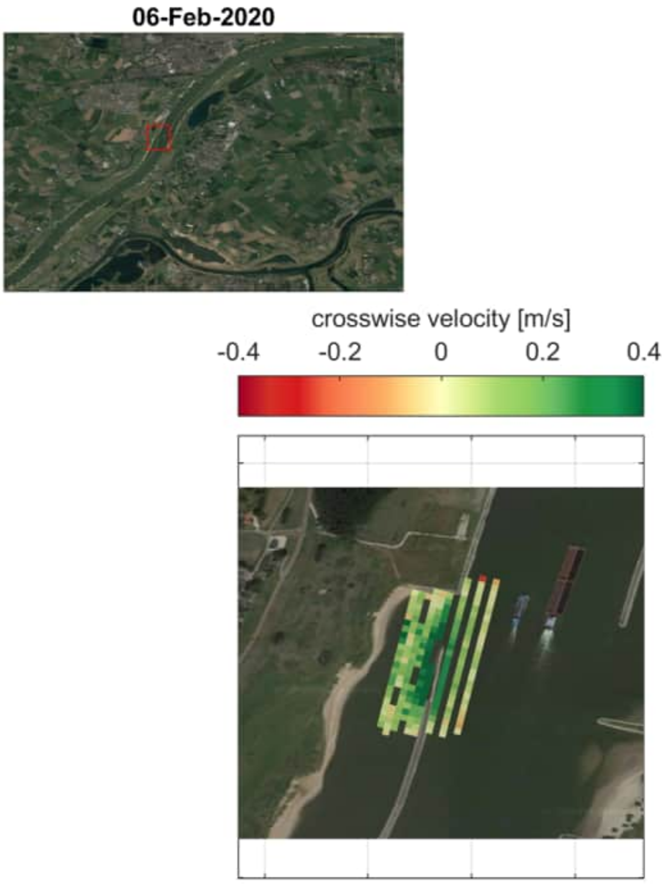

Figure D.136 Depth-averaged velocity field considering the top 2 m on 06-02-20 (discharge at Lobith at 12:00 equal to 4885 m^3/s).

D.5.1.9 02-04-20

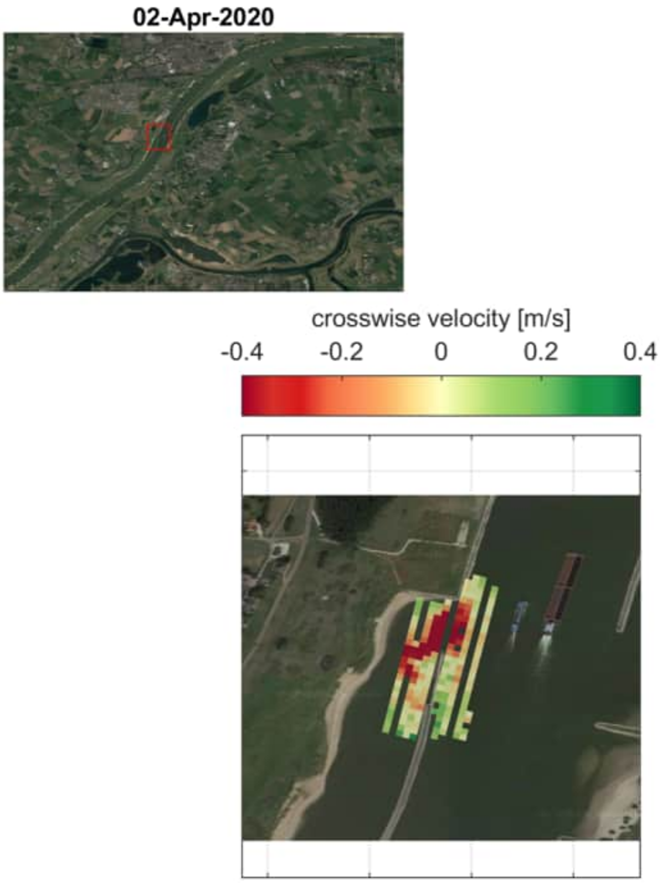

Figure D.137 Depth-averaged velocity field considering the full water column on 02-04-20 (discharge at Lobith at 12:00 equal to 1891 m^3/s).

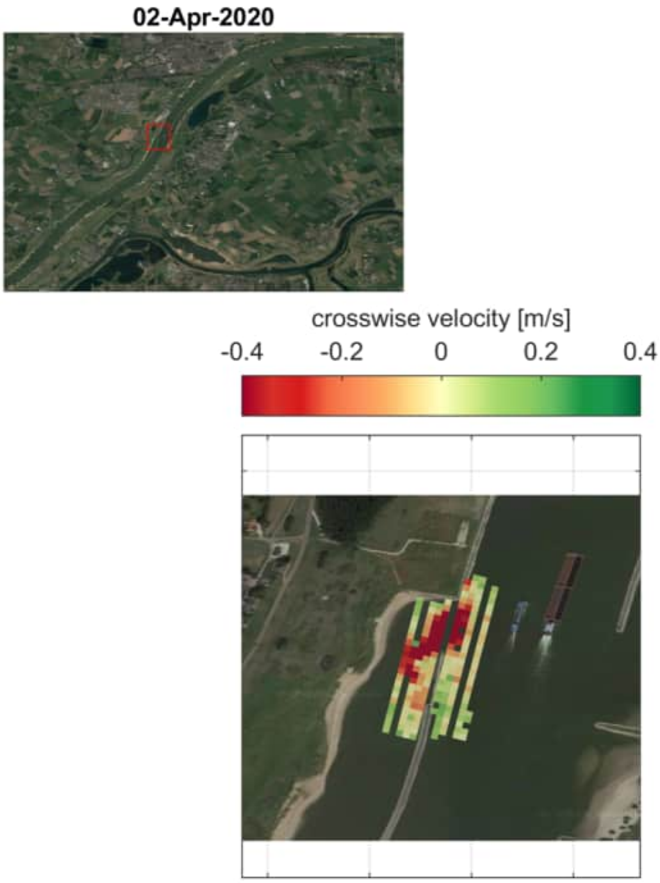

Figure D.138 Depth-averaged velocity field considering the top 2 m on 02-04-20 (discharge at Lobith at 12:00 equal to 1891 m^3/s).

D.5.1.10 24-04-20

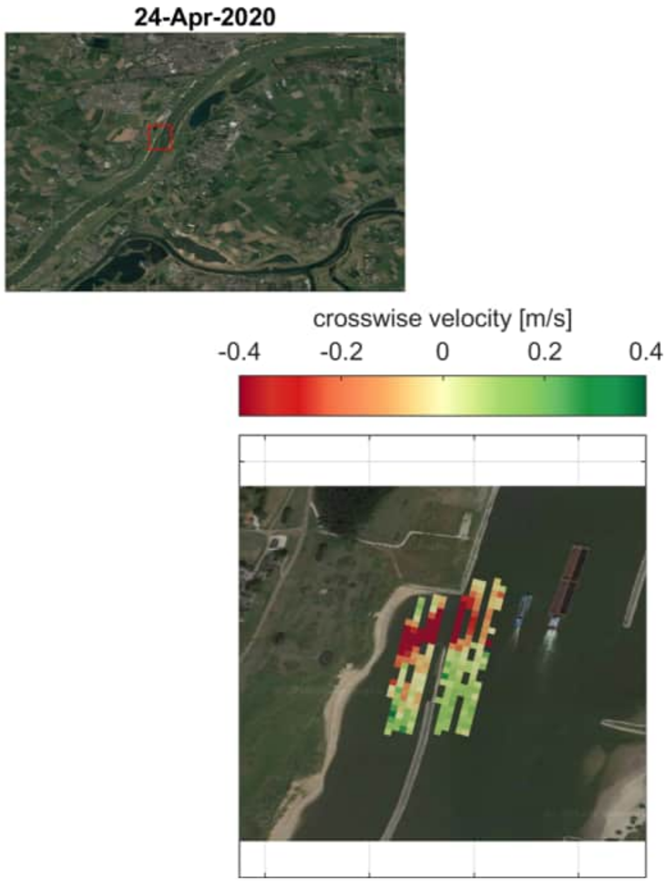

Figure D.139 Depth-averaged velocity field considering the full water column on 24-04-20 (discharge at Lobith at 12:00 equal to 1229 m^3/s).

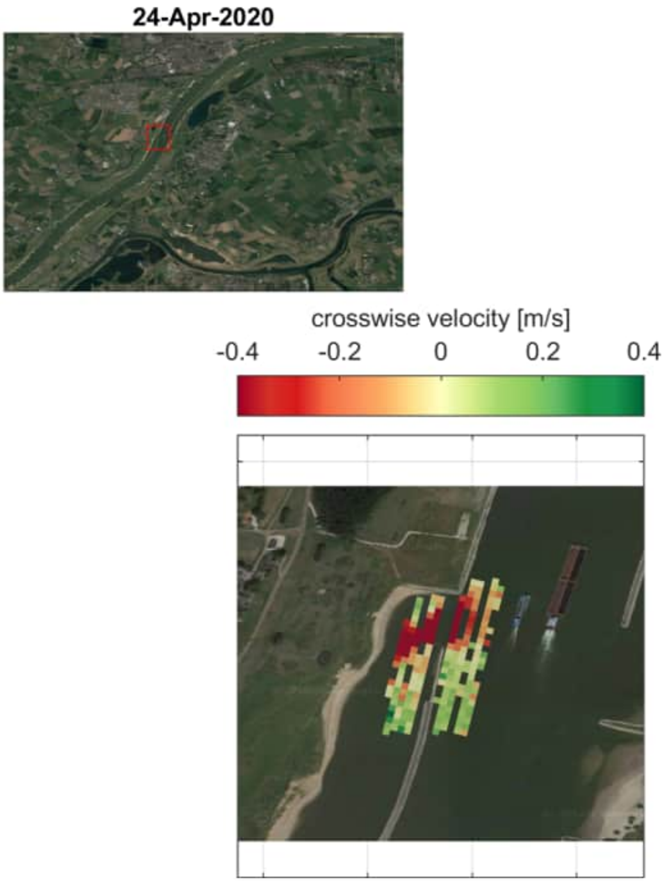

Figure D.140 Depth-averaged velocity field considering the top 2 m on 24-04-20 (discharge at Lobith at 12:00 equal to 1229 m^3/s).

D.5.1.11 01-12-17

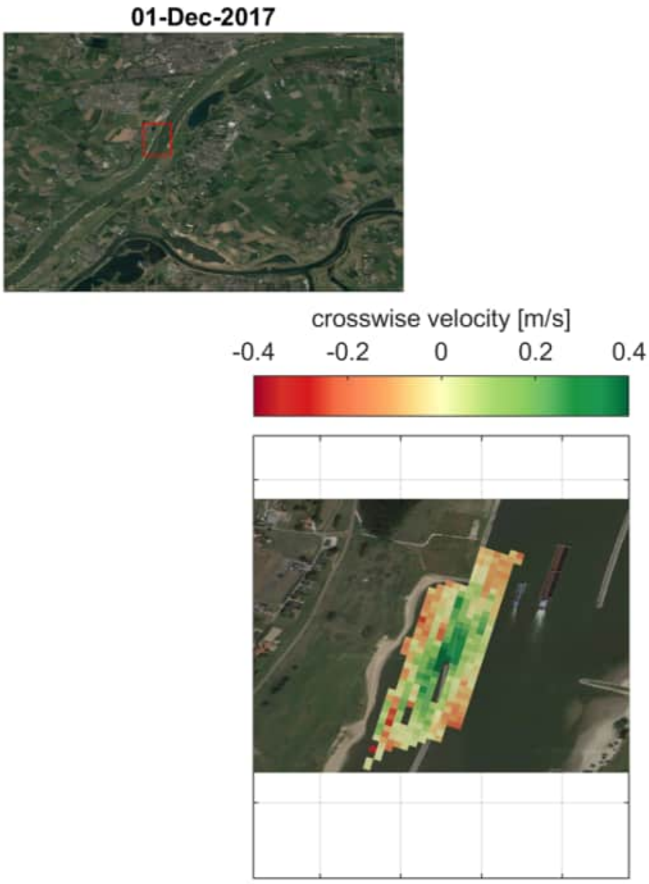

Figure D.141 Depth-averaged velocity field considering the full water column on 01-12-17 (discharge at Lobith at 12:00 equal to 3502 m^3/s).

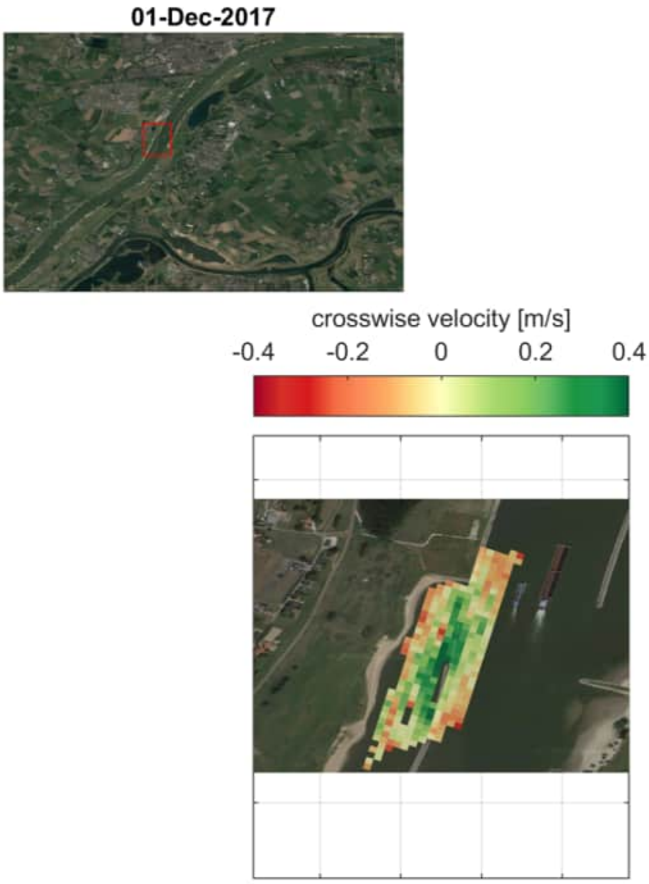

Figure D.142 Depth-averaged velocity field considering the top 2 m on 01-12-17 (discharge at Lobith at 12:00 equal to 3502 m^3/s).

D.5.1.12 02-02-18

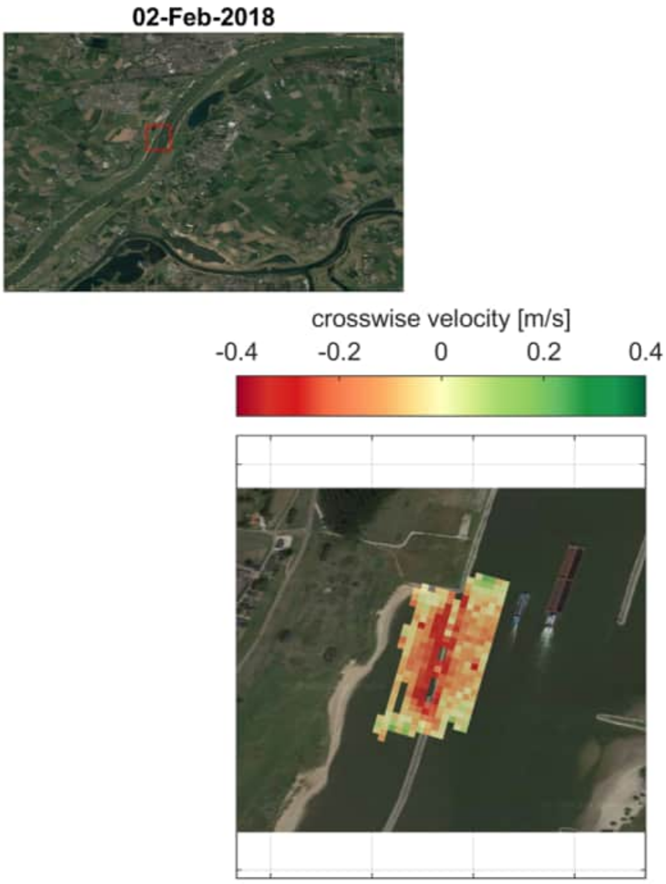

Figure D.143 Depth-averaged velocity field considering the full water column on 02-02-18 (discharge at Lobith at 12:00 equal to 4705 m^3/s).

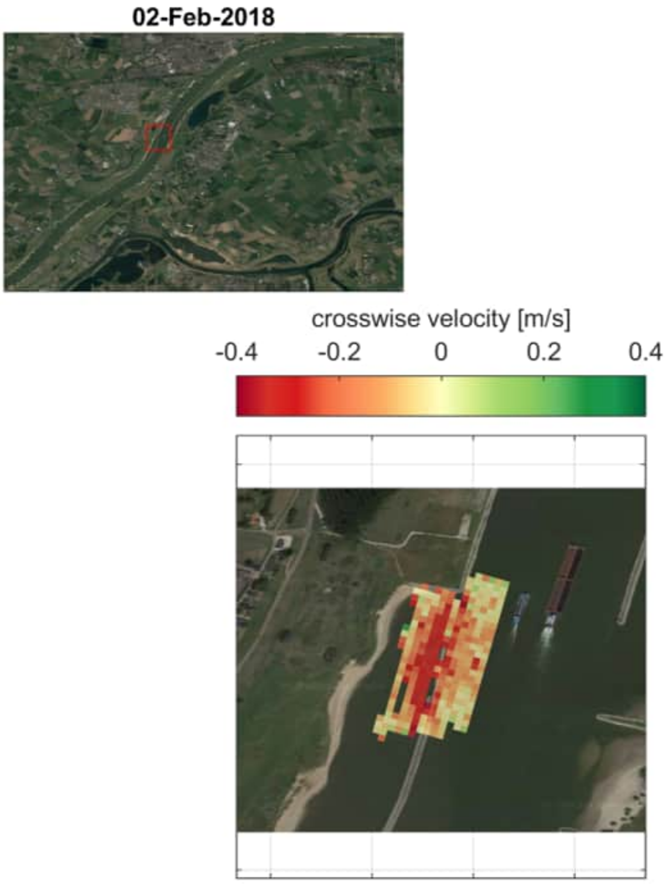

Figure D.144 Depth-averaged velocity field considering the top 2 m on 02-02-18 (discharge at Lobith at 12:00 equal to 4705 m^3/s).

Deltares

D.5.1.13 16-02-18

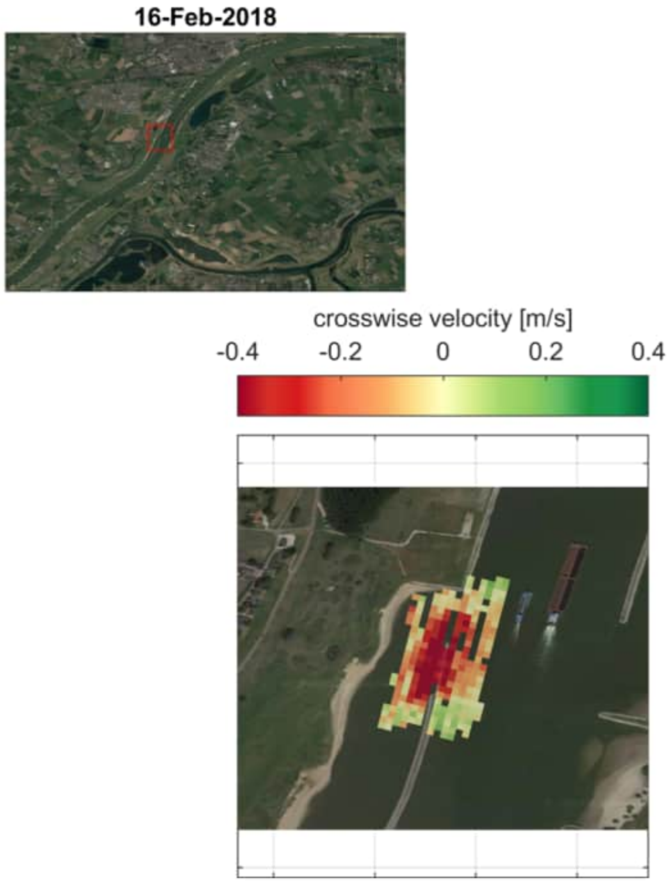

Figure D.145 Depth-averaged velocity field considering the full water column on 16-02-18 (discharge at Lobith at 12:00 equal to 2549 m^3/s).

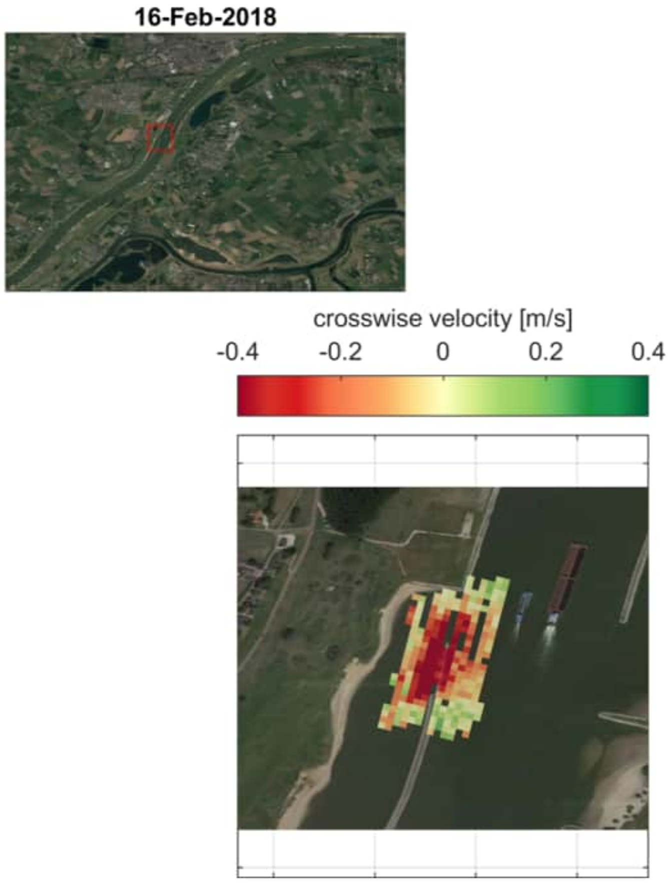

Figure D.146 Depth-averaged velocity field considering the top 2 m on 16-02-18 (discharge at Lobith at 12:00 equal to 2549 m^3/s).

D.5.1.14 07-03-18

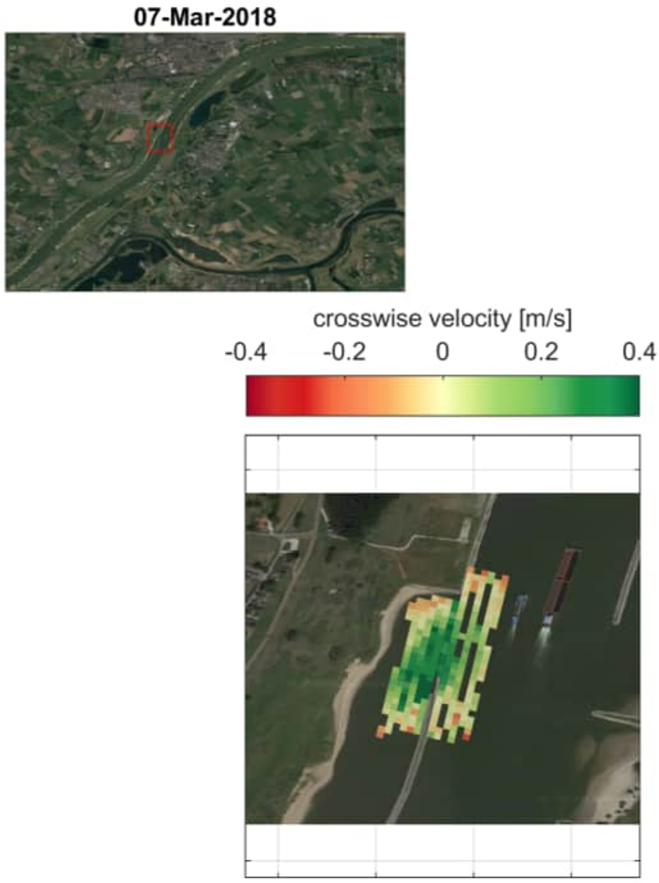

Figure D.147 Depth-averaged velocity field considering the full water column on 07-03-18 (discharge at Lobith at 12:00 equal to 1929 m^3/s).

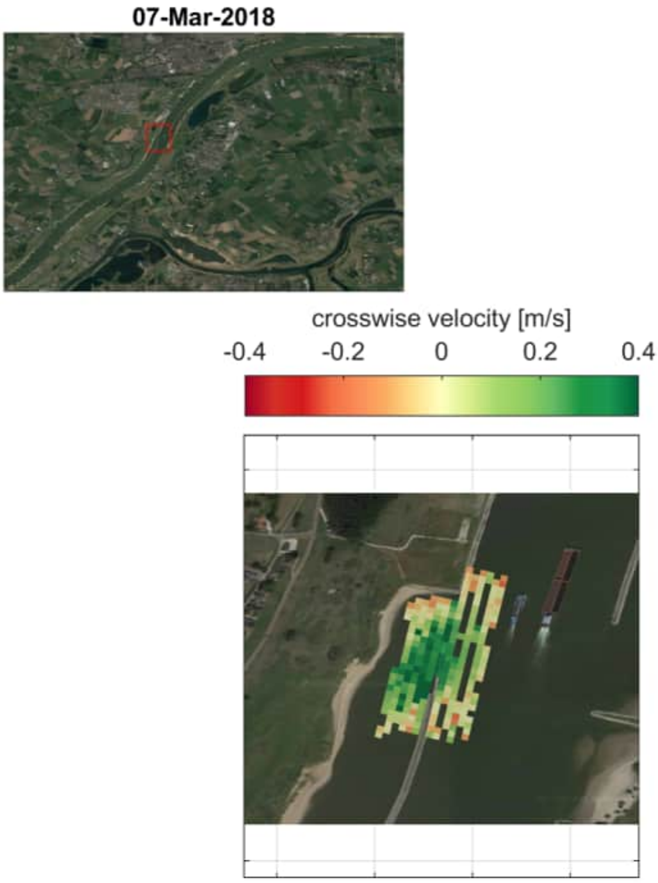

Figure D.148 Depth-averaged velocity field considering the top 2 m on 07-03-18 (discharge at Lobith at 12:00 equal to 1929 m^3/s).

D.5.2 Wamel inlet 1

D.5.2.1 07-12-17

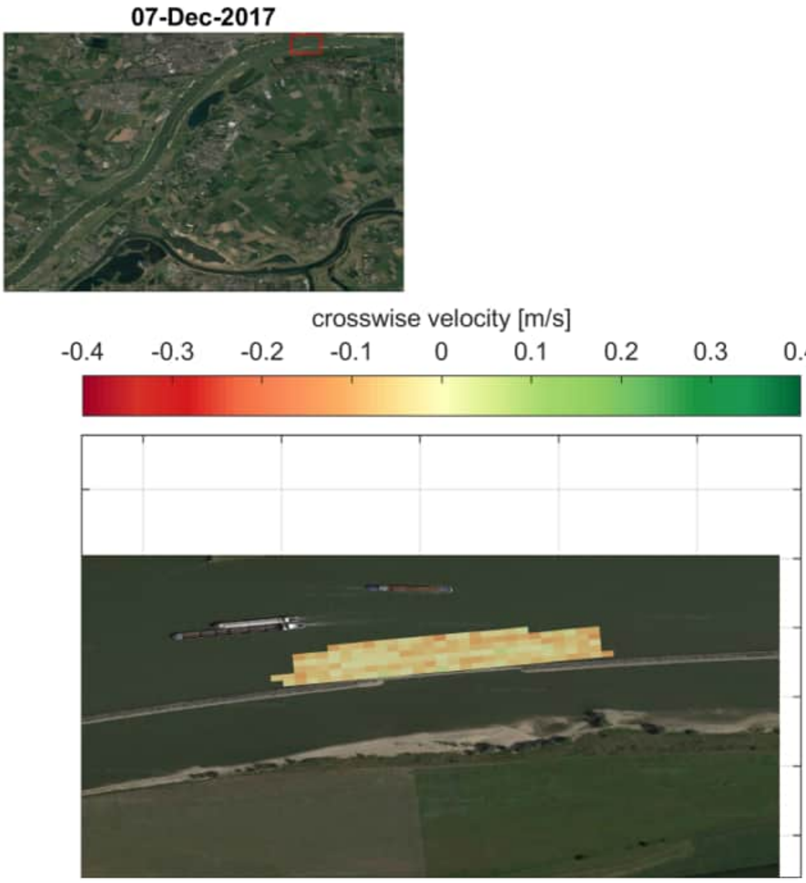

Figure D.149 Depth-averaged velocity field considering the full water column on 07-12-17 (discharge at Lobith at 12:00 equal to 2358 m^3/s).

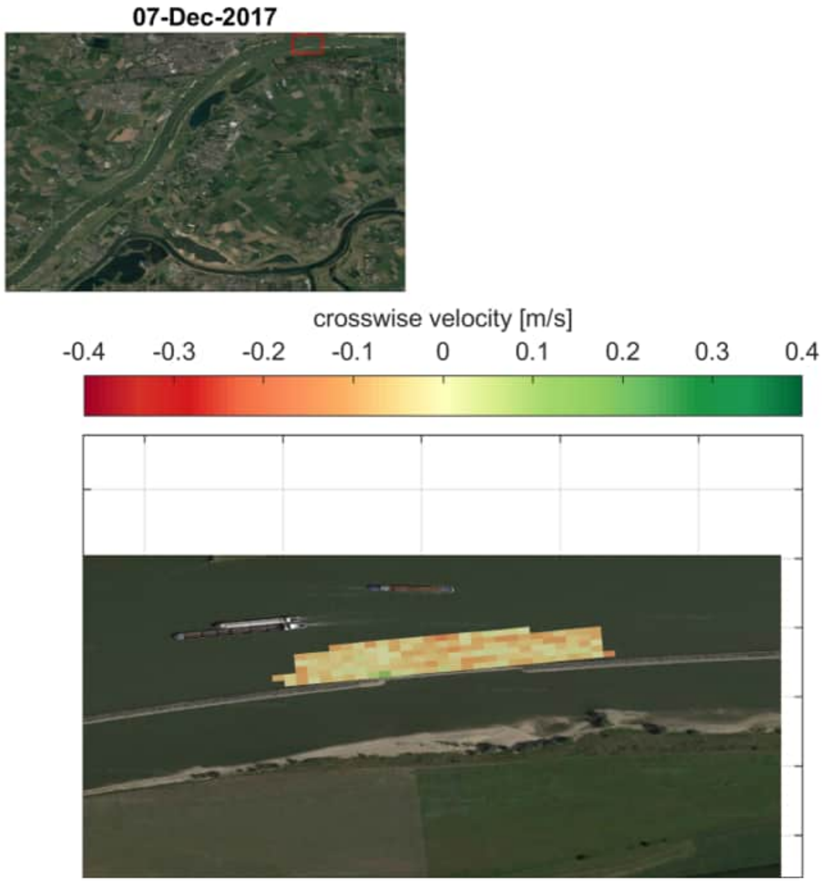

Figure D.150 Depth-averaged velocity field considering the top 2 m on 07-12-17 (discharge at Lobith at 12:00 equal to 2358 m^3/s).

D.5.2.2 07-12-17

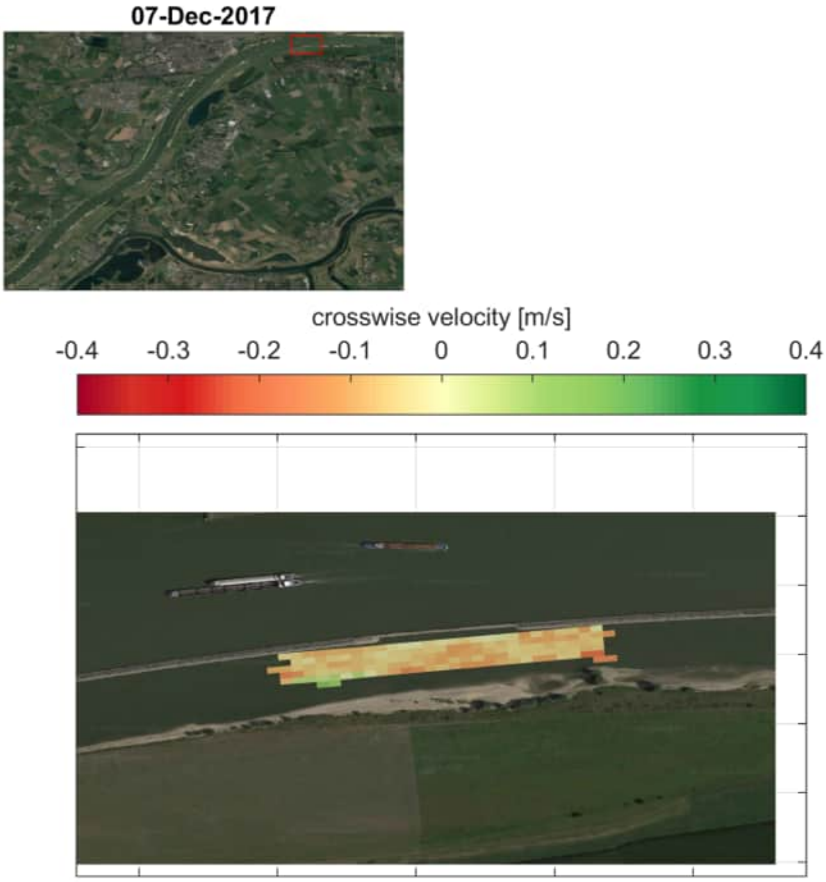

Figure D.151 Depth-averaged velocity field considering the full water column on 07-12-17 (discharge at Lobith at 12:00 equal to 2358 m^3/s).

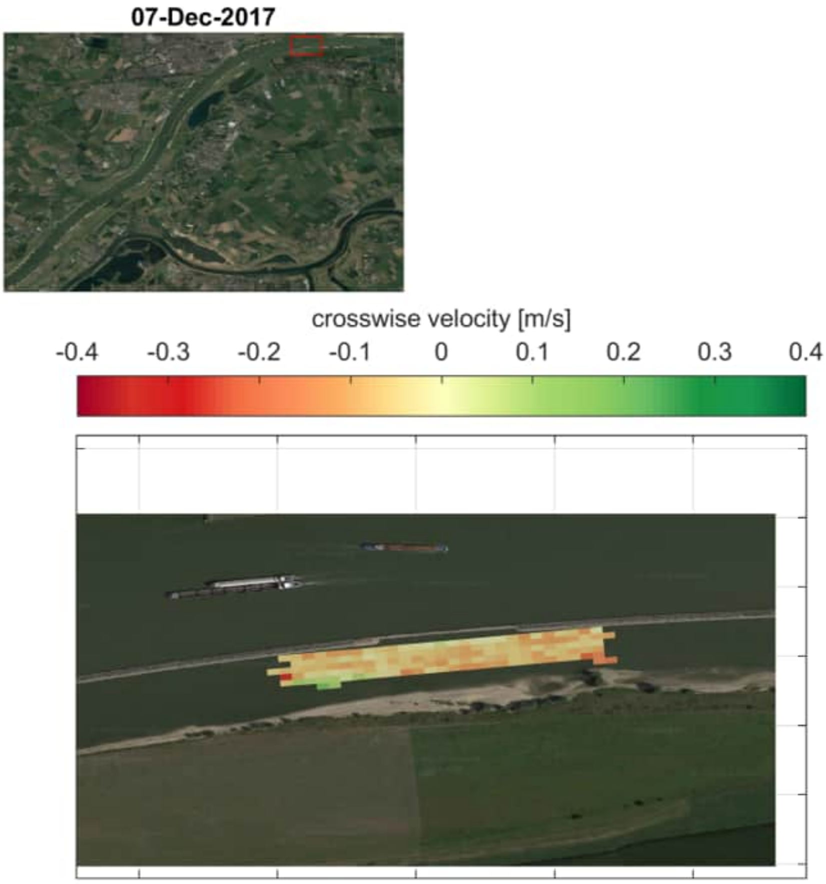

Figure D.152 Depth-averaged velocity field considering the top 2 m on 07-12-17 (discharge at Lobith at 12:00 equal to 2358 m^3/s).

D.5.3 Wamel inlet 2

D.5.3.1 07-12-17

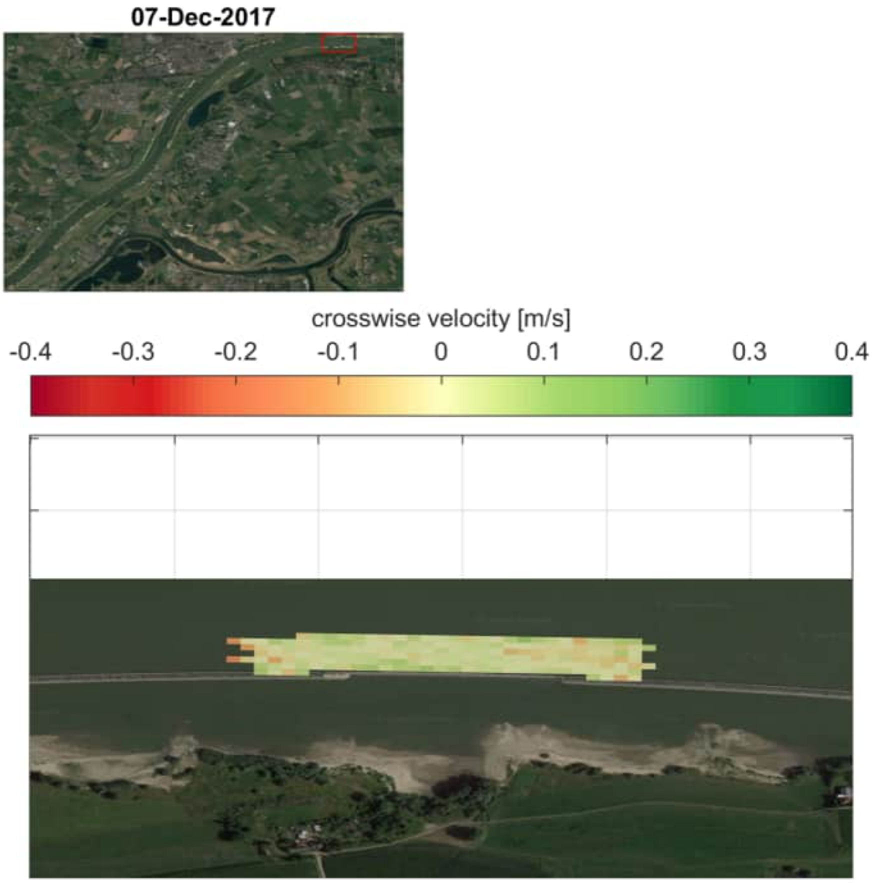

Figure D.153 Depth-averaged velocity field considering the full water column on 07-12-17 (discharge at Lobith at 12:00 equal to 2358 m^3/s).

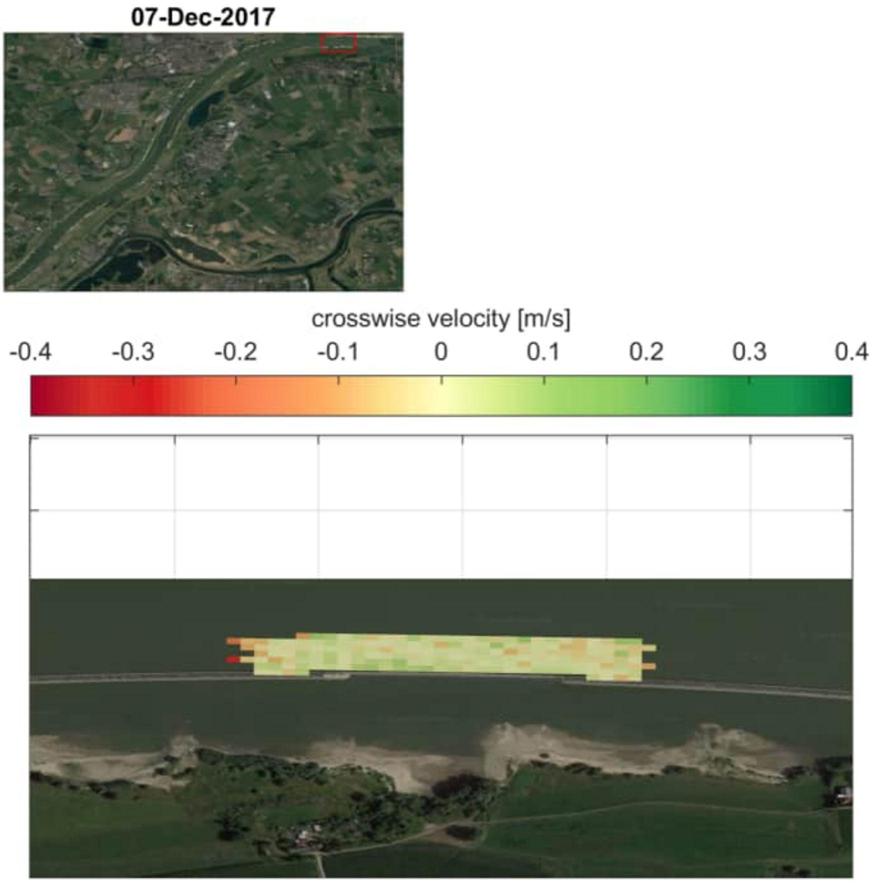

Figure D.154 Depth-averaged velocity field considering the top 2 m on 07-12-17 (discharge at Lobith at 12:00 equal to 2358 m^3/s).

D.5.3.2 07-12-17

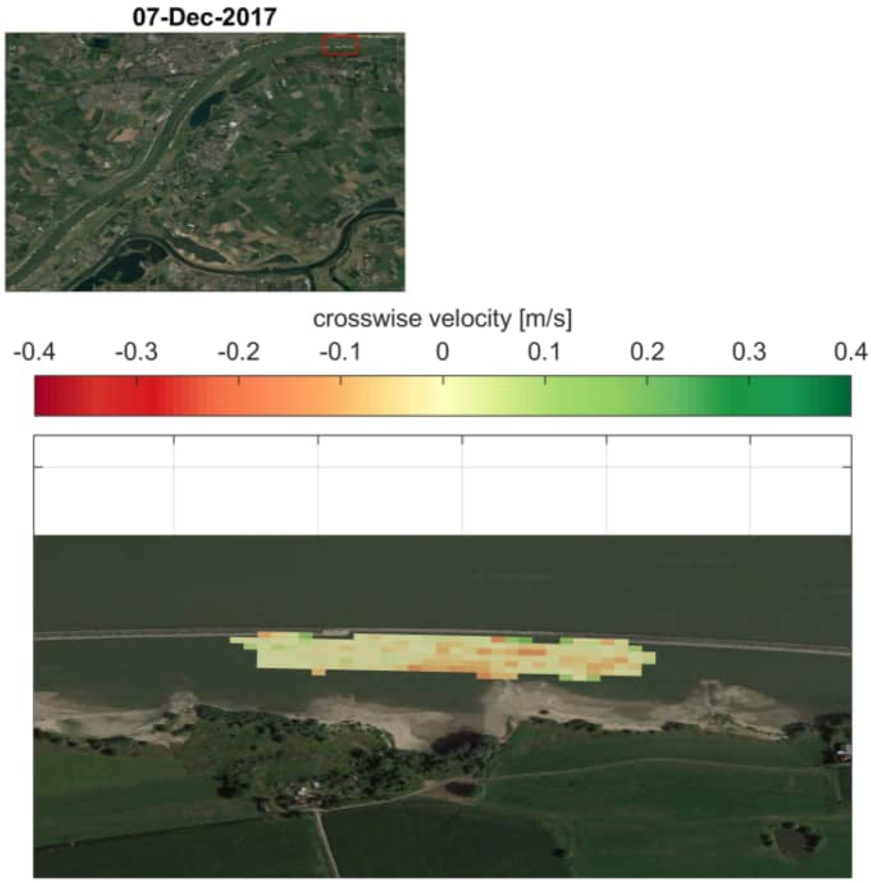

Figure D.155 Depth-averaged velocity field considering the full water column on 07-12-17 (discharge at Lobith at 12:00 equal to 2358 m^3/s).

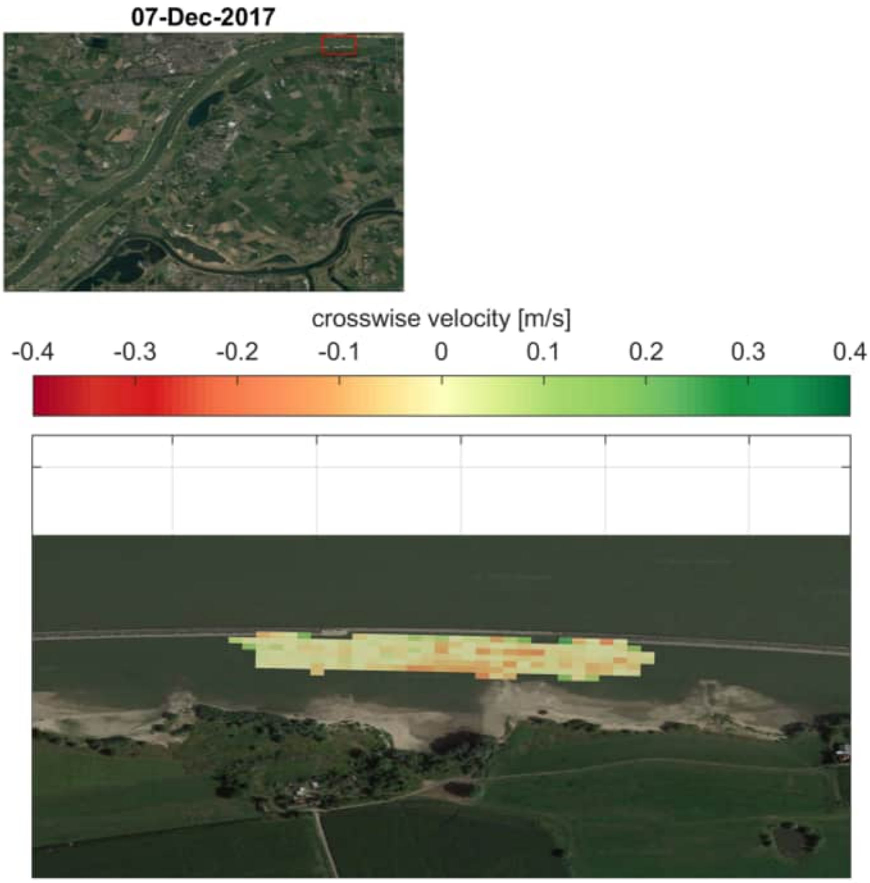

Figure D.156 Depth-averaged velocity field considering the top 2 m on 07-12-17 (discharge at Lobith at 12:00 equal to 2358 m^3/s).

D.5.4 Wamel upstream

D.5.4.1 04-01-19

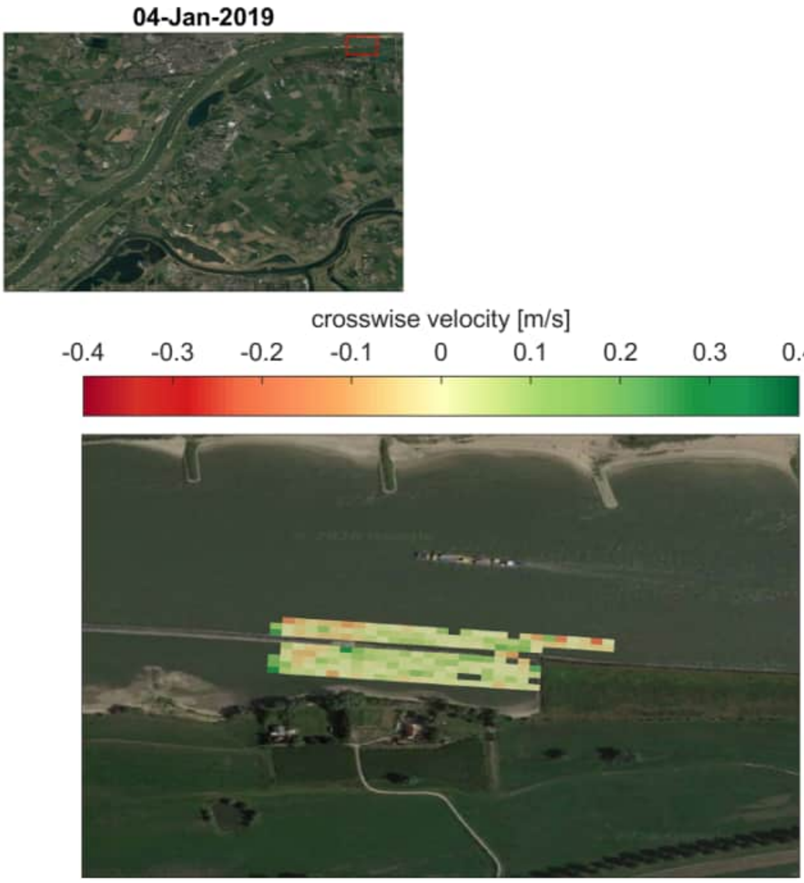

Figure D.157 Depth-averaged velocity field considering the full water column on 04-01-19 (discharge at Lobith at 12:00 equal to 1841 m^3/s).

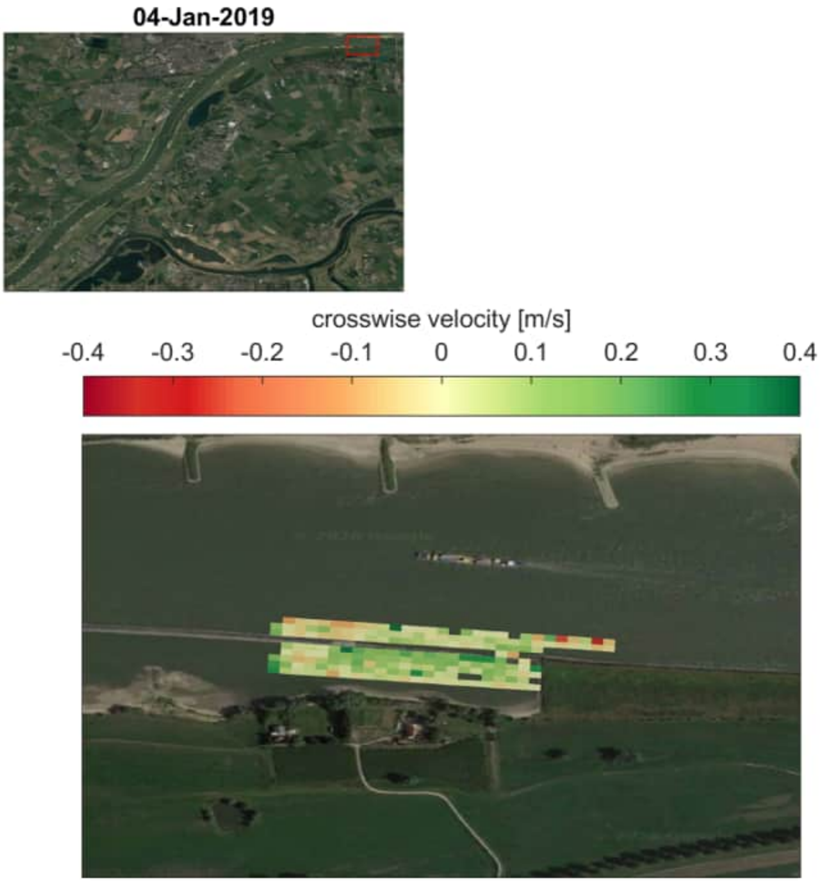

Figure D.158 Depth-averaged velocity field considering the top 2 m on 04-01-19 (discharge at Lobith at 12:00 equal to 1841 m^3/s).

D.5.4.2 04-03-19

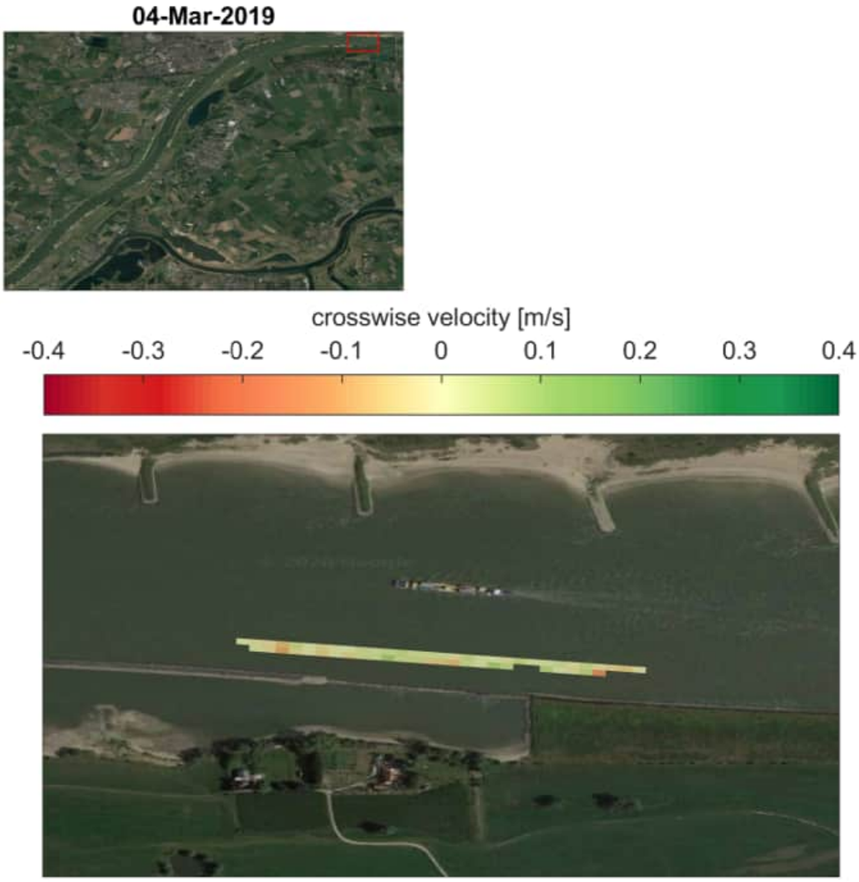

Figure D.159 Depth-averaged velocity field considering the full water column on 04-03-19 (discharge at Lobith at 12:00 equal to 1604 m^3/s).

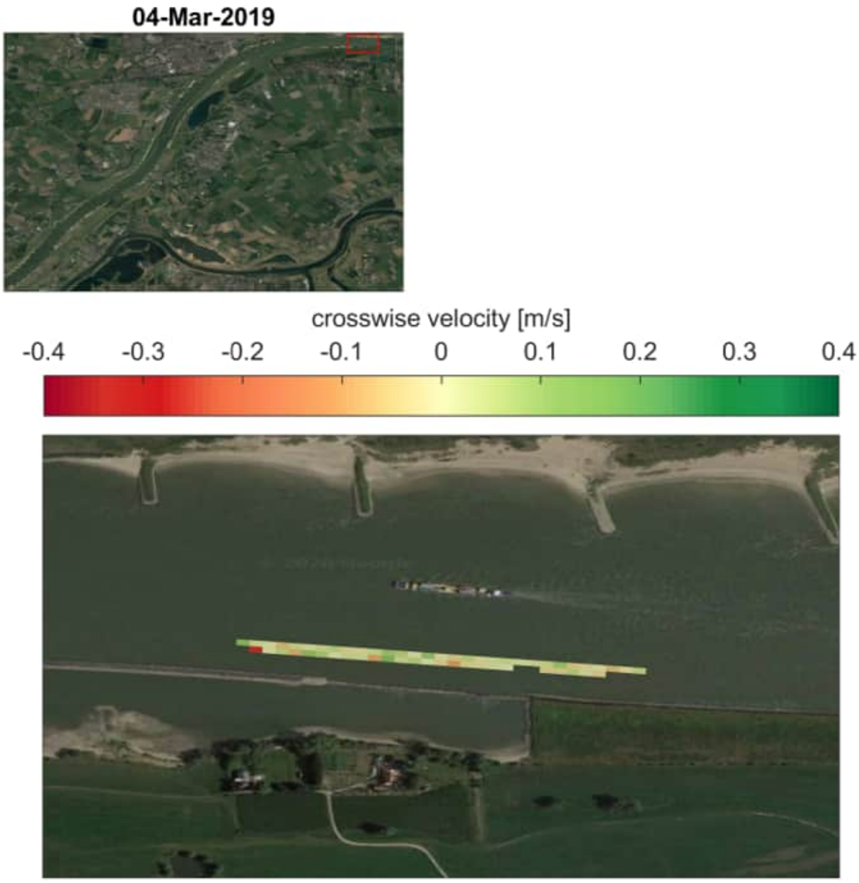

Figure D.160 Depth-averaged velocity field considering the top 2 m on 04-03-19 (discharge at Lobith at 12:00 equal to 1604 m^3/s).

D.5.4.3 20-03-19

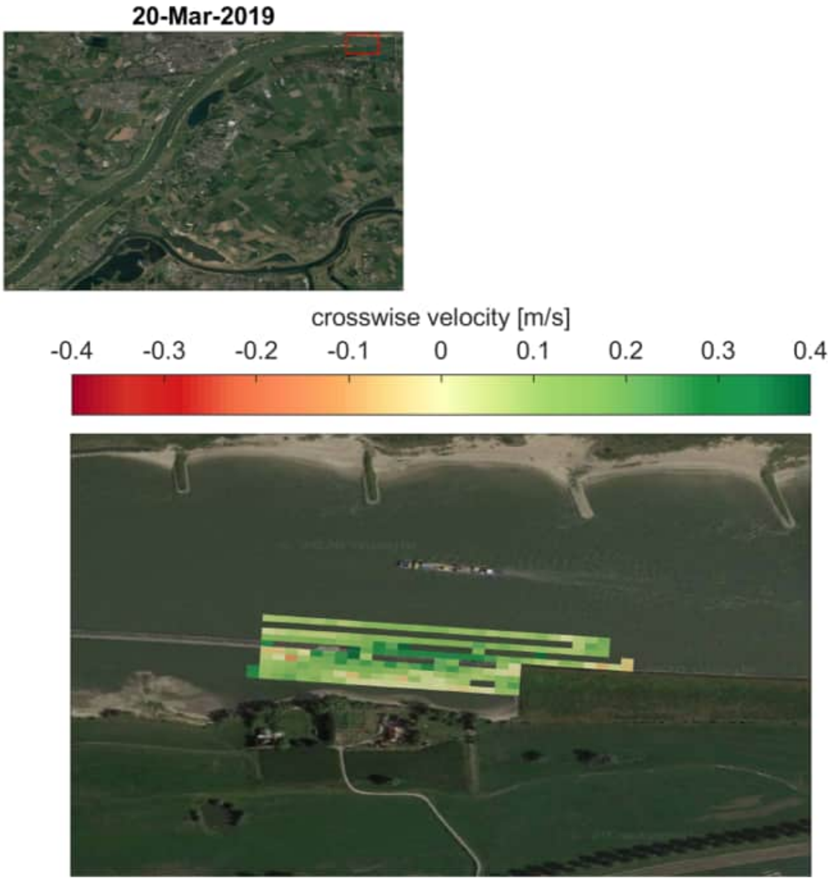

Figure D.161 Depth-averaged velocity field considering the full water column on 20-03-19 (discharge at Lobith at 12:00 equal to 5050 m^3/s).

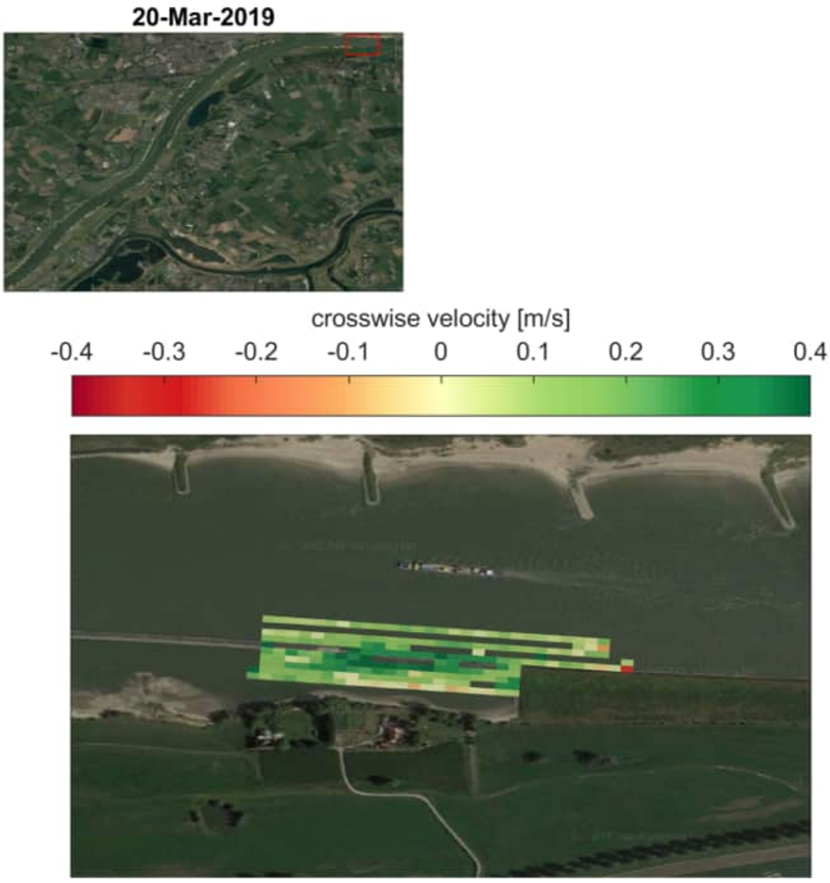

Figure D.162 Depth-averaged velocity field considering the top 2 m on 20-03-19 (discharge at Lobith at 12:00 equal to 5050 m^3/s).

D.5.4.4 26-03-19

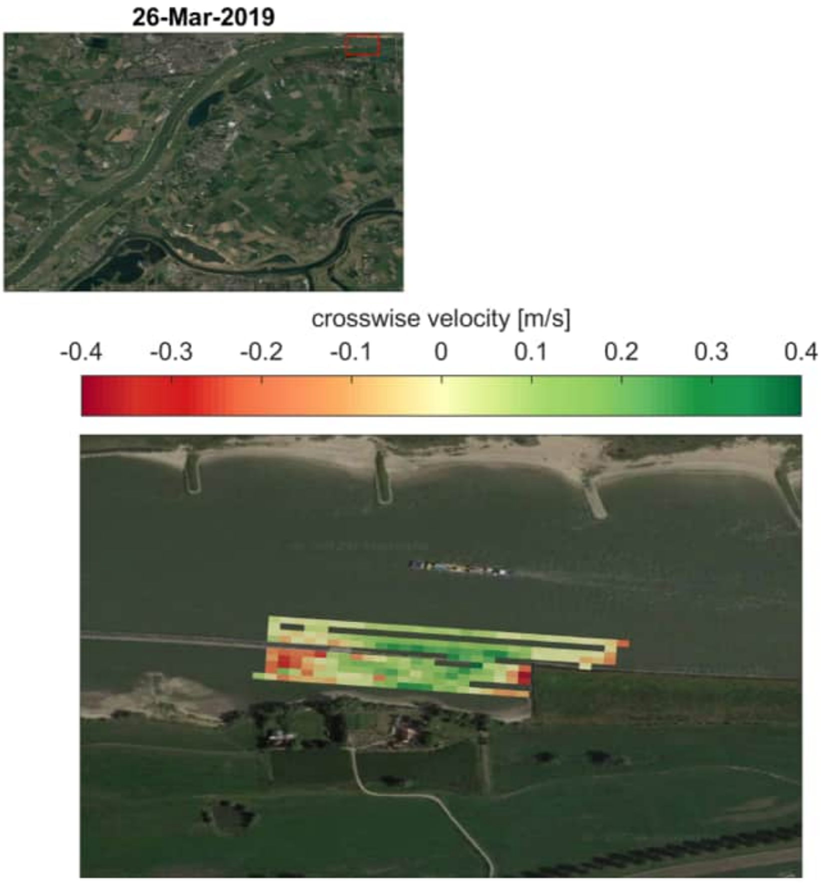

Figure D.163 Depth-averaged velocity field considering the full water column on 26-03-19 (discharge at Lobith at 12:00 equal to 2599 m^3/s).

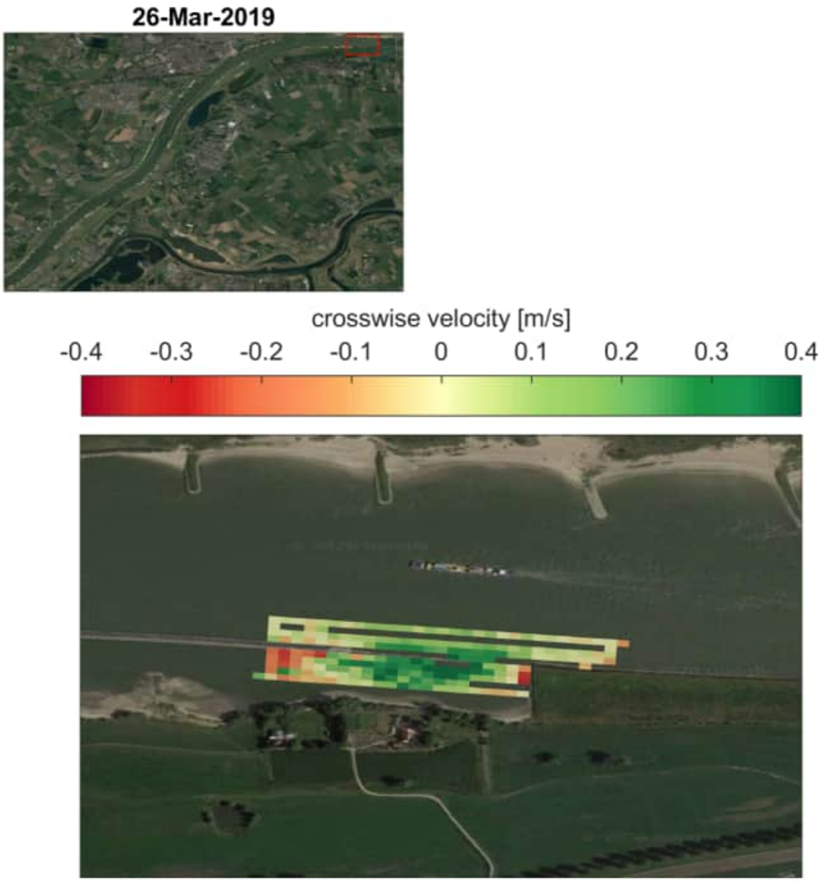

Figure D.164 Depth-averaged velocity field considering the top 2 m on 26-03-19 (discharge at Lobith at 12:00 equal to 2599 m^3/s).

D.5.4.5 25-09-19

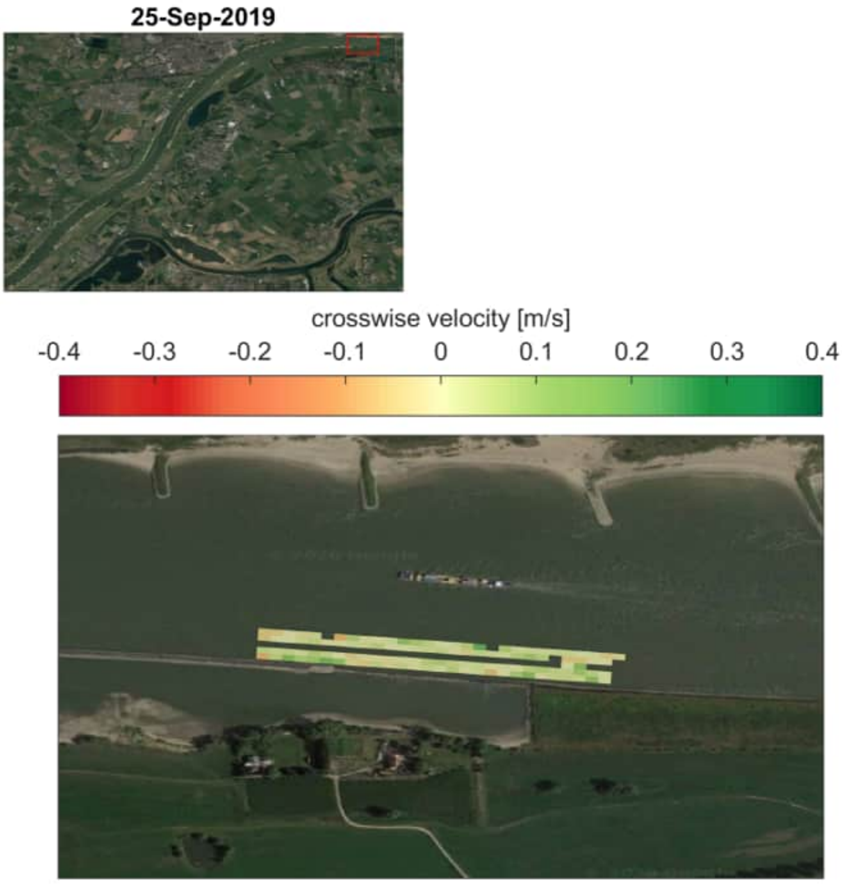

Figure D.165 Depth-averaged velocity field considering the full water column on 25-09-19 (discharge at Lobith at 12:00 equal to 1077 m^3/s).

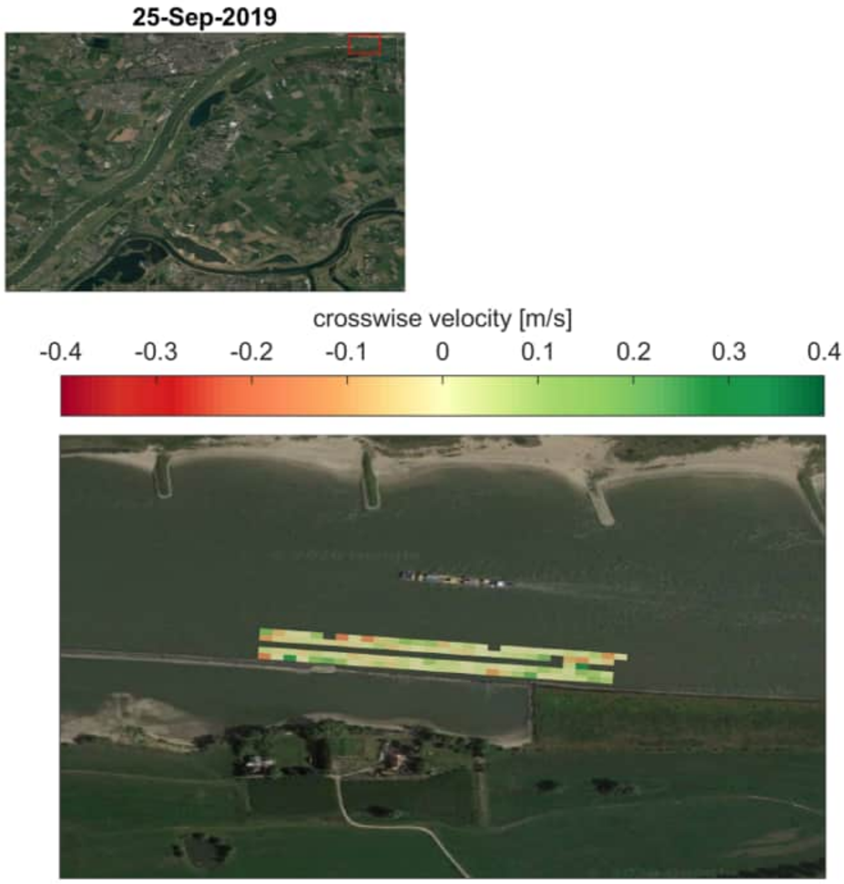

Figure D.166 Depth-averaged velocity field considering the top 2 m on 25-09-19 (discharge at Lobith at 12:00 equal to 1077 m^3/s).

D.5.4.6 19-12-19

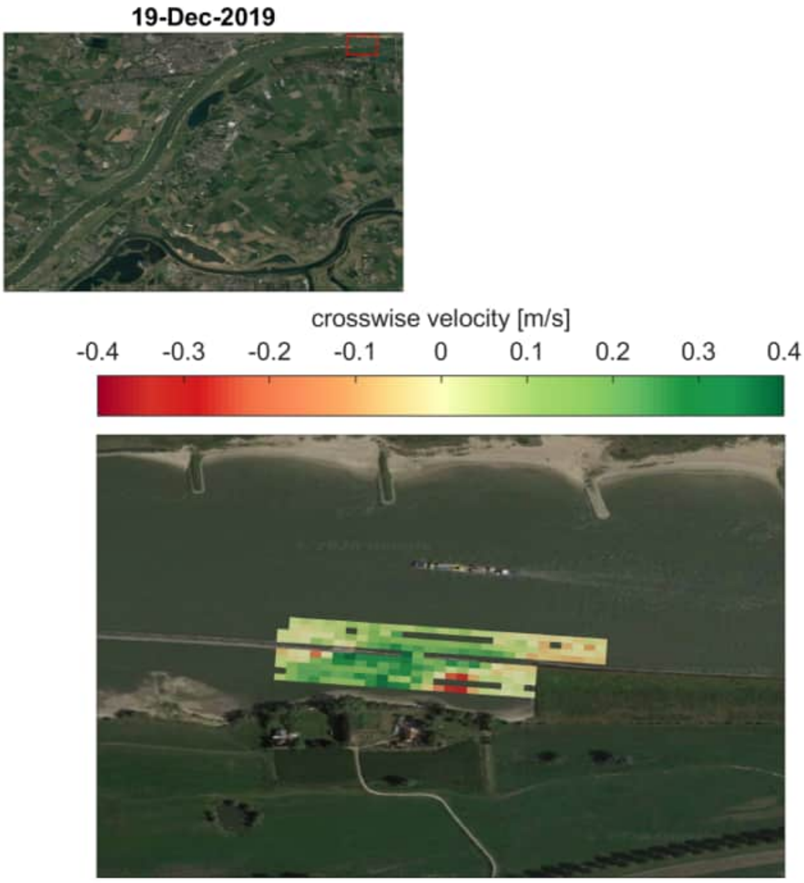

Figure D.167 Depth-averaged velocity field considering the full water column on 19-12-19 (discharge at Lobith at 12:00 equal to 3549 m^3/s).

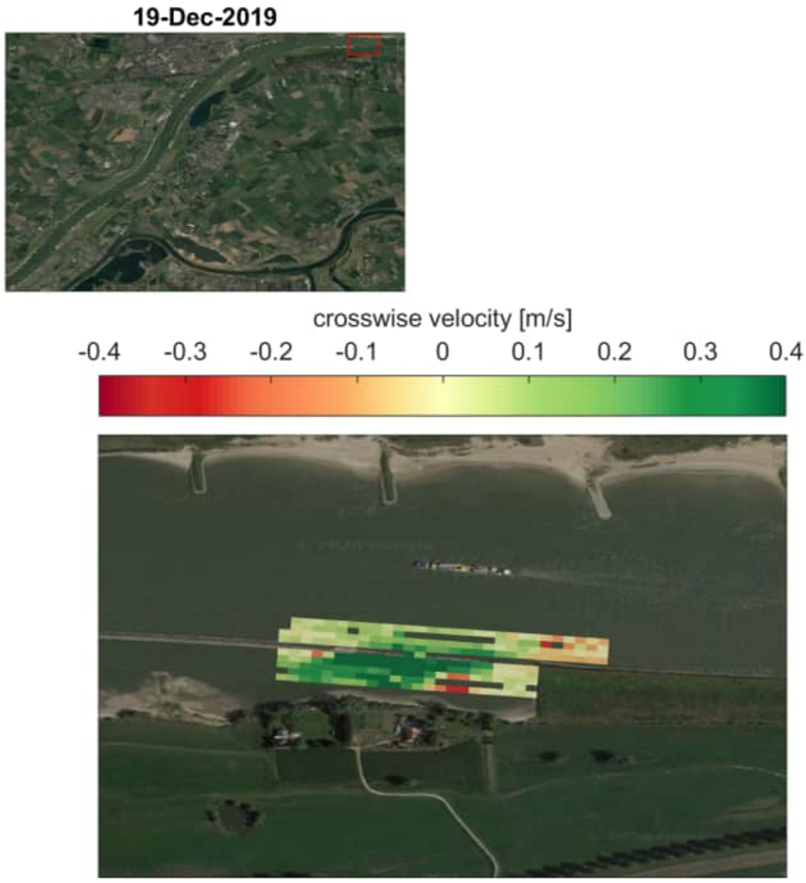

Figure D.168 Depth-averaged velocity field considering the top 2 m on 19-12-19 (discharge at Lobith at 12:00 equal to 3549 m^3/s).

D.5.4.7 05-02-20

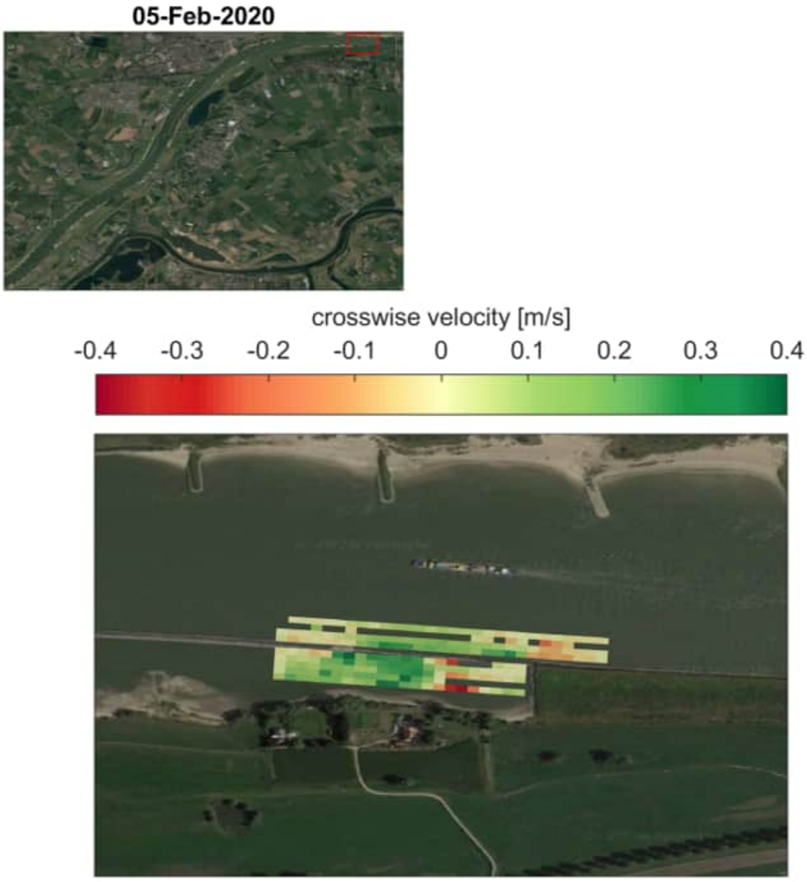

Figure D.169 Depth-averaged velocity field considering the full water column on 05-02-20 (discharge at Lobith at 12:00 equal to 3647 m^3/s).

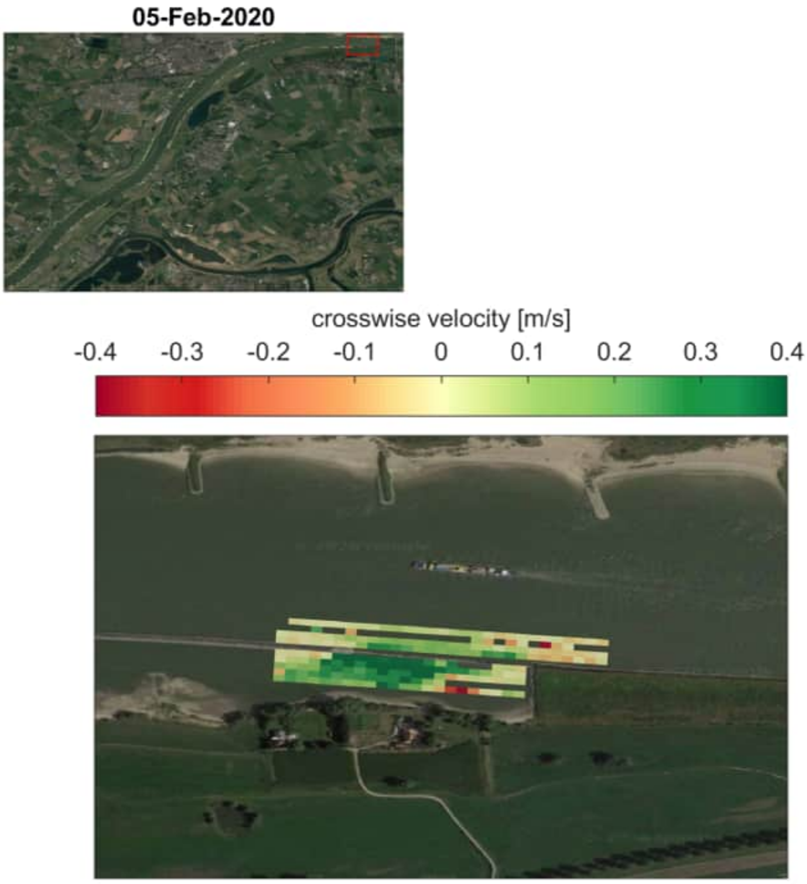

Figure D.170 Depth-averaged velocity field considering the top 2 m on 05-02-20 (discharge at Lobith at 12:00 equal to 3647 m^3/s).

D.5.4.8 06-02-20

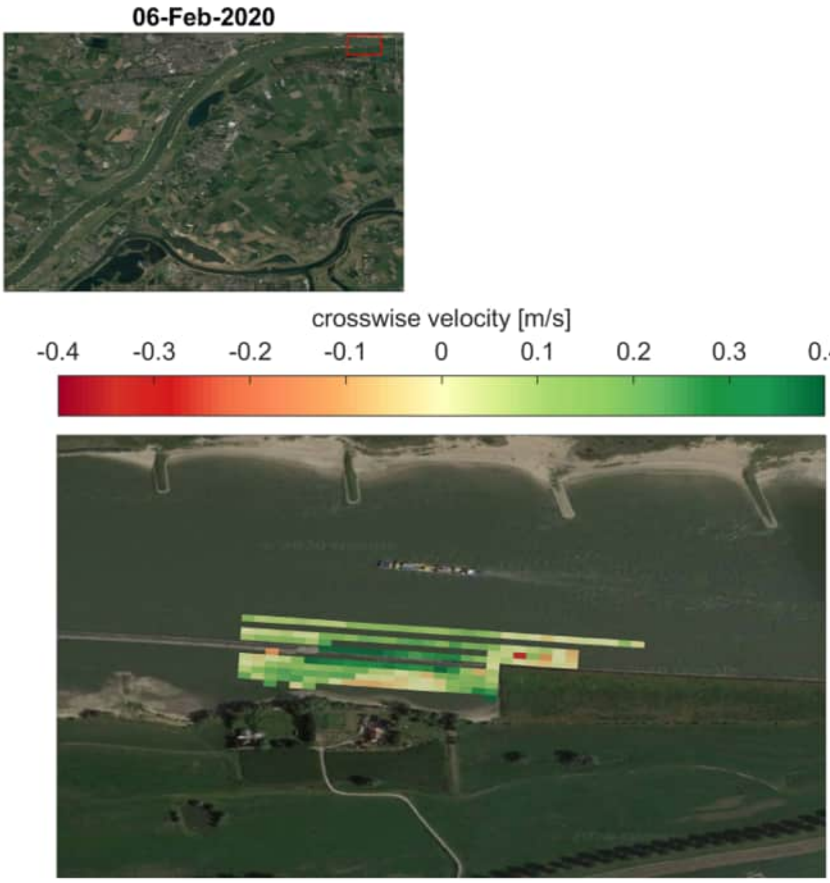

Figure D.171 Depth-averaged velocity field considering the full water column on 06-02-20 (discharge at Lobith at 12:00 equal to 4885 m^3/s).

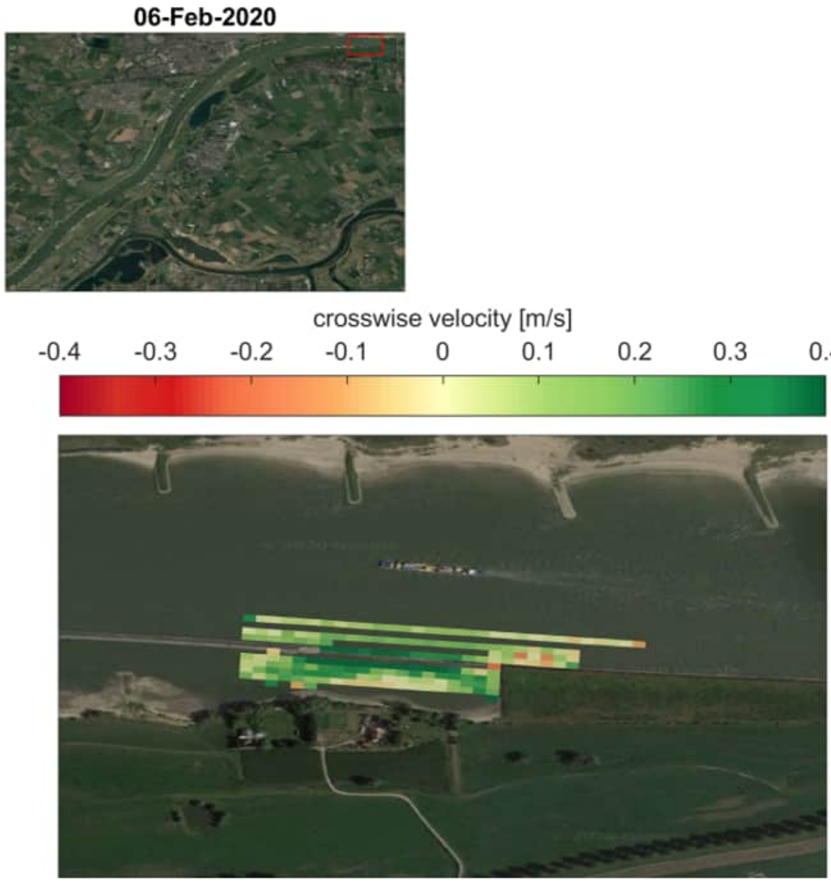

Figure D.172 Depth-averaged velocity field considering the top 2 m on 06-02-20 (discharge at Lobith at 12:00 equal to 4885 m^3/s).

D.5.4.9 02-04-20

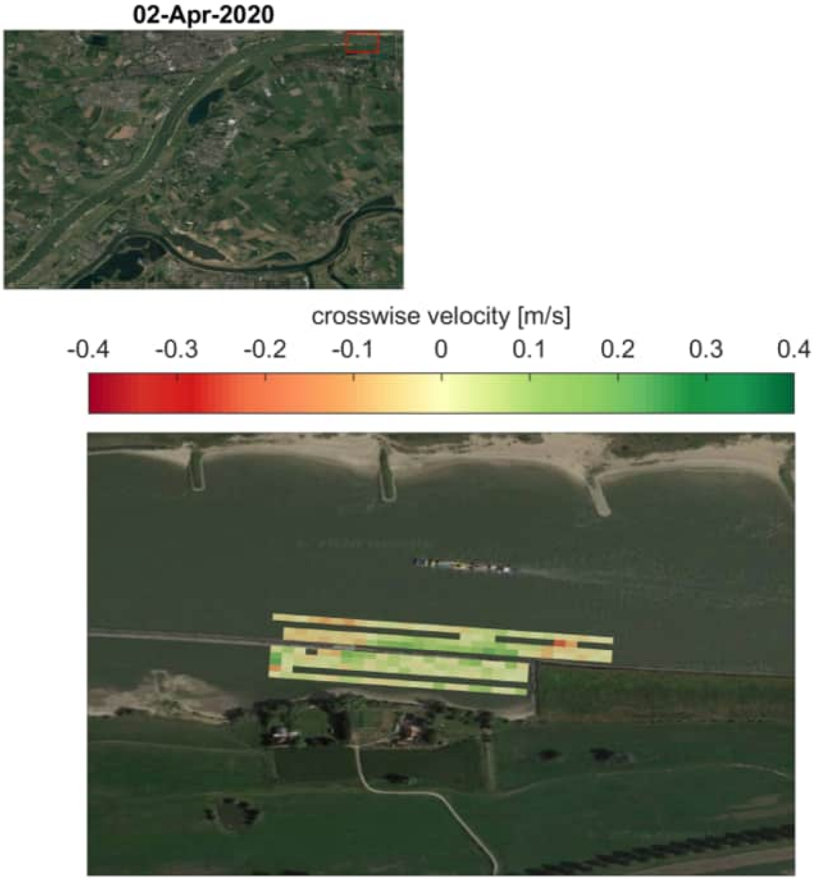

Figure D.173 Depth-averaged velocity field considering the full water column on 02-04-20 (discharge at Lobith at 12:00 equal to 1891 m^3/s).

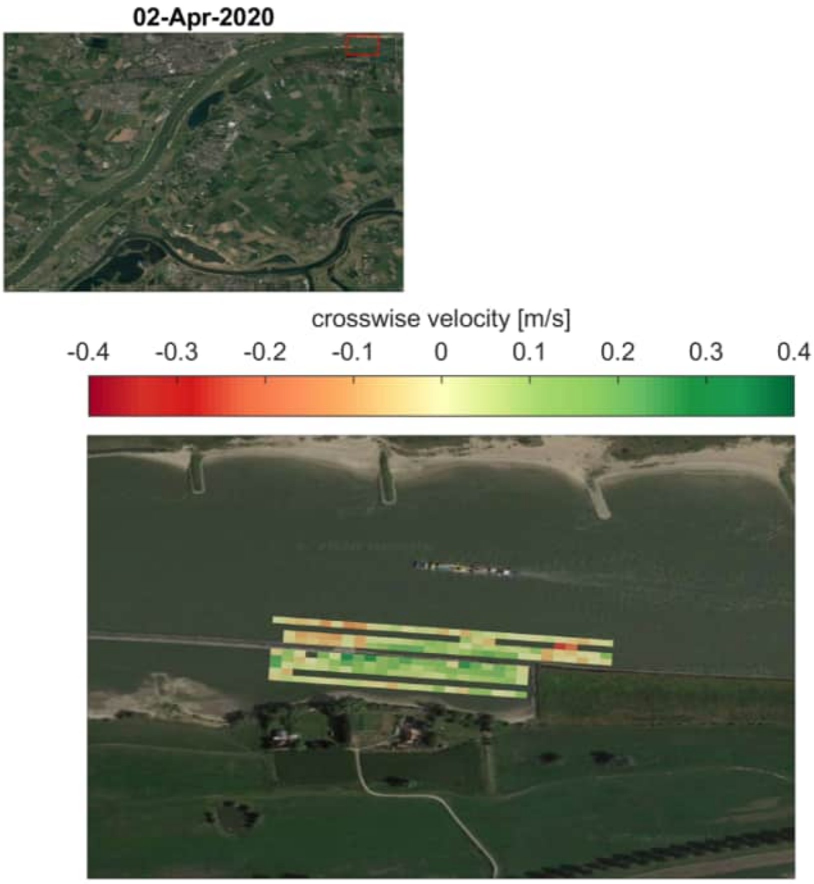

Figure D.174 Depth-averaged velocity field considering the top 2 m on 02-04-20 (discharge at Lobith at 12:00 equal to 1891 m^3/s).

D.5.4.10 21-04-20

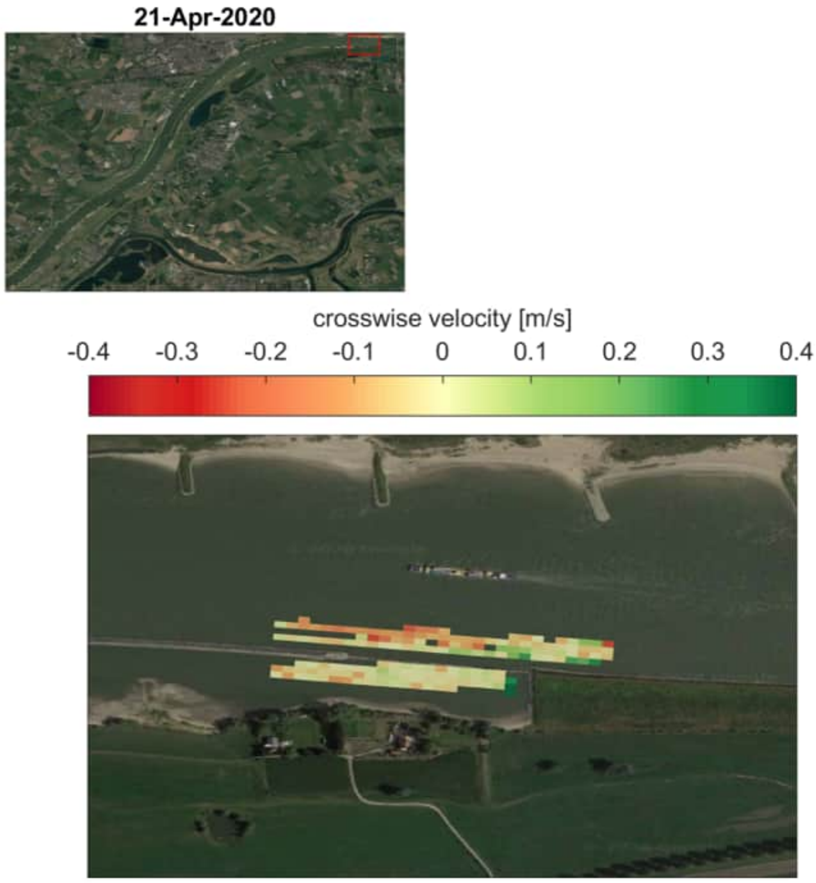

Figure D.175 Depth-averaged velocity field considering the full water column on 21-04-20 (discharge at Lobith at 12:00 equal to 1255 m^3/s).

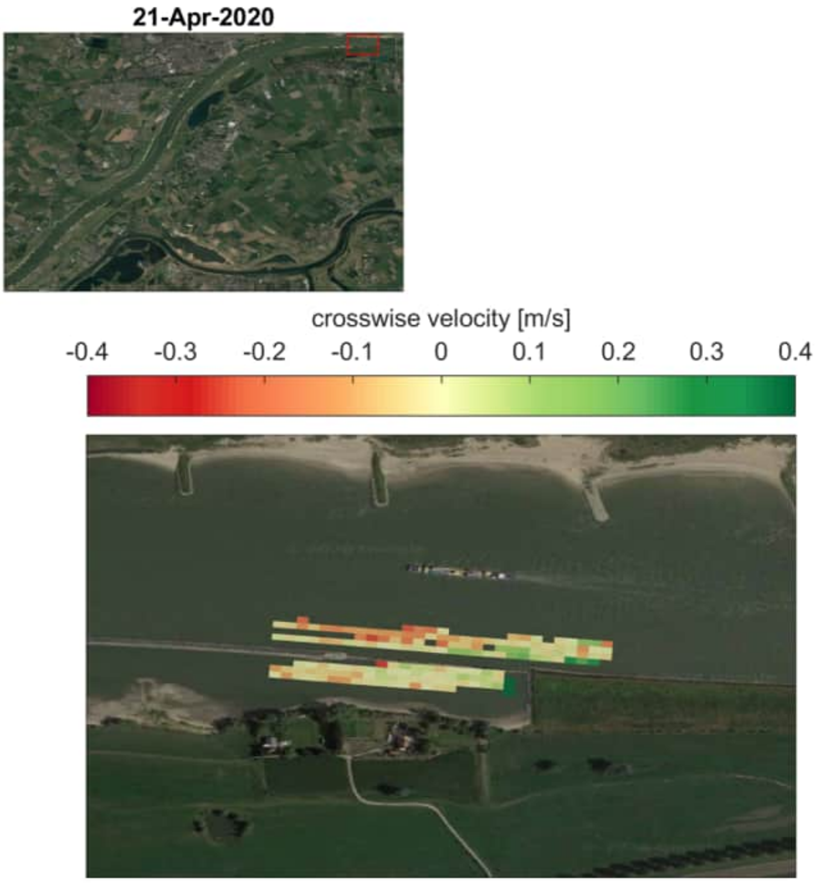

Figure D.176 Depth-averaged velocity field considering the top 2 m on 21-04-20 (discharge at Lobith at 12:00 equal to 1255 m^3/s).

D.5.4.11 01-12-17

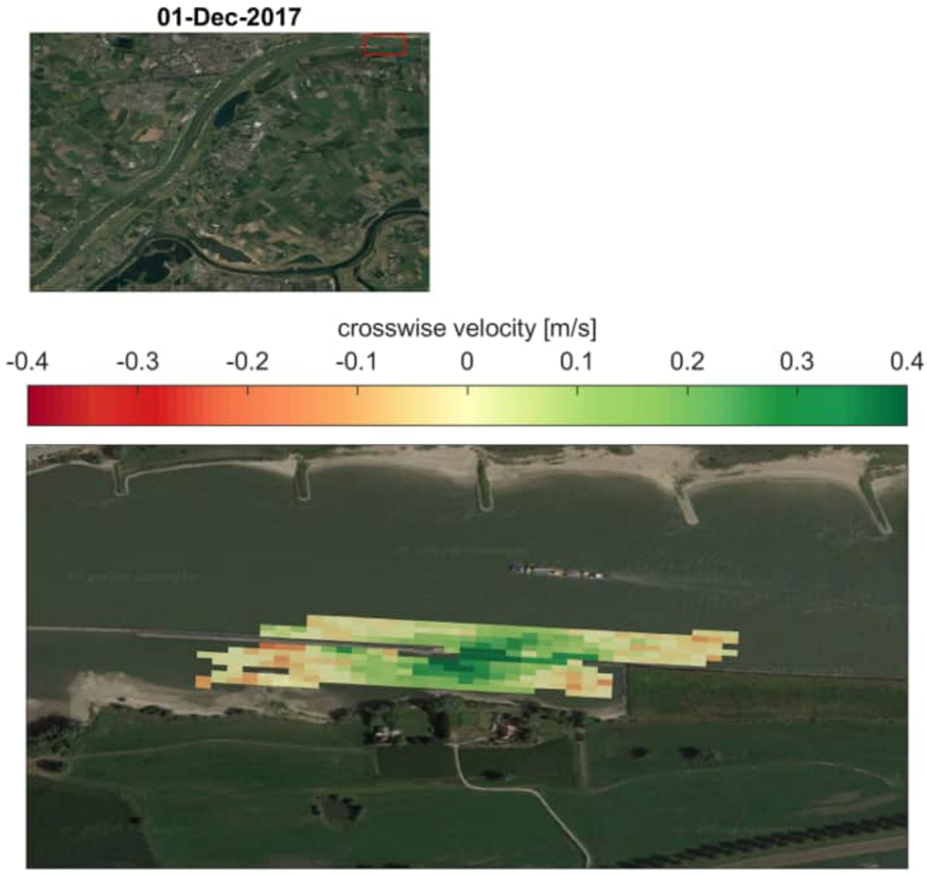

Figure D.177 Depth-averaged velocity field considering the full water column on 01-12-17 (discharge at Lobith at 12:00 equal to 3502 m^3/s).

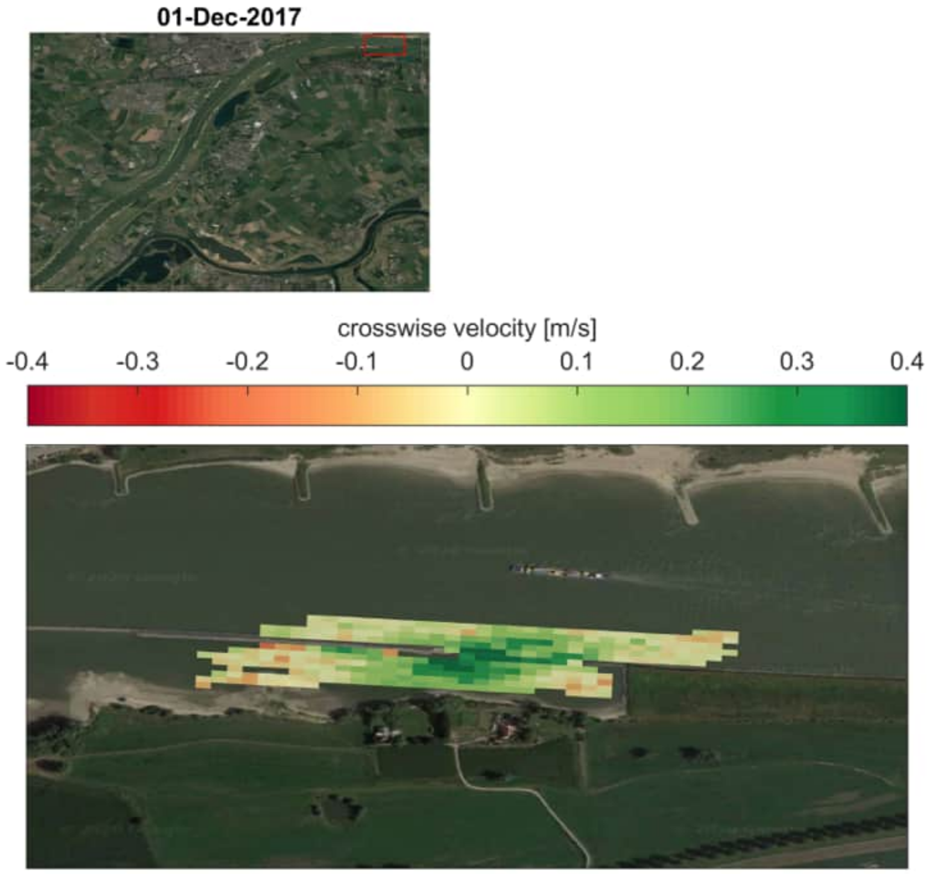

Figure D.178 Depth-averaged velocity field considering the top 2 m on 01-12-17 (discharge at Lobith at 12:00 equal to 3502 m^3/s).

D.5.4.12 02-02-18

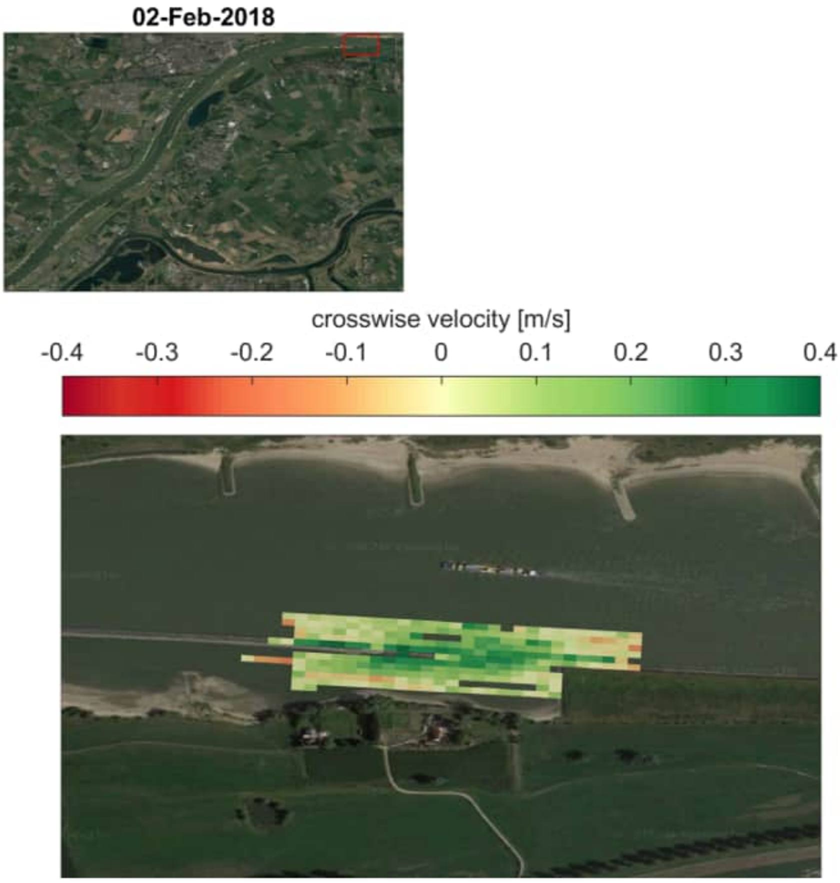

Figure D.179 Depth-averaged velocity field considering the full water column on 02-02-18 (discharge at Lobith at 12:00 equal to 4705 m^3/s).

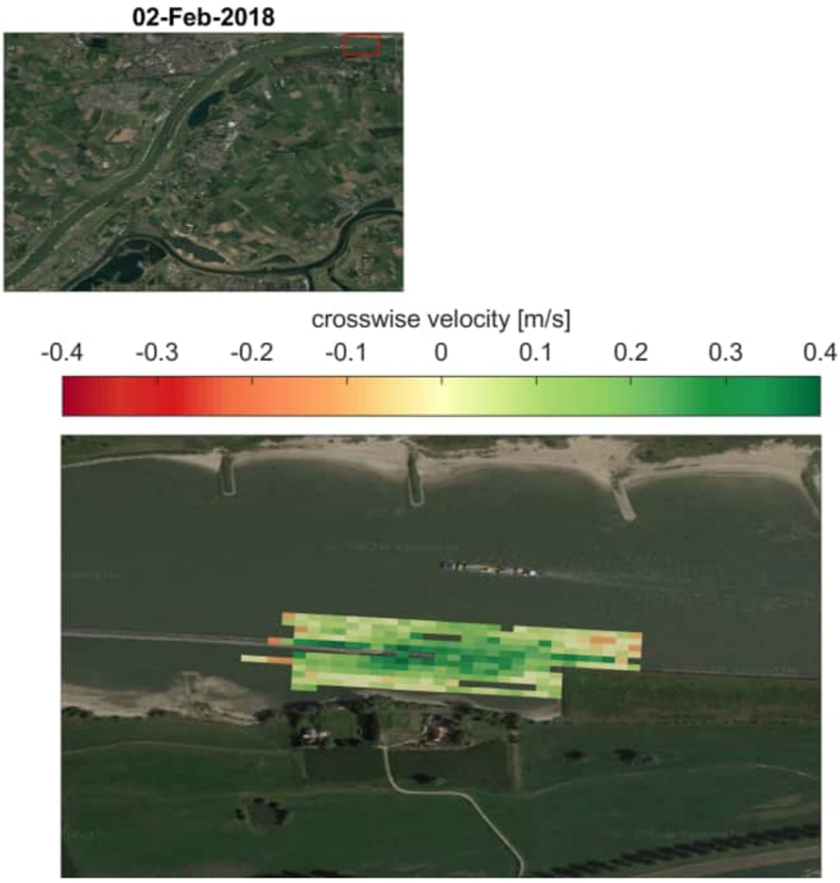

Figure D.180 Depth-averaged velocity field considering the top 2 m on 02-02-18 (discharge at Lobith at 12:00 equal to 4705 m^3/s).

D.5.4.13 16-02-18

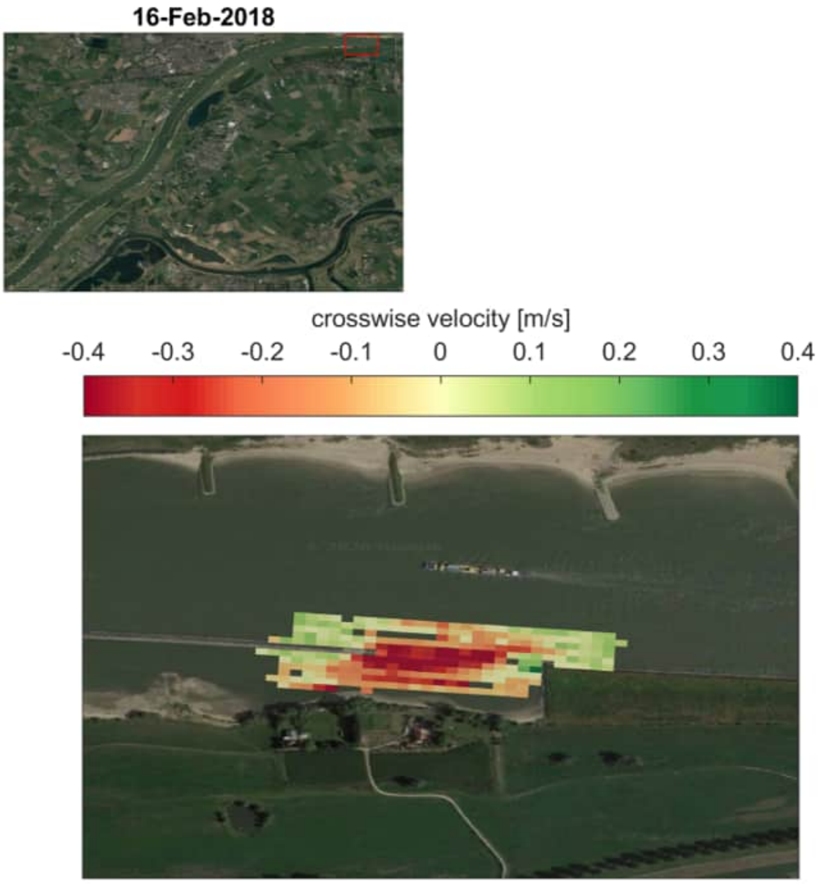

Figure D.181 Depth-averaged velocity field considering the full water column on 16-02-18 (discharge at Lobith at 12:00 equal to 2549 m^3/s).

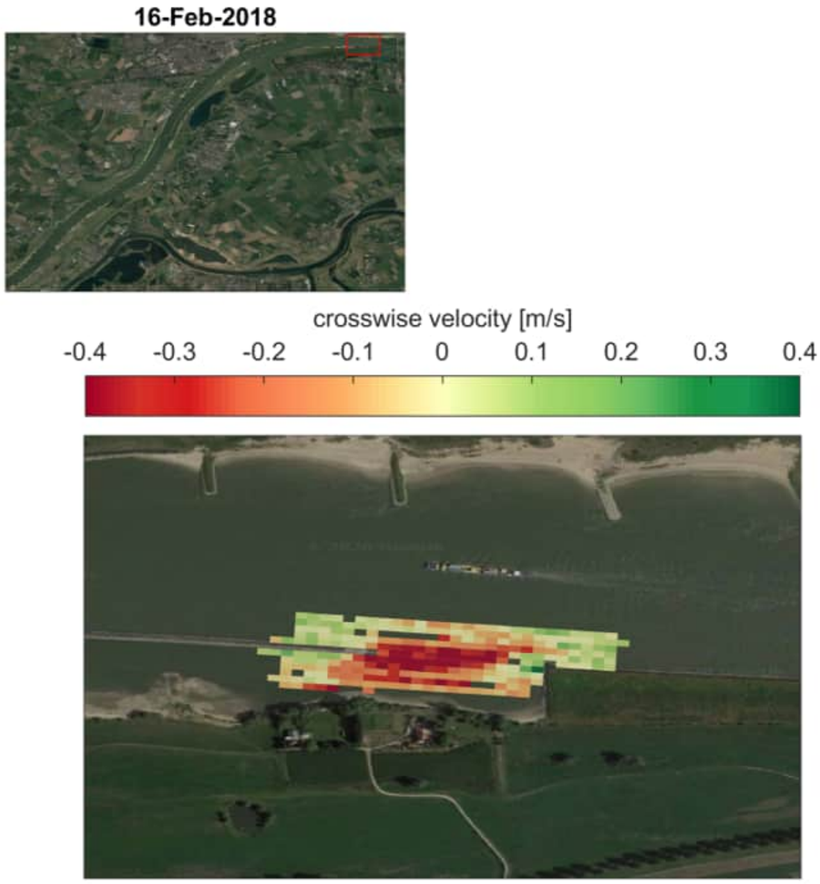

Figure D.182 Depth-averaged velocity field considering the top 2 m on 16-02-18 (discharge at Lobith at 12:00 equal to 2549 m^3/s).

D.5.4.14 07-03-18

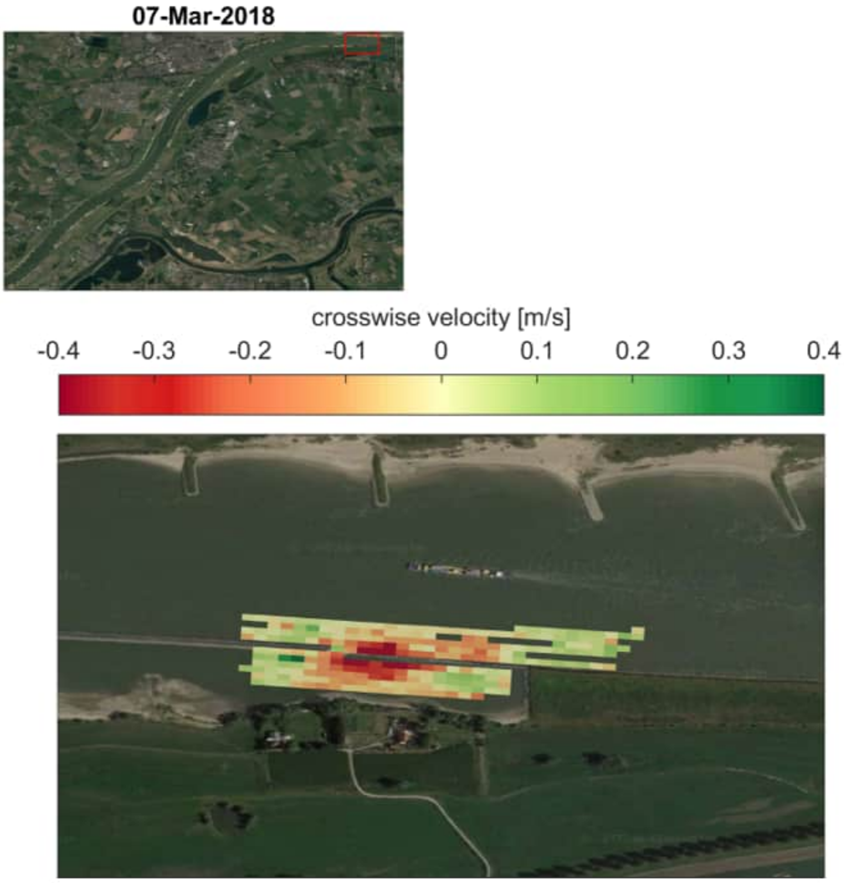

Figure D.183 Depth-averaged velocity field considering the full water column on 07-03-18 (discharge at Lobith at 12:00 equal to 1929 m^3/s).

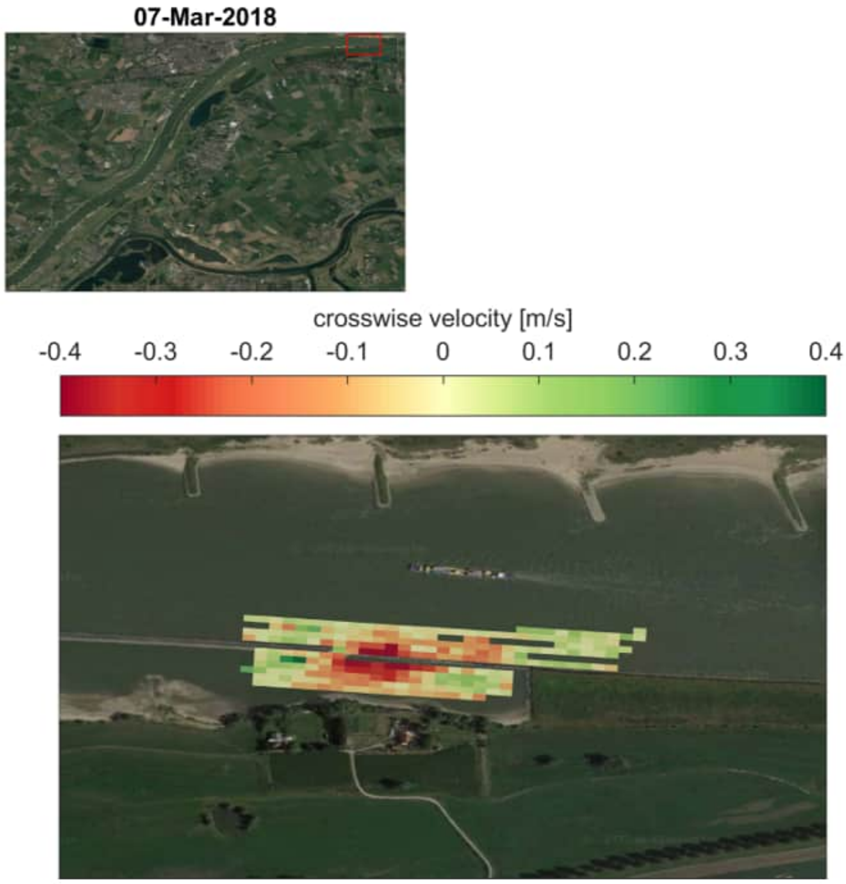

Figure D.184 Depth-averaged velocity field considering the top 2 m on 07-03-18 (discharge at Lobith at 12:00 equal to 1929 m^3/s).

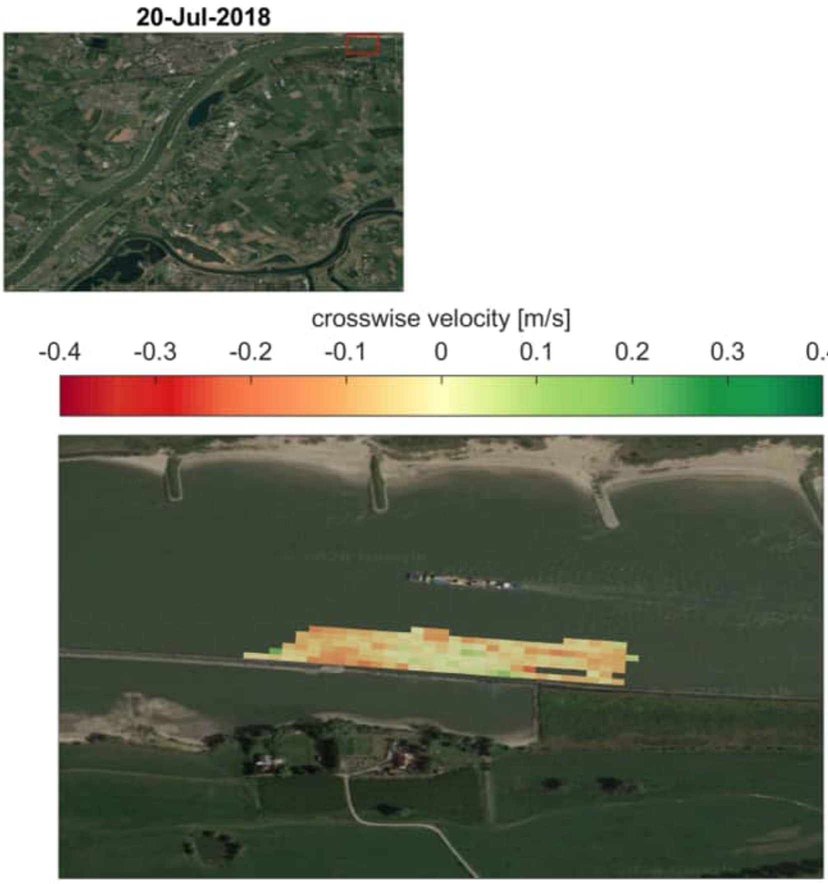

Figure D.185 Depth-averaged velocity field considering the full water column on 20-07-18 (discharge at Lobith at 12:00 equal to 1092 m^3/s).

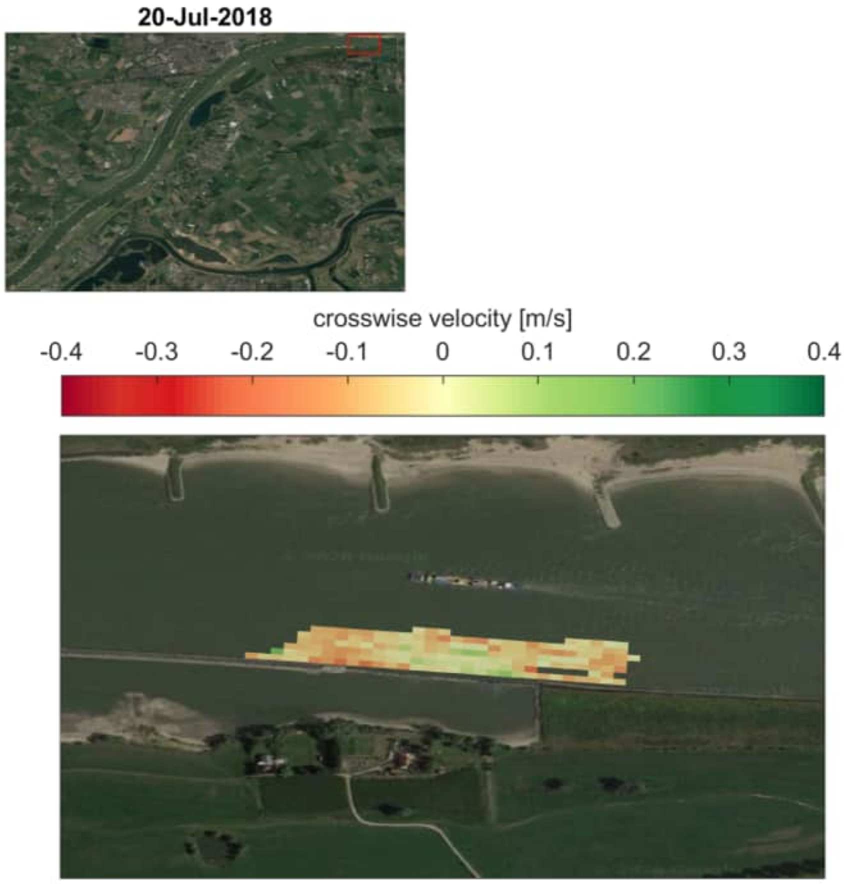

Figure D.186 Depth-averaged velocity field considering the top 2 m on 20-07-18 (discharge at Lobith at 12:00 equal to 1092 m^3/s).

D.5.5 Wamel-Dreumel

D.5.5.1 04-01-19

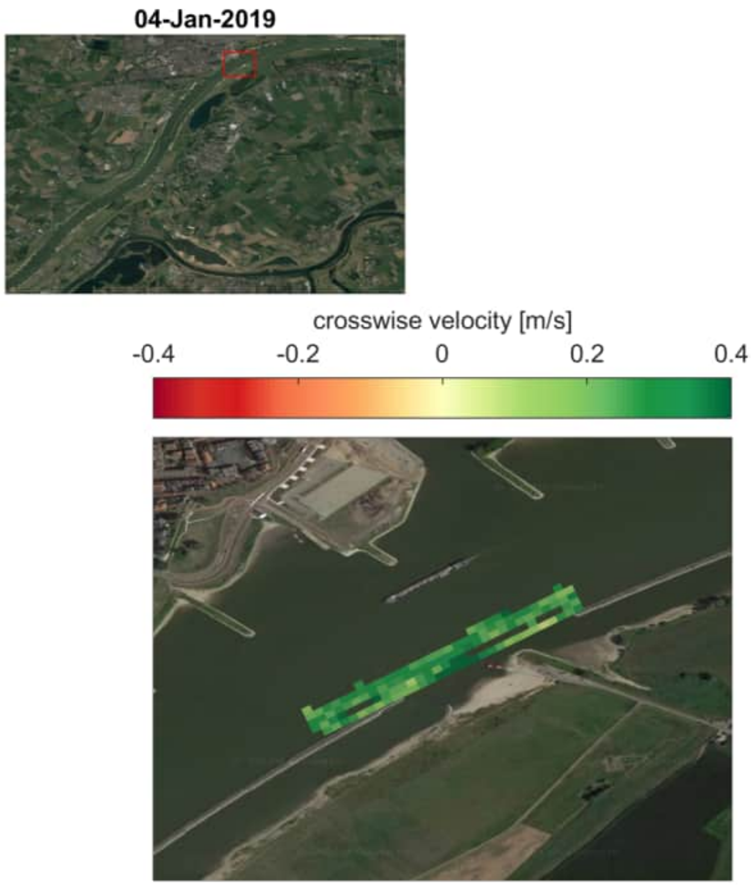

Figure D.187 Depth-averaged velocity field considering the full water column on 04-01-19 (discharge at Lobith at 12:00 equal to 1841 m^3/s).

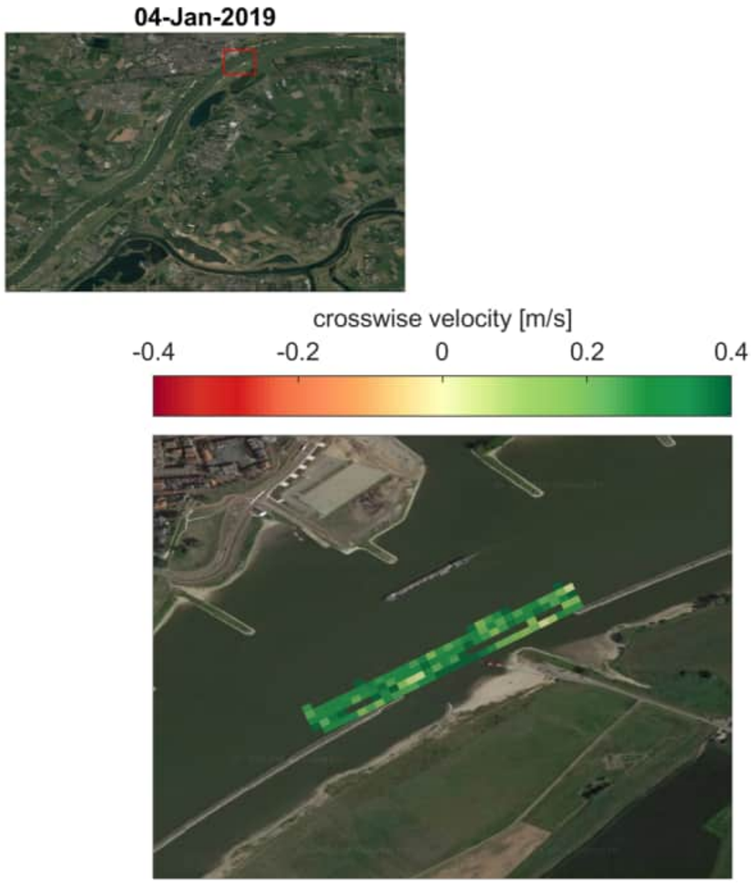

Figure D.188 Depth-averaged velocity field considering the top 2 m on 04-01-19 (discharge at Lobith at 12:00 equal to 1841 m^3/s).

D.5.5.2 09-01-19

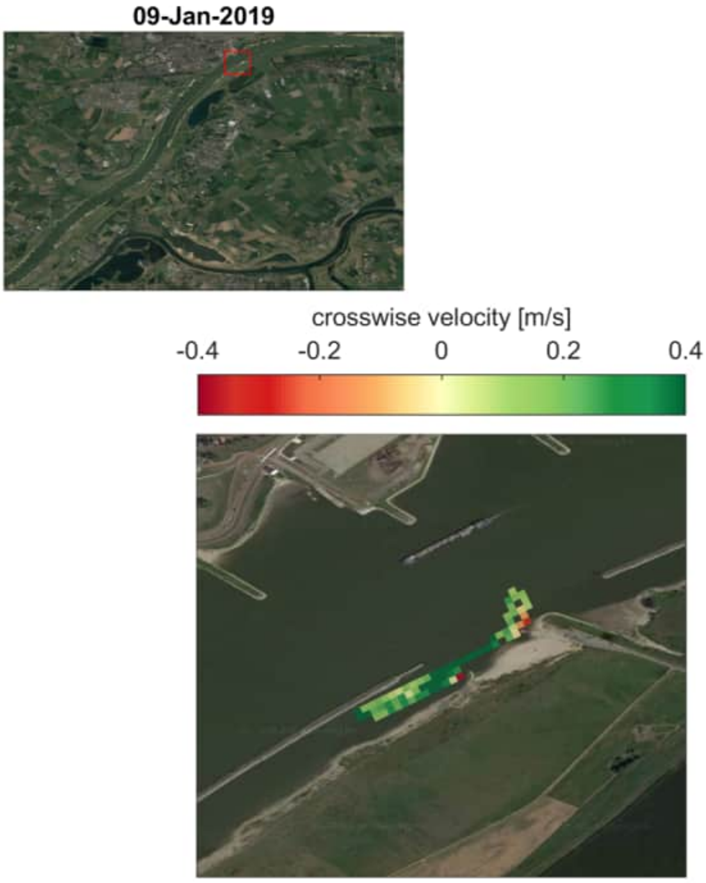

Figure D.189 Depth-averaged velocity field considering the full water column on 09-01-19 (discharge at Lobith at 12:00 equal to 1976 m^3/s).

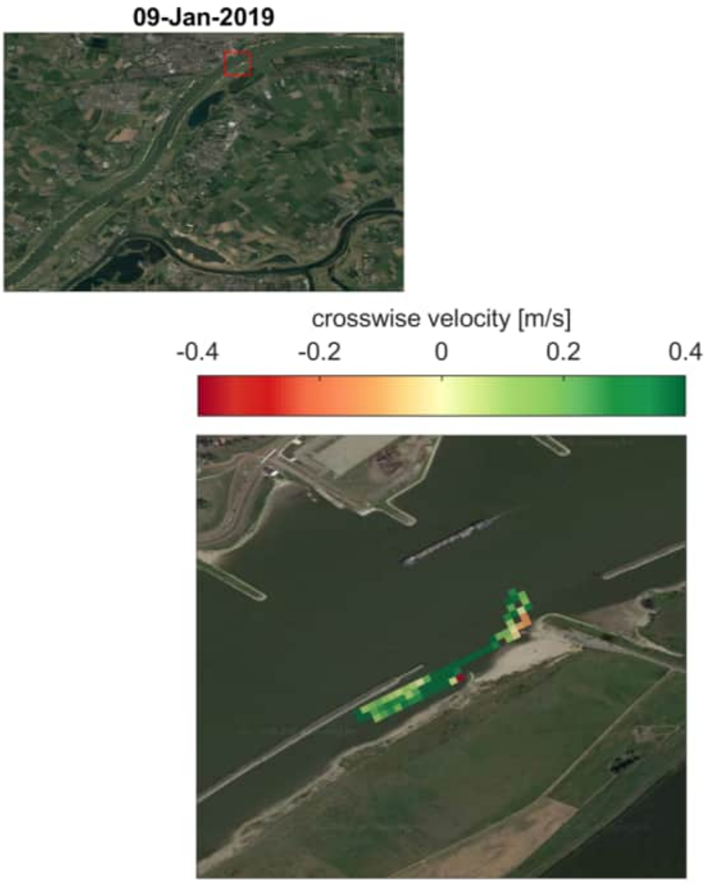

Figure D.190 Depth-averaged velocity field considering the top 2 m on 09-01-19 (discharge at Lobith at 12:00 equal to 1976 m^3/s).

D.5.5.3 27-02-19

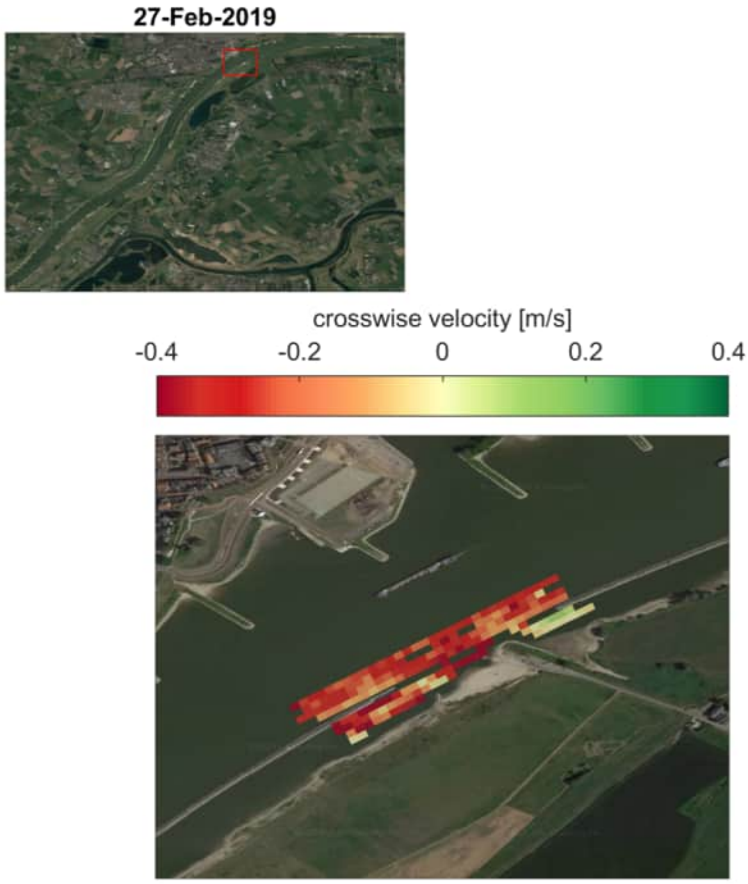

Figure D.191 Depth-averaged velocity field considering the full water column on 27-02-19 (discharge at Lobith at 12:00 equal to 1682 m^3/s).

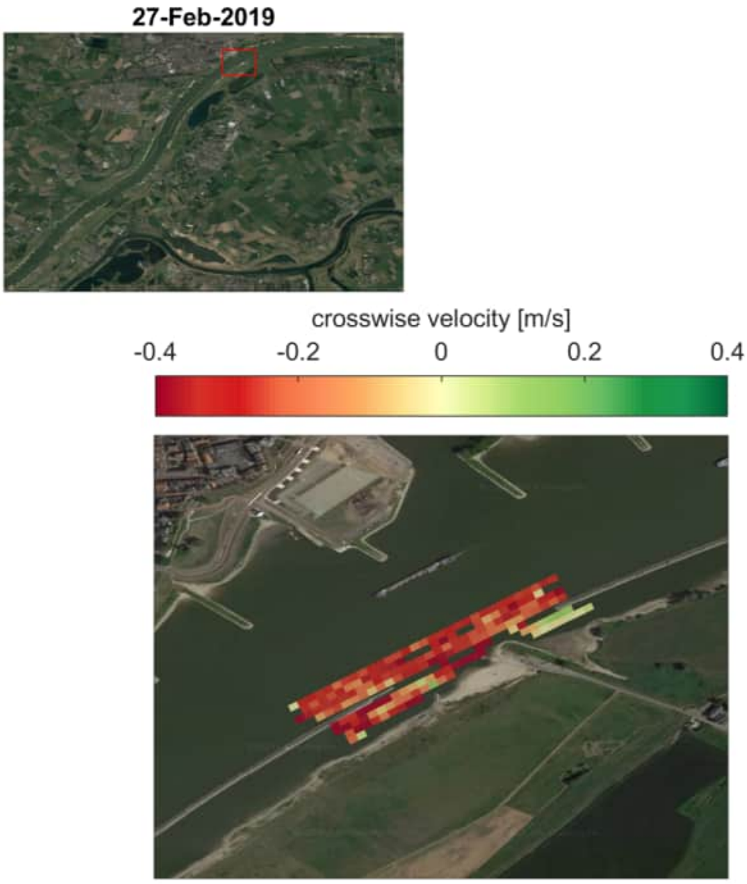

Figure D.192 Depth-averaged velocity field considering the top 2 m on 27-02-19 (discharge at Lobith at 12:00 equal to 1682 m^3/s).

D.5.5.4 20-03-19

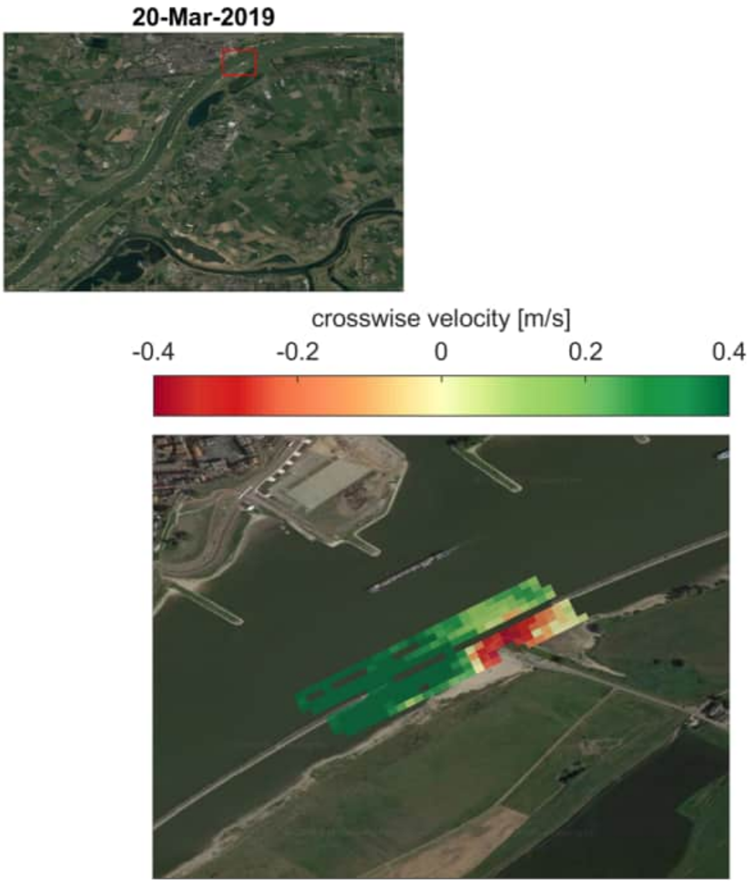

Figure D.193 Depth-averaged velocity field considering the full water column on 20-03-19 (discharge at Lobith at 12:00 equal to 5050 m^3/s).

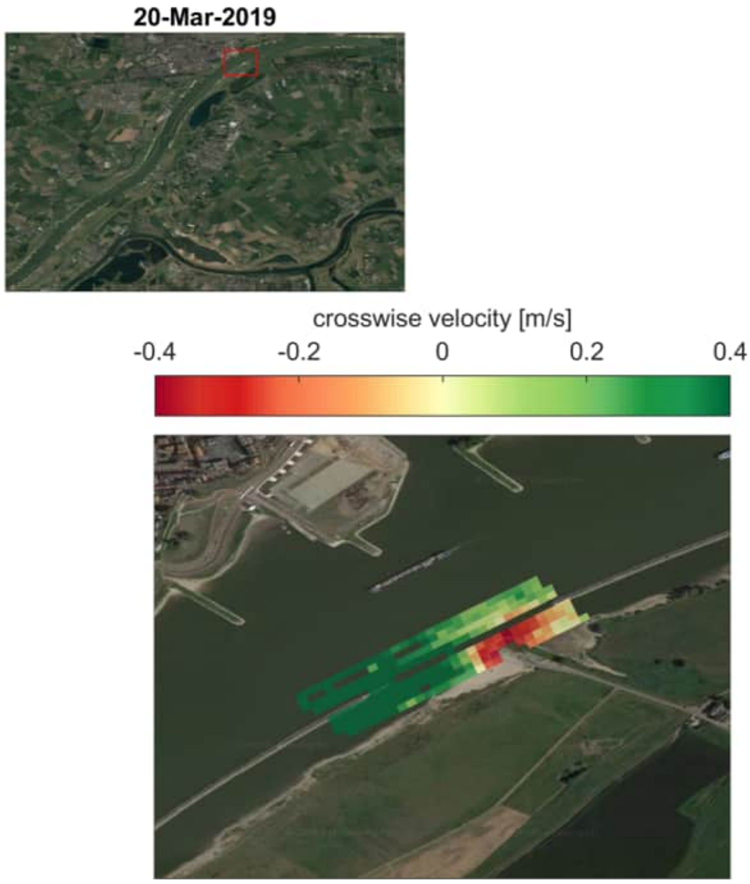

Figure D.194 Depth-averaged velocity field considering the top 2 m on 20-03-19 (discharge at Lobith at 12:00 equal to 5050 m^3/s).

D.5.5.5 27-03-19

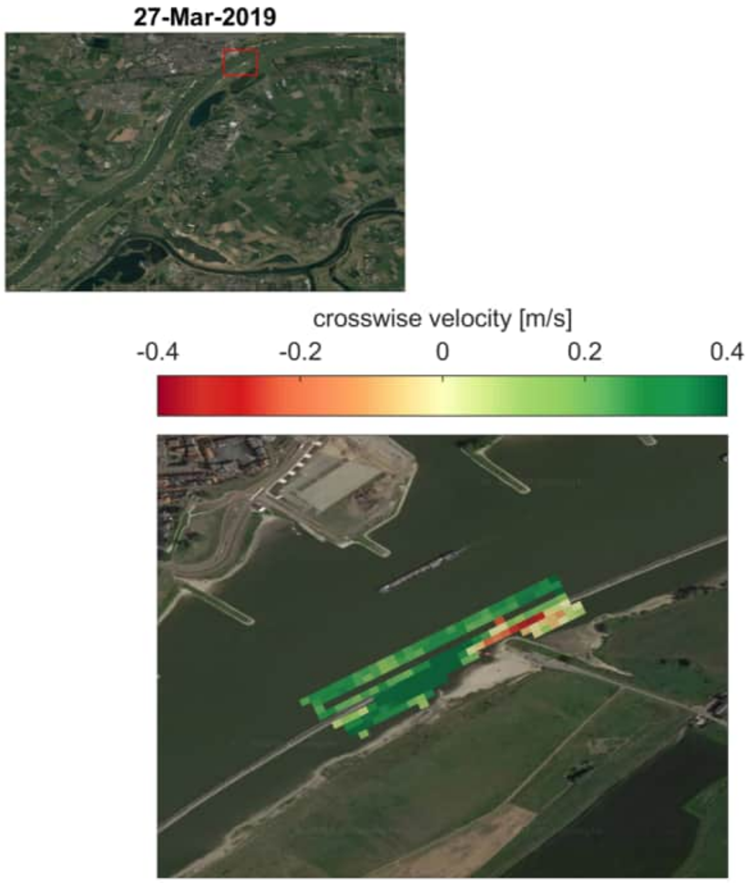

Figure D.195 Depth-averaged velocity field considering the full water column on 27-03-19 (discharge at Lobith at 12:00 equal to 2434 m^3/s).

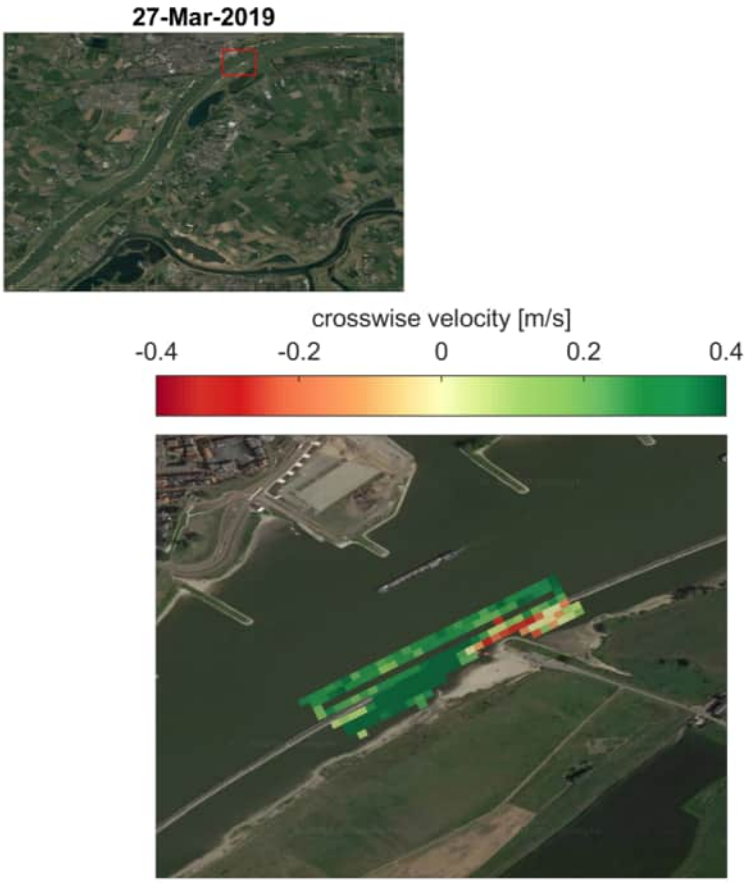

Figure D.196 Depth-averaged velocity field considering the top 2 m on 27-03-19 (discharge at Lobith at 12:00 equal to 2434 m^3/s).

D.5.5.6 26-09-19

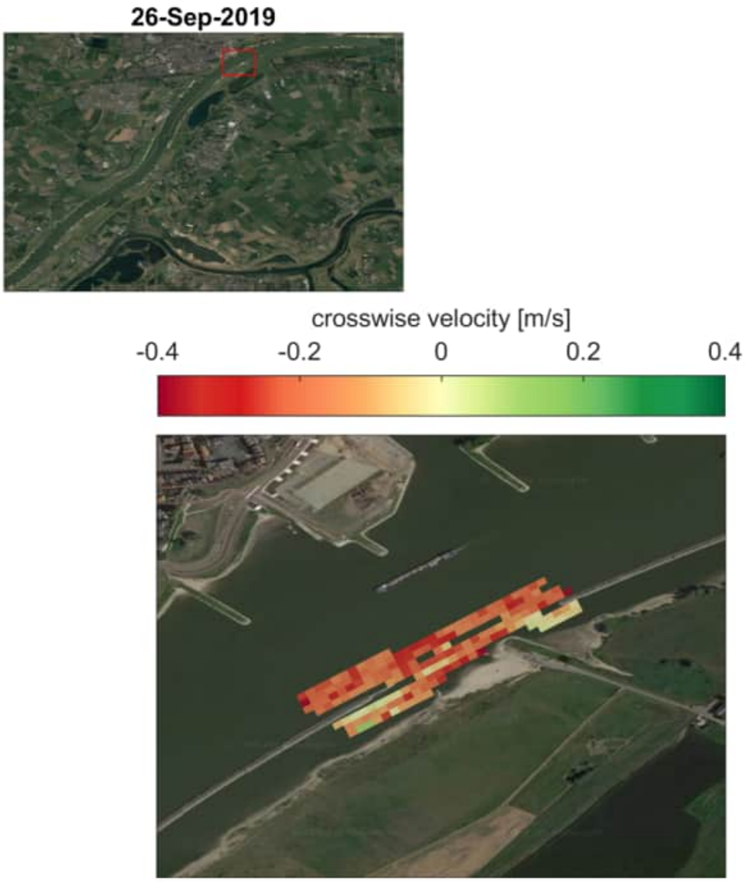

Figure D.197 Depth-averaged velocity field considering the full water column on 26-09-19 (discharge at Lobith at 12:00 equal to 1077 m^3/s).

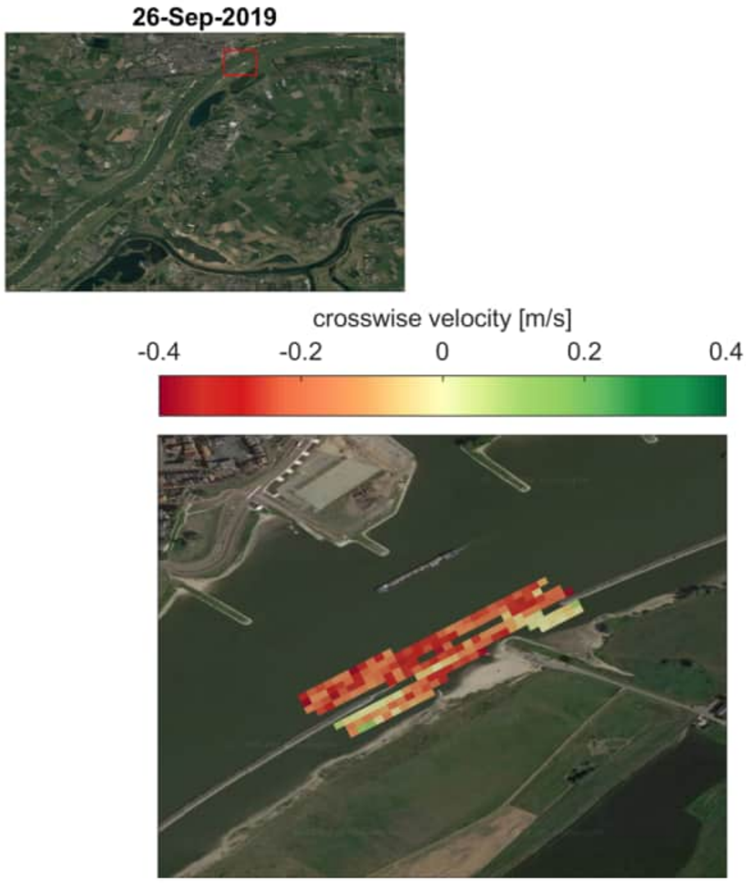

Figure D.198 Depth-averaged velocity field considering the top 2 m on 26-09-19 (discharge at Lobith at 12:00 equal to 1077 m^3/s).

Deltares

D.5.5.7 19-12-19

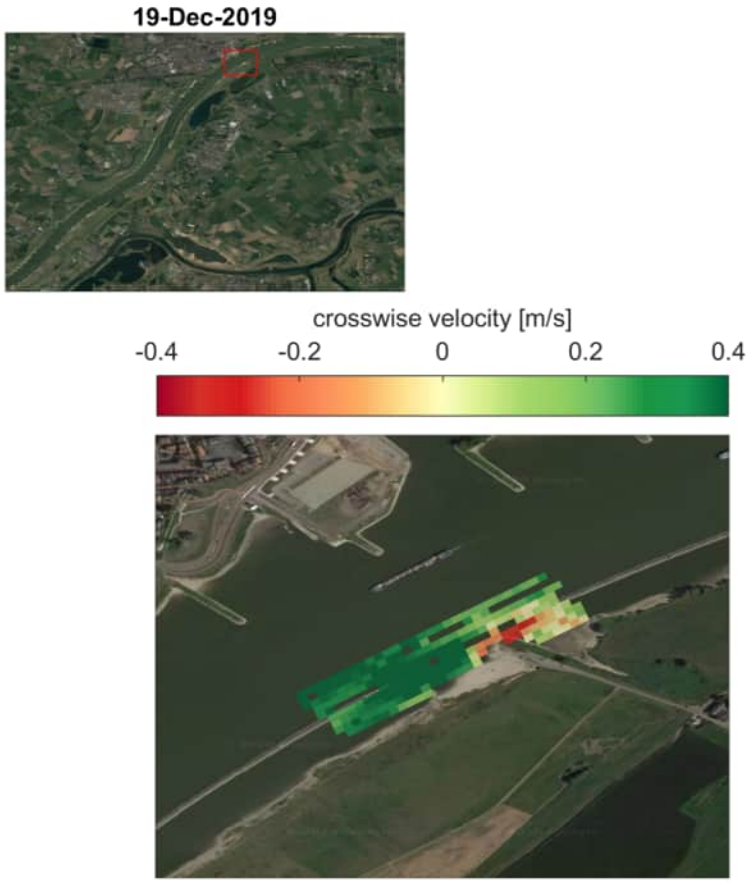

Figure D.199 Depth-averaged velocity field considering the full water column on 19-12-19 (discharge at Lobith at 12:00 equal to 3549 m^3/s).

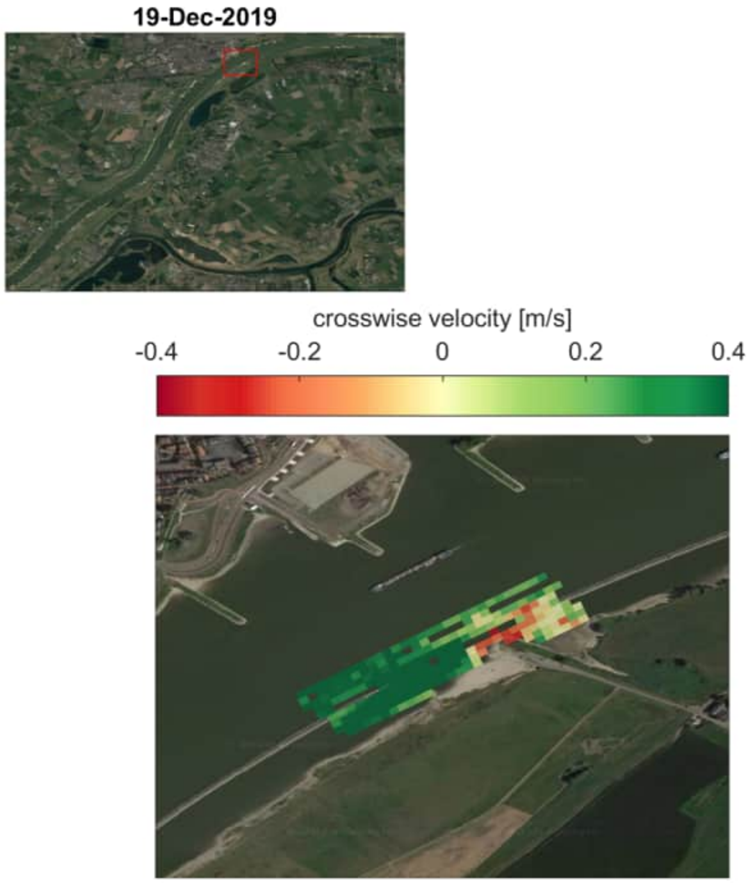

Figure D.200 Depth-averaged velocity field considering the top 2 m on 19-12-19 (discharge at Lobith at 12:00 equal to 3549 m^3/s).

D.5.5.8 05-02-20

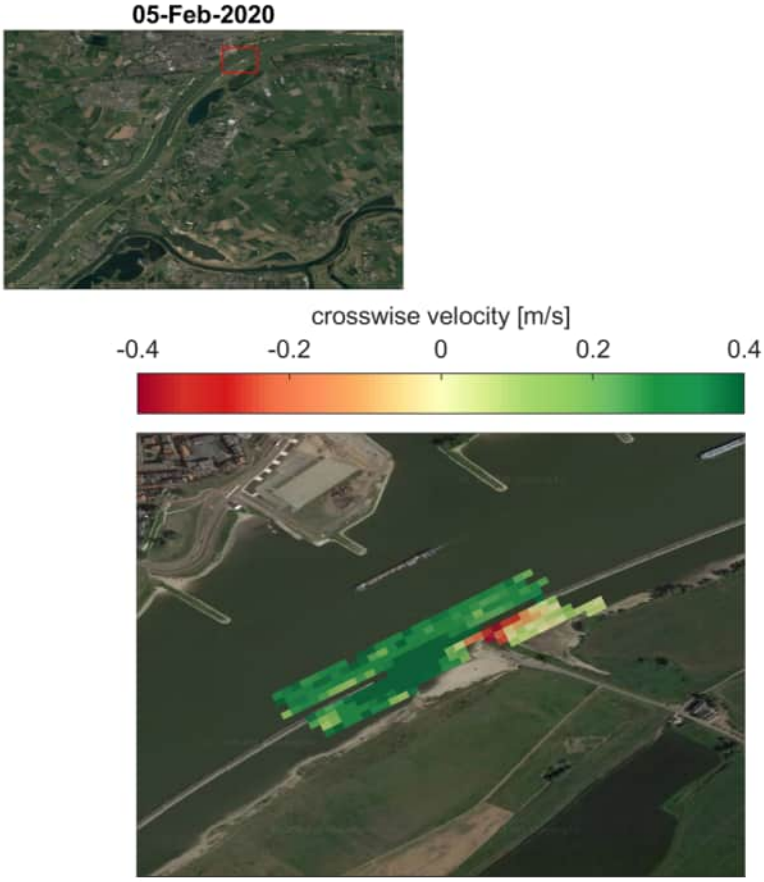

Figure D.201 Depth-averaged velocity field considering the full water column on 05-02-20 (discharge at Lobith at 12:00 equal to 3647 m^3/s).

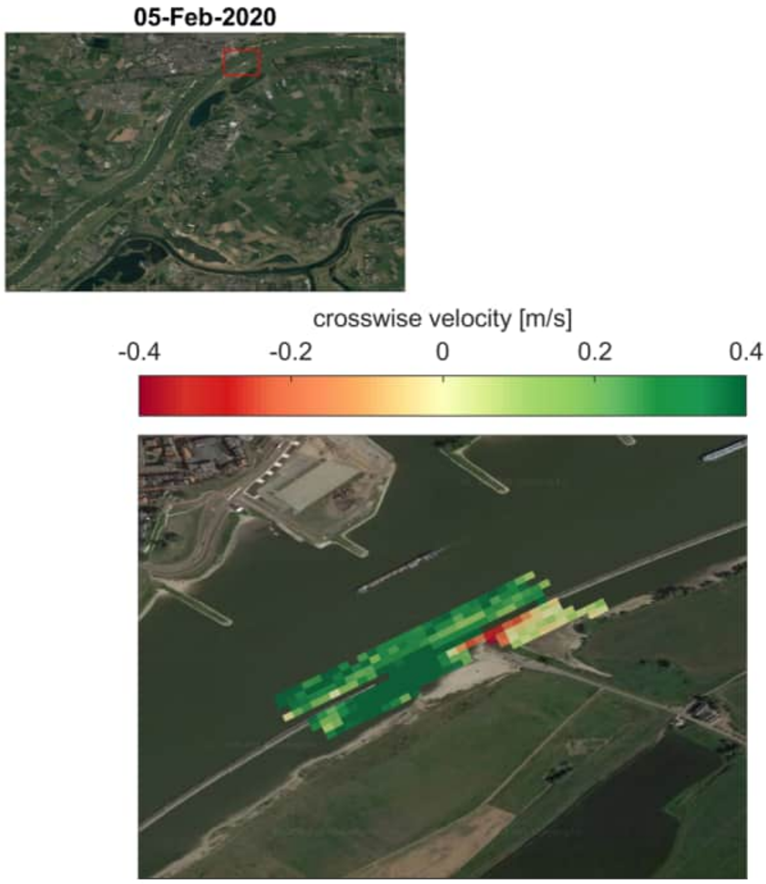

Figure D.202 Depth-averaged velocity field considering the top 2 m on 05-02-20 (discharge at Lobith at 12:00 equal to 3647 m^3/s).

Deltares

D.5.5.9 06-02-20

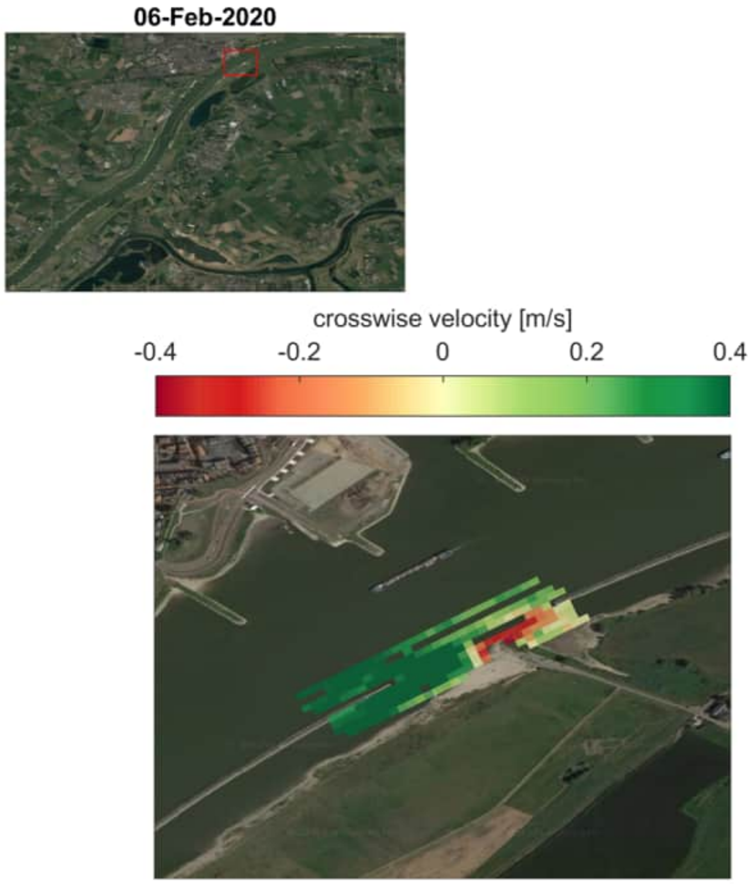

Figure D.203 Depth-averaged velocity field considering the full water column on 06-02-20 (discharge at Lobith at 12:00 equal to 4885 m^3/s).

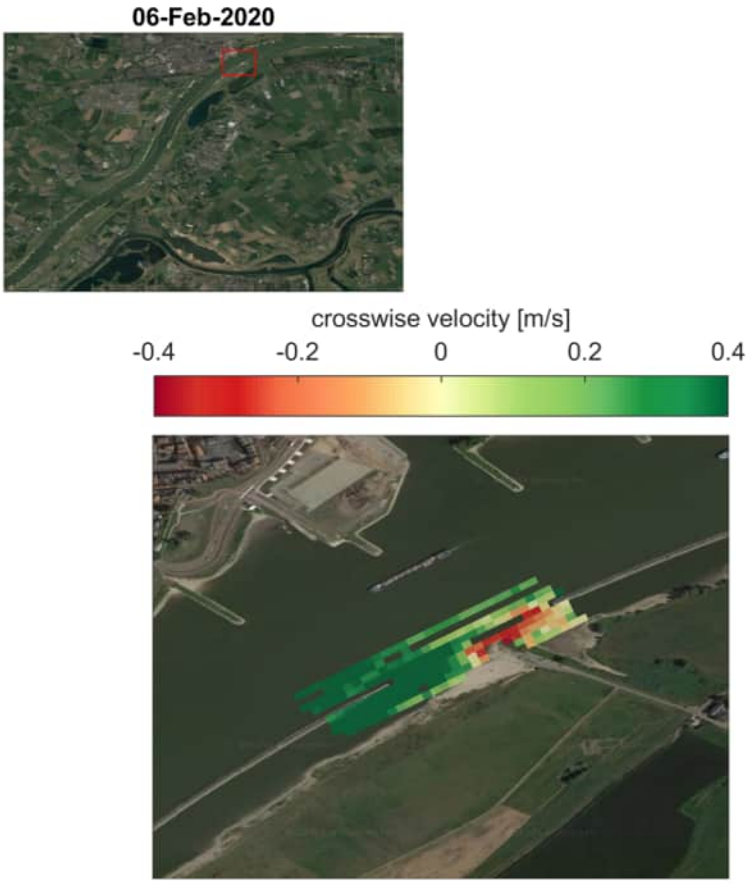

Figure D.204 Depth-averaged velocity field considering the top 2 m on 06-02-20 (discharge at Lobith at 12:00 equal to 4885 m^3/s).

D.5.5.10 03-04-20

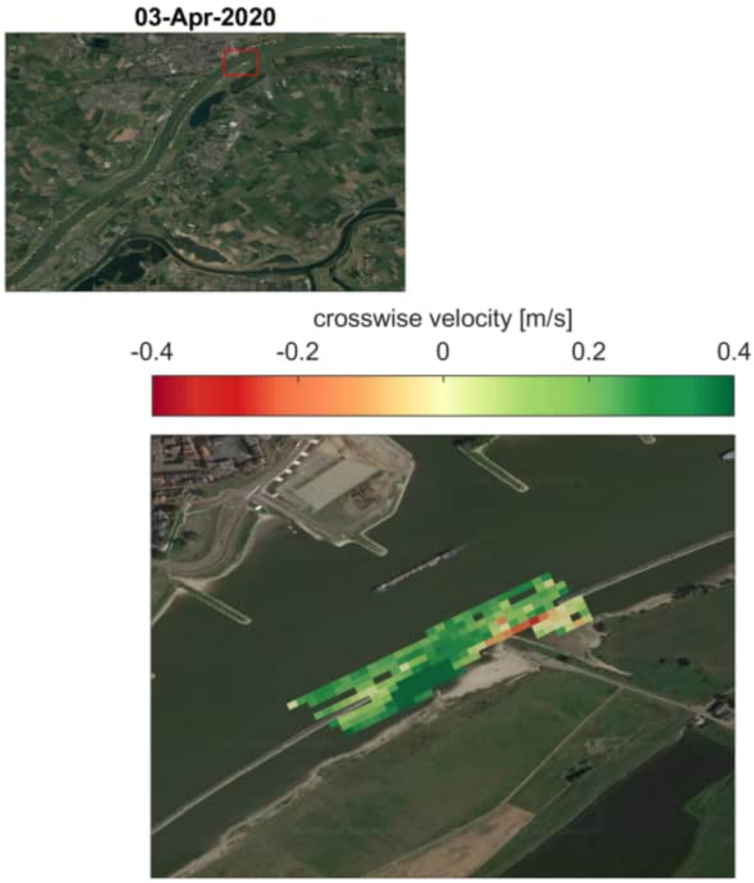

Figure D.205 Depth-averaged velocity field considering the full water column on 03-04-20 (discharge at Lobith at 12:00 equal to 1862 m^3/s).

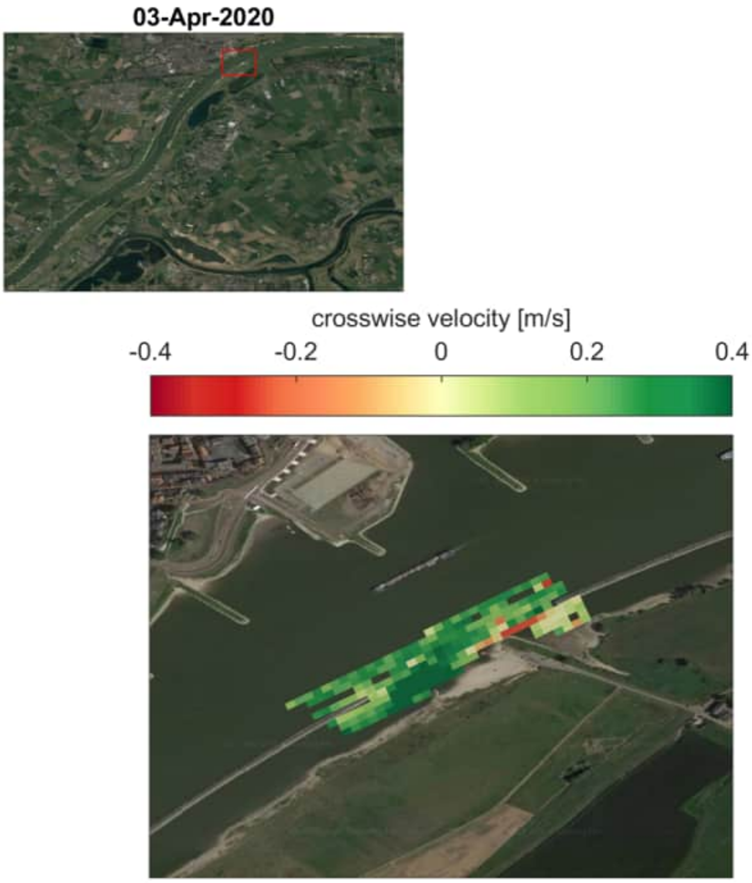

Figure D.206 Depth-averaged velocity field considering the top 2 m on 03-04-20 (discharge at Lobith at 12:00 equal to 1862 m^3/s).

D.5.5.11 23-04-20

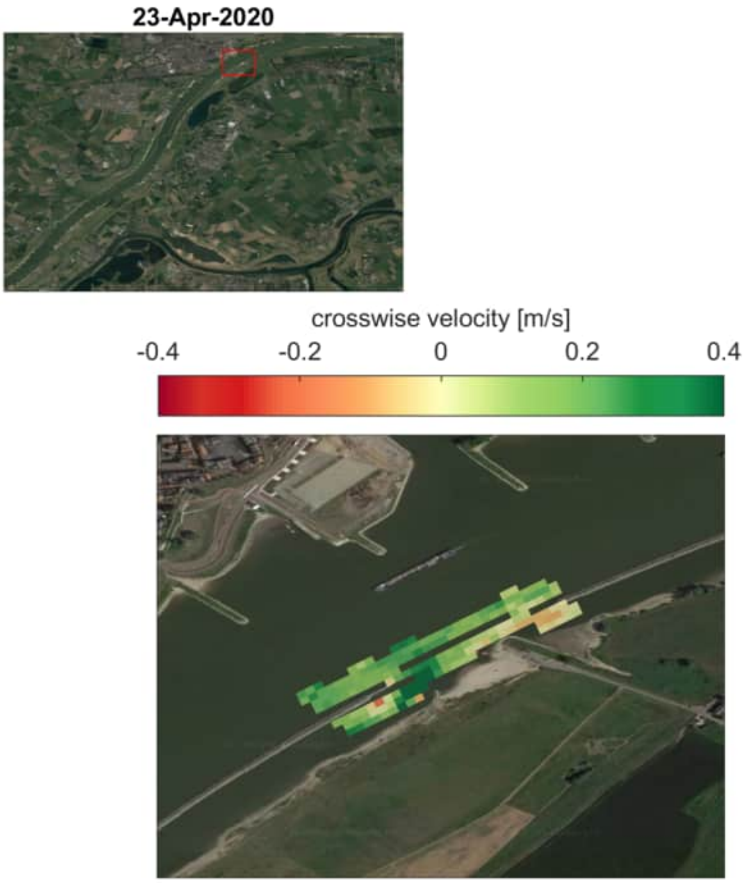

Figure D.207 Depth-averaged velocity field considering the full water column on 23-04-20 (discharge at Lobith at 12:00 equal to 1261 m^3/s).

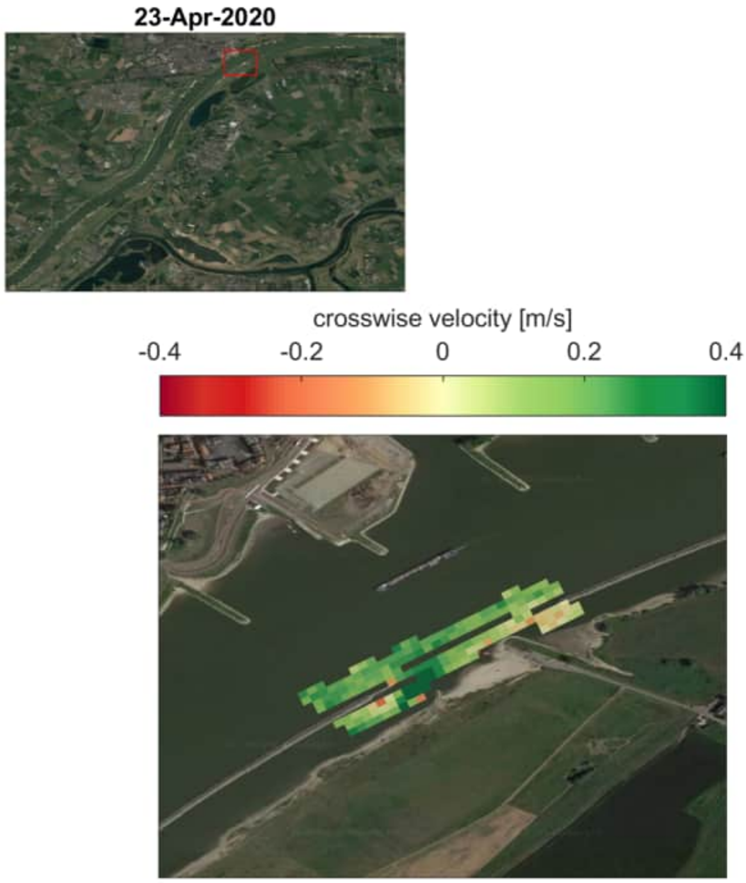

Figure D.208 Depth-averaged velocity field considering the top 2 m on 23-04-20 (discharge at Lobith at 12:00 equal to 1261 m^3/s).

D.5.5.12 01-12-17

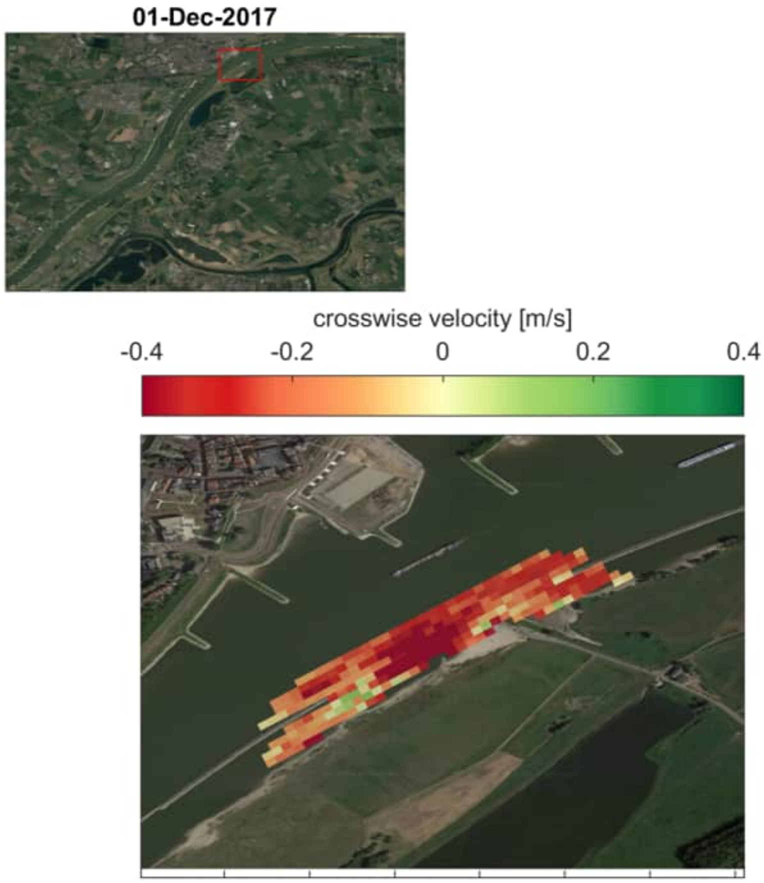

Figure D.209 Depth-averaged velocity field considering the full water column on 01-12-17 (discharge at Lobith at 12:00 equal to 3502 m^3/s).

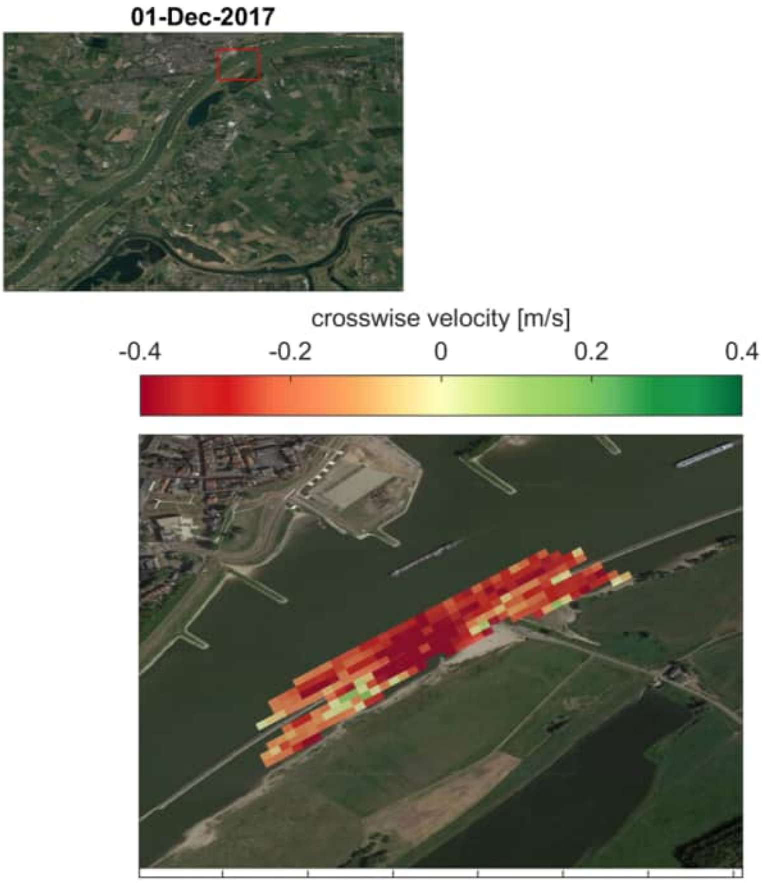

Figure D.210 Depth-averaged velocity field considering the top 2 m on 01-12-17 (discharge at Lobith at 12:00 equal to 3502 m^3/s).

D.5.5.13 02-02-18

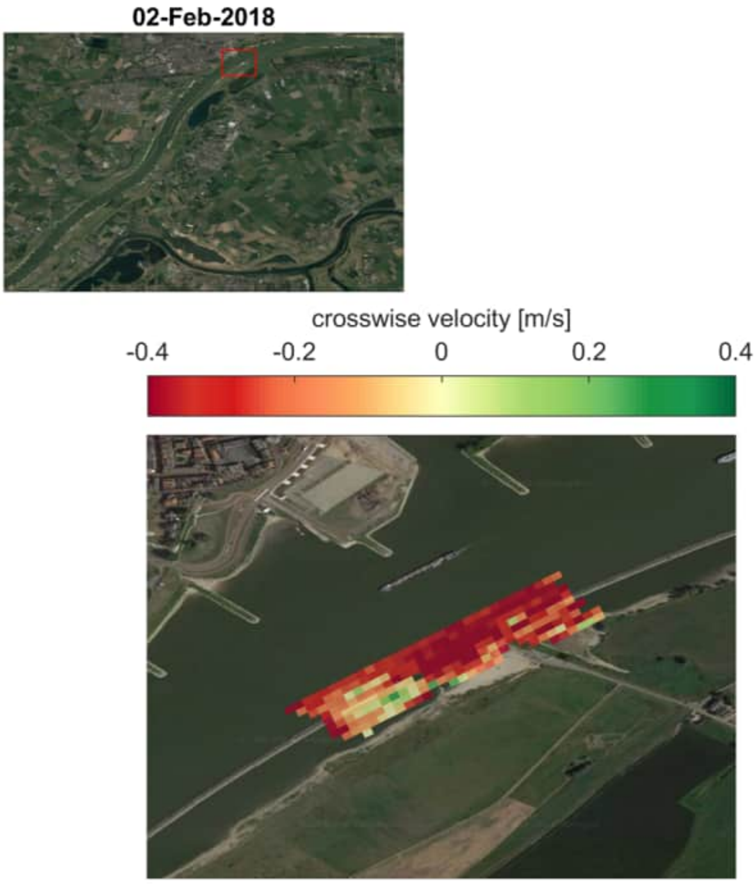

Figure D.211 Depth-averaged velocity field considering the full water column on 02-02-18 (discharge at Lobith at 12:00 equal to 4705 m^3/s).

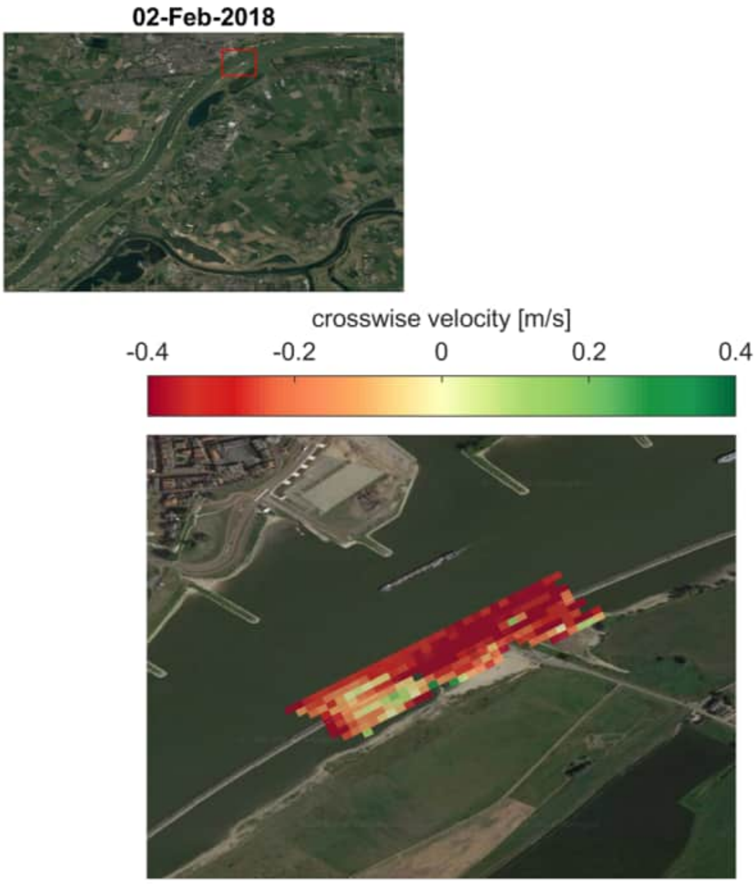

Figure D.212 Depth-averaged velocity field considering the top 2 m on 02-02-18 (discharge at Lobith at 12:00 equal to 4705 m^3/s).

Deltares

D.5.5.14 16-02-18

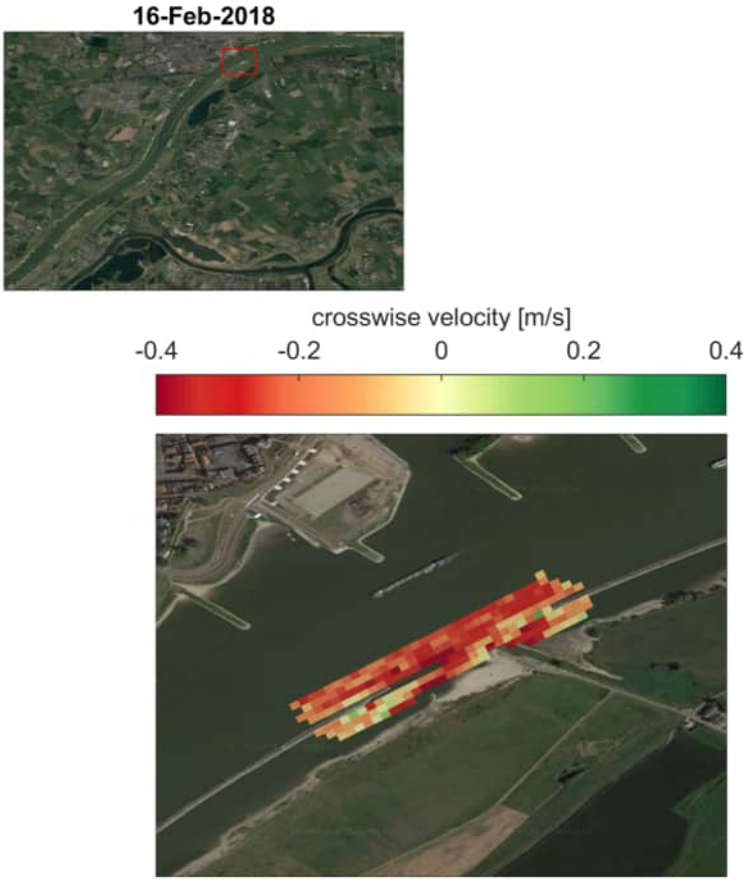

Figure D.213 Depth-averaged velocity field considering the full water column on 16-02-18 (discharge at Lobith at 12:00 equal to 2549 m^3/s).

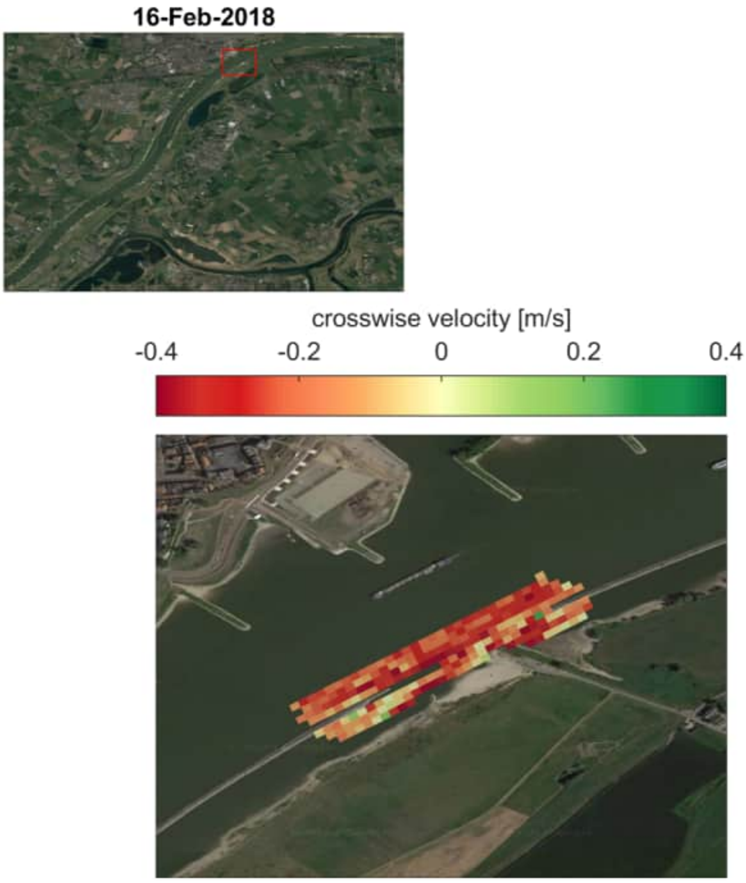

Figure D.214 Depth-averaged velocity field considering the top 2 m on 16-02-18 (discharge at Lobith at 12:00 equal to 2549 m^3/s).

D.5.5.15 07-03-18

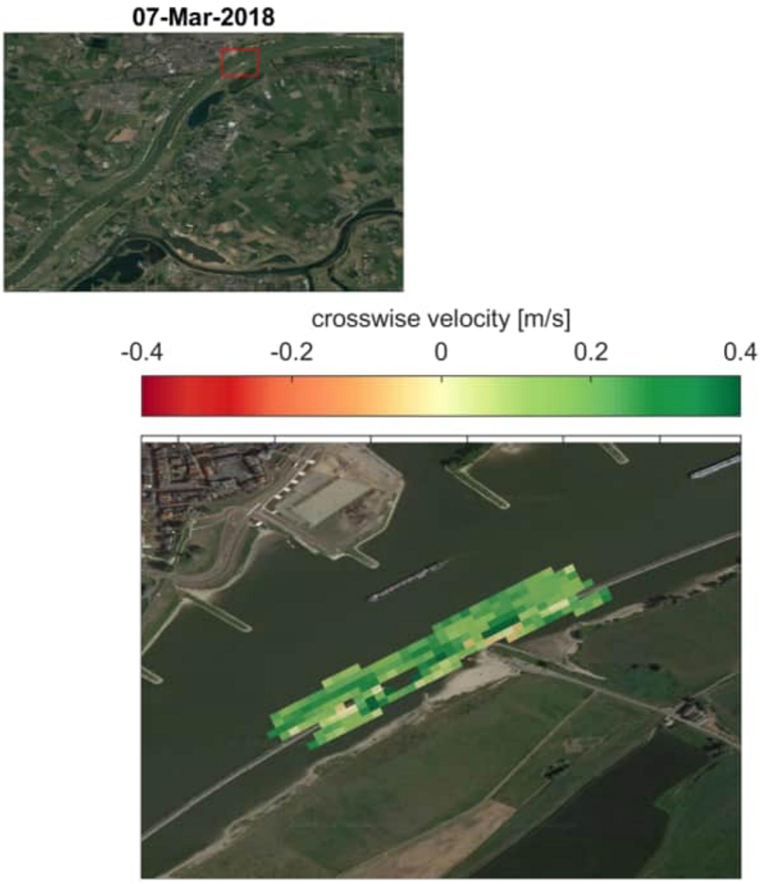

Figure D.215 Depth-averaged velocity field considering the full water column on 07-03-18 (discharge at Lobith at 12:00 equal to 1929 m^3/s).

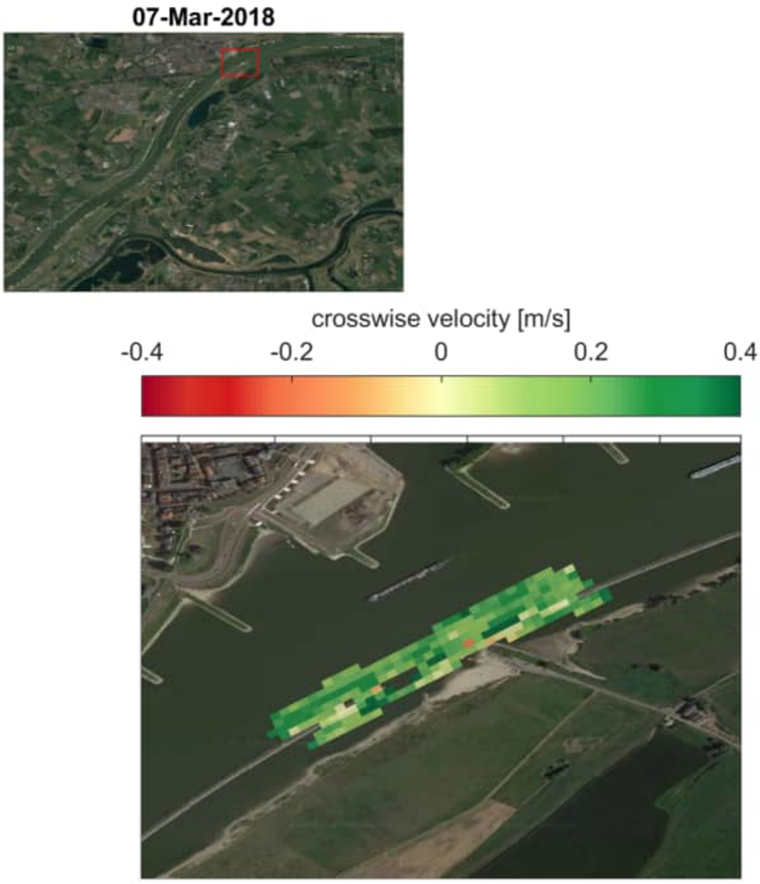

Figure D.216 Depth-averaged velocity field considering the top 2 m on 07-03-18 (discharge at Lobith at 12:00 equal to 1929 m^3/s).

D.5.5.16 20-07-18

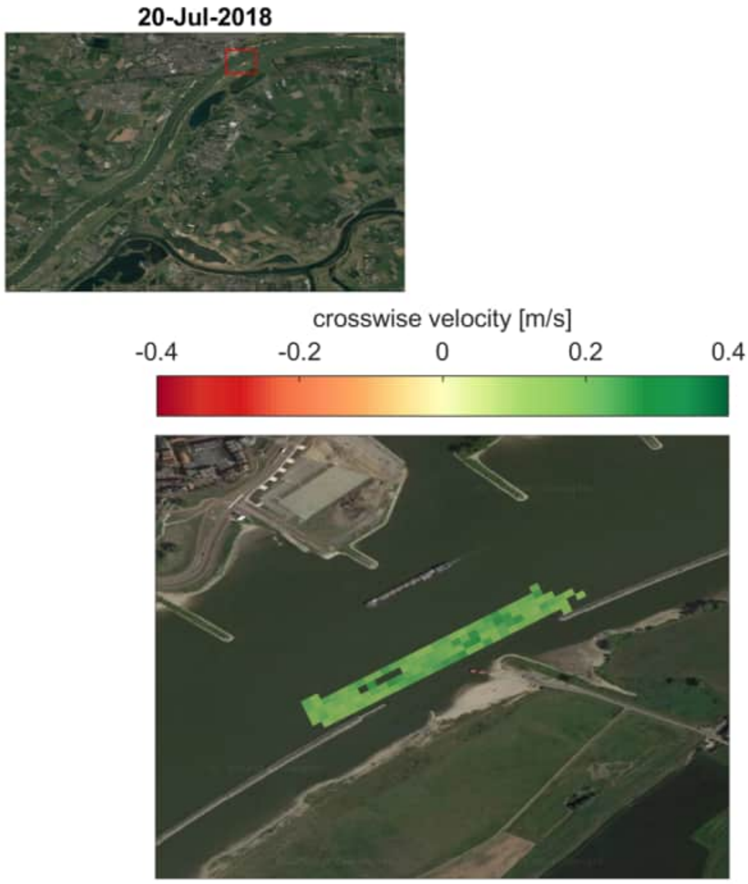

Figure D.217 Depth-averaged velocity field considering the full water column on 20-07-18 (discharge at Lobith at 12:00 equal to 1092 m^3/s).

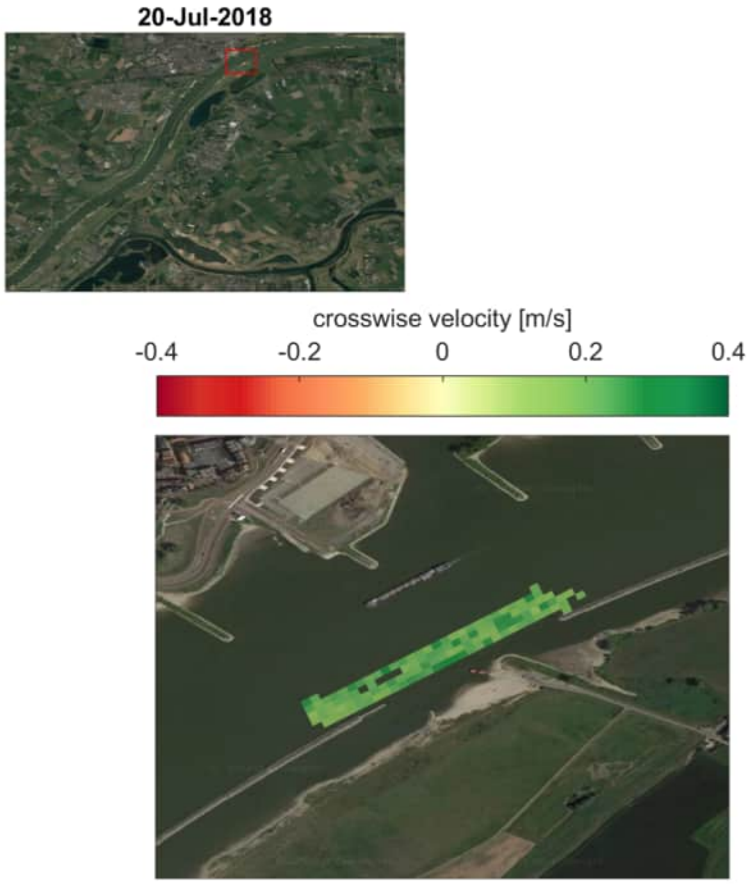

Figure D.218 Depth-averaged velocity field considering the top 2 m on 20-07-18 (discharge at Lobith at 12:00 equal to 1092 m^3/s).

D.6 Discharge partitioning between auxiliary channel and main channel

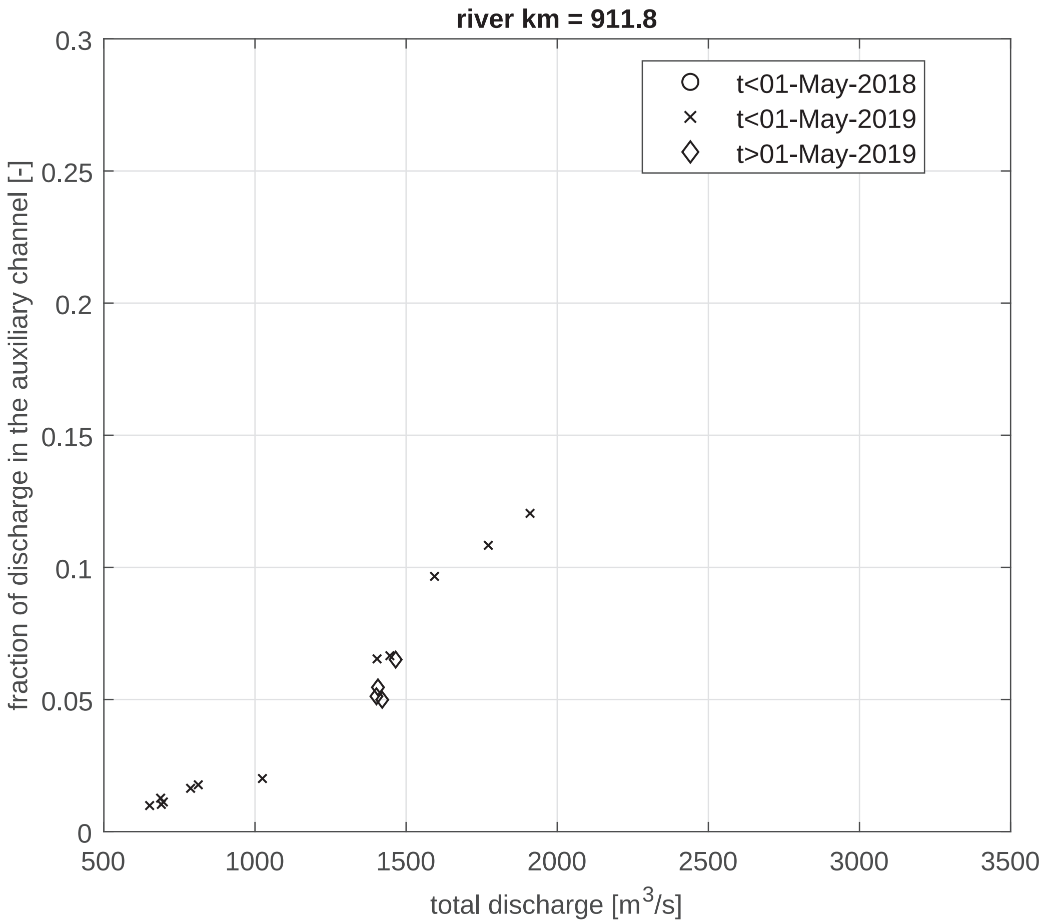

Figure D.219 Fraction of discharge in the auxiliary channel as a function of the total discharge for the measurements at river km 911.8

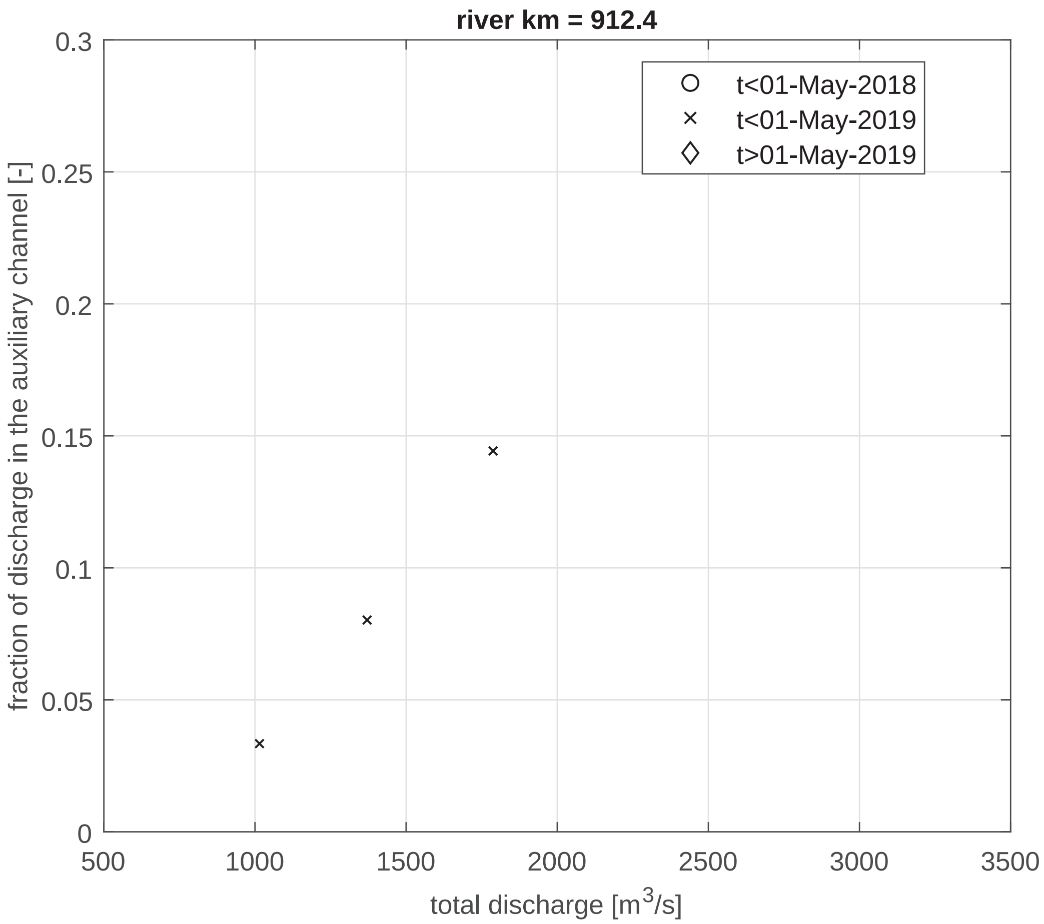

Figure D.220 Fraction of discharge in the auxiliary channel as a function of the total discharge for the measurements at river km 912.4

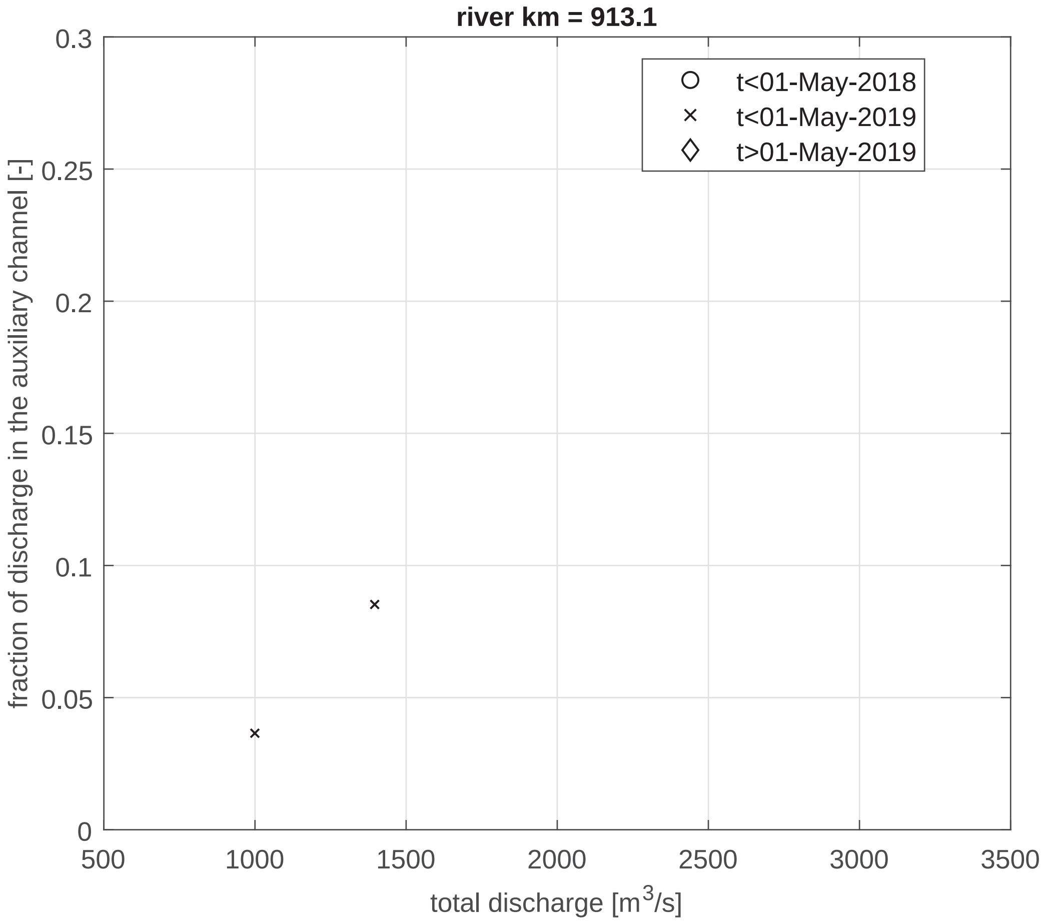

Figure D.221 Fraction of discharge in the auxiliary channel as a function of the total discharge for the measurements at river km 913.1

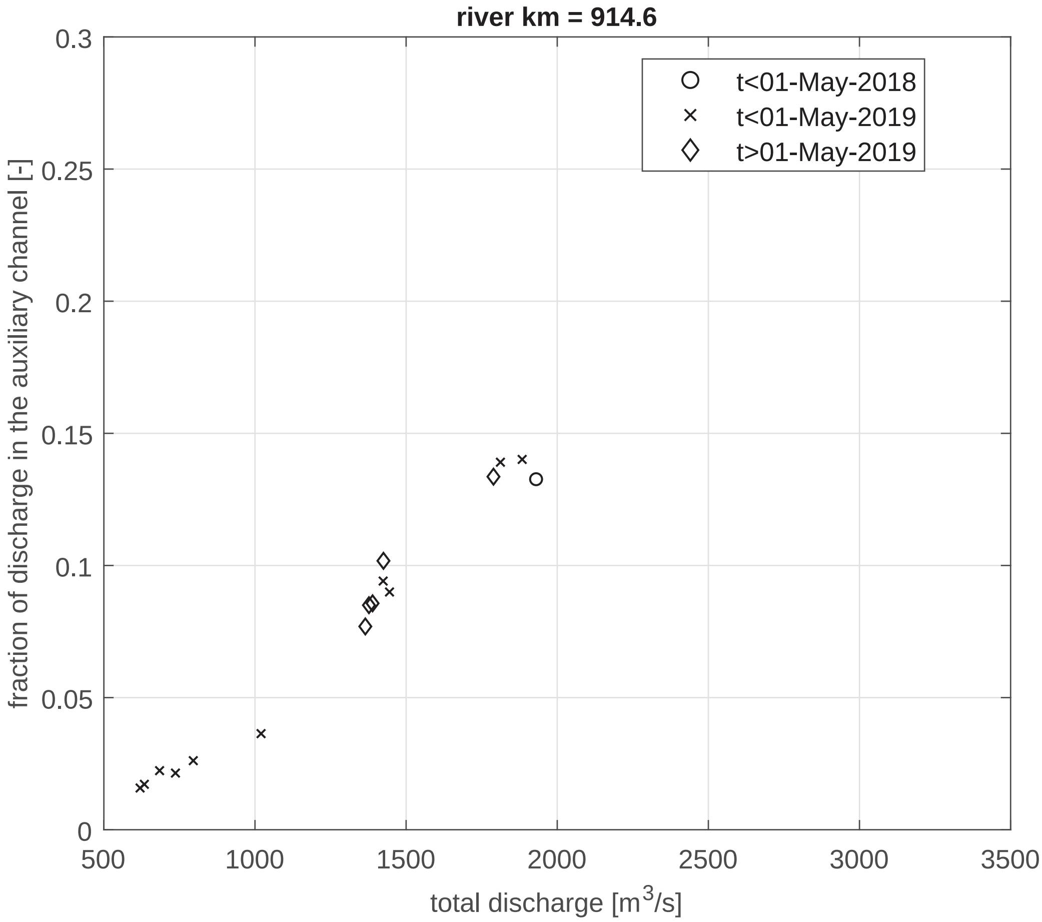

Figure D.222 Fraction of discharge in the auxiliary channel as a function of the total discharge for the measurements at river km 914.6

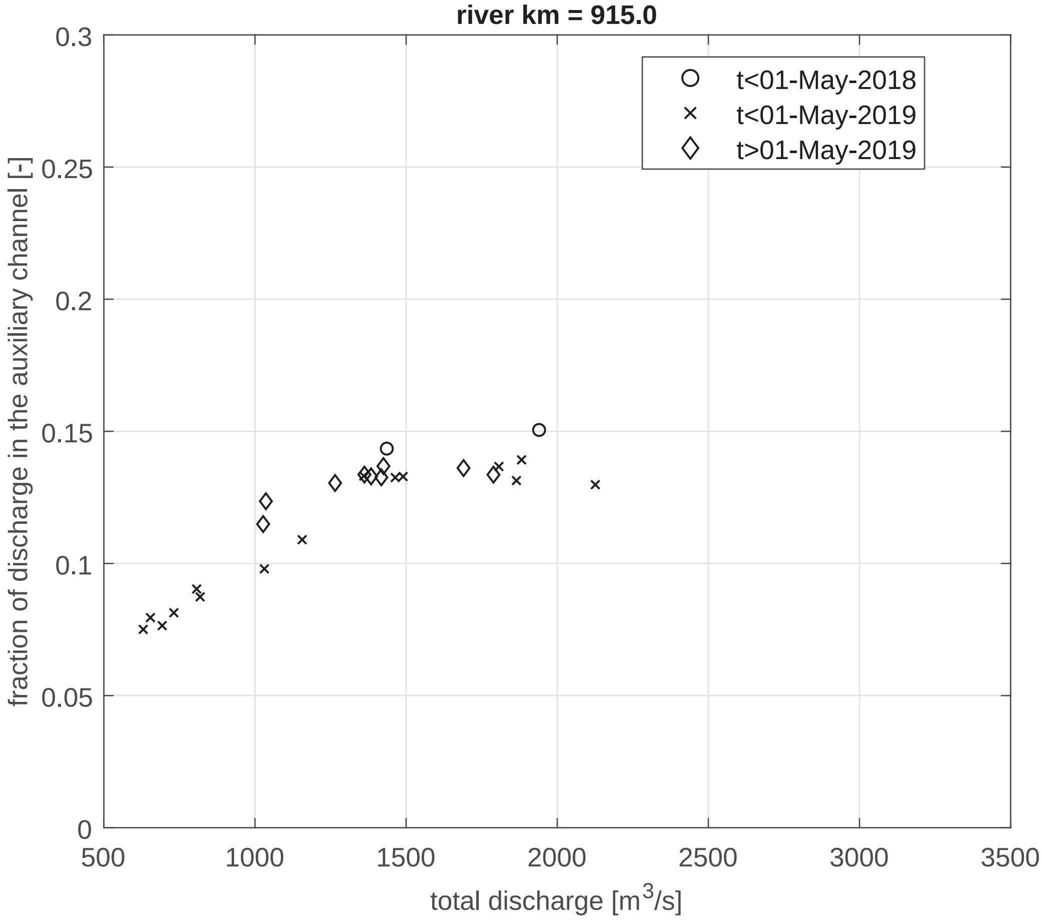

Figure D.223 Fraction of discharge in the auxiliary channel as a function of the total discharge for the measurements at river km 915.0

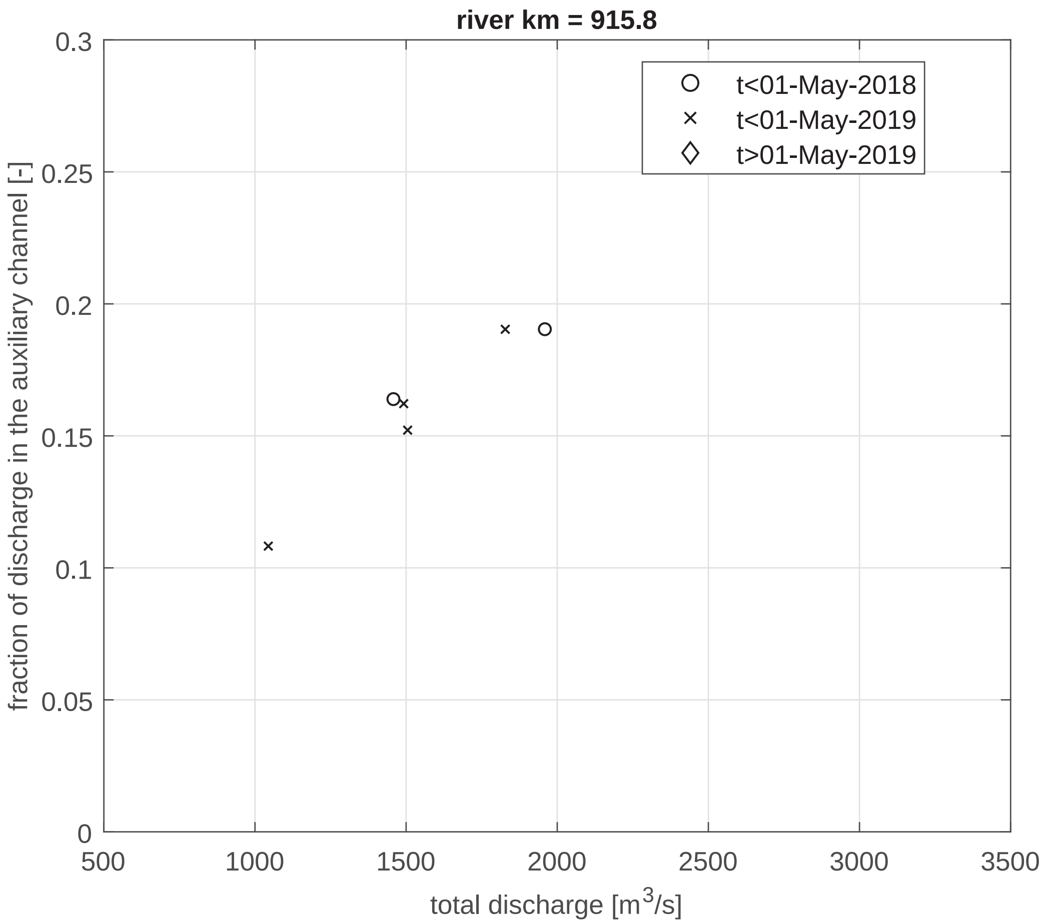

Figure D.224 Fraction of discharge in the auxiliary channel as a function of the total discharge for the measurements at river km 915.8

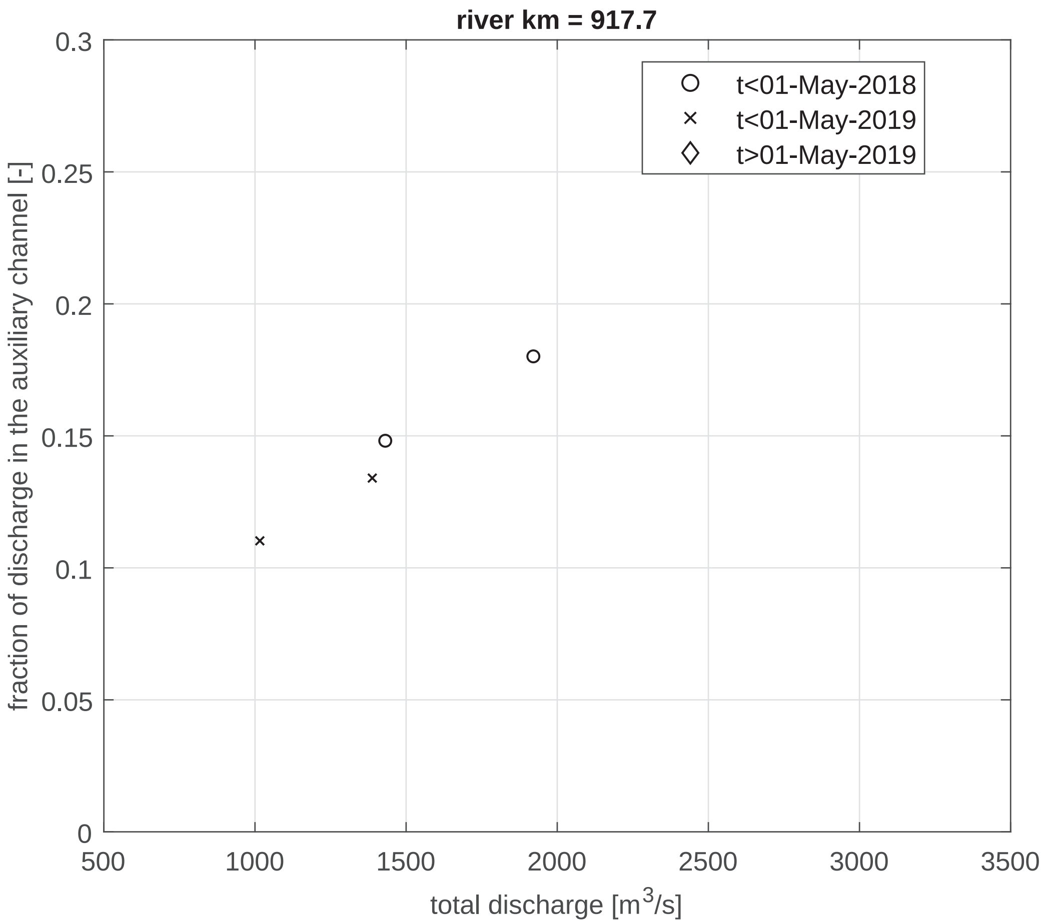

Figure D.225 Fraction of discharge in the auxiliary channel as a function of the total discharge for the measurements at river km 917.7

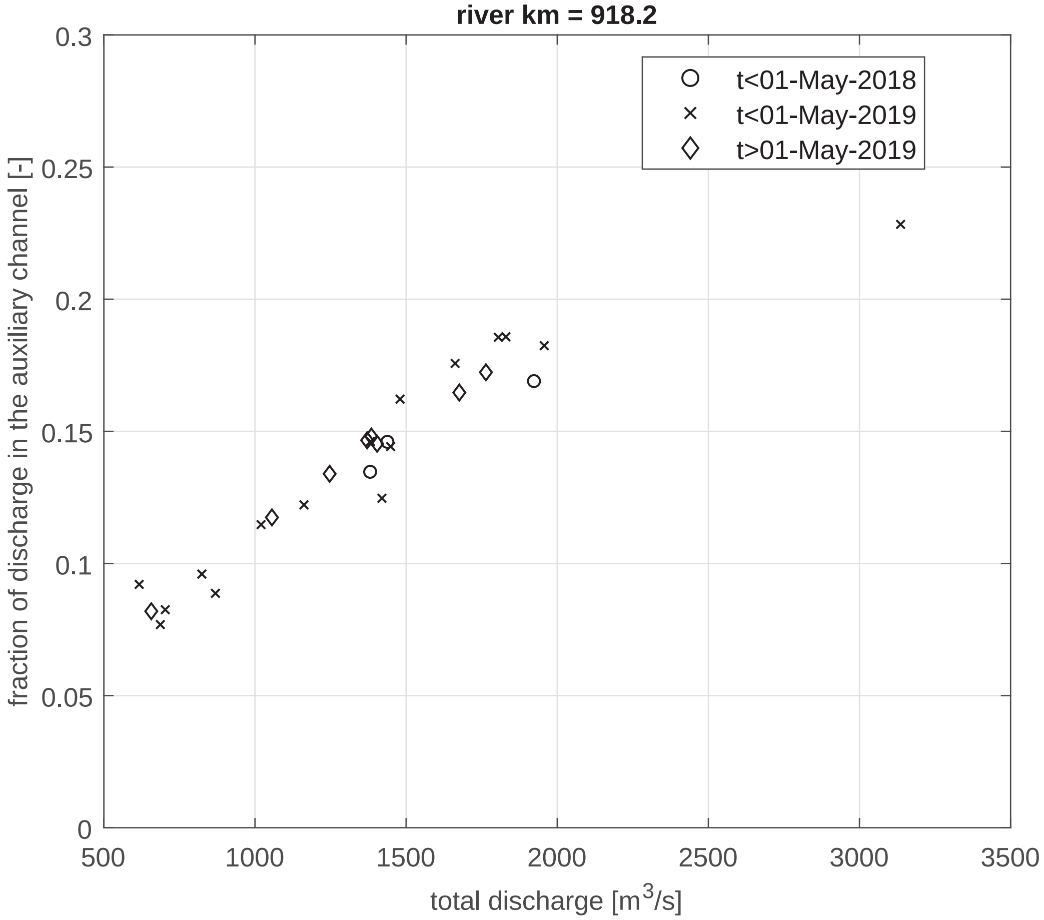

Figure D.226 Fraction of discharge in the auxiliary channel as a function of the total discharge for the measurements at river km 918.2

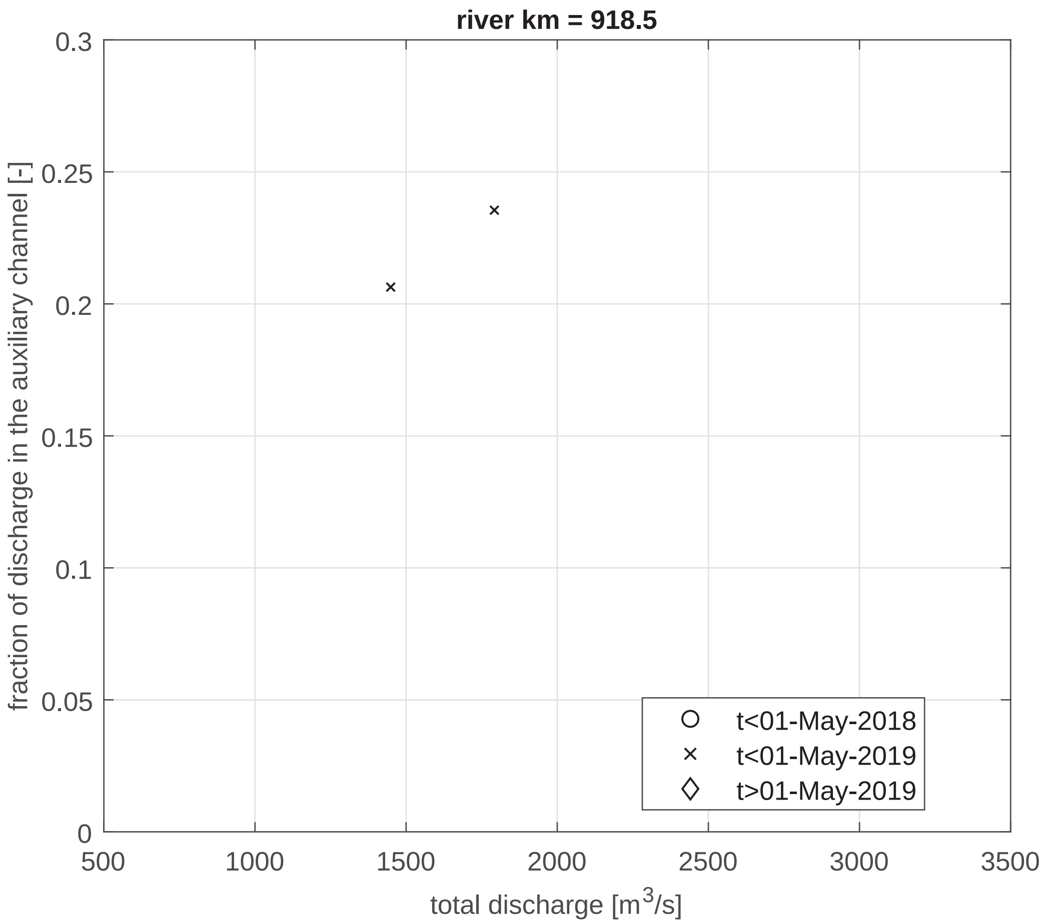

Figure D.227 Fraction of discharge in the auxiliary channel as a function of the total discharge for the measurements at river km 918.5

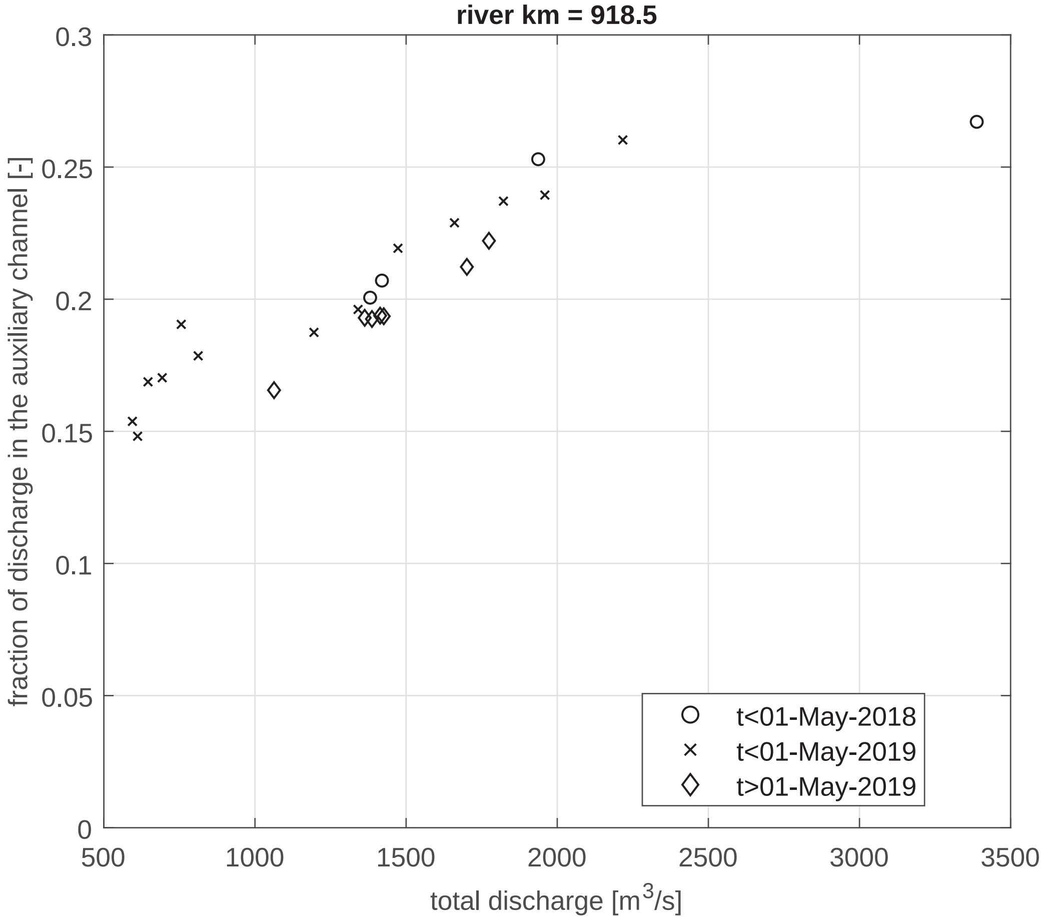

Figure D.228 Fraction of discharge in the auxiliary channel as a function of the total discharge for the measurements at river km 918.5

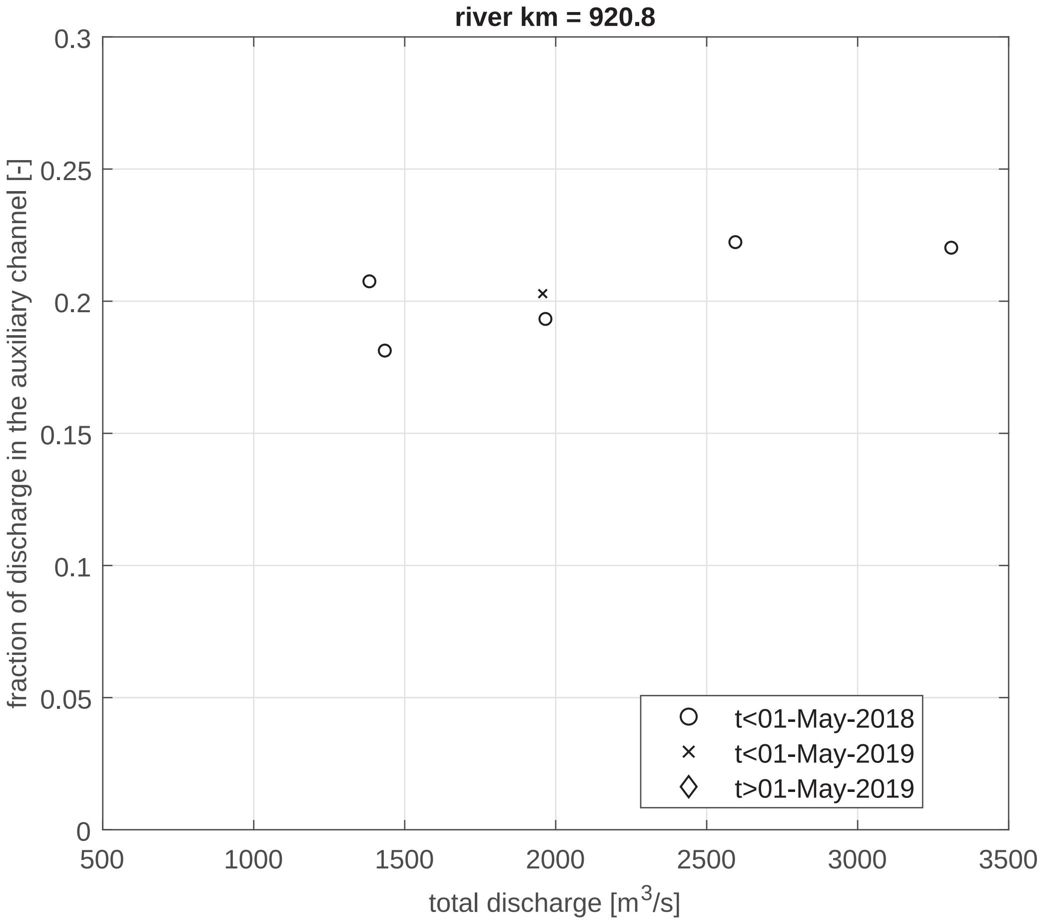

Figure D.229 Fraction of discharge in the auxiliary channel as a function of the total discharge for the measurements at river km 920.8

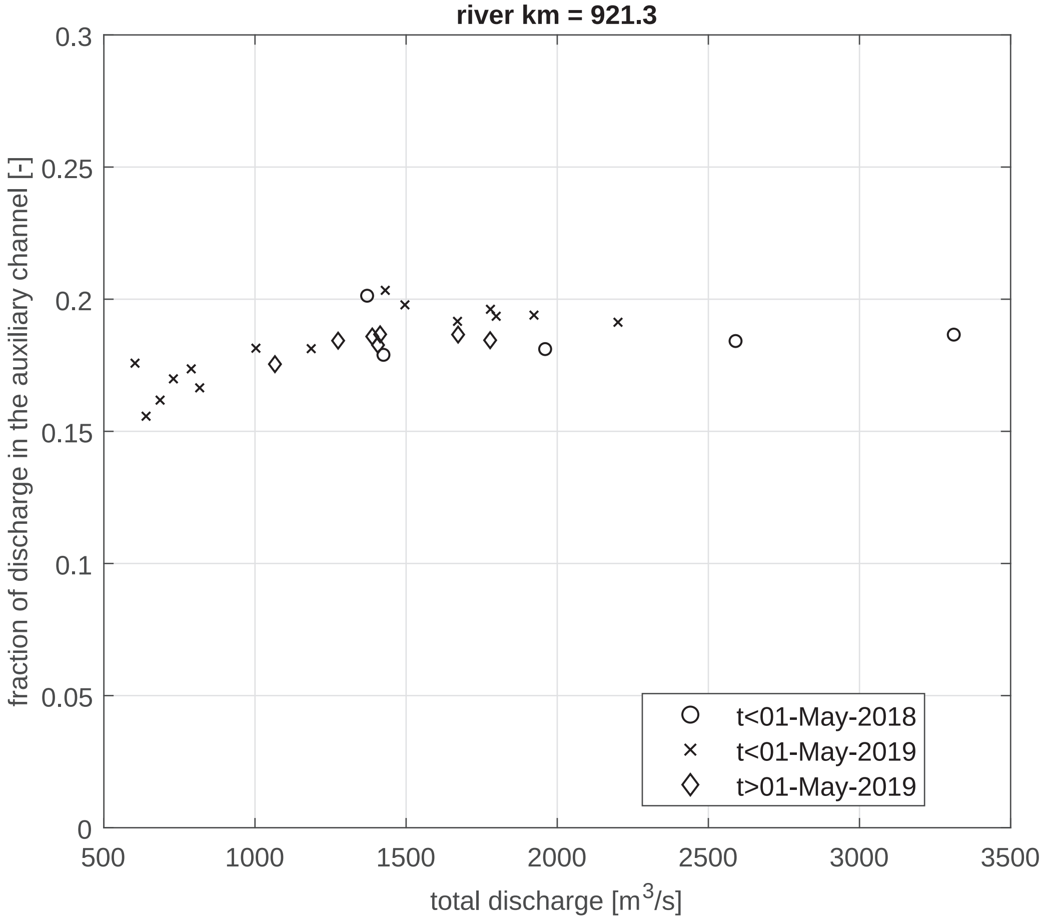

Figure D.230 Fraction of discharge in the auxiliary channel as a function of the total discharge for the measurements at river km 921.3

E Bed level

E.1 Pre-defined sections for bed level analyses

As specified by RWS several polygons are generated for the bed level analyses. The figures below show the extend of the different type of polygons.

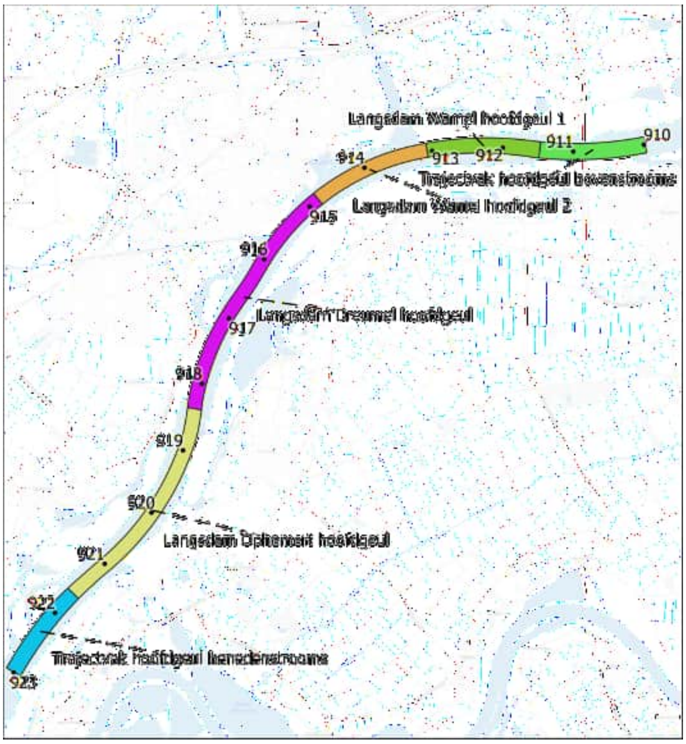

Figure E.1 Polygons as used in bed level analyses (part 1/4).

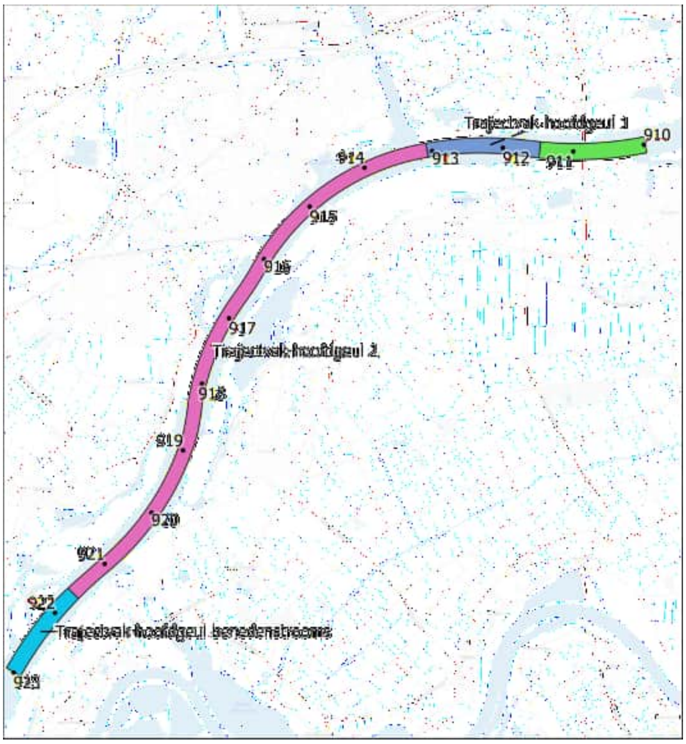

Figure E.2 Polygons as used in bed level analyses (part 2/4).

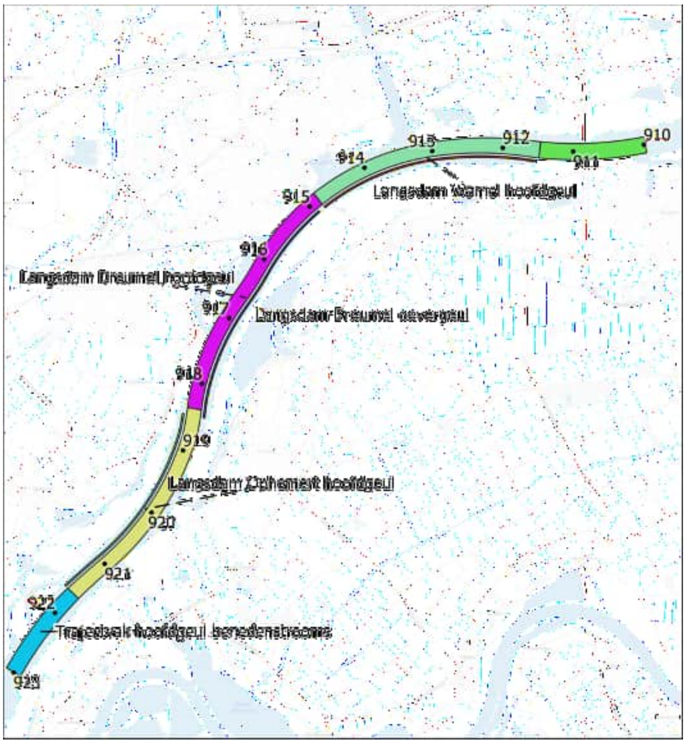

Figure E.3 Polygons as used in bed level analyses (part 3/4).

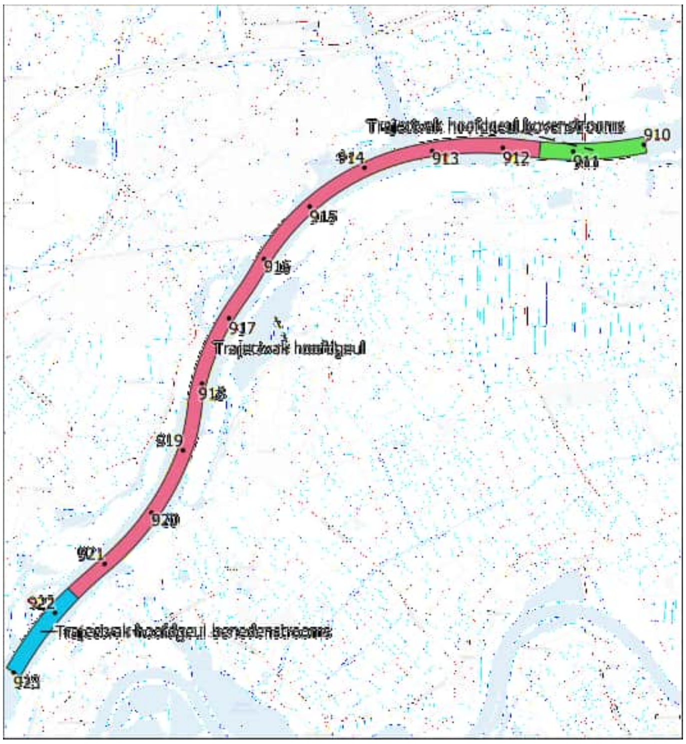

Figure E.4 Polygons as used in bed level analyses (part 4/4).

E.2 Comparison to the findings of Czapiga *et al.* (2021)

To check the results, the averaging approach was also compared to the work of Czapiga *et al.* (2021). Figure E.5 shows that the trends in the bed level in the current study and in Czapiga *et al.* (2021) are the same.

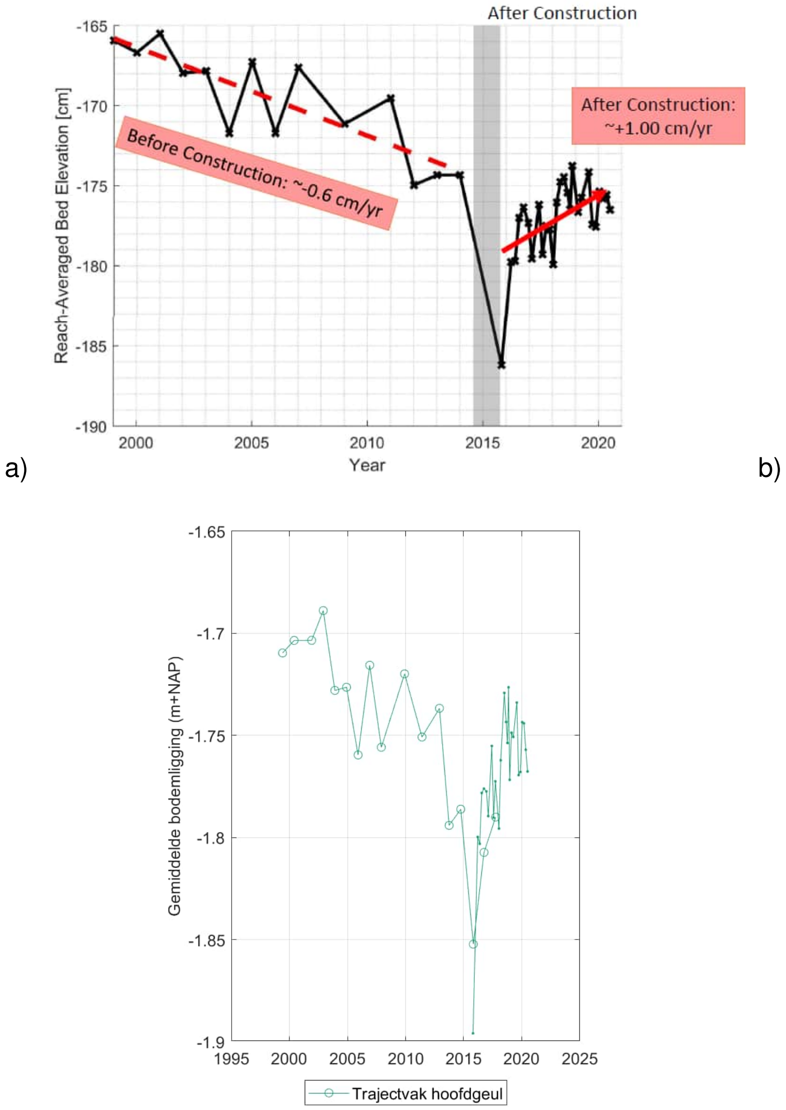

Figure E.5 Reach averaged bed level from a) Czapiga *et al.* (2021) and b) this study

Figure E.6 and Figure E.7 show the response of the river initially after construction and after adjustment of the sill levels, respectively. The results are in line with the observations in Figure 4.13 and Figure 4.14.

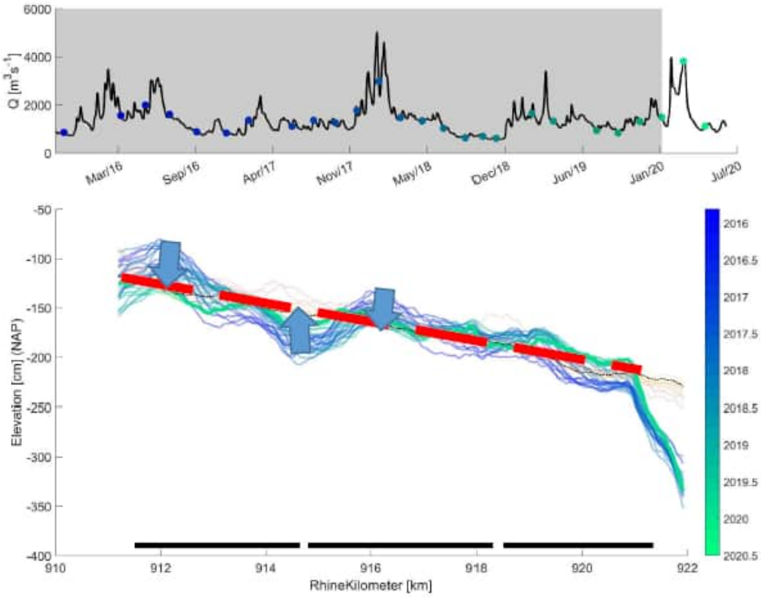

Figure E.6 Bed level over time from Czapiga *et al.* (2021) before April 2018 showing the initial response to the longitudinal training wall

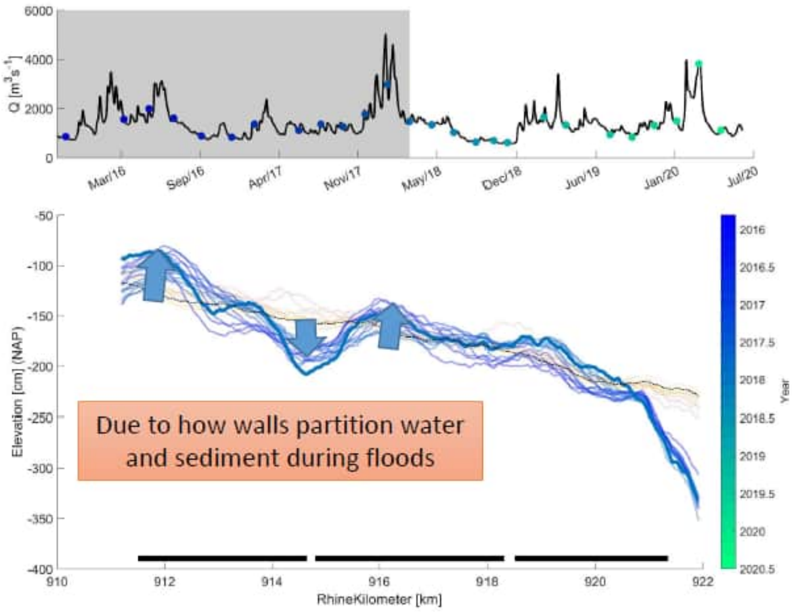

Figure E.7 Bed level over time from Czapiga *et al.* (2021) after April 2018 showing the effect of the adjustment of the sill level.

E.3 Development in main channel for different reaches

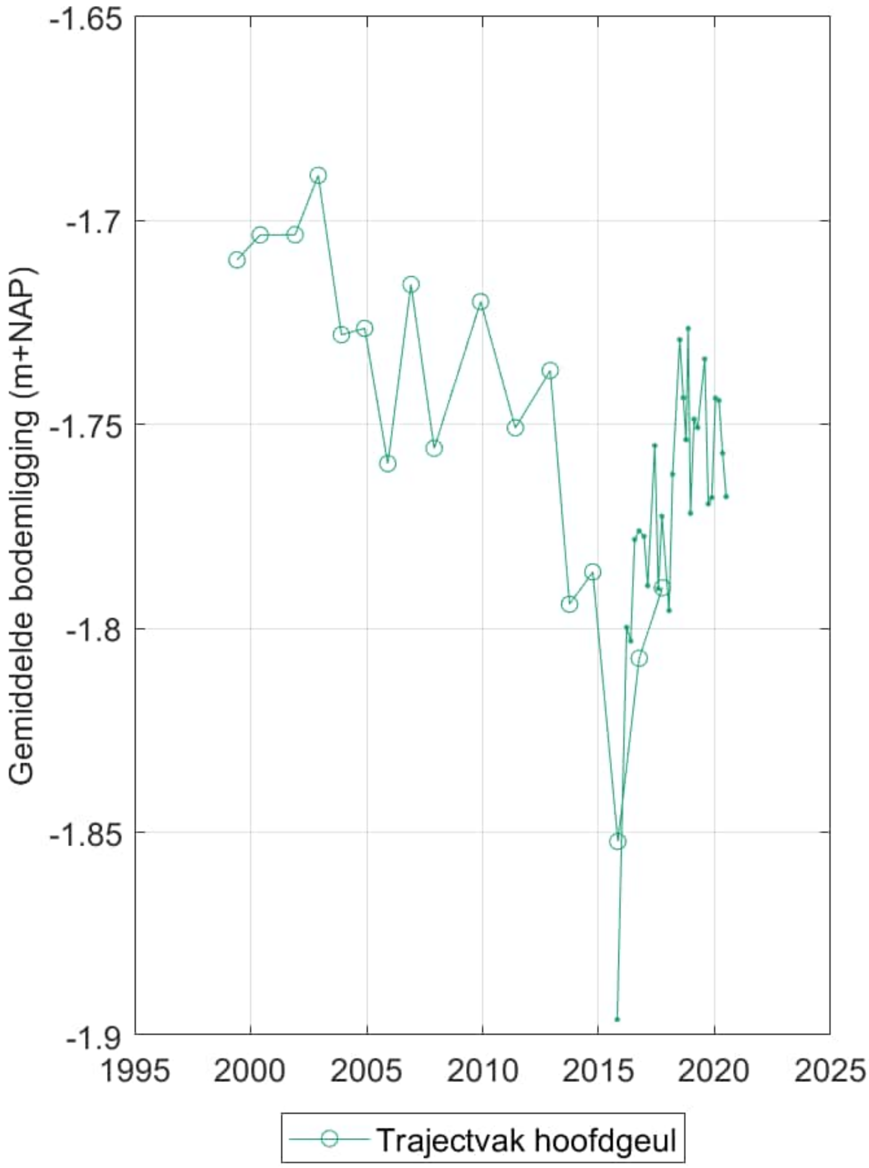

Figure E.8 Average bed level in the main channel in the reach of the LTW (see figure E.4).

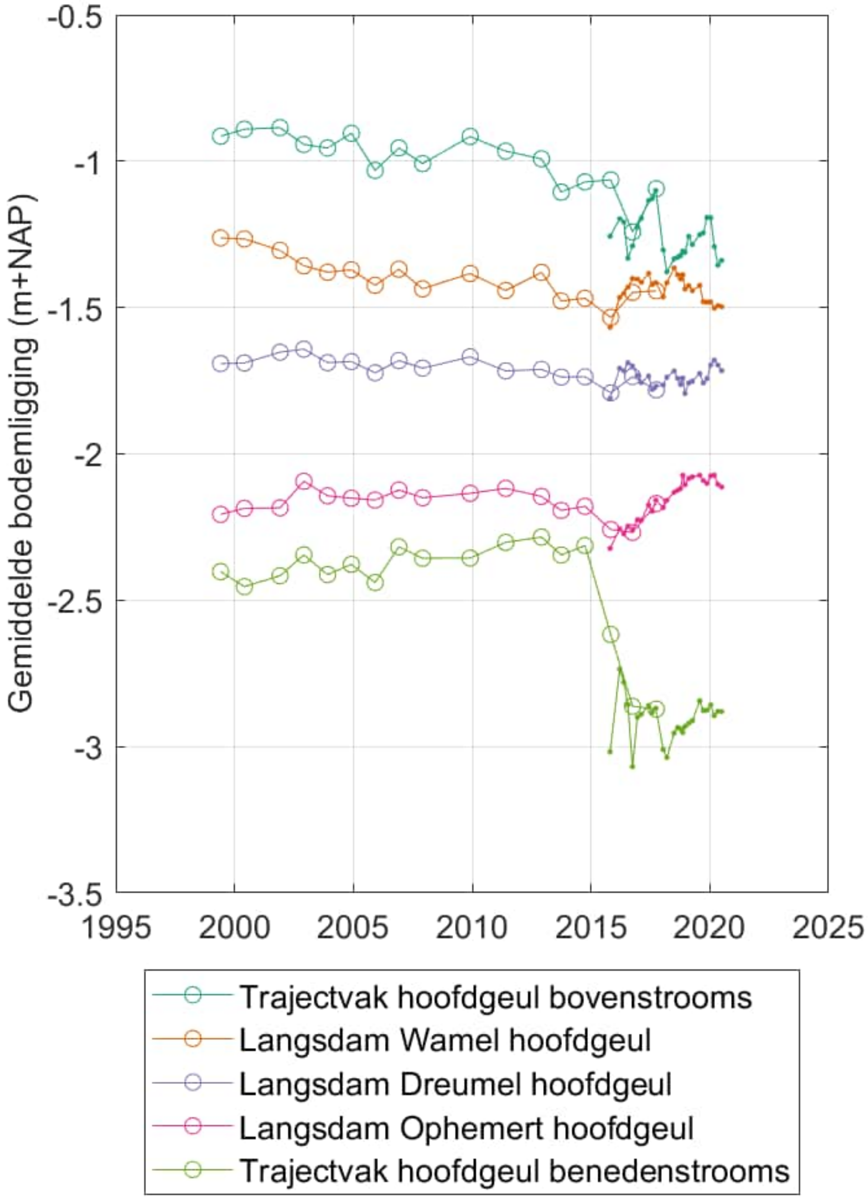

Figure E.9 Average bed level in the main channel for reaches at each LTW (see figure E.3).

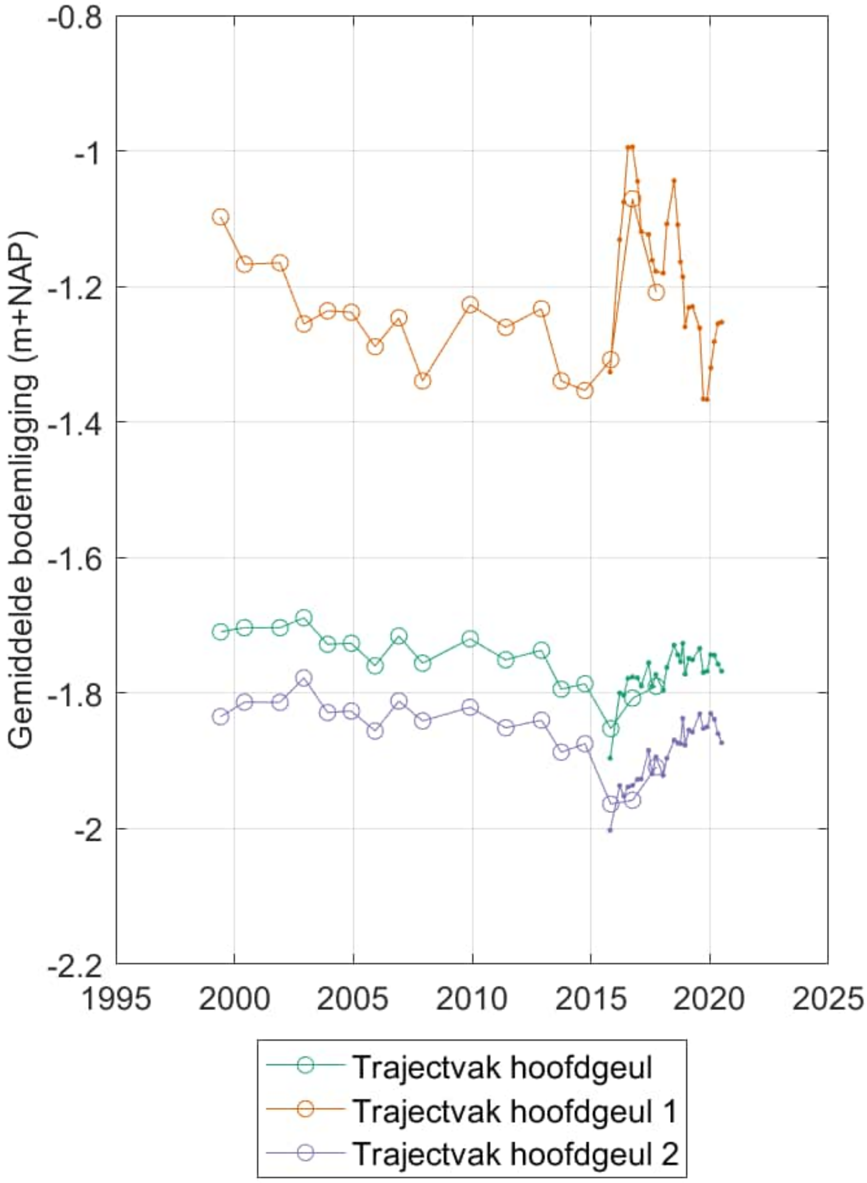

Figure E.10 Average bed level in the main channel in the reach of the LTW. And for the main channel split at the Amsterdam-Rijnkanaal (see figure E.2).

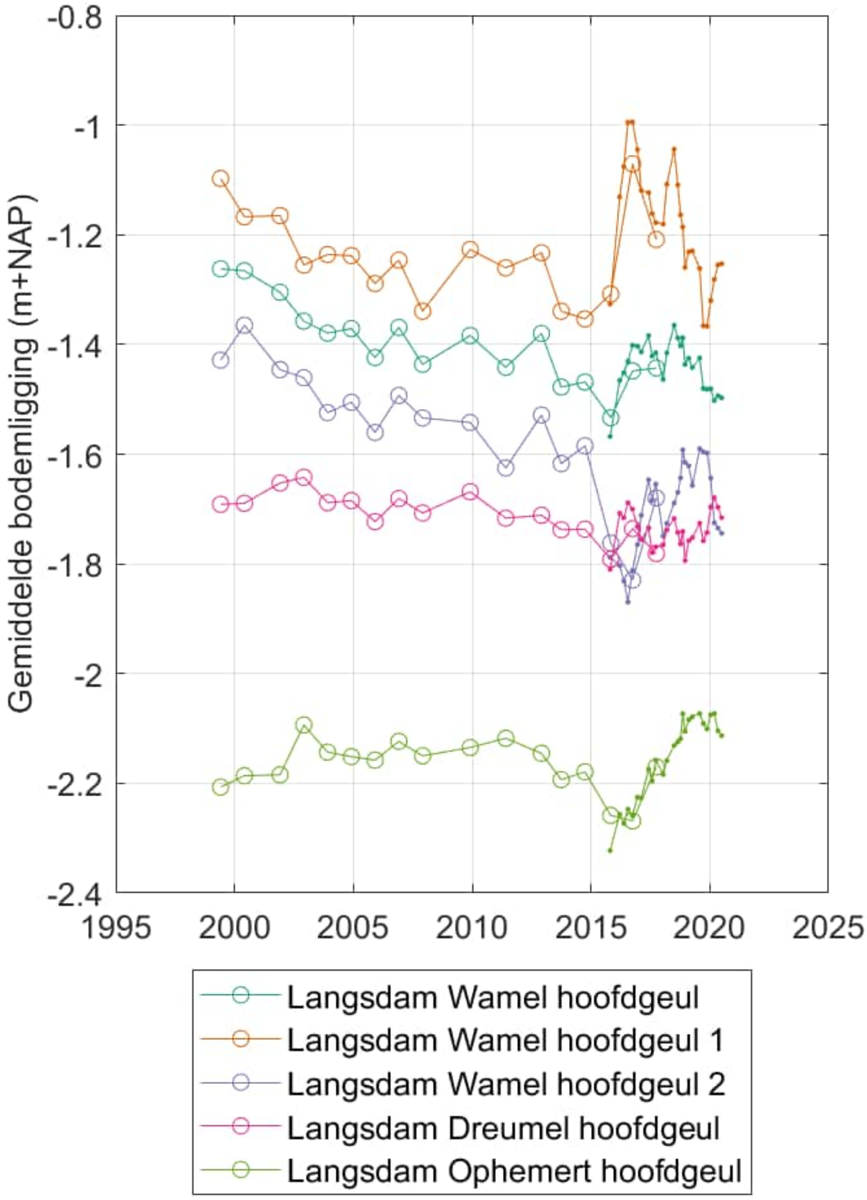

Figure E.11 Average bed level in the main channel for reaches at each LTW, where Wamel is also included as split at the Amsterdam-Rijnkanaal (see figure E.1).

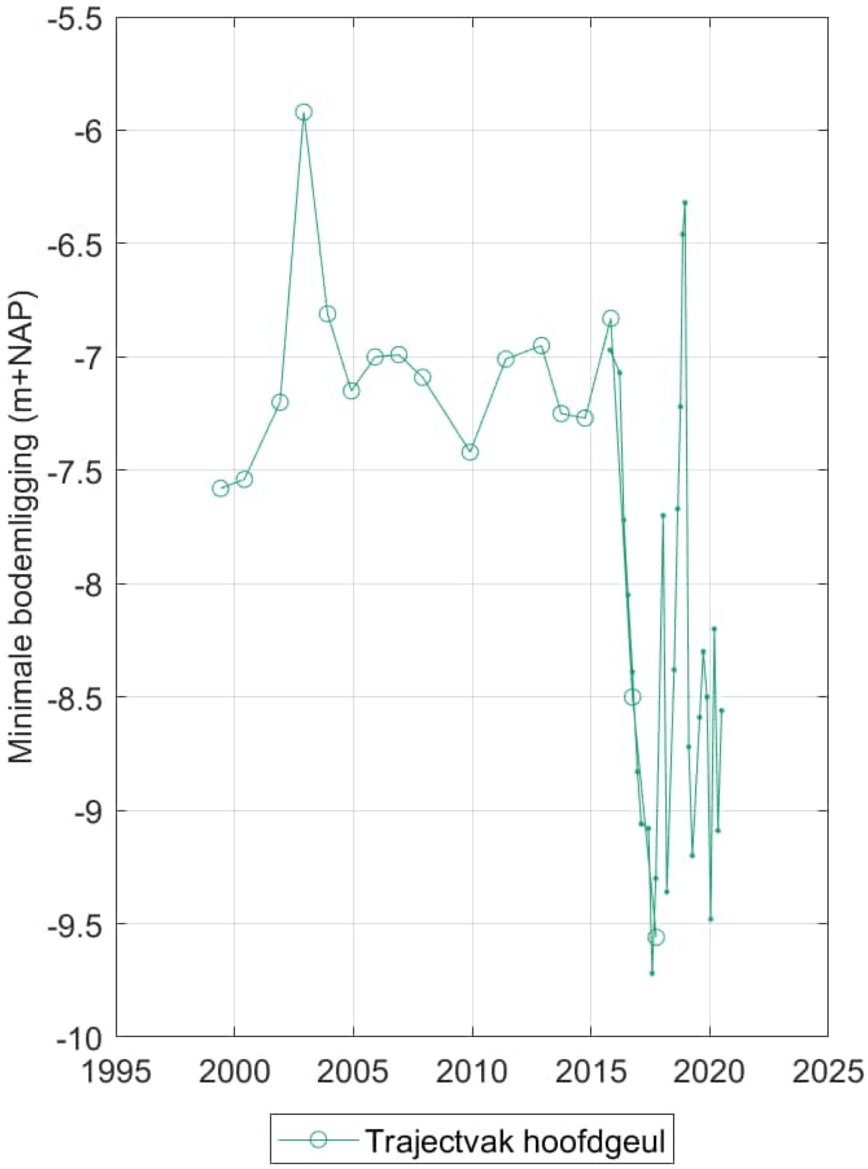

Figure E.12 Minimum bed level in the main channel in the reach of the LTW (see figure E.4).

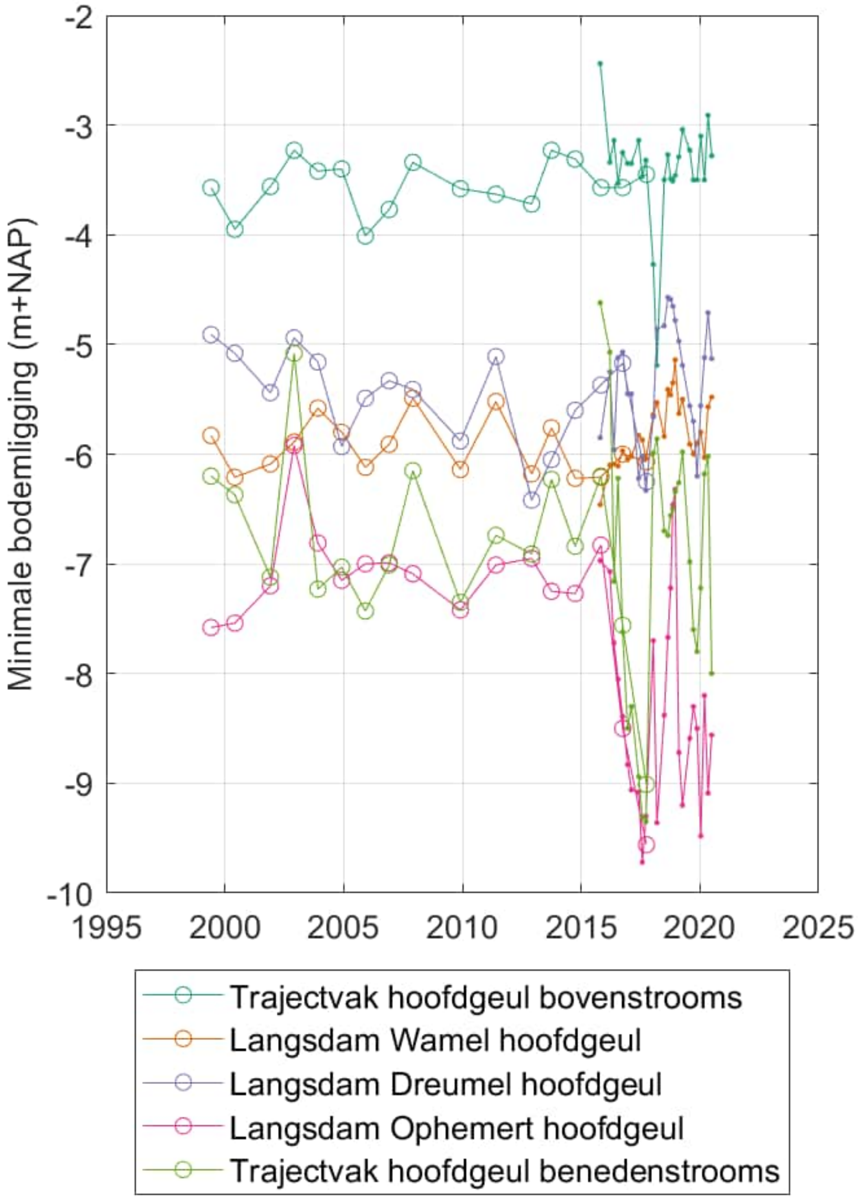

Figure E.13 Minimum bed level in the main channel for reaches at each LTW (see figure E.3).

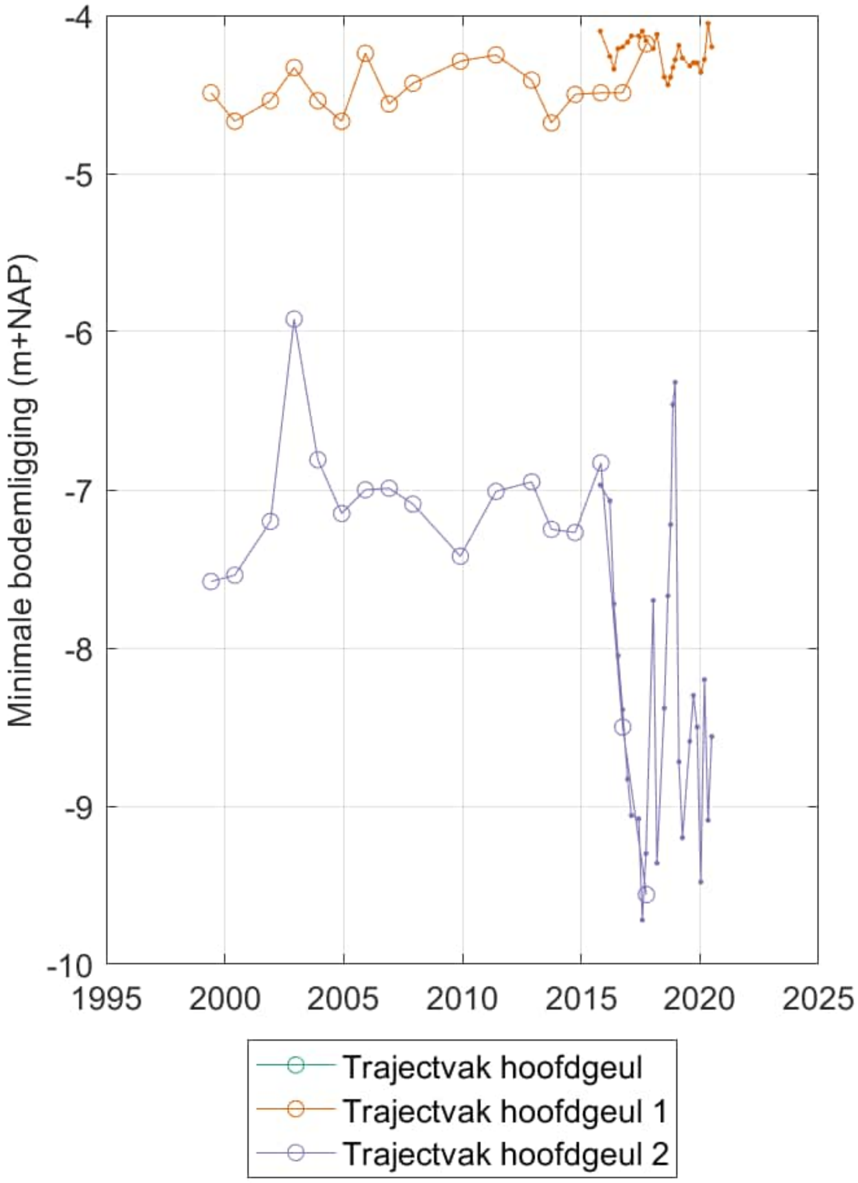

Figure E.14 Minimum bed level in the main channel in the reach of the LTW. And for the main channel split at the Amsterdam-Rijnkanaal (see figure E.2).

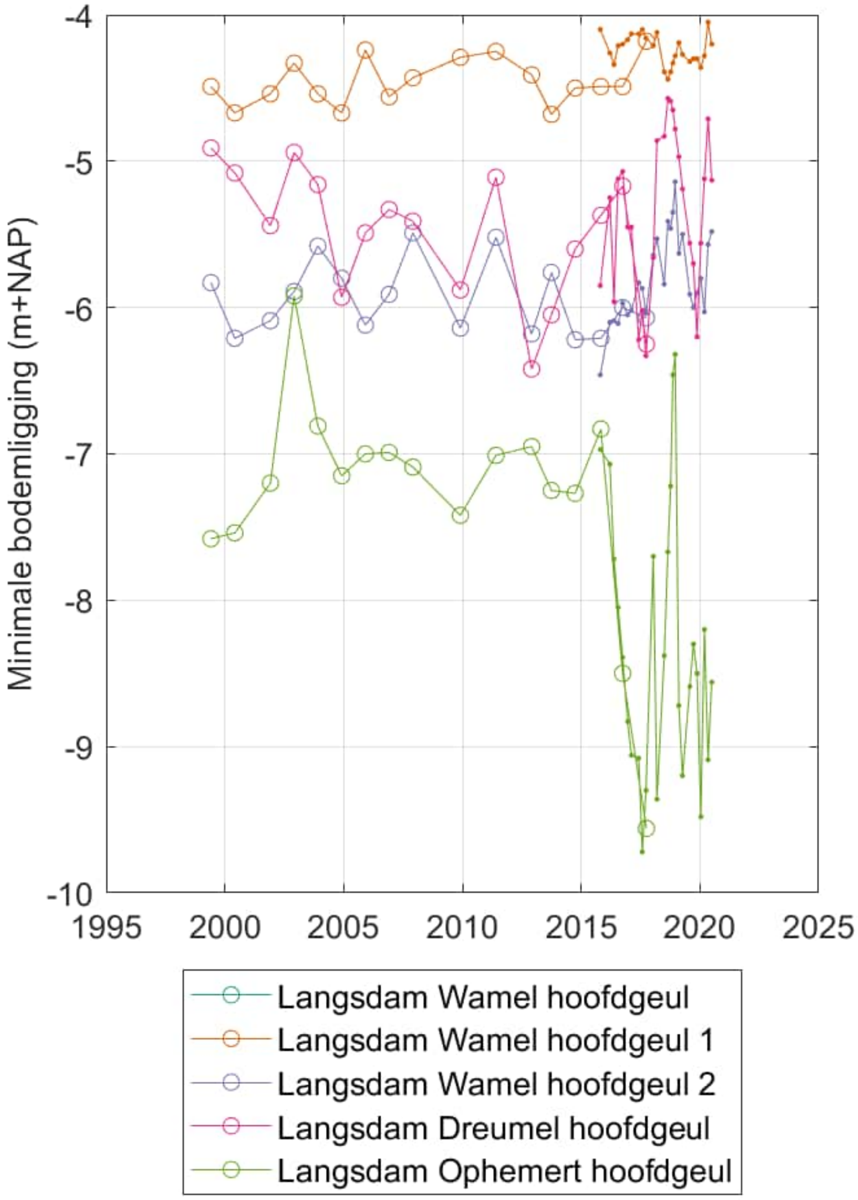

Figure E.15 Minimum bed level in the main channel for reaches at each LTW, where Wamel is also included as split at the Amsterdam-Rijnkanaal (see figure E.1).

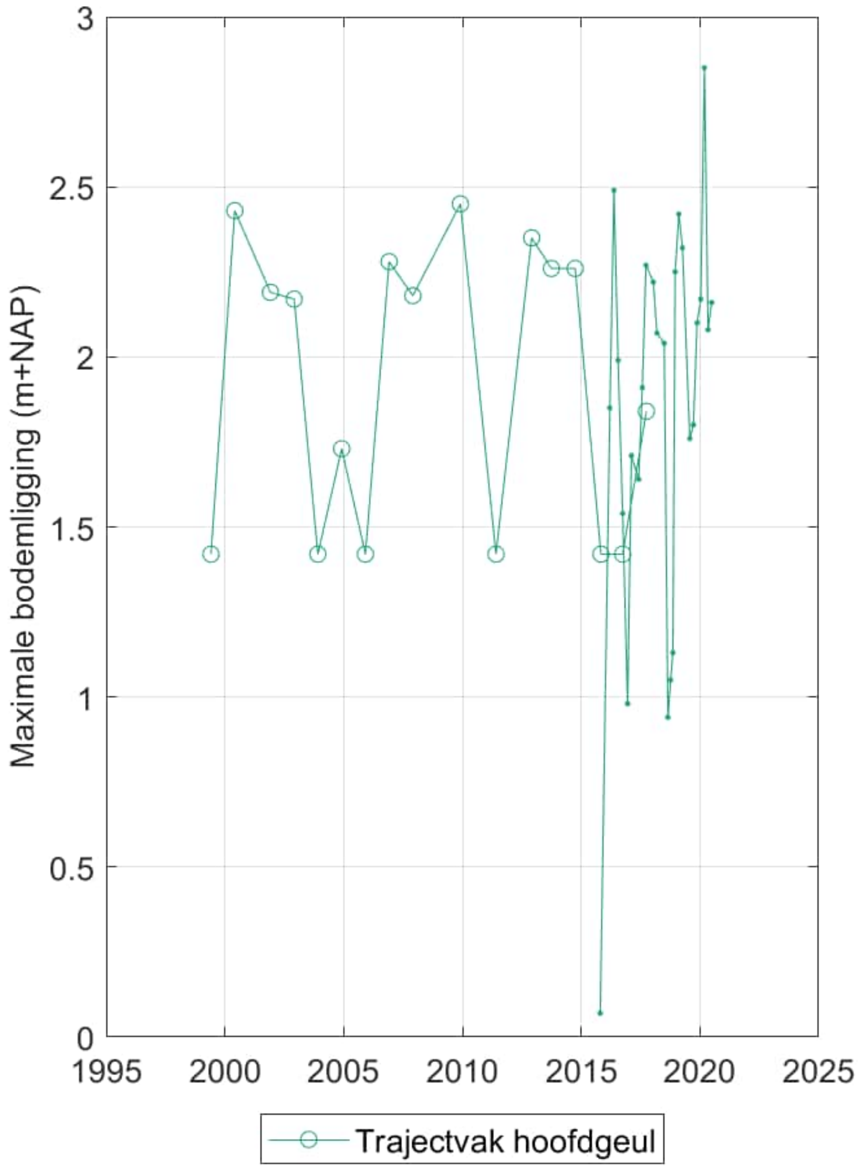

Figure E.16 Maximum bed level in the main channel in the reach of the LTW (see figure E.4).

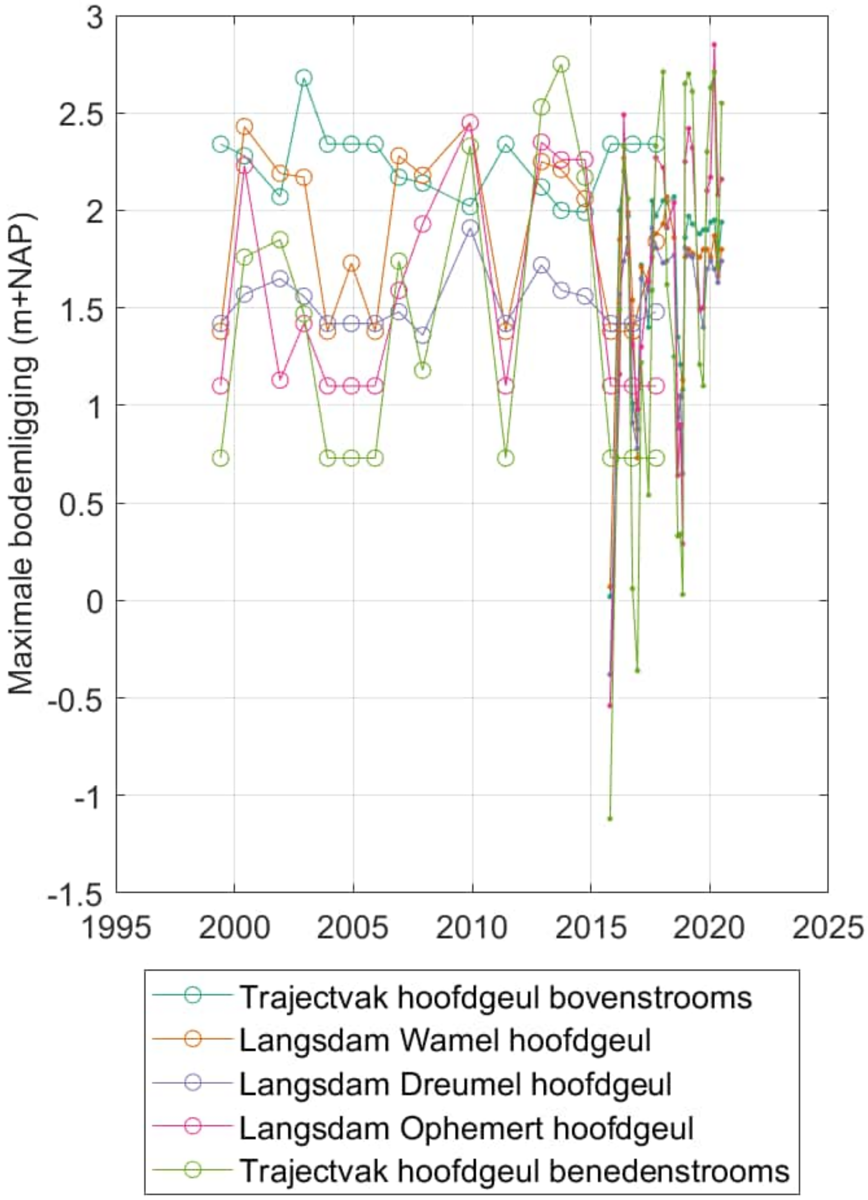

Figure E.17 Maximum bed level in the main channel for reaches at each LTW (see figure E.3).

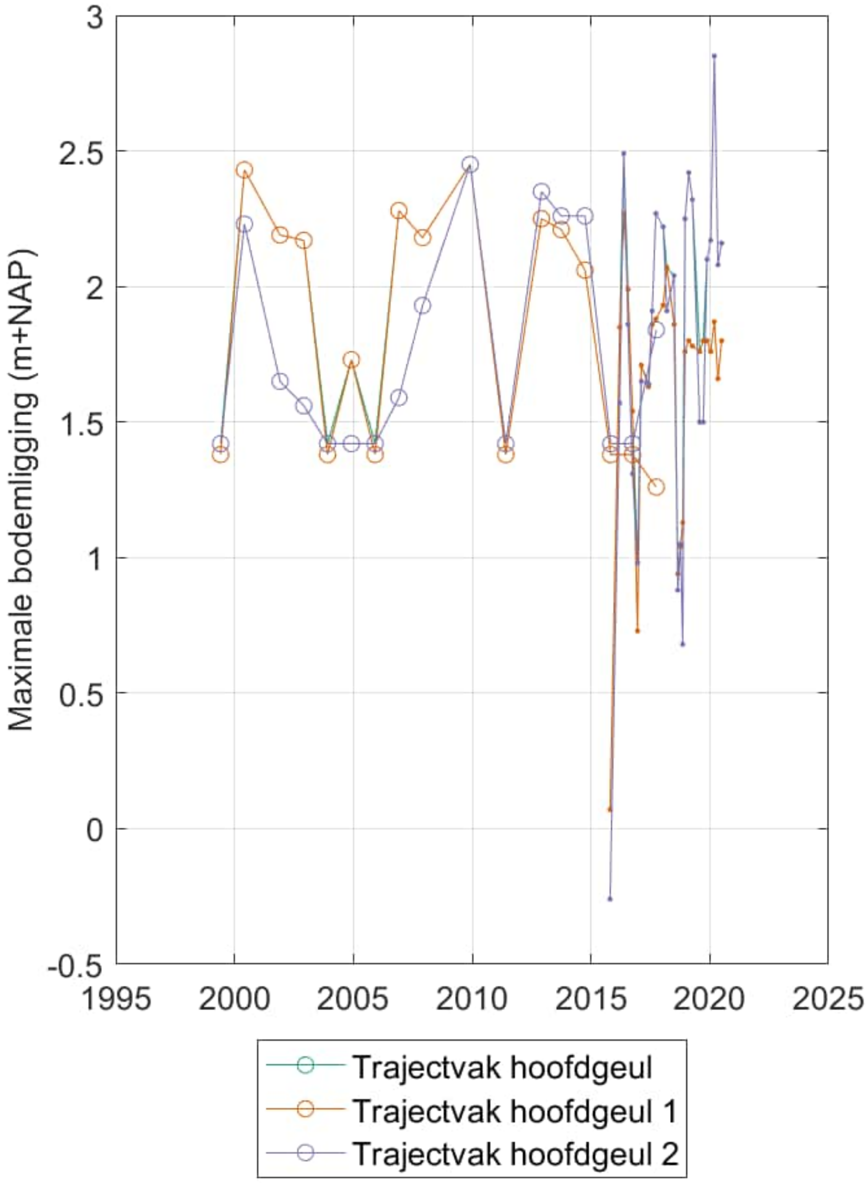

Figure E.18 Maximum bed level in the main channel in the reach of the LTW. And for the main channel split at the Amsterdam-Rijnkanaal (see figure E.2).

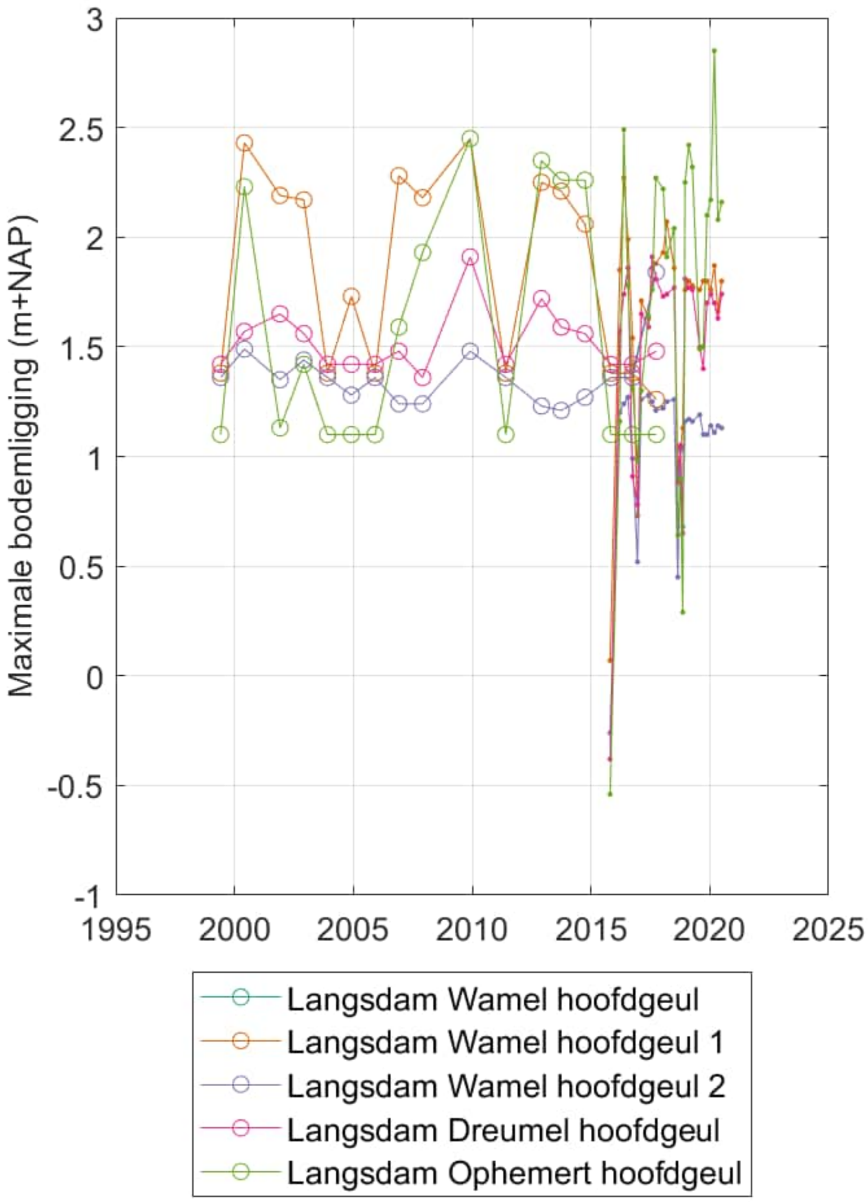

Figure E.19 Maximum bed level in the main channel for reaches at each LTW, where Wamel is also included as split at the Amsterdam-Rijnkanaal (see figure E.1).

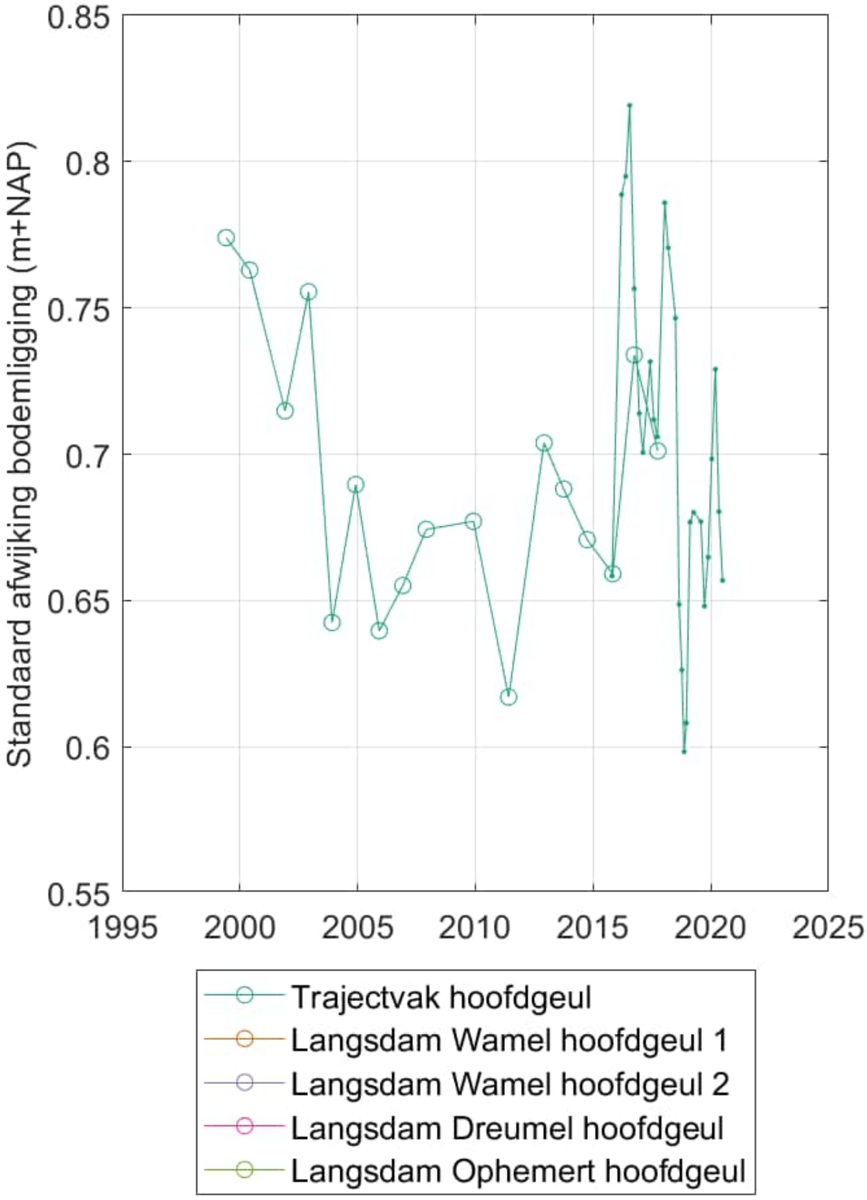

Figure E.20 Standard deviation bed level in the main channel in the reach of the LTW (see figure E.4).

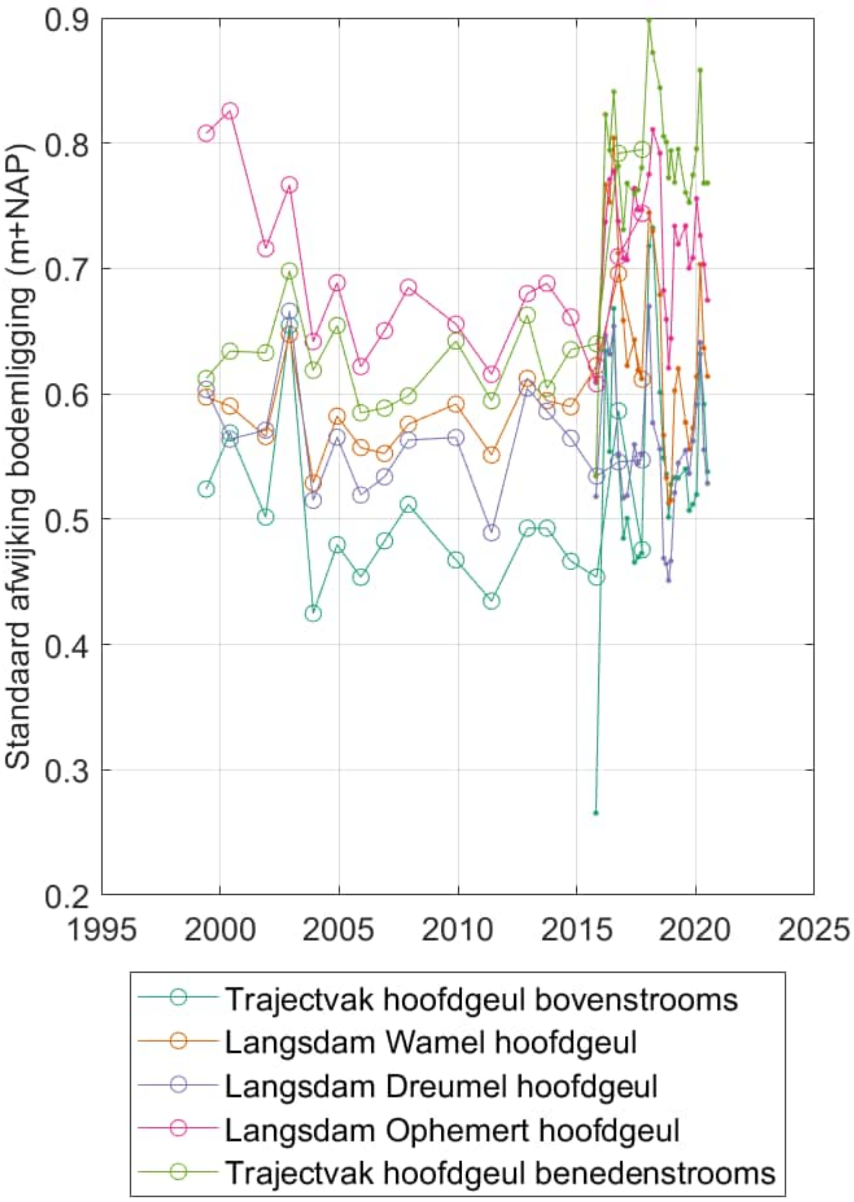

Figure E.21 Standard deviation bed level in the main channel for reaches at each LTW (see figure E.3).

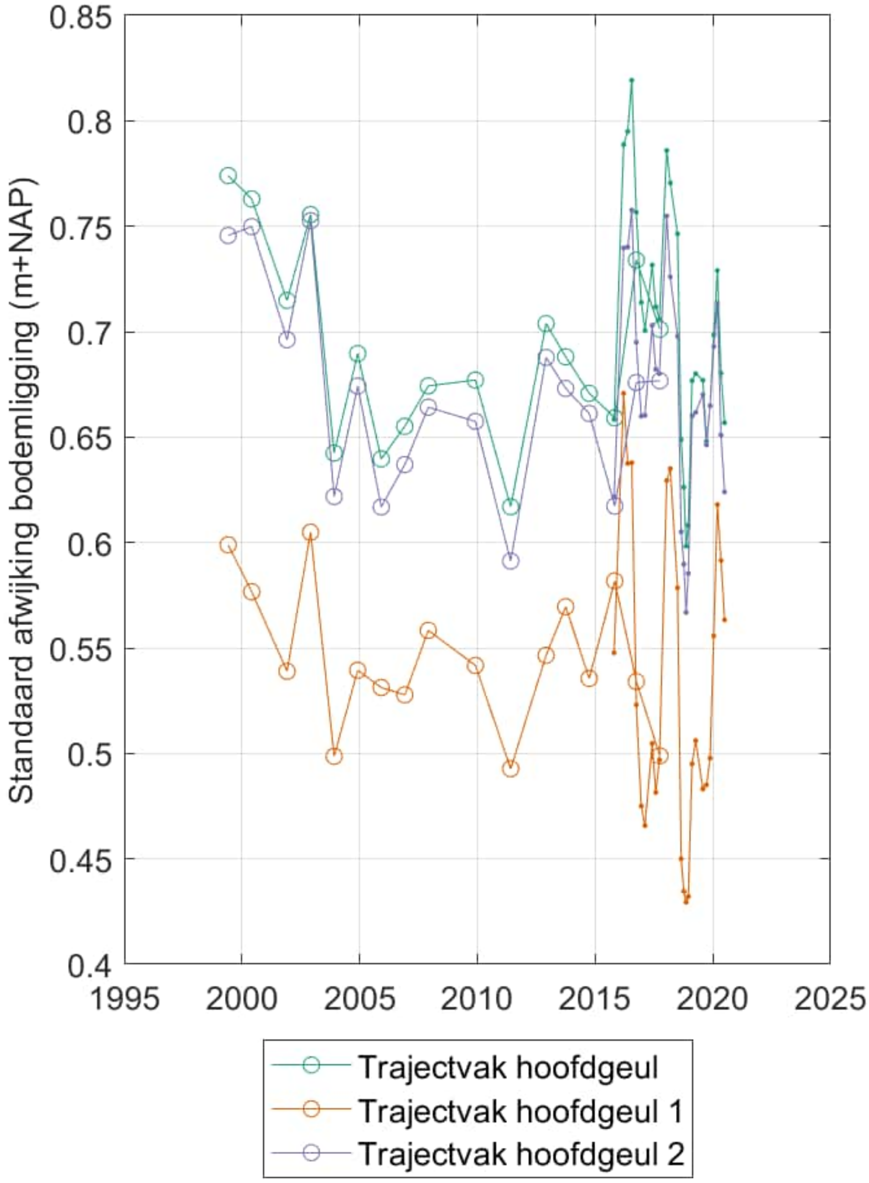

Figure E.22 Standard deviation bed level in the main channel in the reach of the LTW. And for the main channel split at the Amsterdam-Rijnkanaal (see figure E.2).

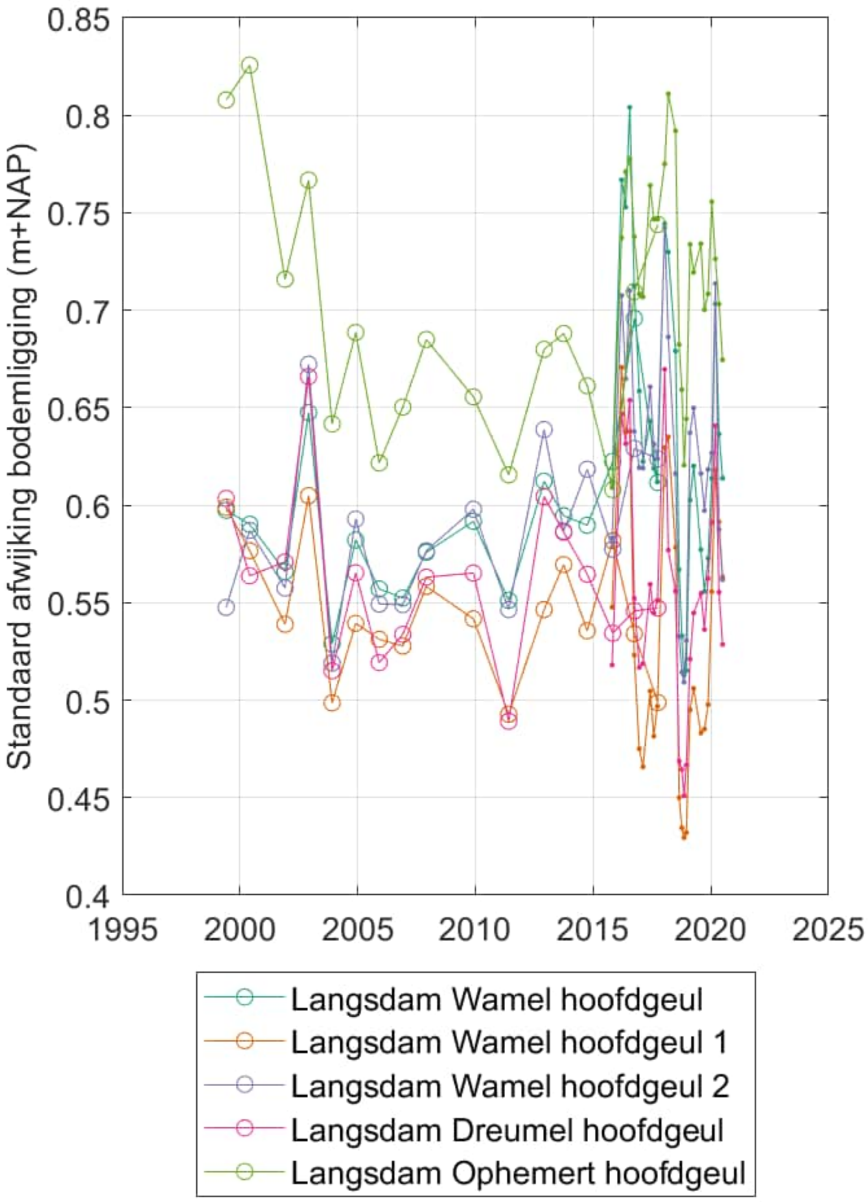

Figure E.23 Standard deviation bed level in the main channel for reaches at each LTW, where Wamel is also included as split at the Amsterdam-Rijnkanaal (see figure E.1).

Table E.15 Mean bed level (m+NAP) in polygon

	Trajectvak hoofdgeul benedenstrooms	Trajectvak hoofdgeul bovenstrooms	Trajectvak hoofdgeul	Trajectvak hoofdgeul 1	Trajectvak hoofdgeul 2	Langsdam Wamel hoofdgeul	Langsdam Wamel hoofdgeul 1	Langsdam Wamel hoofdgeul 2	Langsdam Dreumel hoofdgeul	Langsdam Ophemert hoofdgeul	Langsdam Wamel oevergeul	Langsdam Dreumel oevergeul	Langsdam Ophemert oevergeul
2020_26	-2.88	-1.34	-1.77	-1.25	-1.87	-1.50	-1.25	-1.74	-1.72	-2.11	-0.18	-0.37	-1.52
2020_18	-2.88	-1.35	-1.76	-1.25	-1.86	-1.49	-1.25	-1.73	-1.70	-2.10	-0.22	-0.34	-1.51
2020_10	-2.89	-1.29	-1.74	-1.28	-1.84	-1.50	-1.28	-1.73	-1.68	-2.07	-0.17	-0.28	-1.53
2020_02	-2.86	-1.19	-1.74	-1.32	-1.83	-1.48	-1.32	-1.64	-1.70	-2.08	-0.32	-0.35	-1.52
2019_46	-2.88	-1.19	-1.77	-1.37	-1.85	-1.48	-1.37	-1.60	-1.74	-2.10	-0.35	-0.40	-1.57
2019_38	-2.88	-1.24	-1.77	-1.37	-1.85	-1.48	-1.37	-1.60	-1.76	-2.09	-0.36	-0.38	-1.62
2019_30	-2.84	-1.25	-1.73	-1.26	-1.83	-1.42	-1.26	-1.59	-1.73	-2.07	-0.34	-0.34	-1.55
2019_14	-2.91	-1.28	-1.75	-1.23	-1.86	-1.44	-1.23	-1.66	-1.75	-2.08	-0.32	-0.32	-1.54
2019_06	-2.92	-1.26	-1.75	-1.23	-1.85	-1.43	-1.23	-1.62	-1.76	-2.08	-0.31	-0.40	-1.54
2018_50	-2.93	-1.31	-1.77	-1.26	-1.88	-1.44	-1.26	-1.61	-1.79	-2.11	-0.26	-0.52	-1.61
2018_45	-2.95	-1.31	-1.73	-1.19	-1.84	-1.39	-1.19	-1.59	-1.74	-2.07	-0.28	-0.51	-1.65
2018_40	-2.94	-1.32	-1.75	-1.16	-1.87	-1.40	-1.16	-1.64	-1.76	-2.12	-1.21	-0.72	-2.76
2018_34	-2.93	-1.33	-1.74	-1.11	-1.87	-1.39	-1.11	-1.67	-1.74	-2.12	-1.21	-0.72	-2.76
2018_26	-2.95	-1.33	-1.73	-1.04	-1.87	-1.36	-1.04	-1.69	-1.72	-2.13	-0.26	-0.47	-1.49
2018_10	-3.04	-1.38	-1.76	-1.11	-1.90	-1.42	-1.11	-1.73	-1.74	-2.16	0.06	-0.23	-1.49
2018_02	-3.01	-1.30	-1.80	-1.18	-1.92	-1.46	-1.18	-1.75	-1.76	-2.18	-0.05	-0.27	-1.73
2017_38	-2.87	-1.10	-1.77	-1.18	-1.89	-1.41	-1.18	-1.65	-1.77	-2.16	-0.22	-0.29	-1.80
2017_30	-2.88	-1.13	-1.79	-1.16	-1.92	-1.42	-1.16	-1.68	-1.78	-2.20	-1.21	-0.72	-2.76
2017_22	-2.86	-1.13	-1.76	-1.12	-1.88	-1.38	-1.12	-1.65	-1.73	-2.17	-0.23	-0.21	-1.77
2017_06	-2.89	-1.20	-1.79	-1.12	-1.93	-1.41	-1.12	-1.71	-1.76	-2.23	-0.22	-0.22	-1.81
2016_50	-2.90	-1.22	-1.78	-1.04	-1.93	-1.40	-1.04	-1.76	-1.73	-2.23	-0.33	-0.21	-1.80
2016_39	-3.07	-1.29	-1.78	-0.99	-1.94	-1.40	-0.99	-1.81	-1.70	-2.26	-0.34	-0.16	-1.78
2016_29	-2.86	-1.33	-1.78	-1.00	-1.94	-1.43	-1.00	-1.87	-1.69	-2.25	-0.19	-0.06	-1.75
2016_20	-2.78	-1.21	-1.80	-1.08	-1.95	-1.45	-1.08	-1.83	-1.72	-2.27	-0.36	-0.18	-1.93
2016_11	-2.74	-1.20	-1.80	-1.13	-1.94	-1.47	-1.13	-1.80	-1.71	-2.26	-0.51	-0.19	-1.96
2015_42	-3.02	-1.26	-1.90	-1.33	-2.00	-1.57	-1.33	-1.79	-1.81	-2.32	-1.21	-0.72	-2.76
jmp2017	-2.87	-1.09	-1.79	-1.21	-1.91	-1.44	-1.21	-1.68	-1.78	-2.17	-0.69	-1.33	-1.09
jmp2016	-2.86	-1.24	-1.81	-1.07	-1.96	-1.45	-1.07	-1.83	-1.74	-2.27	-0.69	-1.33	-1.09
jmp2015	-2.62	-1.06	-1.85	-1.31	-1.96	-1.53	-1.31	-1.76	-1.79	-2.26	-0.69	-1.33	-1.09
jmp2014	-2.31	-1.07	-1.79	-1.35	-1.87	-1.47	-1.35	-1.58	-1.74	-2.18	0.15	-0.19	-0.56
jmp2013	-2.35	-1.11	-1.79	-1.34	-1.89	-1.48	-1.34	-1.62	-1.74	-2.19	1.03	0.27	-0.35
jmp2012	-2.28	-0.99	-1.74	-1.23	-1.84	-1.38	-1.23	-1.53	-1.71	-2.15	1.38	0.67	-0.30
jmp2011	-2.30	-0.97	-1.75	-1.26	-1.85	-1.44	-1.26	-1.63	-1.72	-2.12	-0.69	-1.29	-1.09
jmp2009	-2.36	-0.92	-1.72	-1.23	-1.82	-1.38	-1.23	-1.54	-1.67	-2.13	0.40	-0.33	-0.37
jmp2007	-2.36	-1.01	-1.76	-1.34	-1.84	-1.44	-1.34	-1.53	-1.71	-2.15	1.02	0.12	-0.62
jmp2006	-2.32	-0.95	-1.72	-1.25	-1.81	-1.37	-1.25	-1.49	-1.68	-2.12	0.19	-0.22	-0.38
jmp2005	-2.44	-1.03	-1.76	-1.29	-1.86	-1.42	-1.29	-1.56	-1.72	-2.16	-0.69	-1.33	-1.10
jmp2004	-2.38	-0.90	-1.73	-1.24	-1.83	-1.37	-1.24	-1.51	-1.68	-2.15	-0.68	-1.30	-1.01
jmp2003	-2.41	-0.95	-1.73	-1.24	-1.83	-1.38	-1.24	-1.52	-1.69	-2.14	-0.69	-1.33	-1.08
jmp2002	-2.35	-0.94	-1.69	-1.26	-1.78	-1.36	-1.26	-1.46	-1.64	-2.09	-0.15	-0.98	-0.89
jmp2001	-2.42	-0.89	-1.70	-1.17	-1.81	-1.30	-1.17	-1.45	-1.65	-2.18	-0.65	-0.95	-0.98
jmp2000	-2.45	-0.89	-1.70	-1.17	-1.81	-1.27	-1.17	-1.37	-1.69	-2.19	-0.30	-0.84	-0.74
jmp1999	-2.40	-0.91	-1.71	-1.10	-1.83	-1.26	-1.10	-1.43	-1.69	-2.21	-0.69	-1.33	-1.09

Table E.16 Min bed level (m+NAP) in polygon

	Trajectvak hoofdgeul benedenstrooms	Trajectvak hoofdgeul bovenstrooms	Trajectvak hoofdgeul	Trajectvak hoofdgeul 1	Trajectvak hoofdgeul 2	Langsdam Wamel hoofdgeul	Langsdam Wamel hoofdgeul 1	Langsdam Wamel hoofdgeul 2	Langsdam Dreumel hoofdgeul	Langsdam Ophemert hoofdgeul	Langsdam Wamel oevergeul	Langsdam Dreumel oevergeul	Langsdam Ophemert oevergeul
2020_26	-8.00	-3.28	-8.56	-4.20	-8.56	-5.48	-4.20	-5.48	-5.13	-8.56	-3.71	-4.60	-3.96
2020_18	-6.02	-2.91	-9.09	-4.05	-9.09	-5.57	-4.05	-5.57	-4.71	-9.09	-3.61	-4.59	-3.95
2020_10	-6.18	-3.50	-8.20	-4.28	-8.20	-6.03	-4.28	-6.03	-5.12	-8.20	-3.59	-2.13	-4.21
2020_02	-7.22	-3.10	-9.48	-4.36	-9.48	-5.80	-4.36	-5.80	-5.56	-9.48	-3.97	-2.24	-4.01
2019_46	-7.80	-3.50	-8.50	-4.30	-8.50	-5.90	-4.30	-5.90	-6.20	-8.50	-4.00	-4.60	-4.00
2019_38	-7.60	-3.50	-8.30	-4.30	-8.30	-6.00	-4.30	-6.00	-5.70	-8.30	-3.70	-4.60	-3.90
2019_30	-6.98	-3.23	-8.59	-4.32	-8.59	-5.91	-4.32	-5.91	-5.56	-8.59	-3.66	-4.55	-3.86
2019_14	-5.98	-3.04	-9.20	-4.27	-9.20	-5.50	-4.27	-5.50	-5.19	-9.20	-3.75	-2.02	-3.89
2019_06	-6.26	-3.29	-8.72	-4.19	-8.72	-5.63	-4.19	-5.63	-4.97	-8.72	-3.86	-3.87	-3.72
2018_50	-6.34	-3.46	-6.32	-4.28	-6.32	-5.14	-4.28	-5.14	-4.78	-6.32	-3.64	-4.60	-3.84
2018_45	-6.50	-3.51	-6.46	-4.33	-6.46	-5.35	-4.33	-5.35	-4.65	-6.46	-3.62	-4.53	-3.84
2018_40	-6.56	-3.49	-7.22	-4.39	-7.22	-5.46	-4.39	-5.46	-4.59	-7.22	-3.34	-2.97	-3.96
2018_34	-6.74	-3.27	-7.67	-4.44	-7.67	-5.41	-4.44	-5.41	-4.57	-7.67	-3.34	-2.97	-3.96
2018_26	-6.70	-3.50	-8.38	-4.39	-8.38	-5.84	-4.39	-5.84	-4.83	-8.38	-3.65	-4.36	-3.91
2018_10	-5.86	-5.19	-9.36	-4.12	-9.36	-5.53	-4.12	-5.53	-4.86	-9.36	-3.53	-3.09	-4.60
2018_02	-5.99	-4.27	-7.70	-4.21	-7.70	-5.64	-4.21	-5.64	-5.66	-7.70	-3.12	-2.22	-3.90
2017_38	-9.35	-3.32	-9.30	-4.16	-9.30	-6.04	-4.16	-6.04	-6.33	-9.30	-3.53	-3.07	-4.14
2017_30	-9.31	-3.47	-9.72	-4.10	-9.72	-5.87	-4.10	-5.87	-6.02	-9.72	-3.34	-2.97	-3.96
2017_22	-8.94	-3.14	-9.08	-4.13	-9.08	-5.83	-4.13	-5.83	-6.22	-9.08	-3.48	-3.07	-3.96
2017_06	-8.30	-3.35	-9.06	-4.13	-9.06	-6.02	-4.13	-6.02	-5.45	-9.06	-3.25	-3.05	-4.15
2016_50	-8.50	-3.35	-8.83	-4.17	-8.83	-6.05	-4.17	-6.05	-5.45	-8.83	-3.34	-3.08	-4.02
2016_39	-7.62	-3.25	-8.39	-4.20	-8.39	-5.97	-4.20	-5.97	-5.07	-8.39	-3.26	-3.07	-3.77
2016_29	-6.22	-3.53	-8.05	-4.21	-8.05	-6.11	-4.21	-6.11	-5.12	-8.05	-3.37	-1.98	-3.64
2016_20	-7.16	-3.14	-7.72	-4.34	-7.72	-6.09	-4.34	-6.09	-5.96	-7.72	-3.32	-2.60	-3.90
2016_11	-5.07	-3.34	-7.07	-4.26	-7.07	-6.10	-4.26	-6.10	-5.25	-7.07	-3.29	-2.61	-3.86
2015_42	-4.62	-2.44	-6.97	-4.10	-6.97	-6.46	-4.10	-6.46	-5.85	-6.97	-3.34	-2.97	-3.96
jmp2017	-9.01	-3.45	-9.56	-4.18	-9.56	-6.07	-4.18	-6.07	-6.25	-9.56	-1.90	-3.52	-3.46
jmp2016	-7.56	-3.57	-8.50	-4.49	-8.50	-6.00	-4.49	-6.00	-5.17	-8.50	-1.90	-3.52	-3.46
jmp2015	-6.20	-3.57	-6.83	-4.49	-6.83	-6.21	-4.49	-6.21	-5.37	-6.83	-1.90	-3.52	-3.46
jmp2014	-6.84	-3.31	-7.27	-4.50	-7.27	-6.22	-4.50	-6.22	-5.60	-7.27	-1.38	-2.74	-3.35
jmp2013	-6.23	-3.23	-7.25	-4.68	-7.25	-5.76	-4.68	-5.76	-6.05	-7.25	-2.00	-3.43	-2.82
jmp2012	-6.91	-3.72	-6.95	-4.41	-6.95	-6.18	-4.41	-6.18	-6.42	-6.95	-1.39	-2.40	-2.69
jmp2011	-6.74	-3.63	-7.01	-4.25	-7.01	-5.52	-4.25	-5.52	-5.11	-7.01	-1.90	-3.52	-3.46
jmp2009	-7.35	-3.58	-7.42	-4.29	-7.42	-6.14	-4.29	-6.14	-5.88	-7.42	-1.77	-2.95	-2.70
jmp2007	-6.15	-3.34	-7.09	-4.43	-7.09	-5.49	-4.43	-5.49	-5.41	-7.09	-2.16	-3.38	-2.76
jmp2006	-7.01	-3.77	-6.99	-4.56	-6.99	-5.91	-4.56	-5.91	-5.33	-6.99	-2.61	-2.65	-3.37
jmp2005	-7.43	-4.01	-7.00	-4.24	-7.00	-6.12	-4.24	-6.12	-5.49	-7.00	-1.90	-3.52	-3.46
jmp2004	-7.03	-3.40	-7.15	-4.67	-7.15	-5.80	-4.67	-5.80	-5.93	-7.15	-1.90	-3.52	-2.86
jmp2003	-7.23	-3.42	-6.81	-4.54	-6.81	-5.58	-4.54	-5.58	-5.16	-6.81	-1.90	-3.52	-3.46
jmp2002	-5.08	-3.23	-5.92	-4.33	-5.92	-5.89	-4.33	-5.89	-4.94	-5.92	-3.08	-14.49	-14.25
jmp2001	-7.12	-3.56	-7.20	-4.54	-7.20	-6.09	-4.54	-6.09	-5.44	-7.20	-1.80	-4.10	-3.46
jmp2000	-6.37	-3.95	-7.54	-4.67	-7.54	-6.21	-4.67	-6.21	-5.08	-7.54	-1.79	-3.49	-2.63
jmp1999	-6.20	-3.57	-7.58	-4.49	-7.58	-5.83	-4.49	-5.83	-4.91	-7.58	-1.90	-3.52	-3.46

Table E.17 Max bed level (m+NAP) in polygon

	Trajectvak hoofdgeul benedenstrooms	Trajectvak hoofdgeul bovenstrooms	Trajectvak hoofdgeul	Trajectvak hoofdgeul 1	Trajectvak hoofdgeul 2	Langsdam Wamel hoofdgeul	Langsdam Wamel hoofdgeul 1	Langsdam Wamel hoofdgeul 2	Langsdam Dreumel hoofdgeul	Langsdam Ophemert hoofdgeul	Langsdam Wamel oevergeul	Langsdam Dreumel oevergeul	Langsdam Ophemert oevergeul
2020_26	2.55	1.94	2.16	1.80	2.16	1.80	1.80	1.13	1.74	2.16	3.43	2.11	3.12
2020_18	1.71	1.73	2.08	1.66	2.08	1.66	1.66	1.14	1.63	2.08	2.42	1.25	1.99
2020_10	2.71	1.95	2.85	1.87	2.85	1.87	1.87	1.11	1.70	2.85	5.57	2.45	3.49
2020_02	2.63	1.94	2.17	1.76	2.17	1.76	1.76	1.14	1.74	2.17	3.07	2.33	2.42
2019_46	2.30	1.90	2.10	1.80	2.10	1.80	1.80	1.10	1.70	2.10	3.00	2.30	2.40
2019_38	1.10	1.90	1.80	1.80	1.50	1.80	1.80	1.10	1.40	1.50	1.90	1.40	1.20
2019_30	1.21	1.88	1.76	1.76	1.50	1.76	1.76	1.19	1.50	1.49	2.10	1.70	1.60
2019_14	2.61	1.93	2.32	1.78	2.32	1.78	1.78	1.16	1.76	2.32	2.85	2.22	2.05
2019_06	2.70	1.97	2.42	1.80	2.42	1.80	1.80	1.17	1.77	2.42	3.79	2.52	2.77
2018_50	2.65	1.86	2.25	1.76	2.25	1.76	1.76	1.16	1.81	2.25	2.94	2.20	1.95
2018_45	0.03	1.08	1.13	1.13	0.68	1.13	1.13	0.68	0.65	0.29	0.97	0.65	0.15
2018_40	0.34	1.21	1.05	1.04	1.05	1.04	1.04	1.03	1.05	0.90	0.97	0.69	0.00
2018_34	0.33	1.35	0.94	0.94	0.88	0.94	0.94	0.45	0.88	0.64	0.97	0.69	0.00
2018_26	1.25	2.07	2.04	1.86	2.04	1.86	1.86	1.26	1.77	2.04	2.20	1.76	1.68
2018_10	1.62	2.04	2.07	2.07	1.91	2.07	2.07	1.25	1.74	1.91	2.95	2.15	2.09
2018_02	2.71	2.05	2.22	1.93	2.22	1.93	1.93	1.22	1.73	2.22	4.43	1.96	2.93
2017_38	2.33	1.97	2.27	1.88	2.27	1.88	1.88	1.21	1.81	2.27	3.05	1.98	2.33
2017_30	1.59	2.05	1.91	1.86	1.91	1.86	1.86	1.25	1.91	1.76	0.97	0.69	0.00
2017_22	0.54	1.40	1.64	1.63	1.64	1.63	1.63	1.28	1.59	1.64	2.16	1.40	1.33
2017_06	1.22	1.72	1.71	1.71	1.65	1.71	1.71	1.26	1.65	1.30	2.72	1.72	1.21
2016_50	-0.36	0.88	0.98	0.73	0.98	0.73	0.73	0.52	0.78	0.98	1.62	1.43	0.54
2016_39	0.06	1.01	1.54	1.54	1.31	1.54	1.54	0.99	0.91	1.31	1.72	1.42	0.37
2016_29	2.06	1.97	1.99	1.99	1.86	1.99	1.99	1.27	1.86	1.78	3.34	3.03	2.13
2016_20	2.33	2.20	2.49	2.27	2.49	2.27	2.27	1.24	1.74	2.49	3.82	2.96	2.73
2016_11	1.49	2.00	1.85	1.85	1.57	1.85	1.85	1.20	1.57	1.16	3.37	2.78	2.41
2015_42	-1.12	0.02	0.07	0.07	-0.26	0.07	0.07	-0.26	-0.38	-0.54	0.97	0.69	0.00
jmp2017	0.73	2.34	1.84	1.26	1.84	1.84	1.26	1.84	1.48	1.10	0.45	1.26	-0.12
jmp2016	0.73	2.34	1.42	1.38	1.42	1.38	1.38	1.36	1.42	1.10	0.45	1.26	-0.12
jmp2015	0.73	2.34	1.42	1.38	1.42	1.38	1.38	1.36	1.42	1.10	0.45	1.26	-0.12
jmp2014	2.17	1.99	2.26	2.06	2.26	2.06	2.06	1.27	1.56	2.26	2.05	2.73	2.58
jmp2013	2.75	2.00	2.26	2.21	2.26	2.21	2.21	1.21	1.59	2.26	4.85	4.66	3.93
jmp2012	2.53	2.12	2.35	2.25	2.35	2.25	2.25	1.23	1.72	2.35	5.14	4.76	3.81
jmp2011	0.73	2.34	1.42	1.38	1.42	1.38	1.38	1.36	1.42	1.10	0.45	1.26	-0.12
jmp2009	2.33	2.02	2.45	2.45	2.45	2.45	2.45	1.48	1.91	2.45	3.92	3.47	2.99
jmp2007	1.18	2.14	2.18	2.18	1.93	2.18	2.18	1.24	1.36	1.93	3.84	3.50	1.92
jmp2006	1.74	2.17	2.28	2.28	1.59	2.28	2.28	1.24	1.48	1.59	2.36	2.13	1.74
jmp2005	0.73	2.34	1.42	1.38	1.42	1.38	1.38	1.36	1.42	1.10	0.45	1.26	-0.12
jmp2004	0.73	2.34	1.73	1.73	1.42	1.73	1.73	1.28	1.42	1.10	1.07	1.26	0.10
jmp2003	0.73	2.34	1.42	1.38	1.42	1.38	1.38	1.36	1.42	1.10	0.45	1.26	-0.12
jmp2002	1.47	2.68	2.17	2.17	1.56	2.17	2.17	1.44	1.56	1.42	2.92	2.62	0.38
jmp2001	1.85	2.07	2.19	2.19	1.65	2.19	2.19	1.35	1.65	1.13	0.45	1.26	0.94
jmp2000	1.76	2.28	2.43	2.43	2.23	2.43	2.43	1.49	1.57	2.23	1.91	2.45	1.67
jmp1999	0.73	2.34	1.42	1.38	1.42	1.38	1.38	1.36	1.42	1.10	0.45	1.26	-0.12

Table E.18 Standard deviation of bed level (m+NAP) in polygon

	Trajectvak hoofdgeul benedenstrooms	Trajectvak hoofdgeul bovenstrooms	Trajectvak hoofdgeul	Trajectvak hoofdgeul 1	Trajectvak hoofdgeul 2	Langsdam Wamel hoofdgeul	Langsdam Wamel hoofdgeul 1	Langsdam Wamel hoofdgeul 2	Langsdam Dreumel hoofdgeul	Langsdam Ophemert hoofdgeul	Langsdam Wamel oevergeul	Langsdam Dreumel oevergeul	Langsdam Ophemert oevergeul
2020_26	0.77	0.54	0.66	0.56	0.62	0.61	0.56	0.56	0.53	0.67	1.02	0.66	0.91
2020_18	0.77	0.59	0.68	0.59	0.65	0.64	0.59	0.59	0.56	0.70	0.99	0.66	0.91
2020_10	0.86	0.63	0.73	0.62	0.71	0.70	0.62	0.71	0.64	0.73	1.18	0.56	0.97
2020_02	0.80	0.52	0.70	0.56	0.69	0.61	0.56	0.63	0.59	0.76	1.05	0.49	0.96
2019_46	0.77	0.51	0.66	0.50	0.66	0.57	0.50	0.62	0.56	0.71	1.01	0.54	0.96
2019_38	0.75	0.51	0.65	0.49	0.65	0.56	0.49	0.60	0.54	0.70	0.97	0.53	0.85
2019_30	0.76	0.54	0.68	0.48	0.67	0.58	0.48	0.62	0.55	0.73	0.97	0.51	0.90
2019_14	0.80	0.53	0.68	0.51	0.66	0.62	0.51	0.65	0.54	0.72	0.95	0.44	0.85
2019_06	0.77	0.53	0.68	0.50	0.66	0.60	0.50	0.64	0.52	0.73	0.88	0.43	0.83
2018_50	0.79	0.53	0.61	0.43	0.59	0.52	0.43	0.53	0.47	0.64	0.75	0.49	0.76
2018_45	0.77	0.50	0.60	0.43	0.57	0.51	0.43	0.51	0.45	0.62	0.67	0.45	0.68
2018_40	0.80	0.54	0.63	0.43	0.59	0.53	0.43	0.51	0.46	0.66	0.85	0.50	0.57
2018_34	0.81	0.55	0.65	0.45	0.61	0.57	0.45	0.53	0.47	0.68	0.85	0.50	0.57
2018_26	0.84	0.60	0.75	0.58	0.70	0.68	0.58	0.62	0.56	0.79	0.73	0.48	0.84
2018_10	0.87	0.73	0.77	0.64	0.73	0.73	0.64	0.69	0.58	0.81	0.91	0.66	0.71
2018_02	0.90	0.72	0.79	0.63	0.75	0.74	0.63	0.74	0.67	0.78	1.00	0.60	0.77
2017_38	0.78	0.47	0.71	0.50	0.68	0.61	0.50	0.62	0.55	0.75	1.05	0.50	0.92
2017_30	0.76	0.47	0.71	0.48	0.68	0.62	0.48	0.63	0.54	0.75	0.85	0.50	0.57
2017_22	0.76	0.47	0.73	0.50	0.70	0.64	0.50	0.66	0.56	0.76	1.05	0.50	0.79
2017_06	0.77	0.50	0.70	0.47	0.66	0.62	0.47	0.62	0.52	0.71	0.98	0.56	0.73
2016_50	0.73	0.48	0.71	0.48	0.66	0.66	0.48	0.62	0.52	0.71	0.89	0.54	0.69
2016_39	0.78	0.55	0.76	0.52	0.69	0.71	0.52	0.64	0.55	0.74	0.90	0.61	0.68
2016_29	0.84	0.67	0.82	0.64	0.76	0.80	0.64	0.71	0.65	0.78	1.10	0.76	0.73
2016_20	0.79	0.55	0.79	0.64	0.74	0.75	0.64	0.66	0.63	0.77	1.14	0.58	0.74
2016_11	0.82	0.63	0.79	0.67	0.74	0.77	0.67	0.71	0.65	0.74	1.01	0.59	0.64
2015_42	0.53	0.27	0.66	0.55	0.62	0.61	0.55	0.58	0.52	0.61	0.85	0.50	0.57
jmp2017	0.79	0.48	0.70	0.50	0.68	0.61	0.50	0.62	0.55	0.74	0.35	0.67	0.59
jmp2016	0.79	0.59	0.73	0.53	0.68	0.70	0.53	0.63	0.55	0.71	0.35	0.67	0.59
jmp2015	0.64	0.45	0.66	0.58	0.62	0.62	0.58	0.58	0.53	0.61	0.35	0.67	0.59
jmp2014	0.64	0.47	0.67	0.54	0.66	0.59	0.54	0.62	0.56	0.66	0.54	0.77	0.66
jmp2013	0.60	0.49	0.69	0.57	0.67	0.59	0.57	0.59	0.59	0.69	1.49	1.34	0.79
jmp2012	0.66	0.49	0.70	0.55	0.69	0.61	0.55	0.64	0.60	0.68	1.68	1.59	0.76
jmp2011	0.59	0.43	0.62	0.49	0.59	0.55	0.49	0.55	0.49	0.62	0.35	0.65	0.59
jmp2009	0.64	0.47	0.68	0.54	0.66	0.59	0.54	0.60	0.57	0.66	1.07	0.92	0.64
jmp2007	0.60	0.51	0.67	0.56	0.66	0.58	0.56	0.58	0.56	0.69	0.93	1.10	0.57
jmp2006	0.59	0.48	0.66	0.53	0.64	0.55	0.53	0.55	0.53	0.65	0.71	0.72	0.65
jmp2005	0.58	0.45	0.64	0.53	0.62	0.56	0.53	0.55	0.52	0.62	0.35	0.67	0.61
jmp2004	0.65	0.48	0.69	0.54	0.67	0.58	0.54	0.59	0.57	0.69	0.37	0.66	0.64
jmp2003	0.62	0.42	0.64	0.50	0.62	0.53	0.50	0.52	0.52	0.64	0.35	0.67	0.58
jmp2002	0.70	0.65	0.76	0.60	0.75	0.65	0.60	0.67	0.67	0.77	1.32	1.08	0.73
jmp2001	0.63	0.50	0.71	0.54	0.70	0.57	0.54	0.56	0.57	0.72	0.37	0.68	0.58
jmp2000	0.63	0.57	0.76	0.58	0.75	0.59	0.58	0.59	0.56	0.83	0.57	0.75	0.57
jmp1999	0.61	0.52	0.77	0.60	0.75	0.60	0.60	0.55	0.60	0.81	0.35	0.67	0.59

E.4 Development in auxiliary channels

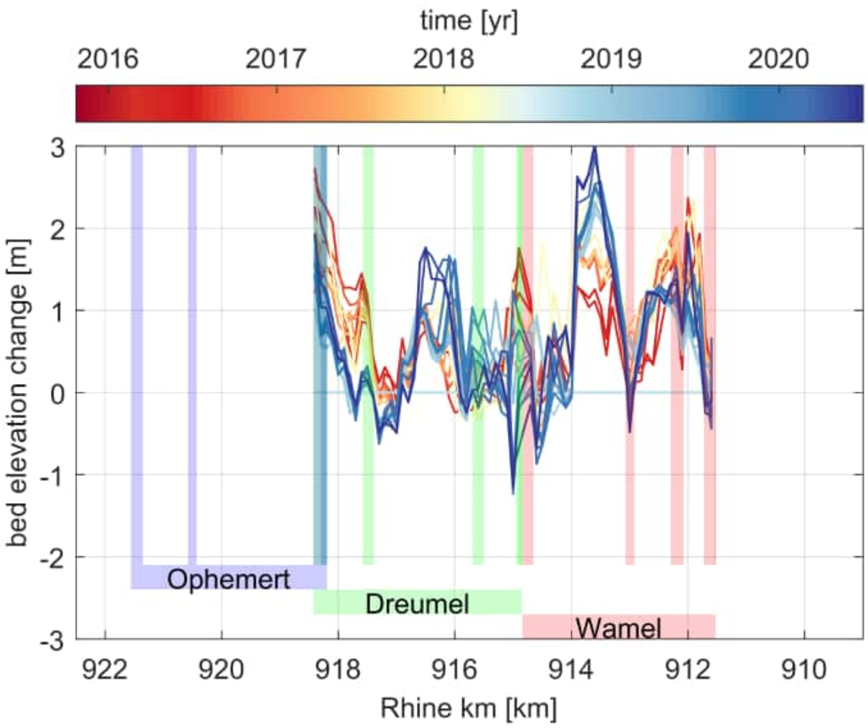

Figure E.24 Bed level change in the near channel zone of the auxiliary channel at the left bank (Bl).

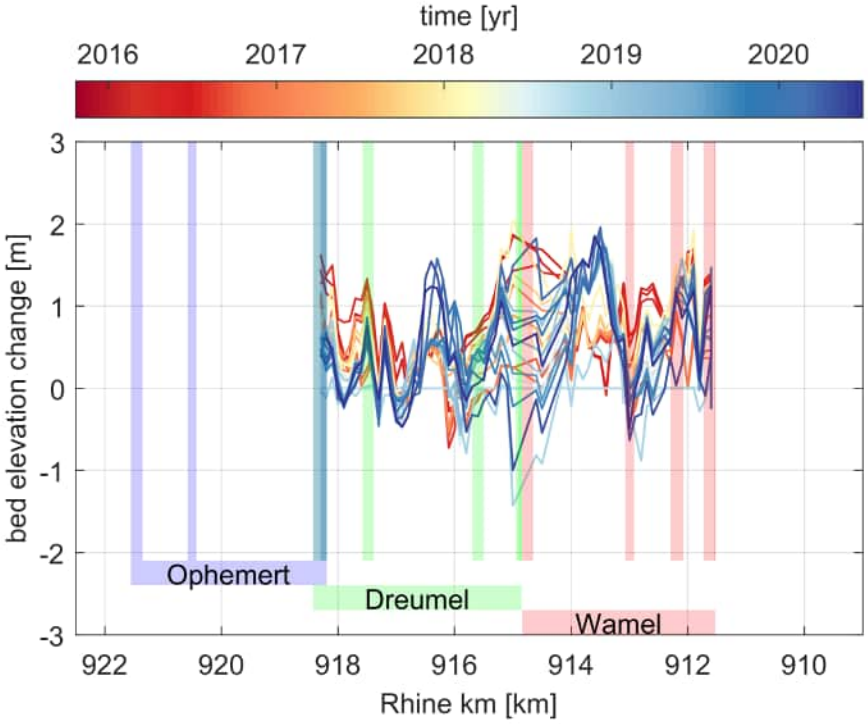

Figure E.25 Bed level change in the near bank zone of the auxiliary channel at the left bank (Cl).

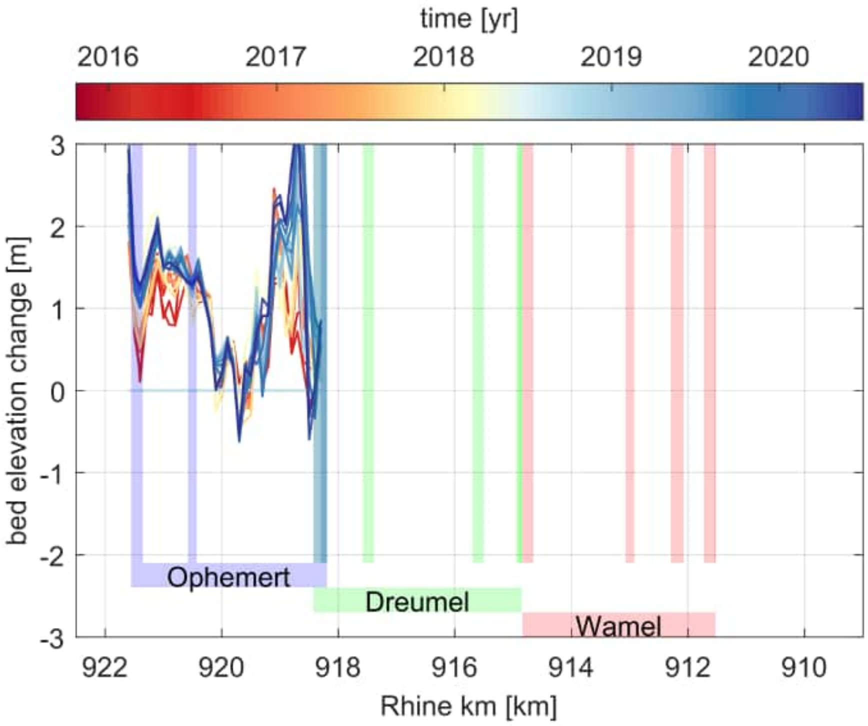

Figure E.26 Bed level change in the near channel zone of the auxiliary channel at the right bank (Br).

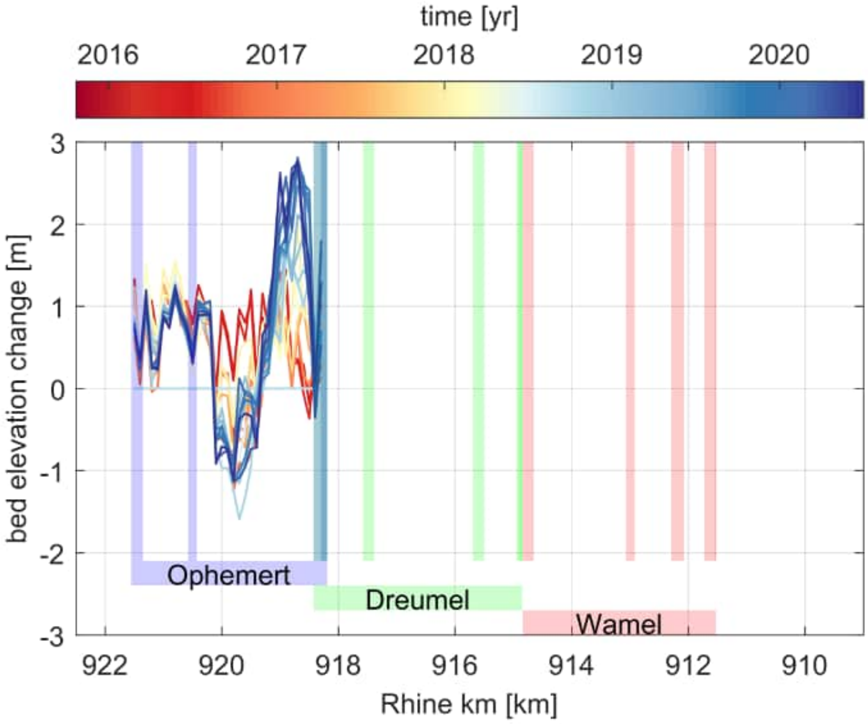

Figure E.27 Bed level change in the near bank zone of the auxiliary channel at the right bank (Cr).

E.5 Analysis of bed levels with respect to OLR

These figures are variants of the figures given in Section 4.4.5. As specified by requirements of RWS the analysis (in the main report for 150 m) is repeated for 170 m and 200 m.

Deltares

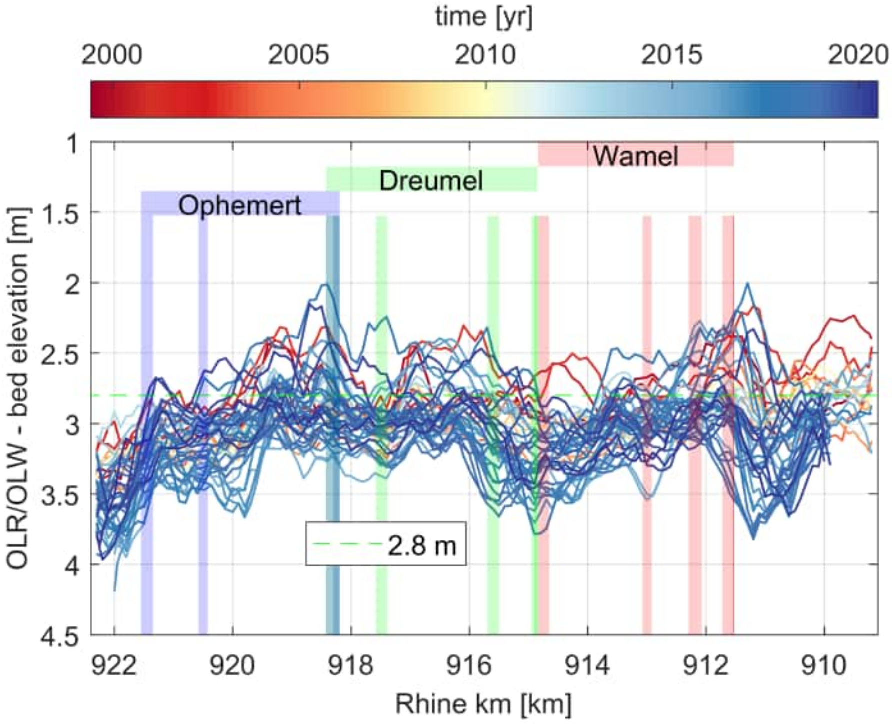

Figure E.28 Minimum depth w.r.t. OLR/OLW in the hectometre area for the *'vaargeul' (150 m)* (averaged over 250 m upstream and downstream)

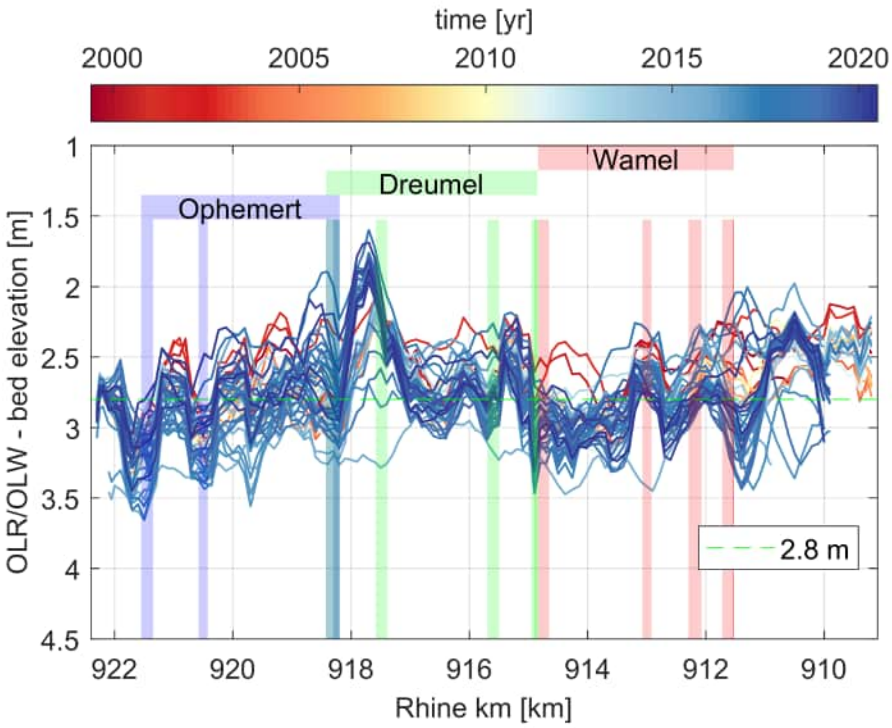

Figure E.29 Minimum depth w.r.t. OLR/OLW in the hectometre area for the *'bevaarbare breedte' (170 m)* (averaged over 250 m upstream and downstream)

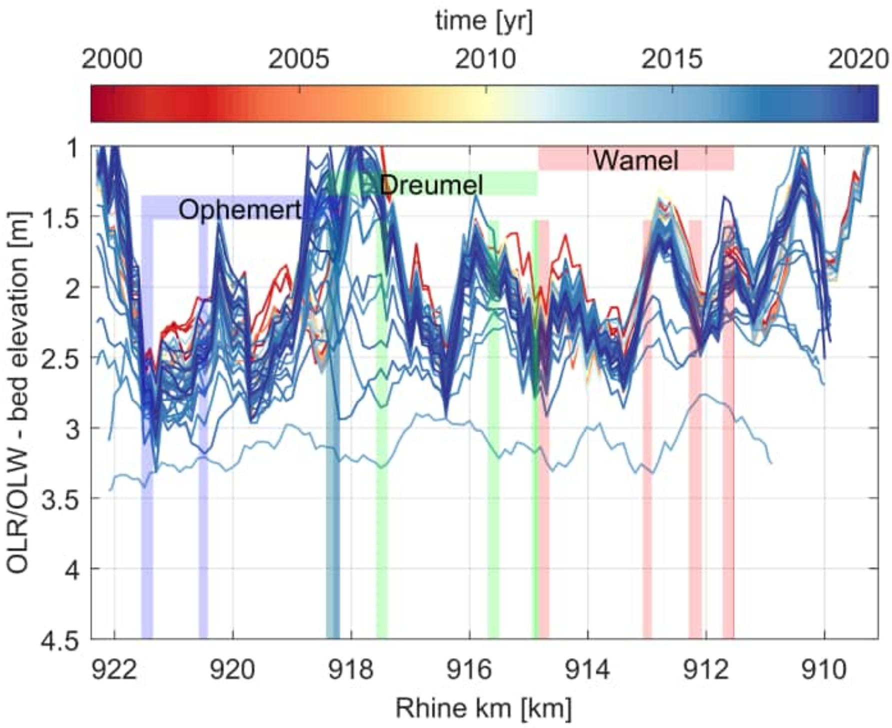

Figure E.30 Minimum depth w.r.t. OLR/OLW in the hectometre area for the *'zomerbed secties' (200 m)* (averaged over 250 m upstream and downstream)

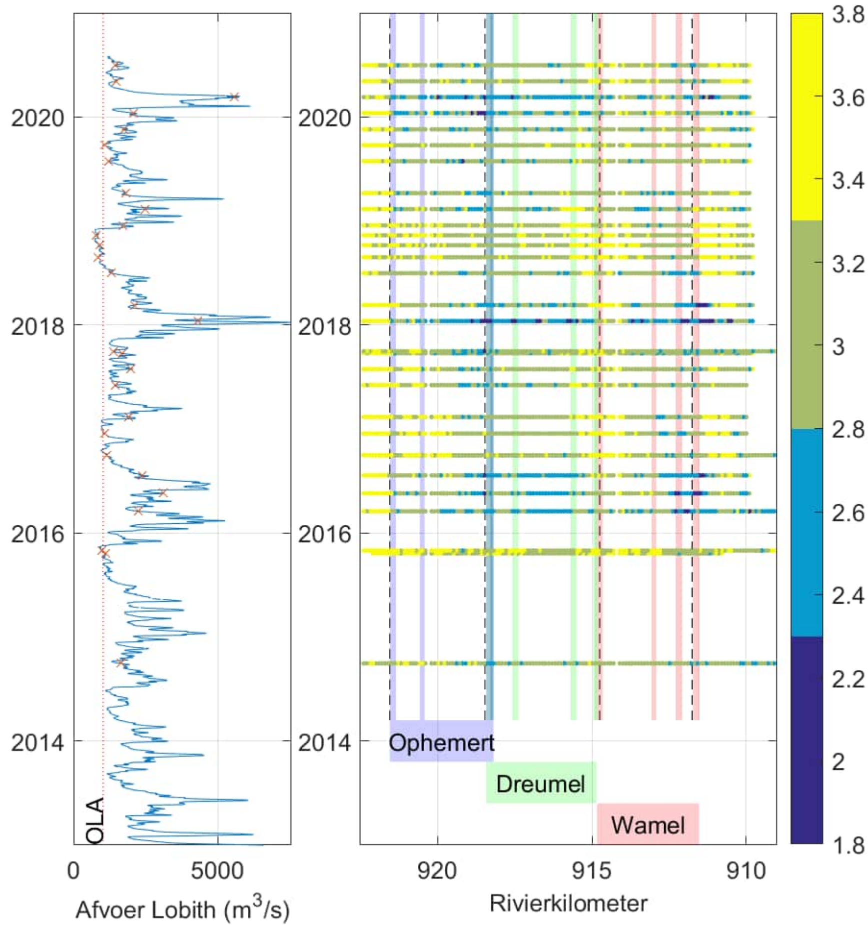

Figure E.31 Minimum depth w.r.t. OLR/OLW in the hectometre area for the *'vaargeul' (150 m)* with comparison to discharge at Lobith

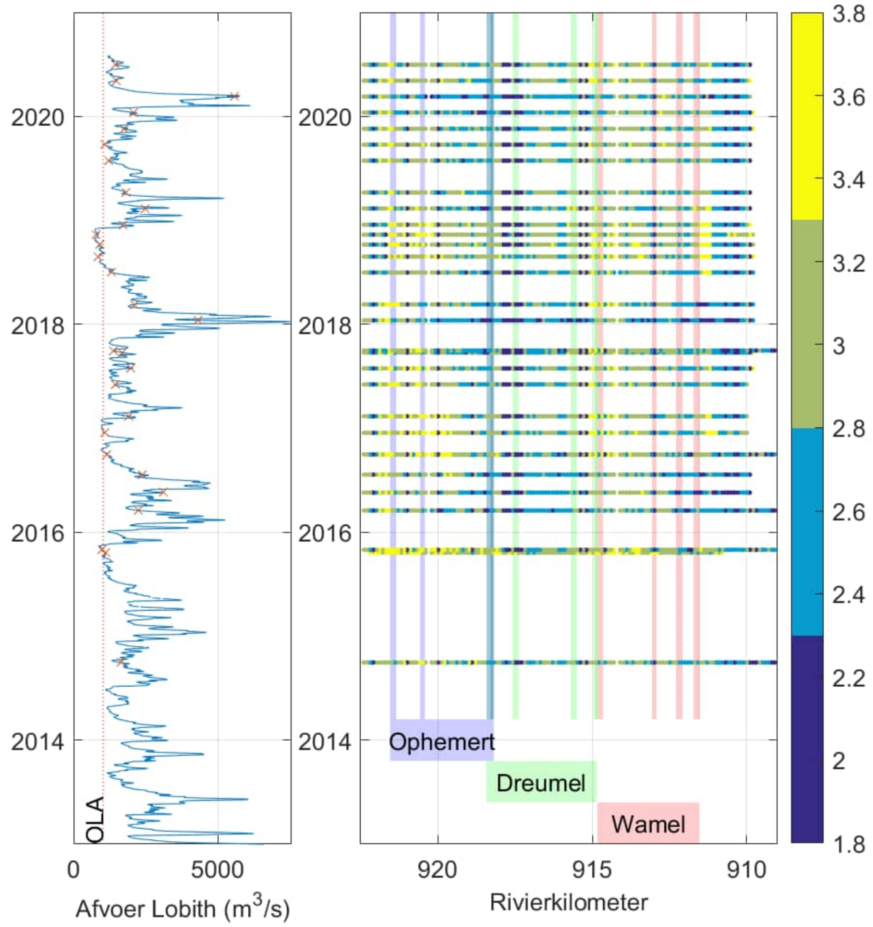

Figure E.32 Minimum depth w.r.t. OLR/OLW in the hectometre area for the *'bevaarbare breedte' (170 m)* with comparison to discharge at Lobith

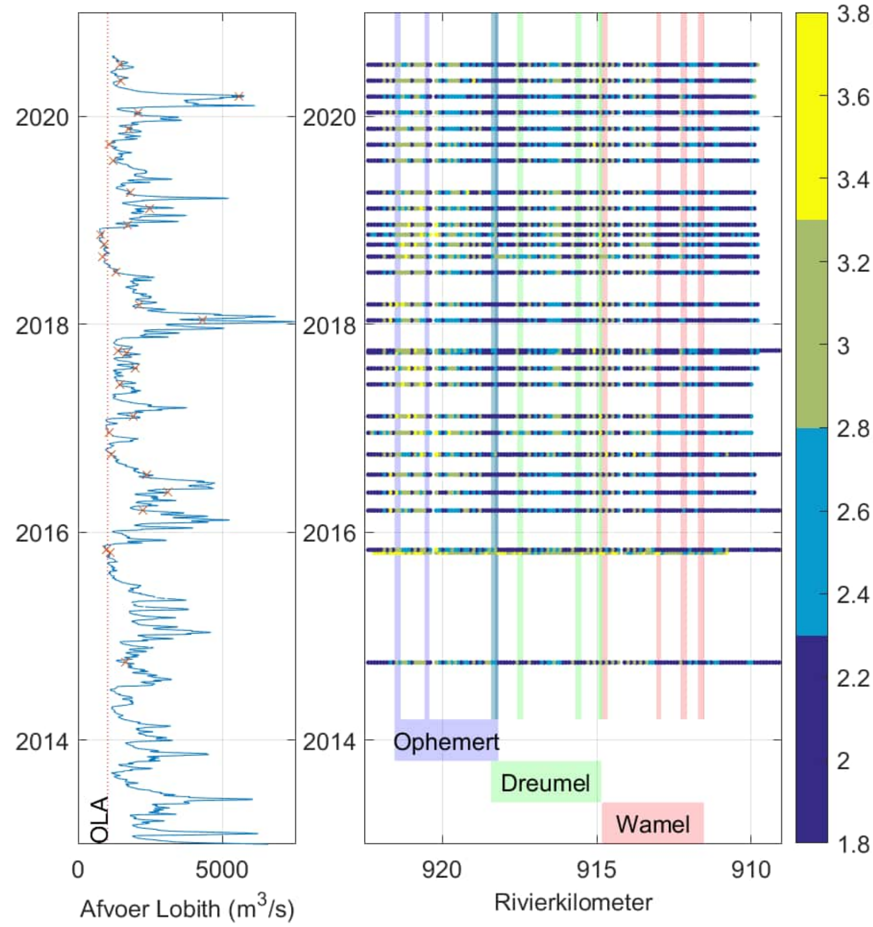

Figure E.33 Minimum depth w.r.t. OLR/OLW in the hectometre area for the *'zomerbed secties' (200 m)* with comparison to discharge at Lobith

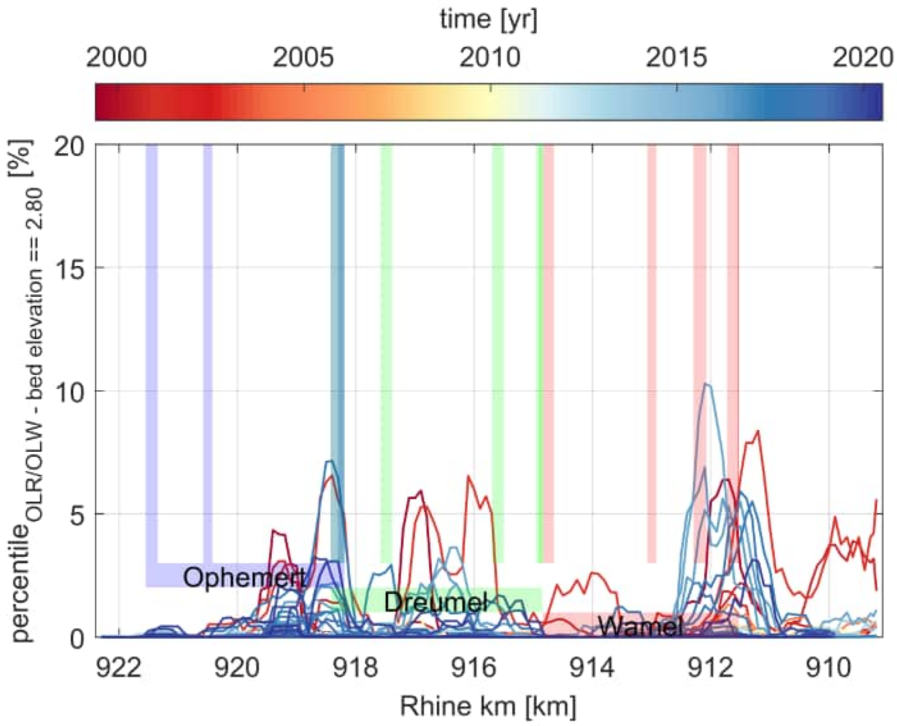

Figure E.34 Percentage of the hectometre area for the *navigation channel (150m)* at which the depth is less than 2.80 w.r.t. OLR/OLW (averaged over 250 m upstream and downstream)

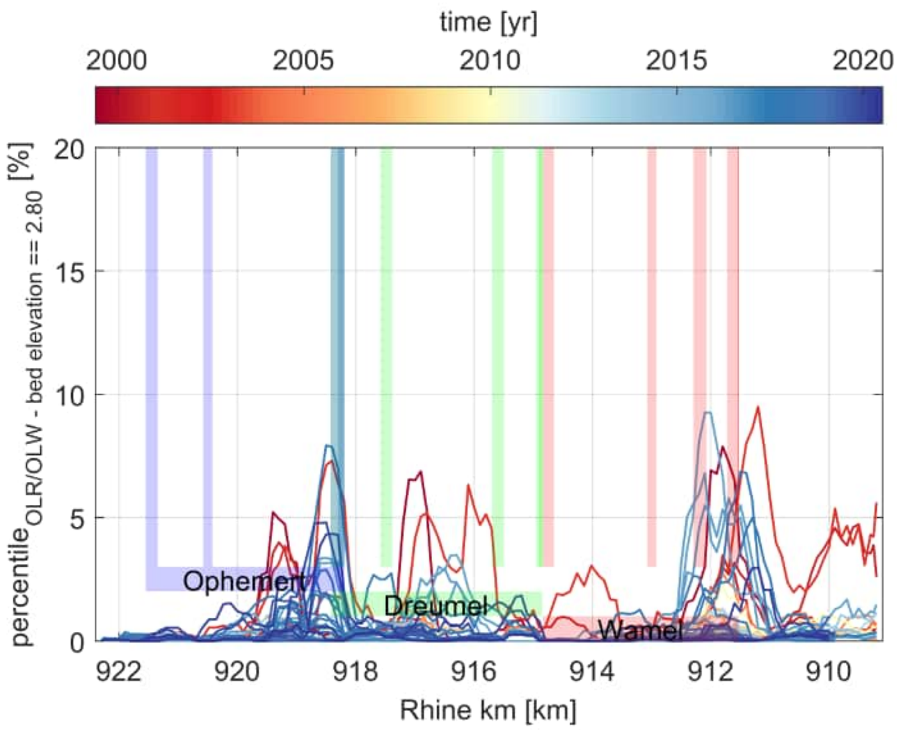

Figure E.35 Percentage of the hectometre area for the *navigable width (170m)* at which the depth is less than 2.80 w.r.t. OLR/OLW (averaged over 250 m upstream and downstream)

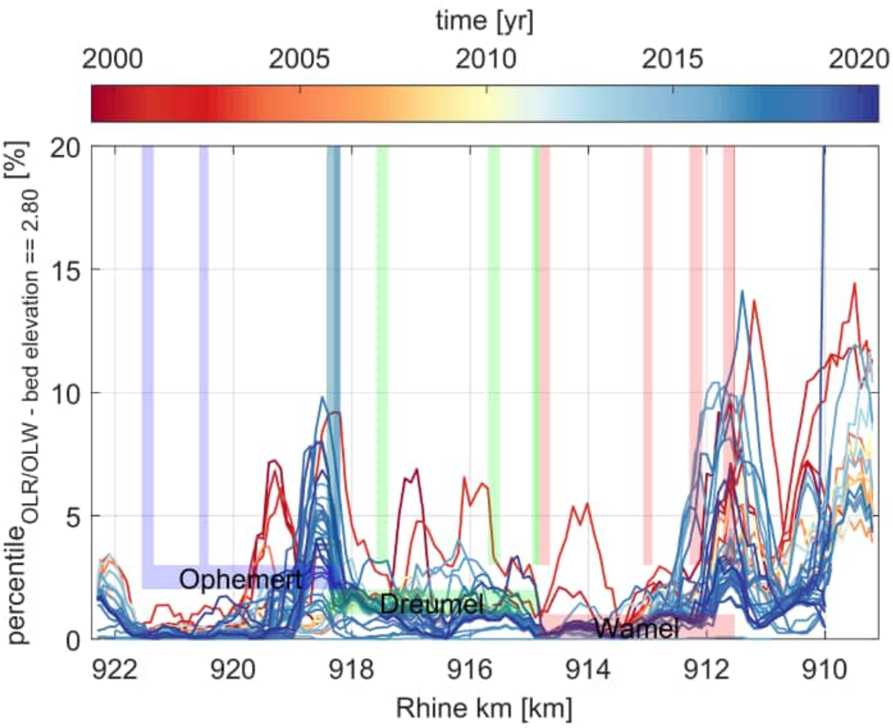

Figure E.36 Percentage of the hectometre area for the *main channel section (200m)* at which the depth is less than 2.80 w.r.t. OLR/OLW (averaged over 250 m upstream and downstream)

E.6 Wamel inlet

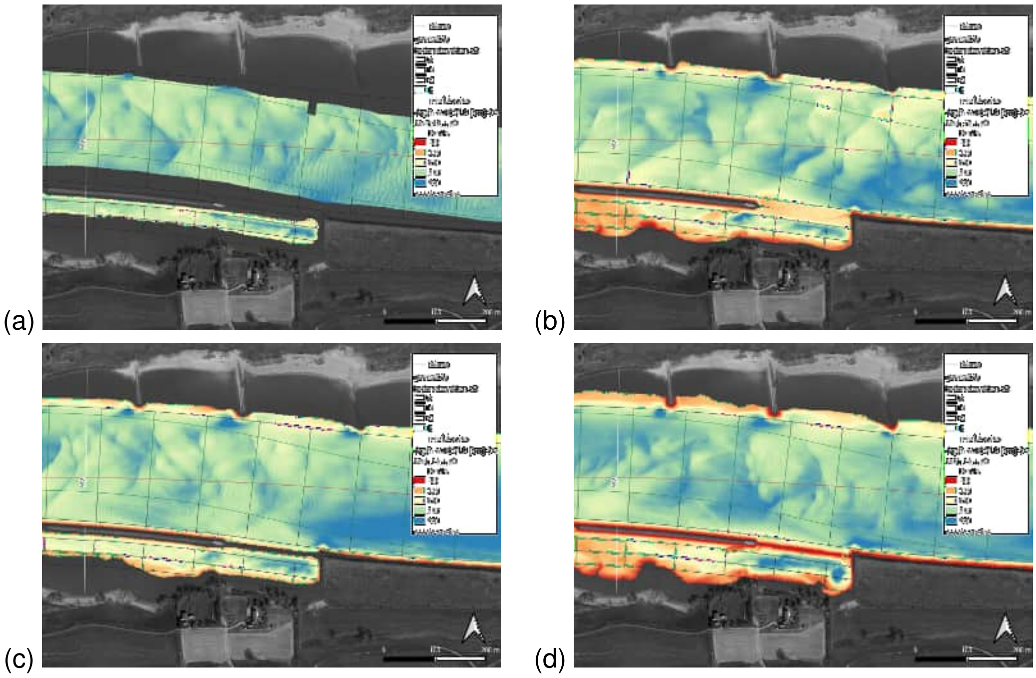

Figure E.37 Depth w.r.t. OLR at the Wamel inlet (a) 2015 week 42, (b) 2018 week 10, (c) 2018 week 26 and (d) 2020 week 26.

E.7 Dreumel inlet

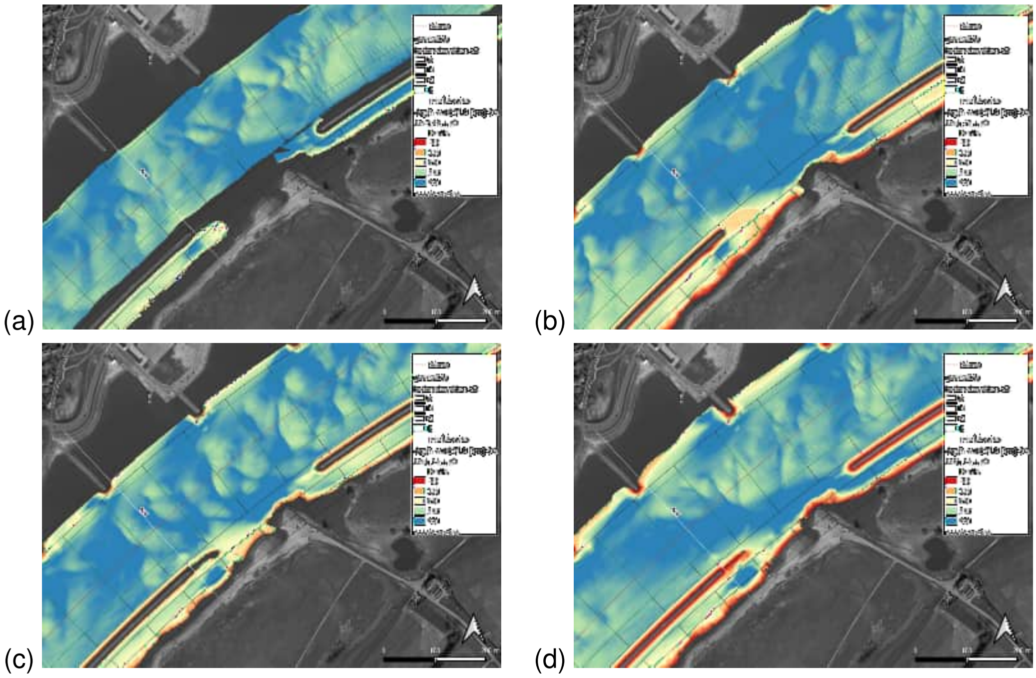

Figure E.38 Depth w.r.t. OLR at the Dreumel inlet (a) 2015 week 42, (b) 2018 week 10, (c) 2018 week 26 and (d) 2020 week 26.

E.8 Ophemert inlet

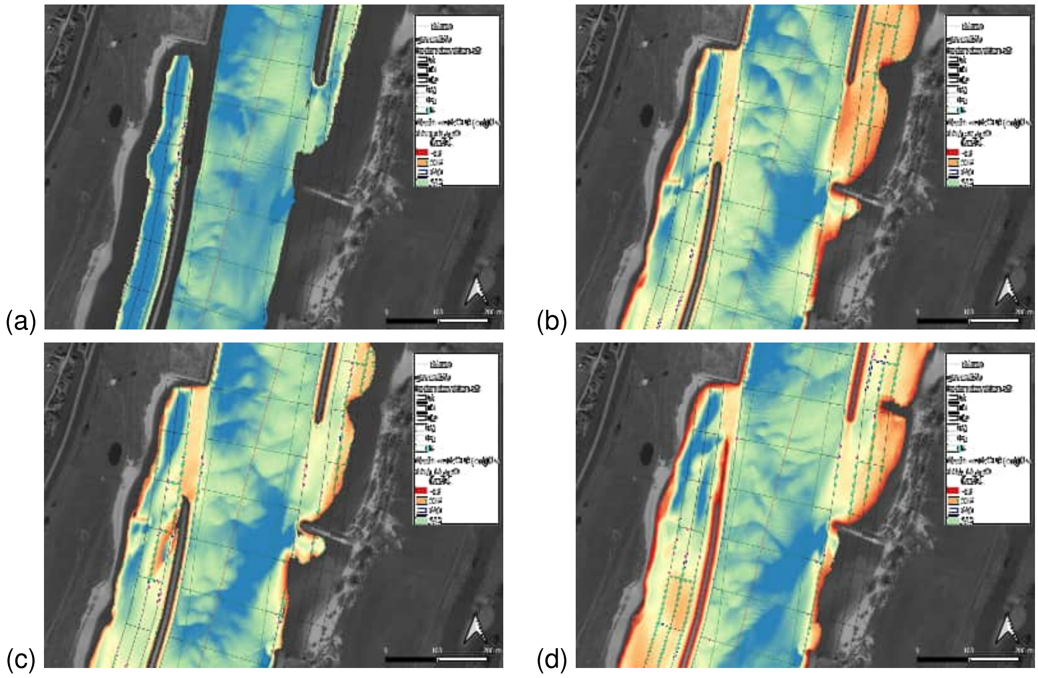

Figure E.39 Depth w.r.t. OLR at the Ophemert inlet (a) 2015 week 42, (b) 2018 week 10, (c) 2018 week 26 and (d) 2020 week 26.

E.9 Overall sedimentation erosion

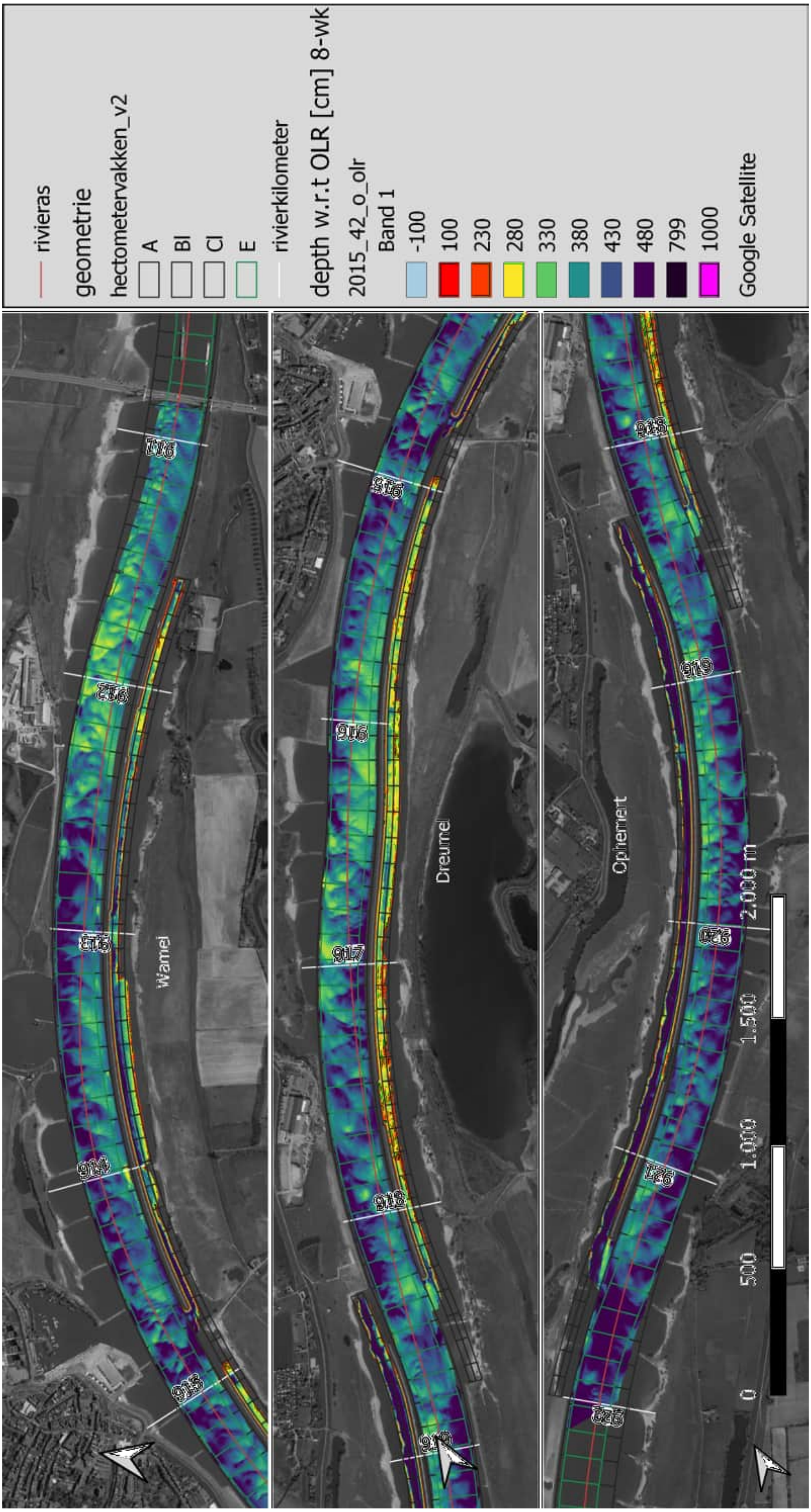

Figure E.40 Depth w.r.t. OLR in 2015 week 42.

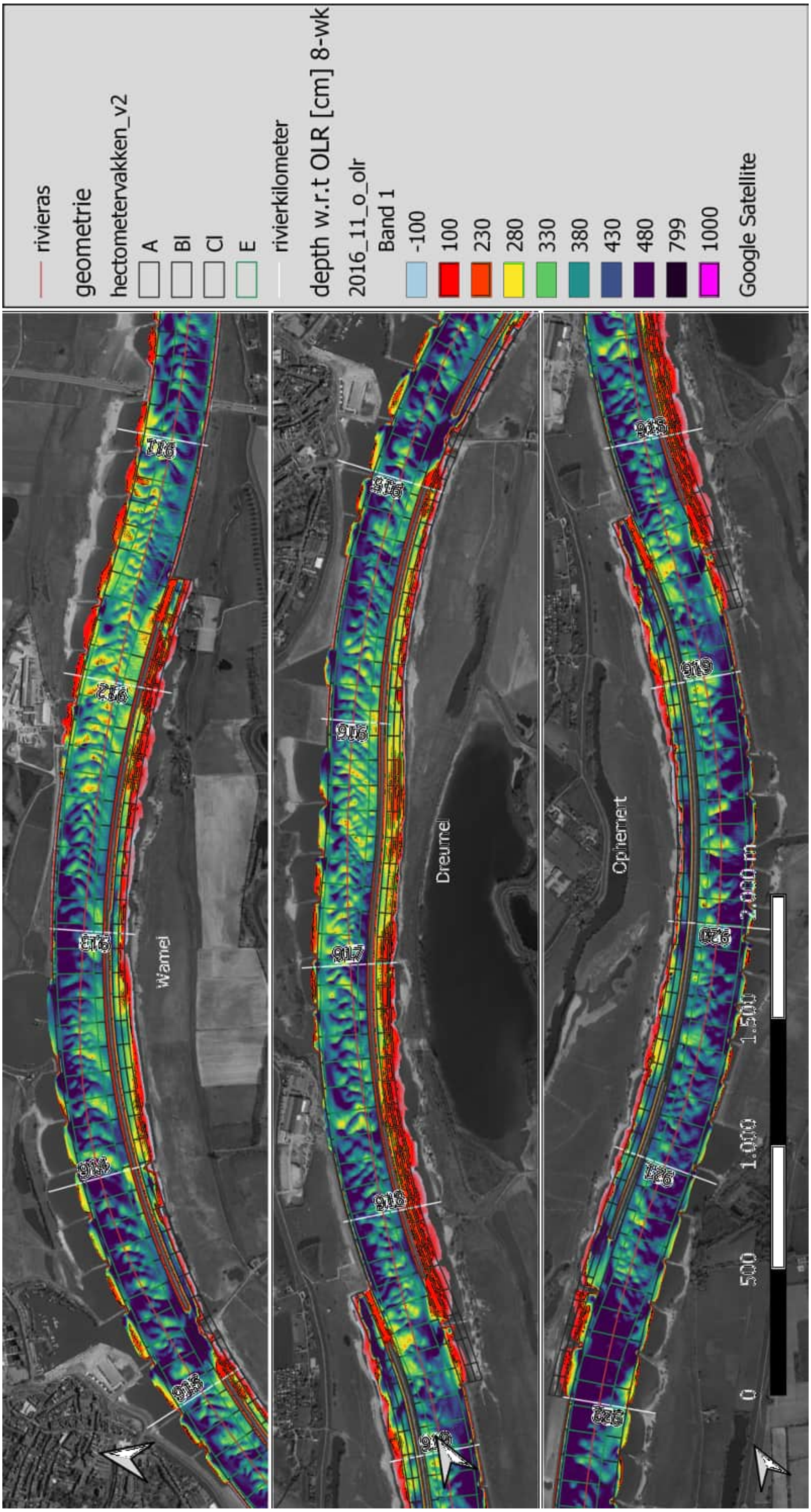

Figure E.41 Depth w.r.t. OLR in 2016 week 11.

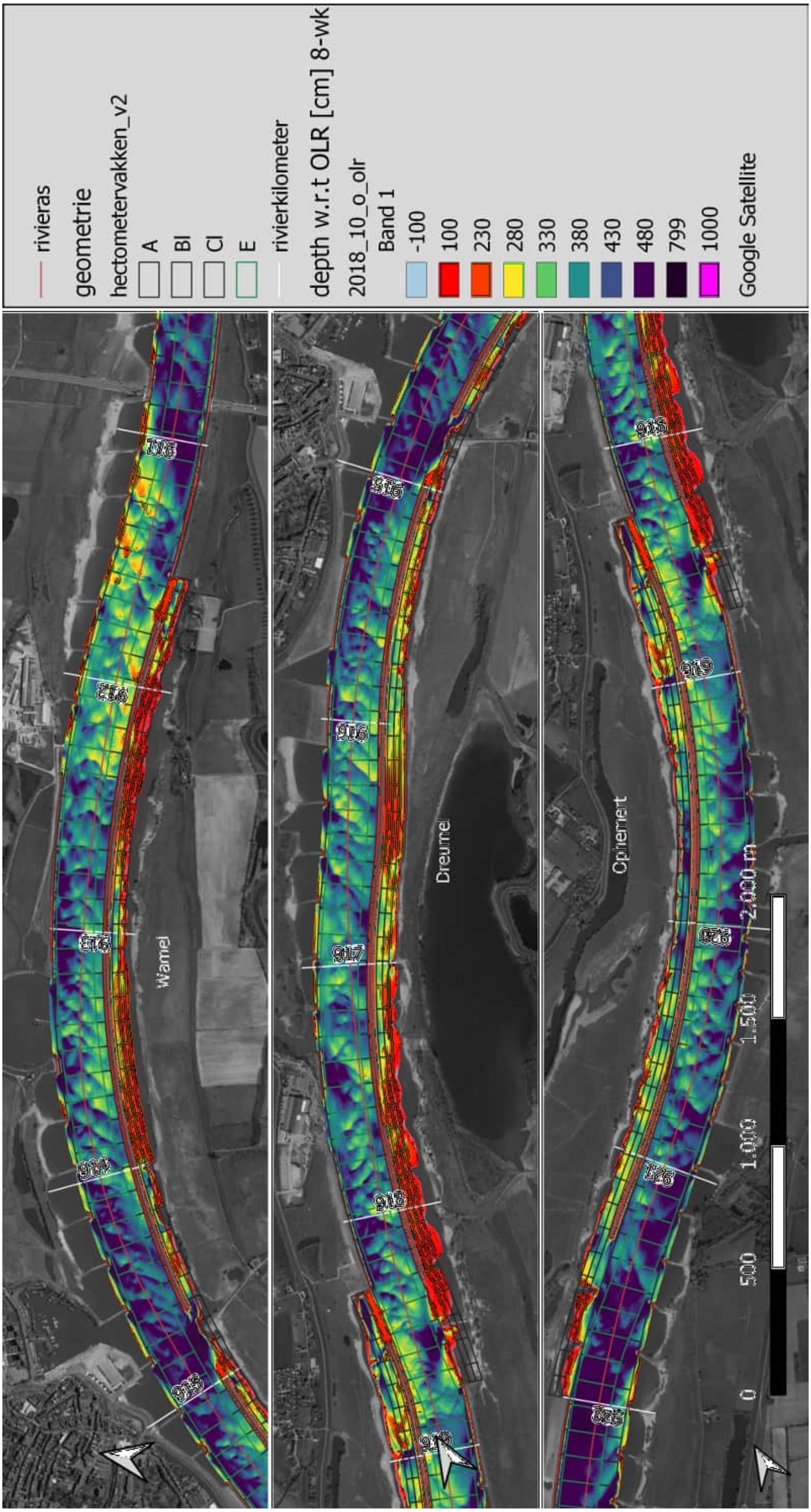

Figure E.42 Depth w.r.t. OLR in 2018 week 10.

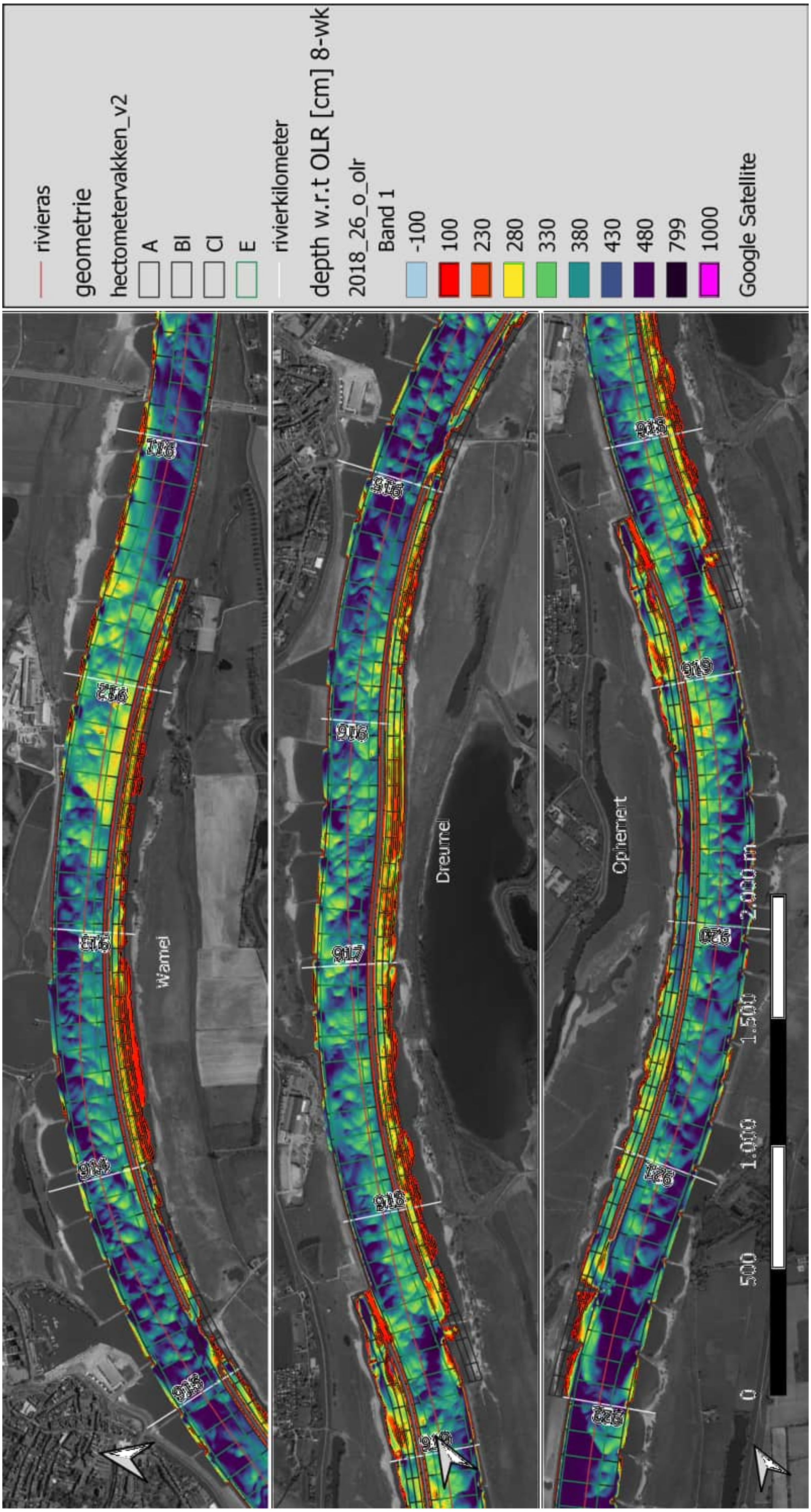

Figure E.43 Depth w.r.t. OLR in 2018 week 26.

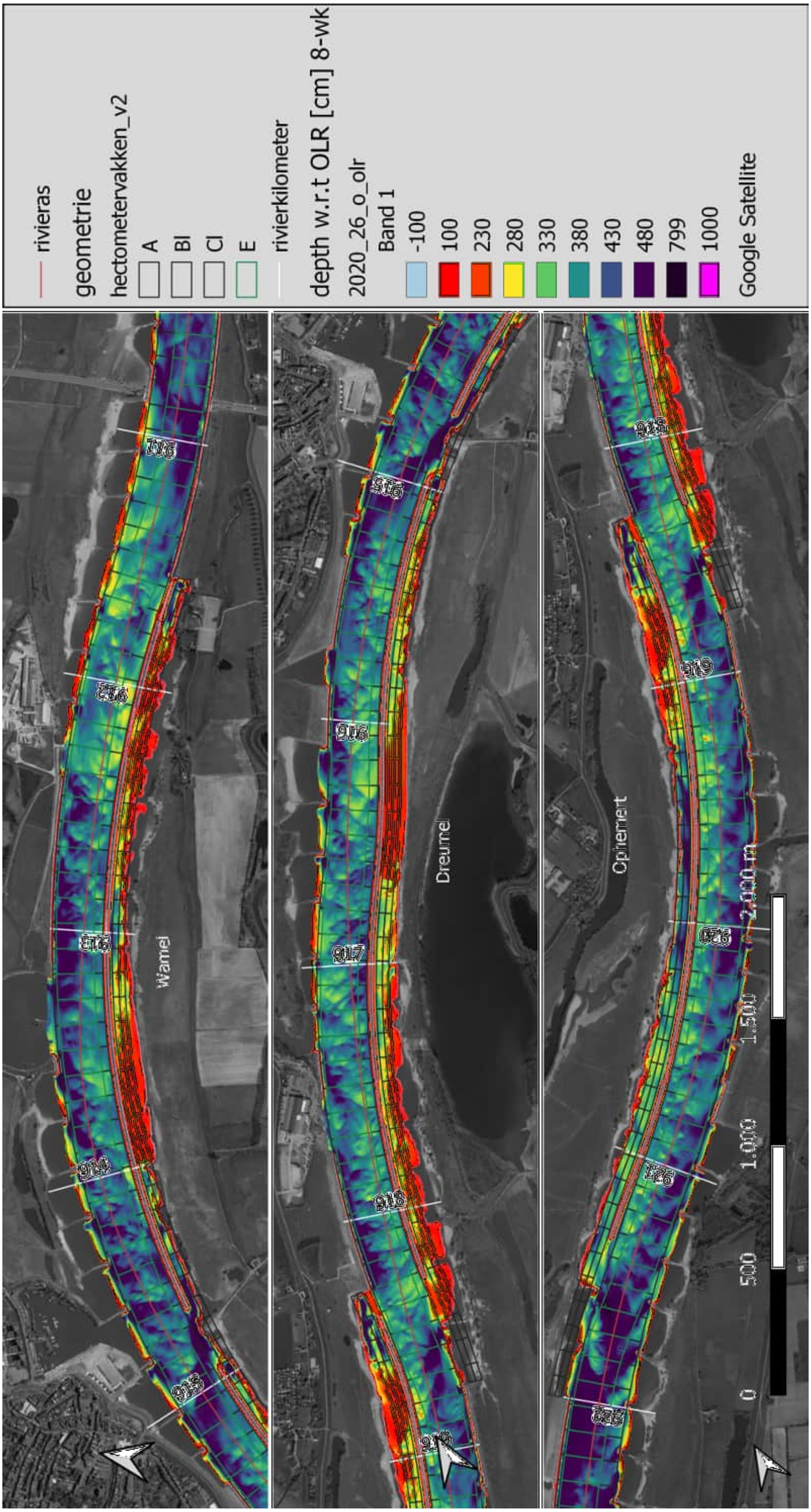

Figure E.44 Depth w.r.t. OLR in 2020 week 26.

Deltares

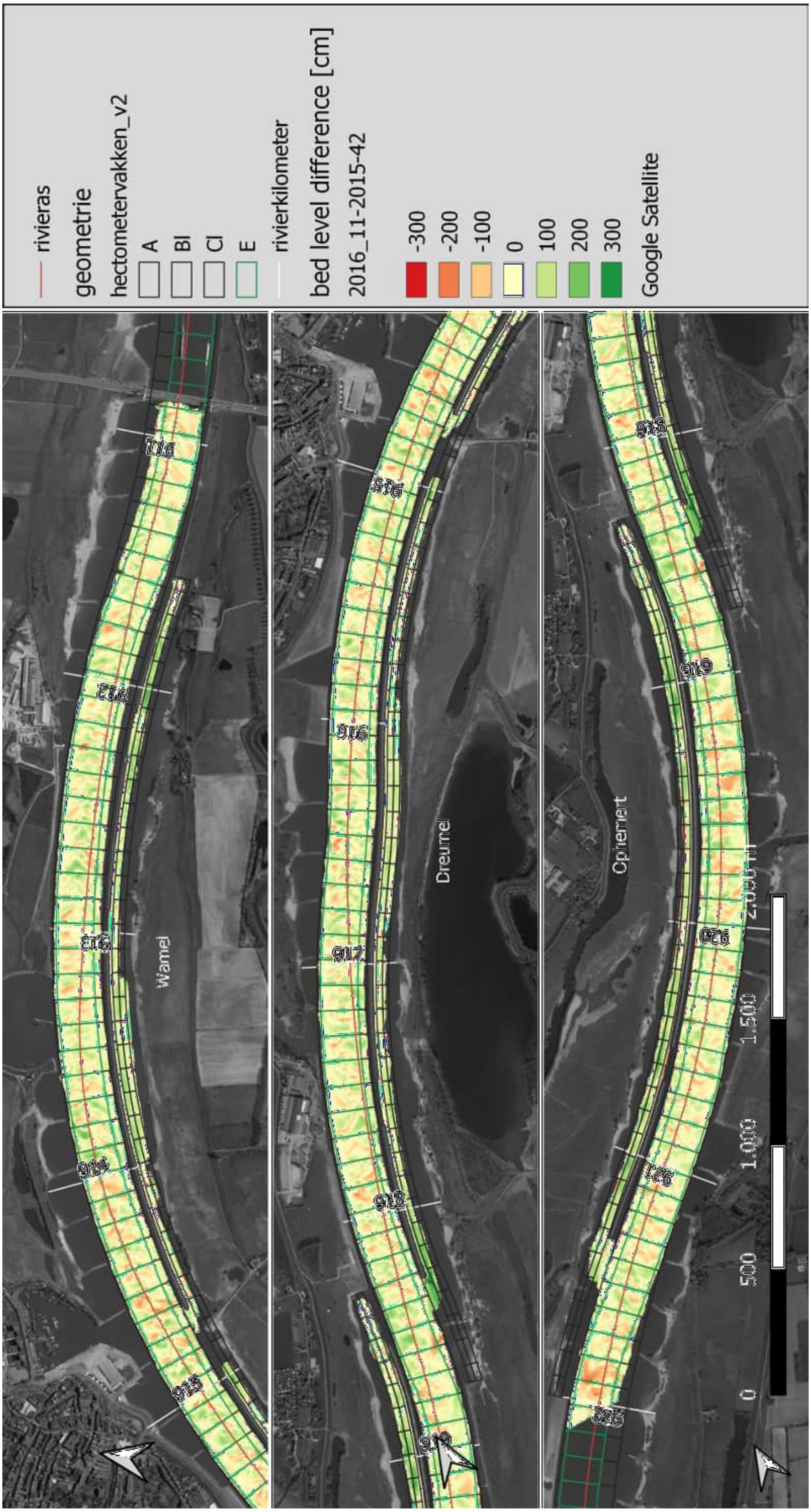

Figure E.45 Initial erosion 2016 week 10 minus 2015 week 42.

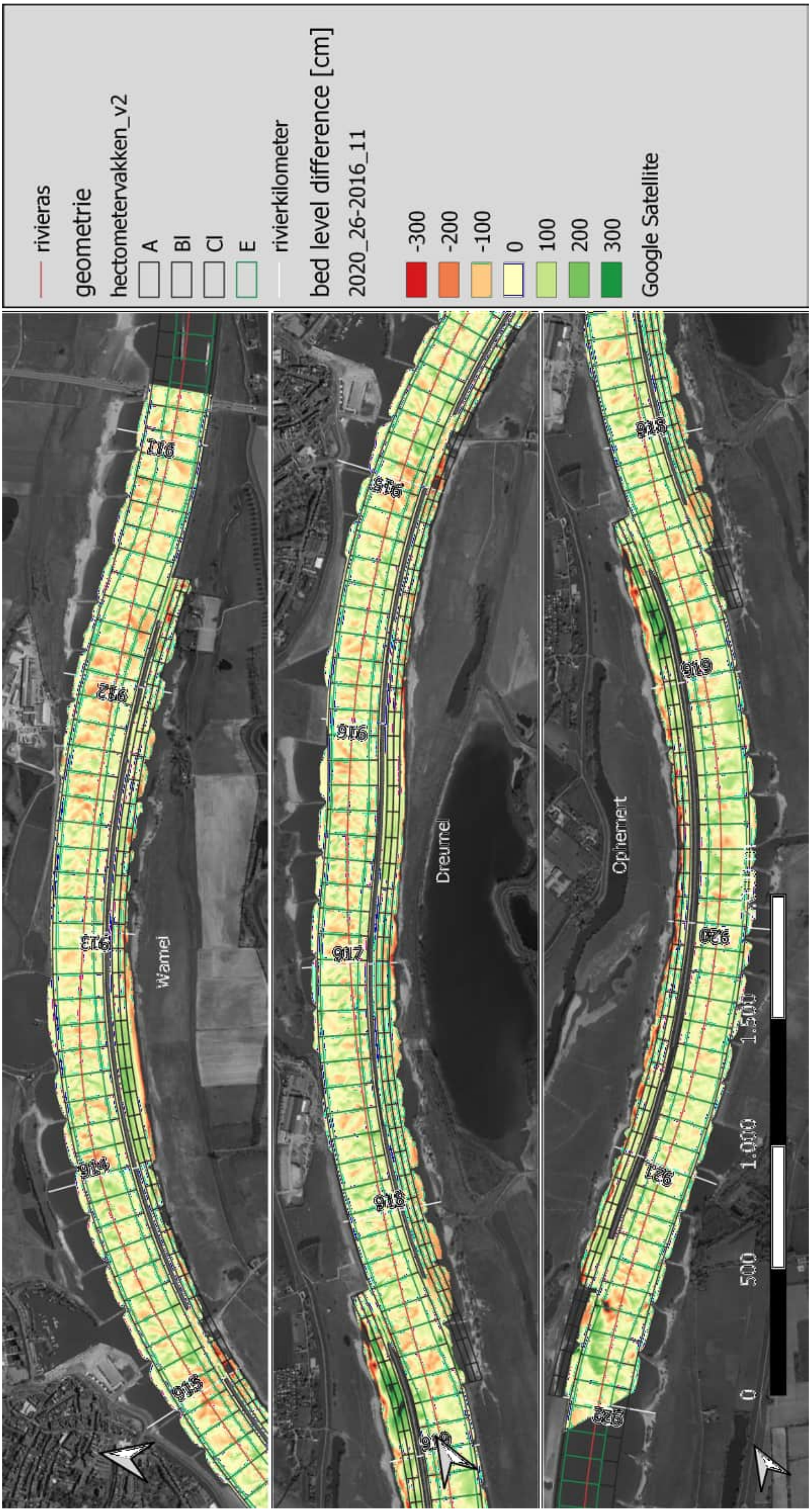

Figure E.46 Initial erosion 2020 week 26 minus 2016 week 10.

F MGD registrations

In this appendix the MGD registrations are given in a longitudinal plot of the Waal. The registrated depth is reduced to bins of 50 cm. In 2015 and 2016 only one MGD for the entire Waal was registered. From 2017 onwards the Waal was segmented in multiple reaches and MGD are since then reported for each of those reaches. For comparison the MGD-data is reduced to only the minimum MGD in figures F.5 and F.6

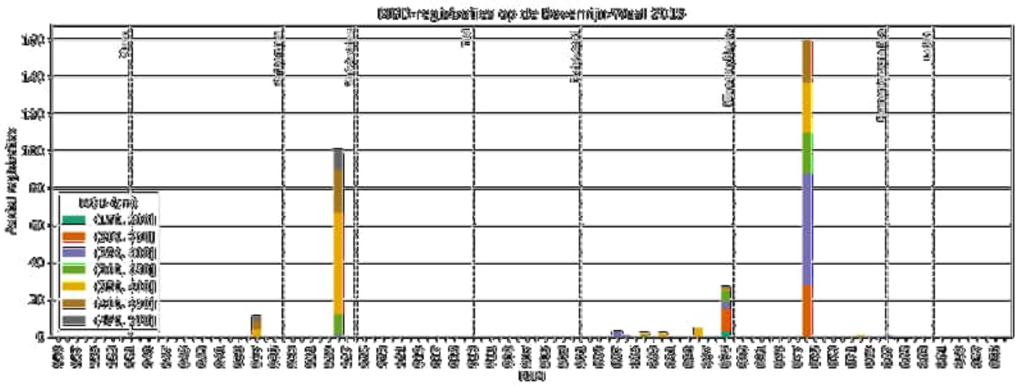

Figure F.1 Registrations of the MGD in 2015.

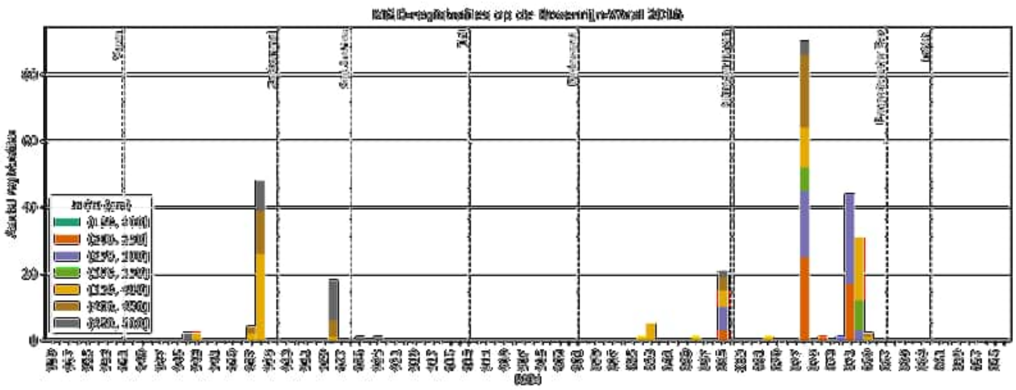

Figure F.2 Registrations of the MGD in 2016.

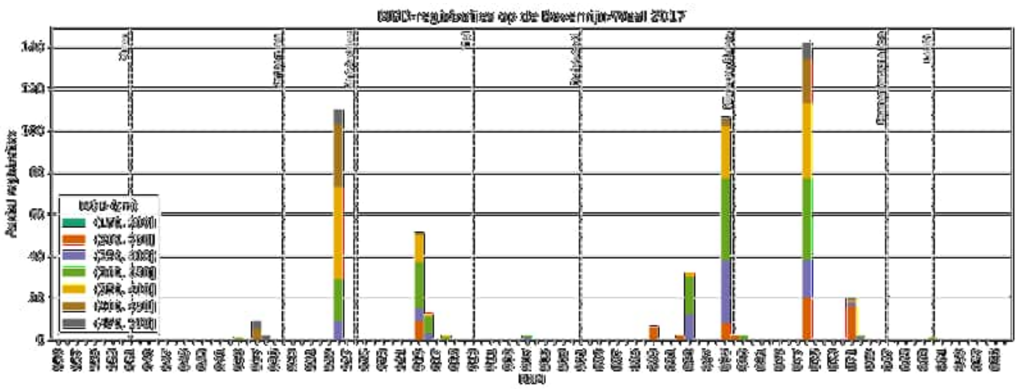

Figure F.3 Registrations of the MGD in 2017.

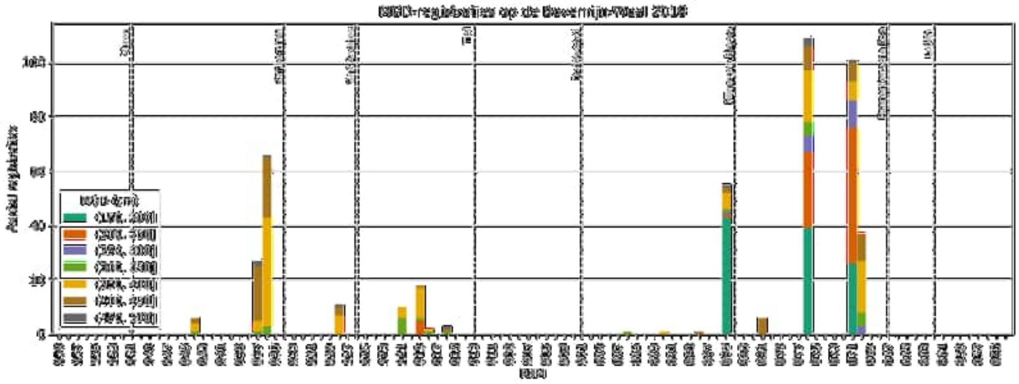

Figure F.4 Registrations of the MGD in 2018.

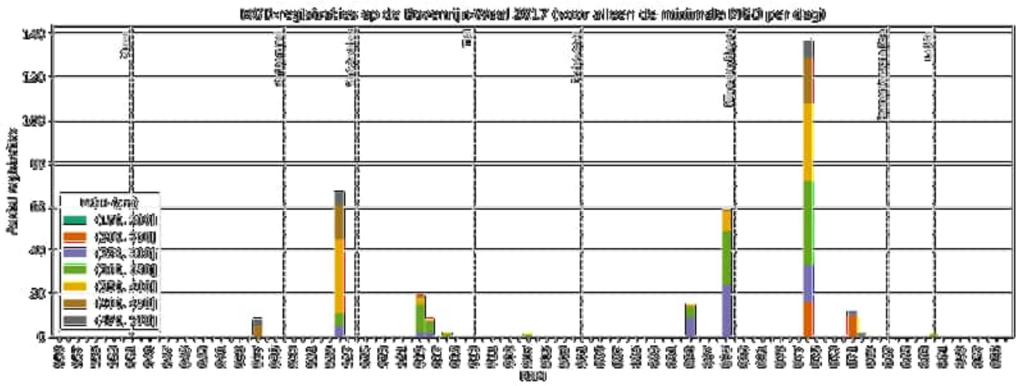

Figure F.5 Registrations of the MGD in 2017. Only showing the minimum MGD for each day.

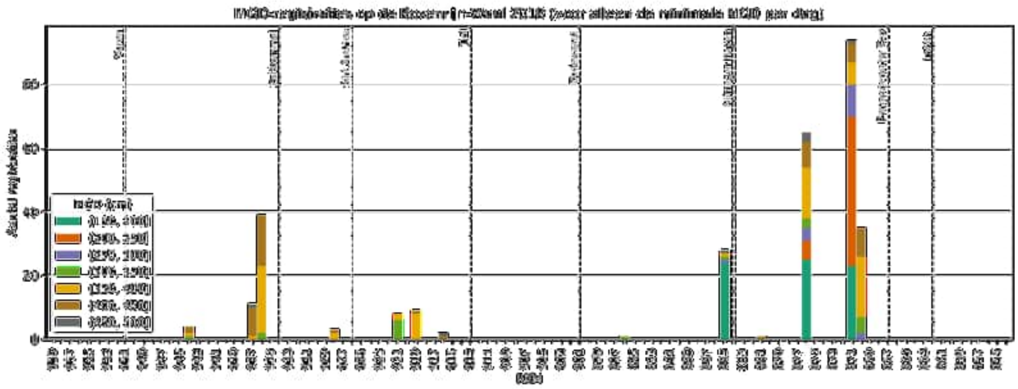

Figure F.6 Registrations of the MGD in 2018. Only showing the minimum MGD for each day.